A STUDY OF COLUMN SEPARATION ACCOMPANYING PRESSURE TRANSIENTS IN AN AVIATION KEROSENE PIPELINE

by

John Arthur Swaffield, B.Sc., M.Phil., Grad. R.Ae.S.

A thesis submitted for the degree of Doctor of Philosophy in Mechanical Engineering of The City University, London.

Mechanical Engineering Department,
The City University,
London.

November, 1970.

TEXT CUT OFF IN THE ORIGINAL

PAGE NUMBERS ARE CLOSE TO THE EDGE OF THE PAGE.

SOME ARE CUT OFF

SUMMARY

Column separation on both the upstream and downstream sides of a valve in an aviation kerosene pipeline was the subject of an investigation involving the method of characteristics to solve the partial differential equations governing pressure transient propagation. Particular attention was given to obtaining accurate velocity results at the instant the predicted pressure at a section reached vapour pressure.

A test rig utilizing L.56 aluminium alloy fuel piping and other aircraft standard components and pumping Aviation Kerosene Specification 2494, was employed to investigate the phenomenon and test the computing procedures.

For separation upstream of a valve following closure, a comparison of the computed and observed results indicated an accuracy within 3% for the first peak following valve closure and 5% for the cavity duration. Computed results within 10% of the observed were obtained for the later peaks following cavity collapse.

Observation and filming of the sequence of events downstream of the valve during and following closure indicated that the air released during initial separation remained out of solution. The effect of this air was significant but could be included, in terms of its partial pressure, in the cavity boundary equations.

The predicted cavity collapse pressures were consistently above those observed. Predicted values of maximum and minimum pressures, and their event times, following valve closure were, at worst, within 10% of the observed results.

Analysis of the released gas indicated that it had normal air composition. Measurement of column velocity from the films and the use of a hot film probe and anemometer supported the assumptions made with reference to column motion. The hot film probe results demonstrated that this flow measurement technique was practical in this application.

ACKNOWLEDGEMENTS

The work reported was carried out at The City University under a Science Research Council award, BSR 5832.

Loans of equipment from the British Aircraft Corporation and Saunders Valve Co., now Flight Refuelling, are gratefully acknowledged.

The author wishes to record his thanks to Mr. J.W.R. Twyman, Senior Lecturer in Mechanical Engineering, for his advice throughout the research. Mr. H.T.C. Boucher, Assistant Chief Systems Engineer, B.A.C. Filton, is to be thanked for his interest and support for the work reported.

Finally the author would like to thank Mrs. Gray and Miss Saunders, Mechanical Engineering Department, for their skill and patience in typing the manuscript.

LIST OF CONTENTS

List of Figures and Tables

Notation

A	Pipe cross sectional area
AIRVOL	Volume of released air
ATM	Atmospheric pressure
a	Overheat ratio
C^+, C^-	Characteristic directions
C_D	Discharge coefficient for venturi meter
C_R	Reflection coefficient
C_T	Transmission coefficient
C_p, C_v	Specific heats of the fluid
c	Transient propagation velocity
c_o	Acoustic velocity for the fluid
c_1	Constant included in wave speed equation to allow for longitudinal stress
D	Pipe bore
d	Wire diameter - anemometer section
E	Young's Modulus pipe material
e	Pipe wall thickness
F( ),f( )	Pressure waves
FUELVOL	Volume of fuel releasing its dissolved air
f	Friction factor based on Reynolds No.
g	Acceleration due to gravity
I	Anemometer current
K	Fluid Bulk Modulus
K^1	Effective Bulk Modulus of the pipe/fluid system
K	Bunsen solubility coefficient
K_f	Thermal conductivity
k_1, k_2	Minor loss coefficients at reservoir inlets
L	Pipe length
ℓ	Wire length - anemometer section

m	Mass of a fluid element
N, N1	Number of sections in a pipe
n	Polytropic coefficient of expansion
P	Power - anemometer section
P	Pressure at a pipe section at time T
PP	Pressure at a pipe section at time T + ΔT
PR	Reservoir pressure, configuration 1
PR1 PR2	Upstream and downstream reservoir pressures respectively in configurations 2, 3
PA	Partial pressure of released air, downstream of the valve
PC1, 2	Maximum pressures attained following the collapse of the first and second cavities downstream of a valve
PM1, 2	Minimum pressures attained during the growth of the first and second cavities. Pressures expressed as variations from steady state
p	Pressure at a pipe section
Q	Flow rate or heat transfer in anemometer section
R	Pipe radius
R	Film resistance at operating temperature
R_o	Film resistance at fluid temperature
Re	Reynolds Number
T, t	Time, measured from start of valve closure
TM1, 2	Minimum pressure time for the first and second cavity formed
TC1, 2	Maximum pressure time following the collapse of the first and second cavities
TS	Time of occurrence of vapour pressure at each of the sections displaying pressures below vapour pressure at the end of a time step
TSMAX	Maximum value of a TS array element for that time step
TC, tc	Valve closure time
TSEP	Instant of column separation
TCLOS	Cavity collapse time for upstream case, maximum returning column velocity time for downstream case

T, To	Film and fluid temperature in anemometer section
tp	Pipe period - 2L/c, defined as the time taken for a transient to return to its source from a system boundary
U	Fluid velocity in anemometer section
V	Anemometer output voltage
VO	Anemometer voltage for zero flow
Vin	Linearizer input voltage
Vout	Linearizer output voltage
V	Mean velocity at a section at time T
VV	Mean sectional velocity at time T + ΔT
Vo	Initial flow velocity
VU, VD	Interface velocities for an internal vapour cavity
VAP	Fluid vapour pressure
VSEP	Initial column velocity on separation
VCLOS	Cavity collapse velocity for upstream case, maximum returning column velocity for downstream separation
VOL	Cavity volume
X, x	Distance along the pipe measured in the initial flow direction
Z	Interpolation constant
α	Pipe inclination, valve open angle
γ	Ratio of specific heats
ΔPo	Pressure drop through an initially fully open valve
Δp	Pressure change across a transient
ΔT, Δt	Time increment
ΔV	Velocity change across a transient
Δx	Length of a pipe section
δs	Length of a control volume

ε	Volumetric strain
ε_1	Unit axial rate of strain
ε_2	Unit circumferential rate of strain
θ	Slope of wave front
λ_1, λ_2	Factors used in the derivation of the characteristic equations
μ	Poisson's ratio
ρ	Fluid density
σ_1	Axial stress
σ_2	Circumferential stress
τ_o	Shear stress
τ	Valve pressure-discharge coefficient

Suffixes

cav	Conditions in the cavity
clos	Cavity closing conditions
cℓ	Centre line
I, i	Pipe section
J	Pipe number
m	Mean values
o	Steady state conditions
T, T-ΔT	Conditions at the time indicated
vap	Vapour pressure

Abbreviations and Definitions

C.T.A.	Constant Temperature Anemometer
O.D.	Oscillator Demodulator unit
L.D.T.	Linear Displacement Transducer
T.M.G.	Time Mark Generator

'rapid valve closure'	a valve closure in less than the pipe period 2L/c calculated from the distance between the valve and the nearest system boundary
'slow valve closure'	a valve closure taking longer than 2L/c
X/L	Position in the pipeline expressed as a % of the pipe length measured from the upstream boundary
Sign convention	Distance is measured +ve in the initial flow direction for both the numerical and graphical methods discussed. This results in an unfamiliar set of equations for the Schnyder Bergeron method as historically distance is measured in the -ve flow direction.

1. INTRODUCTION

Pressure transients will propagate within any pipe network following a change in the steady state conditions of the system. The severity of the subsequent pressure variations will depend on a number of factors including the initial flow velocity and pressure in the pipeline, and the rate of change of the boundary conditions. Among the most common causes of pressure transient problems are inadvertently rapid valve closures or pump failures. Once a transient has been propagated it will continue to be reflected within the system until it damps due to frictional and vibrational effects.

If the pressure at any point in a pipeline falls to the fluid vapour pressure, or in certain circumstances to the gas release pressure, then the fluid column will separate at that section and the separated columns will move under the influence of the prevailing pressure gradients between the cavity and the boundaries of the pipeline. The pressure generated on the collapse of the vapour cavity formed between the separated columns can be of destructive proportions even if any released gas in the region of the cavity is not redissolved by the returning fluid columns. This explains the interest in this particular transient phenomenon.

The roots of pressure transient analysis, or waterhammer as the subject is commonly called, lie in the large scale water distribution and hydro-electric plant field. It is therefore not surprising that all the available work on column separation employed water as the working fluid. Pressure transient phenomena however occur throughout a wide range of engineering applications, from the large scale cases above, through chemical plant and aircraft fuel system applications to small scale installations such as fuel injection systems.

The traditional method of analysis is the Schnyder-Bergeron graphical method first proposed in 1927. The more recent introduction of

digital computing, particularly allied to the numerical "method of characteristics" has enabled complex small scale systems to be accurately analysed without incurring the errors associated with the graphical method.

It was the purpose of the research reported to extend the work on column separation to include its occurrence in aircraft fuel systems and to develop computing procedures capable of predicting the pressure fluctuations during and following cavity collapse in aviation kerosene. A comprehensive series of experiments was devised to investigate column separation on both the upstream and downstream side of a valve following closure, including the use of a high speed camera to record the sequence of events during cavity growth and collapse. Pressure and flow velocity records were made during the existence of the cavity by means of quartz crystal pressure transducers and a hot film constant temperature anemometer. The results obtained from these tests, together with full descriptions of the apparatus, test procedures and the programs and subroutines written in Fortran IV for use on an ICL 1905 computer are presented in this report.

The application of the computing techniques to an analysis of the B.A.C./S.N.A.I.S. Concorde refuelling system is also presented as an appendix to the report.

2. HISTORICAL SURVEY

The number of publications dealing with pressure transient phenomena, or waterhammer as the subject is often called, is vast and covers a period of roughly 80 years. The contributions to the literature range from the purely theoretical treatment of the subject, such as the attempts to use Laplace transform theory to predict pressure variations, through discussions of methods of analysis available at any time, for example the 1933 A.S.M.E./A.S.C.E. symposium, to reports of the occurrence of waterhammer, often destructively, in some particular plant or system.

It would be inappropriate to include much of this literature in the present survey, particularly as there are a number of reviews in print (1, 2, 3). The scope of the present survey will be restricted to the following topics:-

(1) The development of the basic theory of pressure transient analysis and the growth of the methods commonly employed to predict transient pressure effects, either in the design or corrective stages of a system's life.

(2) The development of the method of characteristics in this application, with particular reference to the advances made possible by use of the digital computer.

(3) A review of the literature dealing particularly with column separation following transient propagation. The literature on this sub-topic is limited and it is thought that the survey presented is complete.

The term waterhammer will be used in this survey over the period when it was the common title for the subject, up to about 1960.

2.1 Foundation of waterhammer theory

The first recorded work on waterhammer was carried out by Weber (4) and Michaud (5) who noted the oscillatory nature of the phenomenon and the influence of pipe wall elasticity. However neither realised the connection between the subject and the body of earlier work on sound wave propagation that can be traced back to Euler's solution of the wave equation in 1750 and subsequent work on blood circulation in 1775. During the next 100 years the data on sound wave propagation was extended by D'Alembert, Bernoulli, Thomas Young (1808) Savant and Liscovious (1825) and E.H. and W. Weber (1830). In 1848 Wertheim noted that the acoustic velocity in submerged organ pipes was less than that predicted by the expression:

$$c_o = \sqrt{\frac{K}{\rho}}$$

appropriate for an unconfined mass of fluid. Helmholtz attributed this to the elasticity of the pipe walls in the same year.

In 1878 Korteweg (6) established the equation for acoustic velocity in a fluid/elastic walled pipe system that was to form the basis of much further work:

$$\frac{c}{c_o} = 1/(1 + DK/Ee)^{\frac{1}{2}}$$

Korteweg assumed that the longitudinal and bending stresses set up in the pipe wall could be neglected and that the wavelength of the propagated wave was long in comparison to the pipe bore. Comparisons presented between this equation and contemporary work by Kundt, Lehman and Dvorak display scatter between -10% and +4%.

Lamb (7) extended this work to include the longitudinal stresses by considering the equations of motion along the radius and generating line of a pipe section. By substituting the relevant stress relationships Lamb obtained a cubic expression in c^2. For

long wavelengths Lamb found that the two finite roots of this expression corresponded to two propagation velocities, namely:

(1) the velocity appropriate for the fluid, the value being slightly less than Korteweg's prediction due to the inclusion of longitudinal stress.

(2) a velocity slightly lower than the acoustic velocity of the pipe material, the reduction due to the elasticity of the fluid.

At this time, Joukowsky (8) published the results of a comprehensive series of tests carried out at the Moscow Water Works, together with an independent derivation of Korteweg's wave speed equation.

Joukousky's work is notable as it derived for the first time many of the basic equations for the subject. He realised the significance of the pipe period, i.e. the time taken for a pressure wave to return to its source from a system boundary, and derived the relation between pressure and velocity change during flow stoppage:

$$\Delta p = \rho c \Delta V .$$

In the special case of a flow stoppage in less than one pipe period this expression takes the form

$$\Delta P = \rho c V_o$$

which is known as Joukowsky's equation. Similarly he appreciated the significance of the concept of reflection coefficients at dead ended pipes and reservoirs. The results presented in Simin's translation show a scatter of ±15% on the pressure results and ±2% on the wave velocity records, remarkable in view of the instrumentation available at that time.

Joukowsky's conclusions are of interest as they formed the basis of the modern theory:

(1) The pressure transient is transmitted as a plane wave at constant velocity, the value of this velocity depending on pipe dimensions and elasticity, and the fluid Bulk Modulus and density.

(2) Pressure amplitude remains constant along the pipe.

(3) The concept of transmitted and reflected waves completely explains the periodic nature of the pressure records.

Allievi was also active on waterhammer research and in his Notes 1-4, 1903-1913, (9) he established the Joukowsky relation by making the same assumptions as Joukowsky and Korteweg namely:

(1) Frictionless pipelines.

(2) Uniform pipe dimensions.

(3) Homogeneous wall material.

(4) Longitudinal and bending stresses insignificant.

(5) Uniform velocity distribution in the flow.

From assumption (1) and neglecting the convective terms in the equations of motion and continuity, the wave equation may be expressed as:

$$\frac{\partial^2 p}{\partial x^2} = \frac{1}{c^2} \frac{\partial^2 p}{\partial t^2}$$

which may be solved by a general method proposed by Riemann and d'Alembert yielding:

$$p - p_o = F(t + \frac{x}{c}) + f\ (t - \frac{x}{c})$$

where x is measured in the direction of initial flow, and the functions F, f represent pressure waves propagated in the -ve and +ve x directions respectively.

Allievi used the above relationship to extend Joukowsky's work to slow valve closures by means of a set of interlocked equations intended to predict pressure variations upstream of the valve during and following closure. In order to extend the solution to other points along the pipeline Allievi proposed the first graphical method, which

was cumbersome and impractical but nevertheless served as an illustration of the concept of the F, f travelling waves.

The work of Joukowsky and Allievi has remained the cornerstone of pressure transient analysis. Both predicted a single wave propagation velocity, neither realising the significance of Lamb's work, however in view of the state of communications at that time it is probable that they were unaware of it. Both assumed that the wave was plane, thus neglecting the inertial forces associated with radial fluid motion. Frictional effects were assumed insignificant, as were the mass and inertia of the pipe wall and the longitudinal and bending stresses set up.

Of these assumptions, bending stress has been shown to be insignificant for all but the shortest wavelengths. The neglect of friction would normally result in an over-estimate of any pressure rise, however present graphical and numerical solutions do include friction approximations.

Parmakian (10) proposed an approximation for the effect of longitudinal stress by the inclusion of a factor, c_1, in the Korteweg wave speed equation,

$$c/c_o = 1/(1 + (DK/Ee)\, c_1)^{\frac{1}{2}}$$

where the value of c_1 depended on the pipeline restraint and Poisson's ratio. Halliwell (11) has shown that variations in c_1 have a small effect compared to errors in Young's Modulus E.

Skalak (12) following Lamb's work, assigned the two phase velocities to the propagation of a tensile stress wave in the pipe wall and to the propagation of the main transient in the fluid. The pipe wall stress wave was to be accompanied by a precursor wave travelling ahead of the main transient in the fluid. Experimental verification was provided by Thorley (13), together with evidence of transient dispersion.

Due to its small effect on predicted pressure and wave speed this improved theory is likely to remain of academic interest only.

Thus the basic concepts of waterhammer theory were laid down by 1913, and have proved accurate up to the present time. The means required to analyse any system in terms of the likely waterhammer pressure variations were not available, and the extension of such methods to provide rapid design information on waterhammer had to await the advent of the digital computer.

2.2 Development of waterhammer analysis during the period 1910-1950

It was 1925 before an English translation of Allievi's work was generally available. In this interim period a number of lesser known researchers were active, A.H. Gibson, de Sparre, and Rateau in Europe, Carpenter and Barraclough (14) and Peek (15) in the United States. The first significant contribution was made by Johnson (16) who, in 1915, developed a rigid fluid column theory, and N.R. Gibson (17) who developed Allievi's solution independently in 1920.

In addition to this work, a series of approximate methods were proposed, some derived analytically while others were derived from piecemeal translations of European authors, notably Allievi. The use of these formulae without either a full understanding of their limits of application, or the assumptions made initially, led to a wide range of predicted pressures for any one case.

Two early approximations were due to Vensano and Warren (18). Vensano's approximation was based on Joukowsky's work, however no allowance was included for variation in discharge at a closing valve, so that the theory was reasonable only for high head systems or rapid valve closures. Warren's approximation assumed a uniform pressure rise during closure, and for high head systems predicted a pressure rise on valve closure exactly half that predicted by Vensano.

Contemporary approximations due to Fanning, Talbot and de Sparre were compared by Kerr (3) for a typical valve closure in four pipe periods and result in predicted pressures varying from 65% to 535% above the observed pressure rise.

During this period the number of large scale water distribution systems and hydro-electric schemes built, particularly in the United States, made the provision of an accurate method of analysis vital, and this became available in the early 1930's in the form of the Schnyder-Bergeron graphical method.

This graphical method of waterhammer analysis stemmed from the work of Loewy (20), Schnyder (21) and Bergeron (22, 23), however the origins of the method may be traced as far as Massau's (19) work in the period 1905-1910. For some reason Loewy's contribution has never received attention and the method is generally referred to by the names of its co-founders Schnyder and Bergeron. The method in its present form is outlined in Appendix 1 to this report.

One of the major advantages of the method on its introduction was that frictional losses could be approximated by the inclusion of discrete pressure drops, commonly referred to as "friction joints", at a number of points along the pipeline.

The method did suffer from a number of disadvantages, namely the possibility of cumulative graphical errors, the large time steps and restricted number of friction joints necessary to avoid undue diagram complexity and finally the inability to use the method, prior to its modification for use on a digital computer, as a design tool.

The period between the introduction of the Schnyder-Bergeron graphical method and the widespread use of the digital computer, roughly 1930-50, saw a tremendous increase in interest in waterhammer, particularly in the United States where the A.S.M.E./A.S.C.E. waterhammer

committee held symposia in 1933 (24) and 1937. The graphical method has continued as the main method of analysis up to the present time. Angus, in a series of papers in 1937-40 presented the graphical solutions for the majority of cases likely to be met by the practising engineer (25, 26, 27). More recently, at the I.Mech.E. 1965 Symposium 'Surges in Pipelines', Pearsall (28) and Marples (29) presented papers on the application of the method, while Harding (30) presented a version of the method for use with a digital computer. This 'computerized' version of the method has been successfully employed by a number of authors, including Hayashi and Ransford (31) and has become, following Harding's work, the standard method adopted by the British Hydromechanics Research Association in their transient consulting work, as described by Enever (32).

One of the major problems in this period, 1930-50, was the inability to solve the complete differential equations defining transient propagation. The full equations of motion and continuity will be shown to be:

$$\frac{1}{\rho}\frac{\partial p}{\partial x} + \frac{\partial V}{\partial t} + \frac{V\partial V}{\partial x} + 2f\,\frac{V|V|}{D} = 0$$

$$\rho c^2 \frac{\partial V}{\partial x} + \frac{\partial p}{\partial t} + \frac{V\partial p}{\partial x} = 0$$

It can be seen, if the convective terms $V\partial V/\partial x$ and $V\partial p/\partial x$ are neglected, that the equation of motion is non linear due to the friction term. The simultaneous solution of these equations was considered impossible by some authors (10, 33) and led to the approximations included in the graphical solution of the frictionless wave equation.

The most common approximation of this type considered a single friction joint located at either the upstream (10) or downstream end of the pipeline (34). These hypothetical obstructions were assumed to supply the same pressure loss as the whole pipeline.

This approach was improved on (23) by the introduction of a series of such friction joints at intervals along the pipe. This process was limited by the rapid increase in diagram complexity and the consequent increase in graphical errors.

A number of analytical solutions to the complete equations were proposed (33, 35), involving the linearization of the friction term. Wood introduced Heaviside's operational calculus and presented an example of a simple pipeline and instantaneous valve closure. This work was followed by Rich who proposed the use of Laplace-Mellin transforms. Both solutions involved the linearized friction term, which was a poor approximation for turbulent flow and resulted in complex mathematical solutions for even the simplest practical cases.

Thus, up to about 1950, the best available method was the Schnyder-Bergeron graphical method. The introduction of the digital computer, particularly when allied to the method of characteristics greatly increased the scope and accuracy of waterhammer predictions.

2.3 1950-1970, the introduction of the method of characteristics and improvements in the frictional assumptions made possible by digital computer methods.

The method of characteristics is a general mathematical method that may be used to solve a pair of quasi-linear hyperbolic partial differential equations in two dependent and two independent variables, such as the complete equations defining transient propagation.

The method was first proposed by Riemann in 1860 while he was studying the non linear problem of finite amplitude sound wave propagation in air. Massau in 1900 employed the method in connection with unsteady flow in open channels. The first known application to pressure transients was due to Lamaen (36) in 1947. Two later papers by Gray (37, 38) received wider attention, but neither considered the use of a computer.

Following Gray's work a considerable number of papers were presented in the United States employing the method of characteristics for transient pressure analysis. Among the first contributors were Ezekial and Paynter (39, 40) and more recently Streeter, with several co-authors (41, 42, 43, 44, 45). Paynter severely criticised Streeter and Lai (42) for not quoting Gray's pioneer work, however it would appear that Streeter's contributions were based on a description of the general method by Mary Lister (46), which is also used as a basis for the solutions presented in this report.

Outside the United States a number of papers have been published employing this method, including those by Fox (47, 48), and by the present author (49, 50). Recently Evangelisti (2) presented a complete review of the method and its application to a number of common examples.

Streeter and Lai (42) claimed that the method of characteristics was the equivalent of treating the frictional loss as an uniformly distributed pressure reduction along a pipeline. This is not strictly correct as the choice of finite difference technique effectively reintroduces the concept of 'friction joints'. The improvement lies in the number of such joints, this may be increased indefinitely, the practical limit being supplied by the run time of any program.

The basic assumption is however made that the steady state friction factor equations, depending on the Reynolds Number, based on the mean flow velocity, may be applied to transient flow. The effectiveness of such a quasi-steady approximation for transient viscous effects has been seriously questioned, and it has been shown that the approximation underestimates the frictional damping observed in practice, although the agreement improves for low frequency disturbances or extremely slow valve closures.

The under-estimation of damping is particularly noticeable in transient laminar flow. Although a certain amount of work has been done on this topic, for example Brown and Nelson (51) and Holmboe and Rouleau (52), the results have not been in a form readily applicable to practical pressure transient problems. Zielke (53) presented a method that related the wall shear stress at any section in laminar transient flow to the instantaneous mean velocity and the weighted past mean velocities at that section. As the method of characteristics provides a step by step solution in terms of mean velocity at each pipe section, Zielke's method can be added to a characteristics analysis of a piping system. Robertson (54) and the present author applied Zielke's method to a rapid valve closure in a Shell Tellus 27 pipeline, which proved practical and close agreement was obtained between the predicted and observed pressure variations.

The majority of pressure transient analysis refers to the occurrence of transients in turbulent pipe flow, but little work has been done as yet on an improved frictional representation for the turbulent regime. Wood and Funk (55) proposed a laminar boundary layer model to account for the viscous losses in transient turbulent flow. They assumed inviscid slug flow for the core with all the viscous losses occurring in the boundary layer. Close agreement was achieved for the simple single pipeline rig used, although the authors state that it is necessary to determine the limits of application of the quasi-steady approximation at present commonly employed.

At the present time the use of digital computing methods allied to either the Schnyder-Bergeron graphical method or the numerical method of characteristics allows a reasonably accurate analysis of many transient phenomena to be carried out. As the roots of the subject lie

in the analysis of large scale water distribution systems and hydroelectric schemes it is not surprising that the literature is almost exclusively concerned with water as the working fluid. The occurrence of column separation has received little attention in spite of the destructive consequences of the phenomenon following, for example, a pump failure. The literature on column separation is reviewed separately below.

2.4 Column separation accompanying pressure transients, 1937-1970

The earliest work dealing specifically with column separation was due to Le Conte (56). Le Conte measured the pressure variation immediately upstream of a valve following a rapid closure and during the subsequent cavity formation at the valve. He concluded that the accurate prediction of the cavity collapse pressure rise was dependent on the method employed to calculate the cavity interface velocity. Le Conte assumed that the cavity formed filled the full cross section of the pipeline and that the pressure remained constant at the fluid vapour pressure appropriate for the particular working temperature. Similarly Bergeron (23) analysed the sequence of events following rapid valve closure and presented an estimate of the interface velocities during cavity growth and collapse. The valve boundary conditions in the graphical (p, V) plane were represented by two perpendicular lines, i.e. $V = 0$, and $p = p_{vap}$. The relatively large time steps necessary to avoid an unmanagable graphical solution result in an insufficiently accurate cavity interface velocity, and this in turn results in inaccurate cavity collapse pressures. Usually these collapse pressures are over-estimates of the observed values. Bergeron included a pressure-time trace for this upstream separation case taken from the work of Langevin, 1928, who employed quartz crystal pressure transducers and was possibly the first to use this measurement technique. Unfortunately Bergeron did not present an analysis of Langevin's test case.

Column separation upstream of a valve is the easiest case to analyse as the cavity formation is not affected by flow through the valve during the initial stages of cavity growth. Bunt (57) considered the occurrence of column separation downstream of a closing valve and concluded that pressure fluctuations of waterhammer intensity occurred following the return to the valve of the separated column. Binnie and Thackrah (58) employed a fast action valve to simulate pump shut down and found that column separation could occur downstream of the valve producing severe pressures on cavity collapse. They also noted the repetitive nature of the phenomenon.

Gayed and Kamel (59), employing a test rig similar to Binnie and Thackrah's discovered the presence of a series of secondary pressure waves propagating within the downstream pipeline during the existence of the cavity. These waves have a simple explanation when the pipe is represented by frictionless line terminated by a pair of -1 reflecting surfaces and are merely caused by the reflection within the pipe of the initial negative pressure wave propagated by column separation.

A number of investigators, for example Apelt (60) and Richards (61) have reported on the occurrence of column separation in practice. Apelt and Richards both conclude that the pressures generated on the rejoining of the separated column could be of destructive proportions and Richards particularly stresses the point that the cavity collapse velocity governs the subsequent pressure rise. These conclusions were supported by Duc (62) who photographed cavities formed at a high point in a pump discharge line following a pump failure. Duc observed that low pressures were maintained in the cavities during their growth and decay and that the pressure rise on collapse was very steep if not instantaneous. Duc also confirmed the repetitive nature of the phenomenon. There was no evidence in Duc's work to suggest that air release occurred either at the cavity or in the regions of fluid subjected to pressures below atmospheric pressures.

In many applications the rate of valve closure of pump stoppage is so slow that the movement of a separated fluid column may be approximated by the criteria governing mass oscillations. This was the basis of an approximate method proposed by Kephart and Davies (63) and later expanded by Li (64). Li pointed out, correctly, that not every vapour cavity will result in cavity collapse. The deciding factors include the initial flow velocity, the pipe inclination and the elevation of the source of the transients, i.e. valve or pump, relative to the system boundaries. In some cases the cavity becomes a vapour column between the source and an interface that oscillates before coming to rest at an equilibrium position. In other cases the pipeline simply drains and no high pressures are generated. Li's work and the work reported by the present author refer only to the case where cavity collapse occurs.

Li and Walsh (65) presented equations defining the maximum pressure on cavity collapse in a frictionless pipeline. Li (66) also dealt with the thermal effects of cavity formation and concluded that during cavity collapse the released latent heat raised the temperature and pressure at the cavity interface and vice versa during cavity growth. The net effect is to reduce the cavity size and collapse pressure rise, but the effect was so small as to be insignificant and may be neglected.

In spite of the extreme sensitivity of the cavity collapse pressure to errors in interface velocity the graphical method of Schnyder and Bergeron has been used by a number of authors to predict column separation effects. Lupton (67) described the necessary procedures in 1953 while more recently (1964) Carstens and Hagler (68), drawing on the work of one of their graduate students, describe the sequence of events and the necessary graphical procedures for separation upstream of a rapidly closed valve. They also presented results for column separation following pump failure.

Air or gas release from water is not mentioned by any of the above authors as a factor in column separation calculations. Brown (69)

reported on the effect of entrained air in pump discharge lines and Lawson (70) considered the effect of trapped air in the fire services piping in tall buildings. Brown demonstrated that the presence of entrained air can be included in a solution by the method of characteristics by 'lumping' it at sections along the pipeline. Lawson showed that high pressures can be generated on starting a pump if large quantities of air are trapped in the discharge line. This illustrates the error in the assumption that such air necessarily acts as a cushion for an approaching fluid column. The pressure build up in the trapped air volume is relatively slow so that the approaching fluid column can attain an appreciable velocity before the air pressure becomes sufficient to retard the column. The final pressure generated when the fluid comes to rest can be extremely high, as demonstrated by Lawson's contribution.

All the references quoted up to this point included Le Conte's assumptions that the vapour cavity filled the whole pipe cross section and that the pressure remained at vapour pressure during the growth and decay of the cavity. Baltzer (71) replaced these boundary conditions, for separation upstream of a valve following rapid closure, by assuming that the cavity formed would overlie the fluid and that the flow beneath the cavity would be subject to the viscous, open channel, transient flow equations. The results presented indicate that this model over-estimated both the cavity duration and collapse pressure rise by a factor of about 1.5. The earlier assumptions, when allied to a method of characteristics/ digital computer solution, usually over-estimates cavity collapse pressures but under-estimates cavity duration due to the insufficient frictional damping supplied by the quasi-steady approximation. Baltzer attributed these over-estimates to the release of dissolved air from the water along the whole length of pipeline and supported this by observations of the growth of air bubbles along a glass pipe section during the existence of the cavity at the valve.

In view of the fact that none of the earlier literature mentioned air release and following the present author's own observation of water column separation (72) in a similar test rig, it is the author's opinion that the air bubbles observed by Baltzer were initially entrained in the flow.

Following Baltzer's conclusions Weyler, Streeter and Larsen (73) re-examined the problem, employing the same test rig. They proposed a semi-empirical 'bubble shear stress' which would predict the increased momentum losses under column separation conditions. This 'bubble shear stress' arises from the non-adiabatic expansion and collapse of gas bubbles present throughout the low pressure flow region. The analysis was carried out by means of the method of characteristics, however in order to include the bubble shear stress in the equation of motion it was necessary to introduce a constant C which included all the 'numerical factors and unknown constants', such as the number of bubble nucleation sites per unit wall area. The computer was then programmed to carry out a series of solutions with varying C values until the predicted duration of the first cavity agreed with its observed value, the program then continuing with a complete pressure-time solution. This is at best a dubious procedure as C would be made to automatically include all other potential errors, such as an under-estimate of frictional damping, errors in steady state conditions and the effects of any vibration of the test rig.

The papers referred to in this section are believed to accurately represent the available work on column separation. All the papers refer to water as the working fluid. The release of dissolved air in the region of a vapour cavity is totally neglected, with the exception of Weyler's work which was strictly confined to his test rig.

The object of the work reported in this thesis is the extension of the method of characteristics solution to column separation in an aviation kerosene pipeline. Separation was studied on both sides of a closing valve and procedures are presented, which include the effect of air release from the fuel.

3. THEORY

The theory of pressure transient analysis will be presented in this section, including the derivation of the basic differential equations, their solution in the particular 'no-friction' case and in the general case employing the method of characteristics.

The solution of the full differential equations including a non-linear friction term, pipeline inclination and the convective terms will be presented in a general form applicable to any pair of quasi-linear hyperbolic partial differential equations in two dependent and two independent variables. The necessary computing procedures required to deal with all the system boundary conditions met in the reported research will be outlined together with descriptions of the transient phenomena studied.

Column separation on both sides of a closing valve will be discussed and the application of the method of characteristics to the cavity boundary conditions, including the effect of gas release, will be presented.

3.1 Derivation of the basic differential equations governing the propagation of pressure transients

The propagation of pressure transients within any piping network can be described by a pair of quasi-linear hyperbolic partial differential equations, namely the equations of motion and continuity. In this section these equations will be derived in a form that can either be simplified to allow the description of various transient phenomena or solved in a more complete form by the method of characteristics.

3.1.1 Equation of motion

Figure 1 illustrates the forces acting on an element of fluid in an inclined pipeline. To develop the equation of motion it is necessary to equate the total resolved force in the flow direction to the product of the elements mass and acceleration.

Referring to Figure 1 and resolving parallel to the axis of flow yields an expression for the total force:

$$pA - (p + \frac{\partial p}{\partial x} dx)\ (A + \frac{\partial A}{\partial x} dx) + (p + \frac{1}{2} \frac{\partial p}{\partial x} dx)\ \frac{\partial A}{\partial x}\ dx$$

$$- \tau_o \pi D\ dx + mg\ \sin\alpha = m\ (\frac{V \partial V}{\partial x} + \frac{\partial V}{\partial t}) \qquad (1)$$

made up of two opposing pressure forces, a component of the pressure force due to the change in pipe cross section, friction force and the component of weight, which can be equated to the mass times accelerated term as shown in equation (1).

It is reasonable to assume that changes in fluid density are small compared to the density, ρ, so that:

$$m = \rho\ (A + \frac{1}{2} \frac{\partial A}{\partial x} dx)\ dx$$

Similarly, by assuming that products of small quantities may be ignored in an expansion of (1), the re-arranged terms are:

$$\frac{1}{\rho} \frac{\partial p}{\partial x} + \frac{\partial V}{\partial t} + V \frac{\partial V}{\partial x} - g\ \sin\alpha + \frac{4\tau_o}{\rho D} = 0 \qquad (2)$$

It is customary in pressure transient analysis to assume that the steady state friction factors apply so that:

$$\tau_o = \frac{1}{2} \rho f\ V|V| \qquad (3)$$

where f is the friction factor.

Substituting for τ_o in (2) yields

$$\frac{1}{\rho} \frac{\partial p}{\partial x} + \frac{\partial V}{\partial t} + V \frac{\partial V}{\partial x} - g\ \sin\alpha + 2f \frac{V|V|}{D} = 0 \qquad (4)$$

The equation of motion in the form expressed in (4) will be used throughout this analysis. The modulus or absolute-value sign is introduced in the friction term to ensure that the fluid friction force is always in opposition to the flow direction.

3.1.2 Equation of continuity

Fig. 2 illustrates the flow past two sections of an inclined pipeline δ_s apart. It is assumed that

(i) the pipeline is slightly elastic and obeys Hooke's Law, i.e. δ_s may vary, as may the diameter;

(ii) changes in fluid density may be neglected.

By the principle of continuity, the net mass inflow of fluid per unit time must be equal to the time rate of increase of the mass in the volume it occupies. Referring to Fig. 2 this may be expressed as:

$$\rho AV - (\rho AV + \frac{\partial}{\partial x} (\rho AV)\ \delta_s) = \frac{\partial}{\partial t} (\rho A \delta_s) \qquad (5)$$

Expanding and re-arranging terms yields

$$- V\left(\frac{1}{V}\frac{\partial V}{\partial x} + \frac{1}{A}\frac{\partial A}{\partial x} + \frac{1}{\rho}\frac{\partial \rho}{\partial x}\right) = \frac{1}{\delta_s}\frac{\partial \delta_s}{\partial t} + \frac{1}{\rho}\frac{\partial \rho}{\partial t} + \frac{1}{A}\frac{\partial A}{\partial t}$$

or

$$\frac{\partial V}{\partial x} + \frac{1}{A}\left(V\frac{\partial A}{\partial x} + \frac{\partial A}{\partial t}\right) + \frac{1}{\rho}\left(V\frac{\partial \rho}{\partial x} + \frac{\partial \rho}{\partial t}\right) + \frac{1}{\delta_s}\frac{\partial\ \delta s}{\partial t} = 0 \qquad (6)$$

or, by calculus,

$$\frac{\partial V}{\partial x} + \frac{1}{A}\frac{dA}{dt} + \frac{1}{\rho}\frac{d\rho}{dt} + \frac{1}{\delta_s}\frac{d\ \delta s}{dt} = 0 \qquad (7)$$

The terms in equation (7) represent:

1. the change in velocity between inflow and outlfow, at any instant;
2. the change in pipe cross sectional area;
3. compressibility of the fluid;
4. possible elongation of the pipeline.

These terms must be expressed as functions of the expansion of the pipeline and the compressibility of the fluid, before equation (7) can be transformed into a usable expression.

3.1.3 Compressibility of the fluid:

For a liquid the Bulk Modulus K may be defined as:

$$K = \frac{dp}{dt} \Big/ \frac{1}{\rho} \frac{d\rho}{dt}$$

or in a form suitable for substitution into equation (7):

$$\frac{1}{\rho} \frac{d\rho}{dt} = \frac{1}{K} \frac{dp}{dt} \tag{8}$$

3.1.4 Expansion of the pipeline:

Assuming that ε_2 is the unit circumferential rate of strain, the increase in the radius of the pipeline is:

$$\Delta R = \varepsilon_2 \frac{D}{2}$$

hence the time rate of change of the cross-section of the pipe is

$$\frac{dA}{dt} = \pi D \frac{d\varepsilon_2}{dt} \frac{D}{2}$$

Thus, substituting for the pipe cross sectional area A, yields:-

$$\frac{1}{A} \frac{dA}{dt} = 2 \frac{d\varepsilon_2}{dt}$$

or in a form suitable for substitution into equation (7)

$$\frac{1}{A} \frac{dA}{dt} = \frac{2}{E} \left(\frac{d\sigma 2}{dt} - \mu \frac{d\sigma 1}{dt} \right) \tag{9}$$

where σ_1 is the axial stress, σ_2 is the circumferential stress, μ is the Poisson's ratio and E is the material Young's Modulus.

3.1.5 Elongation of the pipeline

Similarly, the elongation may also be expressed in terms of the stresses in the pipe wall and the material Young's Modulus and Poisson's ratio.

$$\frac{1}{\delta_s} \frac{d\,\delta_s}{dt} = \frac{1}{\delta_s} \frac{d\,\varepsilon 1}{dt}\, \delta_s = \frac{d\,\varepsilon 1}{dt} \tag{10}$$

where ε_1 is the unit axial rate of strain. Expressing (10) as

$$\frac{d\varepsilon 1}{dt} = \frac{1}{E} \left(\frac{d\sigma_1}{dt} - \mu \frac{d\sigma 2}{dt} \right)$$

allows substitution in (7) for the pipe elongation term.

Equation (7), the equation of continuity may now be expressed as:

$$\frac{\partial V}{\partial x} + \frac{1}{K}\frac{dp}{dt} + \frac{1}{E}\left(\frac{d\sigma 2}{dt}(2 - \mu) + \frac{d\sigma 1}{dt}(1 - 2\mu)\right) = 0 \qquad (11)$$

To proceed further it is necessary to make some assumptions with respect to pipe restraint and whether or not the pipeline can be regarded as 'thin walled' in order to obtain expressions for the stresses σ_1 and σ_2.

3.1.6 Effect of pipe restraint

Generally if the ratio of pipe bore to wall thickness is of the order 10 or greater, a pipeline may be regarded as thin walled. It therefore follows from standard theory, which will not be reproduced here, that if the pipe is subjected to a pressure change p then:

1. axial stress $\sigma_1 = \frac{pD}{4e}$ (12)

where D is the pipe bore and e its wall thickness,

and $\frac{d\sigma 1}{dt} = \frac{D}{4e}\frac{dp}{dt}$ (13)

2. circumferential stress $\sigma_2 = \frac{pD}{2e}$ (14)

and $\frac{d\sigma 2}{dt} = \frac{D}{2e}\frac{dp}{dt}$ (15)

Three restraint conditions are commonly considered:

(i) pipeline restrained fully at the upstream end only so that both axial and circumferential stress and strain occur. Thus both equations (13) and (15) apply and equation (11) becomes:

$$\frac{\partial V}{\partial x} + \frac{dp}{dt}\left(\frac{1}{K} + \frac{D}{dE}\left(\frac{5}{4} - \mu\right)\right) = 0 \qquad (16)$$

(ii) pipeline anchored throughout against axial movement,

$$\frac{d\varepsilon 1}{dt} = 0$$

$$\therefore \quad \frac{d\sigma 1}{dt} = \mu\frac{d\sigma 2}{dt}$$

and equation (11) becomes:

$$\frac{\partial V}{\partial x} + \frac{dp}{dt}\left(\frac{1}{K} + \frac{D}{eE}(1 - \mu^2)\right) = 0 \qquad (17)$$

(iii) expansion joints at frequent intervals along the pipe, thus axial stress is zero hence the derivation of equation (11) is altered at equations (9) and (10) as

$\varepsilon_1 = \sigma_1 = 0$

hence equation (11) becomes:

$$\frac{\partial V}{\partial x} + \frac{dp}{dt}\left(\frac{1}{K} + \frac{D}{eE}\right) = 0 \qquad (18)$$

Equations (16), (17), (18) are versions of the continuity equation commonly employed. Normally, it is sufficiently accurate to employ equation (18), however there are cases where the effect of the Poisson's ratio term is significant, these cases basically depending on the relation between the fluid Bulk Modulus, K, and the Young's Modulus, E, of the pipe material.

(i) $E > K$, then the second term in the coefficient of dp/dt is usually smaller than the first, which is itself small, and the effect of μ is not significant.

(ii) $E << K$, then the second term in the coefficient of dp/dt can be considerably greater than the 1/K term and small variations in the multiplier containing μ can be significant.

3.1.7 Velocity of propagation of pressure transients

In an unconfined expanse of fluid the wave speed, c_o, with which sound waves would propagate is given by:

$$c_o = \sqrt{\frac{K}{\rho}} \qquad (19)$$

When the fluid is contained in an elastic pipeline the Bulk Modulus term must be modified to allow for the increase in pipeline dimensions, axial and circumferential. The wave speed in the pipeline can be expressed as

$$c = \sqrt{\frac{K'}{\rho}} \tag{20}$$

where K' is the effective Bulk Modulus term for the fluid/pipeline.

The total volumetric strain ε for the pipeline/fluid combination for a pressure increment p may be expressed as

$$\varepsilon = p\left(\frac{1}{K} + \frac{1}{E}\left(\sigma_2\ (2 - \mu) + \sigma_1\ (1 - 2\mu)\right)\right)$$

$$\text{or} \quad \varepsilon = p\ \frac{1}{K'}$$

Thus for the three restraint cases previously mentioned it is possible to write

$$\frac{1}{K'} = \frac{1}{K} + \frac{D}{eE}\ \left(\frac{5}{4} - \mu\right)$$

$$\frac{1}{K'} = \frac{1}{K} + \frac{D}{eE}\ (1 - \mu^2)$$

$$\frac{1}{K'} = \frac{1}{K} + \frac{D}{eE}$$

Thus, by substituting the appropriate equivalent Bulk Modulus and the corresponding wave velocity in the pipeline into equations (16), (17), (18) it is possible to write the continuity equation in a simplified form:

$$\frac{\partial V}{\partial x} + \frac{1}{\rho c^2}\ \frac{dp}{dt} = 0$$

or, as will be used later in this analysis:

$$\rho c^2\ \frac{\partial V}{\partial x} + \frac{\partial p}{\partial t} + V\ \frac{\partial p}{\partial x} = 0 \tag{21}$$

3.2 Simplification of the basic pressure transient equations

In order to describe some of the basic aspects of pressure transient propagation it is useful to re-write the equations of motion and continuity in the simplified form below:

$$\text{Motion} \qquad \frac{1}{\rho}\frac{\partial p}{\partial x} + \frac{\partial V}{\partial t} = 0 \tag{22}$$

$$\text{Continuity} \qquad \frac{1}{\rho c^2}\frac{\partial p}{\partial t} + \frac{\partial V}{\partial x} = 0 \tag{23}$$

i.e. these equations apply to a horizontal, frictionless pipeline where the convective terms $V\partial V/\partial x$ and $V\partial p/\partial x$ may be neglected with respect to $\partial V/\partial t$ and $\partial p/\partial t$. Equations (22), (23) are a pair of linear differential equations that may be solved directly. By taking the partial derivative of (22) with respect to x and the partial derivative of (23) with respect to t it is possible to eliminate terms in V, hence the equations may be written as:

$$\frac{\partial^2 p}{\partial x^2} = \frac{1}{c^2}\frac{\partial^2 p}{\partial t^2} \tag{24}$$

Similarly, terms in p may be eliminated yielding a second equation:

$$\frac{\partial^2 V}{\partial x^2} = \frac{1}{c^2}\frac{\partial^2 V}{\partial t^2} \tag{25}$$

For the one dimensional wave equation (24) there is an elegant solution known as D'Alembert's solution.

If f is a function possessing a second derivative then:

$$\frac{\partial f}{\partial t}\left(t - \frac{x}{c}\right) = f'\left(t - \frac{x}{c}\right); \quad \frac{\partial f}{\partial x} = -\frac{1}{c} f'\left(t - \frac{x}{c}\right)$$

$$\frac{\partial^2 f}{\partial t^2}\left(t - \frac{x}{c}\right) = f''\left(t - \frac{x}{c}\right); \quad \frac{\partial^2 f}{\partial x^2} = \frac{1}{c^2} f''\left(t - \frac{x}{c}\right)$$

and it is evident that $p = f(t - \frac{x}{c})$ satisfies the equation:

$$\frac{\partial^2 p}{\partial t^2} = c^2 \frac{\partial^2 p}{\partial x^2}$$

Similarly, if F is an arbitrary twice differentiable function, then $p = F(t + \frac{x}{c})$ is likewise a solution to the wave equation. Hence, since (24) is a linear equation, it follows that the sum of F and f is also a solution. If p above is regarded as the pressure change from steady state p_o then the solution of the wave equation takes the generally accepted form:

$$p - p_o = F(t + \frac{x}{c}) + f(t - \frac{x}{c}) \tag{26}$$

Similarly, by substituting for $\partial p/\partial x$ in (22) it follows that:

$$V - V_o = - \frac{1}{\rho c} \left(F(t + \frac{x}{c}) - f(t - \frac{x}{c}) \right) \tag{27}$$

This method of solution of the one dimensional wave equation is named after the French mathematician Jean le Rond D'Alembert (1717 - 1783). The D'Alembert solution is actually not a special method but rather a special application of a general method known as the method of characteristics (74). This form of the solution is particularly useful as it reveals the significance of the parameter c and its dimensions of velocity.

Equations (26) and (27) form the basis of the graphical methods of transient analysis. The Schnyder-Bergeron graphical method is outlined in Appendix 1 to this report.

3.3 Physical significance of the F( ) and f( ) functions and their use to describe simple transient phenomena

The two functions $F(t + x/c)$ and $f(t - x/c)$ are entirely arbitrary and may be selected to satisfy the conditions imposed at the boundaries of the system. Consider the simple pipeline illustrated in Fig. 3 consisting of a single horizontal, frictionless, uniform pipeline of length L terminated at the upstream end by a constant pressure reservoir and at the downstream end by a valve capable of instantaneous closure.

As the F( ) and f( ) functions are arbitrary, the function F( ) may be interpreted as a wave moving in the -x direction, i.e. upstream so that x must decrease at a rate ct. This wave is normally referred to as an F wave and can be propagated by a change in conditions at the downstream end of the pipeline.

Similarly the function f( ) may be interpreted as a wave moving in the +x direction, i.e. downstream. This wave is referred to as an f wave and can be propagated by a change in conditions at the upstream end of the pipeline. The significance of equation (26) is now clear, it implies that at any time t following the initial disturbance, the pressure at a point x in the pipeline may be found from a summation of the travelling F and f waves. It is assumed that these pressure waves travel at a uniform speed c and do not attenuate or change their shape either as they propagate along the pipeline or as they pass each other.

Referring again to Fig. 3 let the disturbance be an instantaneous closure of the downstream valve. As mentioned above an F wave would be propagated upstream from the valve, however as the valve closure is instantaneous the f wave terms in (26), (27) are zero.

Hence applying (26), (27) at the valve at t = 0 yields:

$$p - p_o = F(t + \frac{x}{c}) \tag{28}$$

$$V - V_o = -\frac{1}{\rho c} F(t + \frac{x}{c}) \tag{29}$$

Eliminating F( ) yields

$$p - p_o = -\rho c (V - V_o) \tag{30}$$

where V = 0 as the closure was assumed instantaneous.

Hence the pressure rise at the valve may be expressed as:

$$\Delta P = \rho c V_o \tag{31}$$

This is the maximum pressure rise possible on valve closure and the expression in this form is named after Joukowsky who first demonstrated its validity in 1897.

The equations (28) to (30) apply not only for instantaneous closures but for any valve closure that is completed before the return to the valve of an f type wave from the upstream reservoir, namely any closure completed in less than one pipe period, tp, where

$$t_p = 2L/c \tag{32}$$

The sequence of events following valve closure in the simple pipeline considered may now be described.

At the instant of valve closure (t = 0) the fluid nearest the valve is compressed, brought to rest and the pipe wall is stretched. This process is repeated upstream at the wave speed appropriate for the fluid/pipeline combination, Fig. 3 b, until at a time t = L/c all the fluid is at rest at the uniform pressure $p_o + \rho c V_o$, all the momentum having been lost and all the kinetic energy having been changed into elastic energy. At this time L/c the wave front is at the reservoir inlet so that an unbalanced condition exists, since the reservoir pressure is assumed to be unchanged. This produces a reverse flow of fluid out of the pipeline into the reservoir and an attendant pressure

drop, f type wave, that propagates back downstream. This f wave returns the pressure to its initial p_o value, i.e. a - $\rho c V_o$ wave, and the velocity of the reverse flow behind the f wave is similarly - V_o, Fig. 3 d. The reservoir is thus said to have produced a negative reflection of the incident F wave, and so possesses a - 1 reflection coefficient.

The f wave propagates towards the valve at the sonic velocity c and arrives at the closed valve at time t = 2L/c. At this instant the pressure along the whole pipeline is p_o and the flow velocity is - V_o. Since the valve is closed at this instant no fluid is available to maintain the flow at the valve so that a low pressure, - $\rho c V_o$, F type wave develops and propagates upstream again bringing the flow to rest and resulting in a contraction of the pipeline walls, Fig. 3 f. It has been assumed here that the initial steady state pressure p_o at the valve is sufficient for

$$p_o - \rho c V_o > P_{vap} \tag{33}$$

so that column separation does not occur. If equation (33) is not satisfied the fluid column parts from the closed valve face as a vapour cavity forms and can continue to move upstream for a considerable period before the prevailing pressure gradients reverse the flow and finally close the cavity. The closed valve, fully restrained and in the absence of separation, thus reflects an incident wave with equal magnitude and sign and is thus said to have a + 1 reflection coefficient.

At time t = 3L/c the - $\rho c V_o$, F type, wave arrives at the reservoir, the fluid column is at rest and at a uniform pressure $p_o - \rho c V_o$. An unbalanced condition again exists at the reservoir inlet which again produces an f wave reflection of the incident wave, having a magnitude $\rho c V_o$, which propagates downstream increasing the pressure at each section to its steady state value p_o and re-establishing the

flow, V_o, in the downstream direction, Fig. 3 h. At time 4 L/c this wave reaches the closed valve and conditions are identical to those at the time of the instantaneous valve closure two pipe periods earlier.

This process is repeated completely every 4 L/c. The presence of fluid friction, the imperfect elasticity of fluid and pipe wall together with the possible vibration of the pipeline, particularly at the closed valve, damp out the pressure waves and the fluid eventually comes permanently to rest at reservoir pressure.

The simple pipeline system described can therefore be represented, following valve closure, by an attenuation free line terminated at the upstream end by a - 1 reflector and at the downstream end by a + 1 reflector. This model can be employed to explain many of the pressure transient phenomena encountered.

3.3.1 Pressure variation on either side of a valve positioned between two reservoirs following a rapid closure

Fig. 4 illustrates a simple pipeline system consisting of two pipelines connecting two constant pressure reservoirs and joined at a valve. The pipelines need not have similar properties. The valve closure is assumed to be rapid, i.e. completed in a time less than the period, 2 L/c, of either pipeline.

Consider the pressure variations on the valve upstream face. The maximum pressure rise $\rho c\, V_o$ is generated as equations (28) (29) apply. The pressure rise time is $\frac{1}{2}$ of the upstream pipe period as this is the assumed valve closure time. The pressure variations are illustrated in Fig. 4 and can be explained by use of the reflection coefficients derived previously. It is to be noted that the time taken for the pressure at the valve to fall from $p_o + \rho c\, V_o$ to $p_o - \rho c\, V_o$ is the valve closure time as the f type wave and its F type reflection

are both present at the valve between the times t = 2 L/c and t = 2 L/c + tc where tc is the valve closure time.

Similarly the pressure variation at the mid point of the upstream pipe can be explained by reference to the F, f waves. It is to be noted that the maximum $\rho c\ V_o$ pressure is only generated at this point if the valve closure time, and hence the time taken for the wave front to pass any point, is less than L/c, otherwise the F and f waves overlap and reduce the pressure generated. For the valve closure in ⅜ pipe periods points closer to the reservoir than 3/16 L register a maximum pressure rise progressively less than $\rho c\ V_o$, culminating in a constant pressure at the reservoir inlet.

Pressure variations on the downstream face of the valve are also illustrated in Fig. 4. For convenience the pipelines are considered to be equal in length and properties. Applying equations (26), (27) at the valve downstream face at t = tc, it will be seen that it is an f type wave that is propagated downstream from the valve, the F( ) function may be neglected if tc < 2 L/c, hence:

$$p - p_o = f(t - \frac{x}{c})$$

$$V - V_o = \frac{1}{\rho c} f(t - \frac{x}{c})$$

hence $p - p_o = \rho c\ (V - V_o)$

and as $V = 0$ at $t = tc$

$$p - p_o = - \rho c\ V_o \qquad (34)$$

Subsequent pressure variations are explained by the same methods as outlined for the upstream case. It is to be noted that equation (33) must be satisfied on the downstream face of the valve for the waveform illustrated in Fig. 4 to apply. If equation (33) is not satisfied column separation occurs on the downstream face of the valve.

3.4 Application of the method of characteristics for the solution of the equations of motion and continuity defining transient propagation

The technique described in this section is entirely general (46) and may be employed to obtain the numerical solution to a pair of simultaneous quasi-linear hyperbolic partial differential equations of the first order in two dependent and two independent variables. Linear combinations of the two differential equations, i.e. the equations of motion (4) and continuity (21) will be sought which contain derivatives of the two unknown functions in one direction only. For the type of equation considered there are two such directions, known as characteristic directions, along which finite difference approximations may be applied. Both first and second order finite difference approximations will be discussed.

3.4.1 Derivation of the characteristic equations

The differential equations defining transient propagation have been derived as:

$$L_1 = \frac{\partial p}{\partial x} + \rho \left(V\frac{\partial V}{\partial x} + \frac{\partial V}{\partial t}\right) + \left(2\rho f V\frac{|V|}{D} - \rho g \sin\alpha\right) = 0$$

$$L_2 = V\frac{\partial p}{\partial x} + \frac{\partial p}{\partial t} + \rho c^2 \frac{\partial V}{\partial x} = 0$$

i.e. equations in two independent variables (x, t) and two dependent variables (p, V).

It will be assumed that all the functions involved are continuous and possess as many continuous derivatives as may be required. Further it will be assumed that nowhere does the relation exist that:

$$1 : V = V : c^2 \tag{35}$$

Consider a linear combination of L_1, L_2

$$L = \lambda_1 L_1 + \lambda_2 L_2 \tag{36}$$

$$L = (\lambda_1 + \lambda_2 V)\frac{\partial p}{\partial x} + \lambda_2 \frac{\partial p}{\partial t} + \rho\,\lambda_1 \frac{\partial V}{\partial t}$$

$$+ \rho(\lambda_1 V + \lambda_2 c^2)\frac{\partial V}{\partial x} + \lambda_1\left(2\rho\, f\, V\frac{|V|}{D} - \rho g \sin\alpha\right) \tag{37}$$

Any two pairs of values of (λ_1, λ_2) will yield equations in every respect the equivalent of L_1 and L_2. If $t = t(x)$ is the equation to a curve then dt/dx is the slope of the tangent to the curve at any point, and further, if $p = p(x, t)$ and $V = V(x, t)$ are solutions to L_1, L_2 then it follows by calculus that:

$$dp = \frac{\partial p}{\partial x} dx + \frac{\partial p}{\partial t} dt \tag{38}$$

$$dV = \frac{\partial V}{\partial x} dx + \frac{\partial V}{\partial t} dt \tag{39}$$

The differential expression L now becomes:

$$L = \lambda_2 \frac{dp}{dt} + \rho\lambda_1 \frac{dV}{dt} + \lambda_1 \left(2\rho f \frac{V|V|}{D} - \rho g \sin \alpha\right) \tag{40}$$

if the constants λ_1, λ_2 are chosen so that:

$$\frac{dx}{dt} = (\lambda_1 + \lambda_2 V)/\lambda_2 \text{ from (38)} \tag{41}$$

and

$$\frac{dx}{dt} = (\lambda_1 V + \lambda_2 c^2)/\lambda_1 \text{ from (39)} \tag{42}$$

Thus in the differential expression (40) the derivatives of (p, V) are combined so that their derivatives are in the same direction, namely dt/dx - the characteristic direction.

The ratio λ_1/λ_2 may now be found:

$$\frac{\lambda_1}{\lambda_2} = \frac{dx - V\,dt}{dt} = \frac{c^2\,dt}{dx - V\,dt}$$

hence

$$(dx)^2 - 2V\,dx\,dt + (V^2 - c^2)(dt)^2 = 0 \tag{43}$$

For the case of hyperbolic partial differential equations, two distinct roots of the above quadratic exist. This excludes the exceptional case of all three coefficients vanishing.

The slope $\varepsilon = \frac{dt}{dx}$

may now be introduced, where ε satisfies the equation:

The slope $\varepsilon = \frac{dt}{dx}$

may now be introduced, where ε satisfies the equation:

$$(V^2 - c^2)\,\varepsilon^2 - 2V\varepsilon + 1 = 0$$

hence $\varepsilon = (2V \pm \sqrt{(4V^2 - 4(V^2 - c^2))})/2(V^2 - c^2)$

or $\varepsilon = (V \pm c)/(V^2 - c^2)$

Thus the slope of the two characteristics in the (x, t) plane may be expressed as:

$$\frac{dt}{dx} = \frac{1}{V \pm c} \tag{44}$$

Values of λ_1/λ_2 may now be found, by solving (41), (42) with (44).

Hence if $\frac{dt}{dx} = \frac{1}{V + c}$ then from (41)

$$\frac{\lambda_1}{\lambda_2} = c \tag{45}$$

similarly

$$\frac{dt}{dx} = \frac{1}{V - c} \quad \text{then}$$

$$\frac{\lambda_1}{\lambda_2} = -c \tag{46}$$

Returning to the differential expression (40) and dividing through by $\rho\lambda_1$ yields

$$\frac{\lambda_2}{\rho\lambda_1}\,dp + dV + \left(2f\,V\frac{|V|}{D} - g \sin\alpha\right) dt = 0$$

Substituting for λ_1/λ_2 yields two equations applicable along the two characteristic directions C^+ and C^-:-

$$dV + \frac{1}{\rho c}\,dp + \left(2f\,V\frac{|V|}{D} - g \sin\alpha\right) dt = 0 \tag{47}$$

$$dt = dx/(V + c) \tag{48}$$

C^+

$$dV - \frac{1}{\rho c}\,dp + \left(2f\,V\frac{|V|}{D} - g \sin\alpha\right) dt = 0 \tag{49}$$

$$dt = dx/(V - c) \tag{50}$$

C^-

It will be noted that equations (47) to (50) only contain total derivatices of all the variables. According to the derivation, every solution of the original equations (4), (21) satisfies the system of equations (47) to (50).

It is important to note that the first equation in each pair, i.e. (47), (49) only applies if the second is satisfied, i.e. (48) and (50).

3.4.2 Finite difference approximations

Two finite difference approximations are described below: 1st order finite difference approximation may be expressed in the form

$$\int_{x_o}^{x_1} f(x)\, dx \simeq f(x_o)\ (x_1 - x_o) \tag{51}$$

while the 2nd order expression is:

$$\int_{x_o}^{x_1} f(x)\, dx \simeq \frac{1}{2}\ (f(x_o) + f(x_1))\ (x_1 - x_o) \tag{52}$$

Referring to Figure 5 let P be the point of intersection of the C^+ and C^- characteristics through R and S. The significance of the restriction imposed by equation (35) now becomes apparent as the slope of the C^- line would be infinite if that condition were not satisfied. It is assumed that all (x, t, P, V) values at R and S are known and that it is necessary to solve for (x, t, P, V) at P.

Applying (51), the linear or rectangular rule approximation to (47) - (50) yields:

$$V_P - V_R + \frac{1}{\rho c_R}\ (P_P - P_R) + \left(\frac{2f_R}{D}\ V_R|V_R| - g \sin \alpha_R\right)\ (t_P - t_R) = 0 \tag{53}$$

$$x_P - x_R = (V_R + c_R)(t_P - t_R) \tag{54}$$

and $$V_P - V_S - \frac{1}{\rho c_S}(P_P - P_S) + \left(\frac{2f_S}{D} V_S|V_S| - g \sin \alpha_S\right)(t_P - t_S) = 0 \quad (55)$$

$$x_P - x_S = (V_S - c_S)(t_P - t_S) \quad (56)$$

Similarly, applying (52), the trapezoidal rule approximation to (47) to (50) yields:

$$V_P - V_R + \frac{1}{2\rho}\left(\frac{1}{c_P} + \frac{1}{c_R}\right)(P_P - P_R) + \left(\frac{1}{D}\left((f V|V|)_P + (f V|V|)_R\right) - \frac{g}{2}(\sin \alpha_P + \sin \alpha_R)\right)(t_P - t_R) = 0 \quad (57)$$

$$x_P - x_R = \frac{1}{2}(V_P + c_P + V_R + c_R)(t_P - t_R) \quad (58)$$

and $$V_P - V_S - \frac{1}{2\rho}\left(\frac{1}{c_P} + \frac{1}{c_S}\right)(P_P - P_S) + \left(\frac{1}{D}\left((f V|V|)_P + (f V|V|)_S\right) - \frac{g}{2}(\sin \alpha_P + \sin \alpha_S)\right)(t_P - t_S) = 0 \quad (59)$$

$$x_P - x_S = \frac{1}{2}(V_P - c_P + V_S - c_S)(t_P - t_S) \quad (60)$$

Generally the use of the second set of equations (57) to (60), involves an iterative procedure as the coefficients, particularly f in (57), (59) are no longer independent of the unknowns. In fact f depends on the value of Reynolds Number based on V_P.

3.4.3 Solution of the characteristic equations in the (x, t) plane

There are two common methods available for solving the two sets of equations presented above. One method is the grid of characteristics, which is particularly simple if dx/dt depends on (x, t) only. In this case equations (54), (56) or (58), (60) can be integrated immediately and the grid defined before the calculations for (P, V) commence.

Alternatively the method of specified intervals may be employed in the t direction, the values of (P, V) at the start of each interval being related to those at the end by equations (53), (55) or

(57), (59). In any event the solution will proceed as illustrated in Figure 6, each successive set of points being based on known values one time step earlier and the slopes of the characteristic lines. It will be noted, that in the absence of boundary conditions in Figure 6, the calculations triangulate to an apex point.

3.4.4 Grid of characteristics method

Starting with known conditions at time T_o at a number of points along the pipeline the grid of characteristics results in an irregular mesh pattern as shown in Figure 7. This is due to the varying values of dt/dx at each section. Thus in any calculation employing this method, values of $(x, t)_p$ as well as $(V, P)_p$ have to be calculated at each computing step, resulting in a disorderly computational method.

3.4.5 Method of specified time intervals

In this method Δt and Δx are specified, reducing the calculations to the solution for (V, P), for example at point D1 in Figure 7. The value of Δt must be such that the characteristics through D1 intersect CD and ED within the mesh size, thus:

$$\Delta t \leq \Delta x/(V + c) \qquad (61)$$

An interpolation is therefore required at the start of each calculation step in order that the base values $(V, P)_R$, $(V, P)_S$ are known.

Both methods have their particular applications, for example the grid of characteristic method would be employed for a system including a highly deformable pipe where use of the specified time intervals method would result in large errors following the interpolation procedure. In the majority of transient problems the wave speed c can be considered constant for a uniform length of pipe, hence the use of specified time intervals. This has advantages when dealing with complex pipe networks where various pipes have different wave speeds.

3.4.6 Simplification of the equations

Generally, for the work reported, the simplification that:

$\frac{dx}{dt} = \pm c$ is justified as $c >>> V$, i.e. of the order 400:1. This simplification is the equivalent of neglecting the convective terms $V\partial V/\partial x$ and $V\partial p/\partial x$ in equations (4), (21).

The simplification also means that there is no difference between the grid of characteristics and specified time intervals methods as the slope of the characteristics is constant for any one pipeline. The stability criterion must still be maintained, i.e.

$$\Delta t \leq \Delta x/c$$

Further, if $\Delta t = \Delta x/c$, the characteristics through D1 or B1 intersect the base line at C, E and A, Figure 7.

For the application to be reported the equations may be further simplified by eliminating the pipe inclination terms, $\sin \alpha$, as the pipes used were horizontal.

Thus equations (53) to (56) may be expressed as, referring to Figure 5:-

$$V_P - V_R + \frac{1}{\rho c}(P_P - P_R) + \frac{2}{D}\Delta t\,(fV|V|)_R = 0 \qquad (62)$$

$$\frac{dx}{dt} = c \qquad (63)$$

C^+

and

$$V_P - V_S - \frac{1}{\rho c}(P_P - P_S) + \frac{2}{D}\Delta t\,(fV|V|)_S = 0 \qquad (64)$$

$$\frac{dx}{dt} = -c \qquad (65)$$

C^-

Similarly equations (57) to (60) reduce to:

$$V_P - V_R + \frac{1}{\rho c}(P_P - P_R) + \frac{\Delta t}{D}((fV|V|)_P + (fV|V|)_R) = 0 \qquad (66)$$

$$\frac{dx}{dt} = c \qquad (67)$$

C^+

and

$$V_P - V_S - \frac{1}{\rho c}(P_P - P_S) + \frac{\Delta t}{D}((fV|V|)_P + (fV|V|)_S) = 0 \qquad (68)$$

$$\frac{dx}{dt} = -c \qquad (69)$$

} C^-

3.4.7 Discussion of friction loss

The basic difference between the use of the 1st or 2nd order finite difference approximations is the inclusion of the $(fV|V|)_P$ term in the second case. This is the equivalent of concentrating loss at each section along the pipeline whereas the first method only considers friction losses at the adjacent sections to the one being solved. The inclusion of this term leads to an iterative solution for V_P as $f_P = f(V_P)$ whereas the 1st order approximation results in a pair of equations in $(P,V)_P$, directly solvable.

It can be shown that if the pressure variation at a point is plotted against the number of pipe sections considered, the resulting curve reaches a stable value for about half the number of pipe sections if the 2nd order equations are employed. Against this must be set the slightly more time consuming solution to the equations containing the $(fV|V|)_P$ term.

3.4.8 Magnitude of the time step

The limitation on the size of Δt has already been mentioned, i.e. $\Delta t \leq \Delta x/(V + c)$ so that the characteristics through B1 fall within the segment $AC = 2\Delta x$, in Figure 7. In dealing with systems of more than one pipe it is obvious that an equal time step must be chosen for all the pipes so that the calculation may proceed in an orderly fashion. This is of particular importance at any junction of two or more pipes.

In this report, whenever a system containing more than one pipeline is considered, the time step employed was calculated from:-

$$\Delta t = \left(\frac{\Delta x}{c}\right)_1 = \left(\frac{\Delta x}{c}\right)_2 \quad \text{etc.} \qquad (70)$$

The values of Δx for each pipe are arranged so that (70) is satisfied by suitably arranging the number of sections in each pipeline. This may require slight approximations to the lengths of individual pipes but this is accepted practice.

3.4.9 Effect of employing $\Delta t < \Delta x/c$

In some cases it is necessary to reduce the time step employed, for example if the rate of cavity volume change is excessive errors may occur and result in an unstable solution. The simplest method of reducing the time step is to employ the interpolation technique mentioned above with respect to the method of specified time intervals. Referring to Figure 15, it will be seen that if $\Delta t < \Delta x/c$ the characteristics through P pass through R and S and not A, C. Conditions at R, S may be found by interpolating linearly between AB, BC. This introduces an error as the transients arriving at A, C, B at time T are assumed to effect conditions at R, S at that time. The extent of the error depends on the ratio:

$$Z = \frac{\Delta t^1}{\Delta t_0} = \frac{A.R}{A.B} \qquad (71)$$

and also on the number of time steps calculated in this manner as the error would be cumulative.

The method does, however, approximate to a representation of the spreading or dispersion of the wave front which in fact does occur as the transients propagate along a pipeline.

3.5 Application of the characteristic equations to the solution of various boundary conditions

Figure 8 illustrates a simple pipeline bounded by two unspecified conditions. The limits of solution without reference to the boundary conditions are shown.

All internal points B to F can be solved for (P, V) directly from the C^+, C^- equations previously derived. For the remainder of this report these equations will be used in the form:

$$VV_{J,I} = K1 - K2\ PP_{J,I} \tag{72}$$

for the C^+ characteristic, 1st order finite difference, where

$$K1 = V_{J,I-1}\ (1 - 2f\ \frac{\Delta t}{D}\ |V_{J,I-1}|) + P_{J,I-1}/\rho c_J \tag{73}$$

$$K2 = 1/\rho c_J \tag{74}$$

VV, PP represent conditions at time t + Δt, while V, P represent conditions at time t.

Similarly for the C^- line

$$VV_{J,I} = K3 + K4\ PP_{J,1} \tag{75}$$

where $$K3 = V_{J,I+1}\ (1 - 2f\ \frac{\Delta t}{D}\ |V_{J,I+1}|) - P_{J,I+1}/\rho c_J \tag{76}$$

$$K4 = 1/\rho c_J \tag{77}$$

$$f = 16/Re,\ Re < 2300 \tag{78}$$

for the laminar flow regime and similarly

$$f = 0.079/Re^{\frac{1}{4}},\ Re > 2300 \tag{79}$$

for 'smooth pipe' turbulent flow, and I represents the section number within pipe J.

The simultaneous solution of (72) and (75) for points B - F can be readily programmed and will yield the pressure and velocity (PP, VV) unknowns at these sections at Δt time intervals. The 2nd order equations may be similarly expressed, however this results in terms in (PP, VV, fVV^2).

The problems of programming transient analysis are almost entirely concerned with satisfying boundary conditions. For example

it is necessary to solve the C^+ or C^- equations above with some other (P,V) relation at all pipe boundaries, such as pipe ends, junctions, valves or vapour cavities. The main advantage of the method is that procedures to deal with the solution of the appropriate equations at any boundary may be prepared in isolation from the rest of the system. This makes the method ideal for a subroutine based analysis of any system. In the following section boundary condition solutions will be presented for all the cases met in the research reported.

The analysis presented will assume that the 1st order finite difference are employed. The solutions using the 2nd order equations would follow an identical derivation in each case with the exception that, if the friction factor is calculated at each time step, an iterative procedure would be necessary to obtain a solution in terms of VV_p.

3.5.1 Boundary formed by a valve normally discharging to atmosphere

Figure 9 illustrates a pipeline terminated by a valve which, while open, discharges to atmosphere. The boundary condition at the valve must be dealt with in two parts:-

1. During valve closure:-

The boundary condition is supplied by the valve steady state discharge coefficient:-

$$VV_{N+1} = \tau V_o \sqrt{\frac{PP_{N+1}}{\Delta P_o}} \qquad (80)$$

where ΔPo is the steady state pressure drop across the valve and V_o is the corresponding initial flow velocity.

Note that for this case it is preferable to use gauge pressure for the P, PP arrays, and this is the case for programs SEPP to SEPD.

In practice τ is known as a function of valve open angle. During closure this may be monitored and τ calculated by a cross plotting procedure. See Appendix 2.

Equation (80) may be solved with the C^+ characteristic through sections N at time t and N+1 at $t + \Delta t$, i.e. $VV_{N+1} = K1 - K2\ PP_{N+1}$

Substitution yields a quadratic solvable for VV_{N+1},

$$VV_{N+1}^2 + \frac{K5}{K2} VV_{N+1} - K1 \cdot \frac{K5}{K2} = 0 \qquad (81)$$

where $K5 = (\tau Vo)^2/\Delta Po$

and hence $PP_{N+1} = (VV_{N+1})^2/K5$.

2. Following valve closure:-

The valve boundary is now 'no flow' i.e.:

$$VV_{N+1} = 0 \qquad (82)$$

This assumes no separation or vibration at the closed valve.

Hence $PP_{N+1} = K1/K2$.

3.5.2 Pipeline terminated by a constant pressure reservoir

Figure 10 illustrates a pipeline terminated at both ends by constant pressure reservoirs.

1.) Upstream reservoir.

If there is assumed to be no local loss at the reservoir exit it follows that the pressure at the pipe inlet is the reservoir pressure,

hence $$PP_1 = PR1 \tag{83}$$

and the velocity can be found from the C^- characteristic,

i.e. $$VV_1 = K3 + K4 \cdot PR1$$

If the exit loss is assumed to have the form

$$\Delta P = \frac{1}{2} \rho k_1 VV_1 |VV_1| \tag{84}$$

then

$$PP_1 = PR1 - \frac{1}{2} \rho k_1 VV_1 |VV_1| \tag{85}$$

and substitution of this into the C^- characteristic yields a quadratic to be solved for VV_1.

2.) Downstream reservoir.

The same procedure applies with the modification that it is the C^+ characteristic that must be solved with either

$$PP_{N+1} = PR2 \tag{86}$$

or $$PP_{N+1} = PR2 + \frac{1}{2} \rho k_2 VV_{N+1} |VV_{N+1}| \tag{87}$$

if the inlet loss is considered.

Normally the minor losses are insignificant and need not be included.

3.5.3 Boundary formed by a valve mounted between two pipelines

The particular interest of this system, as illustrated in Figure 11 is that, for a slow valve closure, the presence of the downstream pipeline influences the transients propagating upstream of the valve during closure, and vice versa.

The available equations to be solved for the four unknowns, $(VV, PP)_{1,N1+1}$ and $(VV, PP)_{2,1}$ are:-

1. Valve pressure-discharge coefficient:-

$$VV_{1,N1+1} = \tau Vo_1 \sqrt{((PP_{1,N1+1} - PP_{2,1})/\Delta Po)} \qquad (88)$$

2. Flow continuity:-

$$VV_{1,N+1}\, A_1 = VV_{2,1}\, A_2 \qquad (89)$$

3. C^+ characteristic for pipe 1 between point (1, N1) at time t and point (1, N1+1) at t + Δt.

$$VV_{1,N1+1} = K1 - K2\, PP_{1,N1+1} \qquad (90)$$

4. C^- characteristic for pipe 2 between point (2,2) at time t and (2,1) at t + Δt.

$$VV_{2,1} = K3 + K4\, PP_{2,1} \qquad (91)$$

From (89), (90), (91)

$$PP_{1,N1+1} - PP_{2,1} = \frac{-1}{K2}\,(VV_{1,N1+1} - K1)$$

$$\frac{-1}{K4}\,\left(\frac{A1}{A_2}\, VV_{1,N1+1} - K3\right)$$

also, from (88)

$$PP_{1,N1+1} - PP_{2,1} = \frac{\Delta Po}{(Vo_1\tau)^2}\, VV^2_{1,N1+1} = K5\, VV^2_{1,N1+1}$$

thus a quadratic in $VV_{1,N+1}$ may be formed:

$$VV^2_{1,N1+1} + VV_{1,N1+1}\left(\frac{1}{K5}\left(\frac{1}{K2} + \frac{A_1}{A_2 K_4}\right)\right) - \frac{1}{K5}\left(\frac{K_1}{K_2} + \frac{K_3}{K_4}\right) = 0 \qquad (92)$$

The remaining pressure and velocity terms may be calculated by substitution into (89), (90), (91).

Following valve closure the system must be considered as two separate pipelines. The upstream boundary, in the absence of separation becomes:

$$VV_{1,N1+1} = 0$$

Similarly, in the absence of column separation downstream of the valve the boundary equation becomes:-

$$VV_{2,1} = 0$$

however in low head systems it is likely that separation will occur here, possibly complicated by air release, and this will be dealt with in the 'column separation' section.

3.5.4 Boundary formed by the junction of two pipelines

This case is included as it represents the modification to the test rig caused by the inclusion of a glass observation section downstream of the valve during the later tests reported. Figure 12 illustrates such a junction.

The available equations to be solved for the unknown pressure and velocity terms at $t + \Delta t$ are:-

1. Flow continuity $Q_1 = Q_2$

$$VV_{1,N1+1} A_1 = VV_{2,1} A_2 \qquad (93)$$

2. Pressure continuity:

$$PP_{1,N1+1} = PP_{2,1} \qquad (94)$$

It is assumed that the minor loss at the junction is insignificant.

3. The C^+ characteristic between point (1, N1), at time t, and (1,N1+1) at $t + \Delta t$.

$$VV_{1,N1+1} = K1 - K2\ PP_{1,N1+1} \tag{95}$$

4. The C^- characteristic between points (2,2) at time t and (2,1) at $t + \Delta t$.

$$VV_{2,1} = K3 + K4\ PP_{2,1} \tag{96}$$

It is assumed in this case, as in the previous example that the value of Δt is the same for both pipelines and that the necessary adjustments in section length, Δx, have been made.

Substitution yields:-

$$PP_{2,1} = \frac{K1A_1 - K3\ A_2}{K2A_1 + K4\ A_2} \tag{97}$$

The remaining PP, VV values may now be calculated. It will be seen that the equations apply equally to changes in wave speed, caused by material or pipe thickness changes, or to pipe bore alteration.

In this case it is useful to apply the simplified equations (26), (27) to the junction to obtain an impression of the effect of such a junction on the pressure transients propagating in a pipeline, see Parmakian (10).

Let F_1 be the incident wave at a junction between two infinite pipelines, f_1 be the reflection of F_1 produced at the junction and F_2 be the pressure propagated from the junction along pipe 2. It will be seen that f_2, the reflection of F_2 produced by the upstream system boundary, will be zero as it is assumed that the wave fronts are short compared to the distance to the nearest reflector.

Thus applying (27) and the continuity equation:

$$\Delta Q_1 = \Delta Q_2$$

yields:

$$\frac{A_1}{\rho c_1}(F_1 - f_1) = \frac{A_2}{\rho c_2}\ F_2 \tag{98}$$

Similarly as the pressure at the junction is the sum of the F, f waves present at any time,

$$F_1 + f_1 = F_2 \tag{99}$$

The reflection coefficient may be defined as:

$$C_R = f_1/F_1$$

and the transmission coefficient as

$$C_T = F_2/F_1$$

Eliminating F_2 from (98), (99) yields:

$$(F_1 - f_1)\frac{A_1}{C_1} = \frac{A_2}{C_2}(F_1 + f_1)$$

hence $$C_R = \frac{A_1/c_1 - A_2/c_2}{A_1/c_1 + A_2/c_2} \tag{100}$$

and $$C_T = \frac{2\,A_1/c_1}{A_1/c_1 + A_2/c_2}$$

These equations allow a physical interpretation of the effect of a junction between two pipelines.

3.6 Application of the method of characteristics during column separation

All the analysis previously described in this section was based on the assumption that vapour pressure or air release pressures were not reached anywhere in the piping systems described. Care was taken to include this restriction in both the description of the pressure variations following valve closure, Section 3.3 and during the derivation of the various boundary conditions in Section 3.5.

If the pressure at any point in the fluid column falls to vapour pressure, due to the transients passing through the system, then the fluid column will separate and a vapour cavity or pocket will form. The subsequent growth and collapse of such cavities depends on the system boundary conditions, however such discontinuities in the fluid column can lead to the worst pressure variations to be experienced by a piping system and are therefore of great importance as a design criterion.

The method of characteristics may be employed to calculate the pressure-velocity-time histories of such cavities, and their subsequent collapse pressures. In this section the modifications to the method and the equations needed to define the cavity boundary conditions will be described for the two cases considered in this report, i.e. column separation upstream of a closed valve and downstream of a closing valve, with possible air release in the second case.

3.6.1 Column Separation upstream of a closed valve

Figure 4 illustrated the pressure and velocity variations to be expected on the upstream face of a valve following a rapid closure. If the pressure at a point in the upstream pipeline falls to vapour pressure, a cavity forms and the uniform, repeating waveform of Figure 4 is disrupted. Following a rapid valve closure the pressure in a low

head system is most likely to fall to vapour pressure at the valve itself at the end of the first pipe period, i.e. this coincides with the arrival at the closed valve of the $f = -\rho cV_o$ transient and its reflection as an $F = -\rho cV_o$ transient.

Equation (33) i.e.:-

$$p_o - \rho cVo > p_{vap}$$

described the initial conditions to be satisfied if this separation of the column were to be avoided. Figure 13 illustrates the expected pressure variation if such a cavity formed. The closed valve boundary equation is no longer

$$VV_{N+1} = 0 \qquad (102)$$

but $$PP_{N+1} = \text{Vapour pressure} \qquad (103)$$

referring to Figure 15, as the cavity may be regarded as a constant pressure zone having the same reflective properties as a constant pressure reservoir. The cavity interface velocity will initially be negative, i.e. the column will move towards the reservoir, the magnitude of this velocity being given by solving (103) with the C^+ characteristic between point N at time t and N+1 at time $t+\Delta t$, Figure 15. The column will continue to move towards the reservoir until it is brought to rest by the prevailing adverse pressure gradient. It is then accelerated back towards the closed valve by this same pressure gradient between the cavity and the upstream reservoir.

It is assumed throughout the analysis presented that the total length of a vapour cavity and its drift, for a cavity at some internal pipe section, is small compared to a pipe section Δx. This allows, for example at the valve, the characteristic between N and N+1 to be applied between N and the cavity/fluid interface.

The cavity is also assumed to fill the full cross section of the pipe so that its volume may be calculated from an expression:

$$VOL_T = VOL_{T-\Delta T} - A \frac{\Delta T}{2} (VV + V)_{N+1} \qquad (104)$$

The cavity is considered closed when the result of equation (104) at the end of a time step is zero or negative. The pressure generated on cavity collapse, assuming that there is no released air in the cavity, is given by:

$$\Delta P = \rho c V_{clos} \qquad (105)$$

where V_{clos} is the velocity at the cavity-fuel interface at the instant of collapse.

Following cavity collapse the 'no-flow' boundary equation (102) again applies. The pressure variation in Figure 13 includes a step on the peak recorded at the valve following cavity collapse. This step can be explained by reference to the F, f wave model. At the instant of cavity formation an F wave of maximum magnitude:

$$F = -(p_o - p_{vap})$$

is propagated towards the reservoir and this wave may be imagined to be reflected up and down the pipeline between two constant pressure zones, i.e. - 1 reflectors, representing the reservoir and the vapour cavity, for as long as the cavity exists. As the collapse of the cavity is unlikely to coincide with the end of a pipe period it is likely that the f wave produced at reservoir by the arrival of the F wave above will arrive at the closed valve at some time following cavity collapse. At the instant of cavity collapse the reflection coefficient representing the valve will change from - 1 to + 1 so that the arriving f wave of maximum magnitude:

$$f = (p_o - p_{vap})$$

will be reflected as a + F wave resulting in a step pressure rise at the valve of maximum magnitude 2f.

There are now two systems of pressure waves propagating within the pipeline, namely the system caused by initial valve closure and later modified by the presence of the cavity and a second system caused by the pressure rise $\rho c V_{clos}$ on the first cavity collapse. Such a sequence of events would follow any subsequent cavity collapse resulting in an increasing number of steps on the subsequent pressure peaks, depending on the local time relation between any cavity collapse and the arrival at the valve of the earlier transients still propagating within the system. This leads to the possibility that the peak pressure at the valve following column separation may exceed $\rho c V_o$.

Following the collapse of the final cavity the regular type of wave form will be re-established with a frequency of c/4L, thus the presence of a cavity may be deduced if the phase separation of two consecutive peaks exceed two pipe periods.

3.6.2 Application of the method of characteristics to column separation upstream of a closed valve

The above boundary conditions represent Bergeron's proposals for a graphical solution. Previous papers dealing with solution of transient problems by the method of characteristics have tended to mention these in passing, proposing a simple translation into characteristic notation, Streeter (45) and Fox (47).

In the proposed approach it is intended to examine more carefully the solutions to the characteristic equations obtained during and following the opening of a vapour cavity. It will be assumed that the vapour formed is concentrated at the computing section first displaying vapour pressure, and that the cavity will occupy the full bore of the pipeline at that section.

Following the formation of the vapour cavity a pressure transient of vapour pressure magnitude will propagate along the pipeline.

Depending on the local conditions between the cavity and the reservoir, the pressure for a considerable length of the pipeline will fall to the fluid's vapour pressure. It will be assumed that the length of pipeline so affected remains a continuous liquid column at vapour pressure rather than a mixture of liquid and vapour.

Returning to the example illustrated in Figure 13 following the formation of a cavity at the valve the pressure for a considerable length of the pipeline will fall to vapour formation level, during this process the values of the pressure and velocity at the computing sections produced by the solution of the simultaneous equations (62, 64) or (66, 68) must be treated with caution. Accurate values of velocity can only be obtained if the times at which the pressure at a section reaches the vapour pressure of the fluid corresponds to the end of a computing time step. Normally it is not to be expected that this will occur. For example at a given time the computed value of the pressure at a closed valve may be well below vapour pressure, indicating that the vapour formation level was reached at some intermediate time during the preceding time step. Similarly the computed values of pressure in the pipe section affected by cavity formation may be well below vapour pressure as the numerical solution to the appropriate pair of equations does not suffer from the limitation that the pressure cannot fall below vapour formation level. Replacing the computed values of pressure below vapour pressure by the fluid's vapour pressure and continuing the calculation is not felt to be sufficiently accurate as the computed velocity results would then be in error. The importance of this lies in equation (105) as the magnitude of the cavity closing pressure depends only on the closing flow velocity and so a cumulative velocity error initiated on the opening of the cavity could lead to an error in the cavity closing pressure.

In the proposed approach the time of occurrence of vapour pressure at any of the computing sections is obtained by interpolation between the computed pressure values at the beginning and end of a time step, at section 'i' the time at which vapour pressure was reached would be:-

$$T - TS(i) = T - \Delta T \times (P_{T-\Delta T} - VAP) \; / \; (P_{T-\Delta T} - P_T) \qquad (106)$$

Where $P_T < VAP$, $P_{T-\Delta T} > VAP$.

From this equation it is possible to determine the times at which vapour pressure was reached at each of the sections displaying computed pressures below vapour formation level and thus at which of the sections the pressure first reached vapour pressure, i.e. the section with the maximum TS(i) value, TSMAX. This section can then be considered to be the location of the first vapour cavity and by interpolating all the computed pressure and velocity results back to this time, by using an expression of the form

$$V_{T-TSMAX} = V_{T-\Delta T} + TSMAX \times (V_T - V_{T-\Delta T})/\Delta T \qquad (107)$$

it is considered that a more accurate representation of the conditions in the pipeline at the instant of cavity formation will be obtained. The velocity of opening of the cavity may be calculated from the appropriate characteristic, in this case 62 or 66, Figure 15. It will be seen from the form of these equations that it will be necessary to calculate the values of pressure and velocity at the adjacent section at a time ΔT prior to cavity formation and this can be done by interpolation between values at that section at times $(T-\Delta T)$ and $(T-2\Delta T)$. The cavity drift velocity will be very small compared to the transient propagation velocity and so it is reasonable to assume that the cavity remains stationary.

The above procedure is repeated during each subsequent time step to determine the time of occurrence of vapour pressure at each

of the computing sections lying within the pipe length affected by cavity formation until no new sections display computed pressures below or equal to the fluid's vapour pressure. The solution then continues by full time increments until (104) indicates cavity closure. It is not to be expected that this will correspond to the end of a time increment and interpolation of the conditions back to the instant of cavity closure should yield a more accurate estimate of the conditions prevailing in the pipeline. The whole procedure is repeated until sufficient energy has been dissipated and no new cavities form.

Following slow valve closures, i.e. flow stoppage in a time much longer than a single pipe period it is possible for the first cavity formed to be at some point along the pipeline and not at the closed valve. Figure 14 illustrates this case. The solution above for the valve cavity possibility can be used to deal with this case with one modification. Consider that the first cavity forms at the midpoint of the pipeline. The fluid column at this time will have a direction of flow towards the reservoir. The cavity may be allowed to form but the pipeline must now be split into two sections, upstream and downstream of the cavity. The fluid velocity at the two fluid/cavity interfaces can be found from the C^+ and C^- characteristics at that section solved with (103), Figure 15. The pressure conditions between the cavity and the closed valve will initially be above vapour level but during the subsequent computation steps the pressure in this pipe section will fall to vapour pressure. The sorting and interpolation procedures described above can again be used to determine the time of occurrence of vapour pressure and the correct velocity at each section. The flow direction will be established towards the cavity so that, when the pressure at the closed valve falls to vapour pressure, the 'no flow' boundary condition at the valve can no longer be maintained and a cavity is allowed to form. The solution then continues as before, the volume of the internal cavity being calculated from

$$VOL_T = VOL_{T-\Delta T} - A \times \Delta T \quad \frac{1}{2}(VU_T + VU_{T-\Delta T} - VD_T - VD_{T-\Delta T}) \qquad (108)$$

and the pressure resulting from its collapse by

$$P_T = -(K1 - K3)/2K2 \qquad (109)$$

i.e. simultaneous solution of equations (72), (75).
The value of the flow velocity at that section may then be calculated from either the C^+ or C^- characteristic.

During the growth and collapse of the internal cavity the volume of the valve cavity was monitored by (104) and following the collapse of the internal cavity the solution proceeds as before up to the collapse of the valve cavity.

A complete program SEPD is included in Appendix 3 together with its flow diagram. SEPD incorporates the procedures outlined above together with the 2nd-order approximation in the finite difference equations and friction factor dependence on Reynolds' Number.

3.6.3 Column separation downstream of a closing valve

Figure 16 illustrates the pressure and velocity variations on the downstream face of a valve following closure and subsequent column separation. Figure 17 illustrates the boundary conditions at the valve during such a separation.

The main difference between column separation upstream and downstream of a valve is that the upstream case occurs as a result of the negative reflections produced by the upstream boundaries during and following valve closure, whereas in the downstream case the column separation is caused by the negative pressure waves propagated downstream by valve closure.

If the pressure does fall sufficiently to cause column separation the fluid column breaks at the valve downstream face and the column between the valve cavity and the downstream reservoir is brought to rest

by the adverse pressure gradient and frictional effects. This pressure gradient between cavity and reservoir then acts to drive the liquid back towards the valve, closing the cavity and compressing any released air, which may not necessarily be re-dissolved due to the time scale of events. The pressure finally reached when the column comes to rest at the valve can be of destructive proportions.

The occurrence of column separation downstream of a closing valve is complicated when the working fluid is aviation kerosene by the necessity to include the possibility of air release in the model of the phenomenon.

Air release from aviation kerosene is highly dependent on the degree of agitation supplied to the fuel (75, 76). In the downstream separation case studied, the severe agitation caused by the closing action of the particular type of valve used for the tests, a spherical plug valve, which is widely used in aircraft fuel systems, made the inclusion of air release in the downstream boundary equations imperative.

During the existence of a cavity at the valve downstream face, the pipeline downstream of the valve may be represented by a line terminated by a -1 reflector at each end. In the case of a rapid valve closure, the pressure wave propagated into the downstream pipeline will have a maximum value:

$$f = -(p_o - p_{vap})$$

assuming that equation (33) is not satisfied and that air release does not occur. This wave will therefore be reflected within the downstream pipeline with alternate +f and -f values resulting in a 'saw-tooth' waveform, of frequency c/2L, at any intermediate point along the pipeline. The extreme ends of the line naturally display constant reservoir and vapour pressure respectively. The upper and lower limits of this waveform will be p_o and p_{vap} as the wave front length is assumed to be less than 2L. The actual magnitude of the oscillation will depend on the initial steepness of the pressure drop forming the cavity, thus a cavity formed follow-

ing a slow valve closure would be characterized by a sawtooth waveform oscillating between limits between p_o and p_{vap} but still of frequency $c/2L$.

Column separation downstream of a valve is complicated by the fact that the air release pressure may be reached while the valve is still open. This will result in a mixture of air and fuel plus fuel vapour spreading downstream from the valve as the column separates. This slightly modifies the -1 reflection coefficient at the cavity, as the pressure is not strictly constant but depends rather on the sum of the vapour pressure and the partial pressure of any released air, however the general explanation is still valid.

Following the collapse of the cavity and the stoppage of the returning column the reflection coefficient at the valve reverts to the +1 value appropriate for the 'no flow' case. This means that the secondary oscillation of amplitude $(p_o - p_{vap})$ is made to contribute to the pressure rise at the valve in the same way as was fully described for the upstream separation case. Therefore in the case of a rapid valve closure the pressure recorded at the valve would have a value $\rho c V_{clos} + 2\ (p_o - p_{vap})$ where V_{clos} is the maximum velocity attained by the returning column.

It is also important to note that the presence of released gas in the cavity region does not necessarily act as a cushion to the returning column. The pressure build up due to the air is so slow that the returning column may achieve a relatively high velocity, resulting in high final pressures. As illustrated in Figure 16 the maximum flow velocity for the returning column is reached prior to the major pressure build up, which is in marked contrast to the 'vapour only' case illustrated in Figure 13 where the maximum velocity occurs at the instant of cavity collapse.

3.6.4 Application of the method of characteristics to column separation downstream of a closing valve

Cavity formation downstream of a closing valve was considered with and without an allowance for the effect of any released air.

(1) Cavity boundary conditions, air release neglected.

An initial analysis was carried out using the techniques described in Section 3.6.1, i.e. that the boundary condition at the cavity could be described by:

$$P_{cav} = VAP \tag{110}$$

in the absence of released air.

If the pressure on the valve's downstream face falls to the fluid vapour pressure during closure then the boundary conditions represented by equations (88), (89) may be replaced by:

$$\tau = \frac{VV_{1,N1+1}}{V_{01}} \sqrt{(\Delta P_o/(PP_{1,N1+1} - P_{cav}))} \tag{111}$$

and $$PP_{2,1} = VAP \tag{112}$$

If a cavity does form during closure the vapour is assumed to be concentrated at the valve. The length of the cavity is assumed small in comparison with a section length so that a valid characteristic may be drawn between the cavity/fuel interface, assumed to be at section (2, 1) in Figure 17 and section (2,2).

The two remaining equations are provided by the C^+ line between sections (1, N1 + 1) and (1, N1) and the C^- characteristic referred to above between (2, 1) and (2, 2).

$$VV_{1,N1+1} = V_{1,N1}\left(1 - 2f\frac{\Delta T}{D1}|V_{1,N1}|\right) - \frac{1}{\rho c_1}(PP_{1,N1+1} - P_{1,N1}) \tag{113}$$

and

$$VV_{2,1} = V_{2,2}\left(1 - 2f\frac{\Delta T}{D2}|V_{2,2}|\right) + \frac{1}{\rho c_2}(PP_{2,1} - P_{2,2}) \tag{114}$$

The cavity interface velocity may be calculated directly from (114) while the upstream conditions can be expressed as a quadratic in $PP_{1,N1+1}$.

During valve closure the volume of the cavity may be calculated from an expression:

$$VOL_T = VOL_{T-\Delta T} + A_1 \frac{\Delta T}{2} (VV_{2,1} + V_{2,1} - VV_{1,N1+1} - V_{1,N1+1}) \quad (115)$$

assuming that the pipelines are of equal bore.

Following valve closure the cavity will continue to grow until the separated column is brought to rest by the pressure gradient between the cavity and the downstream reservoir. During this period and the subsequent closing phase of the cavity its volume may still be calculated from (115) with the $(VV, V)_{1,N1+1}$ terms zero. The collapse of the cavity is indicated by equation (115) having a zero or negative value at the end of a time step. The boundary at the closed valve then reverts to the 'no-flow' condition, equation (102) and the generated pressure is obtained directly from the solution of equations (114) and (102), resulting in an instantaneous pressure rise of $\rho c V_{clos}$.

Subsequent cavities open at the valve due to the arrival of negative reflections from the downstream reservoir. This process repeats until sufficient energy has been dissipated.

(2) Cavity boundary conditions including released air

If the vapour cavity at the downstream face of the valve is considered to contain air, or a mixture of gases, then the boundary condition becomes:

$$PP_{2,1} = P_{cav} = VAP + PA \quad (116)$$

where PA is the partial pressure of any released gas within the total volume of the cavity.

The value of PA may be expressed as

$$PA = \left\{ \frac{AIRVOL}{VOL} \right\}^n . ATM \quad (117)$$

where n is the polytropic coefficient of expansion, AIRVOL is the quantity of air released measured at N.T.P. and VOL is the total cavity volume calculated from (115). In view of the introduction of the $p.Vol^n = k$ expression it is necessary to employ absolute pressures in this analysis.

The total volume of air released from an aviation fuel at equilibrium at any particular pressure may be calculated from Henry's Law, and this is assumed to apply in this case. If K is the Bunsen solubility coefficient defined as the volume of gas, at N.T.P., which will dissolve in one unit volume of liquid under a partial pressure of one atmosphere, then the quantity of air released by a unit volume of the fuel at a pressure PK is given by

$$AIRVOL = (ATM - PK) \cdot K/ATM \qquad (118)$$

where ATM = atmospheric pressure and PK < ATM. Fig. 18 illustrates the variation in Bunsen solubility ratio with fuel temperature.

In this approach it will be assumed that the volume of fuel that gives up its dissolved air is the volume of fuel that passes through the valve between the time that the downstream pressure falls below atmospheric pressure and final valve closure. The work reported in (77) supports this as the air is clearly visible while the valve is still closing.

The volume of fuel concerned may be calculated as:

$$FUELVOL_T = FUELVOL_{T-\Delta T} + A_1 \frac{\Delta T}{2} (VV_{1,N1+1} + V_{1,N1+1}) \qquad (119)$$

and the air released from

$$AIRVOL_T = FUELVOL_T \ (ATM - 0.5 \ (PP_{2,1} + P_{2,1})) \frac{K}{ATM} \qquad (120)$$

where the average value of the pressure on the downstream face of the valve during the time step is equated to PK in (118).

During valve closure equations (111), (116), (113) and (114) can be used to determine the velocity and pressure conditions at the valve in the presence of separation. If n = 1 in equation (117) this results in a quartic in $PP_{1,N1+1}$.

If n is taken greater than unity then the equations mentioned above reduce to a pair of equations in $PP_{2,1}$, $PP_{1,N1+1}$ which can be solved by an iterative process, Appendix 4. Appendix 5 includes full flow diagrams and print-out of these programs.

Following valve closure, and within the opening phase of the cavity, pressure and velocity conditions at the cavity interface can be calculated from (114) and (116). Air is assumed to be released from the fuel throughout the opening phase of the cavity.

During the collapse phase of the cavity no air is allowed back into solution. This assumption is again supported by the observations carried out (77) which showed that free air was present in the region of the cavity even at the maximum pressures associated with cavity collapse.

Negative pressure wave reflections produced at the downstream reservoir following cavity collapse lower the pressure at the valve and the cavity re-opens a number of times until sufficient energy has been dissipated.

3.7 Calculation of conditions along the downstream pipeline during and following column separation at the valve

The conditions at the internal points along the downstream pipeline can be calculated from the C^+, C^- equations. During column separation at the valve a considerable length of the pipeline downstream of the cavity may fall to the fluid vapour pressure, this length will be considered as fuel at vapour pressure and not a mixture of fuel and vapour. The sorting and interpolation technique described in section 3.6.2 was applied in all the programs predicting downstream separation to avoid possible velocity errors.

4. APPARATUS

4.1 Properties of Aviation Kerosene Specification 2494

Aviation Kerosene 2494 was employed as the working fluid throughout the tests reported. Relevant properties, taken from an Esso Data Sheet are reproduced below:

Density	800 kg/m^3
Vapour pressure, 15°C	0.7 kN/m^2 abs.
Kinematic viscosity	1.68×10^{-6} m^2/s.
Ratio of specific heat cp/cv at 15°C	1.033
Air solubility, at 15°C	13.6% by volume.
Bulk Modulus (various sources)	$1.03 - 1.38 \times 10^9$ N/m^2.

Due to the scatter on the available Bulk Modulus figures this was measured by an ultrasonic technique at the working temperature.

4.2 Pipeline configurations

Two separate test rig layouts were designed to investigate column separation upstream and downstream of a valve. The L56 aluminium alloy piping had a Young's Modulus of $72.4 \cdot 10^9$ N/m^2 and Poisson's Ratio of 0.3. The glass pipe employed in the observation section downstream of the valve was assumed to have a Young's Modulus of 68.10^9 N/m^2.

4.2.1 Upstream separation, pipeline configuration 1

Figures 19 to 22 illustrate the layout of the 15.24 m test pipeline, made up of five sections of L56 aluminium alloy piping of 50.8 mm O.D. and 0.915 mm wall thickness (20 S.W.G.), supplied by B.A.C. to Concorde standards. The upstream reservoir was a 0.9 m^3 (200 gallon) tank, pressure tested to 500 kN/m^2. The downstream end of the pipeline was terminated by the test valve discharging to atmosphere. An English Electric 24 v. D.C. 28 amp submerged fuel pump was used to return kerosene

to the upstream reservoir tank, Figure 21. Flow measurement was obtained by means of a venturi meter in this return pipeline.

Drain down and supply pipelines were also provided to connect the test system to a storage tank.

4.2.2 Downstream separation, pipeline configuration 2-3

The earlier layout was modified as shown in Figure 23. A second reservoir tank, 0.2 m^3 (45 gallon), also tested to 500 kN/m^2 was mounted at the downstream end of the pipeline, Figure 24. The piping was the same as that used for configuration 1, two pipe sections upstream and three downstream of the valve in configuration 2.

A more powerful Saunders Safran 3 phase A.C. pump was installed to return kerosene to the upstream reservoir. A bypass piping system was devised around this pump to allow the rig to be used for flow in either direction along the test pipeline, Figure 24. Compressed air supplies were connected to both reservoir tanks as shown in Figure 23.

4.2.3 Observation of downstream column separation, pipeline configuration 2G

In order to film and observe the separation of the fluid column downstream of the test valve, a 3.04 m glass observation section, 50.8 mm bore and 4.73 mm wall thickness was mounted downstream of the valve. The need to retain a pressure transducer at the valve and the adapters necessary between the glass pipe and the valve led to a 127 mm solid section between the valve centre line and the start of the glass piping, Figure 25. Figure 26 illustrates the layout of the lights and camera for these tests. The camera used was a Hycam rotating prism high speed 16 mm unit, capable of film speeds up to 10,000 frames per second and film lengths up to 130 m. Figure 27 illustrates the Hycam optical system.

4.3 Test valve design

The valve used for all the tests was a Saunders Aircraft fuel valve, type E60F16, a spherical plug valve of 47 mm bore. Figures 28 and 29 illustrate the design of this valve. Adapters were made to permit the coupling of the valve to the pipeline and the mounting of pressure transducers 50.8 mm on either side of the valve centre line, in pipeline configurations 2 and 3.

The valve was operated by a compressed air ram which, via a lever connection, turned the valve's plug through 90°, Figure 30. For the tests on pipeline configuration 1 the air supply to the ram was controlled by hand via two linked two-way valves. For tests on the later pipeline configurations this method was replaced by a solenoid valve and switch. Using this second method it was found that the ram motion was linear, and that the angle vs. time curve for any series of closures could be expressed solely in terms of the overall valve closure time.

It is to be noted that, with the exception of a few early tests on pipeline configuration 1, the valve closing ram was mounted separately from the valve base plate, as shown in Figures 21 and 25 for configurations 1 and 2 respectively.

The valve could be set to and closed from any open angle by means of an adjustable stop designed to prevent the ram returning to the valve fully open position.

4.4 Pipeline restraint

The test pipelines were supported on a series of wall mounted brackets, Figure 22. It was assumed that only the upstream end of the pipeline was fully restrained, this restraint being provided by the mass of the reservoir. During tests on pipeline configuration 2, extra support members were added bracing the valve base plate to the floor.

4.5 Instrumentation

4.5.1 Layout of transducer stations

Table 1 records the positions of the transducer mounting pads for all the pipeline configurations tested. Two aluminium pads, diametrically opposed on the pipe centre line, were welded to each pipe section, at the mid length point by B.A.C. prior to delivery. These pads were then tapped 14 mm to allow the mounting of either the pressure transducers or the DISA probe support. Adapters were made up for use with the Honeywell transducers used for steady state measurement on pipeline 1.

For pipeline configurations 2, 2G, 3 tappings were also provided 50.8 mm on either side of the valve centre line, the tappings being made into the valve/pipeline adapter sections.

4.5.2 Instrumentation for steady state conditions

The initial flow velocity for all the tests was measured by means of a calibrated venturi meter and mercury manometer mounted in the return pipeline. Two meters were used: a 30.2 mm throat meter in a length of 50.8 mm bore piping in configuration 1, and a 22.8 mm throat meter in a length of 38.1 mm bore piping, that extended for 2 m on either side of the venturi meter, in configurations 2, 2G and 3.

Pressure measurement was obtained at each reservoir tank by calibrated pressure gauges and, for pipeline configuration 1, by a Honeywell inductance transducer and O.D. unit, rated for 0 - 70 kN/m^2, mounted 1 m upstream of the test valve.

4.5.3 Instrumention for transient conditions

Figure 31 illustrates a typical instrumentation system consisting of quartz crystal pressure transducers (Kistler 701A or Vibro-meter 12QP250) linked via piezo amplifiers to a storage oscilloscope, DISA hot film probe and constant temperature anemometer and a Honeywell Linear Displacement Transducer to monitor valve motion. Each of these will be described in detail below.

4.5.4 Pressure transducers

Quartz crystal pressure transducers were employed for all the transient pressure recording tests carried out. Two types were used, Kistler 701A and Vibro-meter 12QP250, both these types were designed for the same specification giving a pressure range extending well beyond the pressures expected in the tests, i.e. pressure up to 1600 kN/m^2. The only difference between the two types lay in the construction of the quartz measuring element, the Vibro-meter version consisting of a cylindrical element made up from a series of discs connected in series while the Kistler type consisted of a similar cylindrical element split up into three 120^o sectors connected in parallel. Both systems were claimed to be equally efficient. Variations in the pressure acting on the quartz elements produced an electrostatic charge output, the well known piezoelectric effect, which could be transformed into a voltage output suitable for display on an oscilloscope. In both cases the measuring element was completely separated from the transducer housing thus eliminating the adverse effects of mechanical stresses and temperature variations.

The Vibro-meter transducers were supplied complete with 14 mm threaded adapter and similar adapters were designed for the Kistler 701 transducers, both types of transducers and their adapters are shown in Figure 32.

The advantages of quartz transducers were found particularly in their great measuring range and also in the fact that they could be statically calibrated. Great care was however required to avoid the effects of damp which produced uncontrollable drifting due to discharge of the electrostatic potential.

4.5.5 Vibro-meter TA-2/C Piezo Amplifier

TA-2/C piezo amplifiers were used in conjunction with the pressure transducers described above, for all the tests reported, together with a TP-220/A power unit, Figure 33. The power unit was supplied directly from the mains. The TA-2/C units were specifically designed for use with quartz transducers and transform the electrostatic charge generated by the transducers into voltage equivalents which could be amplified and displayed on an oscilloscope.

Input sensitivity could be varied by a factor of 1:2000 in eleven calibrated steps. The unit also incorporated a selector switch for static or dynamic measurement which changed the time constant of the instrument. Pressure variations at frequencies less than 10 c/s should be recorded on static mode, although this would not effect the accuracy of recording of any secondary pressure oscillations at frequencies up to 60 c/s.

4.5.6 Tektronix 564 Oscilloscope

This type of oscilloscope was used for all the tests, the main advantage offered being the split screen storage capability which allowed traces to be displayed on either the upper or lower halves of the screen for up to one hour while the other half was used to display other traces for comparative purposes. Alternatively the whole screen could be used in the storage mode or the unit could be operated as a normal oscilloscope. The oscilloscope amplifier and time base units were of the interchangeable plug-in type. The time base normally employed was the

3B3 while both the 4 channel 3A74 amplifier and the 2 channel 3A3 differential amplifier were used. Figures 33 and 34 show the oscilloscope and the storage systems used.

4.5.7 Tektronix time base plug-in unit type 3B3

This plug-in unit was used for all the tests. Internal and external triggering systems were provided for both the normal and delayed time sweeps. The time sweep settings ranged from 1 microsecond to 1 second per division in 20 calibrated steps. The delay sweep operation had a continuous calibrated range from 0.5 microseconds after triggering. Sweep times were checked regularly using a time mark generator. The internally triggered single sweep facility used in conjunction with the screen storage mode was found to be the most useful combination. Careful adjustment of the level control enabled internal triggering to occur at the slightest pressure variation in the fluid.

4.5.8 Tektronix four channel amplifier 3A74

This amplifier was used for all the pressure measuring tests. The unit included four amplifier channels each with its own input coupling, attenuator controls, variable gain, position and a.c./d.c. mode controls. The channels could be used independently to produce a single sweep or together to produce multiple displays, e.g. the pressure variation at four points along the pipeline. Triggering could either be from channel 1 only or alternatively from the first channel to register a disturbance.

Nine calibrated amplification steps were provided from 0.02 volts per division to 10 volts per division. These steps could be checked by means of the step wave output provided by the calibrator unit built into the oscilloscope. These steps were checked regularly by setting the 0.02 volts per division deflection accurately and then comparing the screen deflections for the remaining control positions, the order of accuracy achieved being within 3% of the control settings.

In multiple channel operation there was a choice of two operating modes, chopped or alternate. In the alternate mode the oscilloscope time base generator internally switched channels at the end of each sweep while in the chopped mode an internal oscillator switched the channels at a free running rate of 500 Kc/s, the chopped mode was normally used during the tests. The bandpass was d.c. to 2mc., with a rise time of 0.17 microseconds.

4.5.9 Honeywell Linear Displacement Transducer LD18

A linear displacement transducer was employed to monitor the closing action of the valve, by direct connection to the valve closing ram, Figures 21 and 30. The output was also used to trigger the oscilloscope in the single sweep storage mode.

The LD series of transducers is intended to be used with A.C. excitation. The transducer connects as part of an A.C. bridge, the coils forming two arms, and the output fed, via a demodulator to an appropriate recorder. Figure 35 illustrates a typical arrangement, coils A, B, C being internal, the remainder of the equipment included in the O.D. unit. The transducer was used in conjunction with a Honeywell Oscillator-Demodulator unit, the connections being made with three core screened cable, the screen being earthed at one end.

To maintain linearity it is essential that the slug remain within the transducer throughout its motion, hence a 0.4 m transducer with 200 mm slug was necessary to accommodate the total 177 mm movement of the closing ram.

4.6 DISA hot film probe and constant temperature anemometer

4.6.1 Principle of operation

Hot film anemometry is based on measurements of the convective heat loss to the surrounding fluid from a heated sensing element. The heat loss depends on the temperature, geometrical shape and dimensions of the probe and on the fluid's velocity, temperature, density and thermal properties. Assuming that only one of the fluid parameters varies, the heat loss can be interpreted as a direct measure of the quantity in question.

4.6.2 Probe and anemometer

The sensing element in a hot film probe is a thin metal film deposited on an insulating substrate. The sensor is placed on the leading edge of the probe and is connected by screened cable to the anemometer. The heating current is supplied by the anemometer, consisting of a Wheatstone bridge, in which the sensor forms part of one bridge arm, and an amplifier. The current flowing through the bridge heats the sensor, and the amplifier output voltage is a measure of the heat loss from the sensor.

4.6.3 Static probe characteristics

Due to the complexity of the equations governing convective heat transfer and the further complications arising from heat transfer by natural convection and conduction through the film substrate, it is necessary to determine the relation between fluid velocity and heat transfer experimentally.

The fundamental work on two-dimensional heat transfer from cylinders in incompressible flow was carried out by L.V. King (78) in 1914. King's Law may be expressed as:

$$Q = K_f \ell (1 + \sqrt{(2\pi\rho C_p dU)/K_f}) (T-T_o) \quad (121)$$

where K_f - thermal conductivity

ℓ - wire length

ρ - density fluid

C_p - specific heat of fluid

d - wire diameter

U - fluid velocity

T - wire surface temperature

T_o - fluid temperature.

However King's basic assumptions were not fully valid, as was later demonstrated by Collis and Williams (79). Basically as the ratio ℓ/d normally used is small, compared to the values employed by experimenters to simulate two dimensional heat transfer, the two dimensional assumption breaks down and, as the thermal properties of the fluid were evaluated at the mean wire/fluid temperature, it becomes necessary to calibrate each sensor individually.

The heat loss, Q, through the sensor will equal the power, P, supplied from the electric current, hence

$$Q = P = I^2R \quad (122)$$

For a hot film probe operating at a specific overheat ratio, 'a':

$$a = (R - R_o)/R_o \quad (123)$$

where R, R_o are the operating temperature and fluid temperature wire resistance respectively, the relation between P and fluid velocity U becomes:

$$aI^2 = A + BU^n$$

where A, B, n are determined by calibration. Generally this expression may be written as:

$$V^2 = k_1 + k_2 U^{\frac{1}{2}} \quad (124)$$

where V is the bridge output voltage and k_1, k_2 are found experimentally.

4.6.4 Dynamic probe characteristics

The dynamic probe characteristics give the response of the unit to fluctuating flow. In the constant temperature operating mode the response is greatly influenced by the electronic ciruit. This closed loop response is the response of the entire probe-anemometer system and the frequency response is improved because of the negative feedback employed and the upper frequency limit is increased by a factor of several hundred compared to the constant current mode of operation, depending on anemometer's characteristics. For the 55A01/ 55A82 anemometer/probe combination the upper frequency limit is of the order of 5 kc.

4.6.5 Constant temperature operation

In the constant temperature mode, the resistance of the sensor, and hence its temperature, is kept constant. The bridge voltage provides a measure of the heat transfer, Figure 36.

The bridge is in balance at a certain bridge voltage from the servo-amplifier. A change in the resistance of the sensor due to a change in the heat transfer will result in bridge unbalance, introducing an error voltage at the servo-system input. This voltage is used to adjust the bridge voltage and hence the sensor current so that the bridge is once more in balance. By this means sensor temperature variations are kept to a minimum.

Constant temperature operation is particularly suited for measurements of high frequency flow fluctuations using both hot wire and hot film probes and for measurements of variations between widely different flow magnitudes.

4.6.6 DISA 55D10 Linearizer

The relation between flow velocity U and anemometer output voltage V may be expressed by equation (124), namely

$$V^2 = k_1 + k_2 U^n$$

where k_1, k_2, n are determined experimentally. Examples of this type of relation are given in this report for a 55AB2 hot film probe and 55A01 constant temperature anemometer.

The DISA Linearizer is an electronic analog computer whose basic transfer function at a constant setting of the operating controls can be written as:

$$V_{out} = K (V_{in}^2 - V_{ino}^2)^m \qquad (125)$$

where K, V_{ino} and m are constants.

By putting the anemometer output voltage V equal to the linearizer input voltage V_{in} the following relation is found:

$$V_{out} = K (k_1 + k_2 U^n - V_{ino}^2)^m \qquad (126)$$

Thus for $V_{ino}^2 = k_1$ and $m = 1/n$

the linearizer output voltage will be directly proportional to the flow velocity U.

4.6.7 Disturbing effects

The following points adversely effect the results obtained from the DISA probe.

(1) Temperature changes in the fluid during measurement.

(2) Contamination of the sensor element by dirt particles in the fluid.

(3) Undissolved air in the fluid.

(4) Gas release at the sensor surface.

(5) Film wear due to chemical reaction or electrolysis. This is critical due to the thickness of the film, less than μm.

(6) Vibrations of the probe result in the introduction of noise on the probe signal.

(7) Non alignment of the probe and flow.

4.6.8 DISA 55A82 hot film probe and support

Figures 37 and 38 illustrate the dimensions of the hot film probe used, together with the probe support and traversing device. The probe support was designed to fit the 14 mm threaded pads used for mounting the pressure transducers. A P.V.C. seal and retaining collar was fitted into the base of the upper support, which also carried the traversing screw and a clamping screw necessary to prevent the probe being blown out of the pipeline at high fuel pressures. The lower support was necessary due to the taper on the hot film probe body which would otherwise have made sealing difficult.

4.7 Air collection and analysis

Figure 39 illustrates the apparatus employed to remove and collect the residual gas observed to have been left out of solution following column separation on the downstream side of the valve in pipeline configuration 2G.

The oxygen content of this gas was measured by forcing it through alkaline pyrogallol and measuring volume reduction following oxygen absorption.

4.8 Fire prevention precautions

Due to the danger of sparking across any insulated gap in the pipeline, i.e. neoprene seals etc., caused by the insulating properties of kerosene, care was taken to ensure that the rig presented a continuous electrical circuit, all seals and air gaps being bridged with conducting material. In addition to this electrical bonding care was taken in providing earth connections.

The following precautions were also taken at the request of the G.L.C. fire department:-

(1) Storage tanks positioned outside the building and fire-proofed glass installed in all windows 6m on either side and 10m above the site.

(2) A pull cord operated isolation valve was mounted at the reservoir to test pipeline junction exterior to the building.

(3) Fire warning and 'no smoking' signs as well as a number of fire extinguishers were positioned close to the rig.

5. EXPERIMENTAL METHODS

5.1 Instrument Calibration

5.1.1 Calibration of venturi meter and steady state pressure measuring instrumentation

The venturi meters were calibrated by pumping fuel from the storage tank into the upstream reservoir via the supply and return lines illustrated in Figure 20. The pressure differentials across the meter, measured either by a mercury manometer or by a Honeywell 0 - 35 kN/m^2 inductance transducer, were compared to the flow rate calculated from the filling time of the reservoir tank. Calculation of the C_D of the venturi meter used on pipeline configuration 1 yielded a value of 0.93.

Calibration curves were then drawn for the flow in the test pipeline.

The pressure gauges used to record reservoir pressures were calibrated up to 400 kN/m^2 on the 'dead weight tester' and any variations from the supplied scales noted.

The Honeywell inductance transducers, together with their O.D. units and leads were also calibrated on the dead weight tester up to their maximum permitted pressures.

5.2.1 Linear Displacement Transducer

Figure 40 illustrates the calibration curve for the Linear Displacement Transducer in terms of valve open angle. This curve was produced by noting the oscilloscope screen deflection for a valve movement from 90^o open to some intermediate angle. The calibration of the oscilloscope amplifier channel 1 was checked for calibration prior to these tests by means of the calibrator unit built into the oscilloscope.

The calibration curve obtained allowed angle vs. time data to be extracted from the output of the L.D.T. recorded on the oscilloscope during valve closure.

5.1.3 Quartz crystal pressure transducers

The transient pressure measuring instrumentation was set as shown in Figure 31, with the transducers mounted in a dead-weight pressure tester. After the instrumentation had been allowed to 'warm up' for about 30 minutes the following procedure was carried out:-

(1) The amplification setting for each of the oscilloscope amplifier channels used, 2 - 4, was checked, by use of the calibrator unit, and any necessary adjustments made.

(2) The piezo amplifiers were set in the static mode and the attenuator settings noted.

(3) Each transducer was then calibrated in turn by loading the dead-weight tester and noting the screen deflection. This procedure was repeated for the whole range of pressures expected, the oscilloscope amplifier settings being noted and altered when necessary. By this method an individual calibration curve was obtained for each transducer circuit, i.e. including the cables, piezo amplifier, transducer and the oscilloscope amplifier channel. Each circuit was colour coded to avoid errors arising from the use of an uncalibrated unit.

(4) The gain adjustment controls were adjusted on the piezo amplifiers corresponding to oscilloscope channels 3 and 4 in order to equalise the calibration factors to the measured value for channel 2.

(5) Simultaneous calibration of all three channels was then carried out to ensure that all the transducers had the same factor.

This procedure was repeated at frequent intervals during all the tests reported. The calibration factor for the Kistler 701A or Vibro-meter 12QP250 transducers and associated amplifiers was found to be constant at 450 kN/m^2/volt.

5.1.4 Oscilloscope Time Base

The time base for the Tektronix 564 was checked by means of a Time Mark Generator (TMG). The TMG was plugged into the oscilloscope and the time base set to 10 ms/division. The output from the TMG was also set to one pulse every 10 ms. If the time base was correctly adjusted the pulses should correspond to the screen divisions. A screw adjustment on the oscilloscope could be used to correct the time base calibration if necessary. The procedure was then repeated for a whole series of time base settings to eliminate any error due to a faulty TMG output.

5.1.5 DISA 55A82 hot film and anemometer/linearizer system

Two methods were employed to calibrate the anemometer equipment. The first involved mounting the probe on the valve closing ram, which was directly linked to the Linear Displacement Transducer, and comparing their respective outputs as the ram propelled the probe through a bath of kerosene, Figure 41.

Figure 42 illustrates the type of trace recorded on the oscilloscope, it can be seen that the probe reacts rapidly to the increase in ram velocity, as represented by the slope of the Linear Displacement Transducer output. The low values of overheat ratio were necessary due to the use of the probe in a liquid, comparable tests in air would have required a 1.6 overheat ratio.

A computer program, in Fortran IV, was written to fit a polynomial to the L.D.T. output, by the 'least squares' method, the resulting equation being differentiated to give probe velocity. Direct comparison between these figures and the anemometer output is reproduced in Figure 43. The values of k_1, k_2 and n in equation (124) are now apparent. It was possible to combine the curves in Figure 43 as shown in Figure 44, the 'best line' again being fitted by the least squares program. This cali-

bration was used for the hot-film tests on pipeline configuration 1.

The second method involved mounting the probe in the test pipeline and, by recirculating the fuel through the rig at various flow rates, obtaining a direct comparison between the venturi meter reading and the anemometer output. This method was used in conjunction with a DISA linearizer unit, which resulted in a direct Volts vs. Velocity relation, and the later pipeline configurations 2 and 3. Generally this was simpler than the previous method but did suffer the disadvantage that the velocity measured by the probe was the centre line velocity which could be compared to the mean velocity measurement provided by the ventuir meter, or to a theoretical centre line velocity based on the venturi meter result.

The expression for this from Pao (80) was:-

$$V_{c1} = V_m \, (1 + 3.75 \sqrt{(f/2)}) \qquad (127)$$

where $f = 0.079/Re^{\frac{1}{4}}$.

The value of the exponent m, equation (125), was set by trial and error; the anemometer output was set equal to a particular centre line velocity and the value of m checked by systematically reducing the flow rate and comparing the anemometer output to the new theoretical centre line of velocity from (127) above. A value of 1.98 was found satisfactory, the observed linearity being illustrated in Figure 45, together with the results of equation (127). Figure 45 was used for the hot film tests on pipeline configurations 2 and 3.

5.2 Measurement of basic parameters necessary for a solution by the method of characteristics

5.2.1 Measurement of valve characteristic

The valve pressure-discharge characteristic, τ, forms the necessary boundary condition during valve closure. This characteristic was measured for the test valve in both pipeline configurations 1 and 2 by noting the discharge through, and the pressure drop across the valve for a range of valve open angles, while the rig recirculated fuel continuously under steady conditions. Discharge was measured by means of the venturi meter while the pressure drop in pipeline configuration 1 was measured by a Honeywell 0 - 35 kN/m^2 inductance transducer 1 m upstream of the valve. In pipeline configuration 2 the pressure was measured 1 m on either side of the valve by means of a pair of U-tube manometers, a mercury manometer for the small open angles, i.e. large pressure drop, while a tetrabromoethane manometer was used for the larger open angles. As tetrabromoethane combines with kerosene a 100 mm column of water was used to separate these liquids in each manometer arm.

Figure 46 illustrates the results of these tests together with the open area ratio vs. valve angle curve supplied by the valve manufacturers.

5.2.2 Measurement of the Bulk Modulus of aviation kerosene at room temperature

Due to the difficulty found in obtaining an accurate figure for the Bulk Modulus of the fuel used it was decided to measure this indirectly by an ultrasonic method. Figure 47 illustrates the apparatus used, a Solatron GO1377 pulse generator was used to produce a pulse frequency of 2Mc. These pulses were transmitted through a bath of kerosene by an ultrasonic transducer of PZT4 brush crystal and reflected from a submerged plate. The process was monitored on a storage oscilloscope and measurements of the acoustic velocity of the fluid made from the known separation of the source and reflector. Figures 48 and 49 illustrate the oscilloscope traces recorded.

The above process was repeated with distilled water to monitor the accuracy of the method.

5.3 Test procedures

5.3.1 Measurement of the transient propagation velocity in the test rig

In order to make accurate measurements of the time taken for a transient to pass from one point to another along the pipeline it was necessary to produce a pressure wave front as close as possible to a step profile. It was therefore necessary to employ small initial open angle settings and reasonably high upstream reservoir pressures in pipeline configuration 1 in order to produce as steep a transient as possible on valve closure. The passage of the transients was recorded at two transducer points, T1 - 1.25 m upstream of the valve, and T3 - 7.8 m upstream of the valve. A number of different methods were employed to measure the wave speed, employing the Tektronix 564 storage oscilloscope with and without the time sweep delay facility of the 3B3 plug in time base unit. Table 4 sets out these methods.

5.3.2 Column separation on the upstream side of the valve

By maintaining low pressures in the upstream reservoir tank, Figure 19 and varying the initial open angle of the valve it was possible to carry out a series of tests ranging from the 'no separation' case for low flow rates and small open angle settings up to the production of column separation lasting up to 0.2 seconds following the closure of the test valve from a fully open initial setting.

The test procedure was as follows:

(1) The instrumentation was allowed to warm up for at least 30 minutes. Normally the four channels would be taken up with the L.D.T. on channel 1, acting as a triggering signal, pressure transducers at X/L = 0.918 and 0.498 on channels 2 and 3, and possibly the DISA hot film probe on channel 4.

(2) The fuel was recirculated through the test rig continuously until steady conditions had been achieved. Steady state pressure and velocity values were noted, together with the valve open angle. The flow velocity was controlled by varying the power supply to the D.C. pump.

(3) The valve was closed by operating the pneumatic ram via the linked two-way control valves.

(4) The signal from the L.D.T. produced as soon as the ram started to move triggered the single sweep on the oscilloscope resulting in a presentation of the output from the four channels that could be photographed with a polaroid camera.

(5) The amplification settings of each channel were noted together with the time base and any time delay employed.

The above procedure could be repeated for a series of flow rates or initial valve settings.

5.3.3 Column separation downstream of a valve, pipeline configurations 2, 2G, 3

A similar test procedure to that outlined above was used for these tests. The steady state values of both reservoir pressures and the flow rate were recorded following the establishment of steady state conditions. Three main parameters were varied, namely: the flow rate, the valve closure time and the line pressure. The flow rate was set by a control valve in the return pipeline, Figure 23 , direct pump control was no longer possible on a 3 phase A.C. supply. The valve closure time was controlled by a pressure reducing valve in the ram compressed air supply line. The valve was operated by a solenoid valve and switch.

The line pressure was controlled by a pair of pressure reducing valves in the compressed air supply to the two reservoir tanks. This allowed column separation for constant flow rate and valve closure time to be investigated for a range of absolute line pressures.

The pump feeding the return line was shut down simultaneously with test valve closure to minimize any error arising from a reduction in downstream reservoir pressure, this would occur if the pump continued to pass kerosene from the downstream tank to the upstream reservoir.

5.3.4 Observation of cavity formation downstream of the valve

The procedure outlined above was followed for these tests. The camera and lights were set up as shown in Figure 26. The camera was switched on and the valve closed as soon as the note of the camera drive indicated that the film had reached a steady speed, in these tests 1000 frames/second. The valve closure mode was included in the film by means of a pointer and linking arm that moved through the camera's field of view as the ram moved. Similarly each test film included the steady state conditions for the test on a card mounted on the pipe support, together with a scale marked in cm to give a direct measure of the extent of the separated region.

5.3.5 Residual gas collection and analysis

The gas collection and analysis apparatus illustrated in Figure 39 was used for three separate functions:

(1) Air bleeding during the setting up of steady state conditions. Valve J was opened to allow any air trapped in the pipeline during filling to be removed.

(2) Gas collection. Following test valve closure and the final damping of the transients the residual gas located downstream of the valve was driven through valves A, B, by the downstream reservoir pressure, into the converted 50 cc. burette. With valves C, F, G shut and valves D, E open it was possible to collect the gas in the burette while the displaced kerosene passed out of the system through valves D, E.

Following the complete collection of the residual gas, closure of valves B, E and opening of valve F allowed the volume of the collected gas to be measured at atmospheric pressure by moving the reservoir down.

(3) Gas analysis. Prior to the collection of the released gas in the burette the system was used to draw the alkaline pyrogallol up to valve I by opening valves I, G, D and F and lowering the reservoir, all other valves being shut. With valve I shut kerosene was then forced up to valve I, all displaced air being expelled through valve H.

Procedure (2) above was then carried out. With valves D, F, G, I open and all others shut it was possible to force the released gas into contact with the alkaline pyrogallol, and conversely to return any undissolved gas to the burette, by raising and lowering the reservoir. This process was repeated until no volume change occurred following each contact of the gas and the alkaline pyrogallol.

6. DISCUSSION OF RESULTS

6.1 Presentation of experimental results and discussion of computer programs

The results from the investigation of column separation upstream and downstream of a valve following closure are presented separately. The same general format is employed in each section, namely:

1. Polaroid photographs taken from the storage oscilloscope, or, for the early tests, tracings from such photographs.
2. Comparison between observed and predicted pressure or velocity-time curves at a number of sections along the pipeline.
3. Comparison between the observed and predicted values of certain variables, such as cavity duration or collapse pressure.
4. Tables, where possible compiled by the computer as output, indicating the effects of a variation in computing technique, basic assumption or test condition.

This layout of results is supplemented with data on fuel properties and appendices describing the computer programs.

All the programs written to predict pressure variations during and following column separation were coded in Fortran IV for use on an I.C.L. 1905 digital computer. The university 1905 central processor had a core store of 32,768 24 bit words with a cycle time of 2 microseconds, and a hardware floating point arithmetic unit. Output peripherals consisted of a line printer, 1000 lines/minute maximum speed, and a tape punch. The transient programs SEPP to SEPK required up to 24K store, although efforts were made to reduce this to below the 21K limit set for the use of the computer unit's automated JUNE system which, in theory, gave a turn round time of less than 24 hours on any program.

Full descriptions of the transient programs are presented in Appendices 3 and 5. A number of other programs were employed during the reported research, particularly a curve fitting program based on the 'least squares' method set out by McCraken and Dorn (81) already mentioned in connection with the calibration of the hot film probe. This program formed the basis of the CURFIT subroutine employed in transient programs SEPE-K for valve characteristic manipulation.

6.2 Measurement of the transient propagation velocity

The measured values of acoustic velocity in kerosene and distilled water are shown in Tables 2 and 3. Comparison between the value for distilled water and that quoted by Pearsall (82) was felt to justify the use of the method for the measurement of the acoustic velocity in kerosene at the working temperature (17.5°C).

The Bulk Modulus of kerosene was calculated from the expression:

$$K = \rho c_o^2 \qquad (128)$$

and was found to be $1.26.10^9$ N/m^2. The range of values quoted by Shell, Esso, B.A.C., Saunders Valve Co. and Pearsall (82) was 1.03 to $1.38.10^9$ N/m^2.

Wave speed in the pipeline was calculated from

$$\frac{c}{c_o} = \sqrt{1/(1 + \frac{DK}{Ee} c_1)}$$

where $c_1 = 1.25 - \mu$ and is the value appropriate for a pipeline fully restrained at the upstream end. The value of the wave speed was thus found to be 917.1 m/s. Tables 5 and 6 present the measured values by the four methods employed, Table 4. It can be seen that method 2, employing the time delay facility on the oscilloscope, proved the most accurate. This method involved delaying the internal triggering of the instrument by a set time following the start of valve motion thus enabling a small part of the pressure-time trace to be examined in detail,

in this case that section containing the maximum pressure levels at the two transducer stations, T1-T3, 6.55 m apart. The results obtained by measuring the pipe period at the first transducer, 1.25 m upstream of the valve, displayed a slightly greater scatter. The average observed value of wave speed was found to be 919.85 m/s and this figure was used in the subsequent calculations.

Mention has already been made of the rig modification necessary to avoid the vibrations introduced into the system by the pneumatic ram slamming closed. Figure 50 illustrates the pressure traces adjacent (1.25 m) to the valve for tests before and after the ram was mounted independently. These curves also display the desired characteristic for wave speed measurements, i.e. the maximum pressure levels are attained in less than one pipe period.

6.3 Analysis of column separation upstream of a closed valve

Table 7 summarises the recorded tests. It can be seen that by varying the valve initial open angle, together with the reservoir pressure, a range of flow conditions were obtainable.

Figure 51, Plate 1 illustrates the pressure traces following a rapid valve closure where column separation did not occur due to the low initial flow rate. The traces reproduced illustrate the 2L/c pipe period and the damping due to fluid friction and possible vibration of the pipeline.

Figures 51, 52, 54 and 55 illustrate the effect of increasing the valve closure time for two initial open angle settings, 27^{o} and 90^{o}. The pressure variations recorded during the slower valve closures illustrate the effect of the valve characteristic of spherical plug valves. As can be seen the maximum rate of pressure rise occurs over a relatively small part of the plug rotation and the peak pressure is attained before the valve is fully shut, however it is doubtful whether

a valve of this type passes fuel below an open angle of 15°.

This trend is repeated in Figure 53, illustrating the effect of an increase in initial valve open angle.

As can be seen from Figure 54 the amplification setting of the instrumentation was adjusted so that the first peak following valve closure could be accommodated on the oscilloscope screen. The tables dealing with the measurement of acoustic and transient propagation velocities stressed that readings can only be taken to within ± 0.1 of a screen division under most circumstances and although this represents a small error on the first pressure peak the magnitude of the error will increase for each subsequent peak reaching a maximum of perhaps 10% on the third pressure peak.

The Schnyder-Bergeron graphical method has already been mentioned and Figures 56 and 57 illustrate its application to one particular case, with a valve initial opening of 25°. The smallest time increment practical on the scale used was an eighth of a pipe period. As can be seen from Figure 58 this led to the prediction of excessive pressure peaks, an effect caused by considering time increments that were too large to yield an accurate estimate of the variation in flow velocity at the fluid/vapour interface at the closed valve. Referring to Figure 56 more points between 5A and 6A on the line 0A - 8A would have resulted in more points between 21A and 22A on the 'cavity at closed valve boundary line' which in turn would have given a smoother variation in flow velocity at the cavity. In Figure 58 the graphical results for pressure and velocity variations at the valve are compared to those obtained from the numerical solution via the method of characteristics.

The first program employing this numerical method used to deal with the case mentioned above (Run 3, 13/11/68) assumed that the 1st cavity formed at the valve, employed 1st order or rectangular rule approximation for integration, constant friction factor, the sorting and interpolation procedures outlined previously and a time increment $\Delta T = \Delta x/c$ where Δx was a tenth of the pipelength. As mentioned previously this value of ΔT is the maximum for which a stable solution may be expected but its use can lead to misleading results if the rates of change of pressure are high, for example the instantaneous pressure rise following cavity collapse. This program was known as SEPP and a comparison between its output and the observed results for this test run is shown in Figure 59. As can be seen the output from this program again displayed the peaks predicted by the Schnyder-Bergeron solution, however their magnitude was reduced. Both methods indicate the formation of a second cavity at the valve at $t = 4.5$ pipe periods, this being the result of the high pressures predicted on the collapse of the first cavity. The observed results did not indicate such a cavity as the pressure recorded did not fall to vapour pressure and the 2nd and 3rd observed peaks were two pipe periods apart which could only be possible by transient propagation through a continuous fluid column, no vapour cavities existing anywhere along the pipeline.

The time increment was further reduced by putting Δx equal to a thirtieth of the pipe length resulting in a further decrease in the peaks although they were still predicted. It was therefore decided to reduce the time increment by interpolation by writing $\Delta T = \Delta x/2c$, Δx being a tenth of the pipelength. The results from this modified version of SEPP are also shown in Figure 59, the comparison between observed and computed results now being very close.

The divergence between the observed and predicted pressure variations following 1st cavity collapse and the marked improvement due to the inclusion of an interpolated time step from the instant of cavity formation can be explained by an examination of the assumptions made and the order of events within the pipeline.

Following a rapid valve closure of the type illustrated in Figure 59, the pressure drop at the valve at time 2L/c may be extremely steep, so that the pressure wave propagated upstream as the cavity forms will have a value:

$$F = -(p_o - p_{vap})$$

as mentioned earlier. This wave will be represented within the numerical solution and will be assumed to propagate within the pipeline between two -1 reflectors, at the cavity and the upstream reservoir, until the cavity collapses.

On cavity collapse an instantaneous pressure rise of magnitude $\rho c V_{clos}$ is assumed to propagate upstream from the valve, and the reflection coefficient at the valve reverts to a +1 value appropriate to a zero flow boundary condition.

This pressure rise can be seen in Figure 59 at 2.75 pipe periods. The $(p_o - p_{vap})$ wave, reflected from the upstream reservoir, arrives at the closed valve at some time within the next pipe period and results in a $2(p_o - p_{vap})$ pressure rise at the valve, due to the change in reflection coefficient. In this period, 2.75 - 3.75 pipe periods, the $\rho c V_{clos}$ wave has been reflected at the reservoir and arrives at the valve at 3.75 pipe periods as a $-\rho c V_{clos}$ wave, resulting in a pressure drop of $2\rho c V_{clos}$. These events are clearly illustrated in Figure 59 and are responsible for the peak pressure predicted at 3.75 pipe periods by the numerical solution without interpolation.

The final event of interest following first cavity collapse is the arrival at the valve of a $-(p_o - p_{vap})$ wave from the reservoir at 4.5 pipe periods, Figure 59, which would result in a further pressure drop of $2(p_o - p_{vap})$, and the formation of a second cavity at the valve.

The major assumption in the numerical solution is that the pressure fronts propagate with no change in shape, however the waves do disperse continually from the instant of their propagation. It has been shown by Skalak (12) and Thorley (13) that this dispersion follows an expression:

$$\theta = Kt^{1/3}$$

where θ is the slope of the wave front, t is the time of wave observation measured from the theoretical propagation of the observed transient as a step wave, and K is a constant determined experimentally. Thus both the $(p_o - p_{vap})$ and $\rho c V_{clos}$ pressure waves that produce the pressure variations recorded disperse continually and this can be clearly seen in the observed curve in Figure 59. The sharp peaks predicted are removed as the wave front lengths have increased so that waves of different sign overlap.

The improvement found by reducing the time step by interpolation can now be explained as the interpolation procedure necessary to produce the base conditions for the next time step effectively spreads the wave front. It is implicit in the interpolation that transients arriving at any point at a time T are assumed to influence conditions a given factor of a pipe section ahead of themselves at that time.

From the form of the dispersion equation it can be seen that the rate of dispersion will be more severe the closer the propagated transient is to a step wave, i.e.:

$$\frac{d\theta}{dt} = \frac{K}{3}\frac{1}{t^{2/3}}$$

Thus the beneficial effect of interpolation will be a maximum in cases such as Figure 59 where, following a rapid valve closure, both the $(p_o - p_{vap})$ and $\rho c V_{clos}$ waves are initially steep.

Examination of the computed results for the first series of tests showed that it was insufficient to consider cavities to be formed only at the closed valve. Analysis of slow valve closures, particularly in the cases employing an initially fully open valve setting, predicted vapour pressure first at some point along the pipeline upstream of the valve. SEPP was modified to deal with this possibility by considering the pipeline as two separate fluid columns separated by the vapour cavity and the simultaneous presence of a cavity at the closed valve if the pressure there fell to vapour pressure. The sorting and interpolation procedures designed to ensure correct velocity solutions during cavity formation were employed for both columns, the calculation advancing by a time increment $\Delta x/2c$ following the first indication of vapour pressure. A typical result is shown in Figure 60 where the first cavity is predicted at the mid-point of the pipeline followed by a cavity at the valve. The collapse of the first cavity is shown on the lower trace at a time 3.5 pipe periods after the start of valve closure, the computed and observed results at that time agreeing reasonably. The collapse of the valve cavity occurs 2.5 pipe periods later.

SEPP in this modified form was transferred to magnetic tape and employed for the analysis of all the recorded tests shown in Table 7. Figures 61 to 66 compare the observed and computed results for a number of representative cases while Figures 67 to 71 compare the computed and observed values of the pressure peaks and their phase, at the two transducer stations normally employed i.e. 0.498 and 0.918 of the

pipelength from the reservoir, and the duration of the cavities predicted at the valve.

Generally the agreement was good, within 3% for the magnitude of the first peak following valve closure and the duration of the vapour cavities, within 5% for the phase of the observed pressure peaks and generally within 10% for the amplitude of the pressure peaks following cavity collapse. The solution was found to be sensitive to small errors in the input data, i.e. errors in steady state velocity, reservoir pressure and the valve closure-time curve. It is to be remembered that any errors in this input data will carry through the calculation so that discrepancies in results for the 2nd and 3rd peaks and their phase will be due to some extent to them.

As already mentioned the use of the interpolated time increment $\Delta x/2c$ will produce a cumulative error. Although this method has been accepted for cases involving very high rates of change of pressure and velocity it can lead to errors whose magnitude depend to a large extent on the computation section pipelength. In this analysis the pipe sections considered have been kept to a minimum length, some 1.5 m. This procedure contributes to the discrepancy in the observed and predicted phase of the 2nd and 3rd peaks following valve closure.

These results will also be affected by the magnitude and phase of the first peak. Examination of the computed results showed that generally the first observed peak occurred earlier and had a greater magnitude than that predicted. This in turn would lead to the prediction of a 'weaker' first cavity as the computed pressure changes following the first pressure peak would tend to be less steep than those observed and so a cavity of shorter duration would be predicted bringing forward the phase of successive pressure peaks. This is supported by the results

for the duration of the valve cavity. Generally it was found that in cases such as Run 3, 13/11/68,Figure 59, where close agreement was achieved for the first pressure peak following valve closure, the remainder of the trace also displayed above average agreement.

The predicted magnitudes of the 2nd and 3rd pressure peaks were less accurate, within 10%,with the exception of the 3rd peak observed at X/L = 0.9. These errors illustrate a major weakness in all the methods at present available for the solution of pressure transient problems, namely the correct representation of transient damping. In SEPP the friction factor was assumed constant at its steady state value, however this can not be expected to accurately represent the damping during pressure transient propagation. The effect, if any, of varying friction factor with the Reynolds Number at each pipe section at each time step was investigated by including a procedure based on:

$$f = 16/Re, \quad Re \leq 2300$$

$$f = 0.079/Re^{\frac{1}{4}}, \quad Re > 2300$$

into the existing program, this being known as SEPB. Two representative tests are summarised in Tables 8 and 9. Little effect was found, due to the Reynolds Number range of the tests, 12,000 - 55,000 which would only allow small changes in friction factor, and the pipe section length.

Due to this lack of damping the excessive pressure predicted for the collapse of the first valve cavity would lead to the prediction of a 'strong' second cavity at the valve. Examination of the computed results for those cases displaying excess pressure rise on the collapse of the first cavity showed that the opening of the second cavity at the valve affected conditions for a considerable pipelength, vapour pressure being predicted as far along the pipeline as X/L = 0.5 whereas the observed results showed low pressures approaching vapour pressure but not actually reaching it. This would not preclude the actual formation

of a second cavity at the valve, this was found to occur in most cases as its presence was shown by the phase separation of the 2nd and 3rd peaks observed at X/L = 0.918 and 0.498, i.e. a phase separation greater than two pipe periods. Closure of this predicted cavity would produce a computed pressure rise in excess of the observed value.

The damping supplied by pipeline vibration is neglected in the analysis presented. This could be a significant factor, particularly at a closed valve on cavity collapse. The effect of this vibration is to modify the 'no-flow' boundary equation as the fluid in contact with the valve face will continue to move until the vibration is restrained. Due to the scale of the pressure rise times even a small valve movement can be significant. If this motion continues for longer than one pipe period, the full pressure rise will not be realised due to the arrival of reflected pressure waves from the upstream boundaries of the system. This topic will also be mentioned in the discussion of separation downstream of a valve.

The two programs so far mentioned, SEPP and SEPB employed 1st order or rectangular rule approximation for the friction term. Second order integration was employed in program SEPD, together with the provision of Reynolds Number dependent friction factor. The results from the analysis of three representative cases are again shown in Tables 8 and 9. The basic difference between the 1st and 2nd order approximations is that the first considers friction loss to be concentrated at alternate pipe sections while the second considers friction loss at each section. No appreciable improvement was found, this being due to a number of factors including the short length of each pipe section, the Reynolds Number range and the value of the time increment, i.e. some 0.8 millesecond.

The effect produced by varying the time increment following the formation of the first vapour cavity according to the expression:

$$\Delta T = Z.\ \Delta x/c,\ 0.2 < Z \leqslant 1.0$$

was investigated by SEPC, a program employing the same procedures as SEPB. Tables 10 and 11 illustrate the results obtained. The previously mentioned error arising from the use of this form of decreased time step is clearly shown by the phase of the pressure peaks following valve closure and subsequent cavity collapse. The elimination of the excessive pressure peaks predicted by both the graphical method and the numerical method for Z = 1.0 is also illustrated by these results and indicates one beneficial side effect of employing values of Z < 1.0.

6.4 Measurement of fluid velocity during transient propagation by means of a DISA C.T.A. and hot film probe

Calibration of the DISA 55A01 anemometer and 55A82 hot film probe by mounting the probe on the valve closing ram gave the expected relation between output voltage and probe velocity, namely:

$$\text{Volts}^2 = \sqrt{|\text{Velocity}|}$$

Steady state centre line velocities in the test pipe were measured using this equipment and close agreement was achieved with the corresponding velocity based on the venturi meter reading.

Figures 72 and 73 illustrate the pressure-velocity-time traces obtained for three typical tests. It is apparent that the form of the above relation makes direct reading from the velocity traces impossible. Referring to Figure 72 it will be seen that the velocity reversal times agree with the theoretical 2L/c pipe period. It is important to note that the anemometer is only calibrated for flow

where the hot film forms the leading edge of the probe, thus results during the reverse flow time regions, where the film is in the wake of the probe body, are meaningless. Further the quantity recorded is strictly $|V|^{\frac{1}{4}}$.

It will be seen that the probe output does not approach the zero velocity line during transient propagation. This apparent error is magnified considerably by the form of the recorded output, and further any local secondary flows, which must exist in a transient flow condition, would also contribute to the output voltage of the instrument.

In order to compare the observed and predicted velocity variations it is necessary to repeat the probe results as shown in Figure 74 which is taken from the test illustrated in Figure 73, Plate 1. Reasonable estimates of the maximum velocity of the returning fuel column prior to cavity collapse at 8 pipe periods, and of the flow reversal time, i.e. the start of cavity collapse, at 5.5 pipe periods were obtained. The agreement on the reversal time is possibly surprising as there would be a time lag on the probe results as the flow re-established over the film, however this may be obscured by the fact that centre line velocities are compared to mean velocities and it is likely that the centre line flow would reverse earlier than the predicted mean velocity reversal.

The usefulness of these tests was severely limited by the form of the anemometer output. Later tests on the downstream side of the valve employing a DISA 55D10 Linearizer unit produced more conclusive evidence of the agreement between observed and predicted velocity variations.

Generally the tests indicated that the assumptions made with regard to the movement of the separated column were justified. Further the results confirm that the frequency response of 5 kc quoted for the instrumentation in the C.T.A. mode was sufficient to deal with the oscillations recorded.

6.5 Column separation downstream of a closing valve

6.5.1 Initial tests on pipeline configuration 2

Figure 75 reproduces the pressure-time records obtained at two points downstream of the valve in pipeline 2 following valve closure. Column separation is indicated by the form of these pressure variations, however there are some notable differences between these records and those obtained for separation upstream of a closed valve, e.g. the general smoothness of the traces and the absence of an instantaneous pressure rise on cavity collapse.

As mentioned in Section 3 two basic mathematical models were used, one based on a 'vapour only' cavity and the second based on air release during the opening phase of the cavity.

Figure 76 compares the observed pressure variation downstream of the valve with the results of the 'vapour only' program, SEPE. SEPE employed the 1st order finite difference equations plus Reynold's Number dependent friction factor. Reasonable agreement was achieved for the magnitude of the pressure peaks, however the times of cavity collapse and the general shape of the pressure variations were considerably in error.

In order to improve on the assumptions made for the valve boundary conditions during separation it was decided to observe the separation of the column and to attempt to record on film the actual sequence of events.

6.5.2 Observation of column separation downstream of a closing valve

The observation and filming tests had two main objectives:

1. To gain a qualitative impression of the sequence of events during the duration of the cavity.
2. To measure the velocity of the fluid column during both

the opening and closing phases of the cavity's existence and to link this information with the simultaneous pressure records.

Figure 77 presents both the pressure variation downstream of the valve during and following closure, Plate 1, and the extent of the vapour/gas/fuel mixture Plates a - j. The 16 mm film used did not print and enlarge well, explaining the poor quality of the photographs.

The sequence of events during cavity formation may now be traced.

1. Column separation occurs as a result of pressure reduction downstream of the valve. In the low head piping system employed a sufficiently large pressure drop may be achieved while the valve is still closing. This is confirmed by Plate a, where the valve pointer indicates that the valve is still open, while the presence of the released gas is clearly visible. It must be noted that there was a 127 mm steel section between the valve and the glass pipe, so that by extrapolating the film results it appears that column separation and gas release was initiated as soon as the pressure fell below atmosphere.

2. The separated column is decelerated, by the adverse pressure gradient between the cavity and the downstream reservoir and by friction. Plates b, c, d illustrate this phase and the maximum extent of the mixture.

3. The column is accelerated back towards the valve, collapsing the cavity and compressing any undissolved gas. The final velocity will be less than the initial interface velocity on separation. Plates e, f illustrate this phase.

The shape of the pressure variations in Figure 77 Plate 1 can be explained in terms of the effect caused by the released gas observed.

The returning column initially causes little pressure increase in the released gas, so that the velocity of the column continues to increase. Once the pressure exceeds the downstream reservoir pressure the column is decelerated rapidly, the pressure of the released gas increasing until the column comes to rest. Thus the pressure variation would be expected to display a slow increase from the instant of column reversal, terminated by a smooth but rapid final rise, which agrees with Plate 1, Figure 77.

Reflection of this pressure rise negatively at the downstream reservoir results in a pressure drop at the valve sufficient to re-open the cavity as the reflection coefficient at the valve during the period following cavity collapse was +1. Figure 77 Plates g, h, i illustrate the sequence of events during the second low pressure region on Figure 77 Plate 1. This process is repeated until sufficient energy has been dissipated and the fluid column comes to rest at the reservoir pressure.

A number of points emerged from these tests:

1. Gas release and column separation may occur before the valve is fully closed.

2. Gas remained out of solution throughout the high pressure regions and did not re-dissolve following final damping of the transients. Figure 77, Plate j illustrates this residual gas at the valve, however due to the poor reproduction of the film the extent of this residual bubble overlying the fluid is not well defined in the photograph.

3. The vapour/fuel/released gas mixture was full bore in the pipeline. The buoyancy of the bubbles had no visible effect during the existence of the first two cavities.

4. No gas was observed to come out of solution ahead of the interface between the separated column and the cavity region. This indicated that there was no entrained air in the flow initially and that the agitation supplied at the valve was the deciding factor in the gas release phenomenon.

5. Liberated gas did not go back into solution but remained concentrated at the valve. This explains the subsequent damped pressure traces.

Thus the first objective of these tests was achieved and the program was modified to include the effect of the released gas on the cavity pressure as well as the effect of its continued presence as the new valve boundary condition. Results from the first of these modified programs, SEPF, where n = 1.0 was taken as the polytropic coefficient of expansion, i.e. isothermal conditions, are presented in Figure 76 to provide a direct comparison with both the observed and the predicted 'vapour only cavity boundary' pressure variations. The agreement is seen to be greatly improved.

Figures 78 and 79 compare both the observed values of the volume of the released gas/vapour/fuel mixture and the cavity interface velocity with those calculated by SEPK, a program employing the boundary conditions outlined above plus a modification to allow for the presence of the glass/ aluminium junction 3.04 m downstream of the valve. This boundary condition has already been described in Section 3.5.4.

One of the basic assumptions made in the derivation of the equations defining transient propagation is that the velocity profile is initially uniform and remains so during the passage of a pressure transient. Figure 80 illustrates the probable distortion of the flow through the valve during closure, which quite obviously violates the

above assumption. This explains both volume and interface velocity discrepancies. The velocities measured from the movement of the interface refer, at least while the valve is closing, to a high speed stream of fluid flowing along one side of the pipe. Once the valve has closed it is probable that the velocity assumption becomes more reasonable, as is indicated by the close agreement between the observed and predicted times of maximum cavity volume and cavity collapse. It is interesting to note that a calculation based on the valve open area ratio and the predicted column separation velocity yields a figure comparable to the velocity of the separated column measured from the first frames to record the presence of the gas/fuel mixture.

The observed velocities, Figure 79, for the opening phase of the first cavity were obtained by fitting a polynomial to the observed cavity volume results of Figure 78 and differentiating the resulting equation. Direct velocity measurements from the film were found to be highly inaccurate due to a multiplication of the measurement errors involved.

During the collapse phase of the cavity it is likely that events in the pipe are obscured by a layer of bubbles close to the pipe walls, so no measured velocity values for this phase are included in Figure 79.

The second objective of these tests was therefore only partly achieved however two points were worth noting:

1. The uniform velocity distribution assumption breaks down during the initial opening of the cavity.

2. The mixing that occurs due to the high speed fluid stream passing along one wall of the pipe probably results in gas release from the volume of fluid immediately downstream of the valve.

Figure 81 summarises the maximum extent of the gas/vapour mixture observed from a series of films. Following these tests the pipeline was converted back to configuration 2 and a further series of tests carried out to check the validity of the new boundary conditions included in the analysis.

6.5.3 Further tests on pipeline configuration 2

The difference between the 'vapour only' and vapour plus released gas boundary conditions at the cavity may be summarised by the two equations defining cavity pressure:

$$P_{cav} = P_{vap}$$

for the 'vapour only' case following a pressure reduction to vapour level,

or:

$$P_{cav} = P_{vap} + P_{air}$$

for the released gas case following a pressure drop to below atmospheric pressure,

where

$$P_{air} = \left(\frac{AIRVOL}{VOL}\right)^{n} \quad ATM$$

The necessary solutions and the programs are presented in Sections 3 and Appendices 4, 5.

Figures 76 and 82 confirm that the inclusion of the gas terms is significant, particularly with reference to the times of cavity collapse and the general shape of the pressure variations.

Figures 83 and 84 compare the pressure reduction at the valve during two closure rates. The vapour only assumption predicts a much steeper pressure reduction than was observed. The use of n = 1.0 in the partial pressure calculations is supported by these results and by Tables 12 to 14. This assumption seems reasonable as the volume

of gas involved is small and thoroughly mixed with the fuel which would be likely to act as a heat sink during separation.

The cavity at the valve re-opens a number of times before the fluid finally comes to rest. The inclusion of released gas in the system model improves the decay rate predicted for the duration of these cavities and their collapse pressures, Figure 76.

Solution of the cavity boundary equations involving values of $n > 1$ were carried out by program SEPG, Appendix 5. It was found, for both SEPF and G, that an instability in the results obtained for the peak pressures was possible if the rate of change of cavity volume was too great. The simplest way to avoid this was to reduce the time step, by interpolation, if the change in volume across any time step exceeded half the volume at the start of that time step, thus:

$$IF(VOL_T - VOL_{T-\Delta T} \; . GT. \; 0.5 \; VOL_T) \; \Delta T = \Delta T/2$$

This method was used throughout subsequent tests.

6.5.4 Pressure variation at a point some distance downstream of the valve, in pipeline configuration 2

Pressure variations 4.04 m downstream of the valve are illustrated in Figures 75, 82 and 85 and generally follow the variations at the valve with the exception of the secondary pressure oscillations recorded during column separation at the valve. These have already been explained in terms of the -1 reflection coefficients at the cavity and downstream reservoir. This model must be altered slightly as the cavity pressure is strictly dependent on the gas partial pressure so that as this decreases during the opening phase of the cavity the reflection coefficient is greater than -1 and, conversely, as the air pressure

increases during cavity closure, less than -1. This accounts for the reduction in the amplitude of the oscillations during cavity closure. These secondary oscillations are accurately predicted by the analysis, Figures 82 and 85. The frequency of this wave form is c/2L, or 47.34 c/s for configuration 2 based on a wave speed of 919.85 m/s.

If the flow contained any entrained air, or if any air was released from the fuel along the length of pipeline subjected to pressures below atmosphere, then the wave speed would be drastically reduced. The measured frequency of the secondary oscillations was of the order 45-48 c/s, accurate measurement being difficult, however the change in frequency that would be caused by the presence of free air would be so great as to make these measurement errors insignificant.

Thus the assumption that the effect of the released air can be concentrated at the valve is justified as is the assumption that it is the agitation supplied to the fuel that is responsible for the release of the dissolved air at the valve.

The steepness of these secondary oscillations depend on the rate of valve closure, initial flow velocity and line pressure. Generally the steepness would increase if the initial flow rate or the valve closure rate is increased.

6.5.5 Effect of varying the steady state conditions, pipeline configuration 2.

The tests described above resulted in a program, SEPI, which employed the released gas at the valve as the boundary condition during and following separation, a value of n = 1.0, the time step reduction technique to avoid pressure instability due to rapid cavity volume change and a series of sorting procedures which identified and printed the maximum and minimum pressures and their event times together with the separation velocity and steady state conditions. This program removed the line printer speed limitation imposed on earlier programs and allowed 6 - 10 test cases to be analysed in the time taken to analyse one where all the pressure-velocity results for each time step were printed.

Pipeline configuration 2 was used for a series of tests involving the variation of three steady state parameters, namely the initial flow velocity (1 - 3 m/s), the downstream reservoir pressure (102 - 420 kN/m^2 abs.), and the valve closure time (0.08 - 0.3 s).

Figure 86 Plates 1 - 6 illustrate the effect of varying the valve closure rate. The initial separation velocity decreases with increasing valve closure time, as does the volume of the cavity. The quantity of gas released is also likely to be reduced. Plates 5, 6 illustrate the lower cavity collapse pressures and reduced cavity duration that accompany a reduction in separation velocity. A reduction in the amplitude of the secondary pressure oscillations with increasing valve closure time is also illustrated.

Pressure reduction at the valve during closure and the minimum recorded pressures are illustrated in Figures 87 and 88. The dependence of the minimum pressure on valve closure rate is illustrated. As both cavity volume and separation velocity decrease with increasing valve closure time, the recorded pressure drop decreases with increasing valve closure time.

A decrease in the initial flow velocity reduces both cavity duration and collapse pressure. This effect, plus the secondary pressure fluctuations 4.04 m downstream of the valve are shown in Figure 89.

An increase in the line pressure by controlling the downstream reservoir pressure increases the pressure gradient between the cavity and the reservoir so that cavity duration is reduced, Figure 90.

Results from a series of tests, represented by the above mentioned polaroid photographs, were compared to the theoretical results from SEPI. It is to be noted that the theoretical curves drawn are only valid between the limits shown. For example the cavity collapse pressure vs. initial flow velocity curve could not be drawn through the origin, as at some small initial flow velocity, separation would not occur and the procedures would become invalid.

It is to be noted that the valve closure time is taken to describe the whole valve closing mode as the ram motion is linear and so all the valve open angle vs. time relations during closure belong to the same family of curves.

Figures 91 to 106 illustrate the comparison between observed and predicted values of the maximum and minimum pressures recorded and their event times for the first cavity formed downstream of the valve.

A number of general points are illustrated by these curves and by the results presented in Tables 17, 18, produced as output by SEPI.

(1) The cavity collapse pressure rise displays a dependence on both valve closure rate and downstream reservoir pressure. The pressure generated on cavity collapse is composed of twoccomponents, namely the pressure generated by the stoppage of the returning column and secondly a component arising from the change in valve reflection coefficient from -1 during cavity existence to +1 following cavity collapse.

If the returning column is brought to rest, from the maximum velocity attained, in less than one pipe period, then the pressure generated would have a value $\rho c V_{clos}$, where V_{clos} is the maximum velocity reached by the returning column.

During the existence of the cavity at the valve, the initial transient propagated downstream from the valve on separation will be reflected at the downstream reservoir and at the cavity with a change of sign, resulting in a 'sawtooth' waveform of c/2L frequency. This transient has a maximum value $(p_o - p_{vap})$, which would be generated if the pressure drop producing separation occurred in less than one pipe period.

In the particular test rig employed this maximum pressure drop $(p_o - p_{vap})$ is approximately equal to the downstream reservoir pressure PR2. The contribution of this secondary pressure oscillation to the pressure rise following cavity collapse therefore has a maximum value of 2.PR2, recorded at the valve.

In order to generate the maximum PR2 amplitude secondary pressure oscillations, the pressure drop producing separation should occur, in theory, in less than one pipe period. For a spherical plug valve this condition may be achieved by an overall valve closure in excess of one pipe period due to the valve's closing characteristic.

An increase in the downstream reservoir pressure reduces the critical column separation velocity and the subsequent value of $\rho c V_{clos}$, as indicated in Table 17, for one valve closure rate and flow velocity. The second component, 2PR2, increases with line pressure, so that it would be possible for the peak pressure recorded to remain roughly constant for a range of downstream reservoir pressures, Table 17.

An increase in the valve closure time again reduces the column separation velocity and the $\rho c V_{clos}$ value. The contribution from the

secondary oscillation will also decrease as the amplitude of the secondary oscillation decreases with increasing valve closure time, as illustrated by Figure 86. With reference to Table 17 it can be seen that the sum of ($\rho c V_{clos}$ + 2PR2) is consistently greater than the predicted peak pressure, due to the fact that the secondary wave amplitude does not reach the maximum value ($p_o - p_{vap}$). It is to be noted that the fastest valve closure time, 0.08 seconds, still represents a 3 pipe period closure, Figure 75 illustrates the amplitude of secondary oscillations encountered at this closure rate.

A combination of the above relations explains the form of the collapse pressure curves, Figures 91 to 94.

It will be seen that the maximum and minimum pressures are expressed as variations from the steady state as these were the values recorded during each test.

(2) The cavity duration is highly dependent on the reservoir pressure, due to the influence of the reservoir pressure on the pressure gradient between the reservoir and the cavity that drives the separated column.

(3) The minimum pressure recorded during first cavity growth increases with decreasing valve closure rate.

(4) The time of minimum pressure recorded during the cavity growth is also highly dependent on the reservoir pressure.

Generally the observed results for the first cavity formed were within 5 - 10% of their predicted values, however there is a consistent trend visible throughout the results that warrants further explanation. The pressures generated on cavity collapse were consistently lower and occurred consistently later than those predicted. This comparison tended to improve with increased line pressure or increased valve closure time. A number of factors contribute to this discrepancy.

(i) At low line pressures the possibility of cavitation at either the pump or the control valve in the return pipeline, Figure 23, is increased. Any entrained gas produced in this way and carried into the test pipe would reduce and delay the cavity collapse pressure rise. However, as this would also reduce the wave speed in the test pipeline and as no evidence of this was found on measuring the frequency of the secondary pressure oscillations, this effect may be assumed to be insignificant.

(ii) The vibration of the valve following cavity collapse could produce the reduction in collapse pressure noted. Referring to Figures 86 to 90 it can be seen that the major pressure rise occurs in 5 - 10 ms so that a valve movement of 1 mm in this time would be the equivalent of 0.2 - 0.1 m/s, which could represent 10% of the maximum velocity of the returning column.

Referring to equations (28) to (30), that apply if a fluid column is brought to rest in less than a pipe period it follows that:

$$\Delta P = \rho c \, (V - V_o).$$

If $V \neq 0$, but rather 10% of V_o due to axial valve motion, then the full $\rho c V_o$ pressure rise will not be attained until the valve, and hence the fluid in contact with it is brought to rest by the restraint of the valve supports. If this does not occur prior to the return of a reflection from the system's boundaries then the $\rho c V_o$ value will not be reached.

Recent work by Wood (83) has demonstrated that for a simple reservoir - pipeline - restrained valve system the effect of valve restraint can be predicted if the stiffness of the restraining spring is known. Wood's work confirms earlier work by the present author (84) where the axial motion of a simple gate valve following rapid closure was monitored using a Wayne Kerr vibration meter and the velocity results

obtained compared to the step in the pressure rise to $\rho c V_o$ caused by this valve motion and its subsequent restraint. It was found, for a given valve closure rate and applied restraint, that the ratio of the valve axial velocity to the initial flow velocity remained a constant, having a value up to 20% depending on the applied restraint. The relevance of this can be seen from the cavity collapse pressure rise vs. initial flow velocity curves where the % discrepancy remains a constant over a wide range of initial flow velocity.

Wood's work could not be directly applied to the test rig due to the difficulty in representing the upstream pipeline, valve supports etc. by an equivalent spring system.

The restraint applied at the valve was varied, however this had no noticeable effect and it is probable that the tolerance on the ball of the valve is sufficient to allow the slight axial movement necessary to delay the generation of the maximum pressure until the return of a negative reflection from the downstream reservoir.

(iii) The time of cavity collapse is highly sensitive to the downstream reservoir pressure so that any error in the steady state value fed as data to the program would yield a significant error on the comparison of the cavity duration.

As mentioned in the test procedures care was taken to shut down the pump at the same instant as the valve was closed to ensure that the downstream pressure did not fall during the growth of the cavity. It can be seen from the theoretical curves in the 'carpet graphs', Figures 99 to 104, that an error of the order of 5 kN/m^2 on the downstream reservoir pressure would be sufficient to account for the recorded discrepancy. As the collapse time results were consistently later than those predicted it is likely that the error arose from the pump, during slow down, removing a small quantity of fluid from the reservoir and thus lowering the pressure. The compressed air supply to the tank was controlled

by a two way regulator valve, however it is probable that a drop of 5 kN/m^2 would be insufficient to open the compressed air supply line.

(iv) An underestimate of the air released in the program would have the effect of reducing the predicted cavity duration. The flow visualisation tests indicated that the air release was underestimated by the proposed analysis, due to the flow distortion caused by the closure of the spherical plug valve that resulted in a region of vigorous mixing downstream of the valve, implying that a greater volume of fuel released its air than that passing through the valve between separation and valve closure.

(v) In this reported analysis the gas released is assumed to have the normal 3.76:1 nitrogen-oxygen ratio, however there is evidence (75, 76, 85) that the released gas has a nitrogen to air ratio of 2:1, Figure 107. The assumption that the fuel is saturated with air is supported by Figure 108 reproducing tests carried out for B.A.C. by Shell and R.A.E.

However this data is based on tests reproducing a slow reduction in tank pressure. Poulston and Thomas (76), in a paper discussing gas release and foaming during aircraft climb, state that oxygen has a higher solubility coefficient in fuel than nitrogen, Figure 18, and that the gas dissolved is richer in oxygen than is normal air. It would be expected from "thermodynamic reasoning" that, during slow de-gassing, the gas first evolved would be close in composition to air, but the oxygen concentration of the gas evolved would rise continuously as more gas was released. Therefore it is likely that this data does not apply to a pressure reduction occurring in milli-seconds.

The validity of the steady state air release data was checked by an analysis of the air released from the fuel and the results will be discussed later.

(vi) The pressure in the cavity is governed by both the fluid vapour pressure and the partial pressure of the released air. The value of vapour pressure at normal working temperature, 17.5°C, was taken as 0.7 kN/m^2, however there is evidence (85),Figure 109 to suggest that this could be an underestimate as tests by Shell and R.A.E. (unpublished) have indicated that actual fuel does tend to have a scatter in properties. A small increase in vapour pressure would reduce the driving pressure gradients and delay the collapse of the cavity.

(vii) As already mentioned in both the literature survey and the theory sections, the steady state friction factor is assumed to apply during transient flow. This is accepted practice but results in an underestimate of the damping so that the cavity duration is underestimated and the collapse pressure rise is overestimated.

All the factors mentioned above would tend to act in the same way, confirming the trends on cavity duration and collapse pressure. Points (i), (ii) and (iii) are factors of the rig design. Increasing the overall valve closure time reduced the shock loading on the valve on cavity collapse and the comparison on peak pressure was consequently improved.

Increasing the downstream reservoir pressure would reduce the percentage error on the driving pressure gradients and the comparison on cavity duration would improve.

The remaining factors, with the exception of (vii), could be allowed for in the program, however it was the object of the work reported to employ as far as possible only data readily available from manufacturer's specifications. It was felt that this would be the way any of the computing procedures developed would be used in practice.

Figures 95 to 98 illustrate the minimum pressures recorded at the valve. Scatter on measured values of time of minimum pressure is accounted for by the practical difficulty that the pressure-time curve is very flat in this region even on an increased Y-axis as shown in Figure 87. The minimum pressure results indicate that the air release is a significant factor.

6.5.6 Comparison of the observed and predicted results for the second cavity formed at the valve, pipeline configuration 2.

SEPI was also used to predict the values of maximum and minimum pressures and their times of occurrence for the second cavity formed downstream of the valve, and Figures 110 to 116 illustrate the comparisons achieved.

It is to be noted that any discrepancies caused by points (i) - (vii) for the first cavity above will come through the calculations and adversely effect the results achieved for the second cavity. Thus the comparisons obtained are in the 10 - 20% bracket, however the observed duration of the second cavity would still be within 10% of its predicted value.

5.6.7 Collection and analysis of the released gas, pipeline 2

The residual gas downstream of the valve following final cavity collapse was collected and its volume measured, at atmospheric pressure, for a range of valve closure rates and line pressures and two initial flow rates, Figures 117 and 118. The agreement was found to be reasonable, the volume collected being 1.25 - 1.5 times that predicted, the agreement improving with increased line pressure. This comparison agrees with the observation tests which indicated that the severe mixing immediately downstream of the valve during valve closure led to a greater volume of released gas.

Table 15 records the results of an analysis of the collected gas. When allowance is made for the vapour content of the gas mixture, some 0.6% by volume, it is seen that the gas mixture contained, on average, about the 3.76:1 nitrogen-oxygen ratio of normal air. This supports the assumption that, for a relatively rapid decrease in pressure during and following valve closure, it is reasonable to ignore the possibility of further oxygen release.

6.5.8 Measurement of column velocity with a DISA hot-film probe, in pipeline configuration 2

Following the partial failure of the filming tests to produce values for the velocity of the separated column, during cavity collapse, it was decided to attempt to record these by means of the hot film probe and Constant Temperature Anemometer. In view of the problems encountered during measurements upstream of the valve, concerning the interpretation of the probe output, a DISA 55D10 Linearizer unit was incorporated, Figure 31, and adjusted so that:-

$$\text{Output Volts} = |\text{Centre Line Velocity}|$$

Figures 119 Plates 1 - 4 illustrate two tests on test pipeline 2, involving the hot film probe. Due to the necessity to point the probe 'upstream' relative to any flow to be recorded, each test was repeated with the probe rotated through 180°. Thus Plates 1 and 2, and Plates 3 and 4 refer to two tests.

Figures 120 to 122 were compiled from the oscilloscope traces for a series of such tests. With reference to Figure 120 it will be seen that the assumptions made with reference to the variations in the velocity of the separated column were justified. The steep velocity reduction corresponding to the collapse pressure rise is clearly visible.

A number of assumptions were made in the use of the hot film probe for this purpose:-

(1) The probe was assumed to accurately record velocity as soon as the flow reversed and re-established across the film. In actual tests there would be a time lag while this occurred.

(2) The probe is assumed to line up correctly with the flow direction, whereas in practice secondary flows would be bound to effect the results. This can be seen on Figure 119 Plates 1 - 4 as the probe output does not reach the zero flow line.

(3) The probe records centre line velocity whereas the predicted results refer to the mean velocities.

By the use of two probes and support equipment it would have been possible to record column velocity for both the opening and closing phases of the cavity during a single test, however it is regretted that the second linearizer unit was not available.

6.6 Use of SEPI to provide a design envelope for pipeline configuration 2

SEPI was modified to calculate conditions up to the time at which the column separated downstream of the valve for a series of valve closure rates and line pressures. By repeating the calculations for a series of initial flow velocities from 0.03 m/s upwards in 0.015 m/s steps it was possible to identify and print out the initial velocity at which column separation would first occur for a given valve closure rate and downstream reservoir pressure. This modified program, SEPJ, produced the results illustrated in Figure 123, where the volume $A_1 - A_4$ represents the 'no-separation' conditions for pipeline configuration 2.

As can be seen the design conditions from this envelope would hardly be of practical interest in this case as the flow rates to avoid separation were so small. The program was therefore allowed to continue and to identify and print the initial flow rate for which cavity collapse pressure first exceeded 1000 kN/m^2 above line pressure. It is to be noted that for all these calculations it is assumed that the valve closing ram motion is linear so that the angle-time curve of the valve is described by the overall closure time and the calibration curve of Figure 40.

Figure 123 volume $B_{1-4} \cdot A_{1-4}$ illustrates the new design envelope when column separation is accepted. This procedure could be employed for any piping system and illustrates the vast potential of the method as a design tool.

6.7 Pressure variation upstream of the valve in pipeline configuration 2

Figure 124 Plates 1-3 illustrate the pressure variations upstream of the valve during and following closure. Plates 1, 2 illustrate the expected pressure oscillations following valve closure, and in the absence of column separation, having a frequency of c/4L.

The effect of valve vibration on cavity collapse can be seen, particularly in Plate 2, where an increased amplitude oscillation is introduced into the trace upstream of the valve. This would support the assumption that the ball of the spherical plug valve is displaced axially following downstream cavity collapse.

Figure 124, Plate 3 and Figure 125 reproduce the traces for column separation upstream of the valve, the predicted values being calculated by SEPH, a program identical to SEPF up to valve closure and thereafter dealing only with the upstream pipeline. The cavity boundary conditions were constant vapour pressure, no air release, and full bore cavity growth, effectively the same conditions as employed in the earlier work on upstream separation, Section 6.3.

The pressure rise on valve closure follows the same pattern as previously recorded, Section 6.3. Due to the need to monitor pressure and velocity downstream of the valve, as well as the Linear Displacement Transducer output, pressure variations upstream of the valve were not normally measured during the tests on pipeline configuration 2. Table 16 lists the results of some tests where this pressure was recorded and indicates the degree of accuracy obtained for the peak pressure and peak pressure time.

6.8 Tests on pipeline configuration 3

It was possible to use the second test rig, Figure 23, for flow in either direction along the test pipeline. Figure 126 illustrates the separation upstream and downstream of the valve in configuration 3. Figures 127 and 128 illustrate the observed and predicted values of maximum and minimum pressures and their event times for the first and second cavities formed downstream of the valve for a particular valve closure rate and line pressure. Close agreement is again seen to have been obtained, generally the same comments as made with reference to pipeline configuration 2 apply to these results.

7. CONCLUSIONS AND FURTHER WORK

The results presented indicate that the propagation of pressure transients and subsequent pressure fluctuations in an aviation kerosene pipeline may be accurately predicted by a numerical solution of the wave equations based on the method of characteristics programmed for a digital computer.

The transient propagation velocity in the fuel/pipeline system was found to be within 0.2% of the calculated value. The maximum pressure variation predicted upstream of a valve following closure, and in the absence of column separation, was found to be within 3% of the observed value for a wide range of test conditions.

The tests involving column separation and cavity formation upstream of a closed valve showed that the assumptions that the cavity pressure remained a constant at the fluid vapour pressure and that the cavity volume could be based on a full pipe bore flow interruption were justified.

The predicted duration and collapse pressure rise for the first and second cavities formed were found to be generally within 5% and 10% respectively of the observed values.

Column separation downstream of a valve, both during and following valve closure was studied. The release of dissolved air from the kerosene, due to the agitation supplied by the valve motion, was found to be significant but could be included in the cavity pressure expression in terms of its partial pressure.

Observation of the sequence of events at the valve during and following closure indicated that this released air did not redissolve. A series of programs employing this released air as the valve boundary condition predicted the values of minimum and maximum pressures and their

event times during and following separation to within 10% at worst. The peak pressures observed were consistently below those predicted. A value of n = 1.0 was found to be satisfactory for the coefficient of expansion of this released gas.

Measurement and analysis of the released gas indicated that its nitrogen-oxygen ratio was that of normal air and that its volume was some 1.25 to 1.5 times that predicted by the proposed analysis. This discrepancy was due to the flow distortion at the valve during closure which resulted in severe mixing immediately downstream of the valve.

The filming tests failed to provide an accurate measurement for the interface velocity during cavity collapse. The use of a hot-film probe and Constant Temperature Anemometer to record centre line velocity improved on these results, however it is considered that the use of a linearizer unit is essential in any further work of this type.

Generally the computing procedures developed accurately predicted the column separation phenomena for both the cases studied. The use of these procedures to provide a 'design envelope' for a particular piping system was illustrated. The procedures described in this report have already been applied by the author to an analysis of the Concorde refuelling system.

The work reported on the use of the anemometer equipment indicated that this was practical. Due to the repeatability of the tests it is considered that velocity profile measurements during transient propagation could be obtained, particularly if two probes could be employed to measure flow in opposing directions.

The test rig was not specifically designed to allow observation of the separation, hence the 127 mm solid section between the valve centre line and the glass piping. It would be useful to redesign this part of the apparatus.

Further work, both experimental and analytical is required in connection with the vibration of the valve, following cavity collapse, in order to improve the predictions of pressure and cavity duration decay.

8. REFERENCES

1. Kennedy, J.F. 'A short bibliography of references on waterhammer' Jour. New England Water Works Assn. Vol. 78 1964.
2. Evangelisti, G. 'Waterhammer analysis by the method of characteristics' L'Energia Elletrica Vol. 10, No. 10 - 12 1969.
3. Kerr, S.L. 'Surge problems in pipelines - oil and water' Trans. A.S.M.E. Vol. 98 May 1968.
4. Weber, E.H. 'Theorie der durch wasser oder andere incompressible Flussig-Keiten in elastishen Rohren fortgepflanzten Wellen' Liepzig 1865.
5. Michaud, J. 'Coup de bellier dans les conduites. Etude des moyens pour en attenuer les effets' Bull. Soc. Vaudoise Eng. Arch., Lausanne 1878.
6. Korteweg, D.J. 'Uber die Fortphlanzungsgeschindigkeit des Schalles in elastisches Rohren' Annalen der Physik und Chemie. 5 Floge, Band 5, 1878.
7. Lamb, H. 'On the velocity of sound in a tube as affected by the elasticity of the walls' Mem. Manchester Lit. Phil. Soc. July 1898.
8. Joukowsky, N.E. 'Uber den hydraulisher Stoss in Wasser - leitungsrohren' Memoirs de l'Academie Imperiale des Sciences de St. Petersburgh 1900 Translated by O. Simin as 'Waterhammer' Procs. A.W.W. Assn. Vol. 24, 1904.
9. Allievi, L. Notes I - IV. Translated as 'Theory of waterhammer' E.E. Halmos. Ricardo-Garoni, Rome 1925.
10. Parmakian, J. 'Waterhammer analysis' Longmans Green 1955.
11. Halliwell, A.R. 'Velocity of a waterhammer wave in an elastic pipe' A.S.C.E. Procs. Vol. 89 1963.
12. Skalak, R. 'Extension of the theory of waterhammer' Trans. A.S.M.E. 1956.

13. Thorley, A.R.D. 'Hydraulic transients in pipelines' Trans. A.S.M.E. 1969.

14. Carpenter, R.C. and Barraclough, S.H. 'Some experiments on the effect of waterhammer' Trans. A.S.M.E. 1894.

15. Peek, G.M. 'Pressure in a pipe due to a stoppage of the flowing liquid' Trans. A.S.M.E. 1900.

16. Johnson, R.D. 'Rigid fluid column waterhammer theory' Trans. A.S.C.E. 1915 Vol. 79.

17. Gibson, N.R. 'Elastic fluid column theory' Trans. A.S.C.E. 1920. Vol. 83.

18. Vensano, H.C. and Warren, M.M. 'Waterhammer approximations' Trans. A.S.C.E. 1915.

19. Massau, J. 'Memoirs sur l'integration graphique des equations aux derivees partialles' Ann. Ass. Ingrs. Sortis des Ecoles Speciales de Gand. 23 : 95 - 214. 1900. Translated as 'Unsteady Flow' H.J. Putnam, Rocky Mountain Hydraulic Laboratory, Colorado 1948.

20. Loewy, R. 'Druckschwankungen in druckrohrleitungen' Springer, Wien, 1928.

21. Schnyder, O. 'Waterhammer in pump discharge lines' Schweizerische Bauxeitung Vol. 94 No. 22, 23, 1929.

22. Bergeron, L. 'Variations of flow in water conduits' Comptes rendres des travaux de la soc. hyd. de France, Paris 1932.

23. Bergeron, L. 'Waterhammer in hydraulics and wave surges in electricity' J. Wiley. New York, 1957.

24. A.S.M.E. 'Symposium on waterhammer' 1933.

25. Angus, R.W. 'Simple graphical solution for pressure rise in pipes and pump discharge lines' Journal Eng. Inst. Canada Vol. 18. 1935.

26. Angus, R.W. 'Waterhammer in pipes, including those supplied by centrifugal pumps: a graphical treatment' Procs. I.Mech.E. Vol. 136, 1937.

27. Angus, R.W. 'Waterhammer pressures in compound and branched pipes' Trans. A.S.C.E. Vol. 104, 1939.

28. Pearsall, I.S. 'Waterhammer effects due to branched and stepped pipes' Procs. I.Mech.E. Vol. 180, 1966.

29. Marples, E.I.B. 'The significance of surge diagrams' Procs. I.Mech.E. Vol. 180, 1966.

30. Harding, D.A. 'A method of programming graphical analysis for medium speed computers' Procs. I.Mech.E. Vol. 180, 1966.

31. Hayashi, T. and Ransford, G. 'Sudden opening or closing of an outlet valve on a pipeline' La Houille Blanche, November 1960.

32. Enever, K.J. 'The use of the computerized graphical method of surge analysis' The City University Pressure Transient Symposium, November 1970.

33. Wood, F.M. 'Applications of Heaviside's operational calculus to the solution of waterhammer problems' Trans. A.S.M.E. 1938.

34. Rich, C.R. 'Hydraulic transients' McGraw-Hill 1952.

35. Rich, C.R. 'Waterhammer analysis by the Laplace-Mellin transformation' Trans. A.S.M.E. 1945.

36. Lamoen, J. 'Le coup de belier d'Allievi, compte tenu des pertes de charge continues' Bull. Centre de Etudes, de Recherches et d'Essais Scientifiques des Constructions du Gerrie Civil et d'Hydraulique Fluviale, Tome II, Dosoer, Liege, 1947.

37. Gray, C.A.M. 'The analysis of the dissipation of energy in waterhammer' Procs. A.S.C.E. Vol. 119 1953.

38. Gray, C.A.M. 'Analysis of waterhammer by characteristics' Trans. A.S.C.E. 1954.

39. Ezekiel, F.D. and Paynter, H.M. 'Computer representations of engineering systems involving fluid transients' Trans. A.S.M.E. 1957, Vol. 79.

40. Ezekiel, F.D. and Paynter, H.M. 'Waterhammer in non-uniform pipes as an example of wave propagation in gradually varying media' Trans. A.S.M.E. 1958, Vol. 80.

41. Streeter, V.L. 'Waterhammer analysis with non-linear frictional resistance' Procs. 1st Australasian Conference on Hydraulics and Fluid Mechanics. Pergamon Press, 1963.

42. Streeter, V.L. and Lai, C. 'Waterhammer analysis including fluid friction' J. Hydr. Div. A.S.C.E. Vol. 88, 1962.

43. Streeter, V.L. 'Computer Solution of Surge Problems' Procs. I.Mech.E. Vol. 180, 1966.

44. Streeter, V.L. 'Waterhammer analysis' J. Hydr. Div. A.S.C.E. November 1969.

45. Streeter, V.L. and Wylie, E.B. 'Hydraulic Transients' McGraw-Hill 1967.

46. Lister, M. 'The numerical solution of hyperbolic partial differential equations by the method of characteristics' Mathematical Methods for Digital Computers J. Wiley, New York, 1960.

47. Fox, J.A. 'The use of the digital computer in the solution of waterhammer problems' Proc. I.C.E. Vol. 39, 1968.

48. Fox, J.A. 'Pressure transients in rising mains' The City University Pressure Transient Symposium, November 1970.

49. Swaffield, J.A. 'A study of column separation in a pipeline carrying aviation kerosene' Procs. I.Mech.E. 1970.

50. Doyle, T.J., Swaffield, J.A. and Wood, W.J. 'Pressure transient analysis of the B.A.C./ S.N.A.I.S. Concorde refuelling system' The City University Pressure Transient Symposium, November 1970.

51. Brown, F.T. and Nelson, S.E. 'Step response of liquid lines with frequency dependent effects of viscosity' Trans. A.S.M.E. Series D Vol. 87, 1965.

52. Holmboe, E.L. and Rouleau, W.T. 'The effects of viscous shear on transients in liquid lines' Trans. A.S.M.E. Series D, Vol. 89, 1967.

53. Zielke, W. 'Frequency dependent friction in transient pipe flow' Trans. A.S.M.E. Series D, Vol. 90, 1968.

54. Robertson, J. 'A study of transient laminar flow' The City University M.Sc. thesis 1969.

55. Wood, D.J. and Funk, J.E. 'A boundary layer theory for transient viscous losses in turbulent flow' A.S.M.E. paper No. 70 - FE - 8 1970.

56. Le Conte, J.N. 'Experiments and calculations on the resurge phase of waterhammer' Trans. A.S.M.E. Vol. 59, 1937.

57. Bunt, E.A. 'Preliminary study of valve cavitation in a pipeline' Jour. S.A.I. Mech.E. Johannesburg, Vol. 2, 1953.

58. Binnie, A.M. and Thackrah, M.A. 'Waterhammer in a pumping main and its prevention' Procs. I.Mech.E. Vol. 165, 1951.

59. Gayed, Y.K. and Kamel, M.Y.M. 'Mechanics of secondary waterhammer waves' Procs. I.Mech.E. Vol. 173, 1959.

60. Apelt, C.J. 'Investigations of waterhammer at the University of Queensland' Jour. Inst. of Engrs. Australia, Vol. 28, 1956.

61. Richards, R.T. 'Water column separation in pump discharge lines' Trans. A.S.M.E. Vol. 78, 1956.

62. Duc, J. 'Negative pressure phenomena in a pump pipe line' Sulzer Technical Review. No. 3, 1959.

63. Kephart, J.T. and Davies, K. 'Pressure surges following water column separation' Trans. A.S.M.E. series D, Vol. 83, 1961.

64. Li, W.H. 'Mechanics of pipe flow following column separation' Trans. A.S.C.E. Vol. 128, Part 1, 1963.

65. Walsh, J.P. and Li, W.H. 'Pressure generated by cavitation in a pipe' Procs. A.S.C.E. Vol. 90, 1964.

66. Li, W.H. 'Thermal effect on the growth and collapse of cavities' Paper A-1, Symposium on Cavitation and Hydraulic Machinery, Int. Ass. for Hydr. Research 1962.

67. Lupton, H. 'Graphical analysis of pressure-surge in pumping systems' J. Inst. Water Engrs. Vol. 7, 1953.

68. Carstens, M.R. and Hagler, T.W. 'Waterhammer resulting from cavitating pumps' Procs. A.S.C.E. 1964, Paper 4143.

69. Brown, R.J. 'Watercolumn separation at two pumping plants' Trans. A.S.M.E. series D, Vol. 90, 1968.

70. Lawson, J.D., O'Neill, I.C. and Graze, H.R. 'Pressure surge in fire services in tall buildings' Procs. 1st Australasian Conference on Hydraulics and Fluid Mechanics. Pergamon Press 1963.

71. Baltzer, R.A. 'Column separation accompanying liquid transients in pipes' Trans. A.S.M.E. Paper 67-WA/FE - 16 1967.

72. Dorsett, L.R. 'The effect of separation on transient pressures in pipes' The City University B.Sc. report July 1968.

73. Weyler, M.E., Streeter, V.L. and Larsen, P.S. 'An investigation of the effect of the momentum loss in transient pipe flow' Trans. A.S.M.E. Paper No. 70-FE-4 1970.

74. Wylie, C.R. Advanced Engineering Mathematics McGraw-Hill 1960.

75. Derry, L.D., Evans, E.B., Faulkner, B.A. and Jelfs, E.C.G. 'Vapour and air release from aviation fuels' Jour. Inst. Petroleum Vol. 38, 1952.

76. Poulston, B.V. and Thomas, A. 'Inflammability and electrical studies of foams which may occur at altitude by de-aeration of aviation turbine fuels' Jour. R.Ae.S. Vol. 63, 1959.

77. Swaffield, J.A. 'Visualisation of column separation in an aviation kerosene pipeline' Paper 6, 'Symposium on flow visualisation' Borough Polytechnic London, June 1969.

78. King, L.V. 'On the convection of heat from small cylinders in a stream of fluid' Phil. Trans. Roy. Soc., London, Ser. A., Vol. 214, 1914.

79. Collis, D.C. and Williams, M.J. 'Two dimensional convection from heated wires at low Reynolds Numbers' Jour. Fluid Mechanics, Vol. 6, 1959.

80. Pao, R.H.F. 'Fluid Dynamics' Charles E. Merrill Boaks, Columbus, Ohio, 1969.

81. McCraken, D.D. and Dorn, W.S. 'Numerical methods and FORTRAN programming' J. Wiley, 1964.

82. Pearsall, I.S. 'Velocity of waterhammer propagation' Proc. I.Mech.E. Vol. 180, 1966.

83. Wood, D.J. 'The influence of line motion on hydraulic transients' Procs. A.S.C.E., May 1969.

84. Swaffield, J.A. 'A study of the influence of bends on transients in pipelines' M.Phil. thesis 1968, The City University.

85. British Aircraft Corporation 'Effects of increased fuel vapour pressures' SST/B72T-15/6472 June 1969.

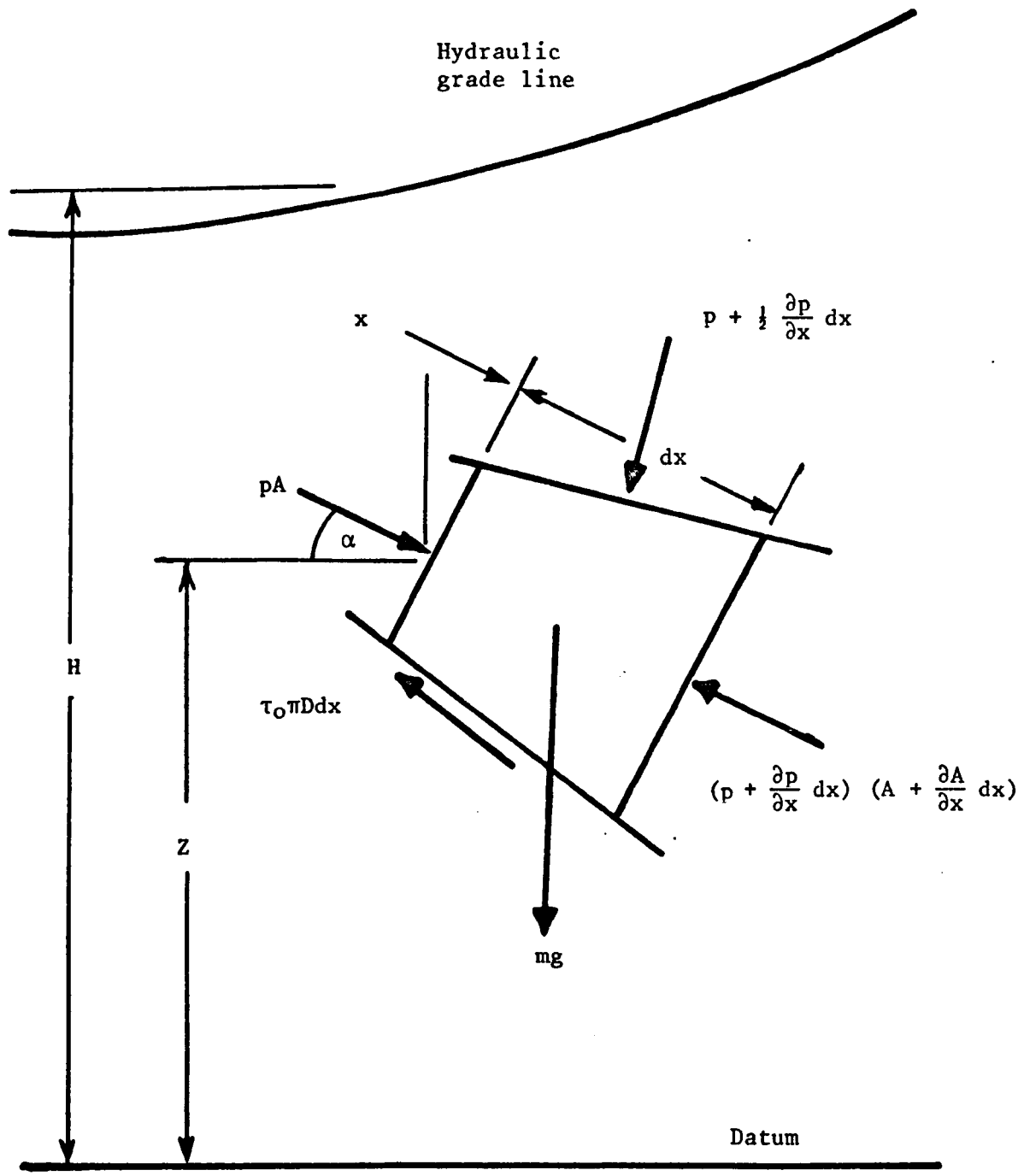

Fig. 1 Free body diagram representing an element of the flow in an inclined pipeline.

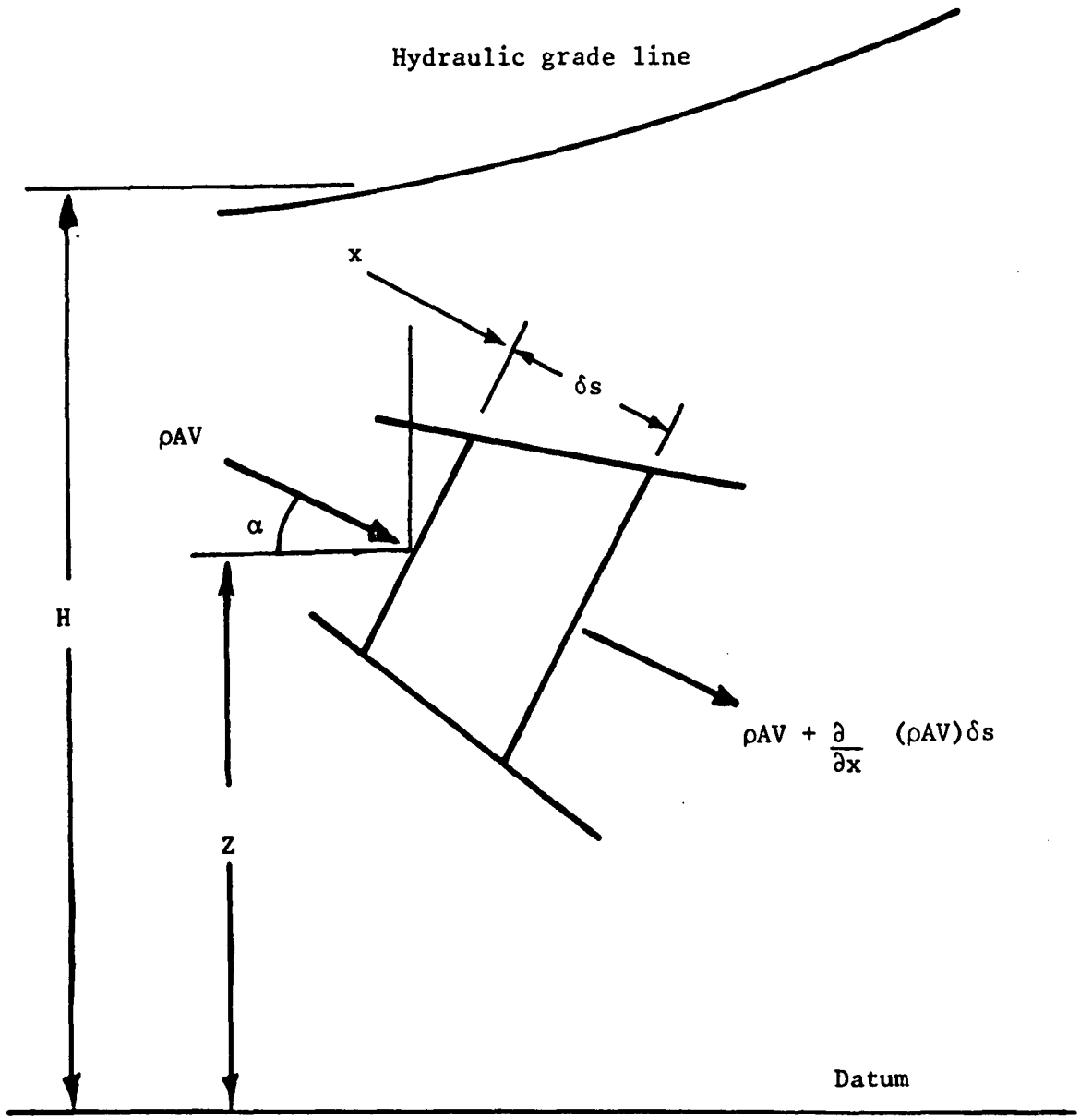

Fig. 2 Free body diagram representing the flow past two points δs apart in an inclined pipeline. Due to pipeline elasticity the length δs may vary.

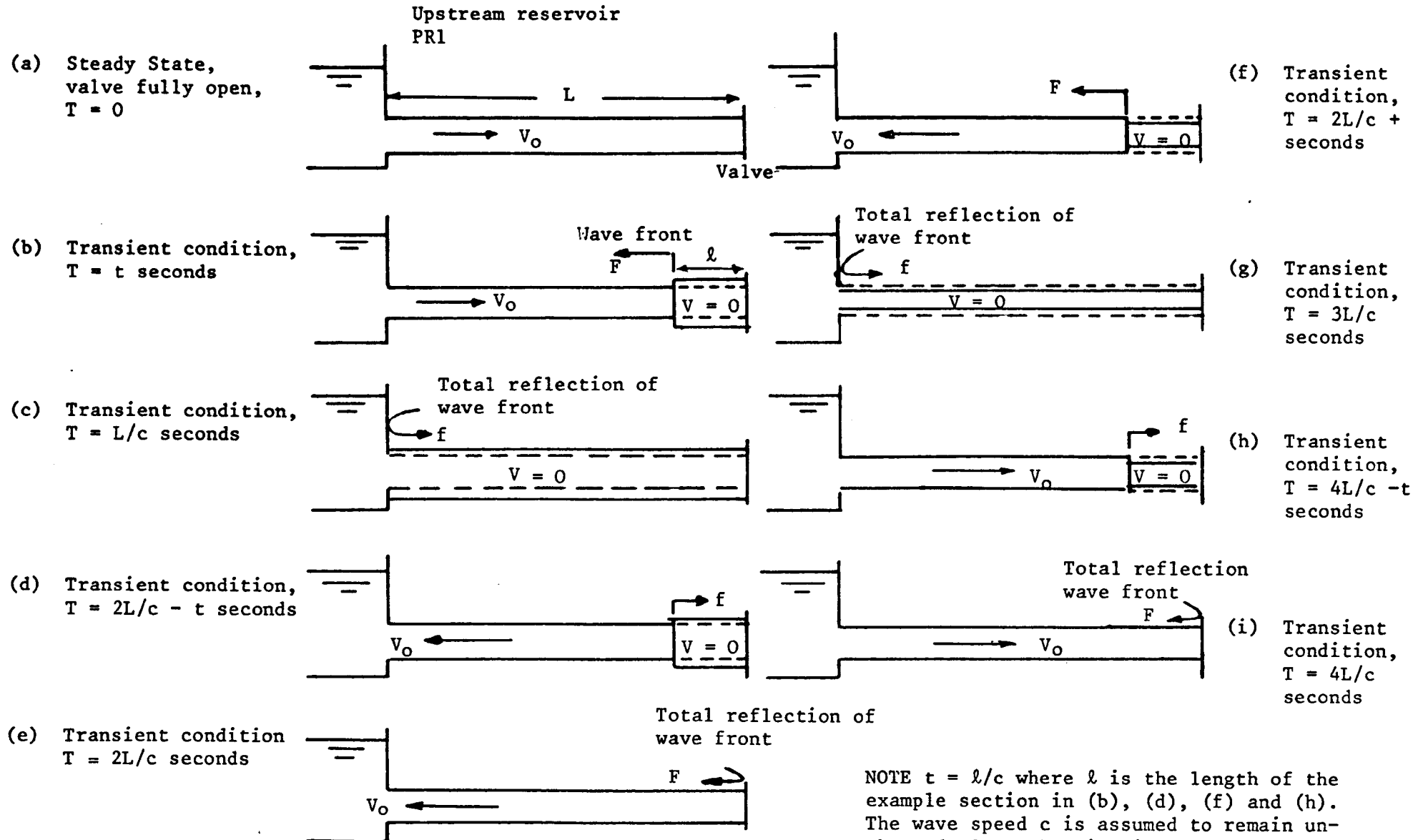

Fig. 3 Propagation of transient pressure waves by an instantaneous valve closure. Note that the reflection coefficient at the reservoir is -1 and +1 at the closed valve in the absence of frictional or vibrational damping or column separation.

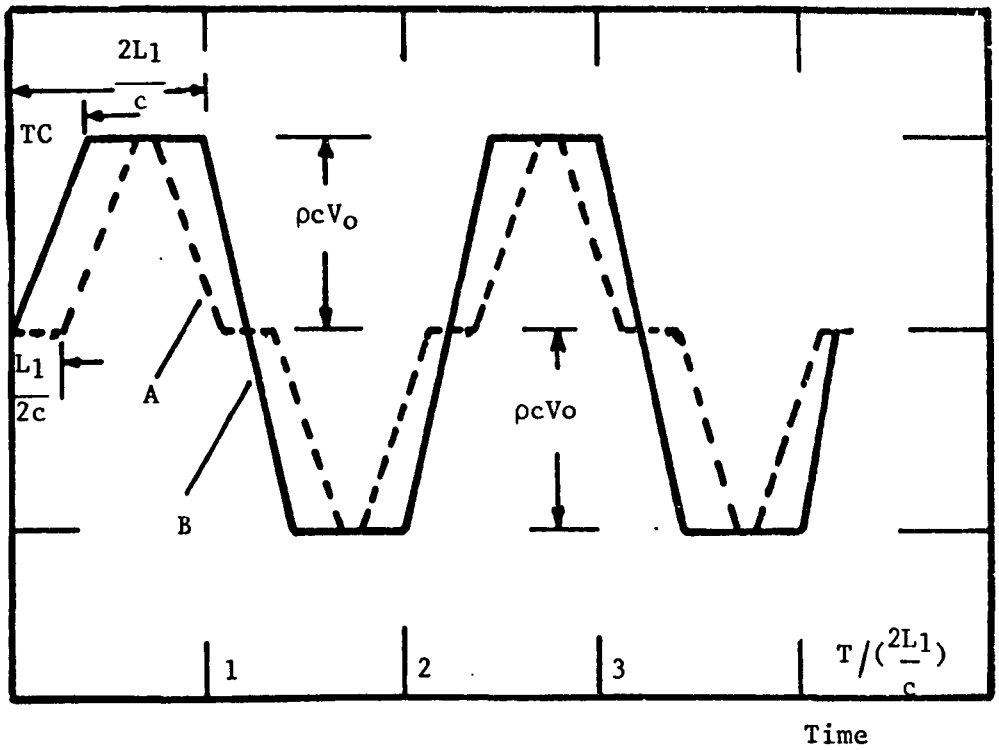

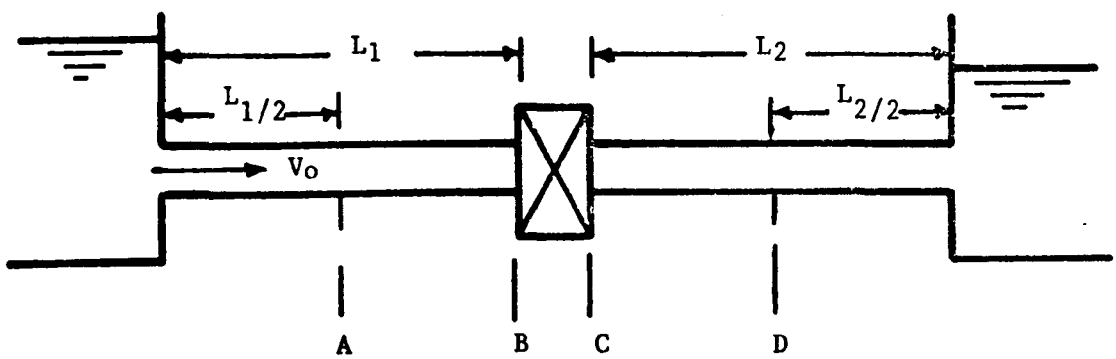

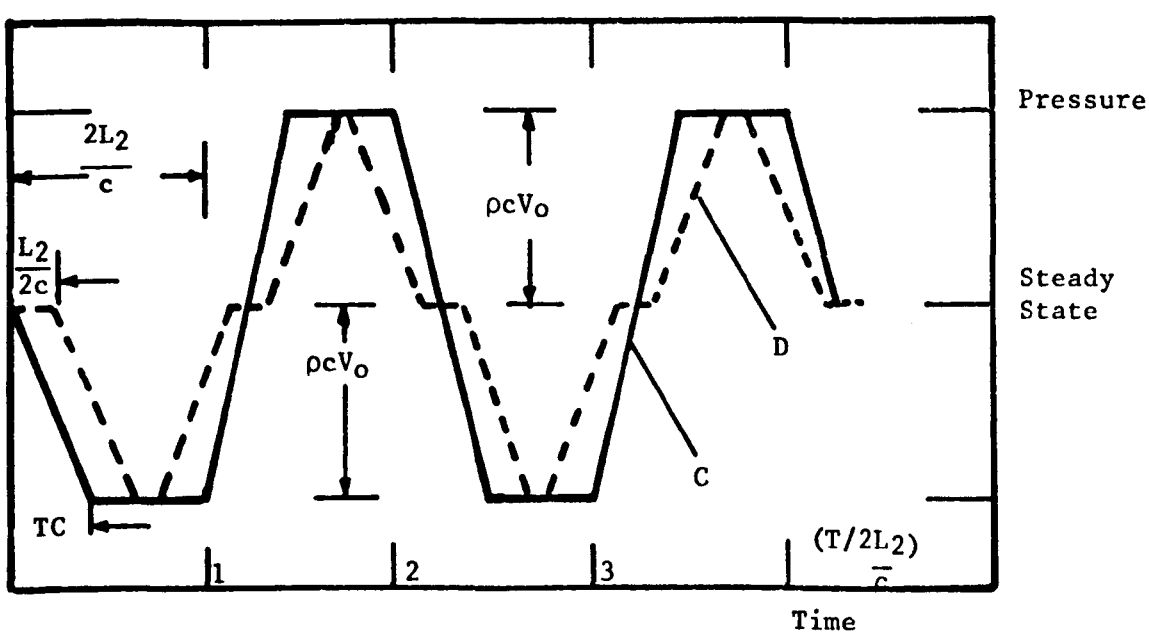

Fig. 4 Pressure variations in the upstream and downstream pipelines following a rapid valve closure and in the absence of column separation and frictional damping.

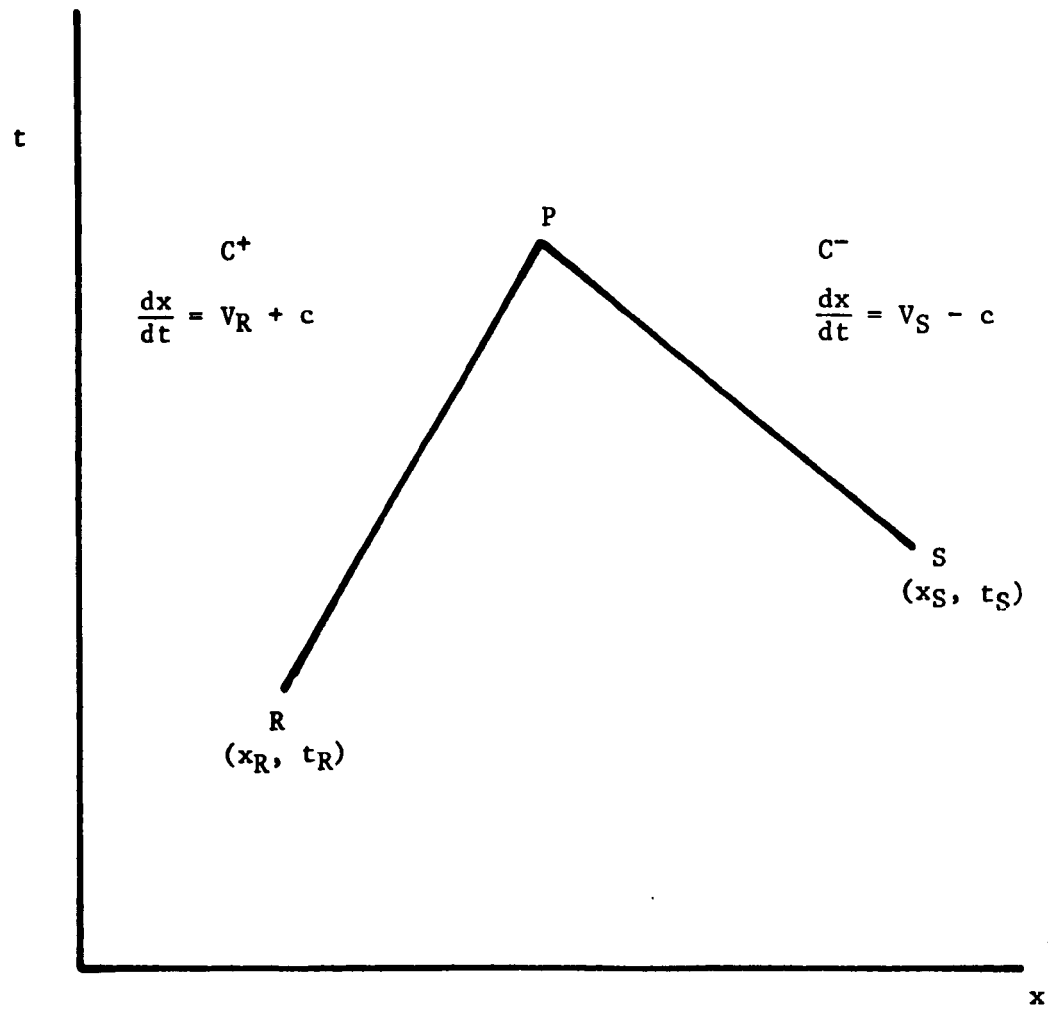

Fig. 5 C^+ and C^- characteristic lines drawn in the (x,t) plane.

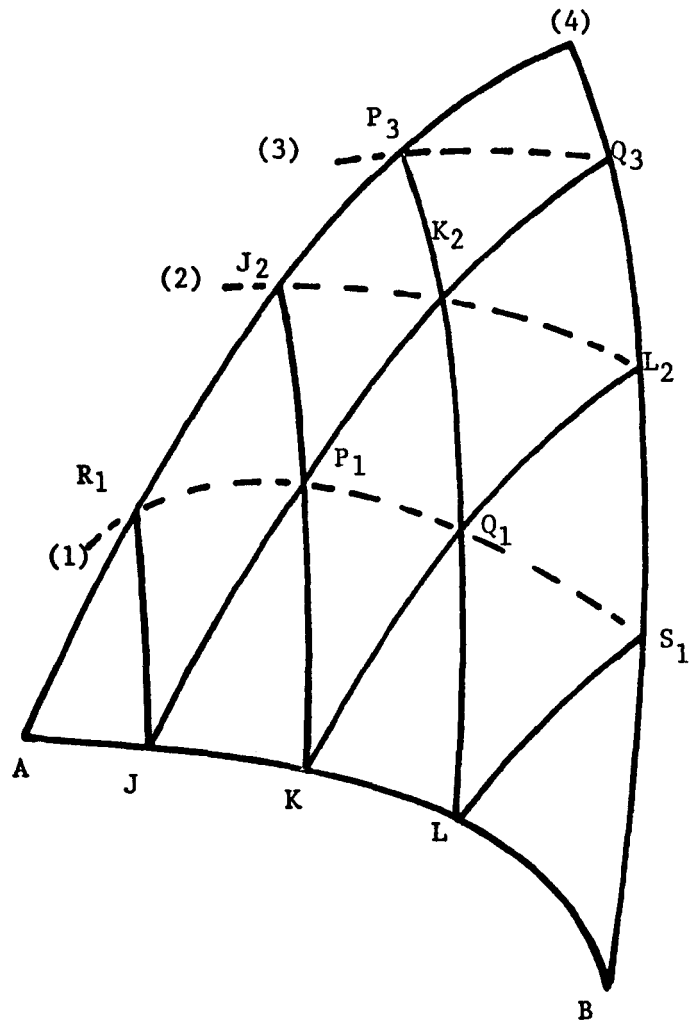

Fig. 6 General solution by the method of characteristics.

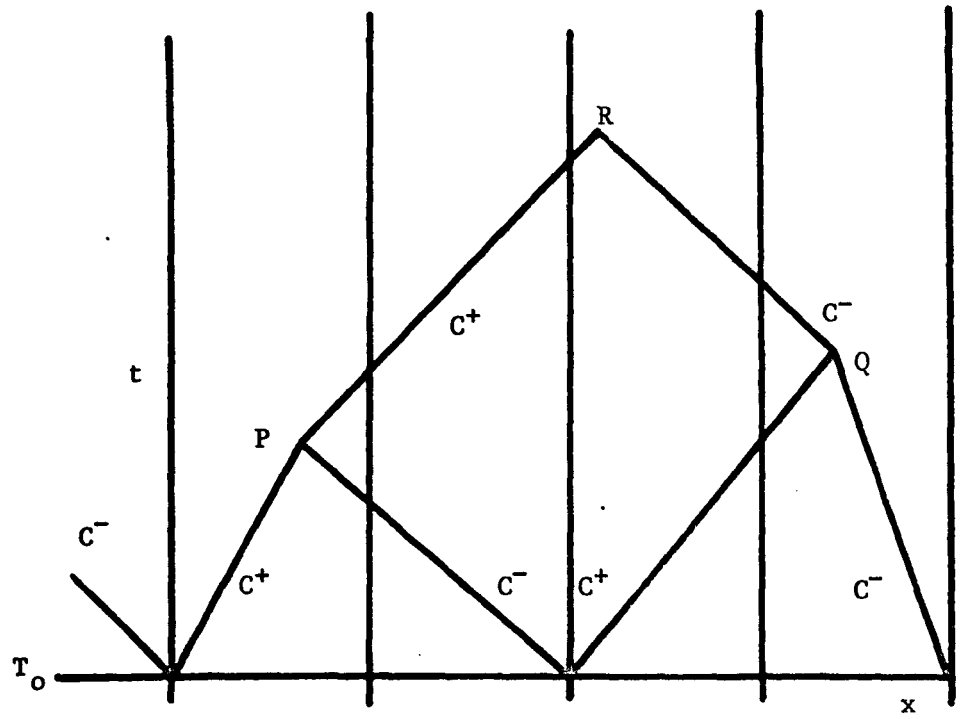

(a) Grid of characteristics.

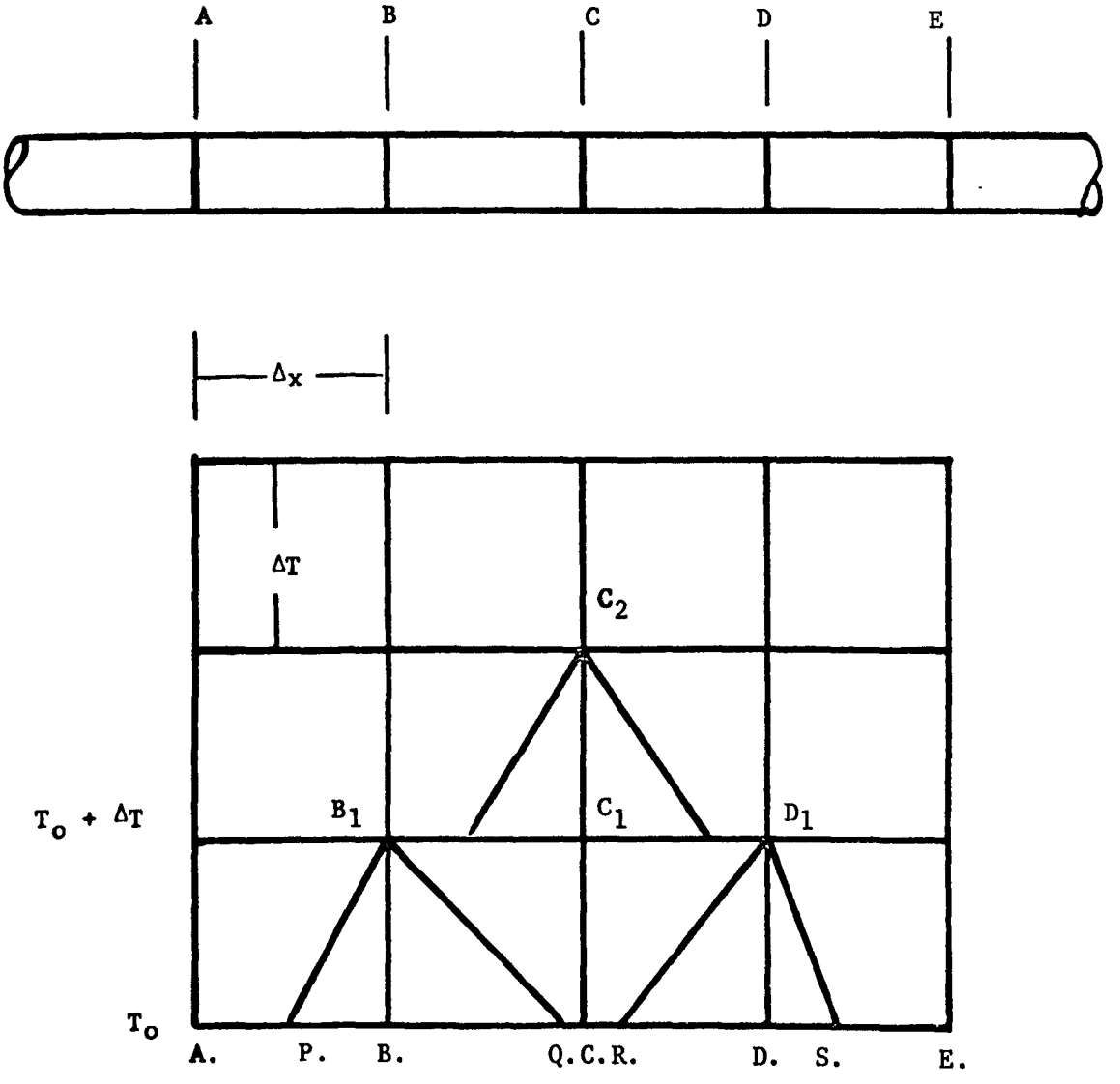

(b) Method of specified time intervals
$\Delta T \leq \Delta_x/(c + V)$

Fig. 7 Comparison between the grid of characteristics, which requires solution for x, t as well as P, V, and the method of specified time intervals.

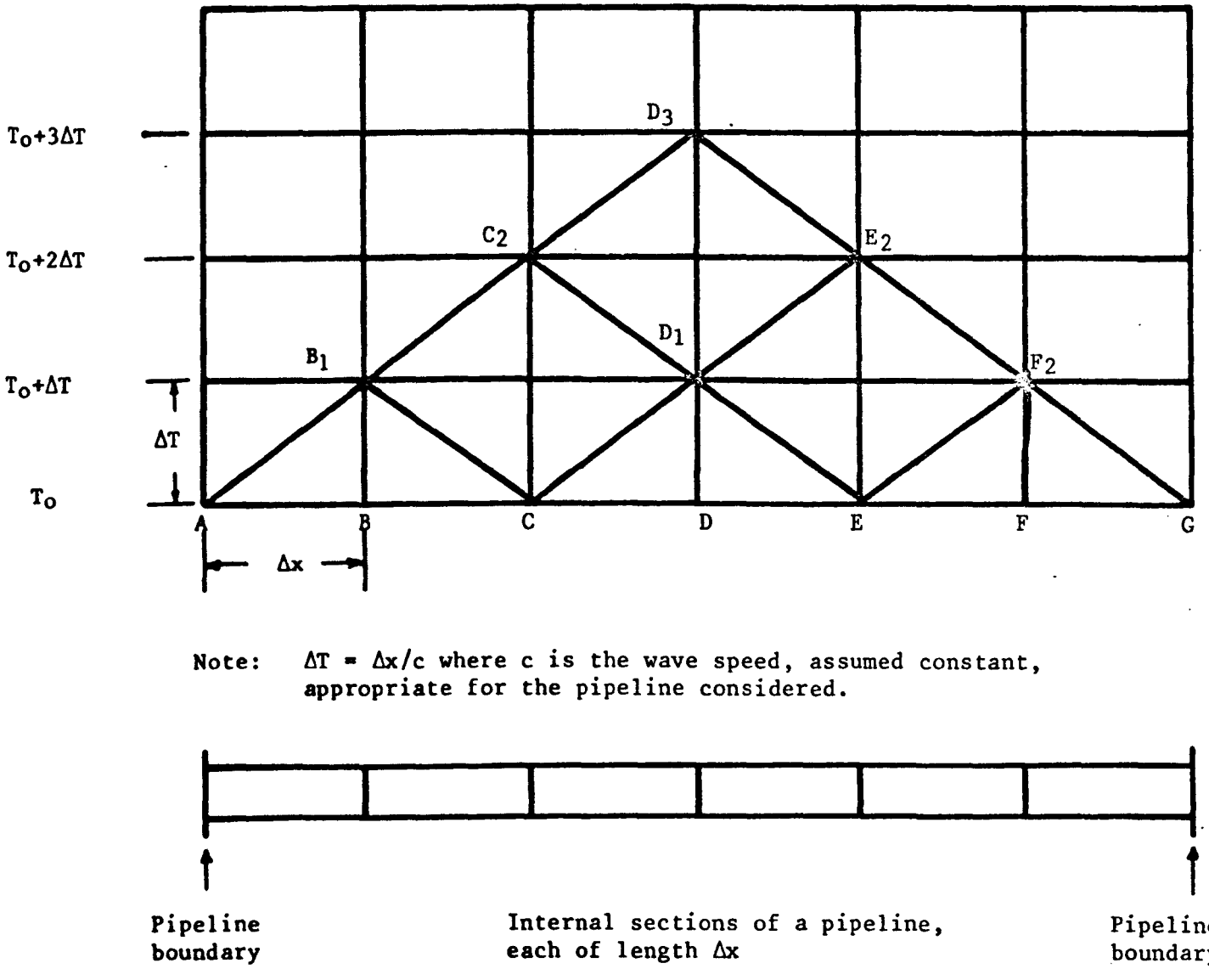

Note: $\Delta T = \Delta x/c$ where c is the wave speed, assumed constant, appropriate for the pipeline considered.

Fig. 8 Limit of solution in the (x,t) plane without reference to either of the pipeline boundary conditions.

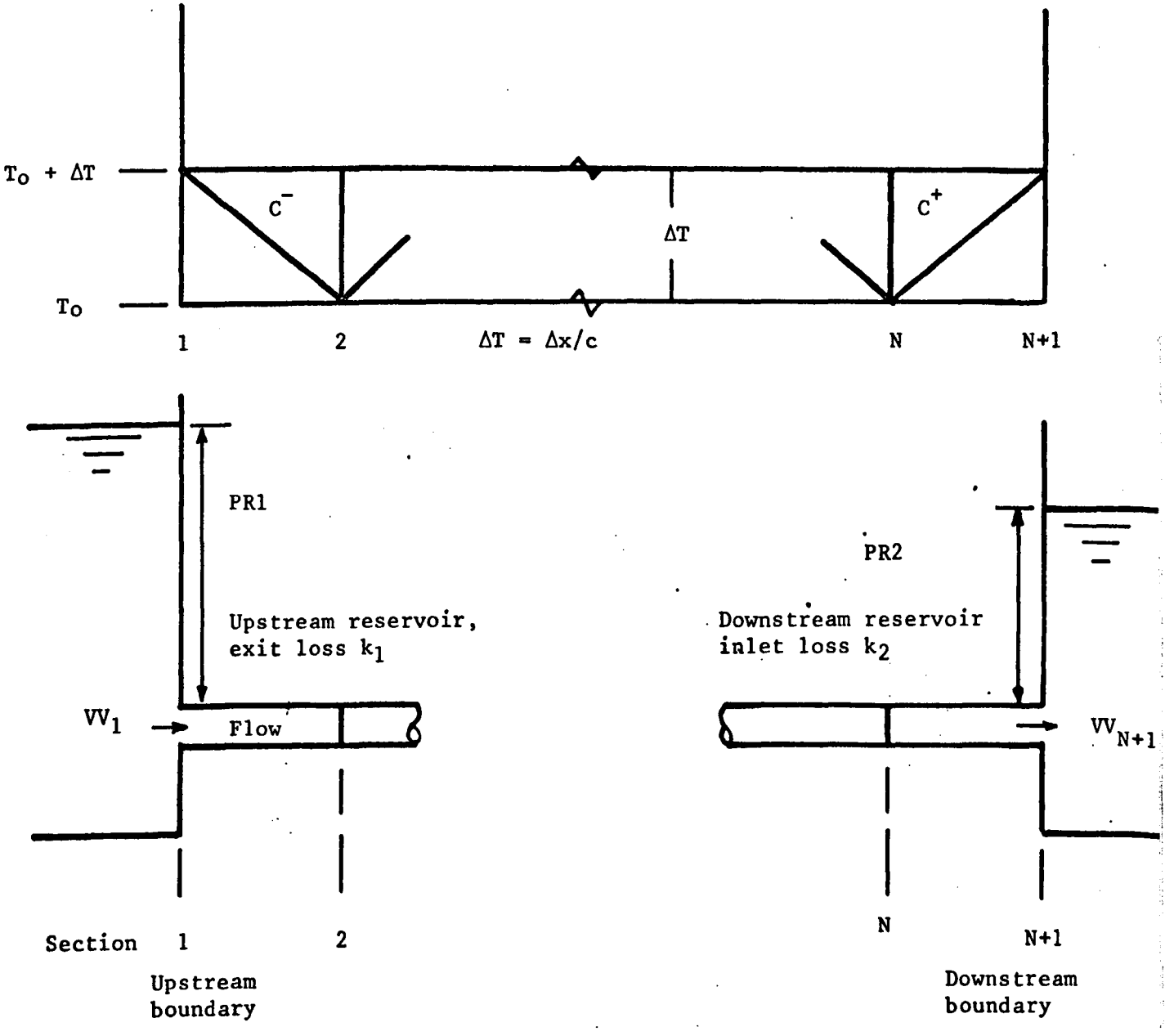

Fig. 10 Boundary conditions for a pipeline terminated at each end by a reservoir.

Upstream boundary, solve C^- characteristic with $PP_1 = PR1 - \frac{1}{2}\rho VV_1^2 k_1$

Downstream boundary, solve C^+ characteristic with $PP_{N+1} = PR2 + \frac{1}{2}\rho VV_{N+1}^2 k_2$

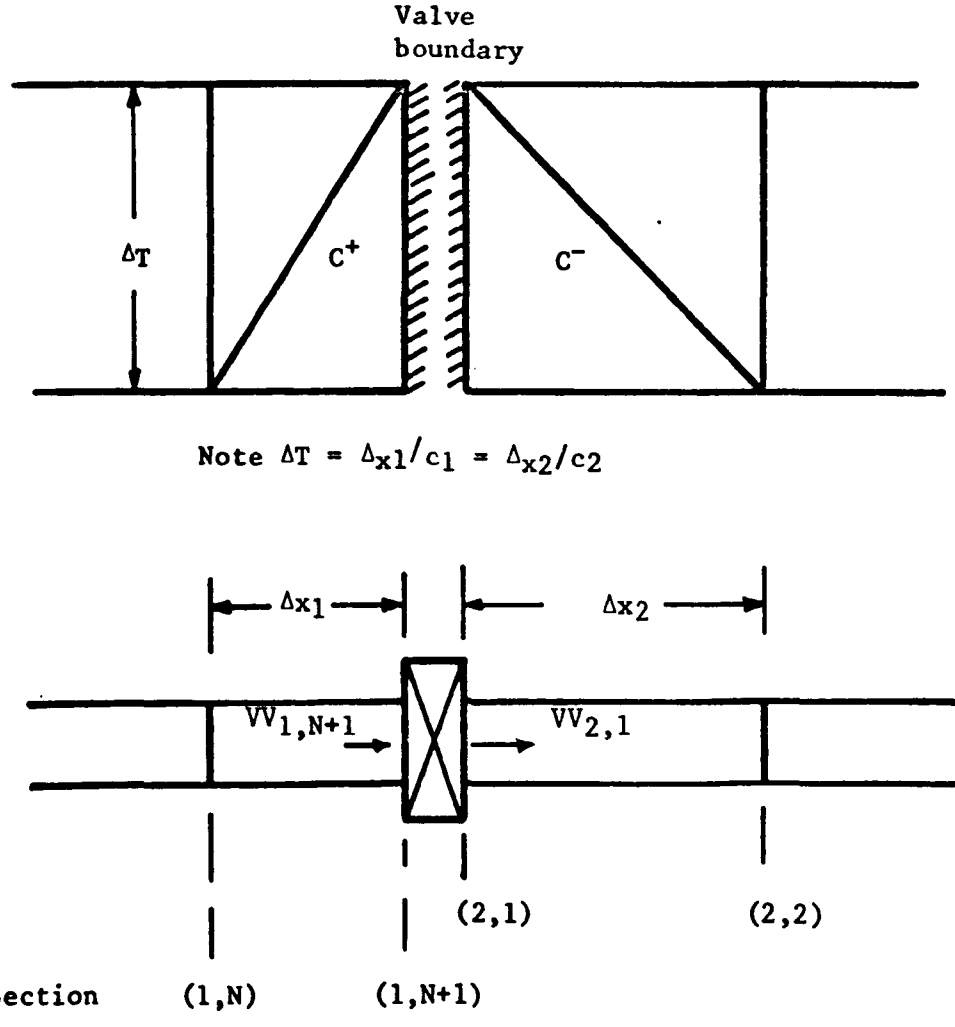

Fig. 11 Boundary conditions for a pipeline with an internal valve.

(a) Open valve, pressure above gas release level. Solve C^+ and C^- characteristics above with $A_1 VV_{1,N+1} = A_2\ VV_{2,1}$

$VV_{1,N+1} = \tau V_{o_1} \sqrt{(PP_{1,N+1} - PP_{2,1})/\Delta P_o}$

(b) Closed valve boundary, no separation on either side,

$VV_{1,N+1} = VV_{2,1} = 0$

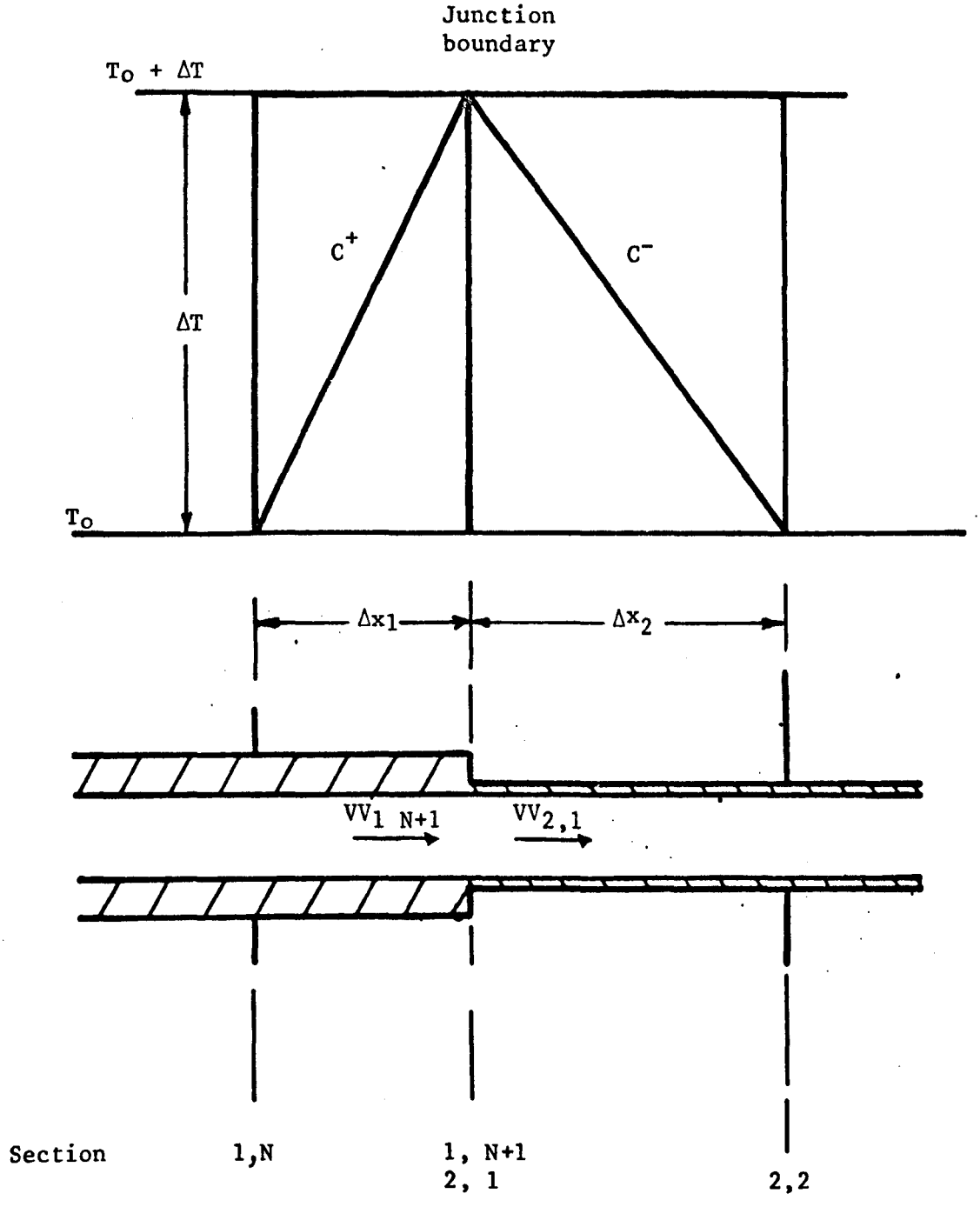

Fig. 12 Boundary conditions at an internal junction of two pipelines.

Solve C^+, C^- characteristics with the pressure and flow continuity equations.

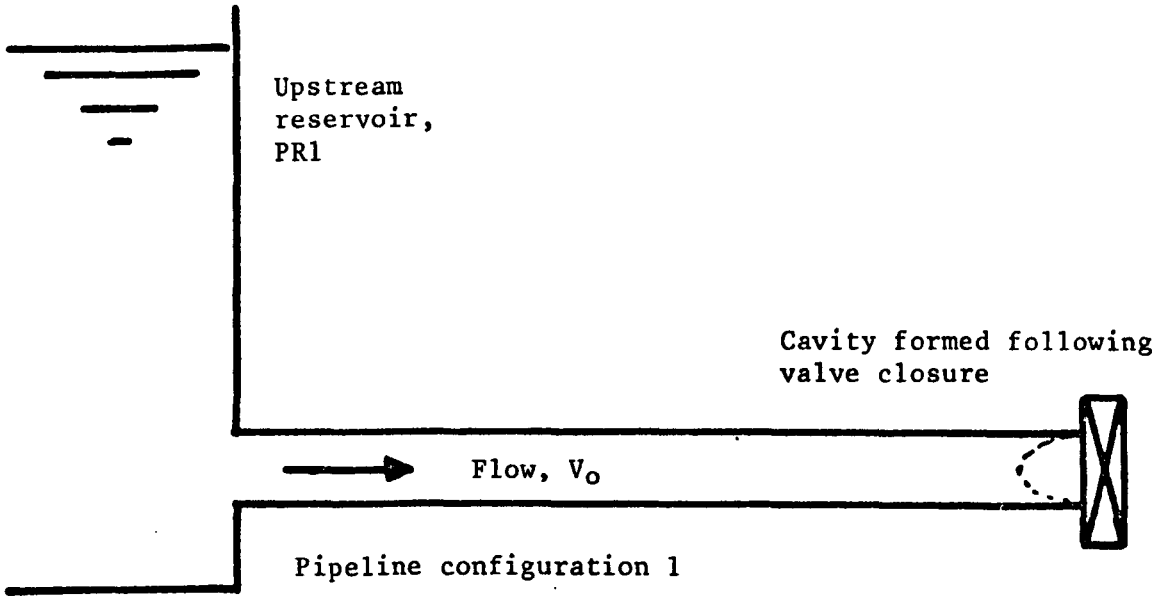

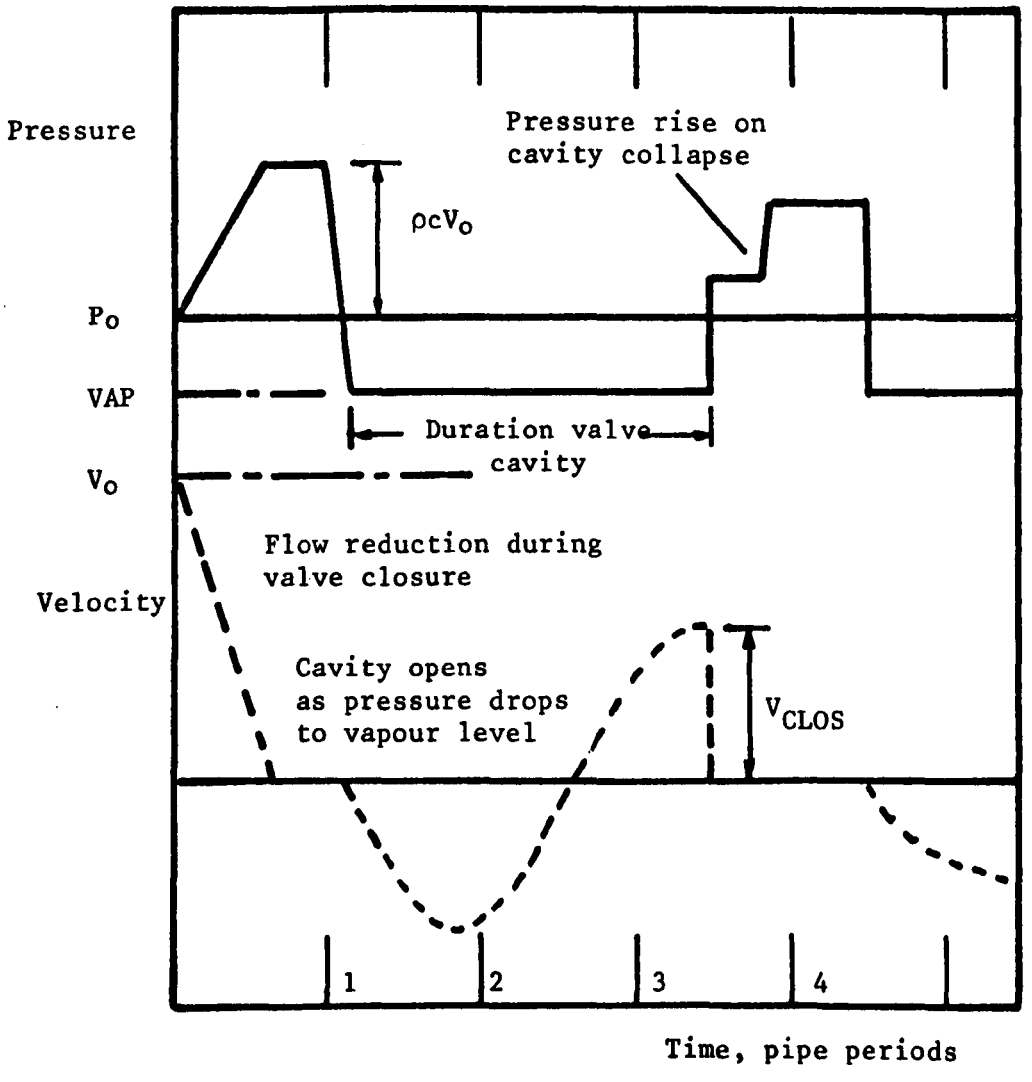

Fig. 13 Column separation on the upstream side of a valve following a rapid closure.

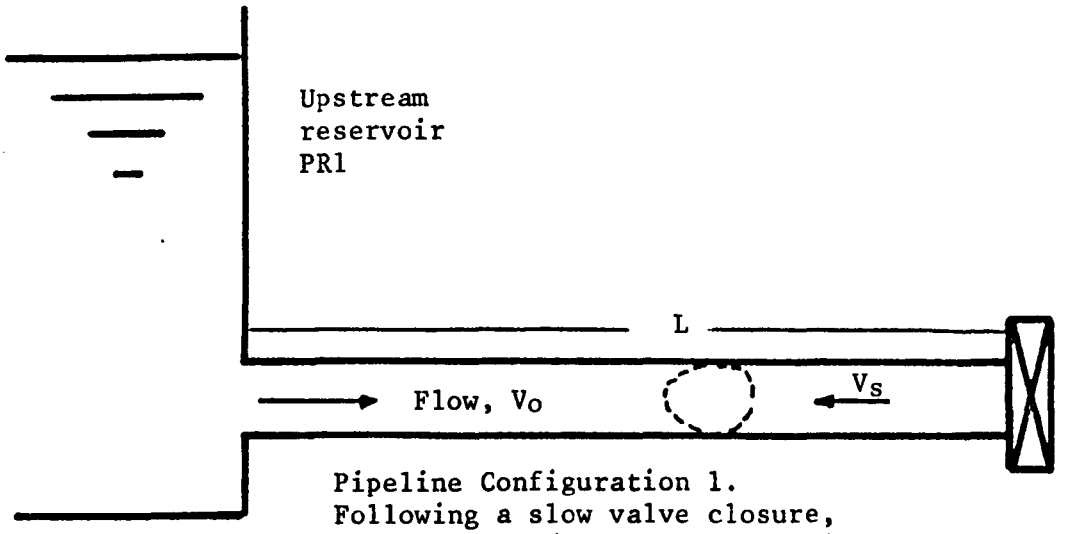

Pipeline Configuration 1.
Following a slow valve closure, i.e. TC >> 2L/c, the first cavity may be formed at an internal pipe section. The flow between the cavity and the valve is then represented by V_s.

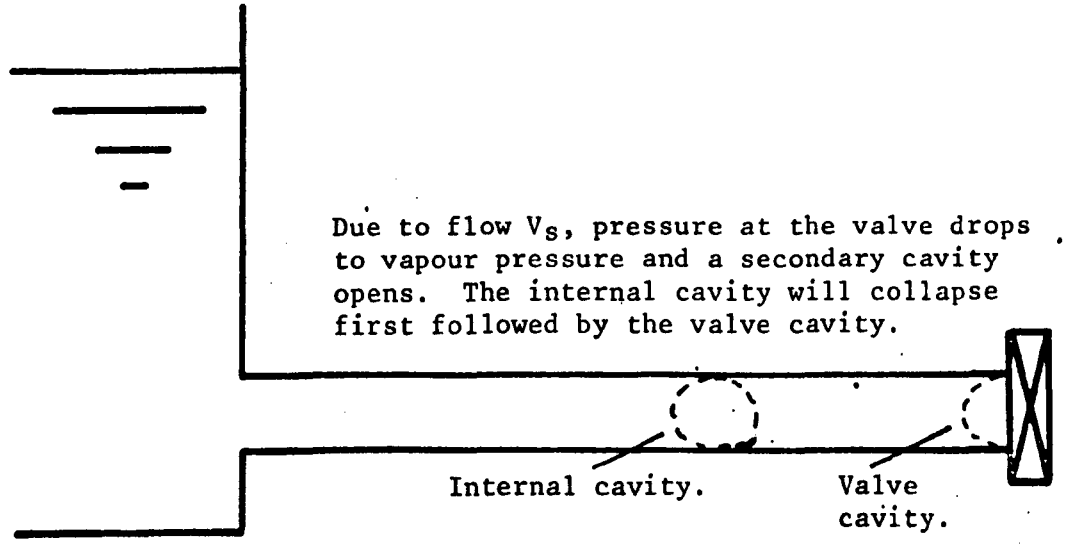

Due to flow V_s, pressure at the valve drops to vapour pressure and a secondary cavity opens. The internal cavity will collapse first followed by the valve cavity.

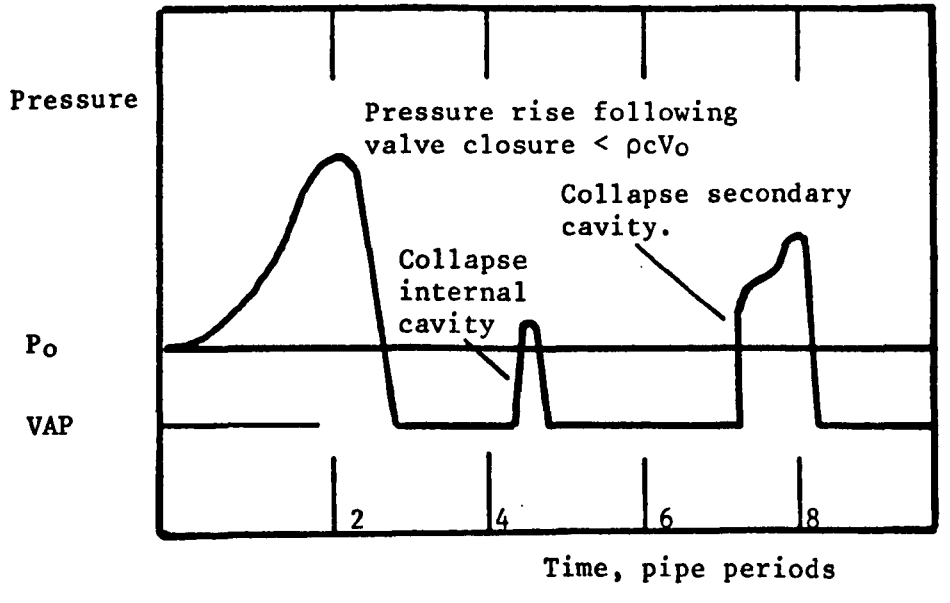

Fig. 14 Column separation upstream of a valve following a slow valve closure.

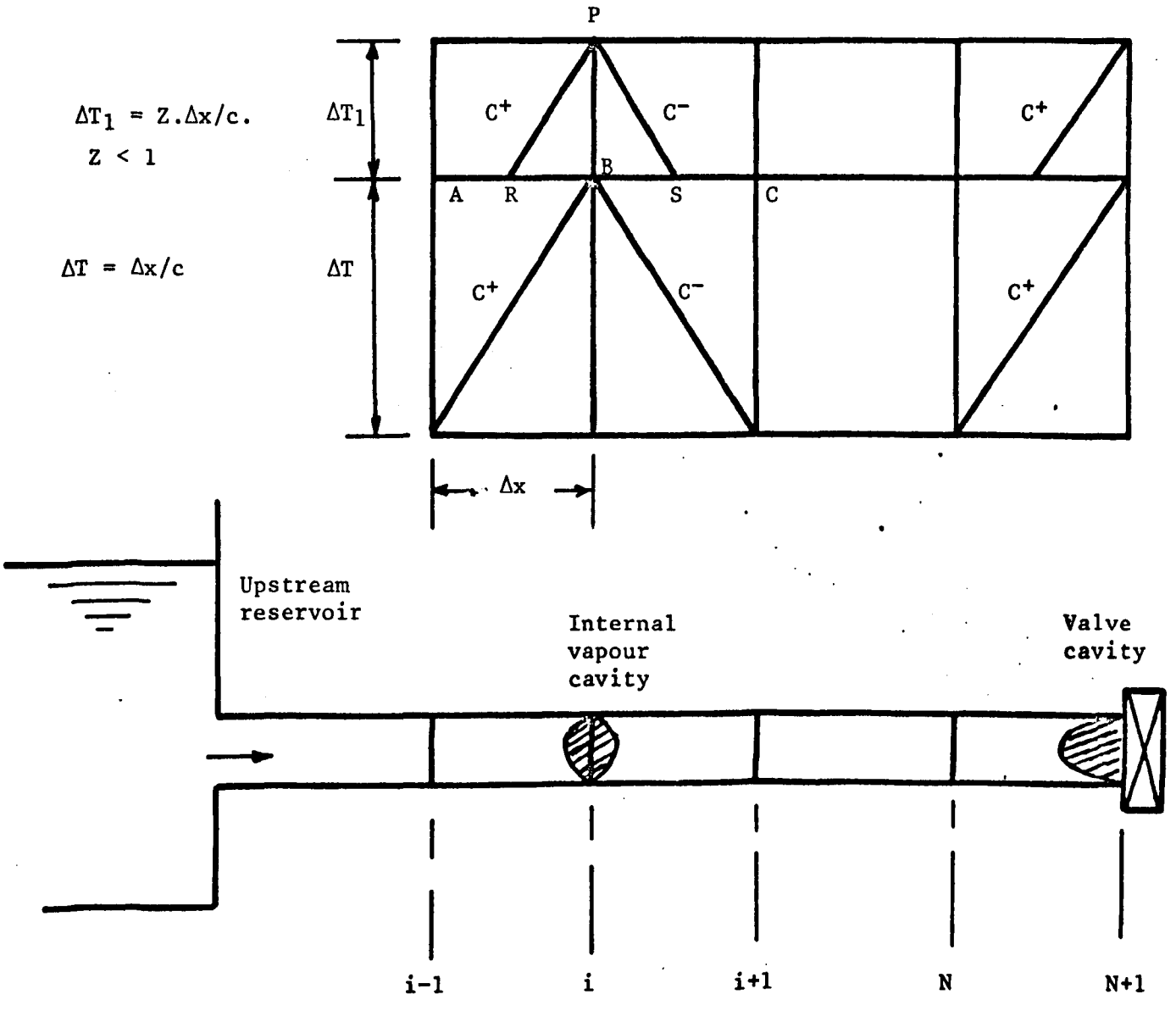

Fig. 15 Boundary conditions in the event of column separation upstream of the valve.

Open cavity boundary, PP_i, PP_{N+1} = VAP

Closed cavity at valve, $VV_{N+1} = 0$

Closed internal cavity, solution reverts to C^+, C^- characteristics normal for an internal pipe section.

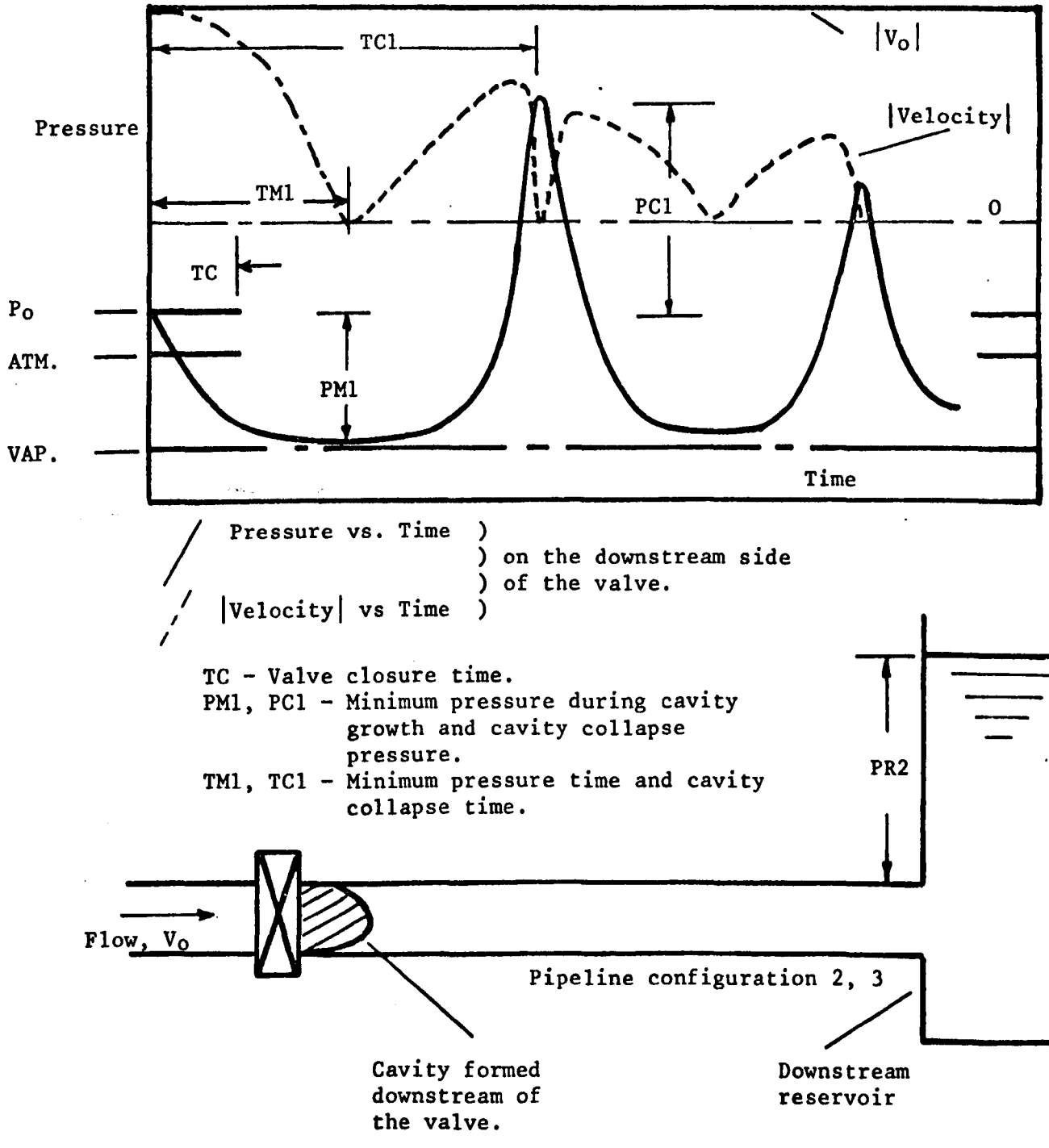

Fig. 16 Column separation on the downstream side of a closing valve.

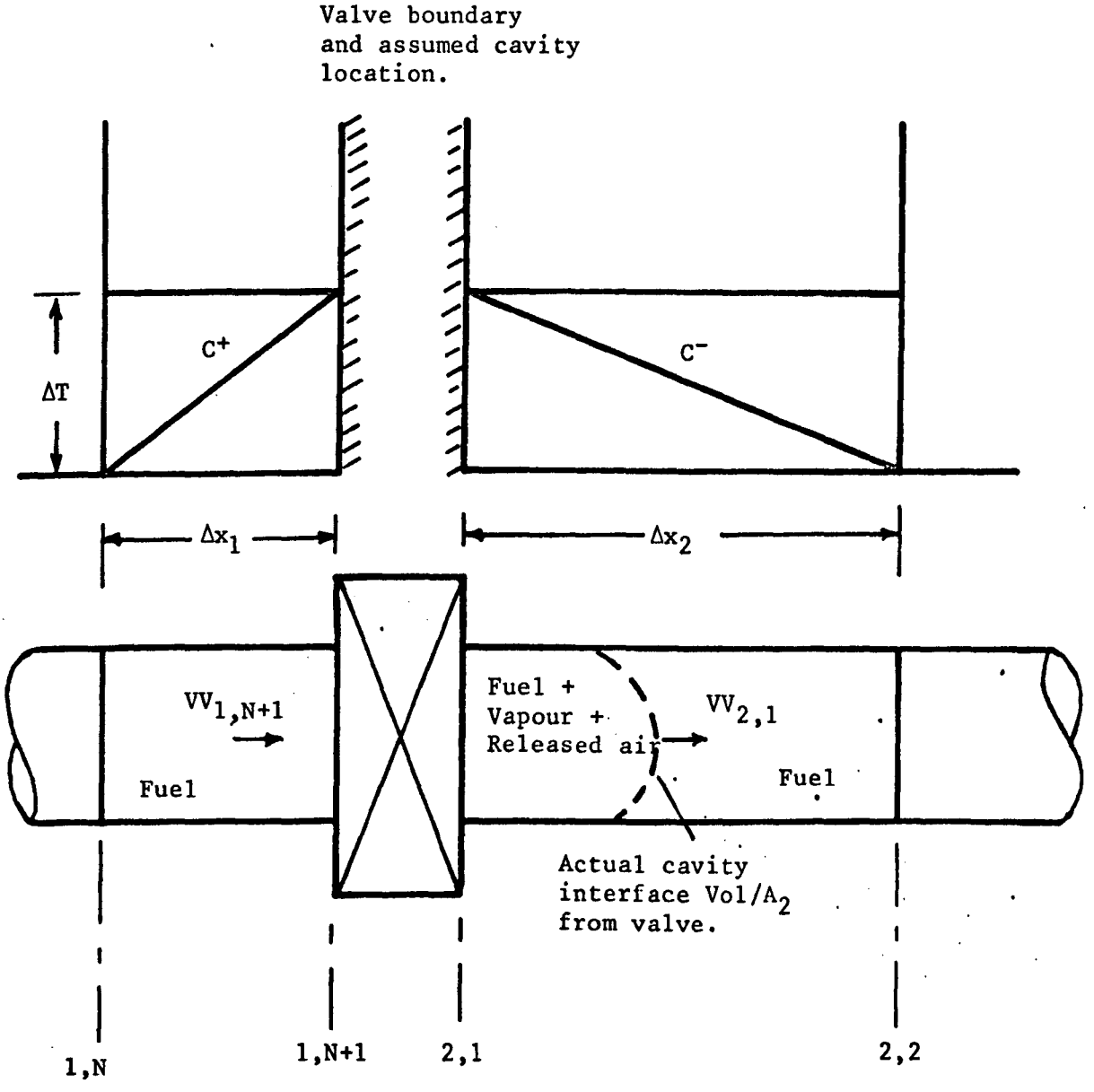

Fig. 17 Separation downstream of a closing valve.

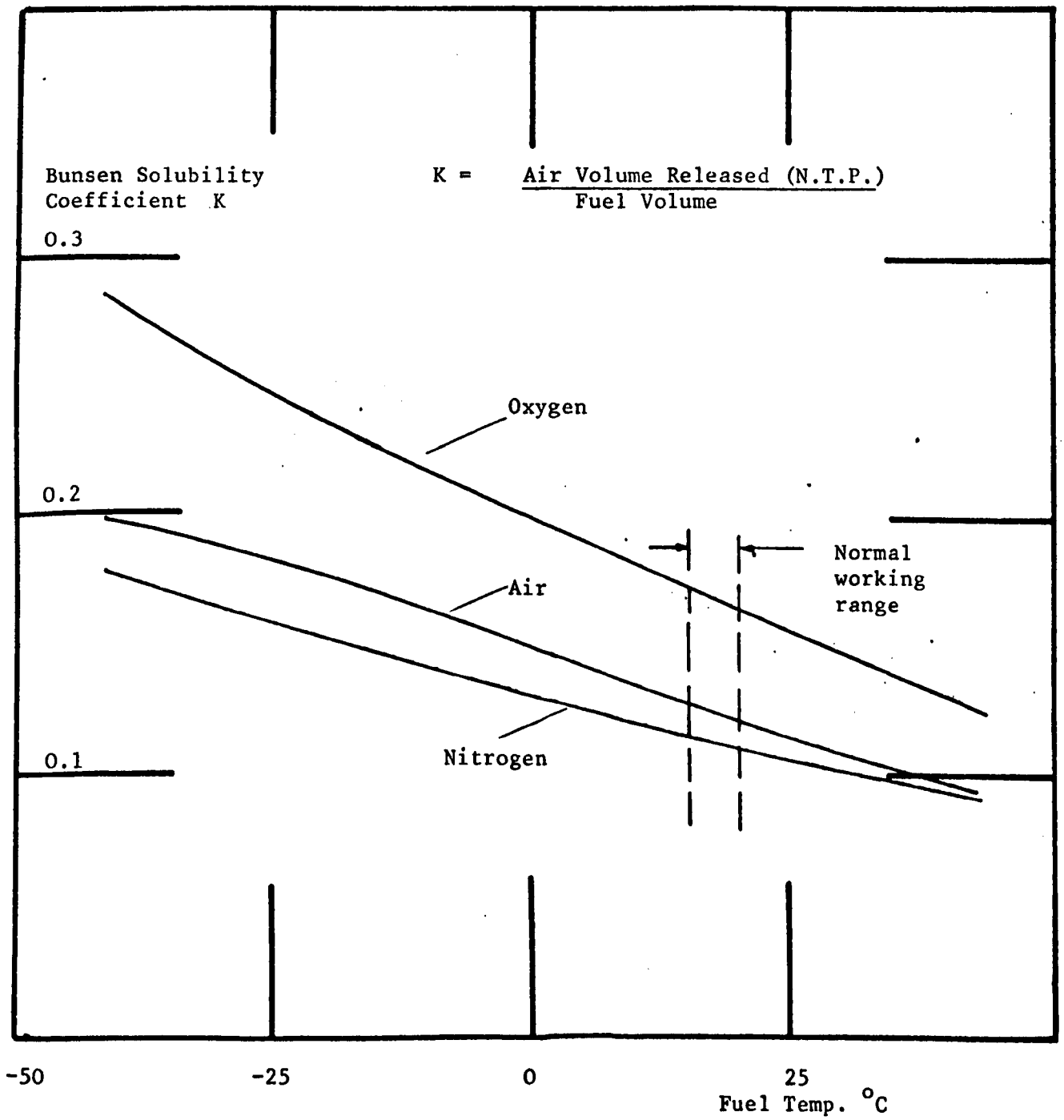

Fig. 18 Air solubility in Aviation Kerosene (Spec. 2494) (B.A.C. data)

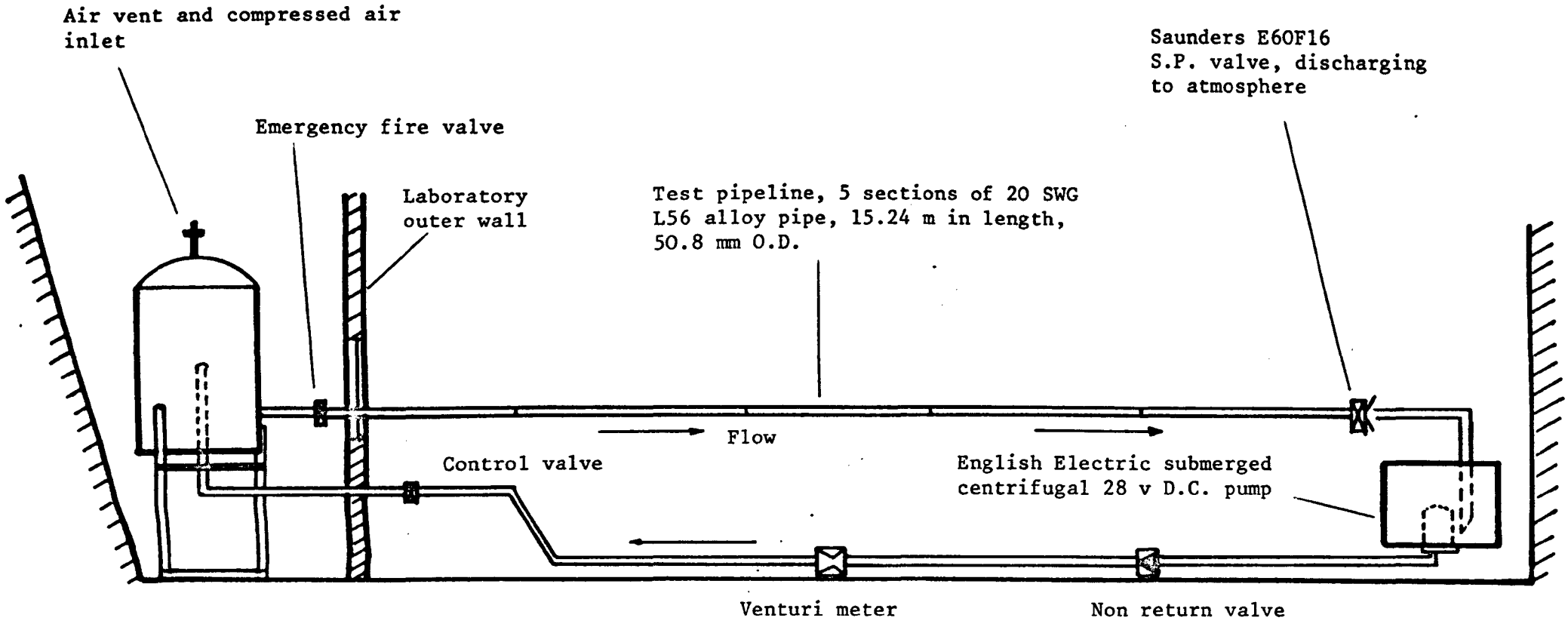

Fig. 19 Layout of test rig, pipeline configuration 1.

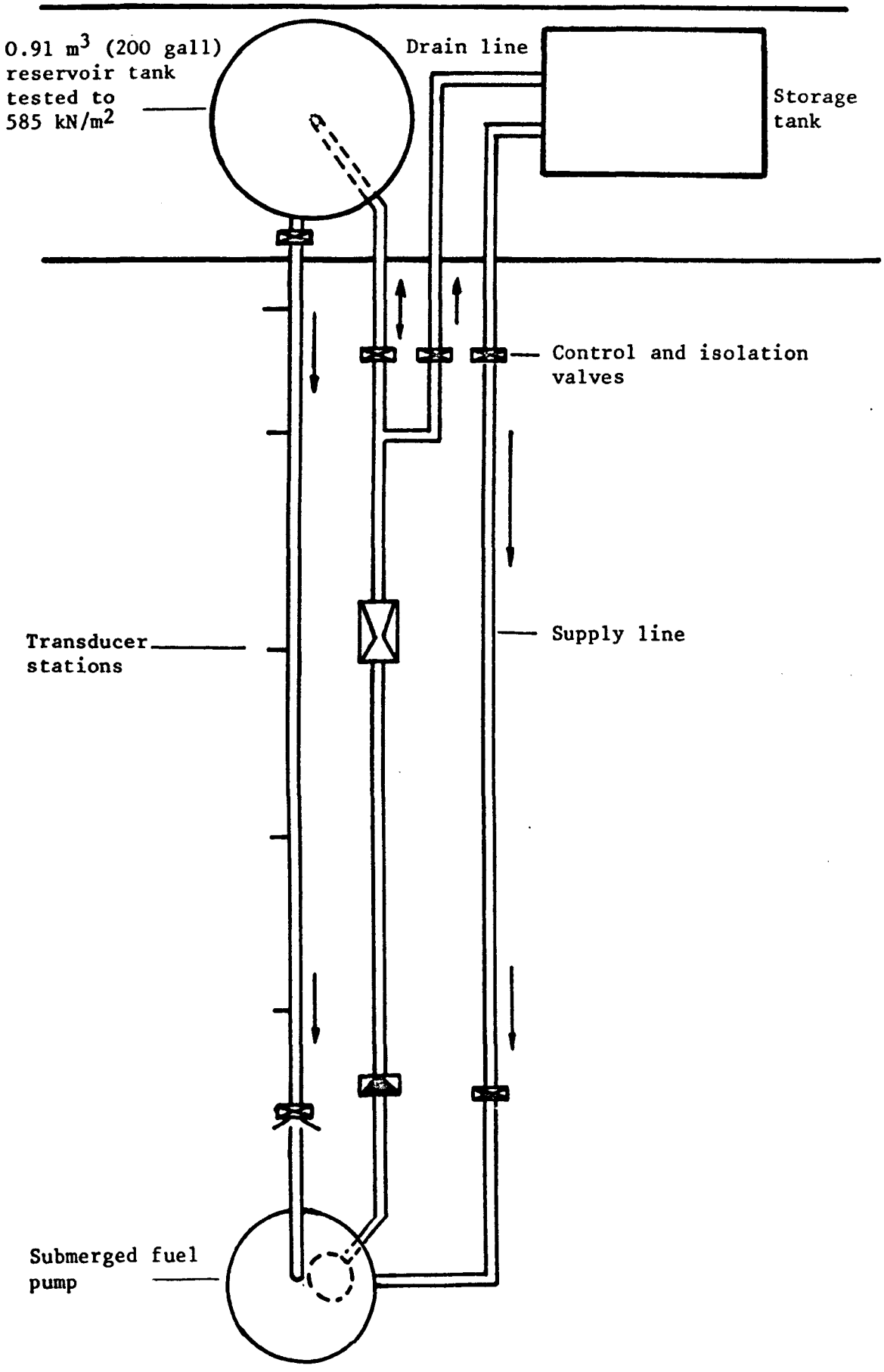

Fig. 20 Plan view of pipeline configuration 1 illustrating drain and supply lines and storage tank.

Fig. 21 Valve end of pipeline configuration 1, illustrating the independently mounted valve closing ram and the submerged fuel pump.

Fig. 22 View upstream from the valve in pipeline configuration 1, illustrating the pipe support brackets.

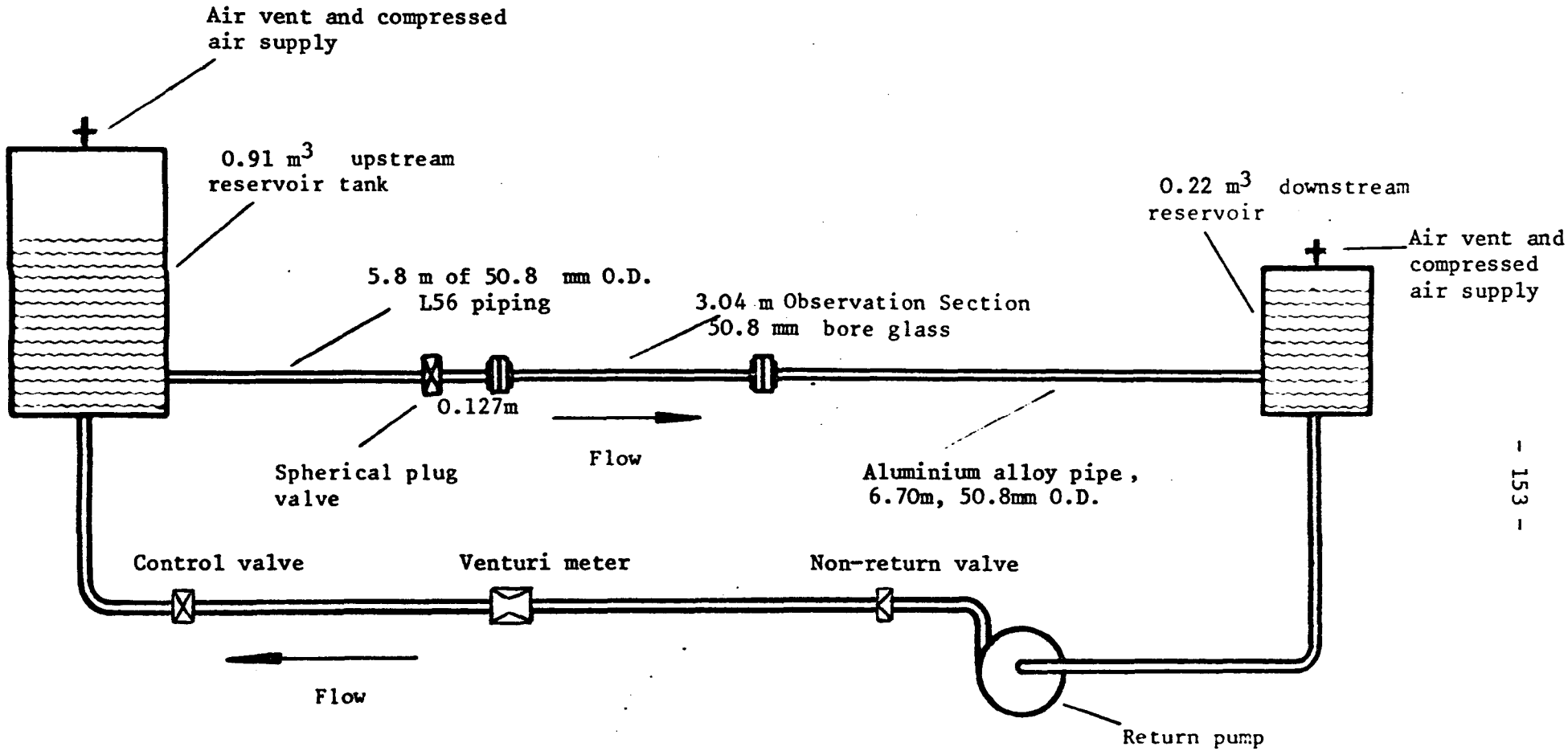

Fig. 23 Layout of test pipeline configuration 2G, illustrating the position of the glass observation section. Pipeline configuration 2 is as above but with the glass replaced by a standard L56 section of the same length.

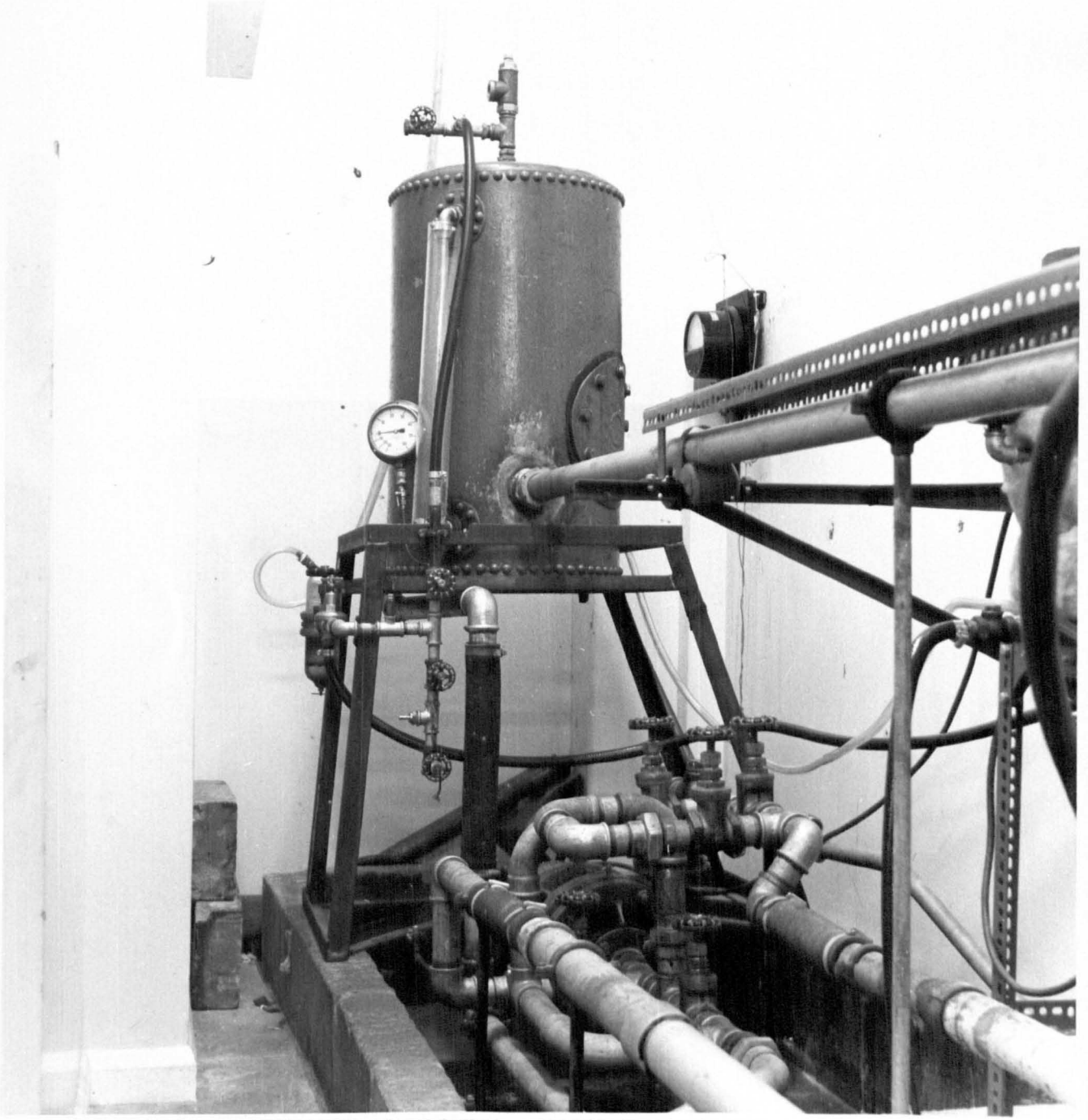

Fig. 24 Downstream reservoir, pipeline configuration 2, illustrating the compressed air supply and the pump bypass piping.

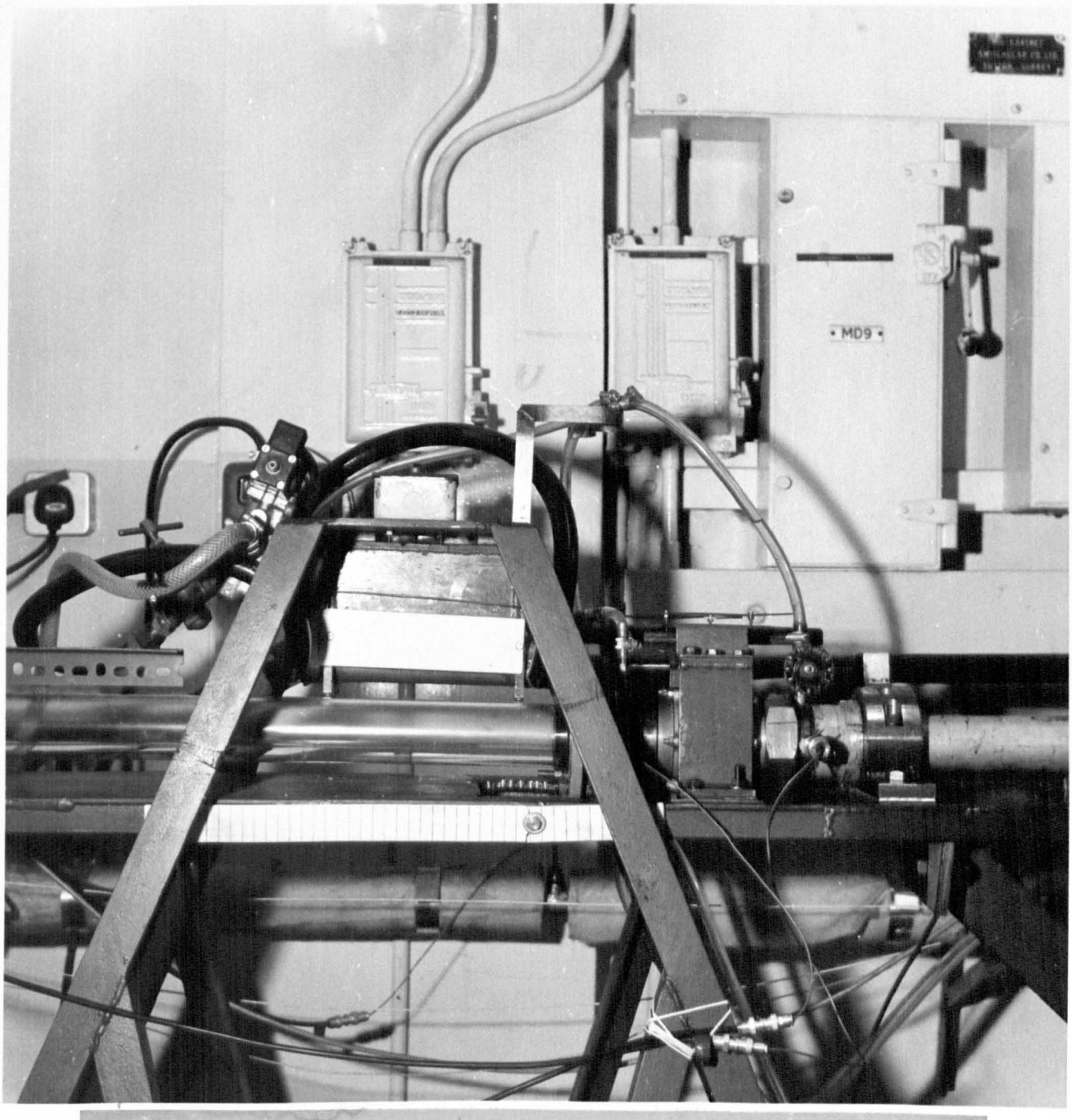

Fig. 25 Valve mounting, pipeline configuration 2, illustrating the glass pipe and the independently mounted valve closing ram.

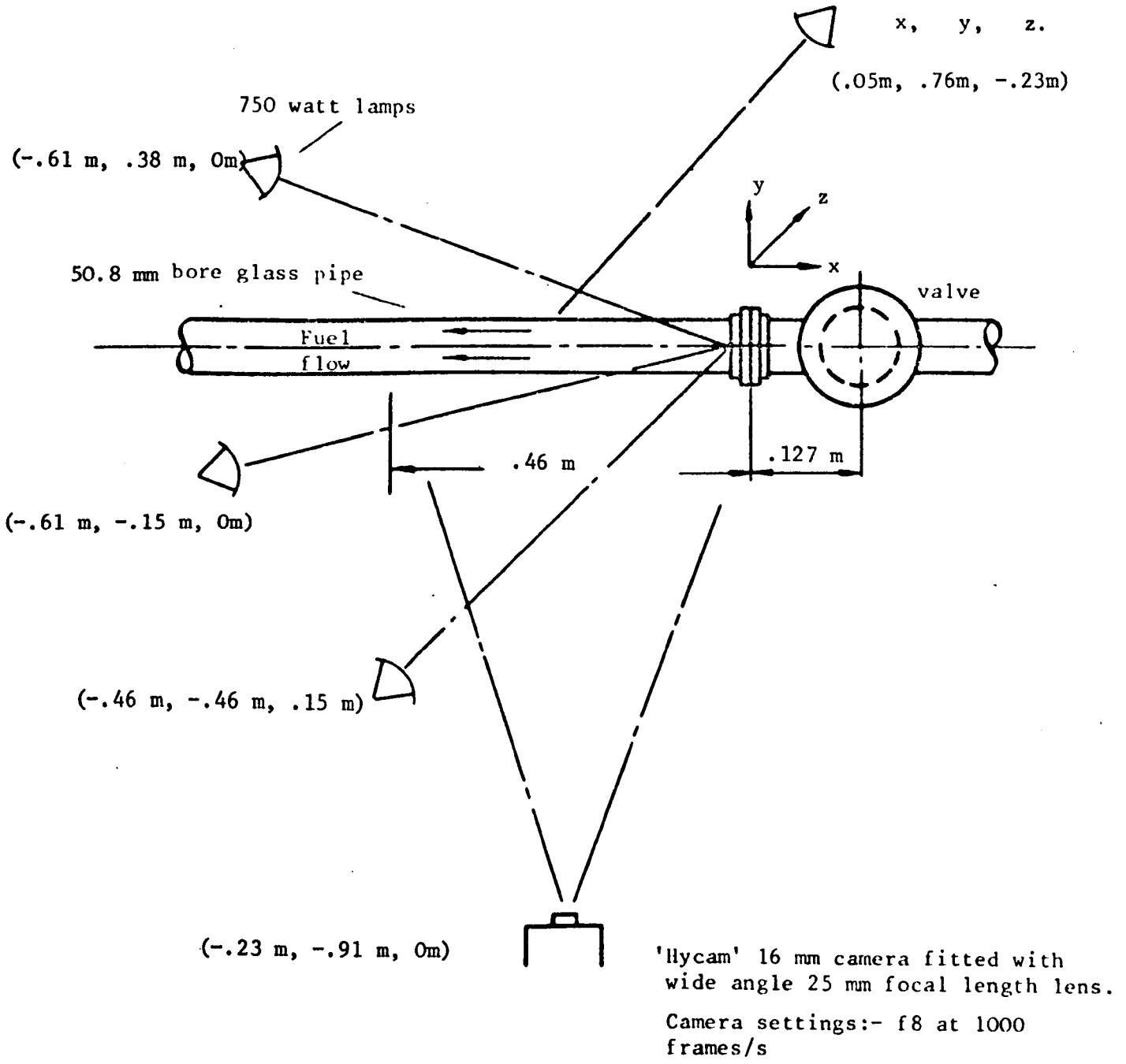

Fig. 26 Arrangement of camera and lights - plan view.

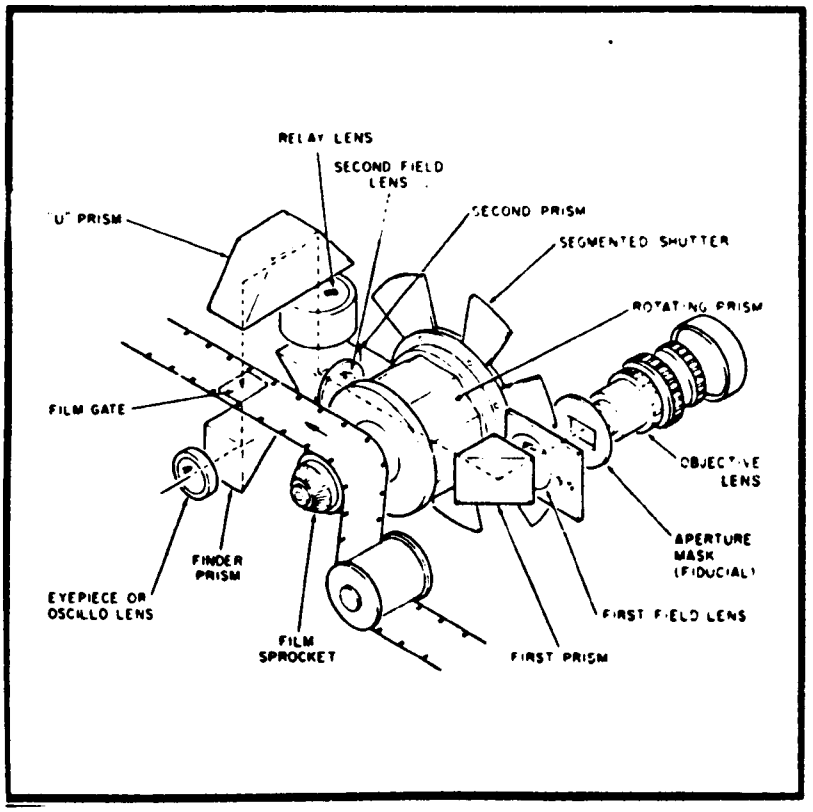

Fig. 27 Schematic layout of the Hycam optical system.

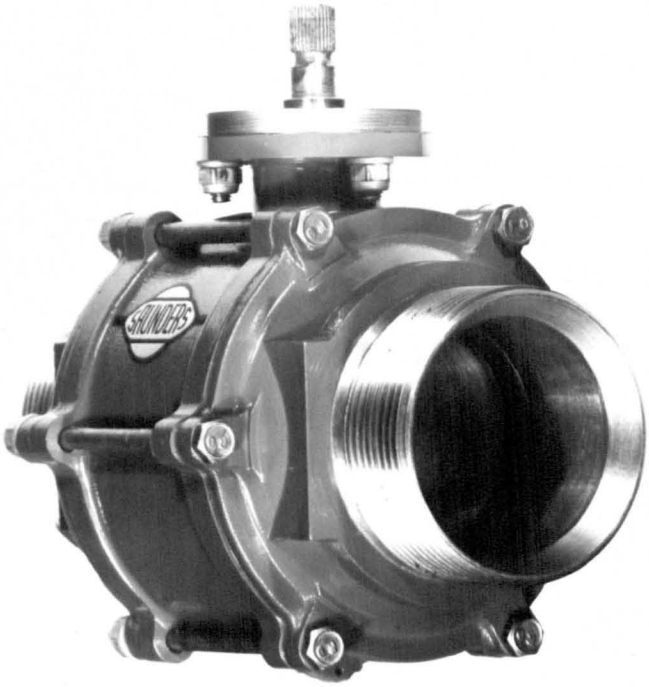

Fig. 28 Saunders Aircraft Fuel Valve, Type E60F16, a spherical plug valve used for all the tests reported.

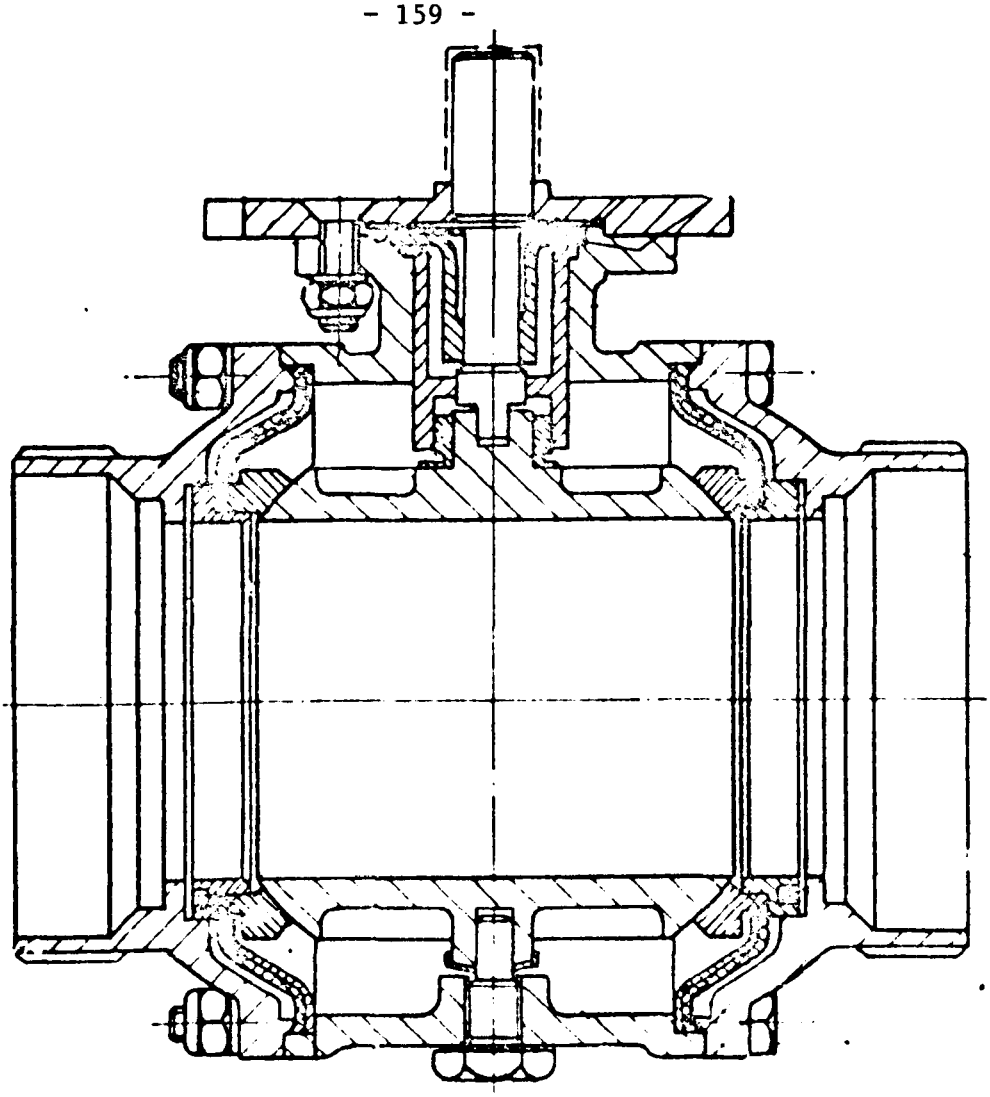

Scale: Full Size

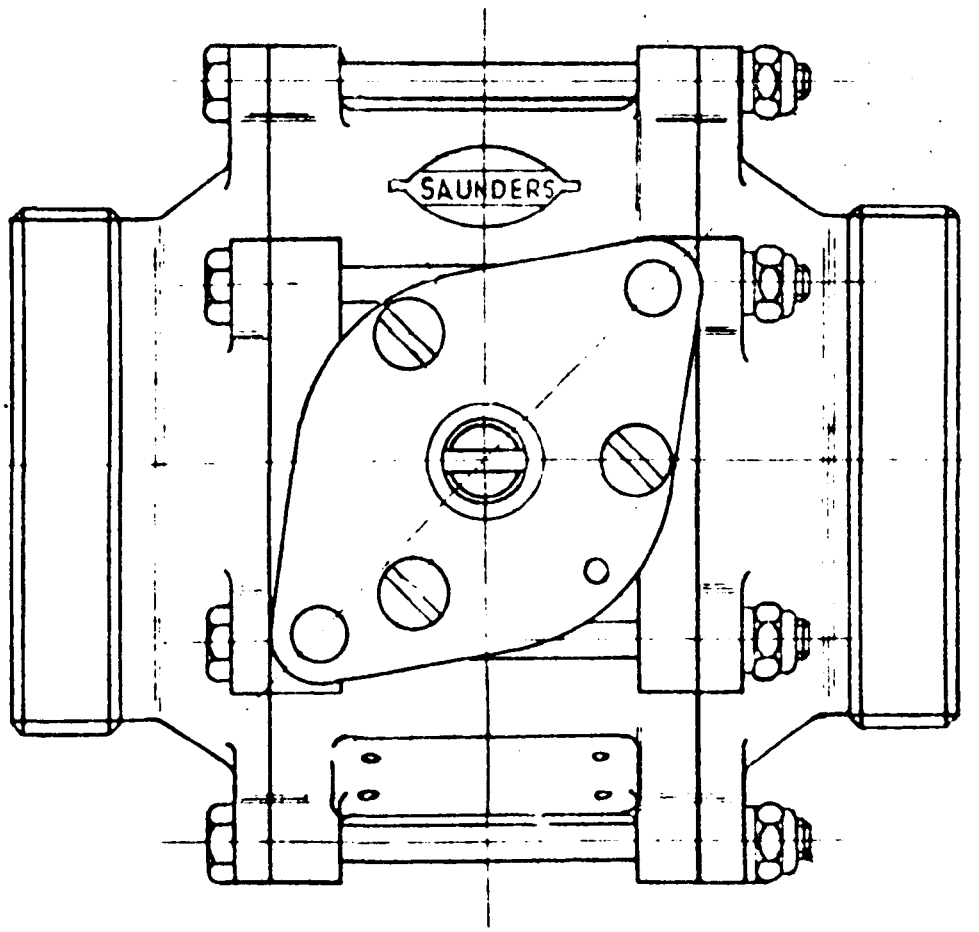

Fig. 29 Side view section and plan view of Saunders E60F16 spherical plug valve used for all the tests reported.

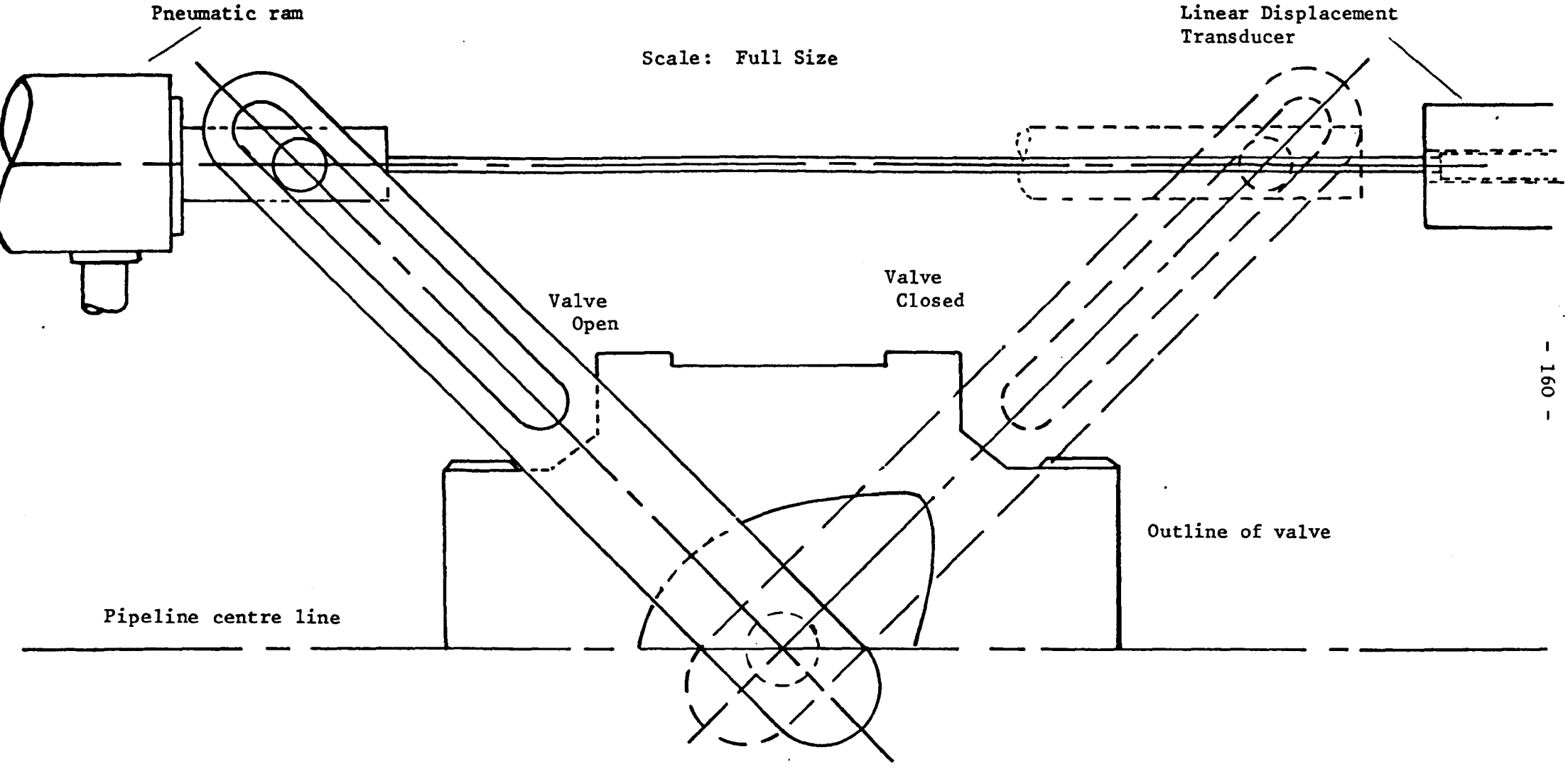

Fig. 30 Plan view of valve closure mechanism.

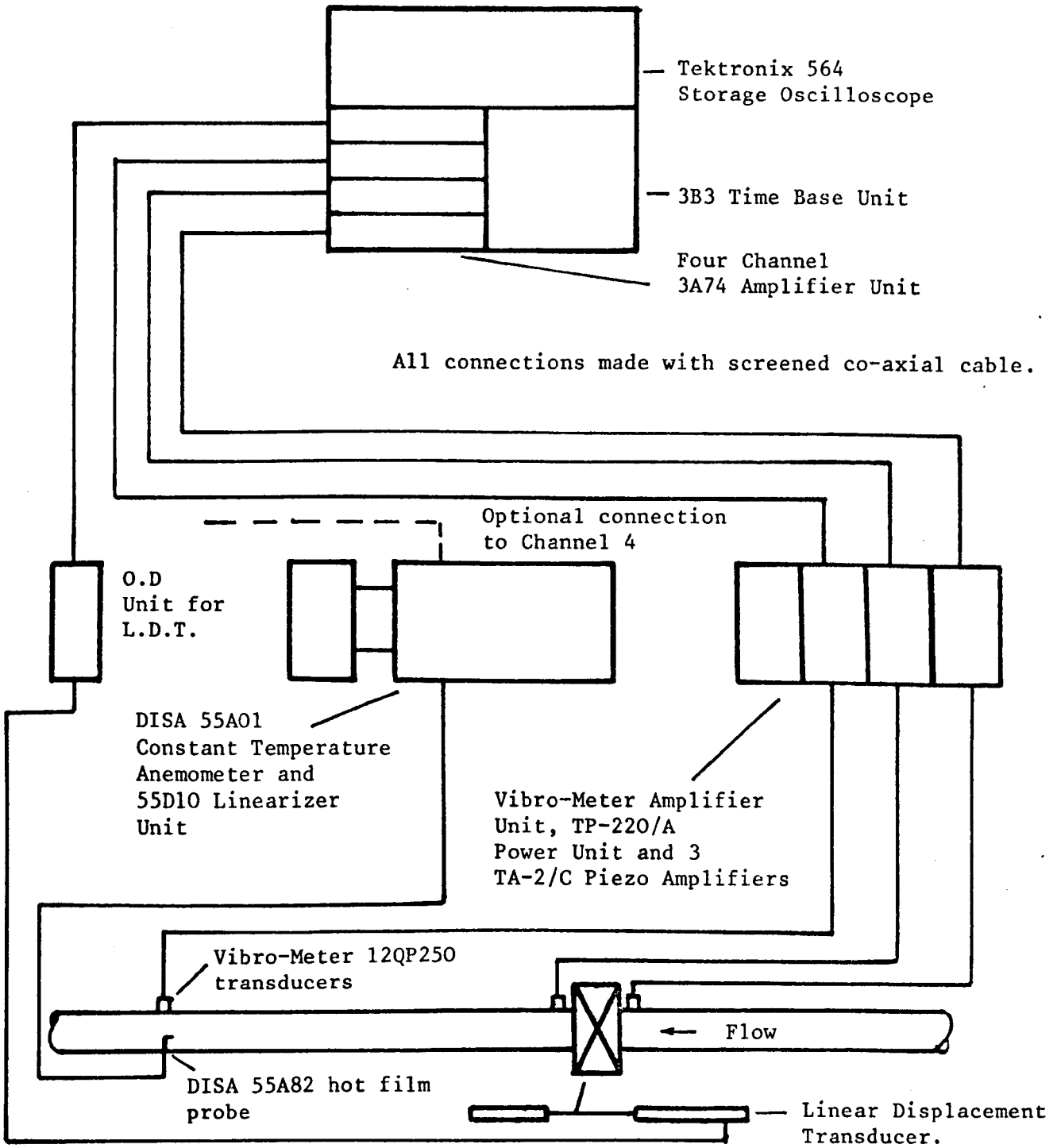

Fig. 31 Typical instrumentation layout on pipeline configuration 2.

Fig. 32 Vibro-meter 12QP250 and Kistler 701A quartz crystal pressure transducers.

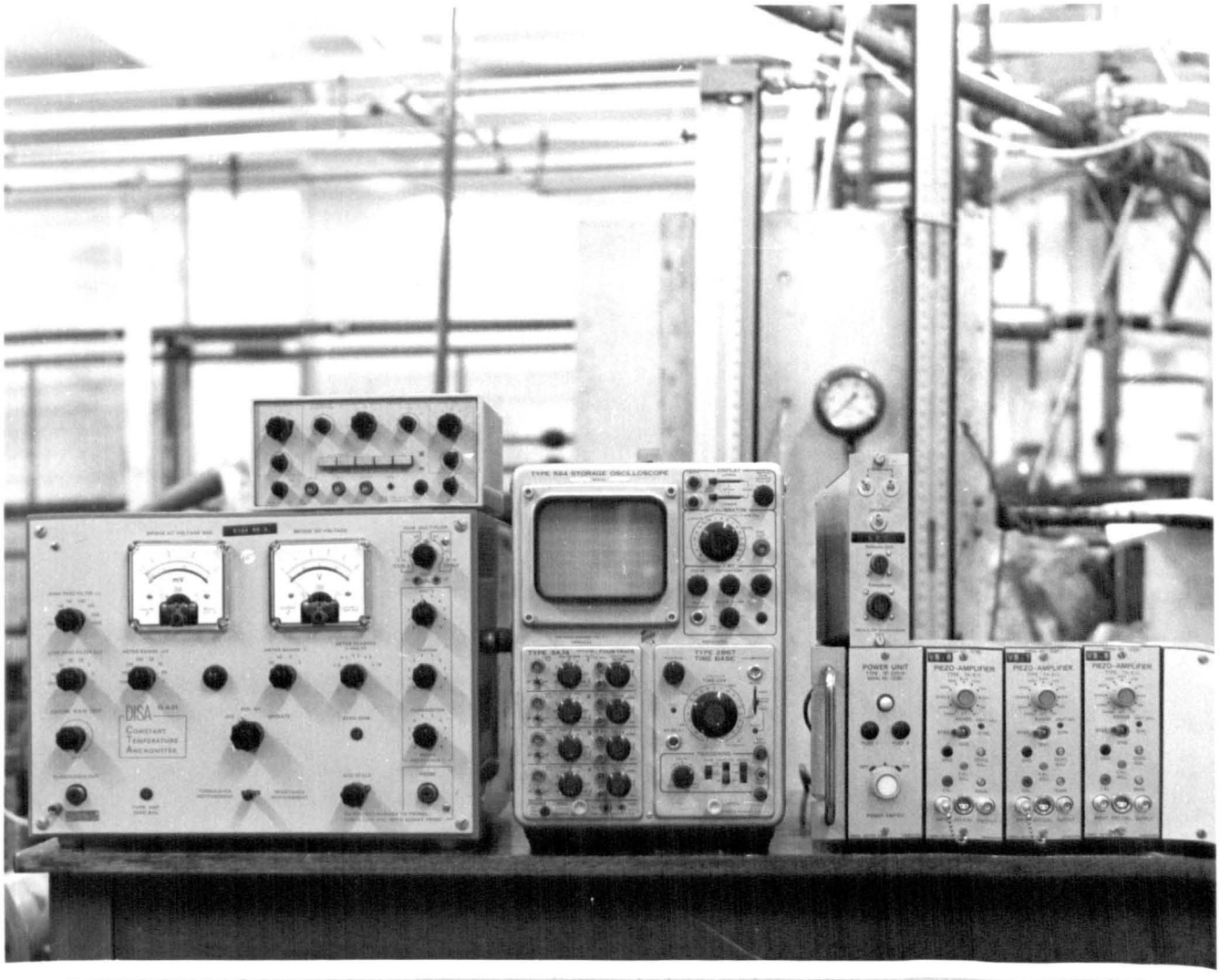

Fig. 33 General view of the instrumentation employed, left to right: DISA 55A01 C.T.A. and 55D10 Linearizer, Tektronix 564 oscilloscope, Vibrometer TA-2/C piezo amplifiers and the Honeywell O.D. unit.

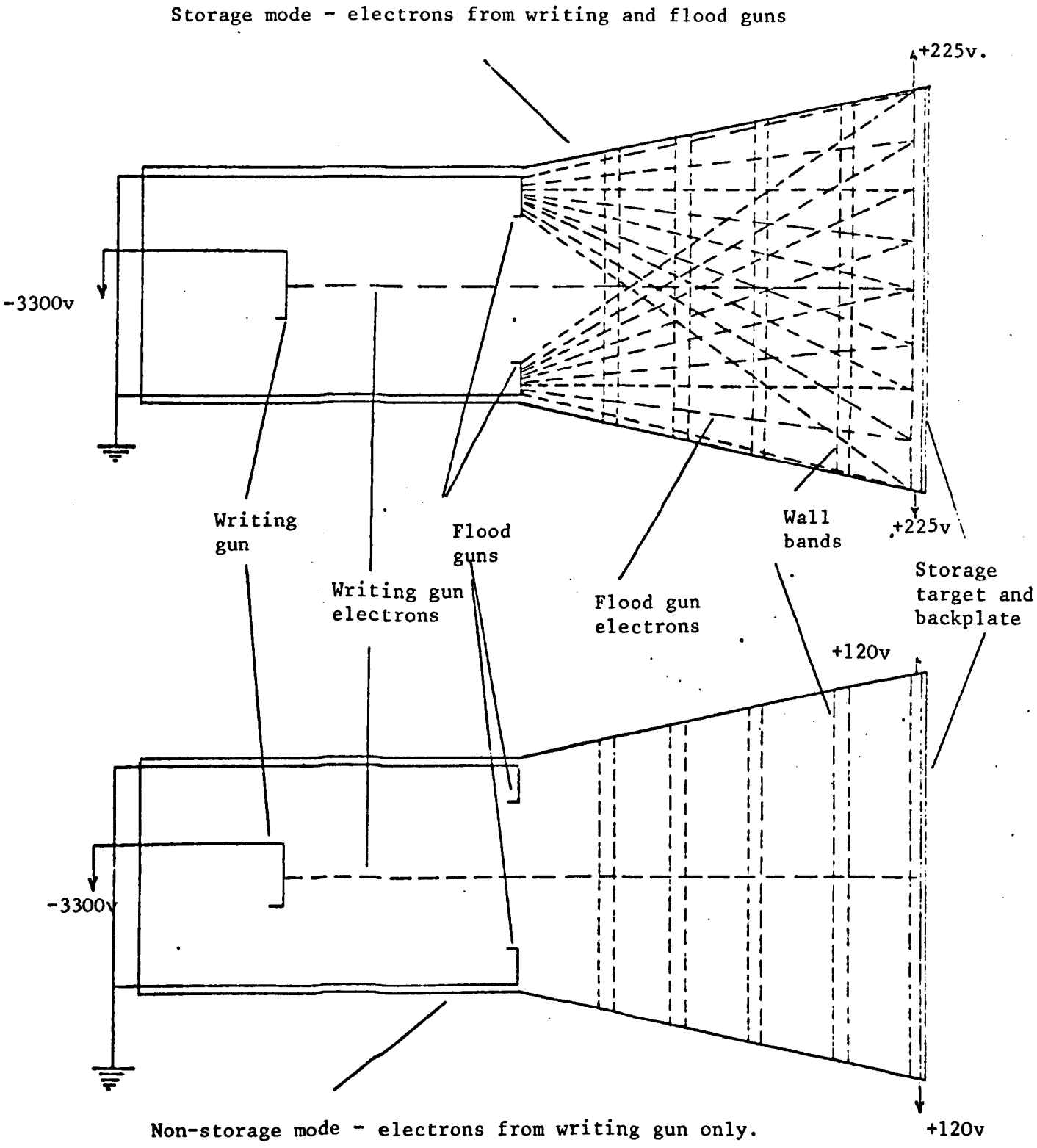

Fig. 34 Schematic view of the Tektronix 564 storage system.

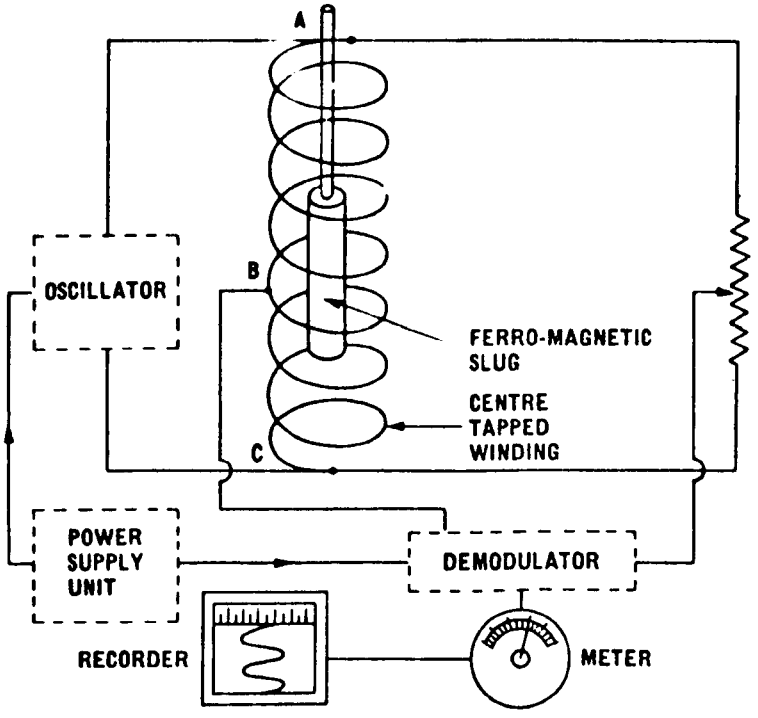

Fig. 35 Typical arrangement of Honeywell Linear Displacement Transducer, O.D. unit and recorders.

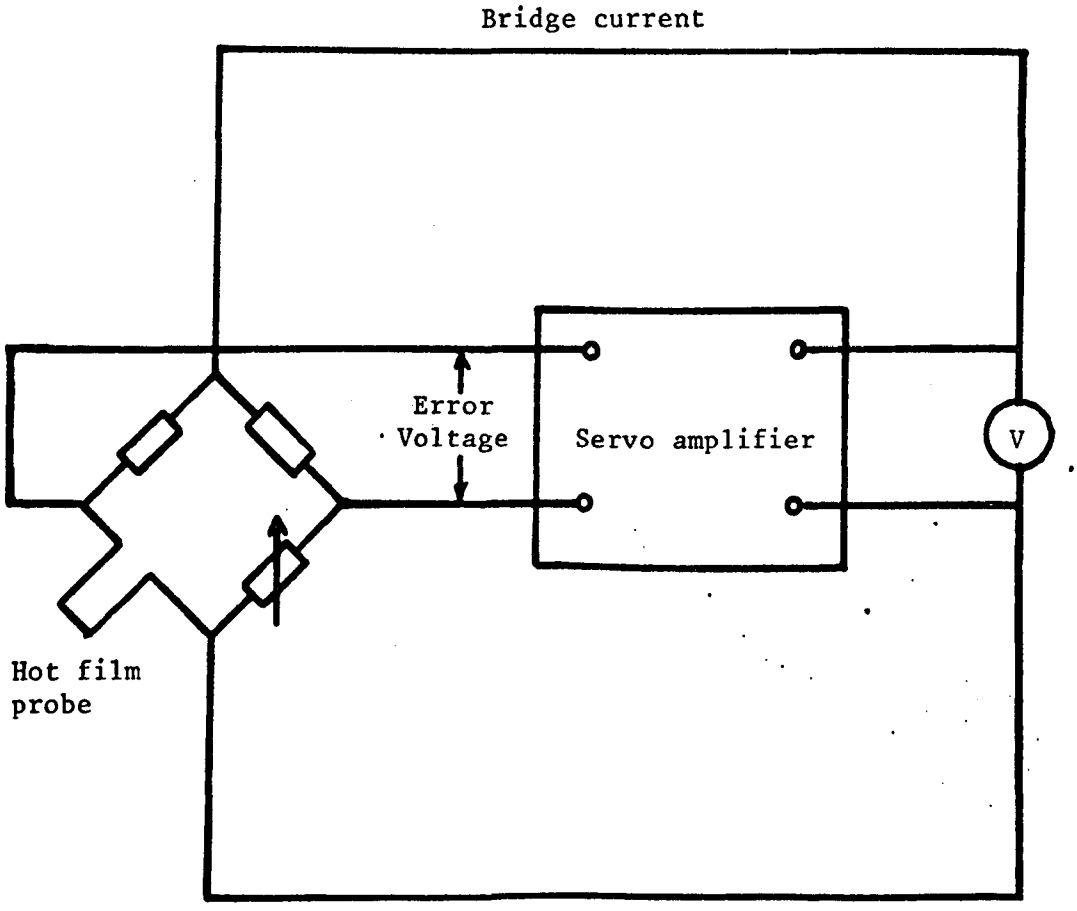

Fig. 36 Schematic layout of DISA 55A01 Constant Temperature Anemometer and 55A82 hot film probe.

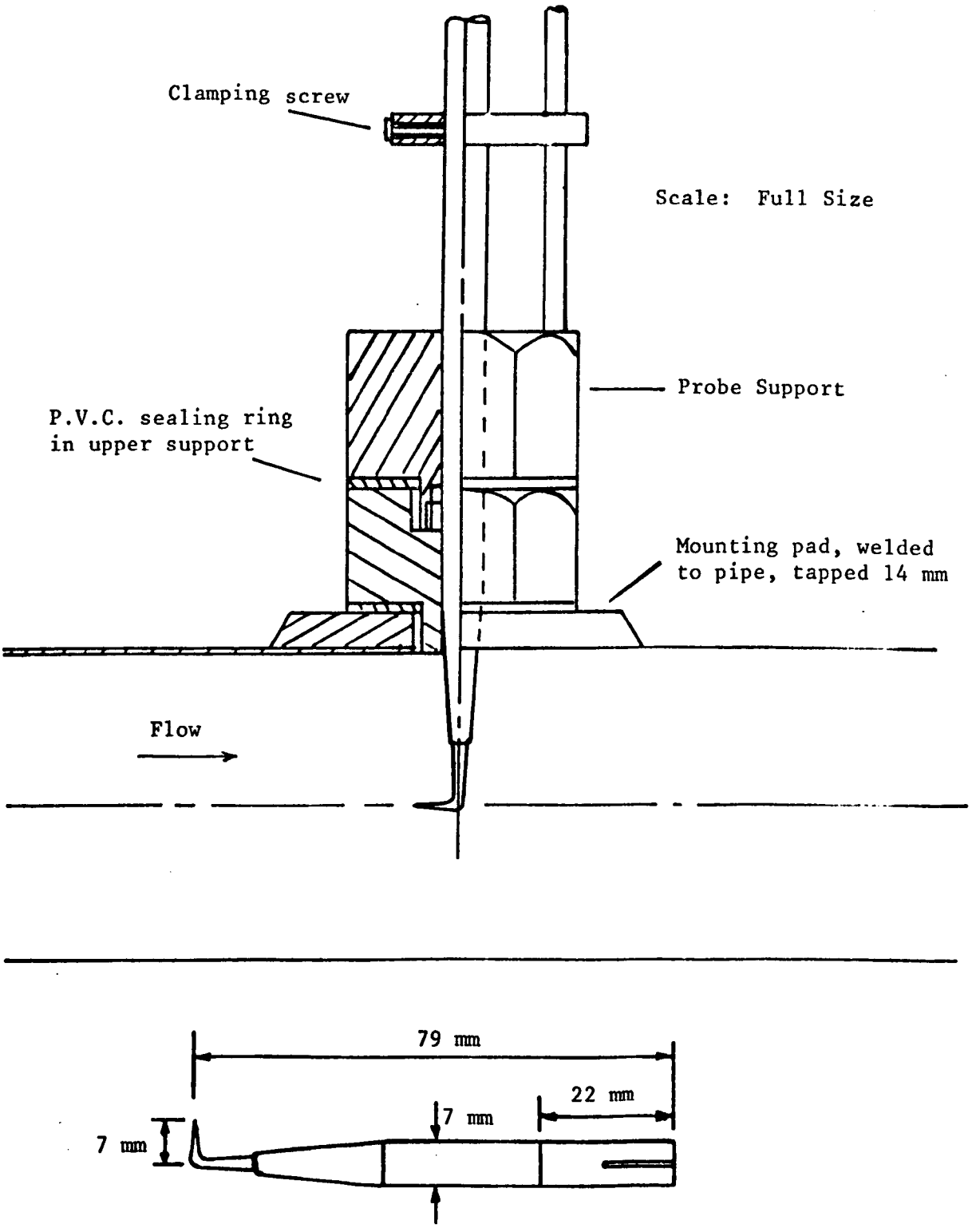

Fig. 37 DISA 55A82 hot film probe and support mounted on the pipeline.

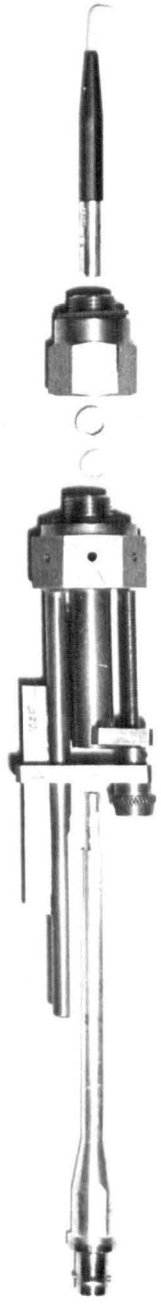

Fig. 38 DISA hot film probe : top to bottom: 55A82 probe, lower 14 mm adaptor, P.V.C. seal and retaining collar, upper adaptor with traversing screw and clamping device, and DISA probe support and cable connector.

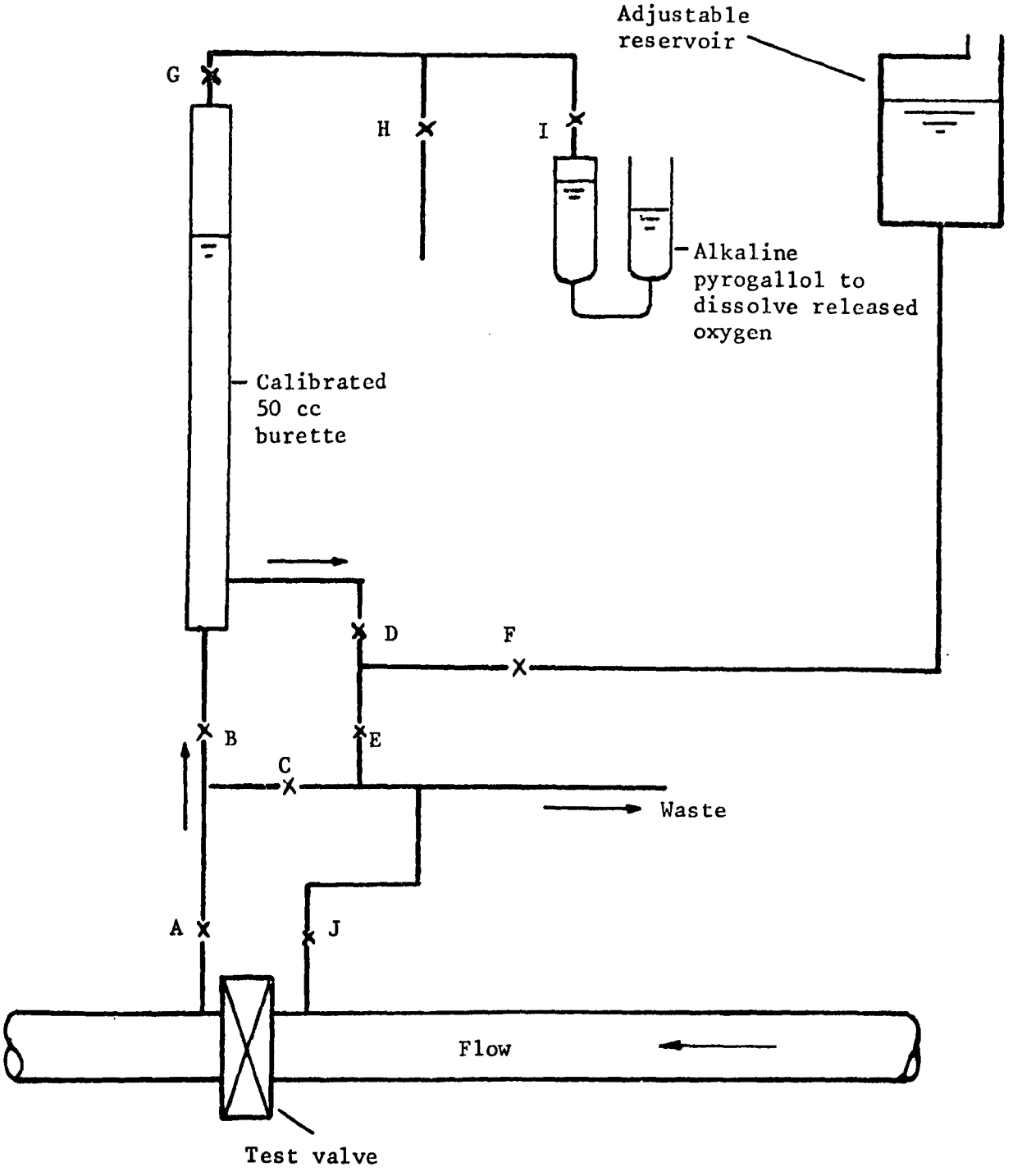

Fig. 39 Air collection apparatus as used in tests on pipeline configuration 2

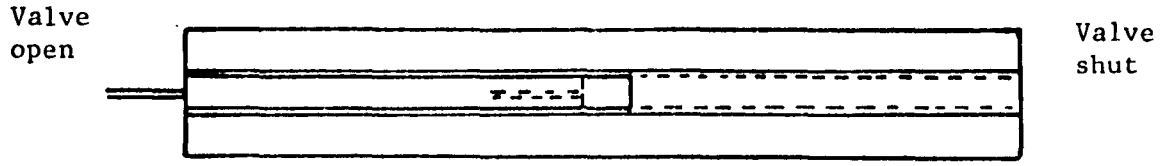

Transducer travel = 177 mm

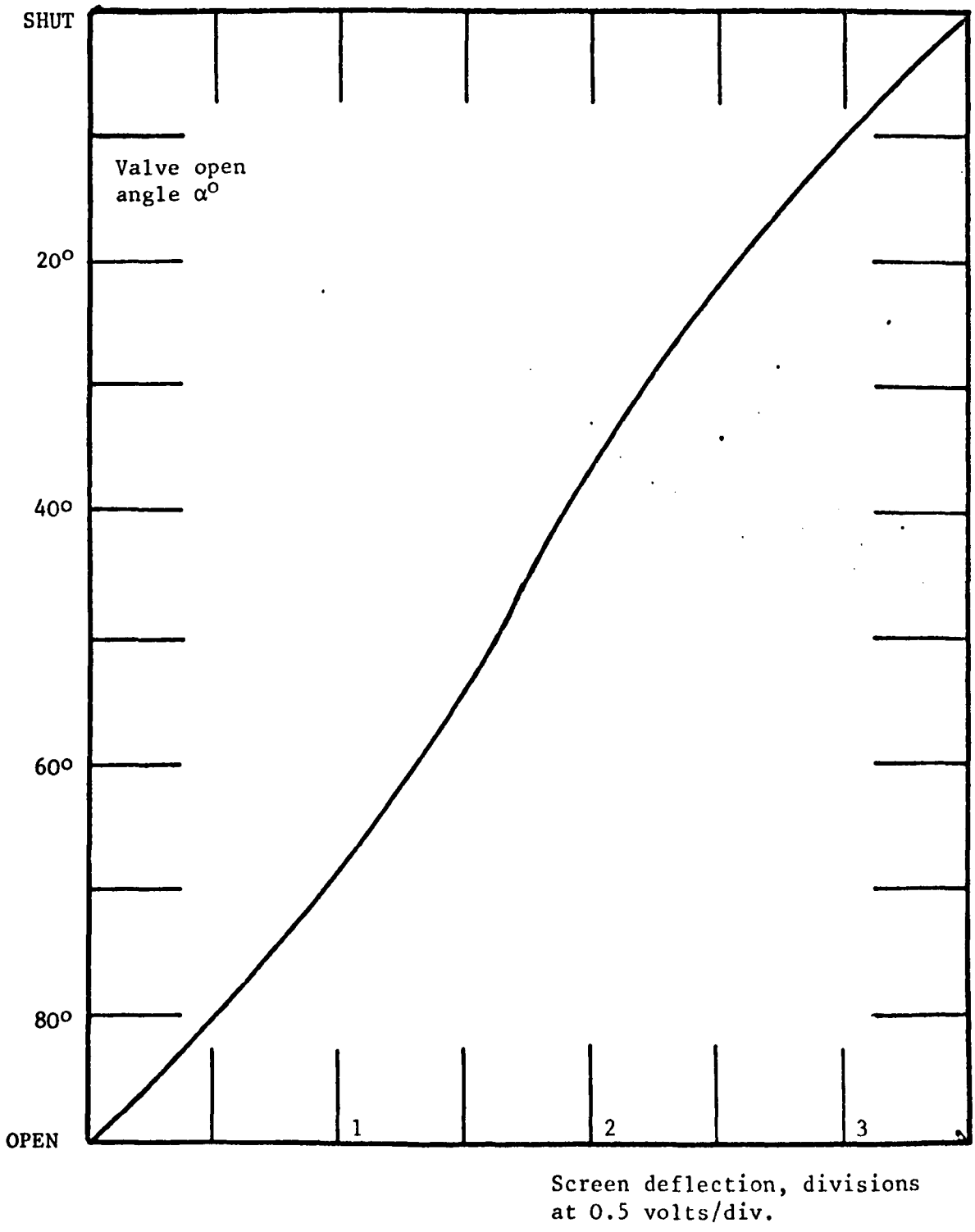

Fig. 40 Calibration curve for linear displacement transducer.

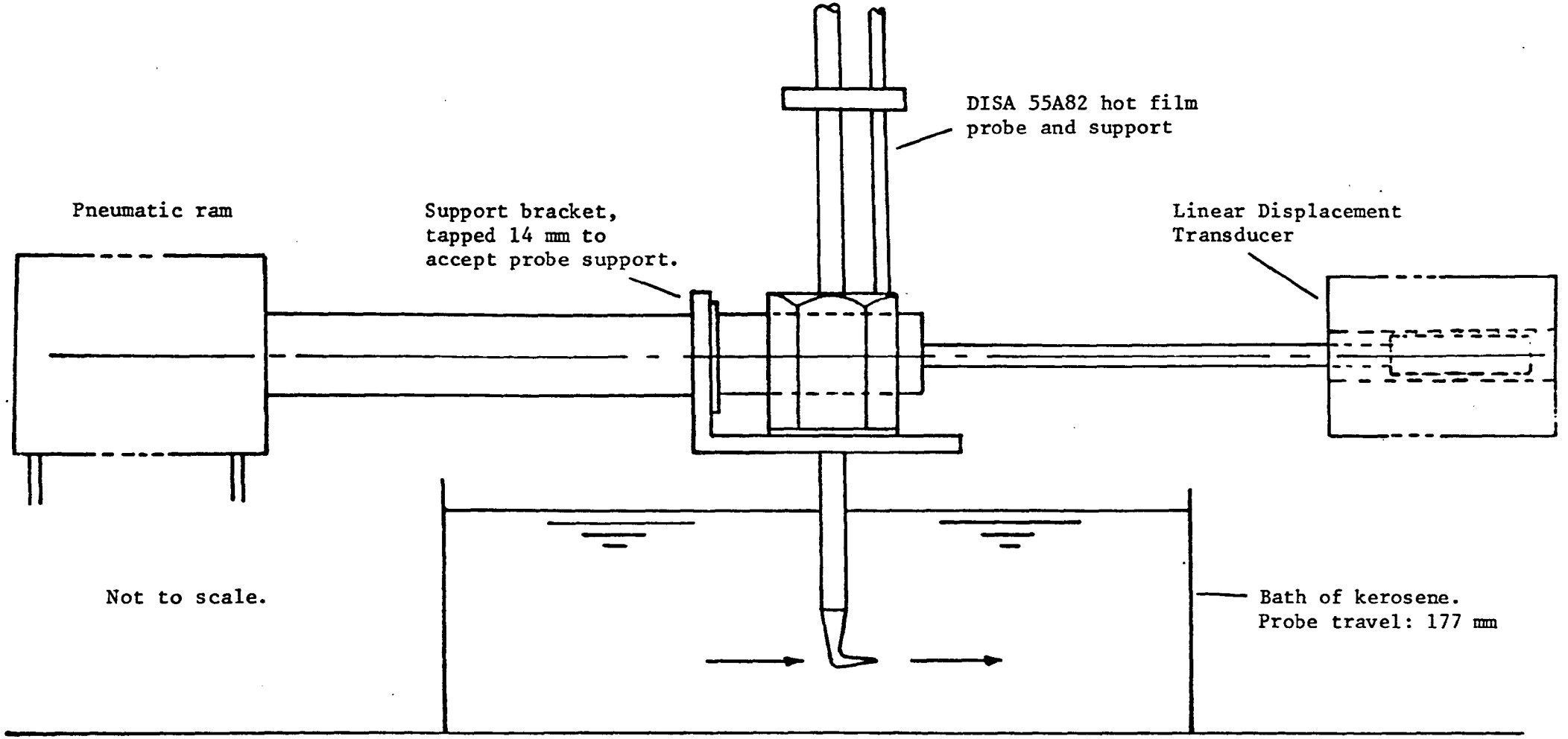

Fig. 41 Schematic layout of DISA hot film probe calibration attachment mounted on valve closing ram.

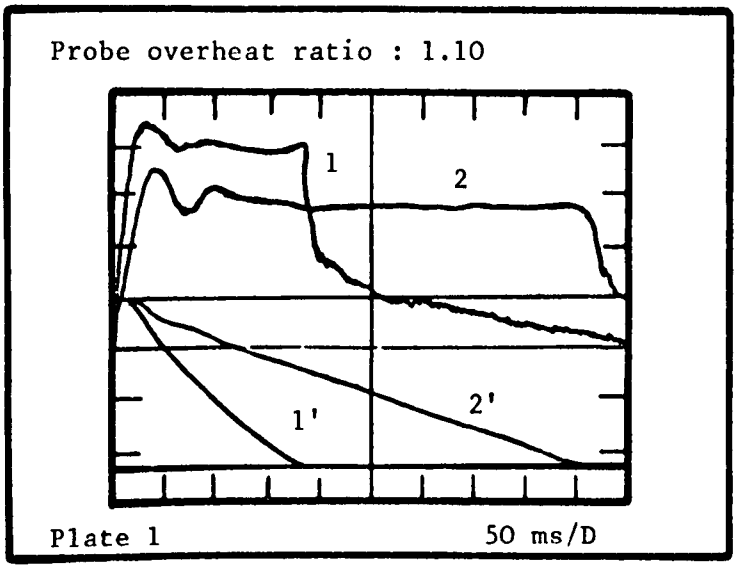

Fig. 42 Plates 1, 2 illustrate the results employed for the calibration of the unlinearized DISA 55A82 hot film probe. Direct comparison between the probe output and the L.D.T. yields a relation of the form $VOLTS^2 \alpha VEL.^{\frac{1}{2}}$

Traces 1', 2' - L.D.T. - 0.5 volts/Div.

1 ,2 - DISA - 2 volts/Div.

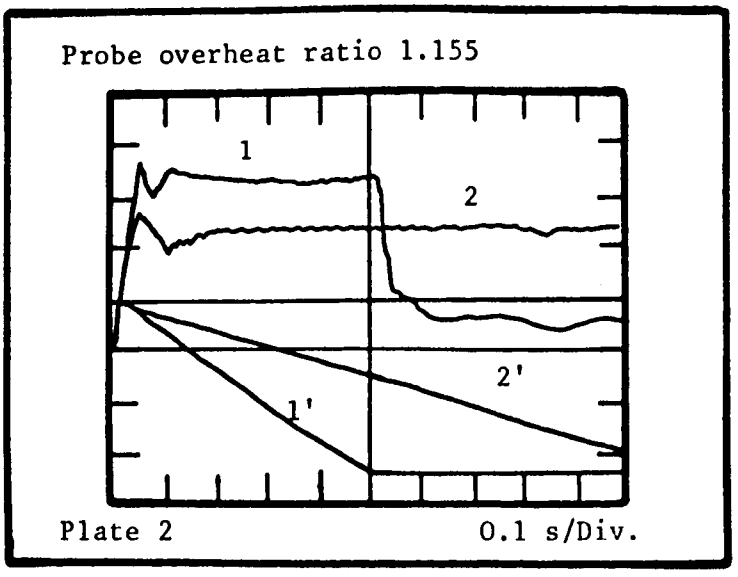

Note - total L.D.T. travel - 177 mm.

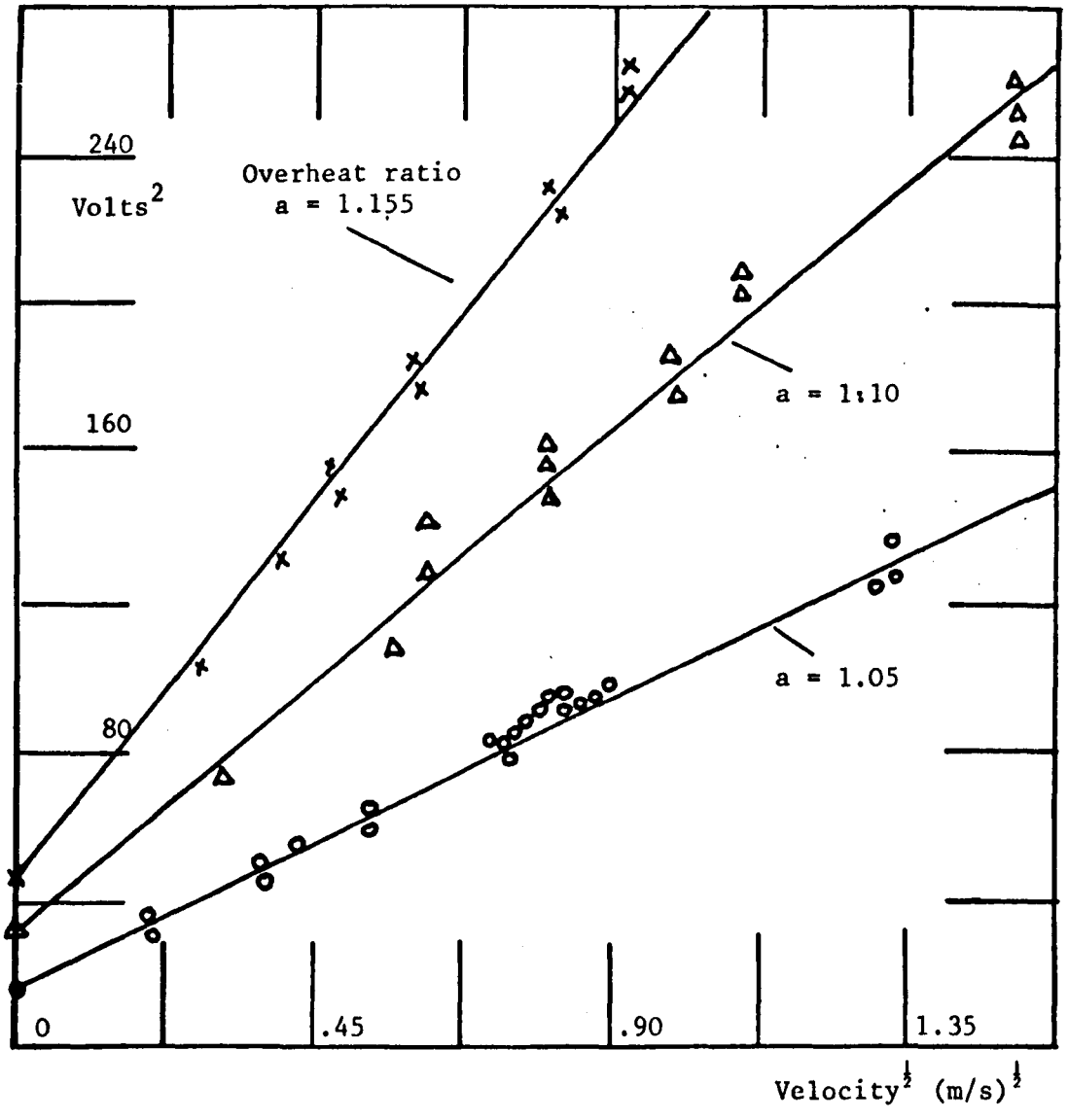

Fig. 43 Calibration curves for DISA 55A82 hot film probe obtained by means of the probe mounting attachment fitted to the valve closing ram. Velocity estimated from L.D.T. output. This calibration employed for tests on pipeline configuration 1.

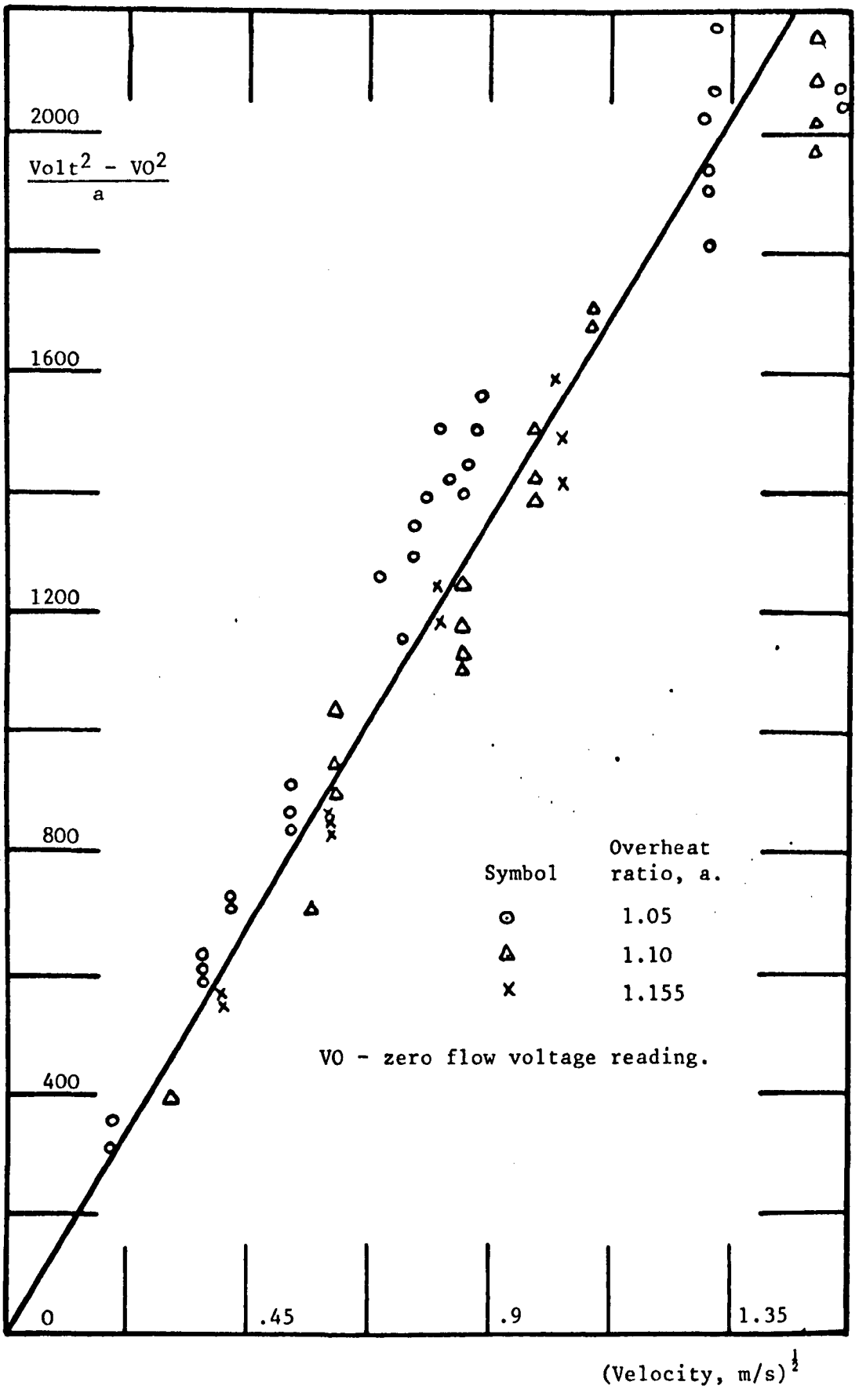

Fig. 44 Calibration curve for DISA 55A82 hot film probe used on pipeline configuration 1.

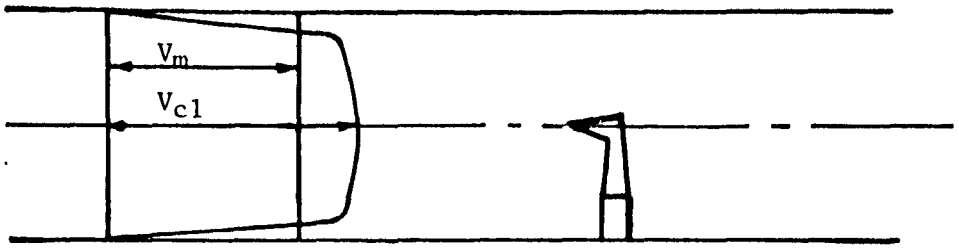

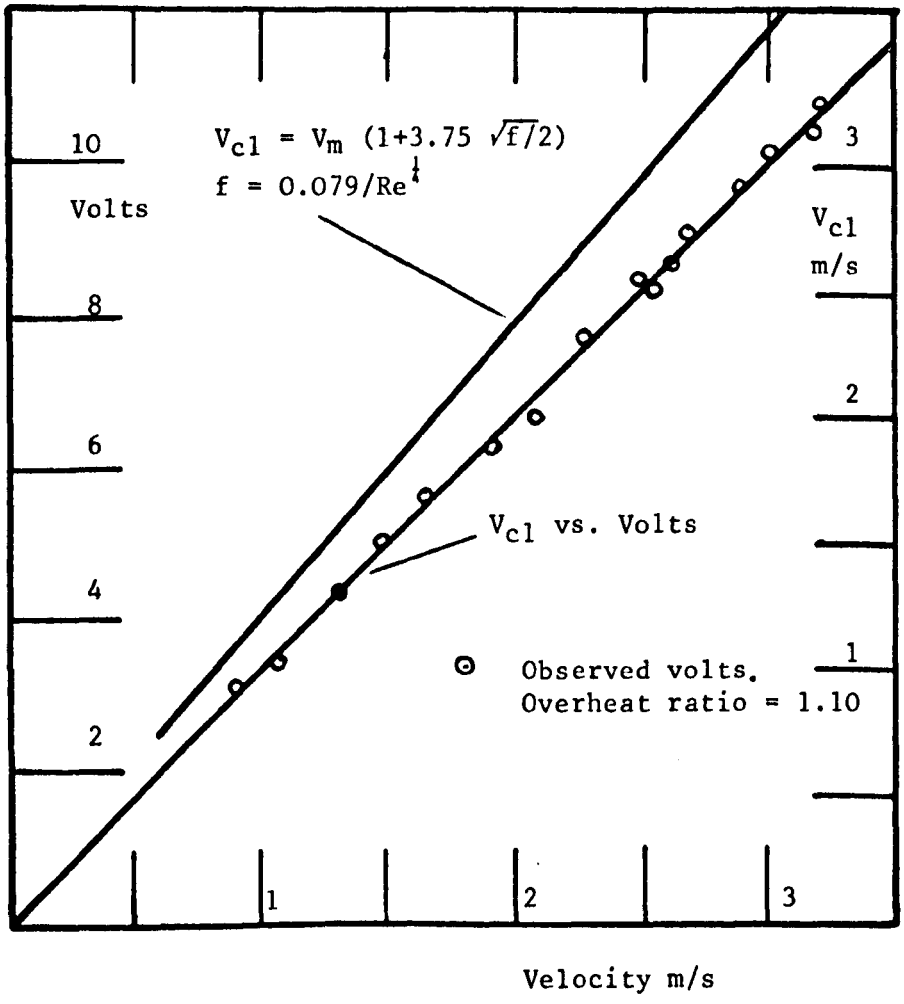

Fig.45 Calibration curve for DISA 55A82 hot film probe and linearizer unit used on pipeline configurations 2 and 3.

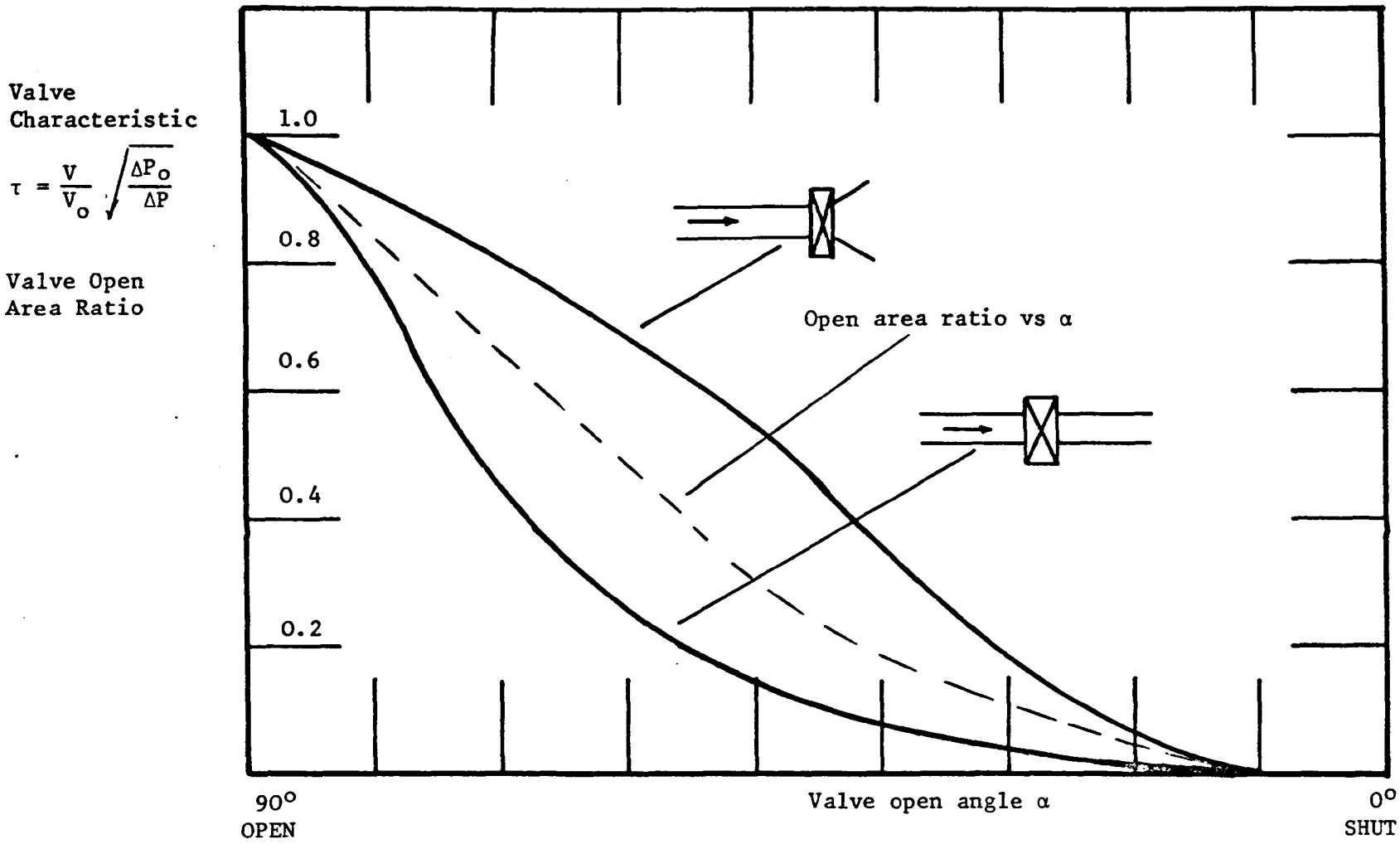

Fig. 46 Valve characteristic and open area ratio vs. open angle.

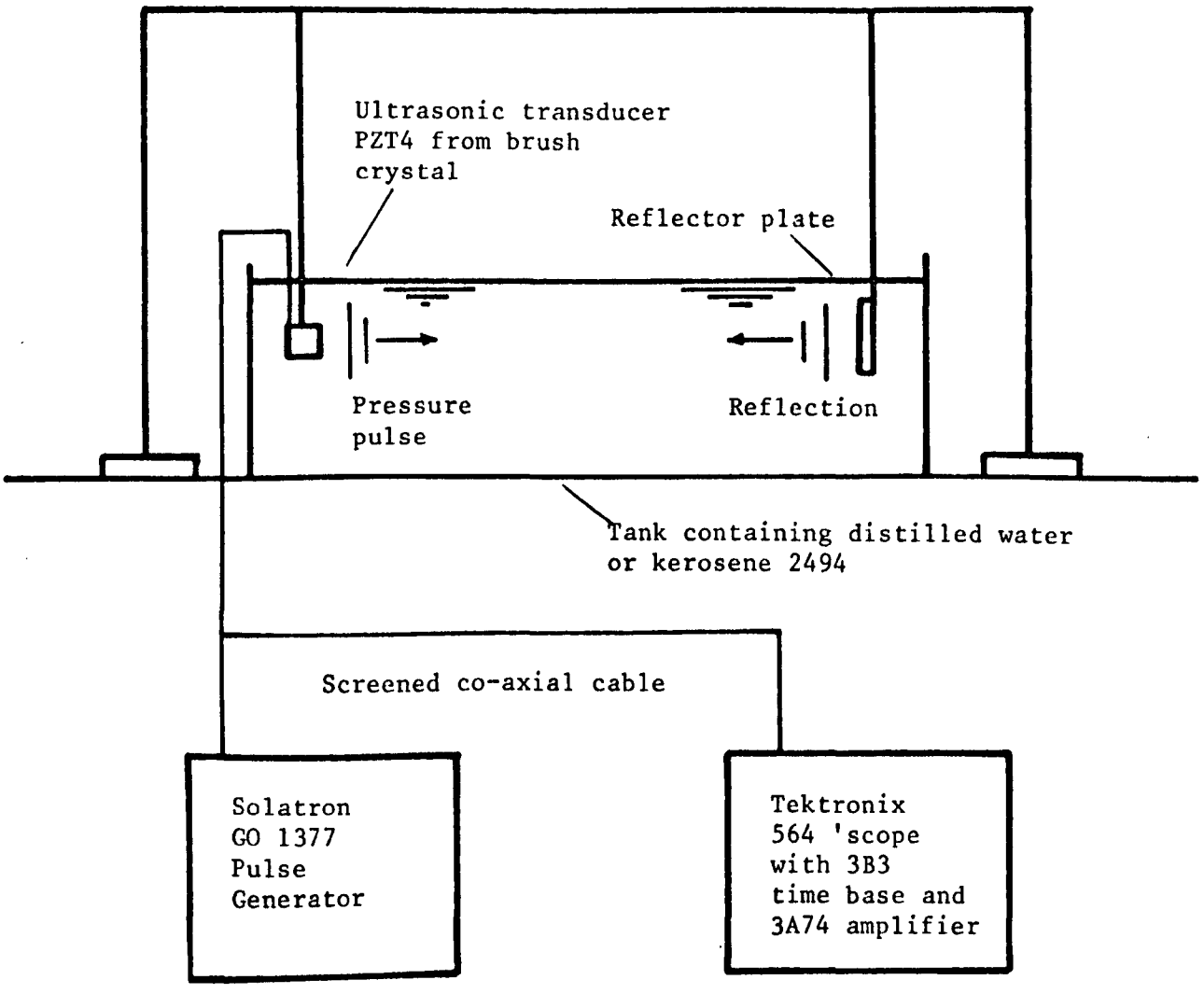

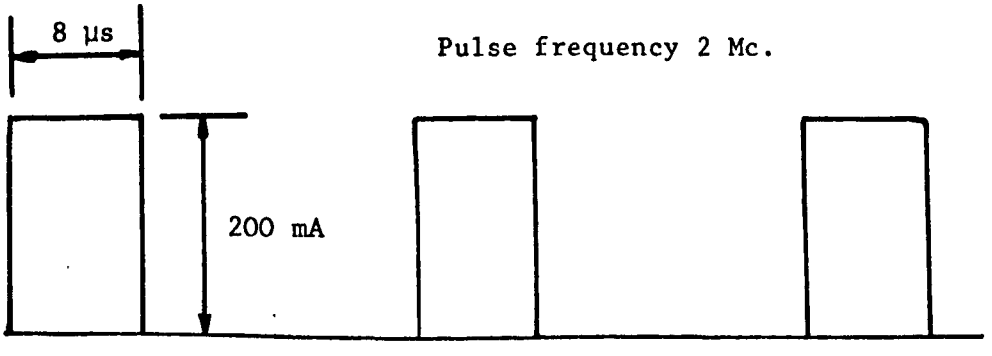

Fig. 47 Layout of apparatus used to estimate the bulk modulus of kerosene at room temperature and atmospheric pressure.

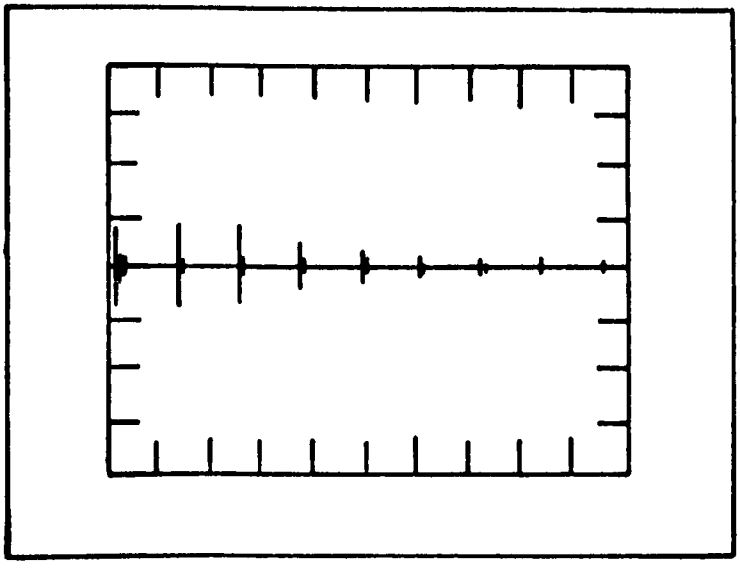

Fig. 48 Initial pulse and 8 reflections in kerosene 2494. Separation transducer -plate 152 mm, time base 0.2 ms/Div, fuel temperature 17.5°C.

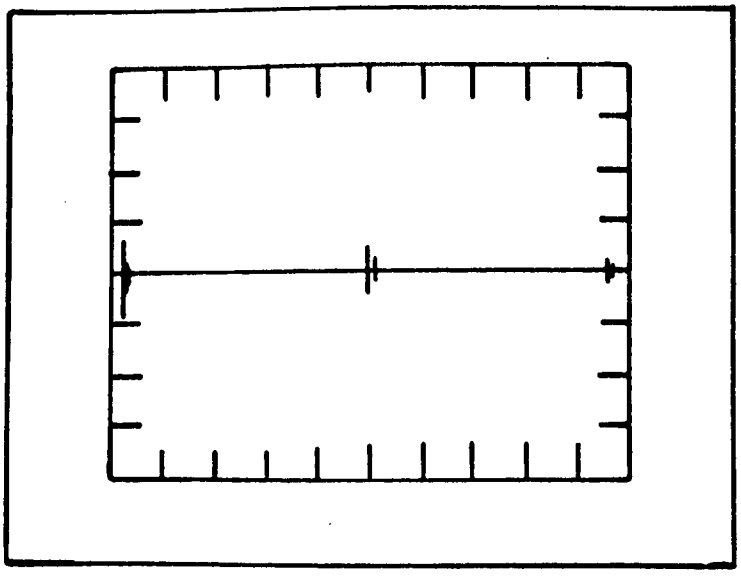

Fig.49 3rd, 4th, 5th reflections in kerosene 2494 measured by use of delay time base. Separation 152 mm, delay time 0.4 ms, time base 50 µs/Div, fuel temperature 17.5°C.

Pipeline configuration 1

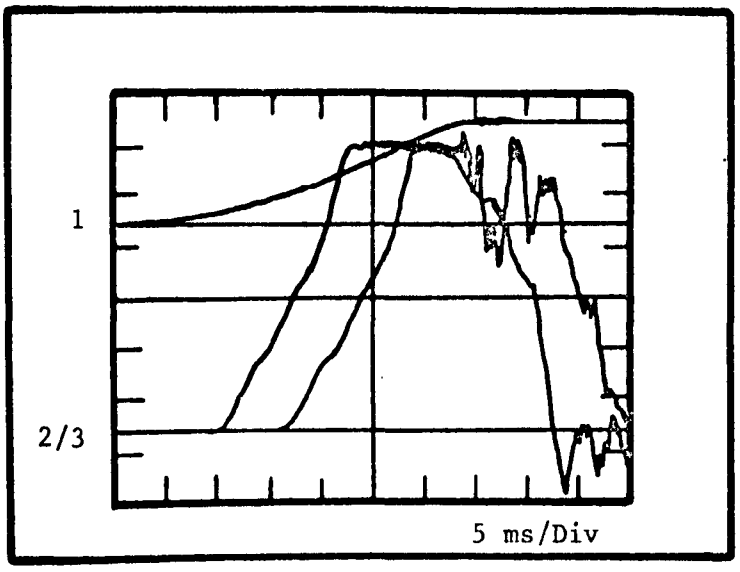

Plate 1: Pneumatic ram and valve on common base.

Fig. 50 Pressure variations at two points upstream of the valve following closure, and illustrating the influence of vibrations transmitted by the closing action of the ram.

Traces
1. L.D.T.
2. Pressure 1.25 m upstream of the valve.
3. Pressure 7.8 m upstream of the valve.

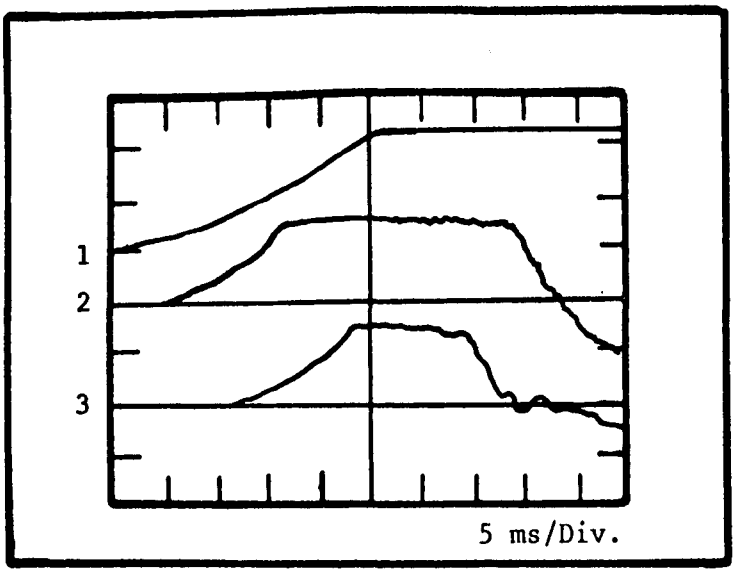

Plate 2: Pneumatic ram mounted separately to eliminate vibrations.

Pipeline configuration 1

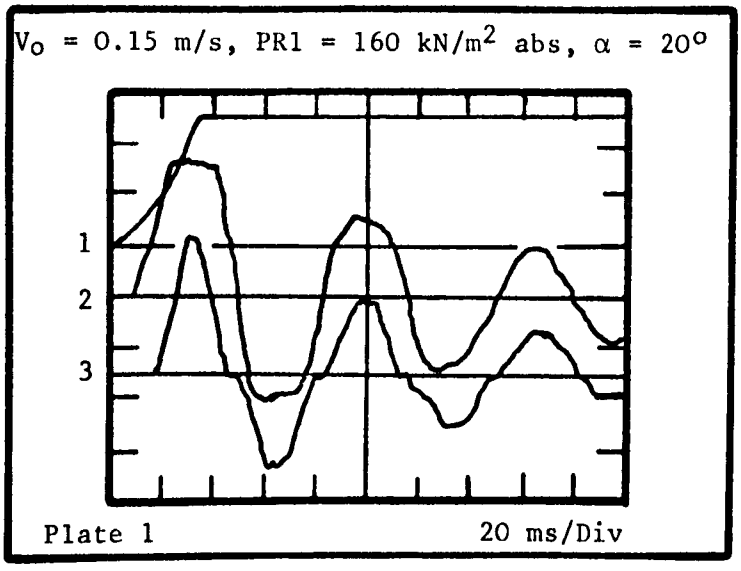

Fig. 51 Pressure variation at two points upstream of the valve following closure.

Traces: 1. L.D.T.
2. Pressure transducer 1.25 m upstream of valve.
3. Pressure transducer 7.8 m upstream of valve.

Pressure scale: 45 kN/m^2/Div (Plate 1)
90 kN/m^2/Div (Plate 2)

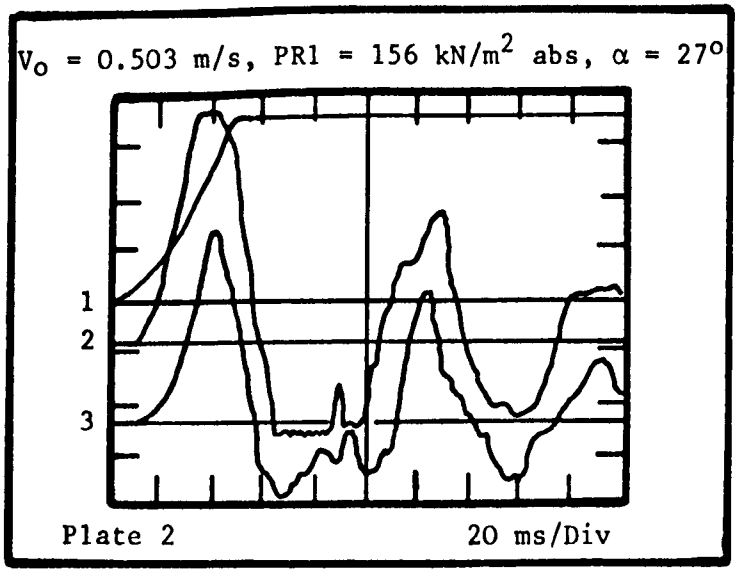

Pipeline configuration 1

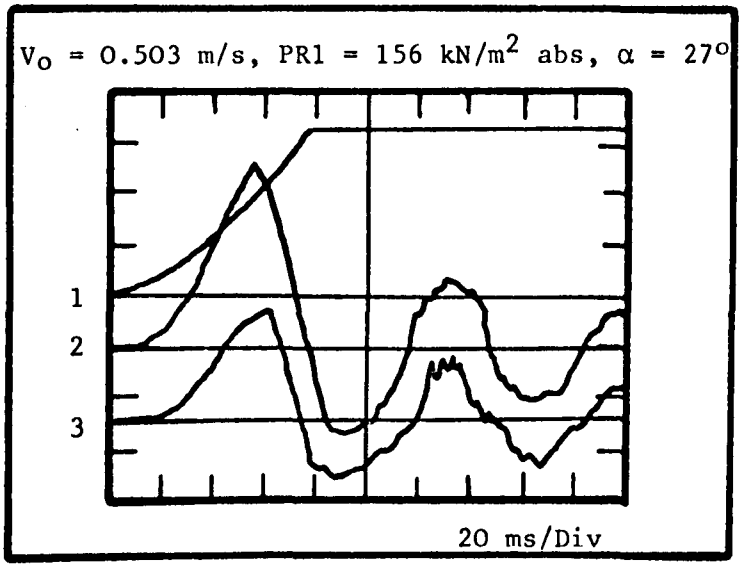

Fig. 52 Pressure variations at two points upstream of the valve following closure.

Traces: 1. L.D.T.
2. Pressure transducer 1.25 m upstream of valve.
3. Pressure transducer 7.8 m upstream of valve.

Pressure scale: 90 kN/m^2/div.

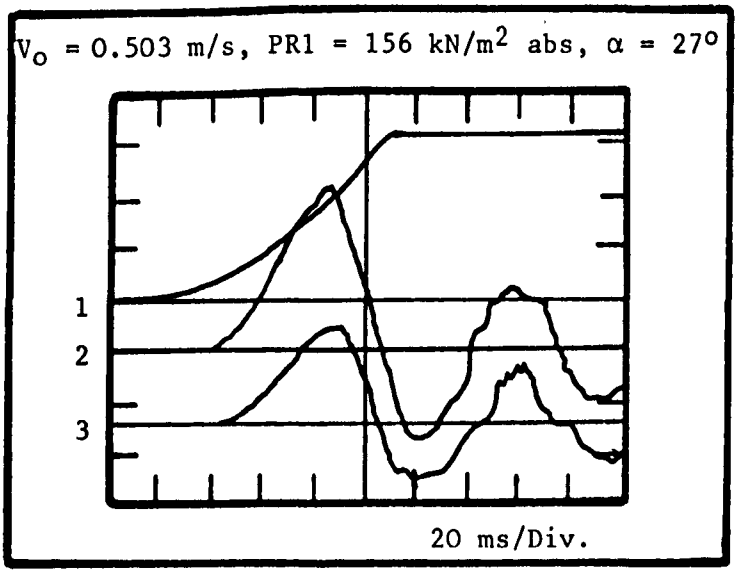

Pipeline configuration 1

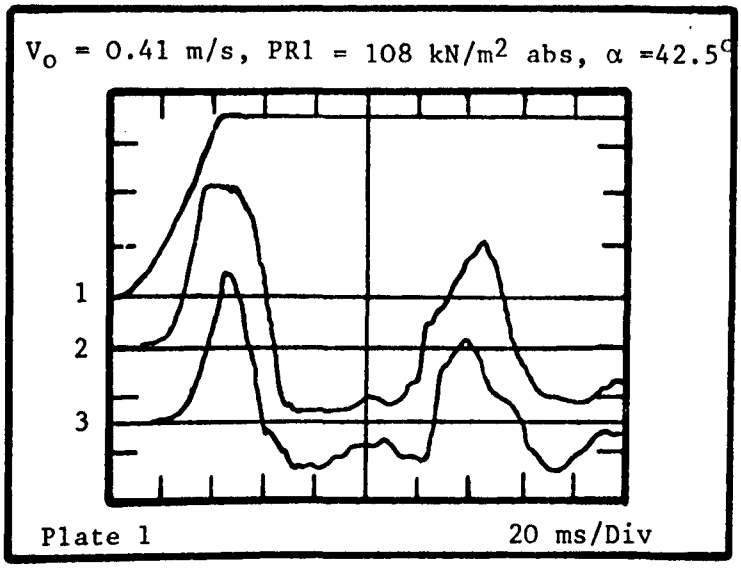

Fig. 53 Pressure variation at two points upstream of the valve following closure.

Traces: 1. L.D.T.
2. Pressure 1.25 m upstream of the valve.
3. Pressure 7.8 m upstream of the valve.

Pressure scale: Plate 1: 90 kN/m^2/Div
Plate 2: 225 kN/m^2/Div.

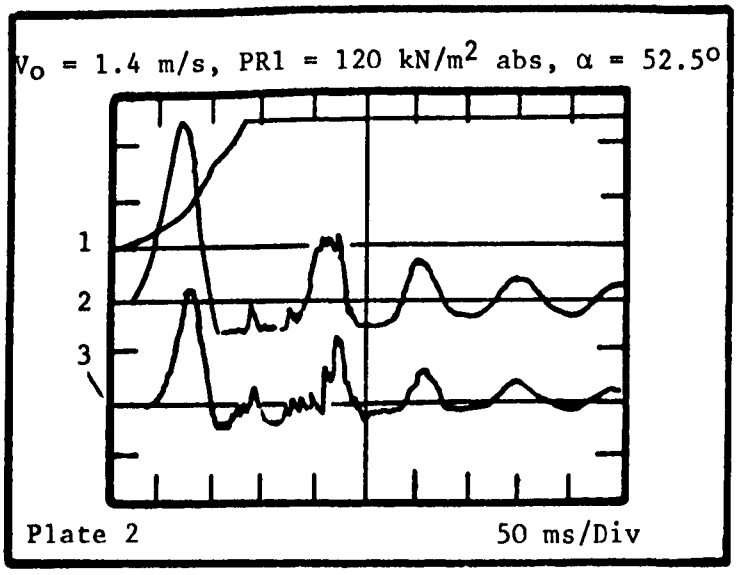

Pipeline configuration 1

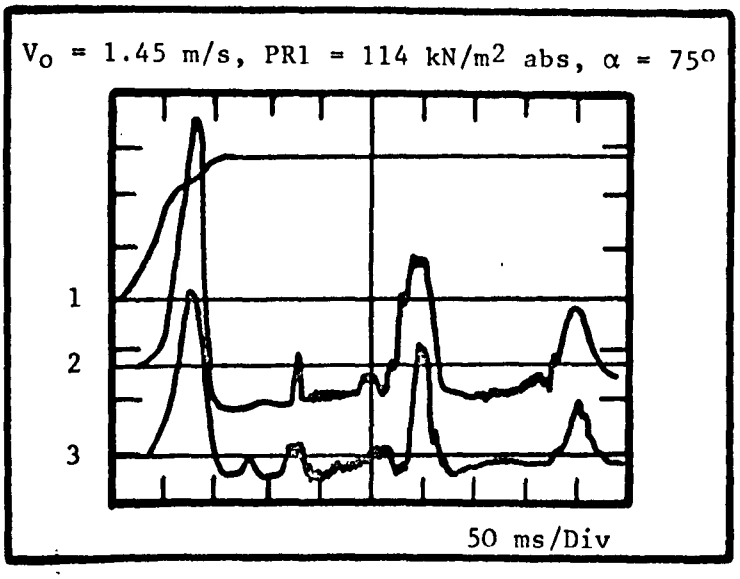

Fig. 54 Pressure variation at two points upstream of the valve following closure.

Traces
1. L.D.T.
2. Pressure 1.25 m upstream of the valve.
3. Pressure 7.8 m upstream of the valve.

Pressure scale: 225 kN/m^2/Div.

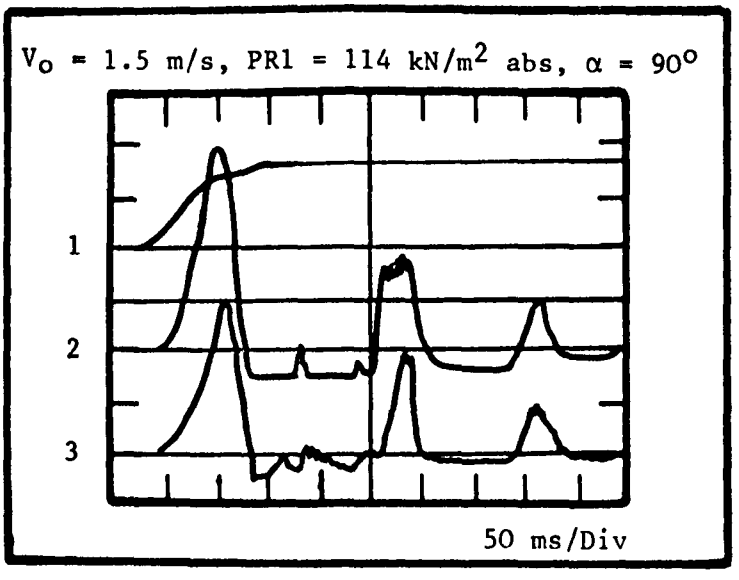

Pipeline configuration 1

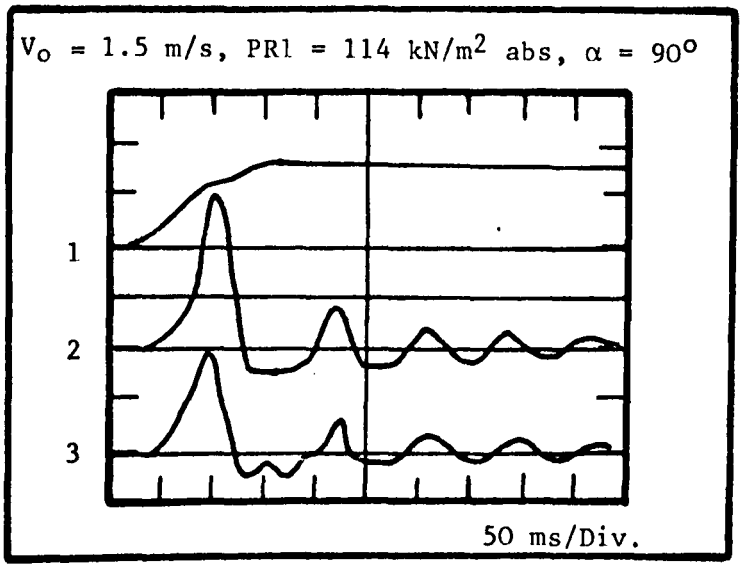

Fig. 55 Pressure variation at two points upstream of the valve following closure.

Traces
1. L.D.T.
2. Pressure 1.25 m upstream of the valve.
3. Pressure 7.8 m upstream of the valve.

Pressure scale: 225 kN/m^2/Div.

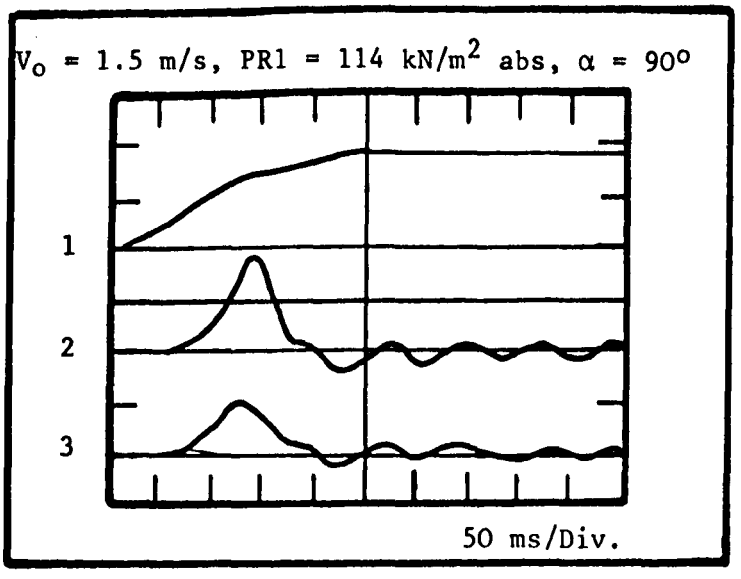

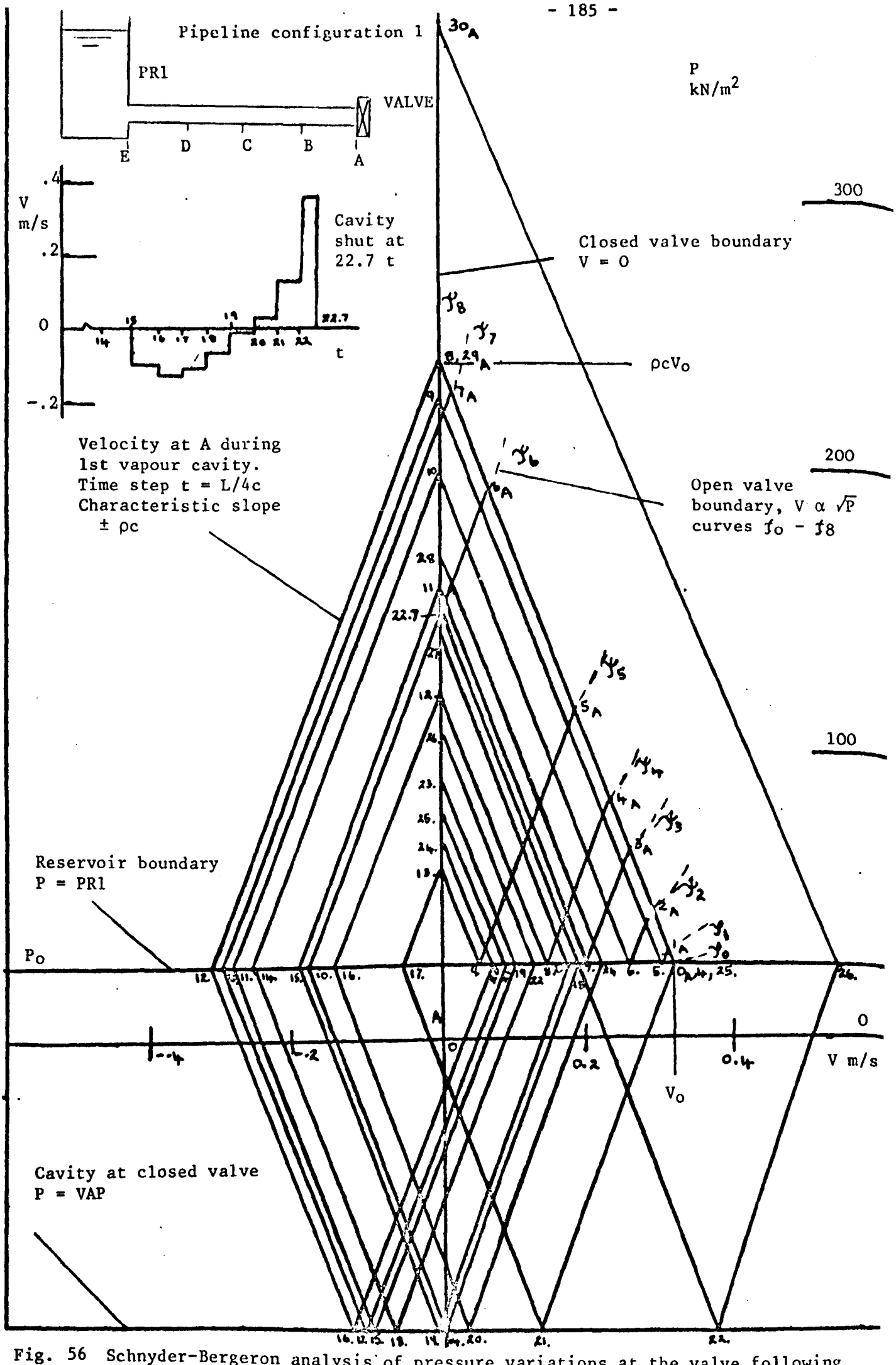

Fig. 56 Schnyder-Bergeron analysis of pressure variations at the valve following a rapid valve closure in 0.03 s. V_o = 0.29 m/s, $\alpha = 25^o$ PR1 = 130 kN/m^2 abs.

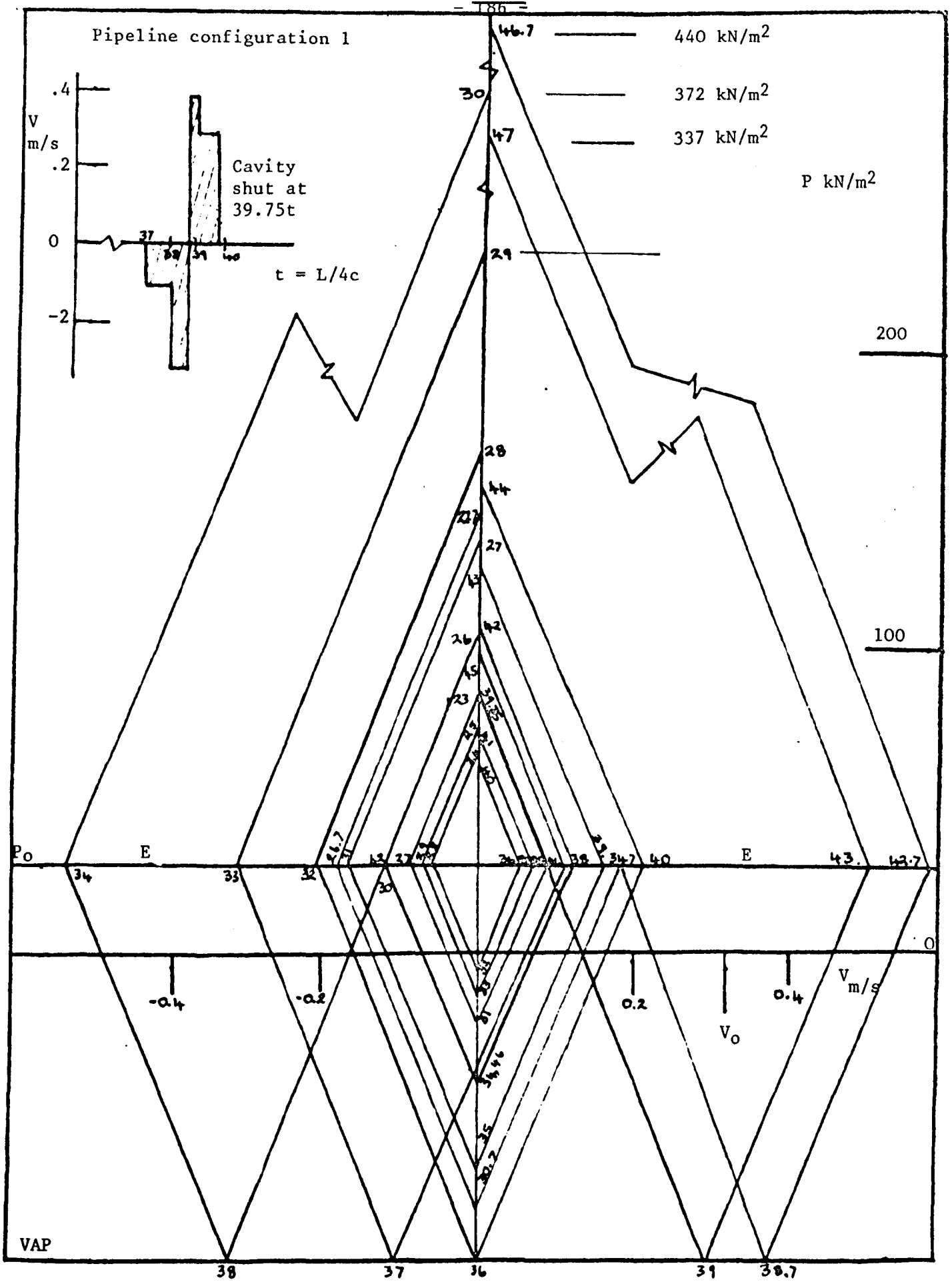

Fig. 57 Continued Schnyder-Bergeron analysis of pressure variation at the valve following a rapid closure in 0.03 s. V_o = 0.29 m/s, α = 25°, PR1 = 130 kN/m^2 abs.

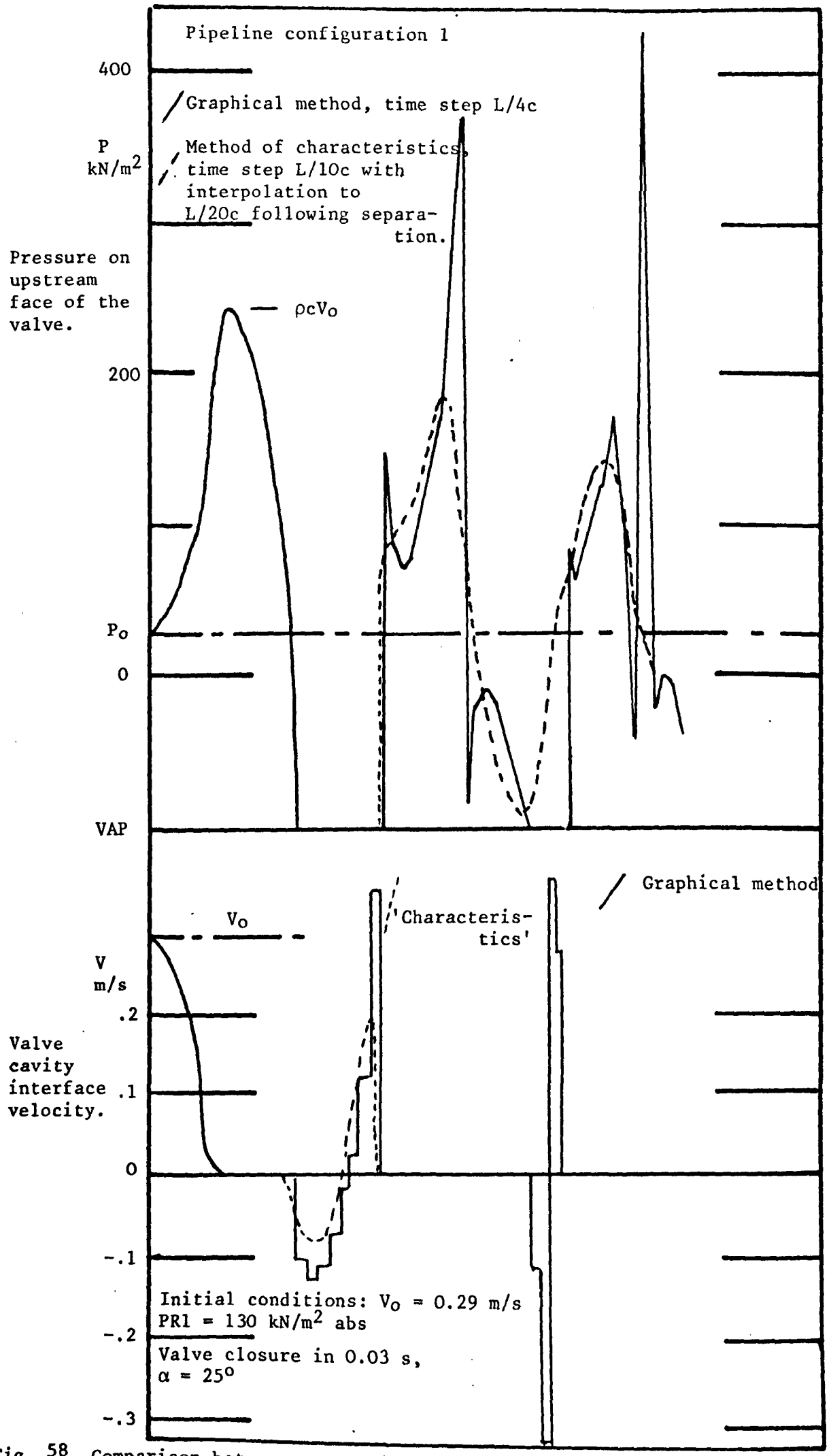

Fig. 58 Comparison between a graphical and numerical analysis of one test case.

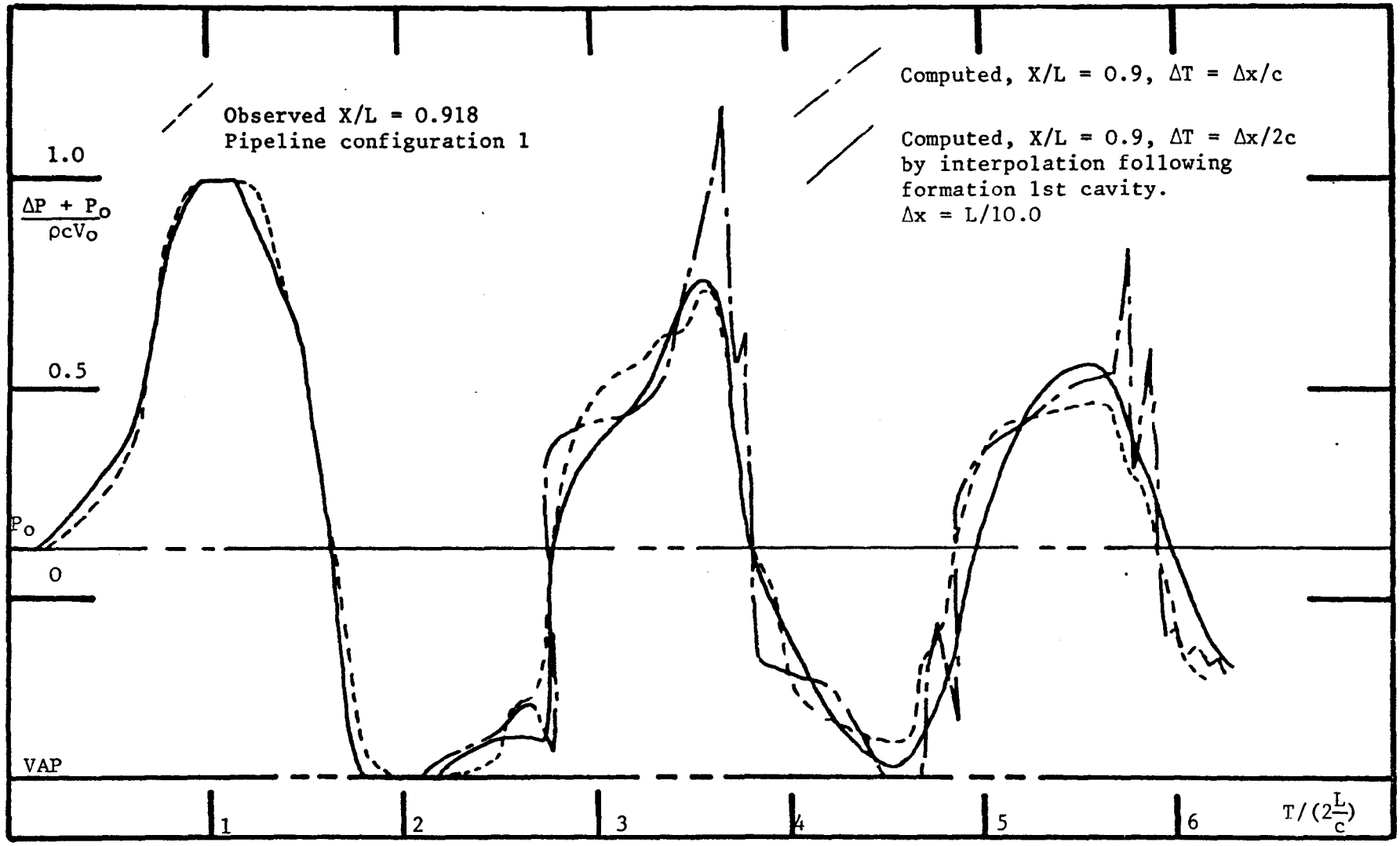

Fig. 59 Effect of reducing the time increment, by interpolation, from $\Delta x/c$ to $\Delta x/2c$, following 1st cavity formation. Pressure variation recorded upstream of the valve. Initial conditions, V_o = 0.29 m/s, PR1 = 130 kN/m^2 abs, $\alpha = 25^o$, 2L/c = 0.0326 s, ρcV_o = 220 kN/m^2, valve closure in 0.03 s. X measured from reservoir.

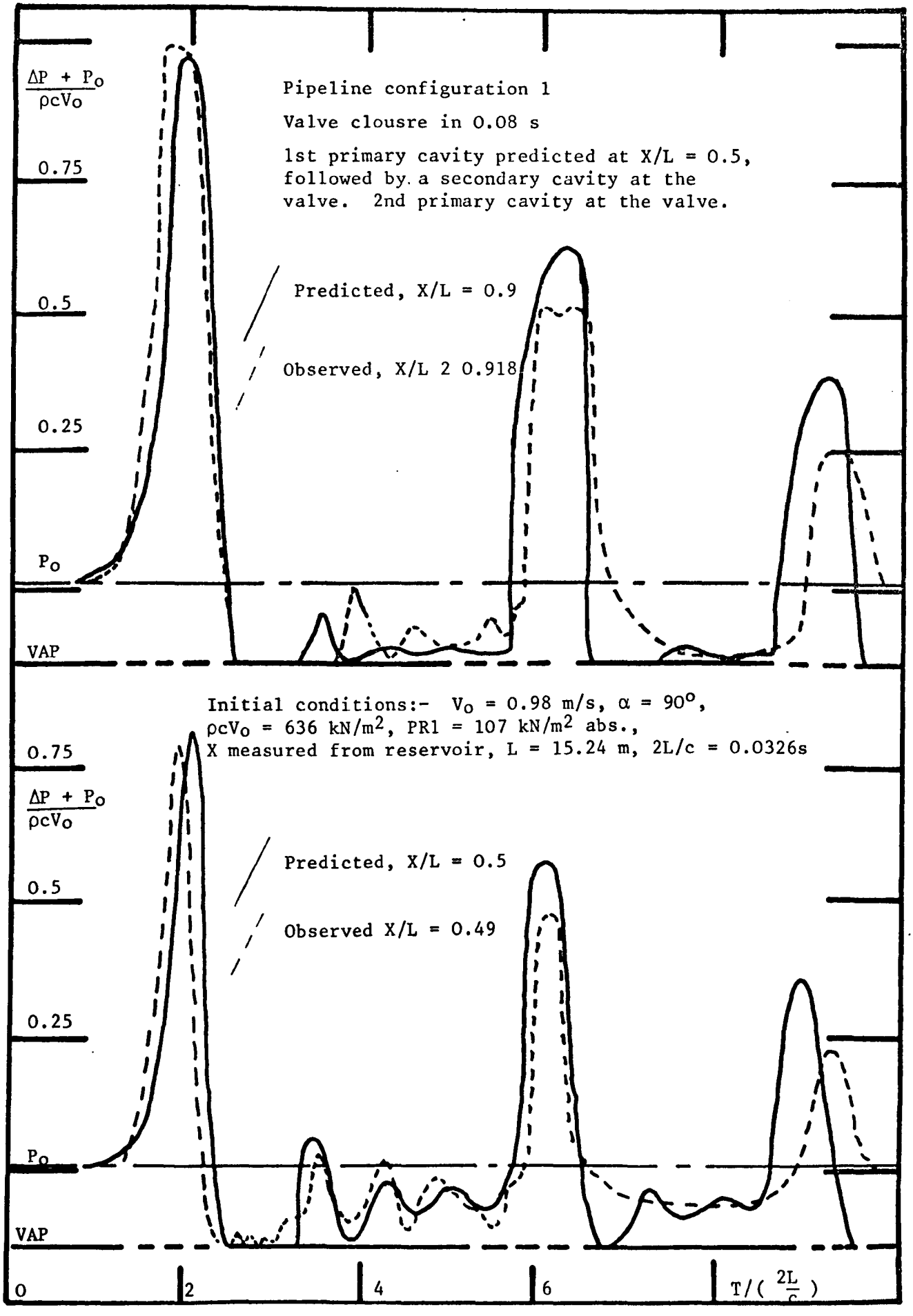

Fig. 60 Pressure variations at two points upstream of the valve following closure compared to the predicted variations.

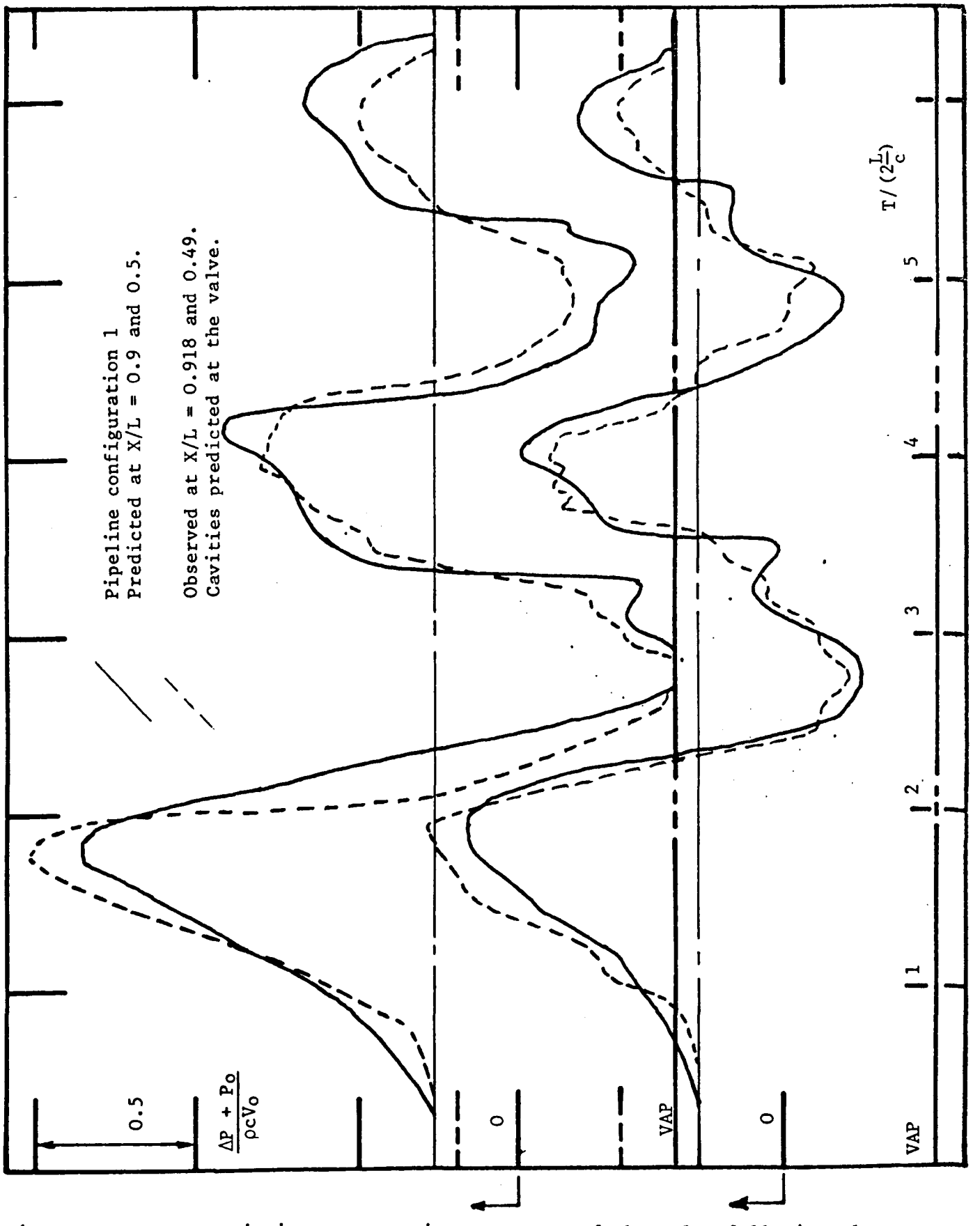

Fig. 61 Pressure variation at two points upstream of the valve following closure. Initial conditions:- V_o = 0.5 m/s, PR1 = 157 kN/m^2 abs, α = 32°, valve closure in 0.07 s, L = 15.24 m, 2L/c = 0.0326 s, $\rho c V_o$ = 370 kN/m^2. X measured from reservoir.

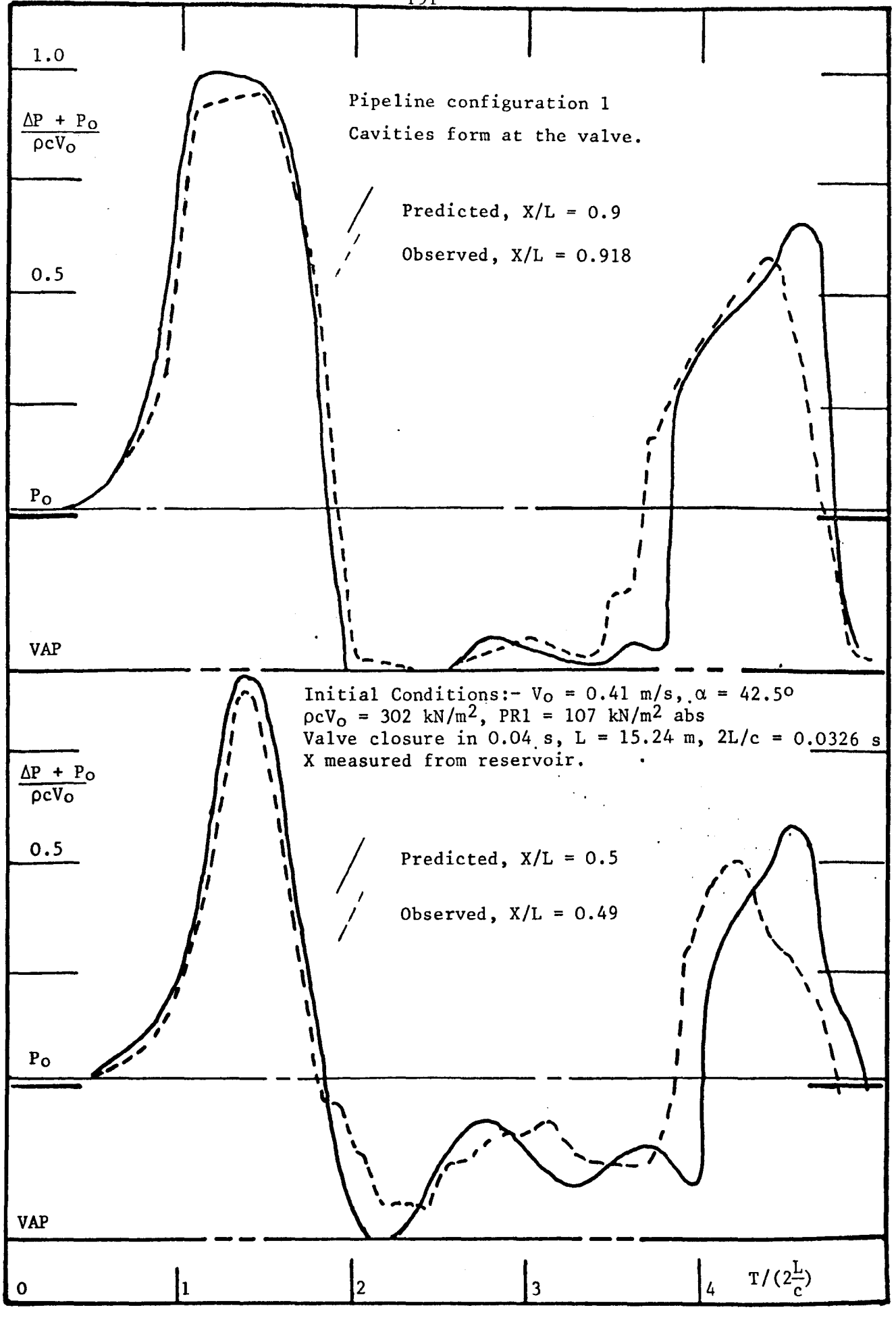

Fig. 62 Predicted and observed pressure variations at two points upstream of the valve.

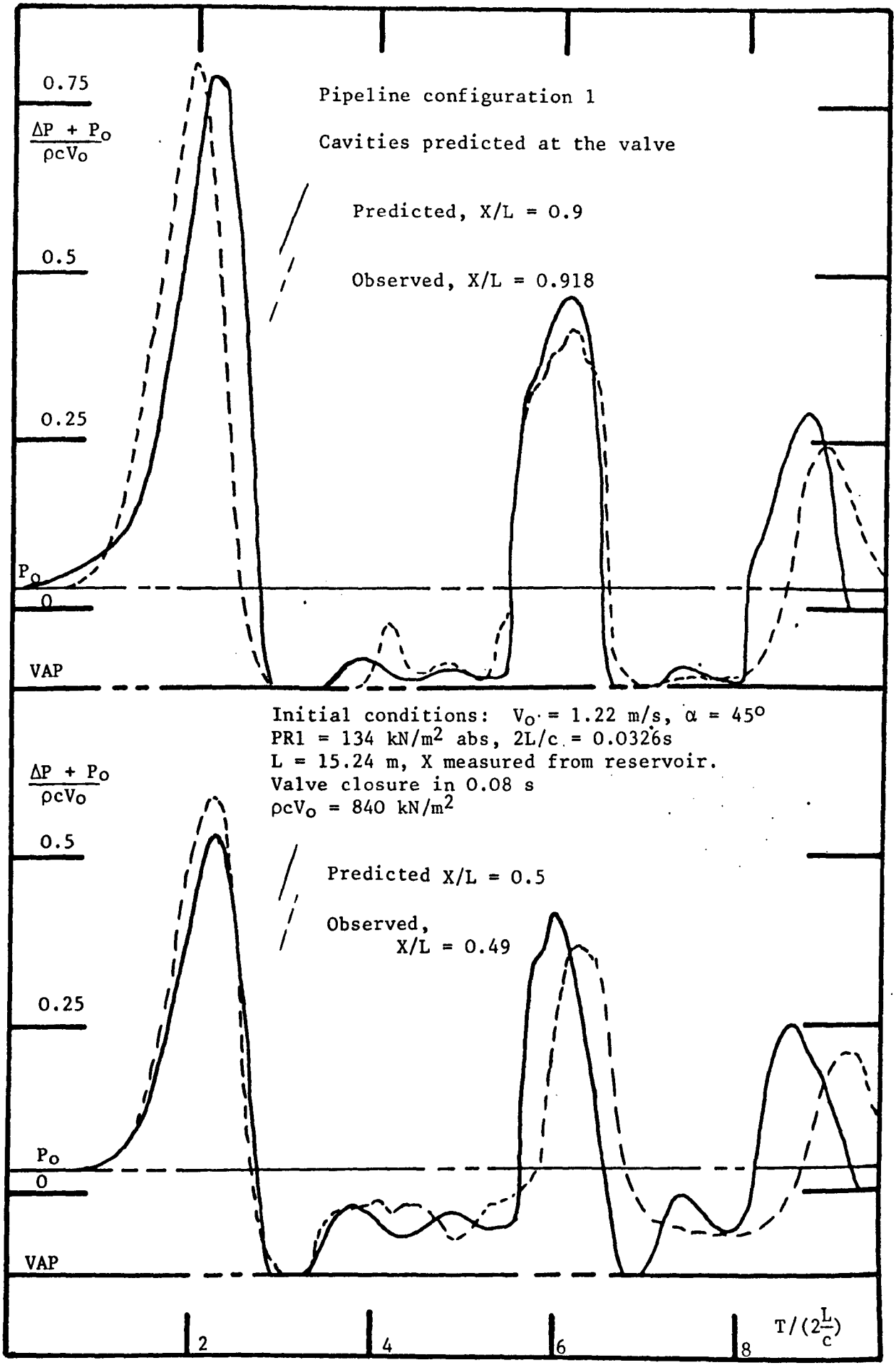

Fig. 63 Pressure variation at two points upstream of the valve following closure.

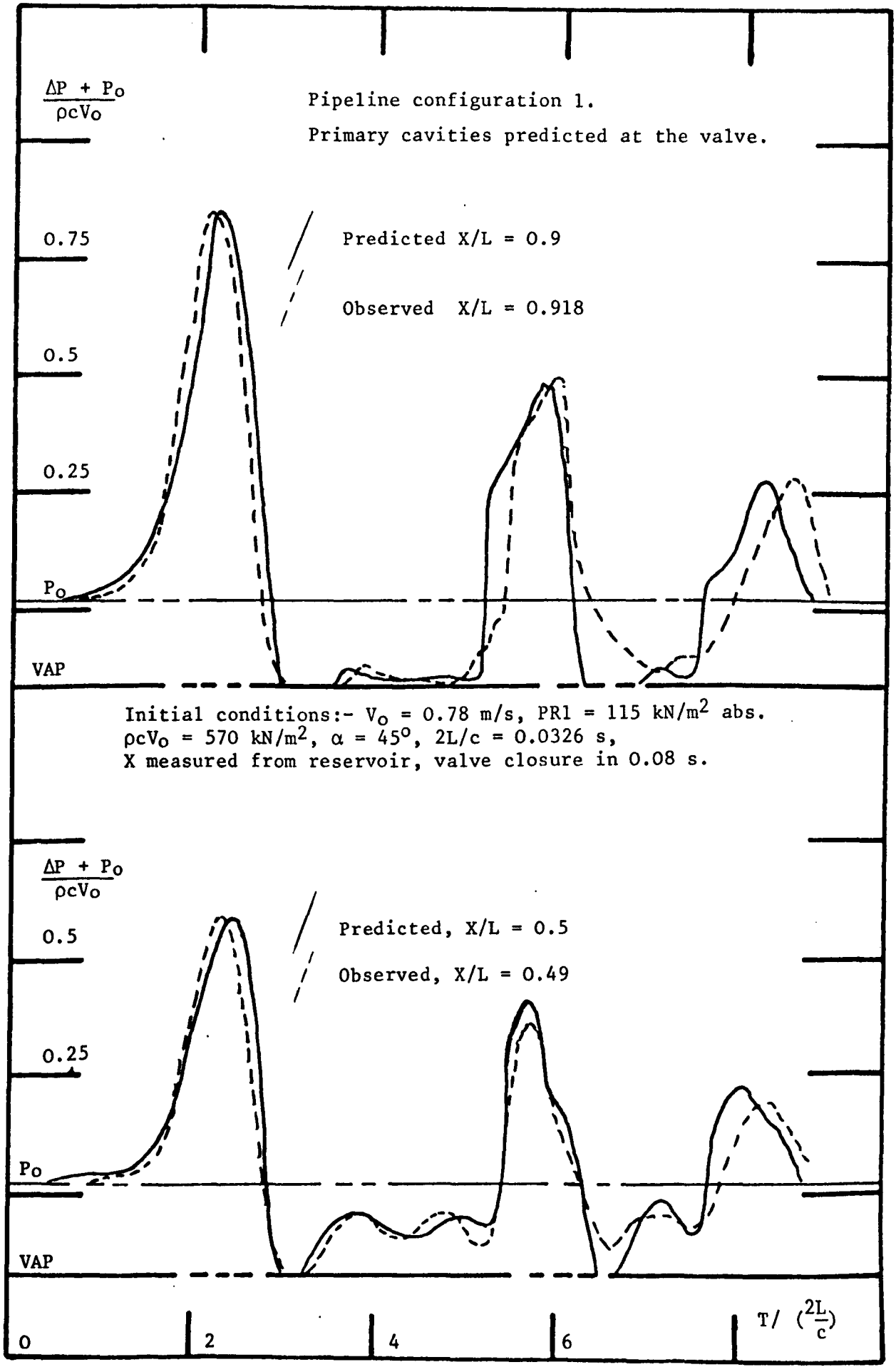

Fig. 64 Predicted and observed pressure variations at two points upstream of the valve following closure.

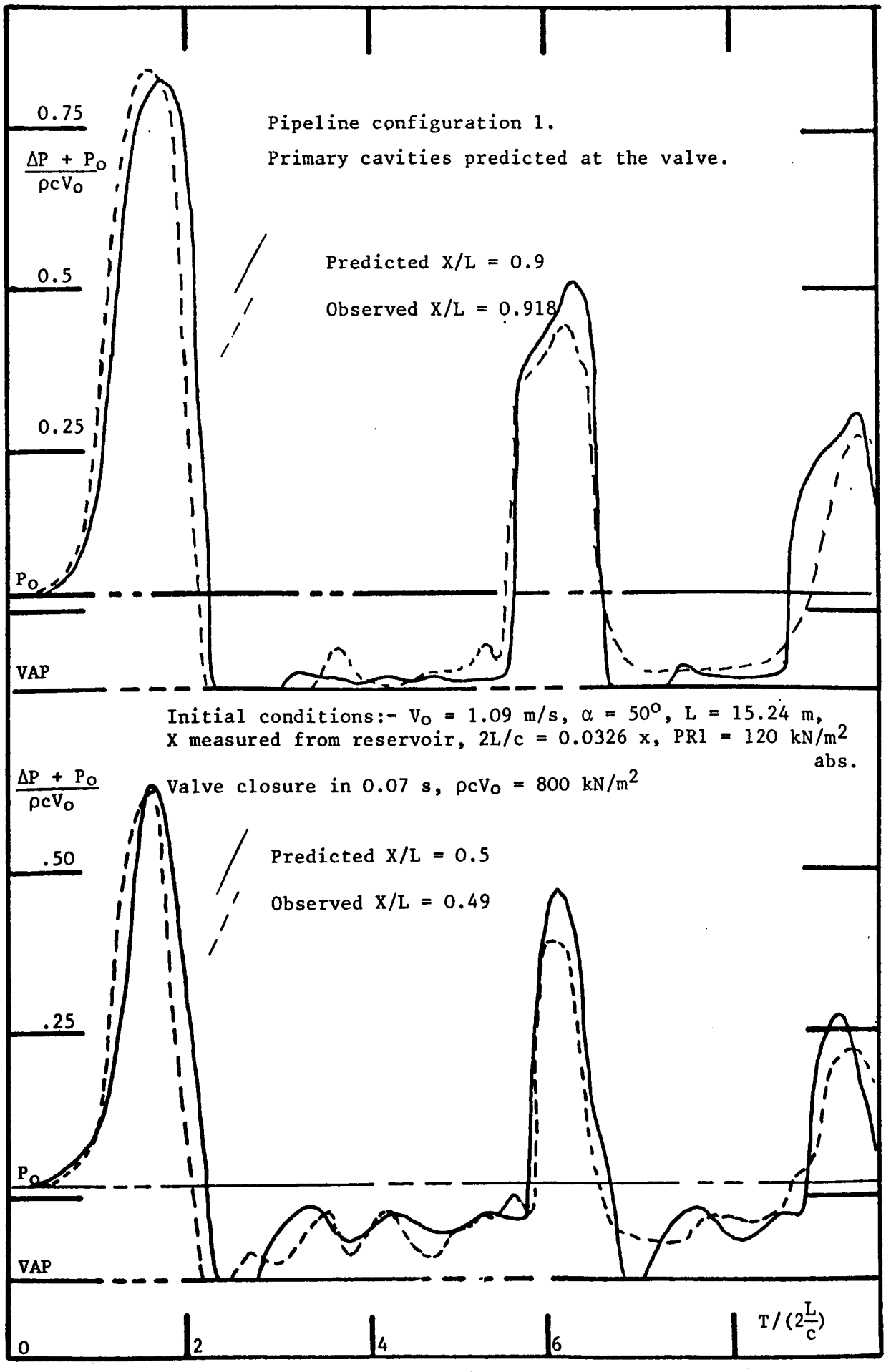

Fig. 65 Predicted and observed pressure variations at two points upstream of the valve following closure.

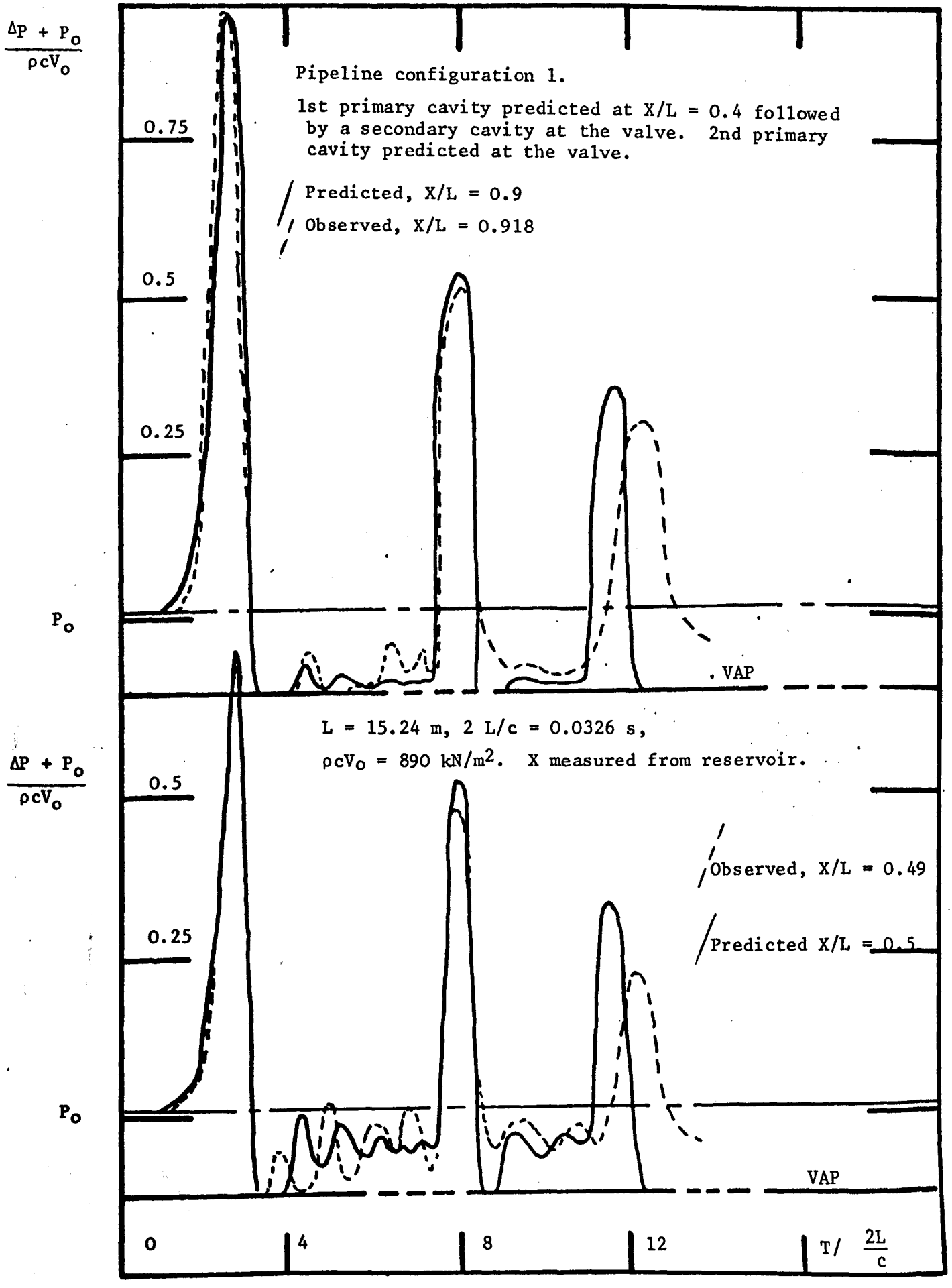

Fig. 66 Comparison between the observed and computed pressure variations at two points upstream of the valve following valve closure. Initial conditions: V_o = 1.22 m/s, PR1 = 113.0 kN/m^2 abs., $\alpha = 65^o$, valve closure in 0.085 s.

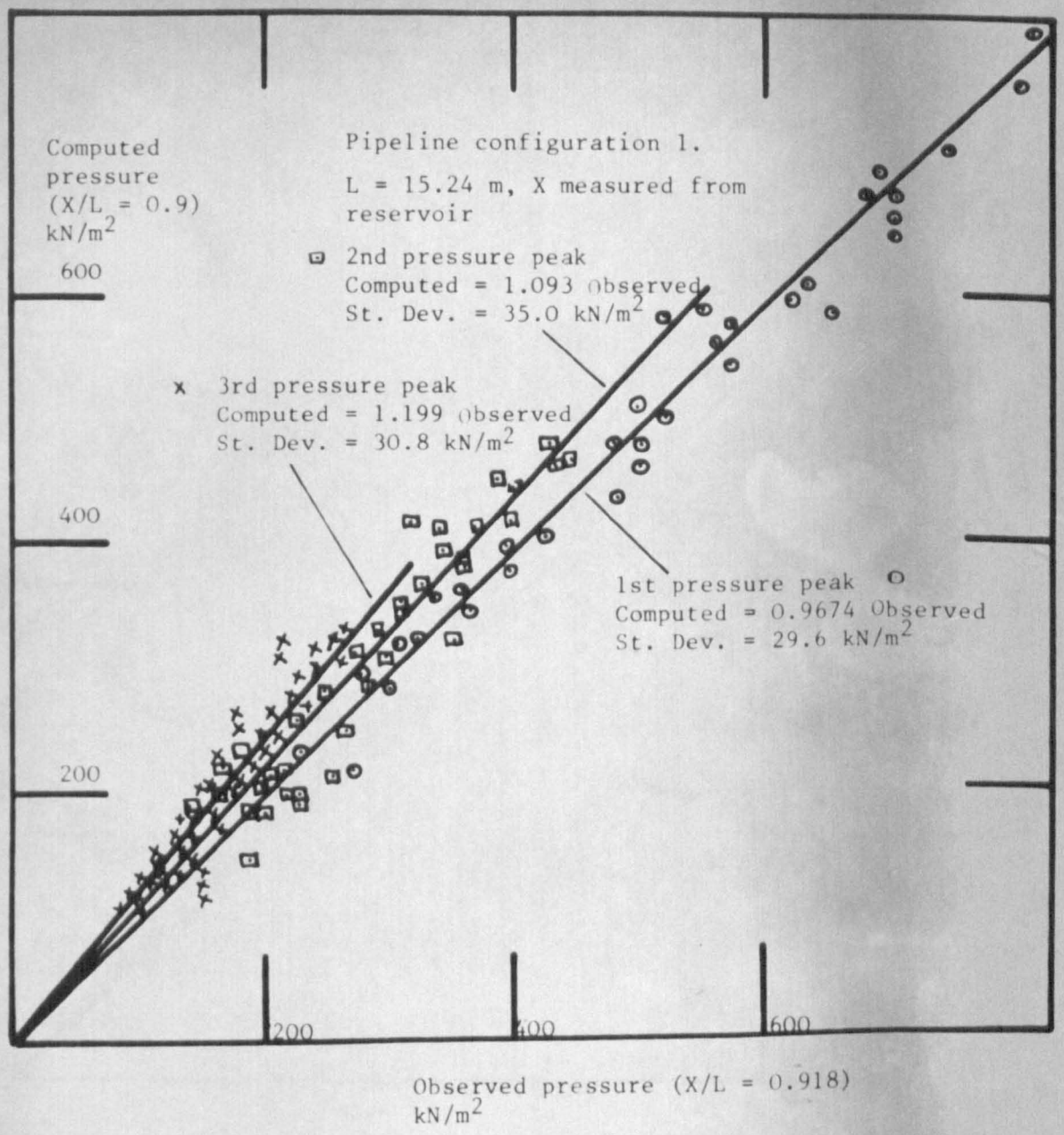

Fig. 67 Comparison between the computed and observed values of the pressure rise above steady state at the 1st and 3rd recorded pressure peaks following valve closure.

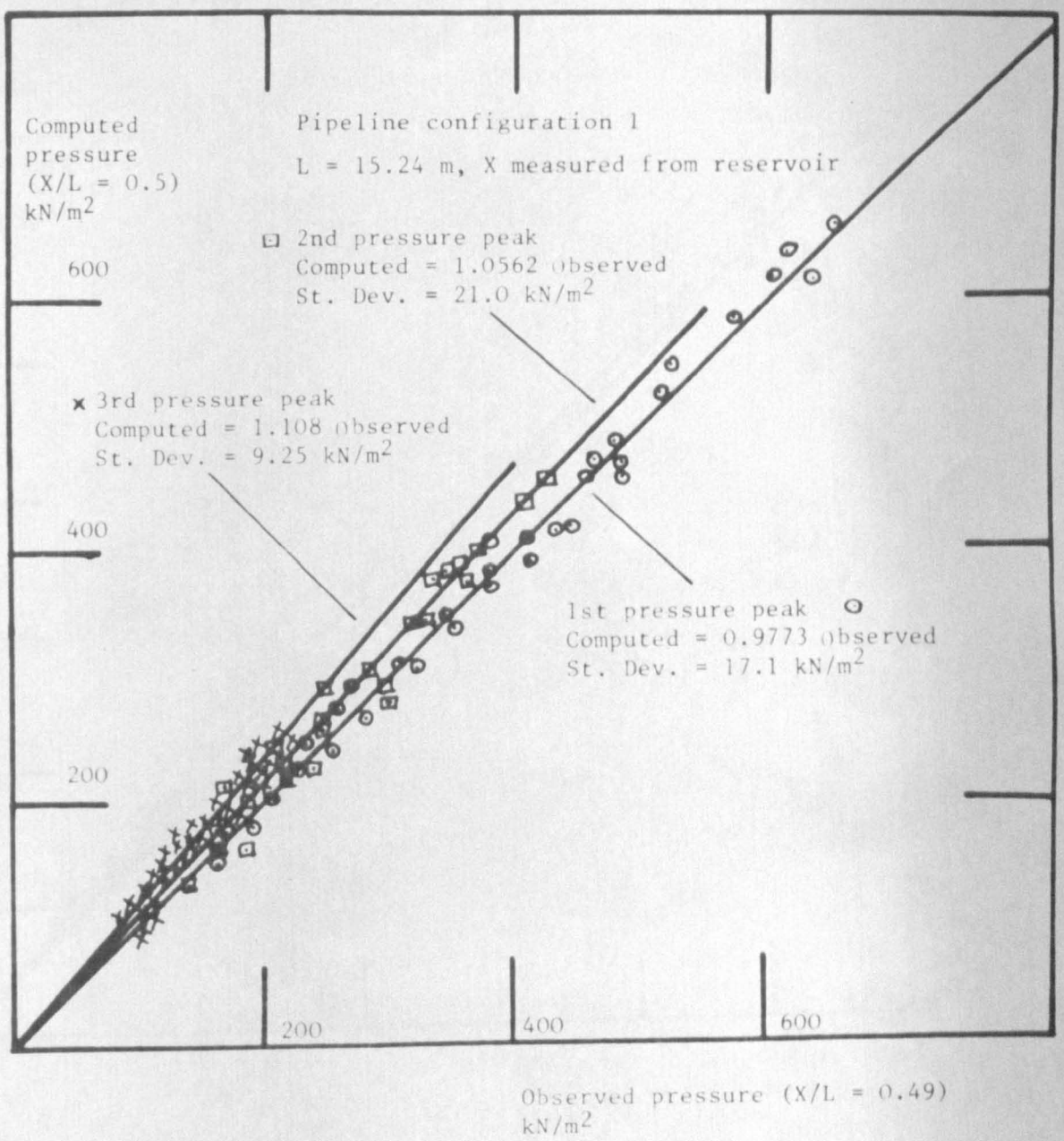

Fig. 68 Comparison between the computed and observed values of the pressure rise above steady state at the 1st to 3rd recorded pressure peaks following valve closure.

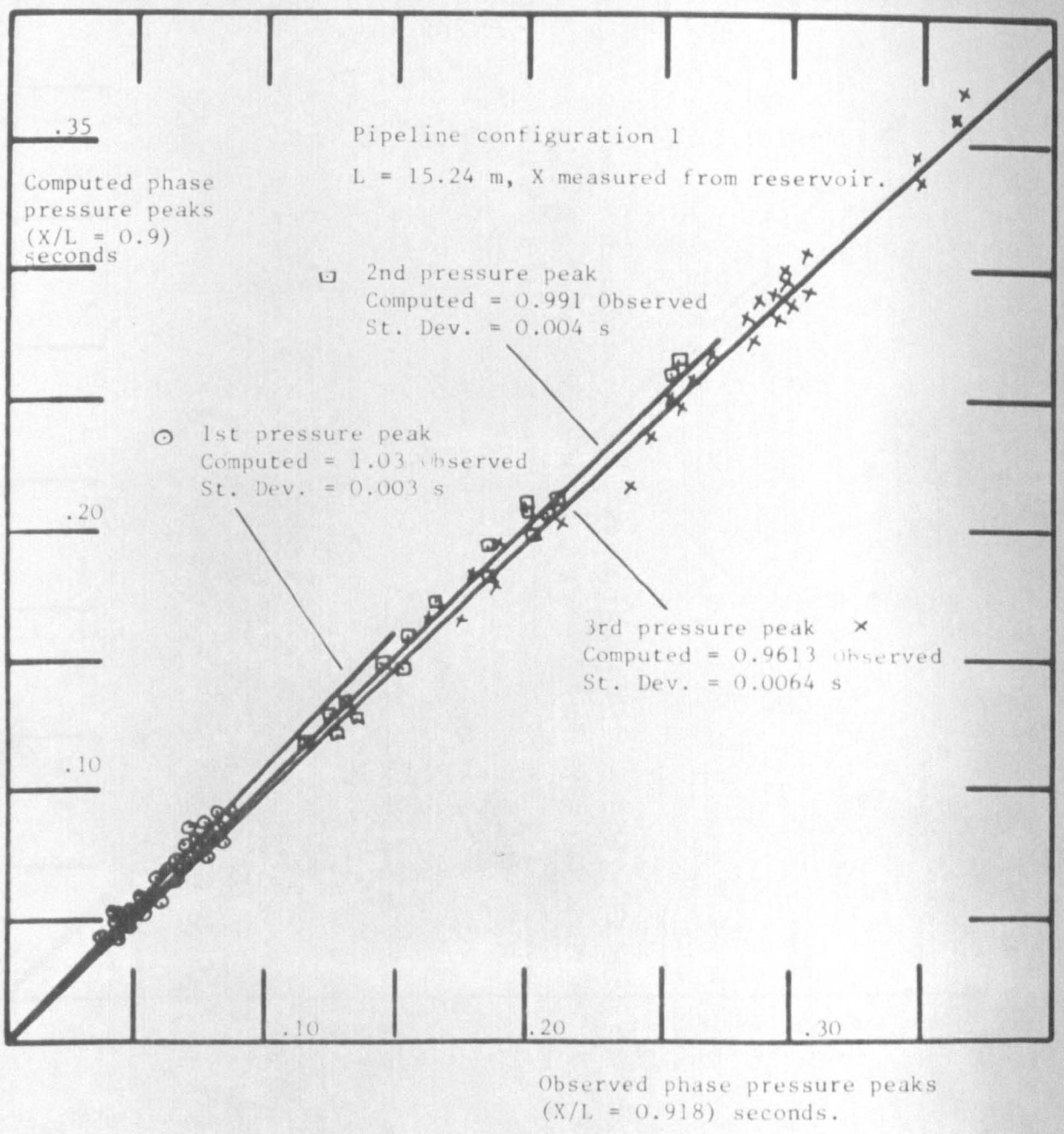

Fig. 69 Comparison between the computed and observed phase of the 1st to 3rd pressure peaks at X/L = 0.9 following valve closure.

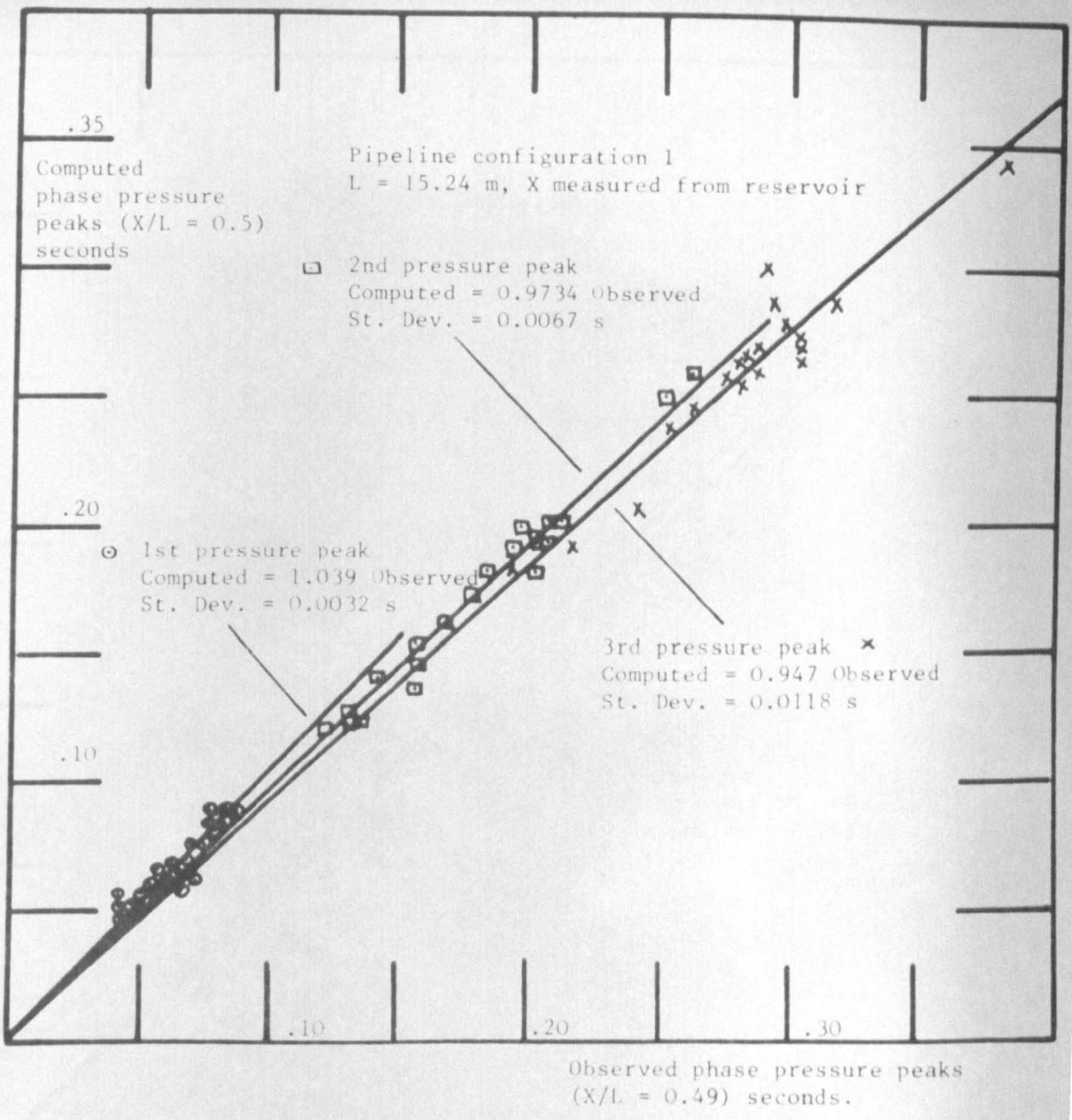

Fig. 70 Comparison between the computed and observed phase of the 1st to 3rd pressure peaks at X/L = 0.5 following valve closure.

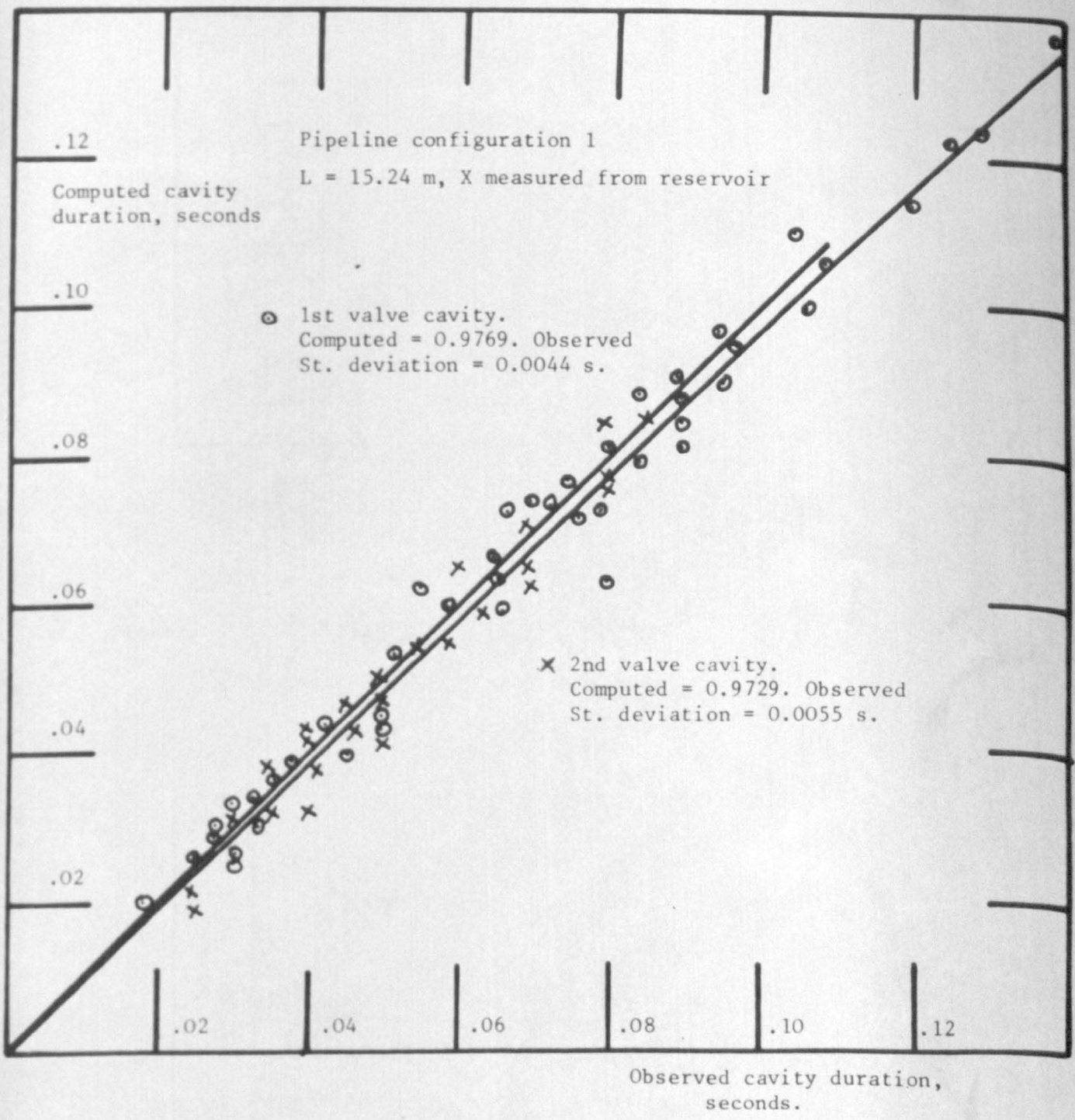

Fig. 71 Comparison between the observed and computed duration of the 1st and 2nd vapour cavities formed upstream of the valve.

Pipeline configuration 1.

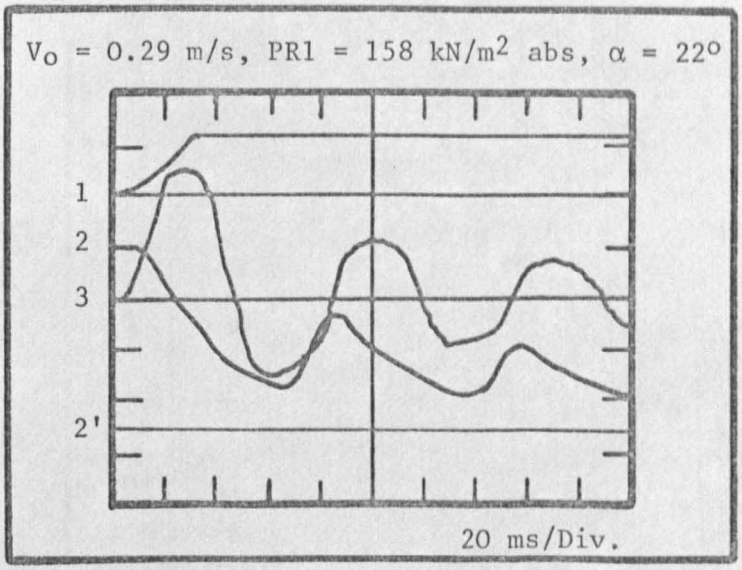

Fig. 72 Pressure and centre line velocity variation following a rapid valve closure recorded 1.25 m upstream of the valve.
DISA. overheat ratio on 55A82 - 1.10

Traces
1. L.D.T.
2. DISA probe, 2' - zero velocity line - 5 volts/Div.
3. Pressure variation - 90 kN/m^2/Div.

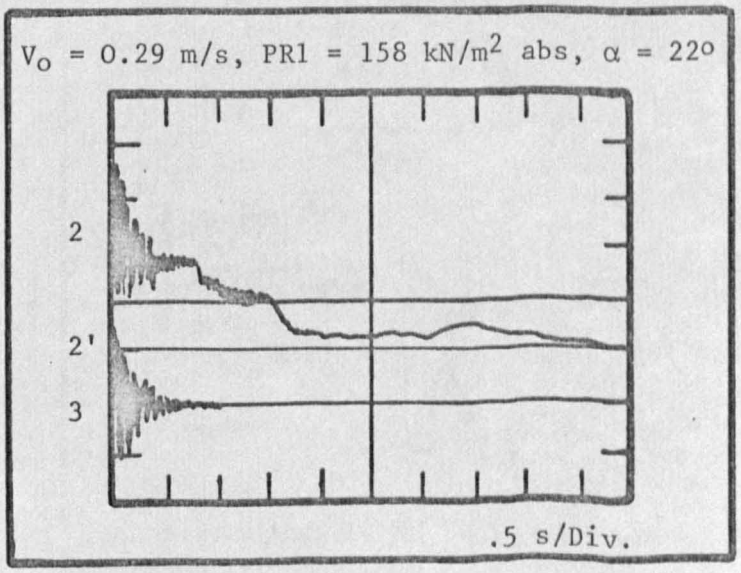

Pipeline configuration 1

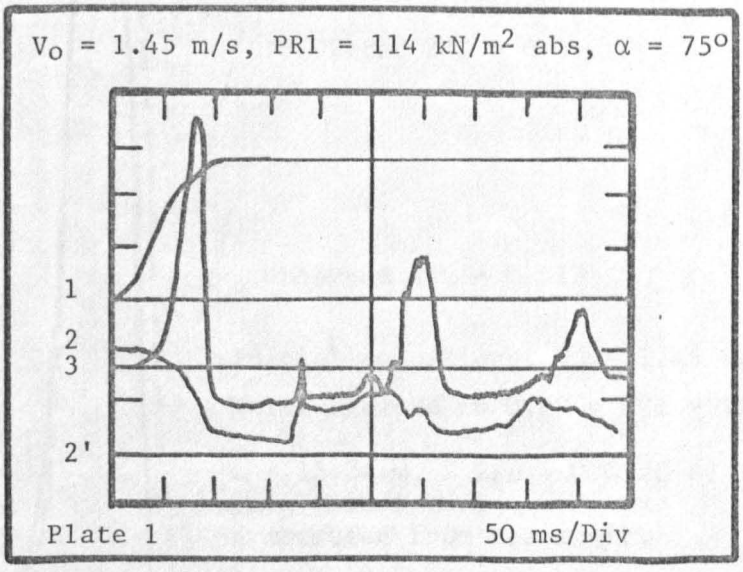

Fig. 73 Pressure and centre line velocity variation 1.25 m upstream of the valve following closure. DISA 55A82 probe used, unlinearized, overheat ratio = 1.10

Traces
1. L.D.T.
2. DISA 55A82, 2' - zero velocity line.
3. Pressure variation.

Scales: Plate 1 225 kN/m^2/Div., 5 volts/Div. DISA
Plate 2 450 kN/m^2/Div., 5 volts/Div. DISA

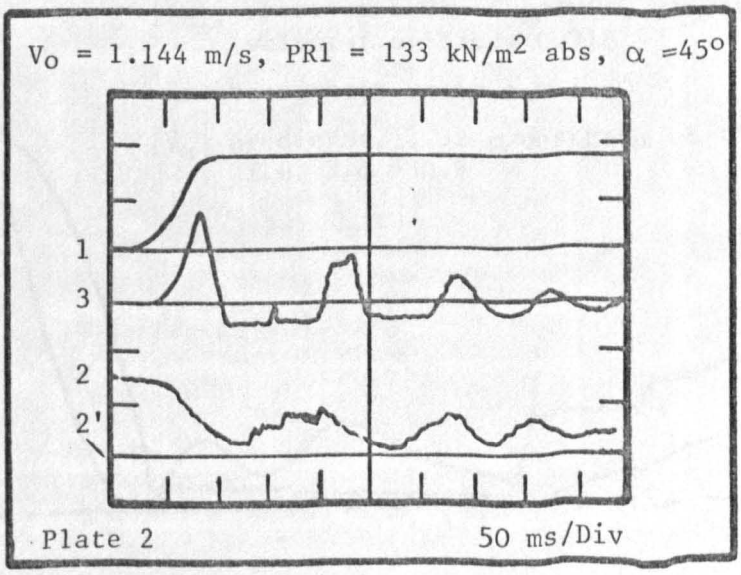

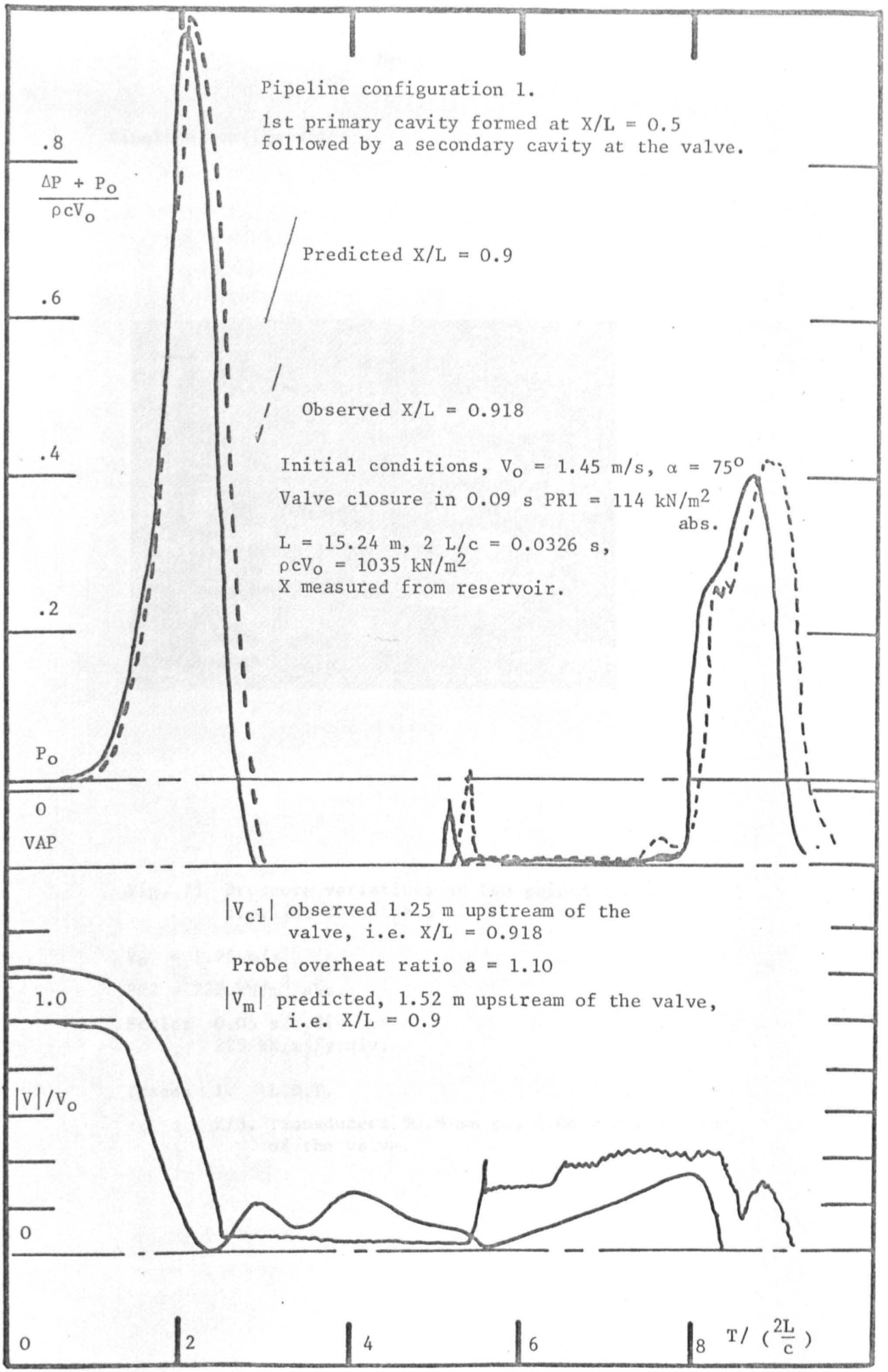

Fig. 74 Pressure and centre line velocity variations compared to those predicted upstream of the valve following closure.

Pipeline configuration 2.

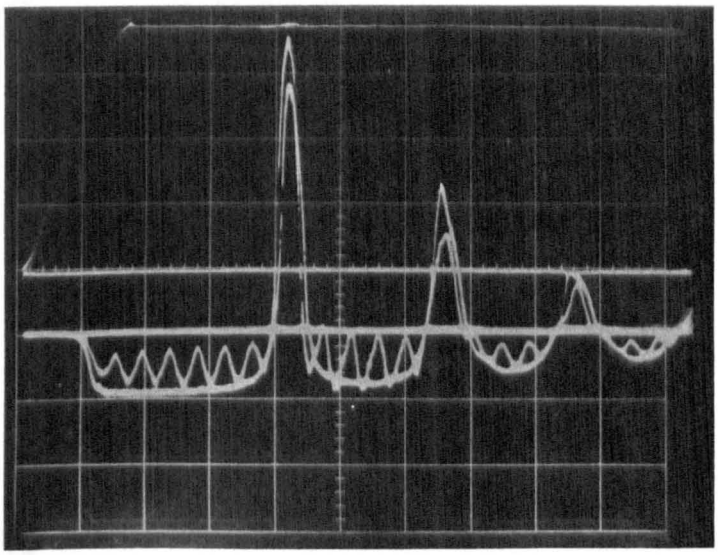

Fig. 75 Pressure variations at two points along the pipeline downstream of the valve.

V_o = 1.75 m/s

PR2 = 222 kN/m^2 abs.

Scale: 0.05 s/x.div.
225 kN/m^2/y.div.

Traces 1. L.D.T.

2/3. Transducers 50.8 mm and 4.04 m downstream of the valve.

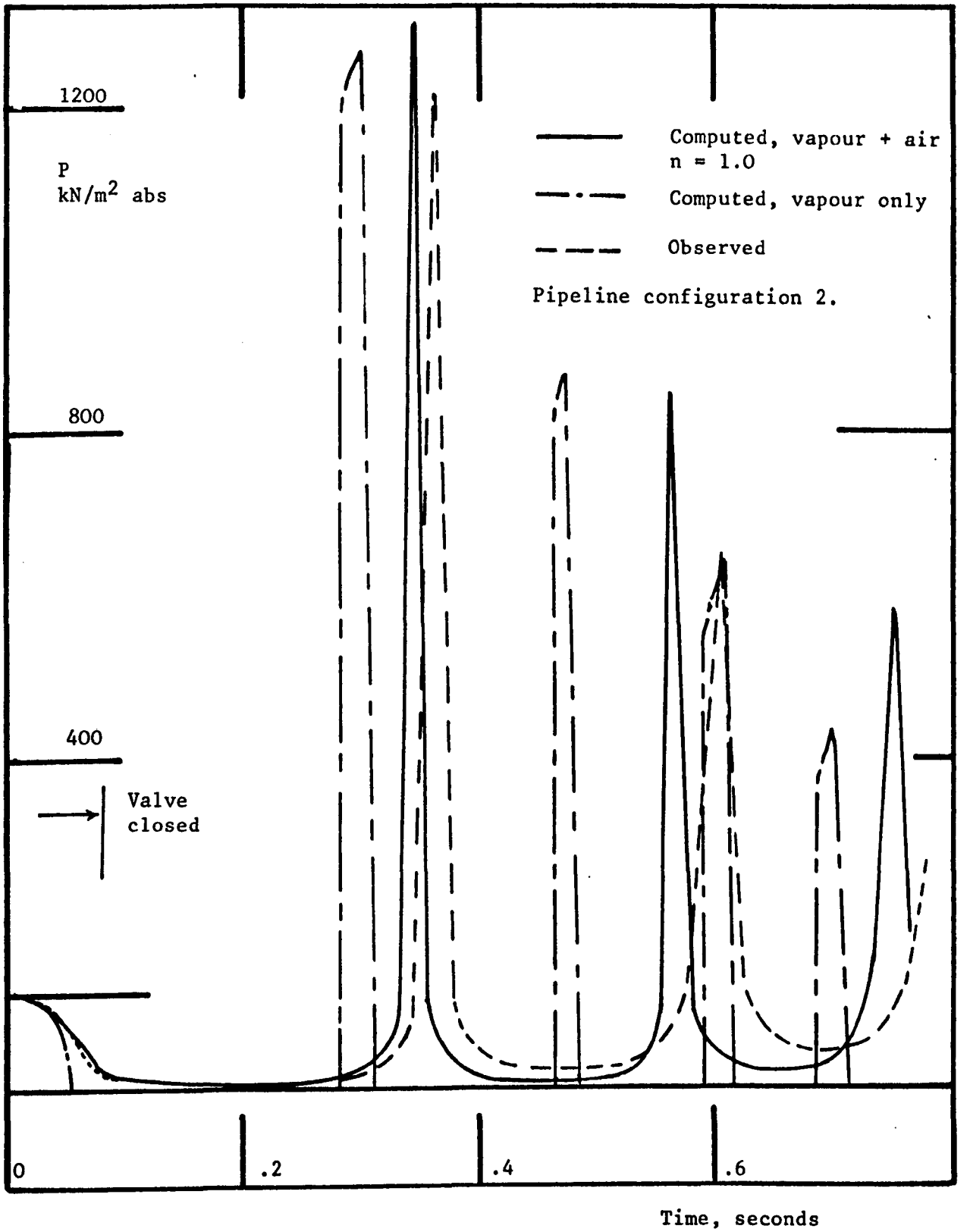

Fig. 76 Comparison between the observed pressure variation at the valve downstream face and the predicted pressure variations from both the vapour only (SEPE) and vapour + air (SEPF) programs. Initial conditions, V_o = 1.75 m/s, PR2 = 102 kN/m^2 abs.

Fig. 77 Plate 1 illustrates the pressure variations recorded on the downstream face of the valve, in pipeline configuration 2G, during closure and subsequent column separation.
Plates a - j are reproduced from the high speed film, 1000 frames/second, made of the column separation at the valve for the same test case as Plate 1. Plates a - i illustrate the growth and collapse of the first and second cavities while Plate j illustrates the residual air at the valve after the transients have damped out.

Pipeline configuration 2G.

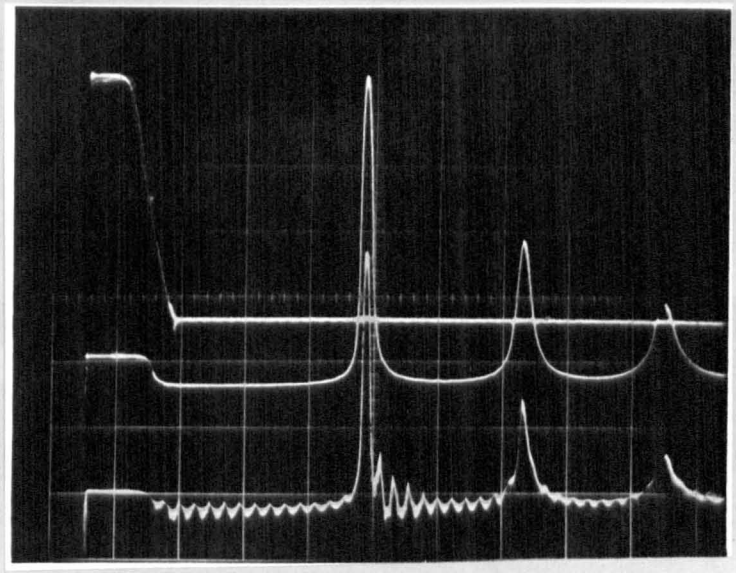

Fig. 77 Plate 1. Pressure variation at two points downstream of the valve.

V_o = 1.75 m/s, PR2 = 102 kN/m^2 abs.,

Traces
1. L.D.T.
2. Transducer 50.8 mm downstream of the valve.
3. Transducer 4.3 m downstream of the valve.

Scales:
225 kN/m^2/y.div.
0.1 s/x.div.

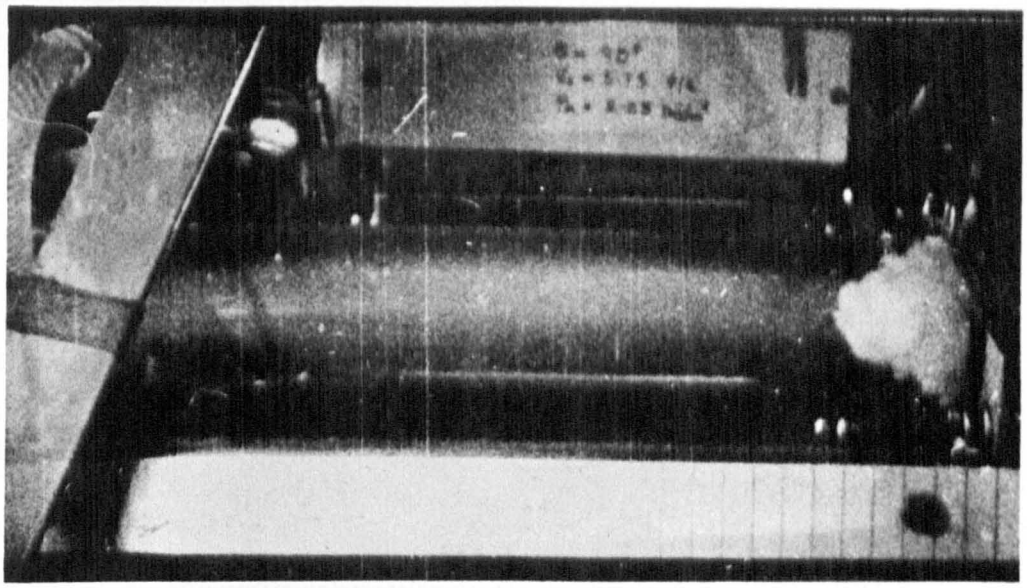

a. 0·054 s.

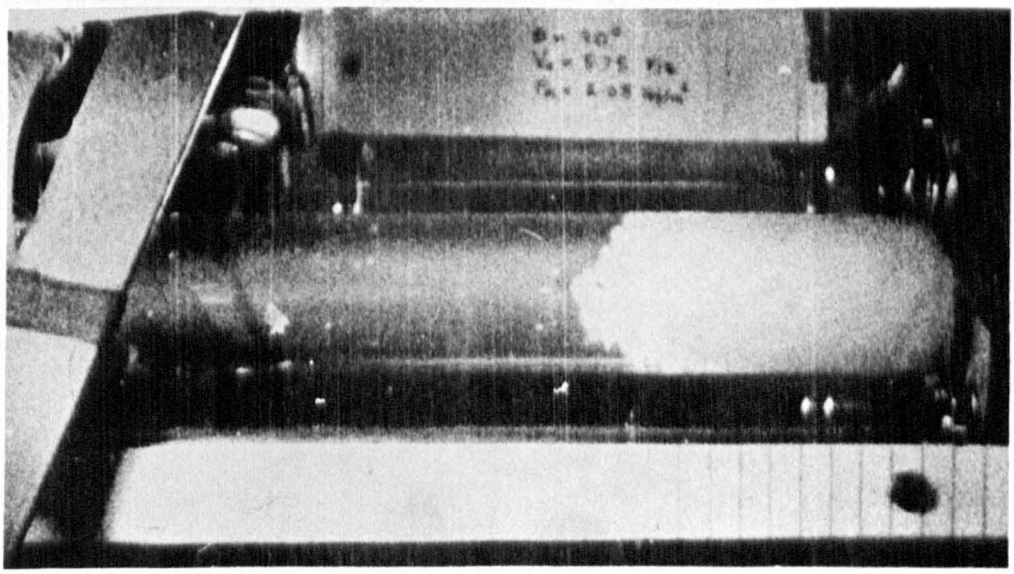

b. 0·096 s.

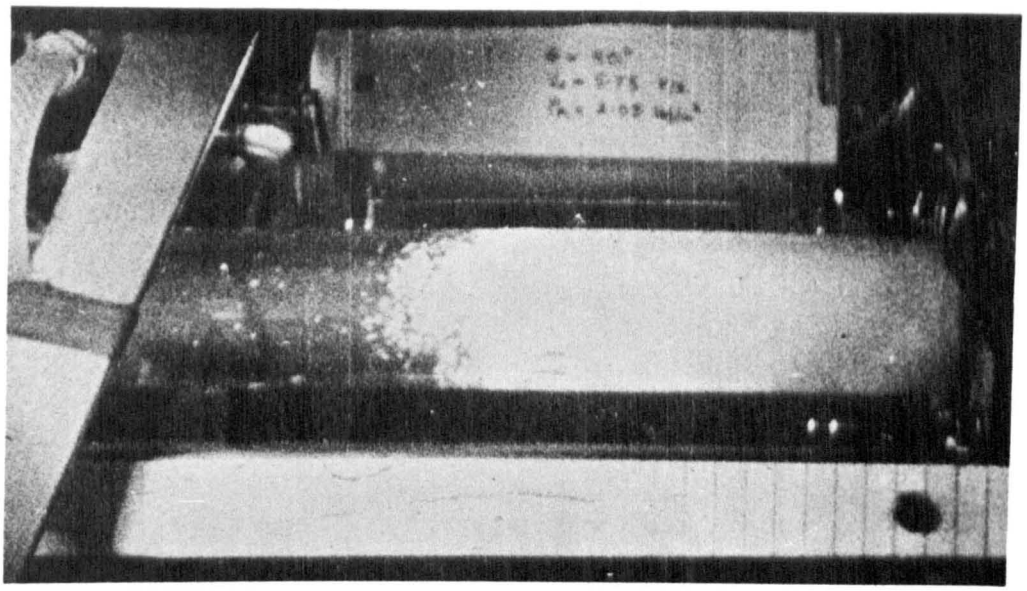

c. 0·164 s.

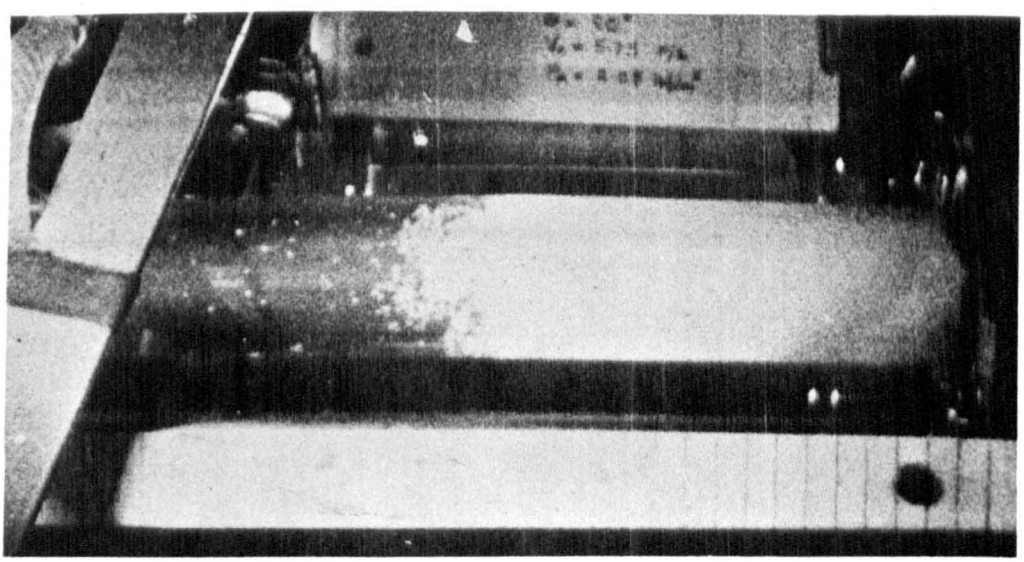

d. 0·236 s.

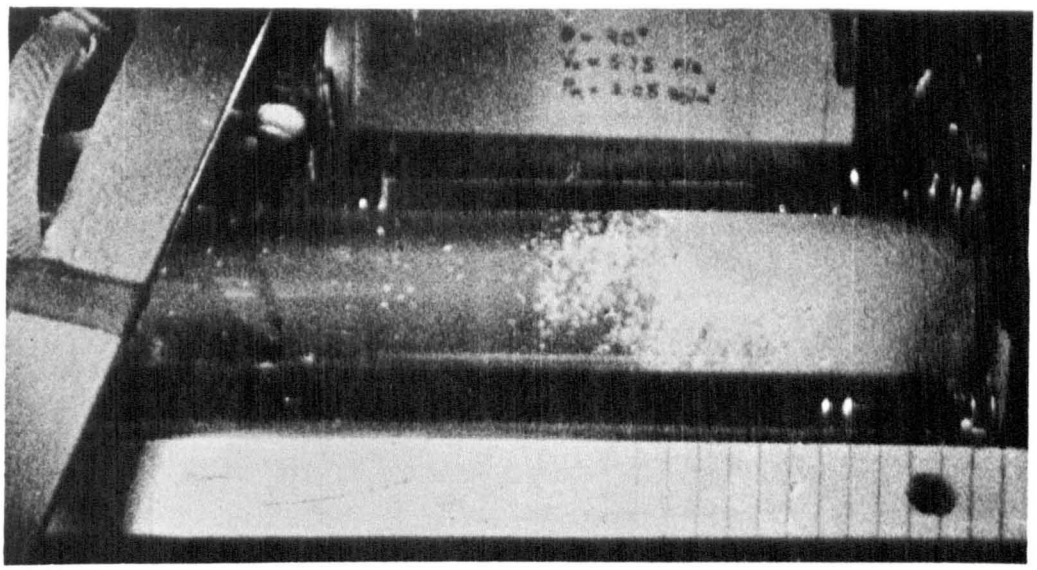

e. 0·284 s.

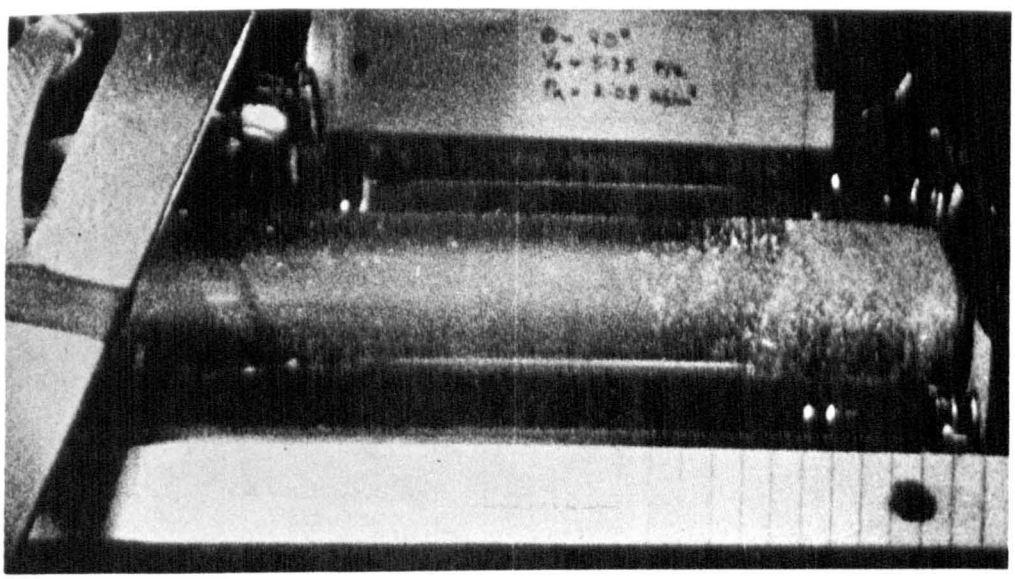

f. 0·314 s.

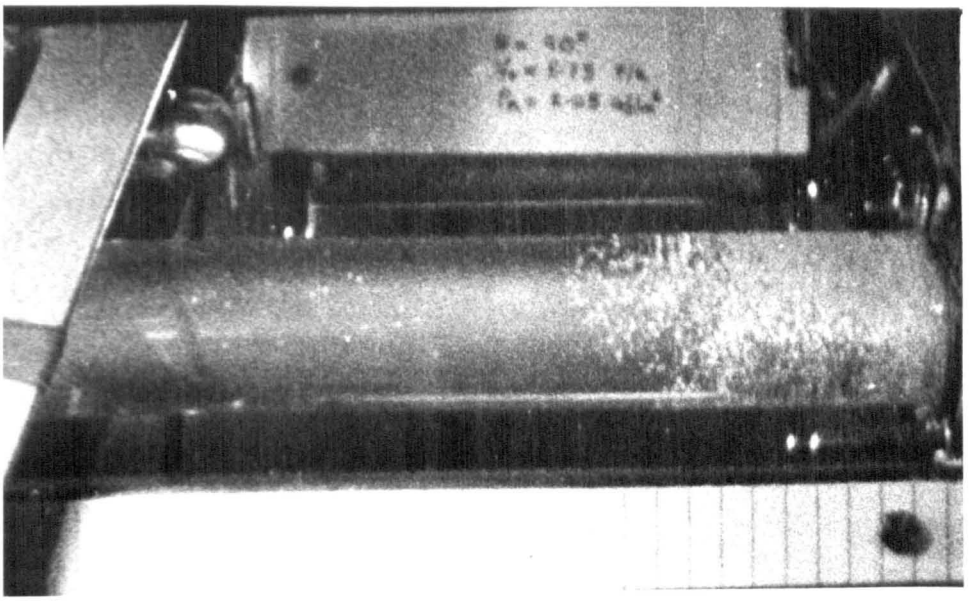

g. 0·47 s.

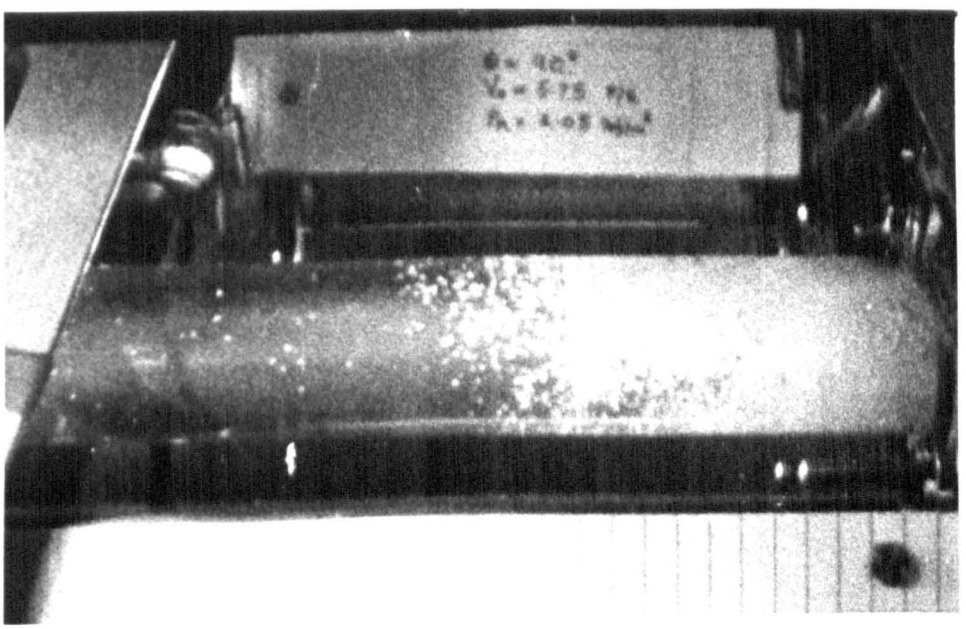

h. 0·52 s.

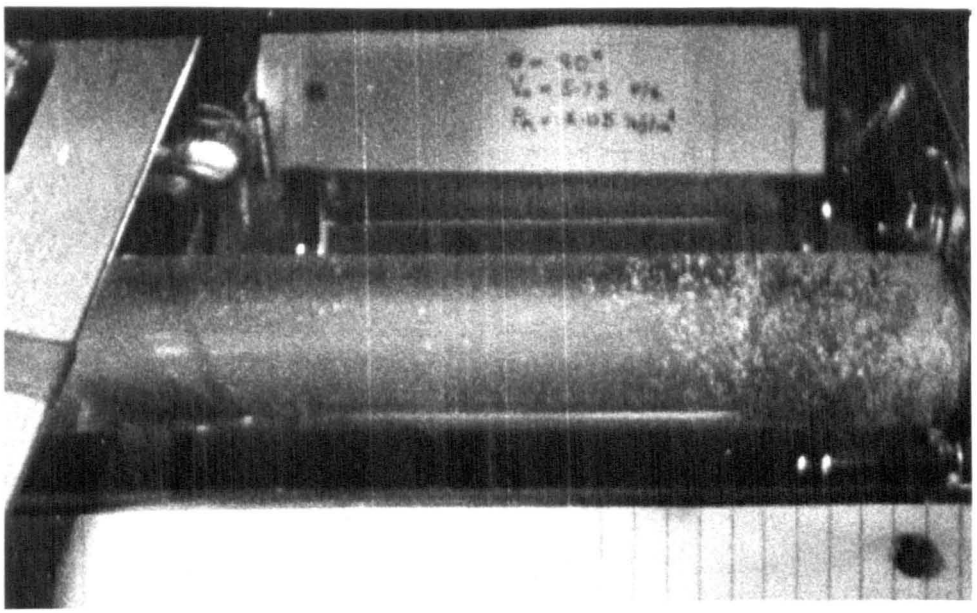

i. 0·58 s.

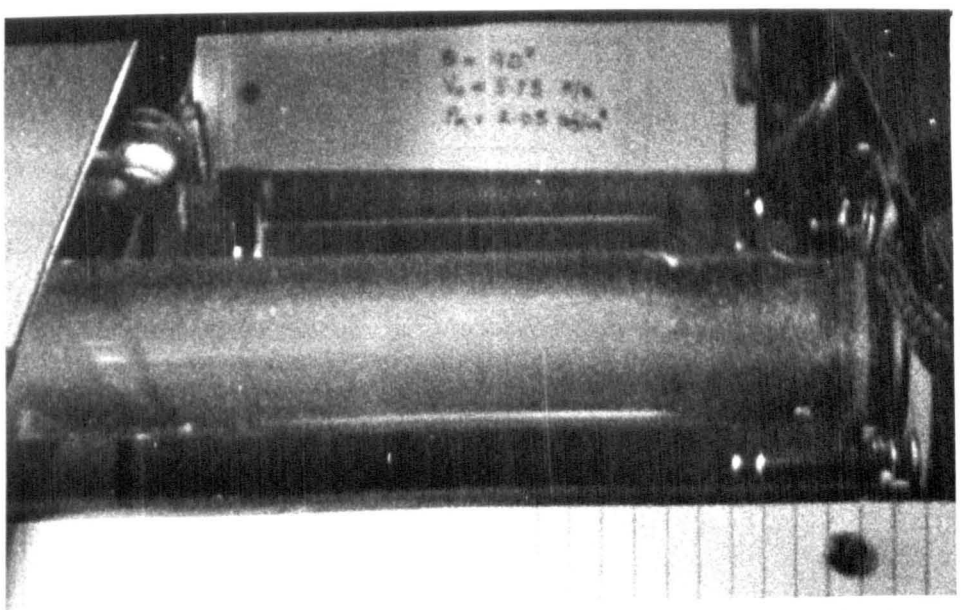

j. 4·0 s.

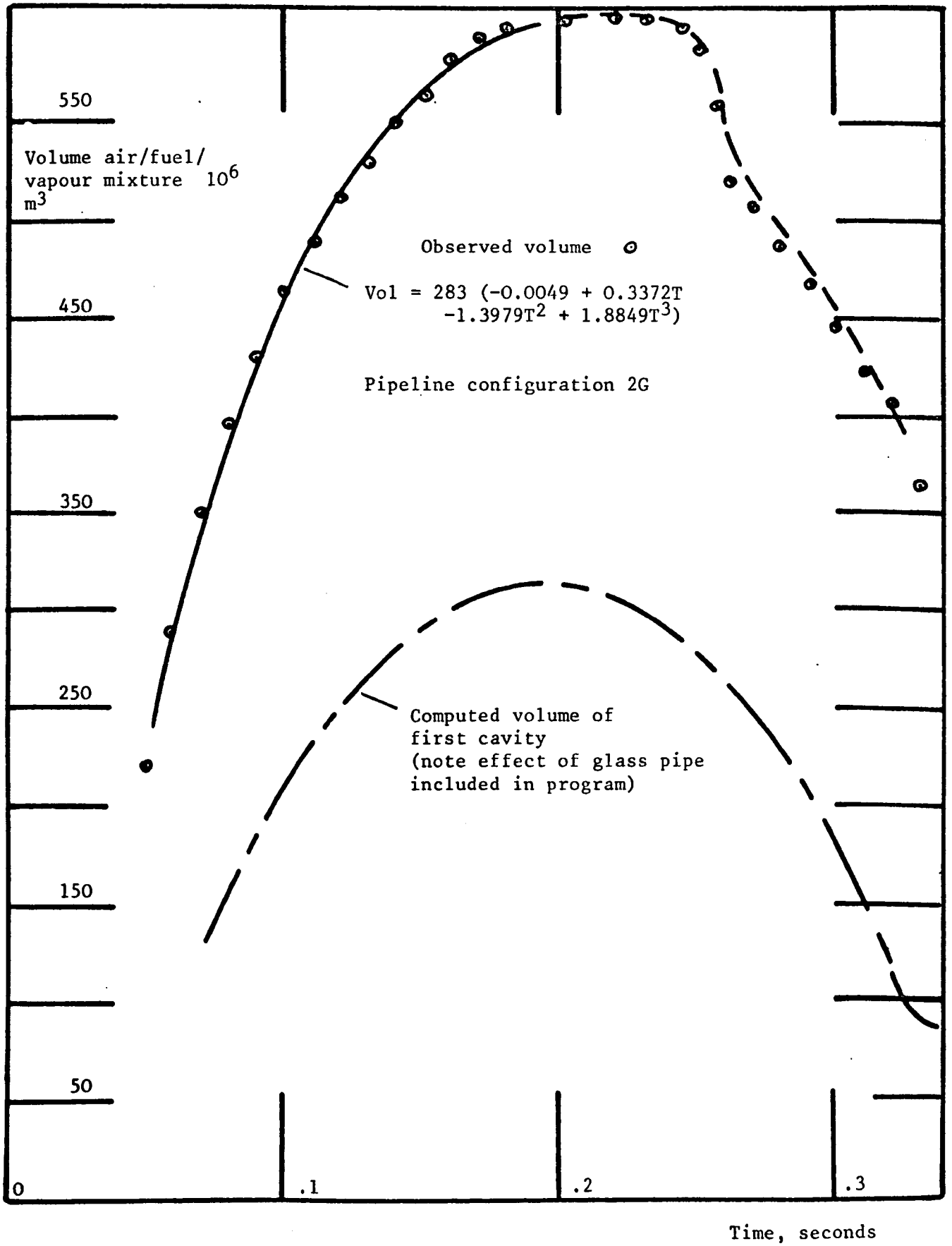

Fig. 78 Comparison between the observed and predicted cavity volume for the first cavity formed following valve closure. Initial conditions, V_o = 1.75 m/s, PR2 = 102 kN/m^2 abs, TC = 0.08 s.

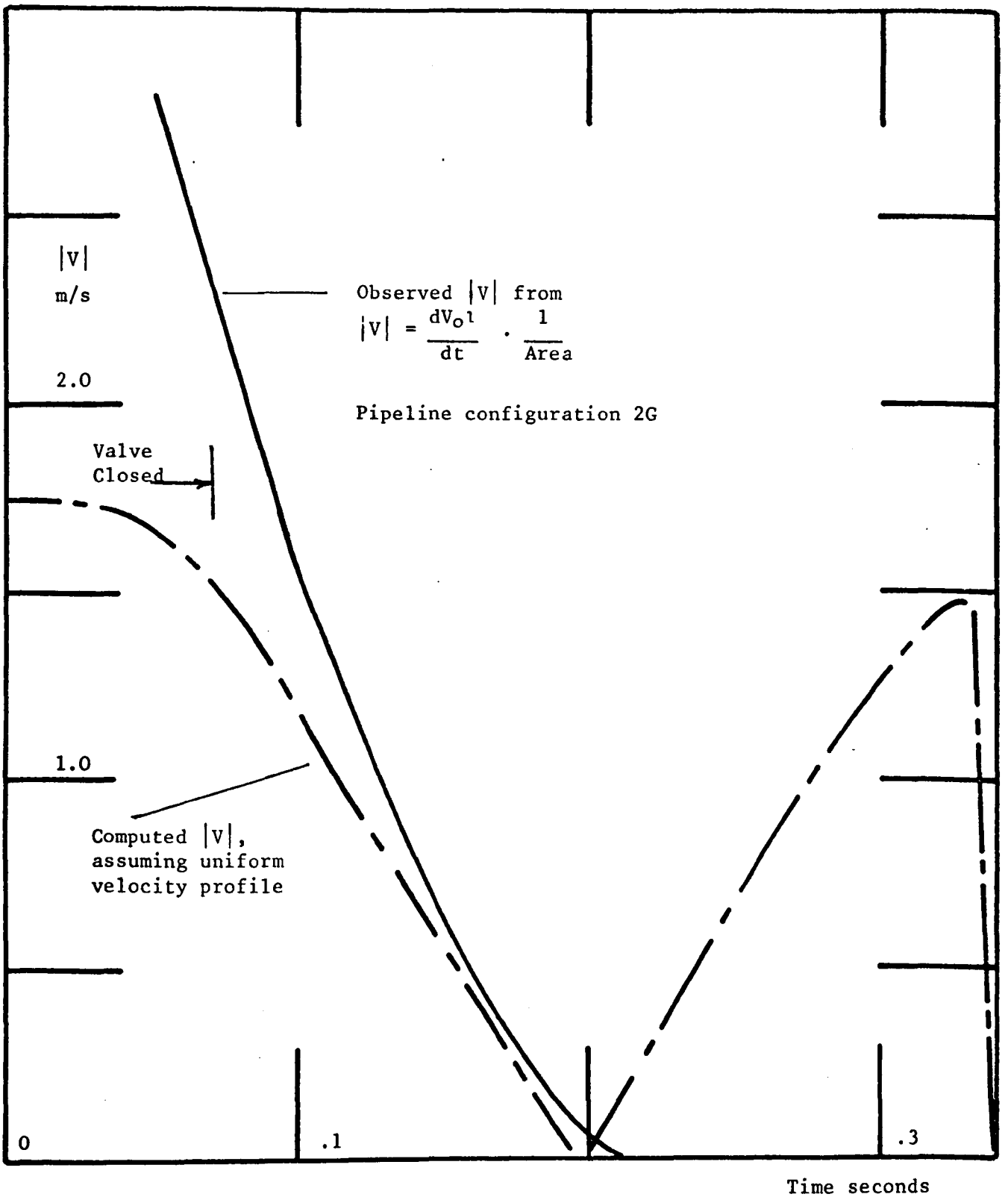

Fig. 79 Comparison between observed and computed fuel - cavity interface velocity for the first cavity formed following valve closure. Initial conditions, V_o = 1.75 m/s, PR2 = 102 kN/m^2 abs, TC = 0.08 s.

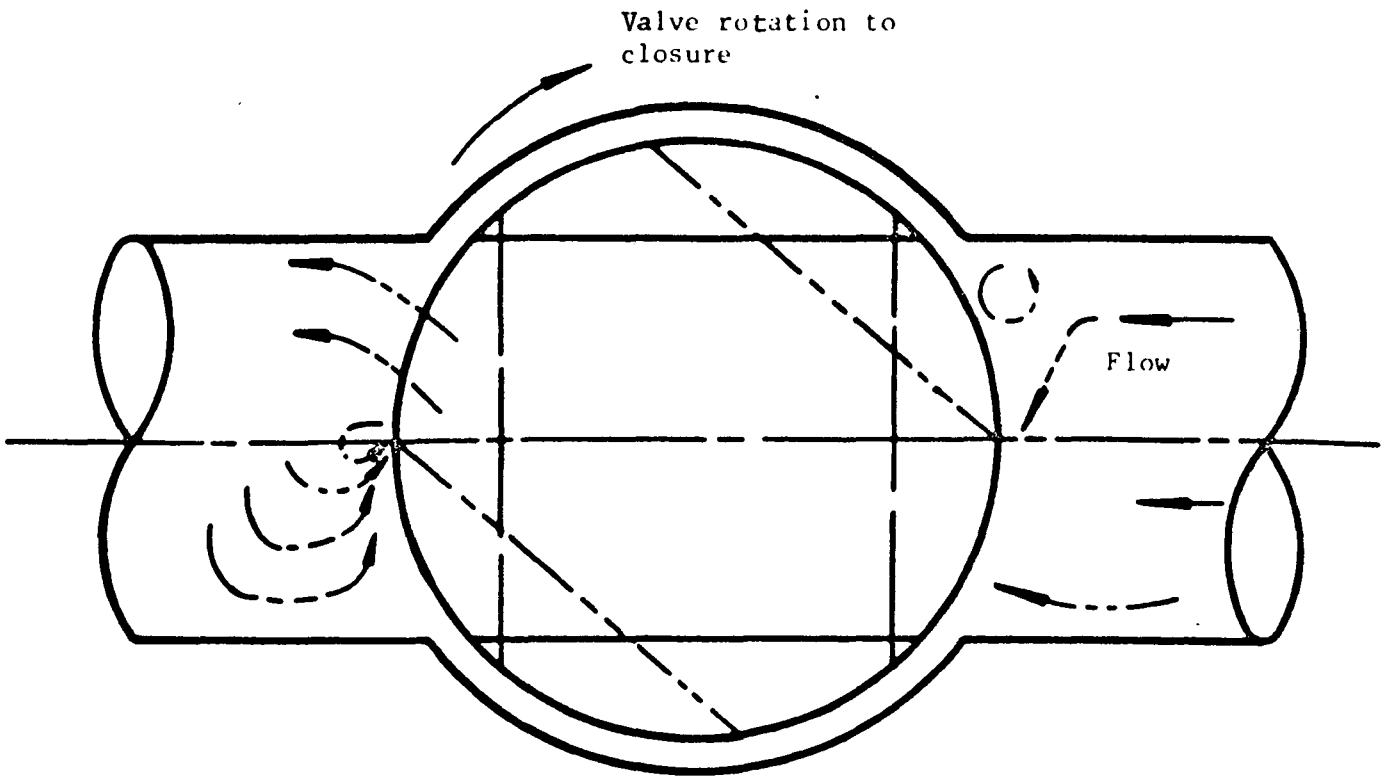

Valve fully open

Valve 45° open

Valve fully shut

Fig. 80 Probable flow through a spherical plug valve during closure

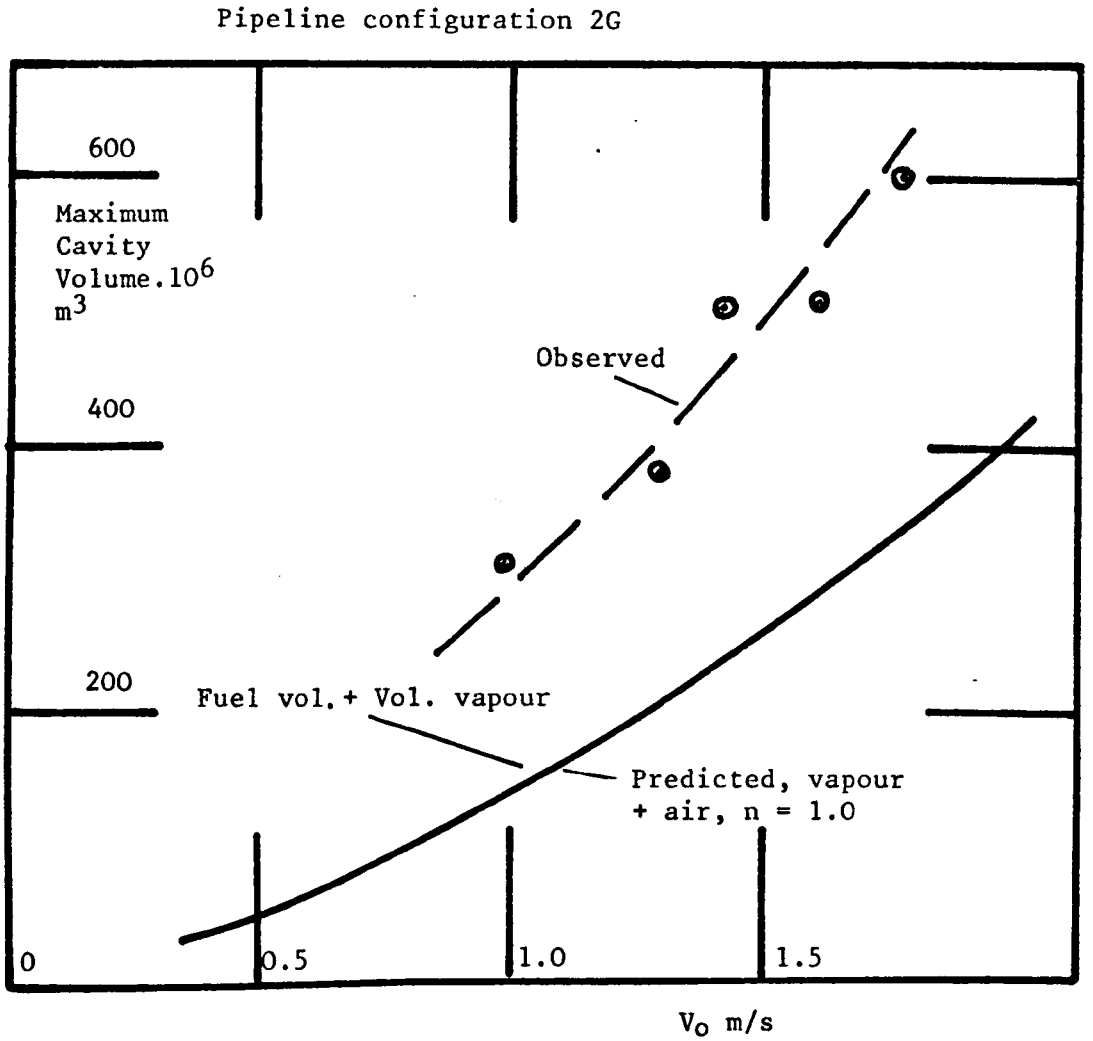

Fig. 81 Comparison between the maximum observed extent of the vapour/fuel/air mixture and that predicted by the analysis of the glass/aluminium pipeline.

Downstream reservoir pressure constant at 102 kN/m^2 abs., valve overall closure in 0.08 s.

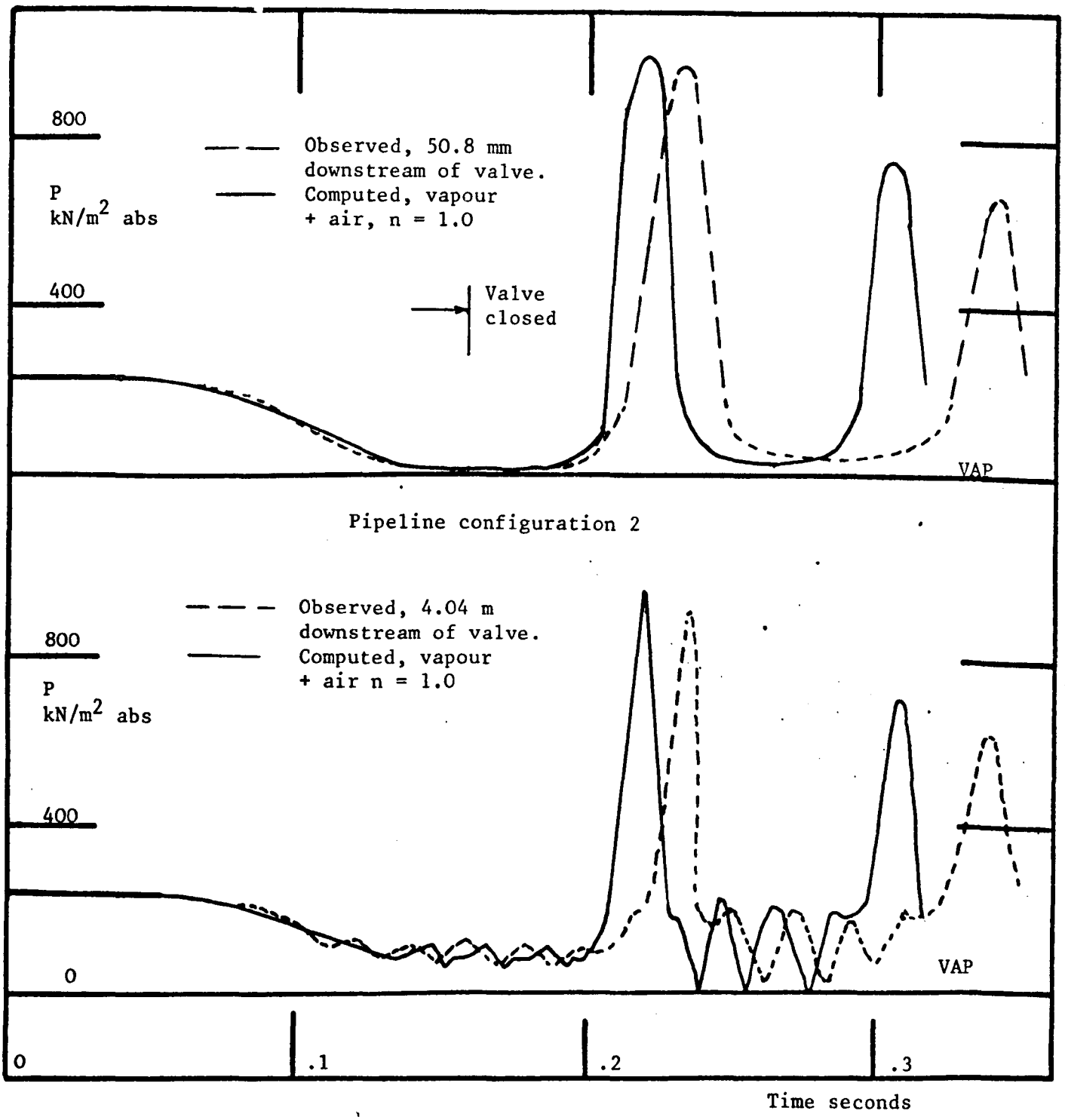

Fig. 82 Comparison between the observed and predicted pressure variations at two points along the pipeline downstream of the valve. Initial test conditions, V_o = 1.75 m/s, PR2 = 222 kN/m^2 abs, and an overall valve closure time of 0.16 s.

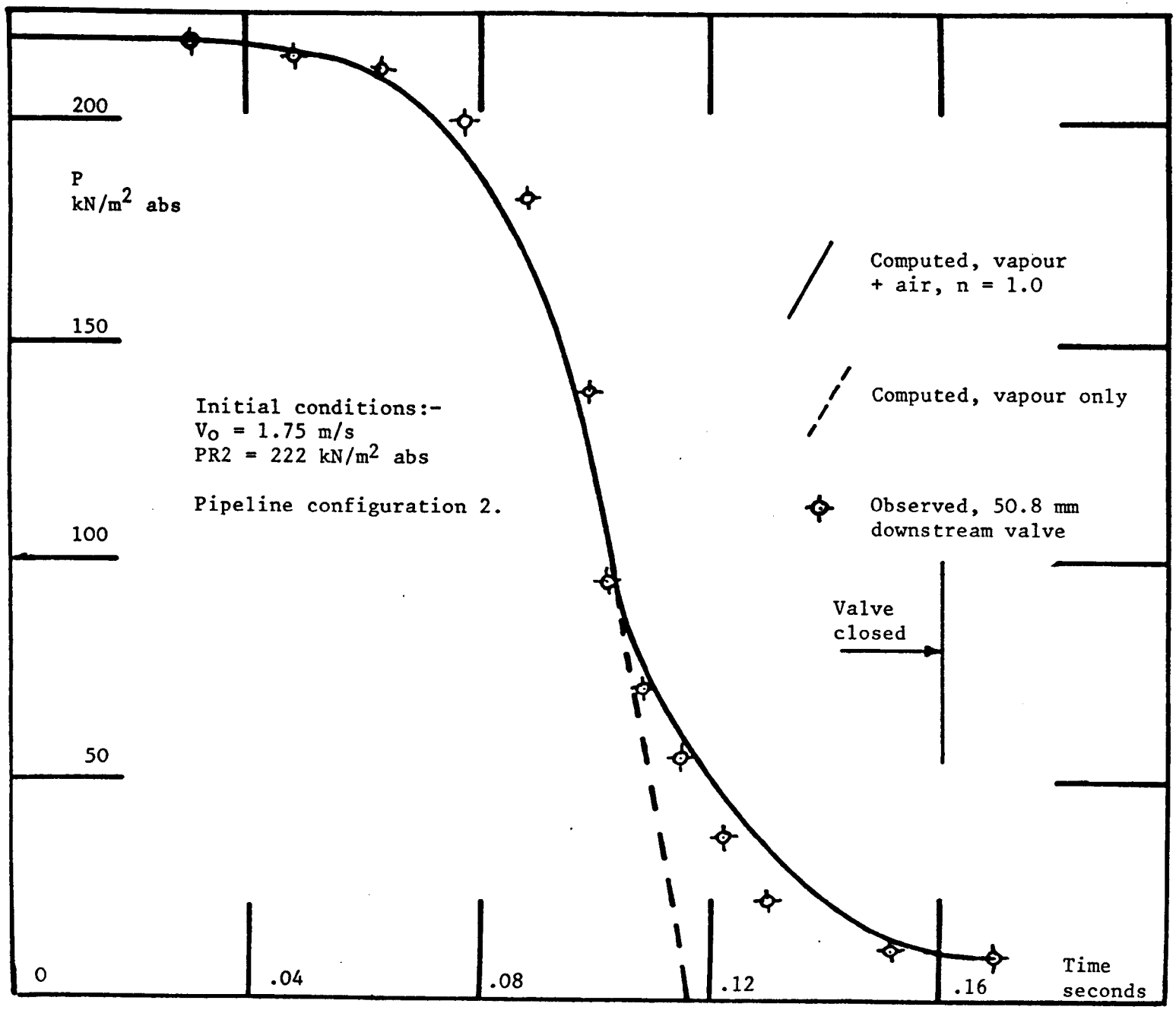

Fig. 83 Pressure reduction at the valve during closure.

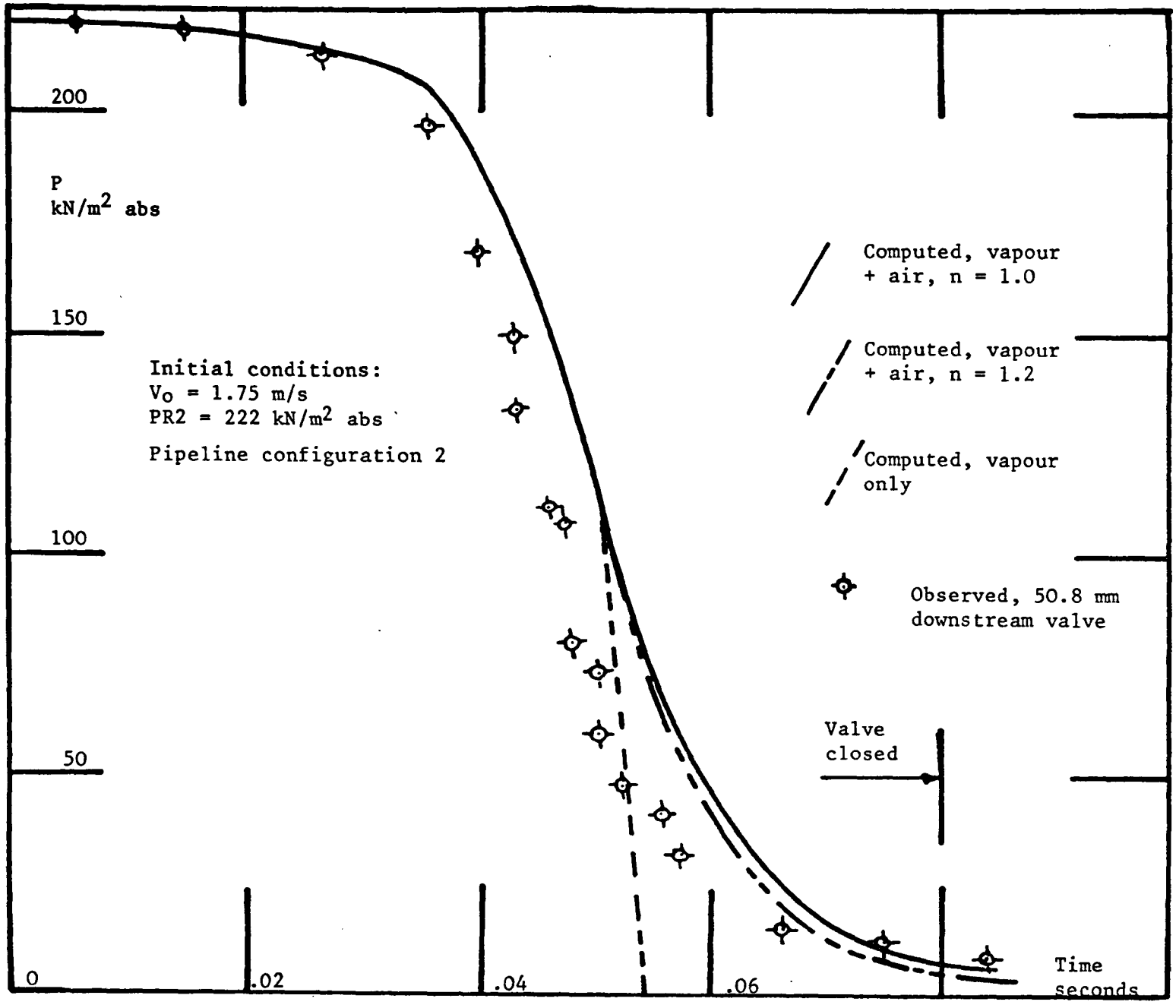

Fig. 84 Pressure reduction downstream of the closing valve.

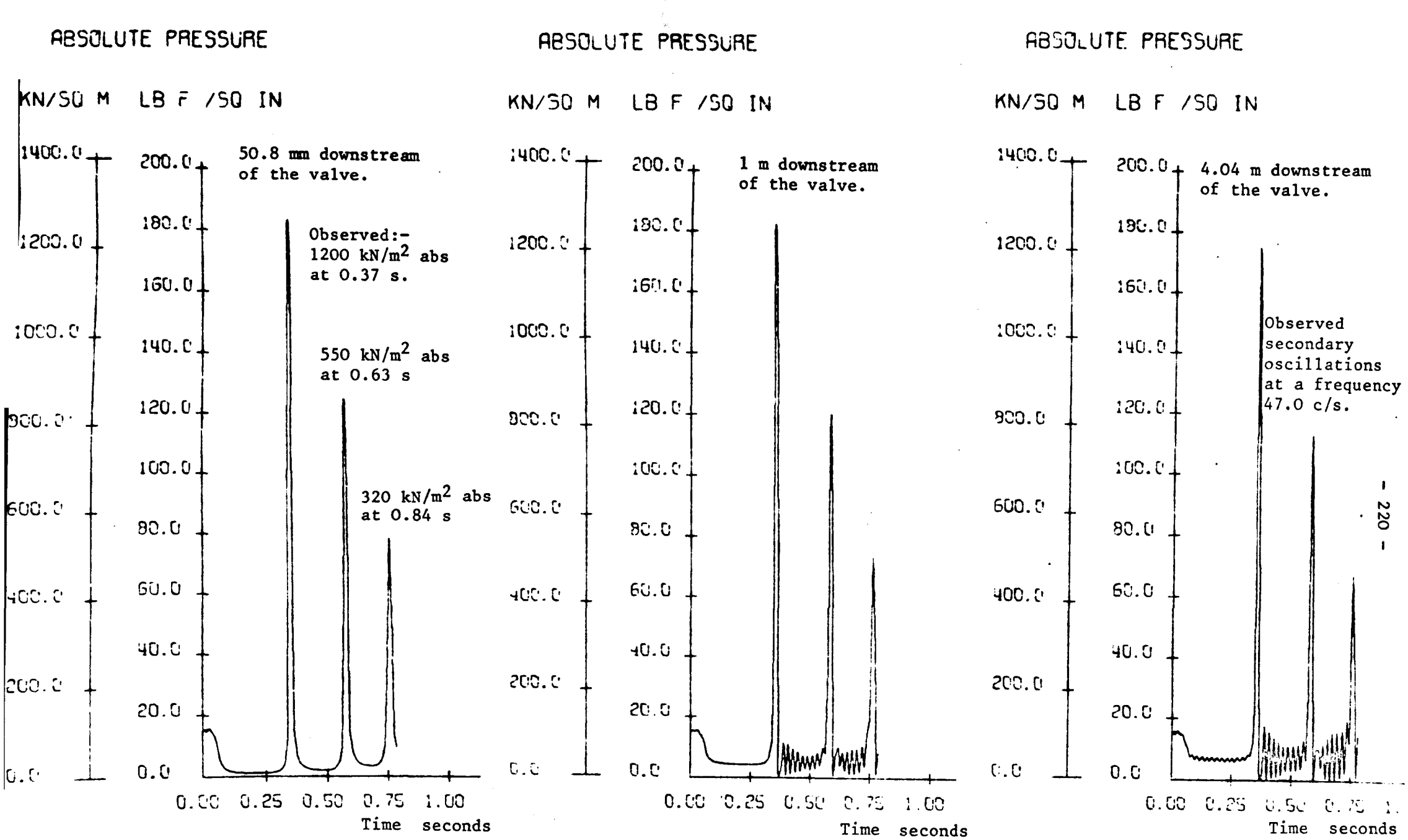

Fig. 85 Predicted pressure variations at three points downstream of the valve in pipeline configuration 2. Initial conditions: V_o = 1.75 m/s, PR2 = 102 kN/m^2 abs, valve closure in 0.08 s. The values of peak pressure and cavity collapse times are indicated above.

Fig. 86 Plates 1 - 6 illustrate the effect of varying the overall valve closure time (TC) for a range of initial flow velocities (V_o) and downstream reservoir pressures (PR2).

Common scales for plates 1 - 6:

1.	L.D.T.	.5 volts/y div.	
2.	Pressure transducers	225 kN/m^2/y div.	
3.	Time base	0.05 sec/x div.	(Plates 1-4)
		0.10 sec/x div.	(Plates 5-6)

Common trace layout from the top of each plate:

1. L.D.T.
2. Pressure transducer 5.08 cm downstream of valve.
3. " " 4.04 m " " "

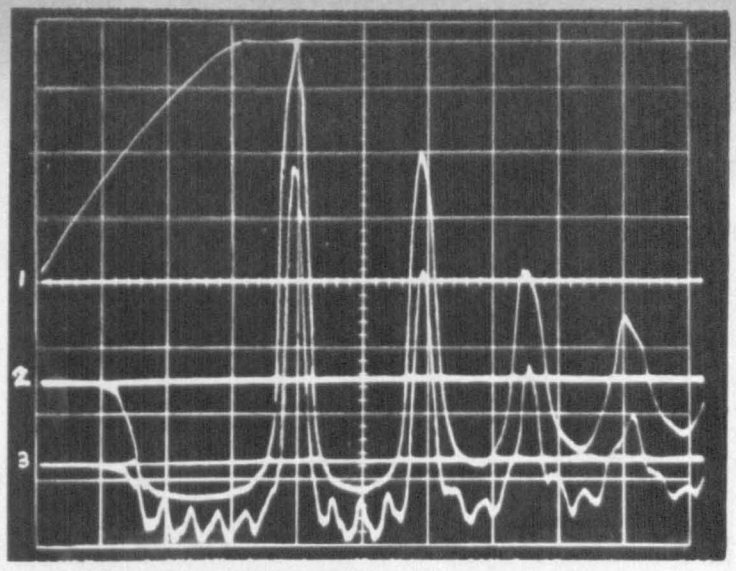

Fig. 86 Plate 1.

V_o = 2.743 m/s
PR2 = 413 kN/m^2 abs.
TC = 0.15 s

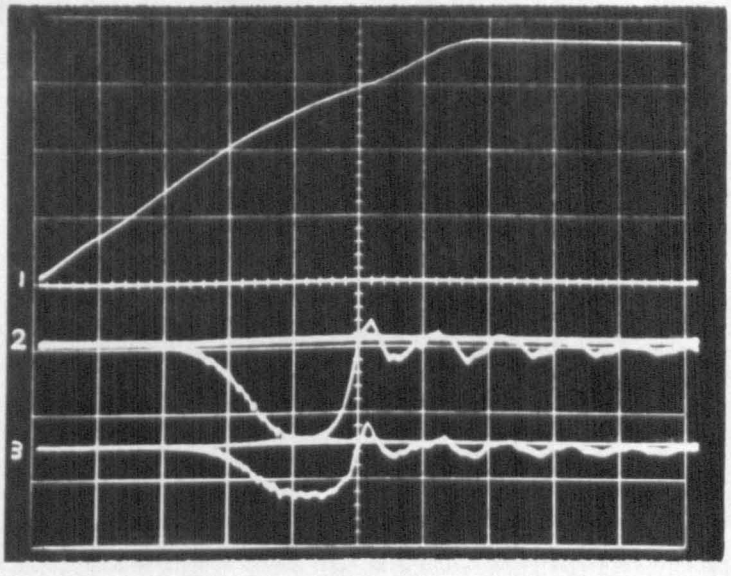

Fig. 86 Plate 2.

V_o = 2.743 m/s
PR2 = 413 kN/m^2 abs.
TC = 0.34 s

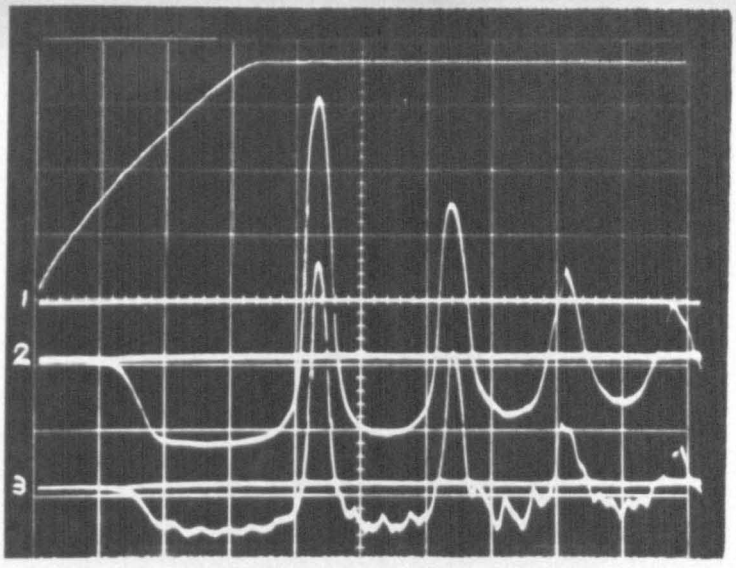

Fig. 86 Plate 3.

V_O = 2.29 m/s
PR2 = 309 kN/m^2 abs.
TC = 0.17 s

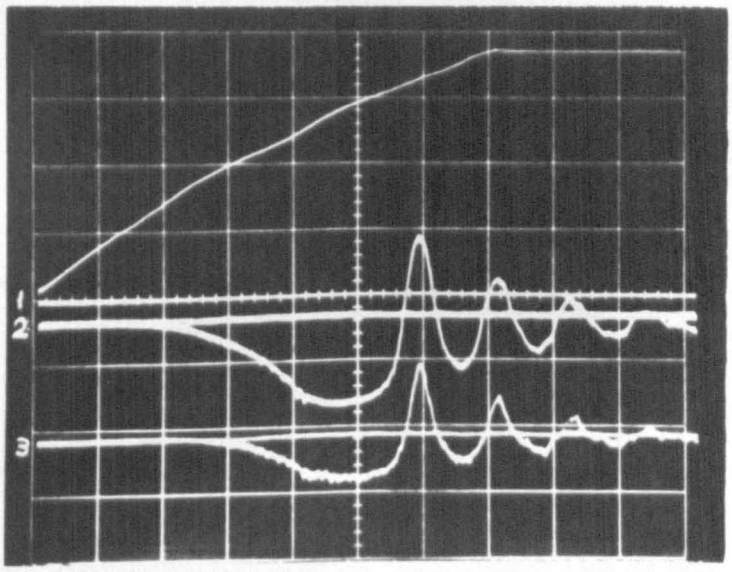

Fig. 86 Plate 4.

V_O = 2.29 m/s
PR2 = 309 kN/m^2 abs.
TC = 0.36 s

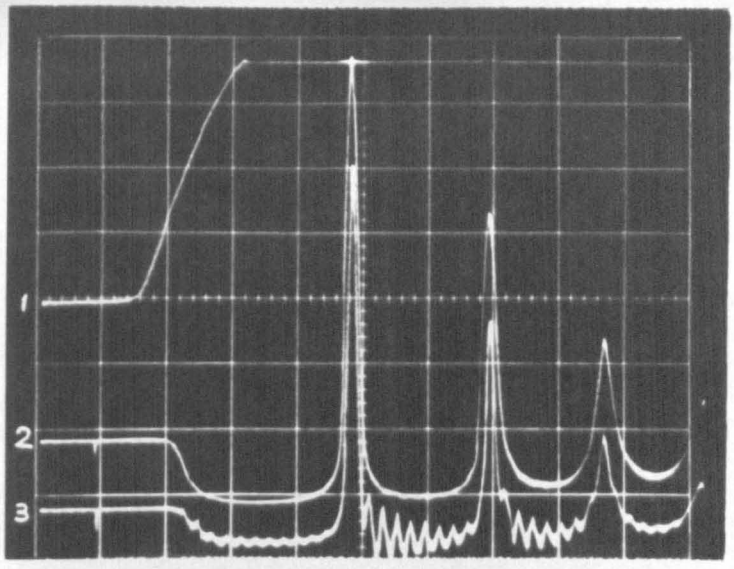

Fig. 86 Plate 5.

V_o = 2.743 m/s
PR2 = 205 kN/m^2 abs.
TC = 0.16 s

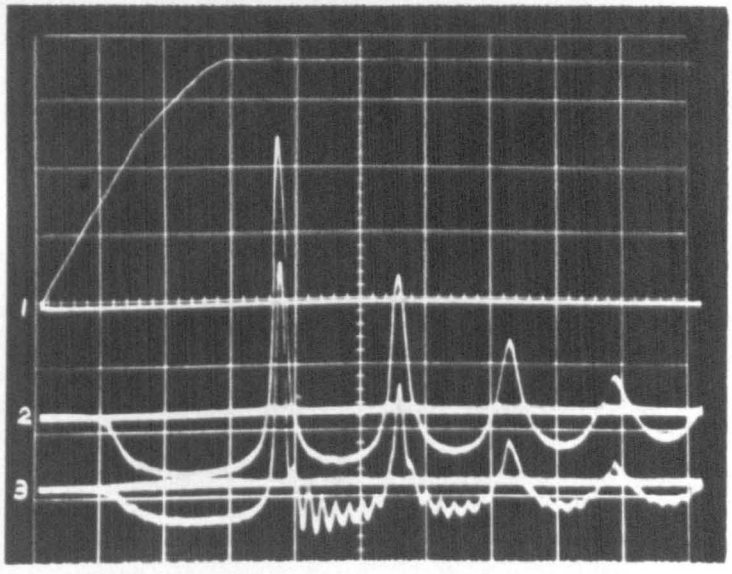

Fig. 86 Plate 6.

V_o = 2.743 m/s
PR2 = 205 kN/m^2 abs.
TC = 0.28 s

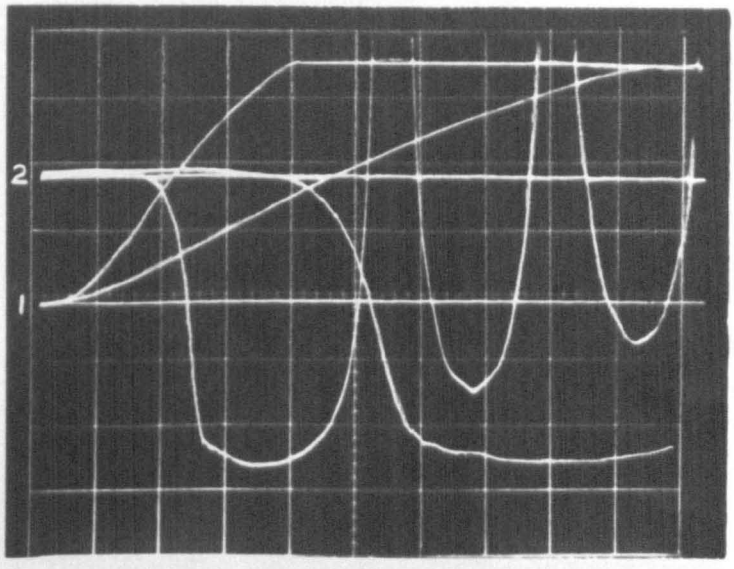

Fig. 87 Pressure variations on the downstream face of the valve during closure. Note that the traces represent the same test repeated with a change in oscilloscope time base.

V_o = 1.75 m/s
PR2 = 222 kN/m^2 abs.

Scale: Time base = 0.05 and 0.02 s/ x div.
45 kN/m^2/y div.

Traces
1. L.D.T.
2. Pressure transducer 5.08 cm downstream of the valve.

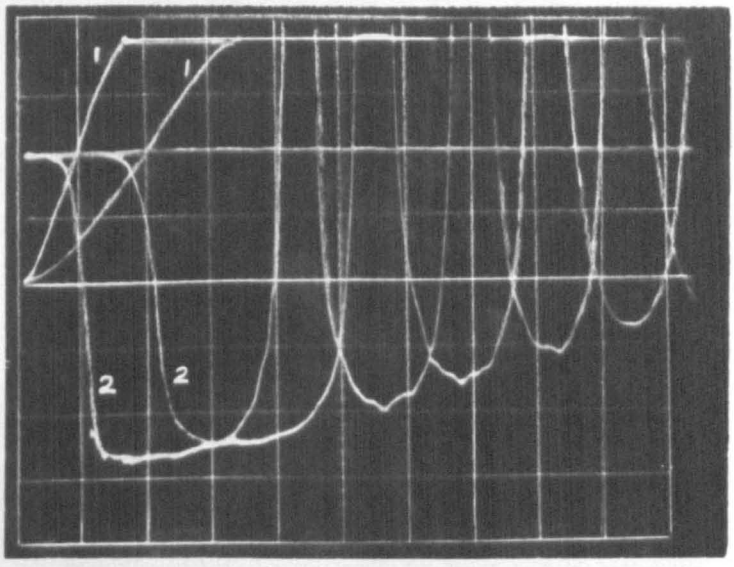

Fig. 88 Minimum pressures recorded at the valve for two overall valve closure times.

V_o = 1.75 m/s
PR2 = 222 kN/m^2 abs.

Scale: 0.05 s / x div.
45 kN/m^2/y div.

Traces
1. L.D.T.
2. Pressure transducer 5.08 cm downstream of the valve.

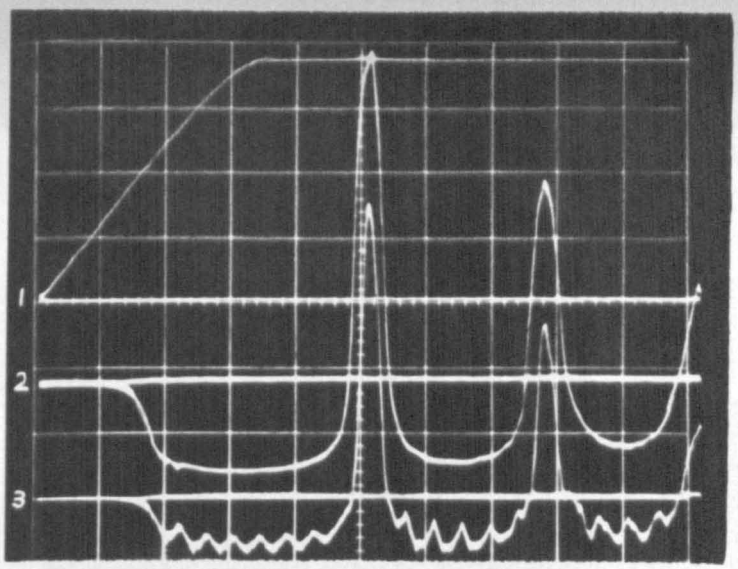

Plate 1. V_o = 2.743 m/s

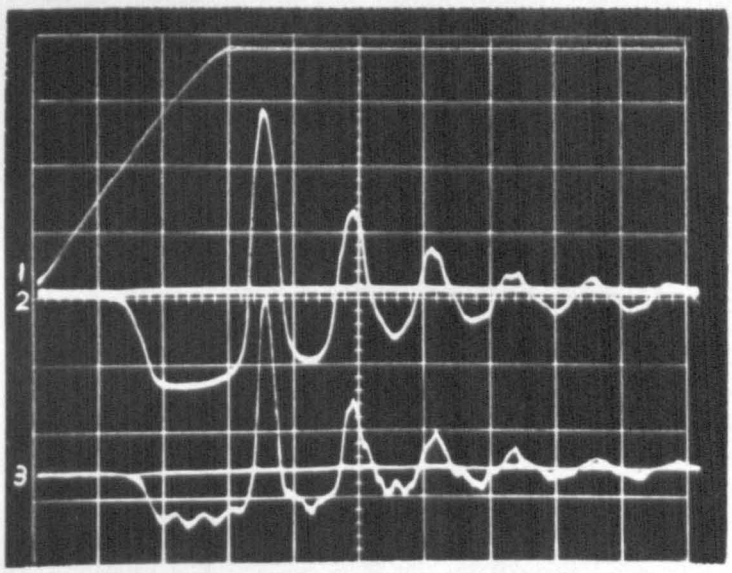

Plate 2. V_o = 1.75 m/s

Fig. 89 Plates 1, 2 above illustrate the effect of a reduction in initial flow velocity for a constant valve closure time (0.16 secs) and downstream reservoir pressure (309 kN/m^2 abs.) Scales and layout as Fig. 86, (Plates 1 - 4)

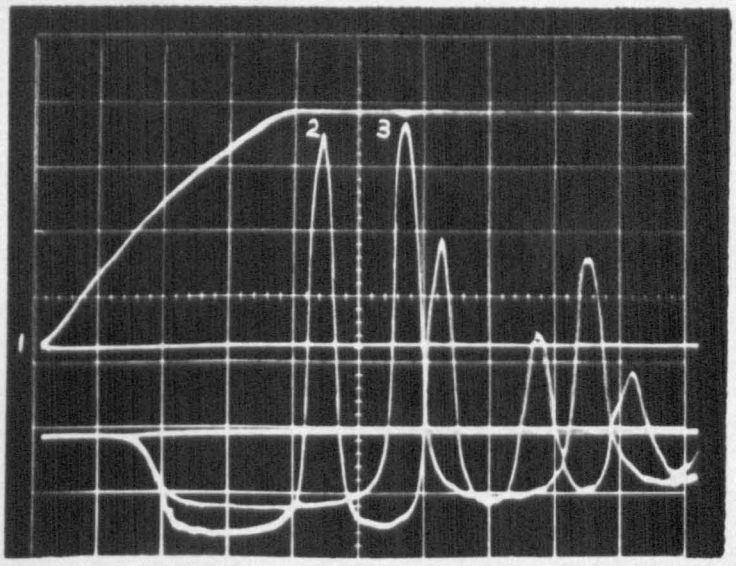

Fig. 90 Pressure variations recorded 5.08 cm downstream of the valve during two consecutive tests illustrating the effect of a variation in downstream reservoir pressure (PR2).

Scale:
L.D.T. .5 volts/y div.
Pressure transducer 225 kN/m^2/y div.
Time base = 0.05 s / x div.

Trace layout
1. L.D.T.
2. Pressure variation, PR2 = 378 kN/m^2 abs.
3. Pressure variation, PR2 = 240 kN/m^2 abs.

Initial velocity for each test, V_o = 2.743 m/s

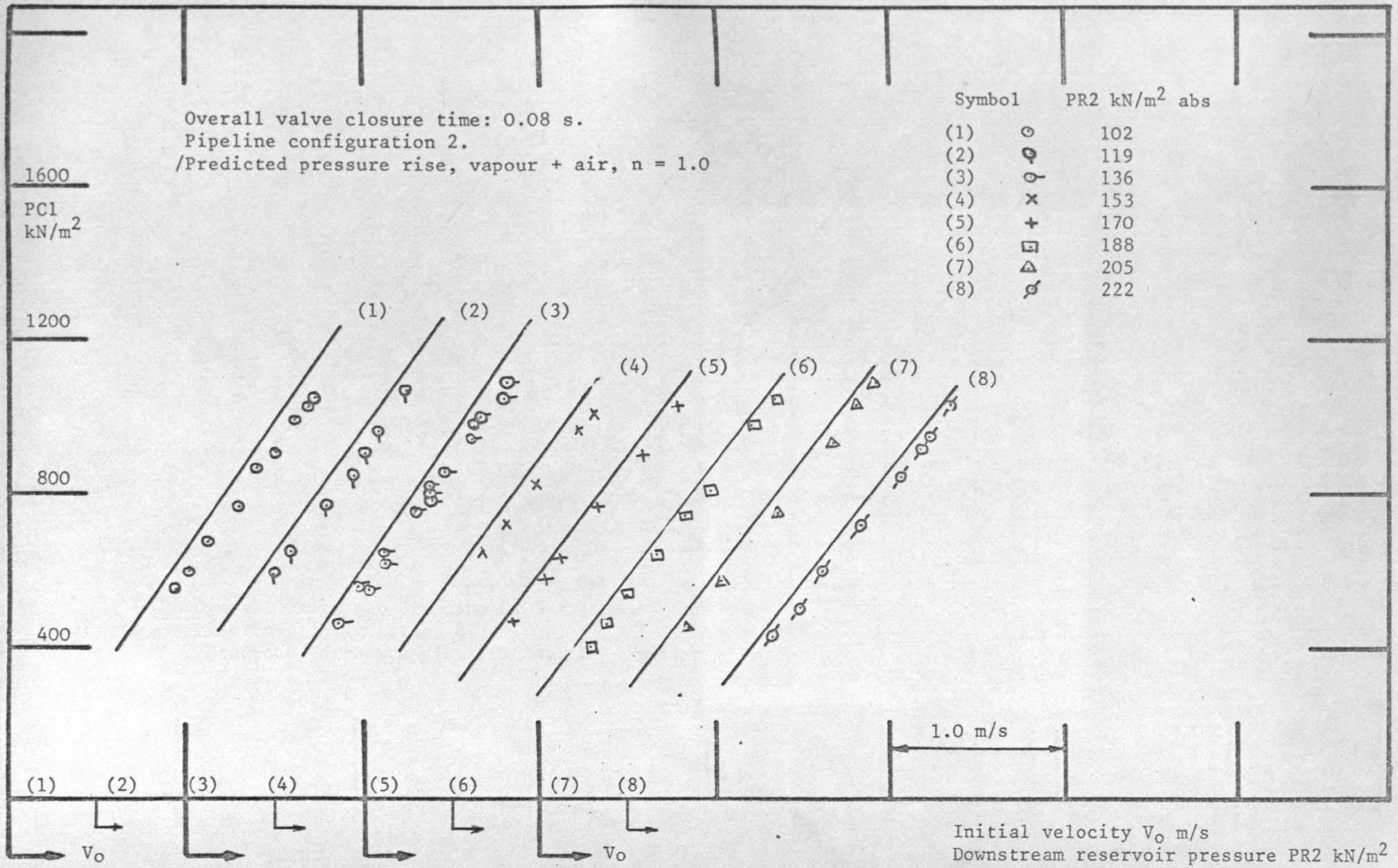

Fig. 91 Pressure rise (PC1), above steady state, on the downstream face of the valve following the collapse of the first vapour cavity, for a range of initial flow velocities (V_o) and downstream reservoir pressures (PR2).

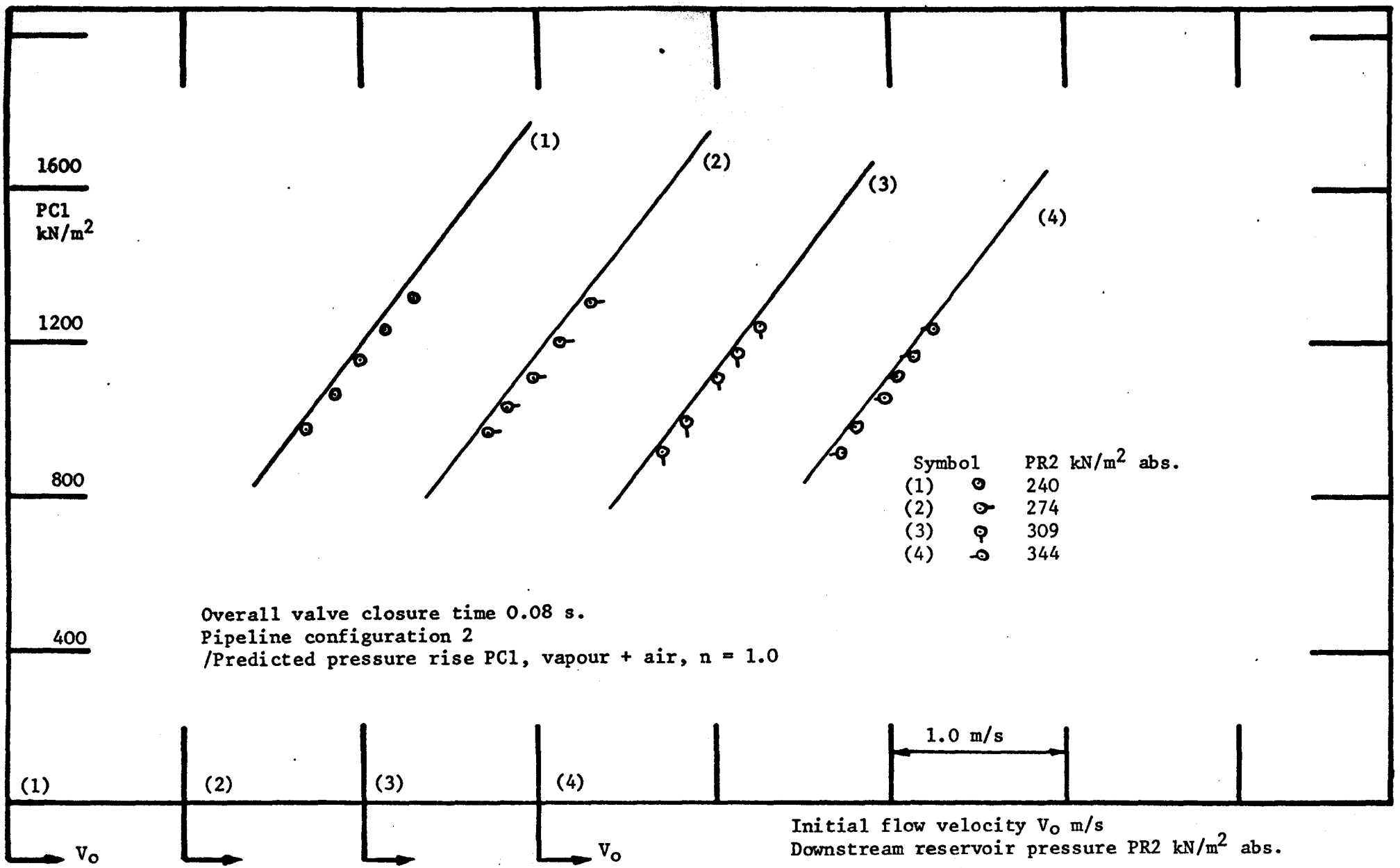

Fig. 92 Pressure rise (PC1) above steady state, on the downstream face of the valve following the collapse of the first vapour cavity, for a range of initial flow velocities (V_o) and downstream reservoir pressures (PR2).

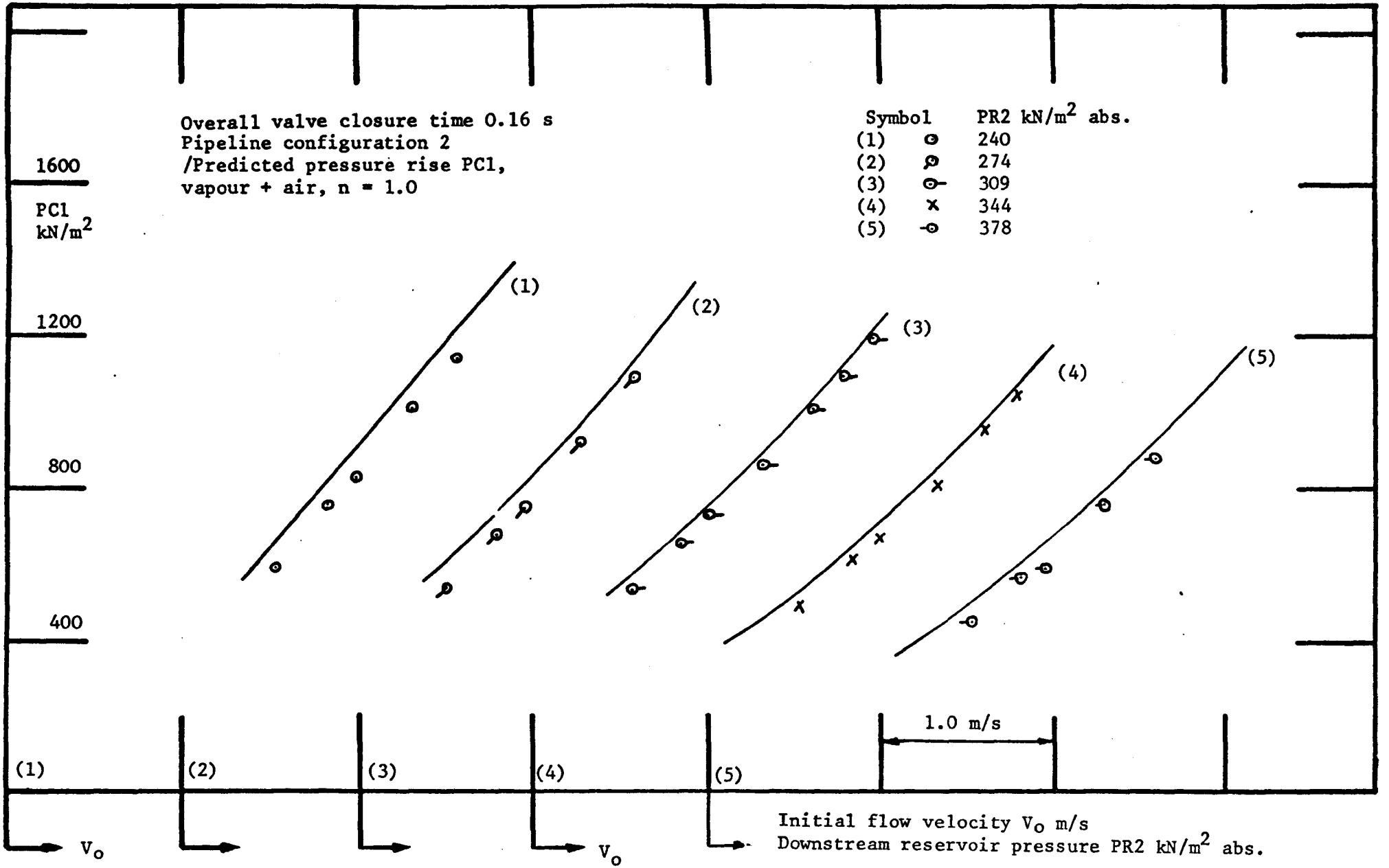

Fig. 93 Pressure rise PC1, above steady state, on the downstream face of the valve following the collapse of the first cavity, for a range of initial flow velocities (V_o) and downstream reservoir pressures (PR2).

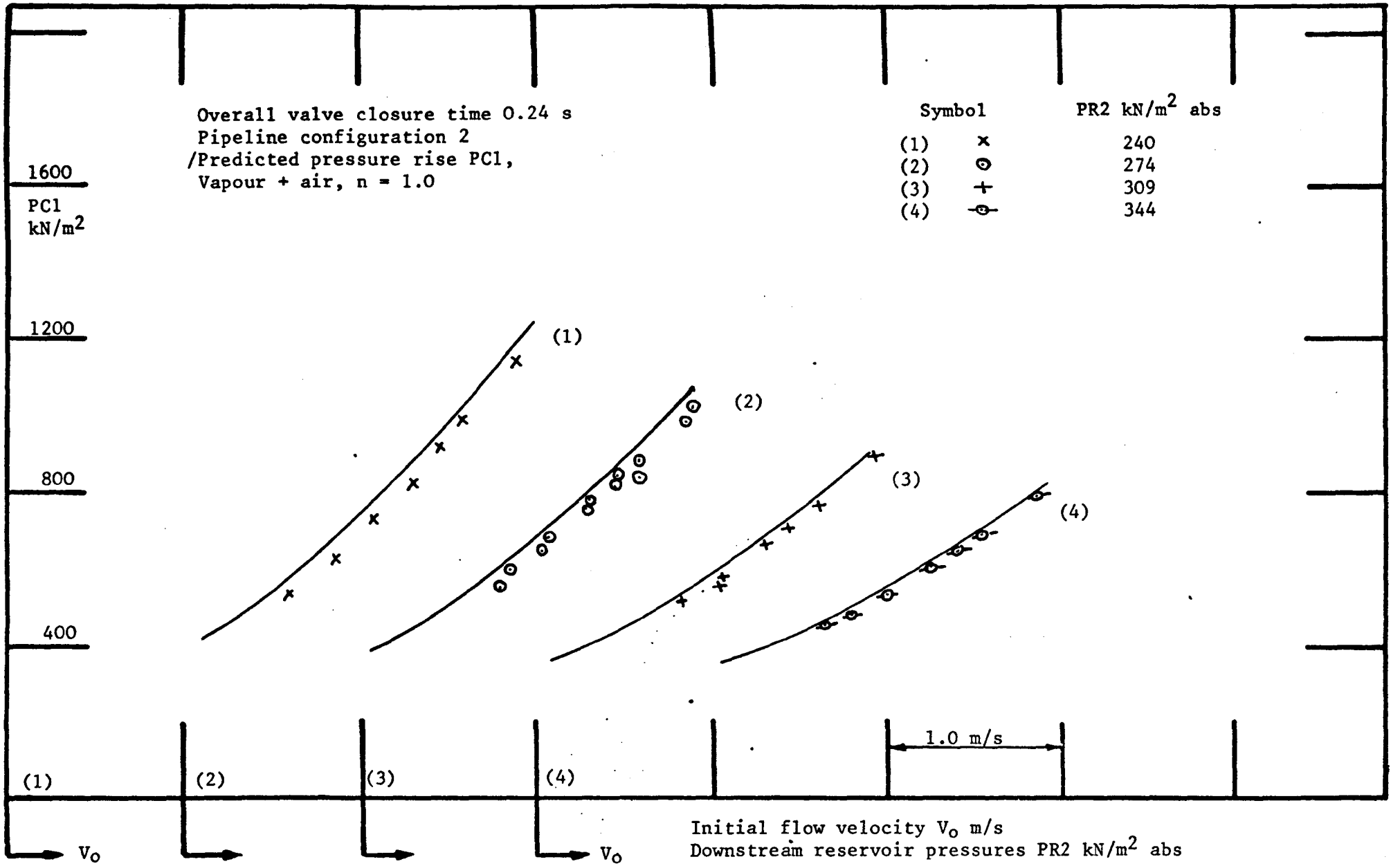

Fig. 94 Pressure rise PC1, above steady state, on the downstream face of the valve, following the collapse of the first vapour cavity for a range of initial flow velocities (V_o) and downstream reservoir pressures (PR2).

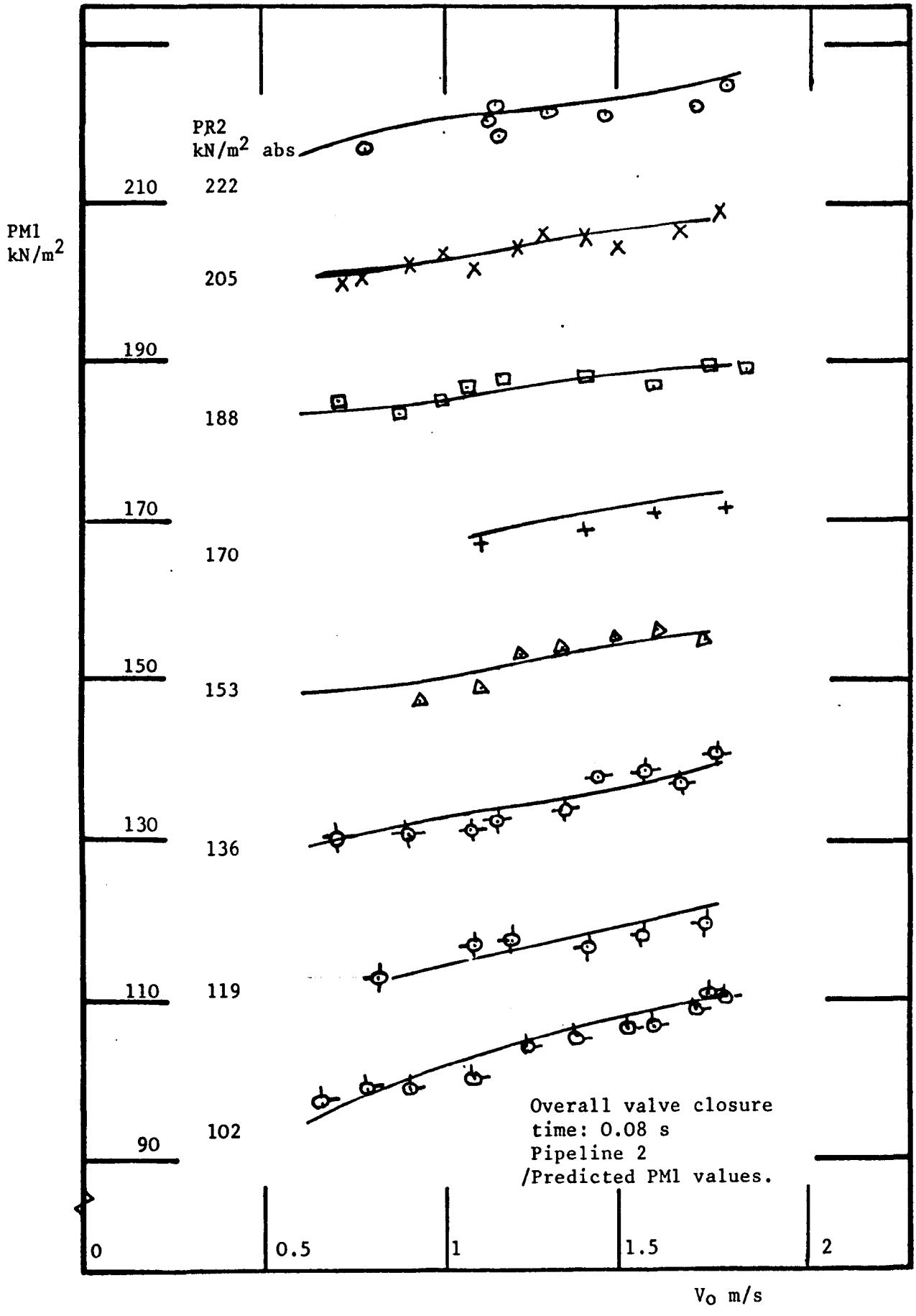

Fig. 95 Minimum pressure (PM1), expressed as a drop below steady state, at the valve downstream face during the growth of the first cavity formed downstream of the valve for a range of initial flow velocities (V_O) and downstream reservoir pressures (PR2).

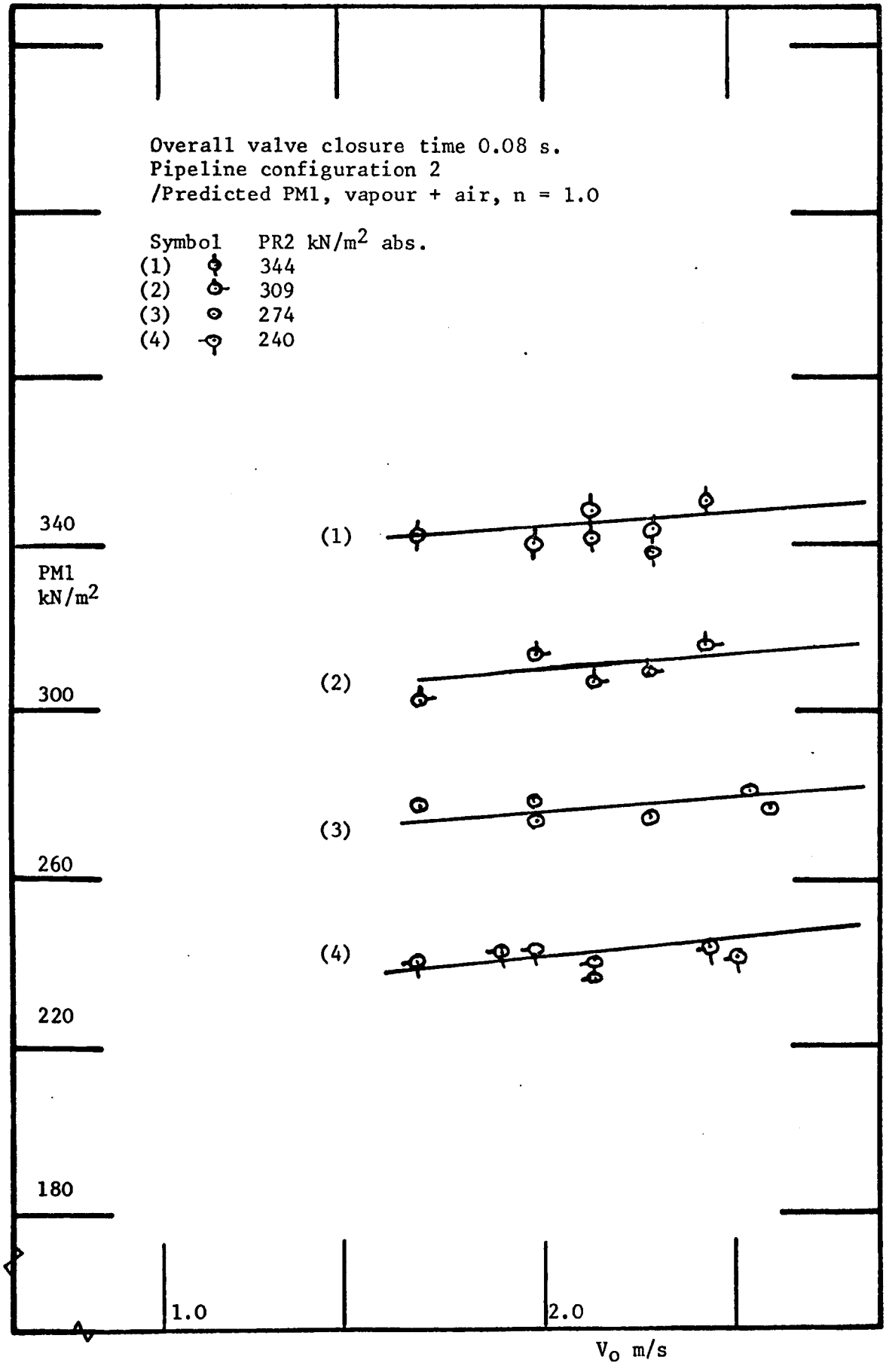

Fig. 96 Minimum pressure PM1 expressed as a drop below steady state, during the growth of the first cavity formed downstream of the valve for a range of initial flow velocities (V_o) and downstream reservoir pressures (PR2).

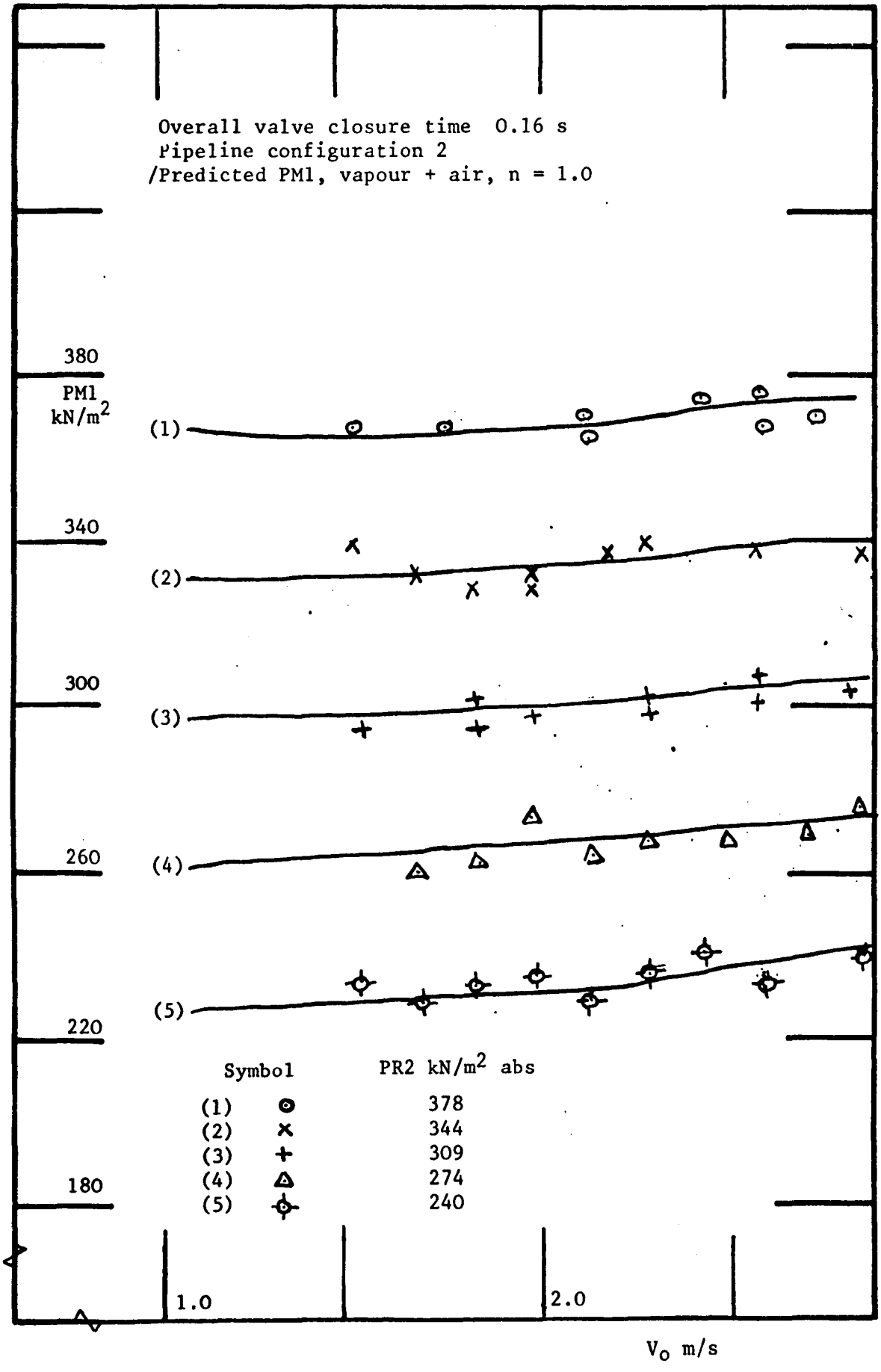

Fig. 97 Minimum pressure PM1, expressed as a drop below steady state, at the valve downstream face during the growth of the first cavity formed downstream of the valve for a range of initial flow velocities (V_o) and downstream reservoir pressures (PR2).

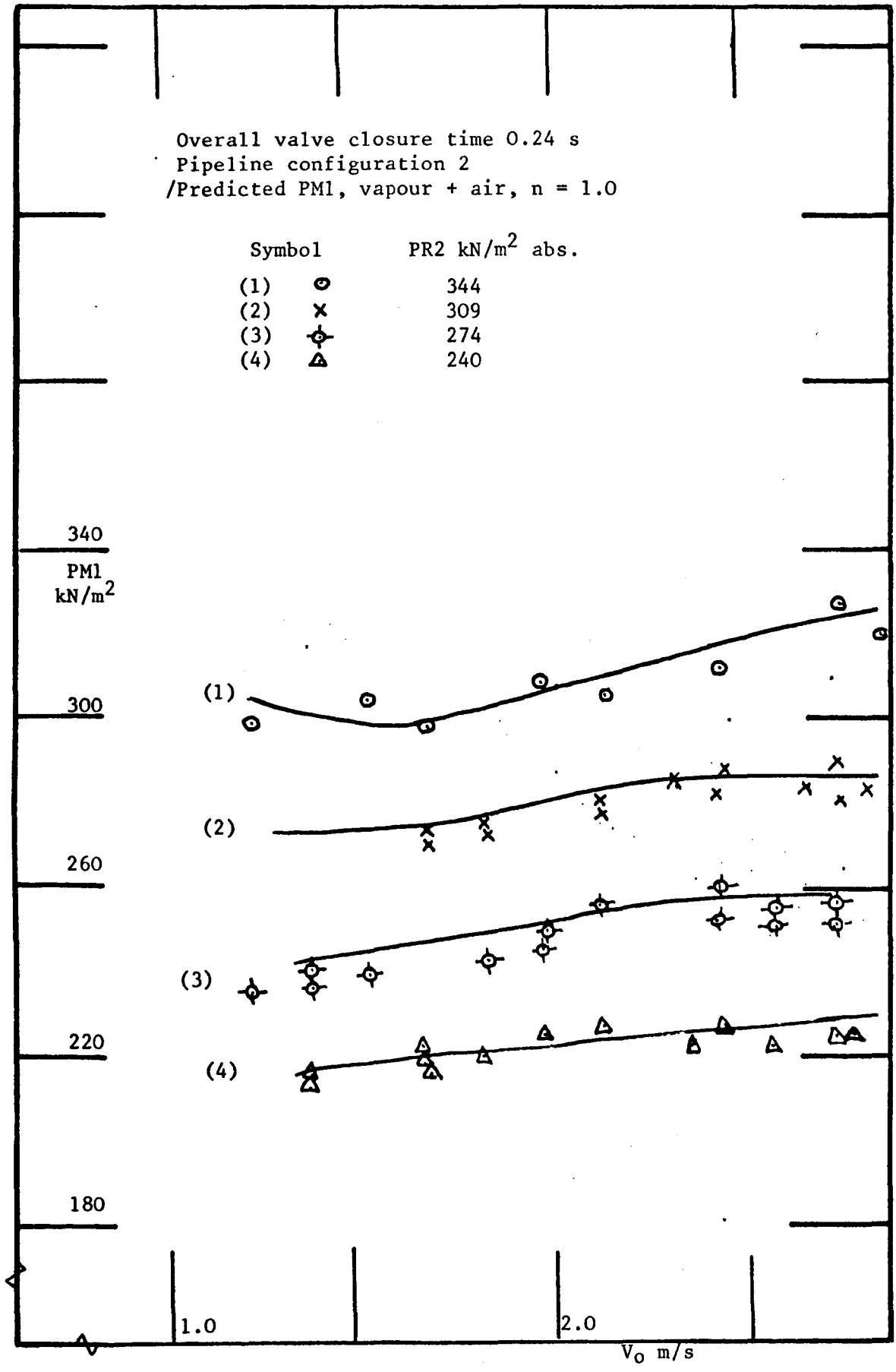

Fig. 98 Minimum pressure (PM1) expressed as a drop below steady state, at the valve downstream face during the growth of the first cavity, for a range of initial flow velocities (V_o), and downstream reservoir pressures (PR2)

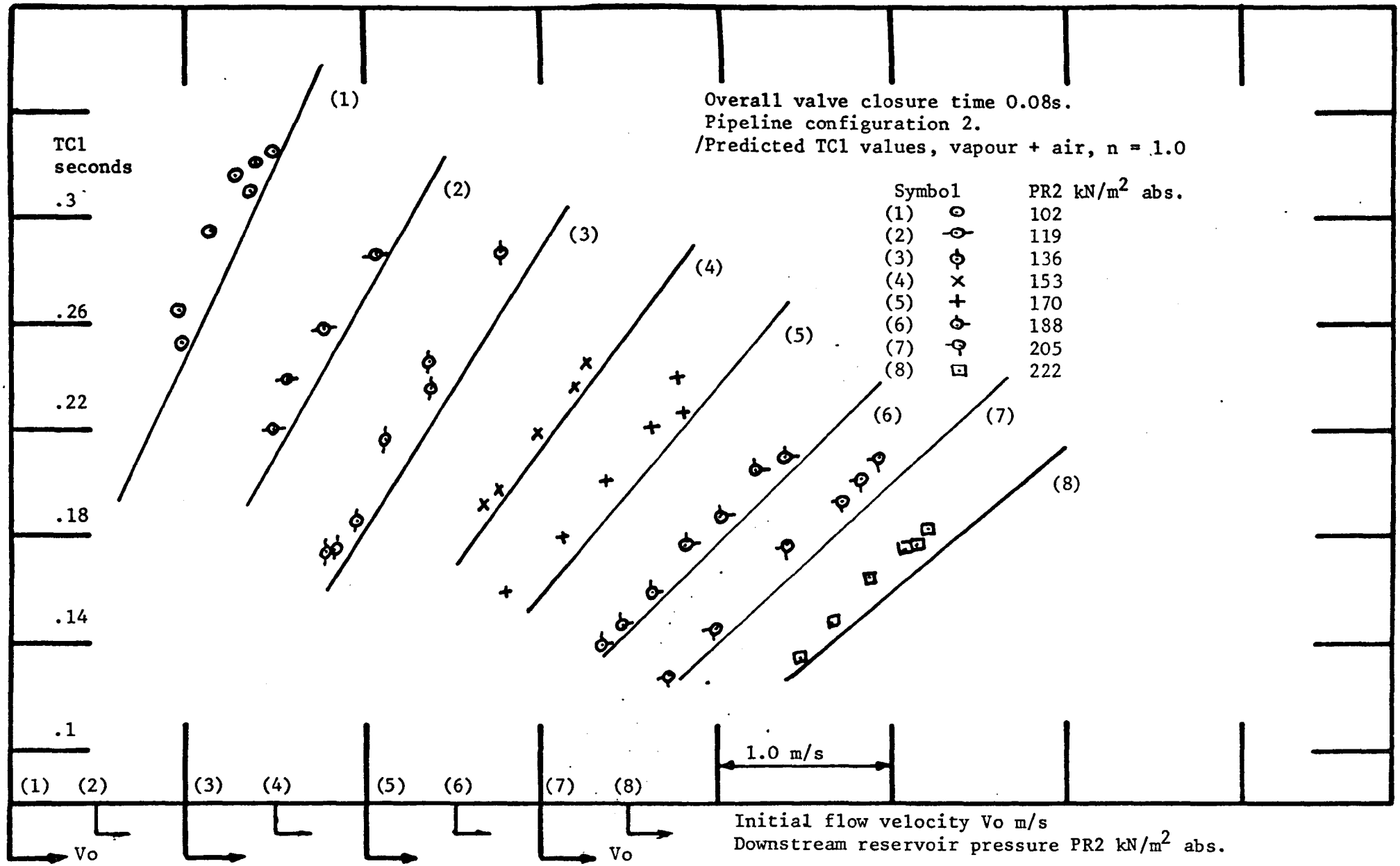

Fig. 99 First cavity collapse time for a range of flow velocities (Vo) and downstream reservoir pressures (PR2).

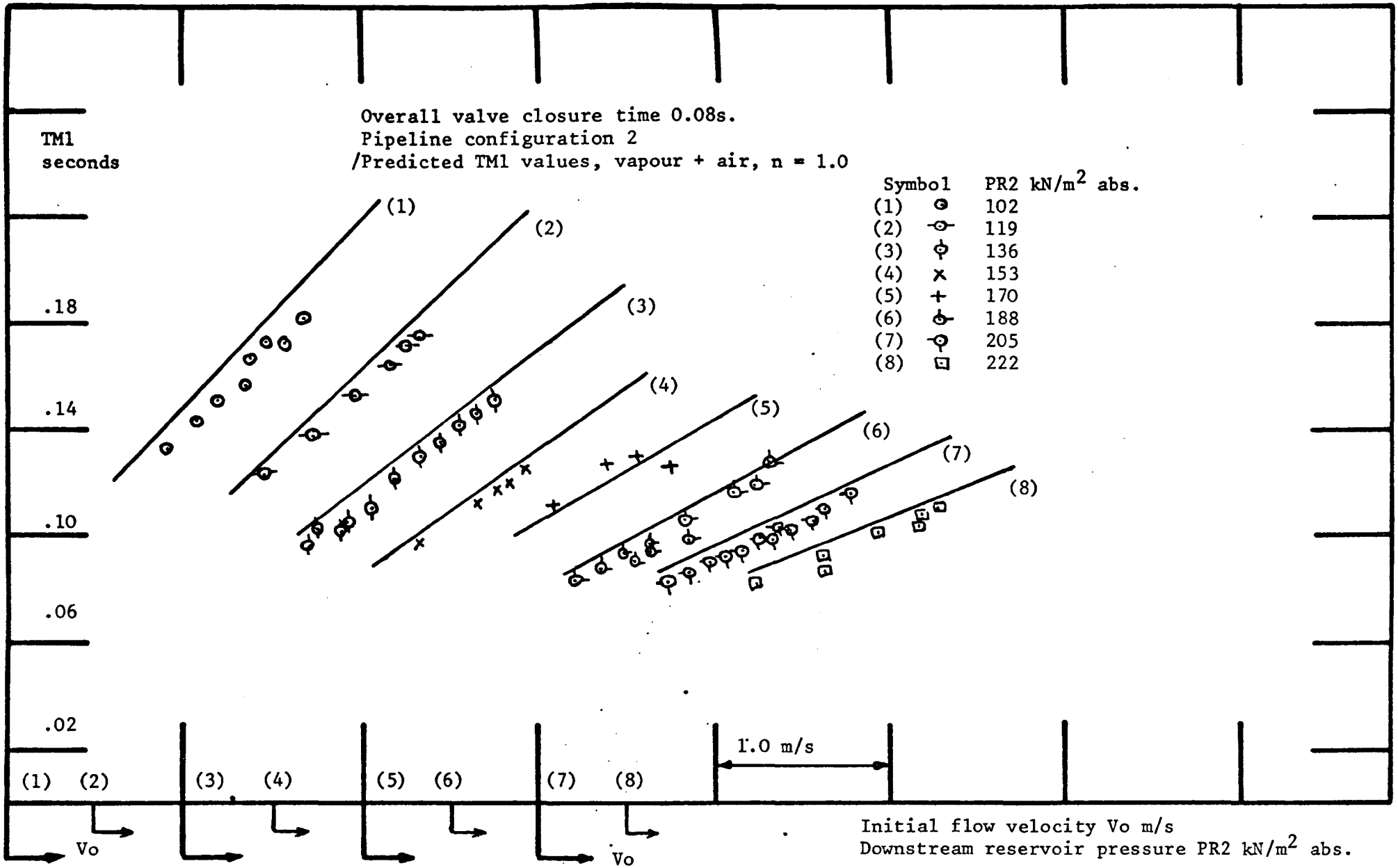

Fig. 100 Time to minimum pressure for the first cavity formed downstream of the valve.

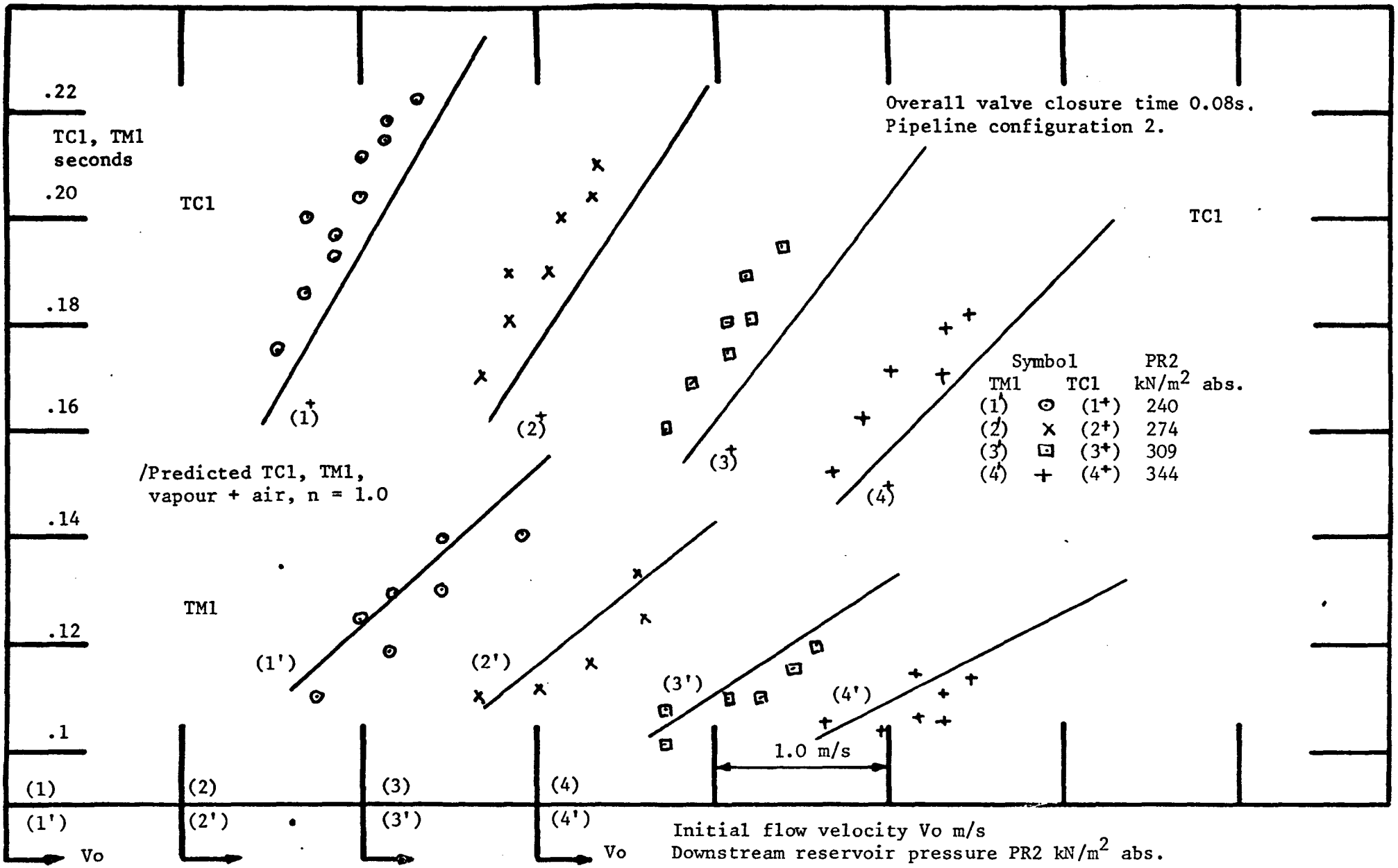

Fig. 101 Time to minimum pressure (TM1) and subsequent cavity collapse (TC1), for the first cavity formed downstream of the valve, for a range of initial flow velocities (Vo) and downstream reservoir pressures (PR2).

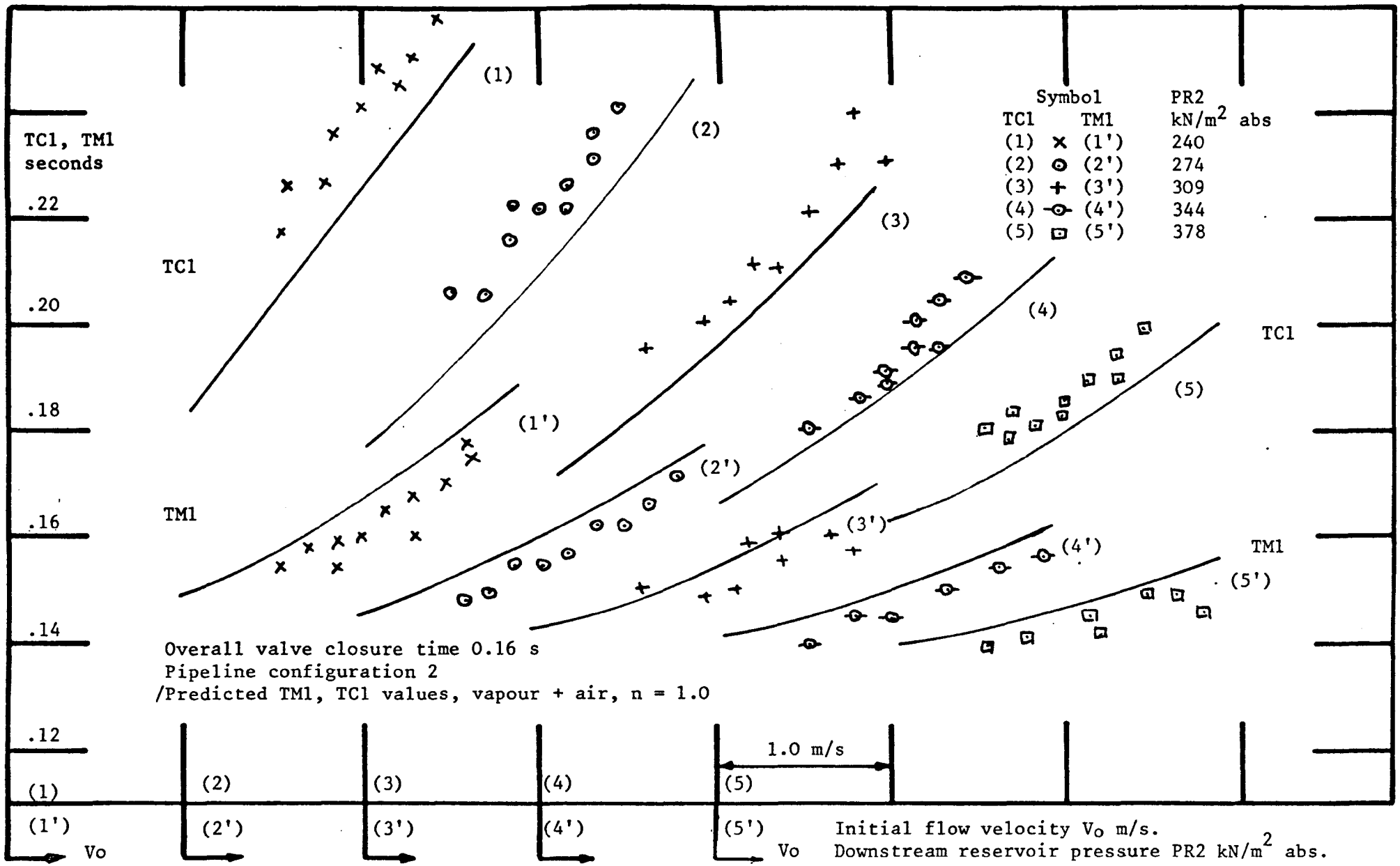

Fig. 102 Time to minimum pressure (TM1) and subsequent cavity collapse (TC1), for the first cavity formed downstream of the valve, for a range of initial flow velocities (V_o) and downstream reservoir pressures (PR2).

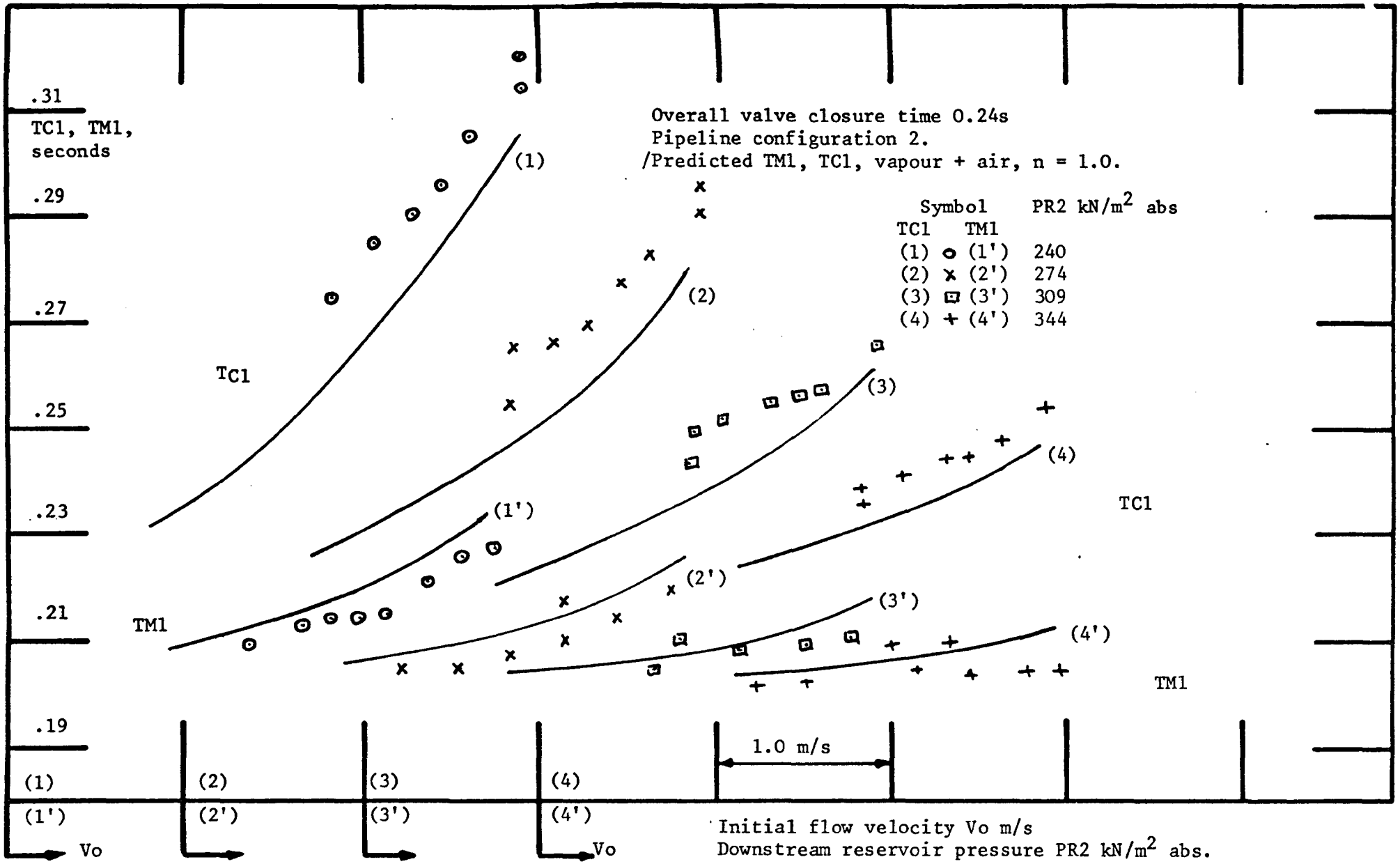

Fig. 103 Time to minimum pressure (TM1), and subsequent cavity collapse (TC1), for the first cavity formed downstream of the valve, for a range of initial flow velocities (Vo) and downstream reservoir pressures (PR2).

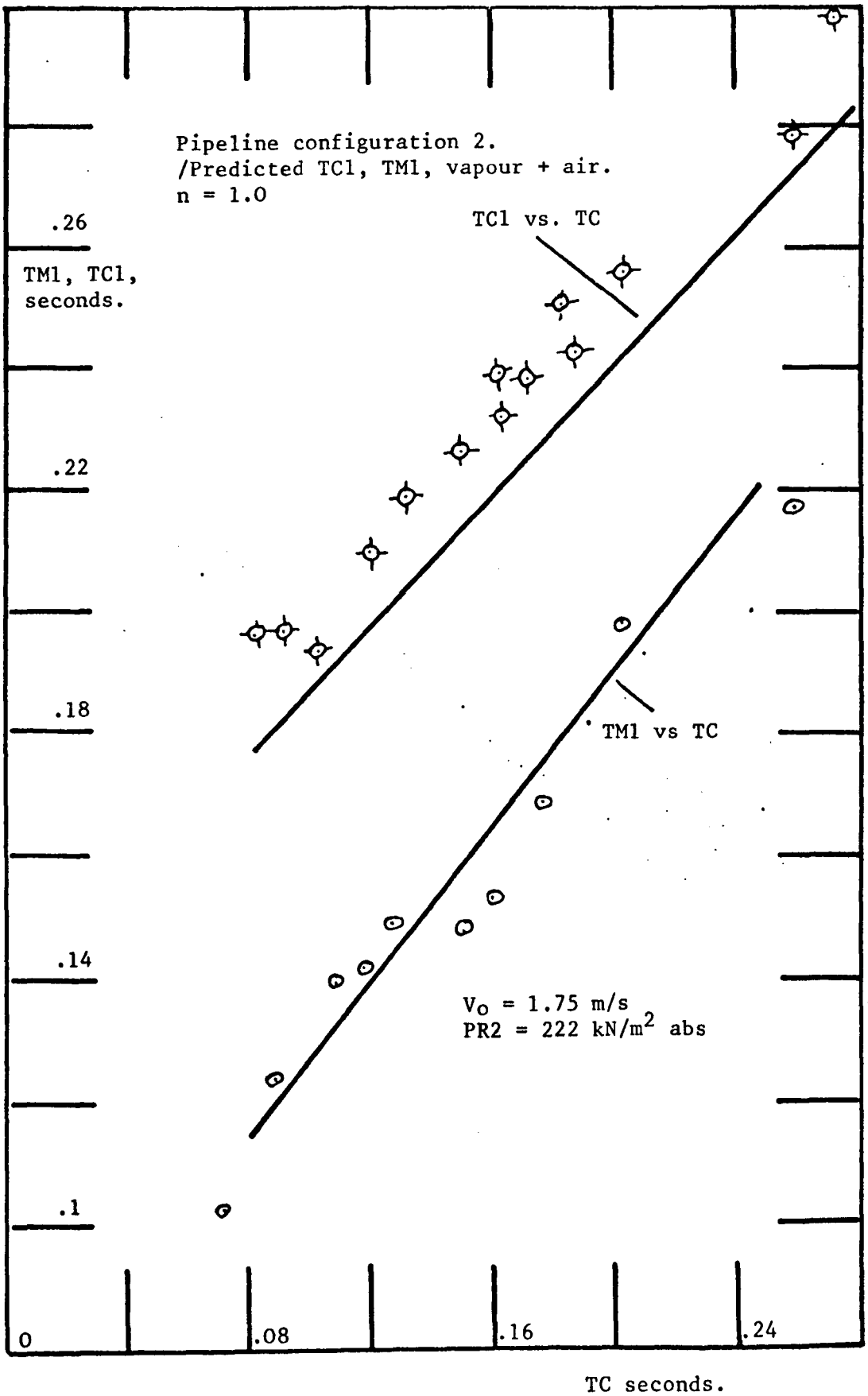

Fig. 104 Minimum pressure (TM1) and subsequent cavity collapse time (TC1) for the first cavity formed downstream of the valve for a range of valve closure rates TC.

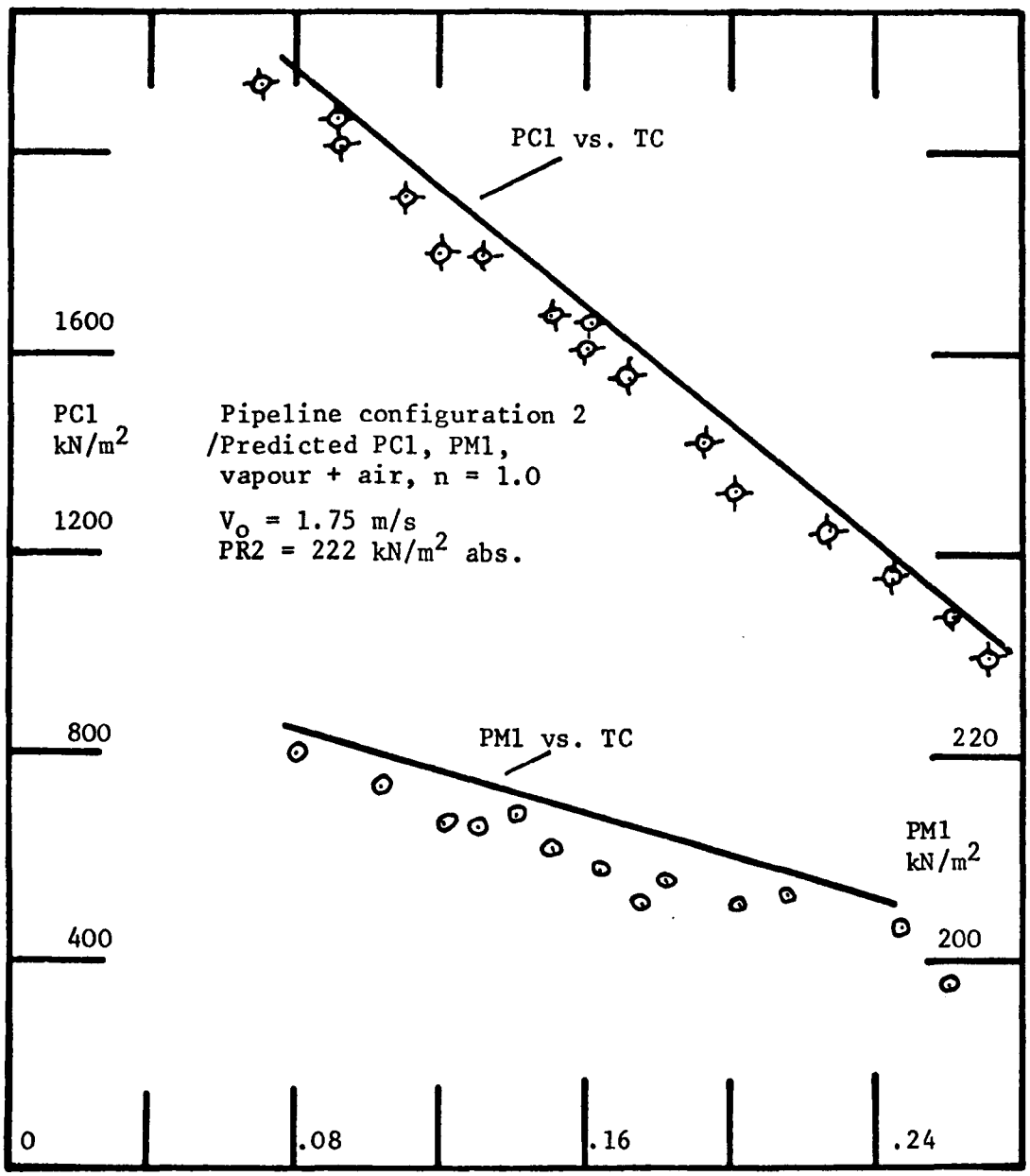

Fig. 105 Minimum pressure and cavity collapse pressure at the valve downstream face, for the first cavity formed for a range of valve closure rates. Pressures expressed as variations from steady state.

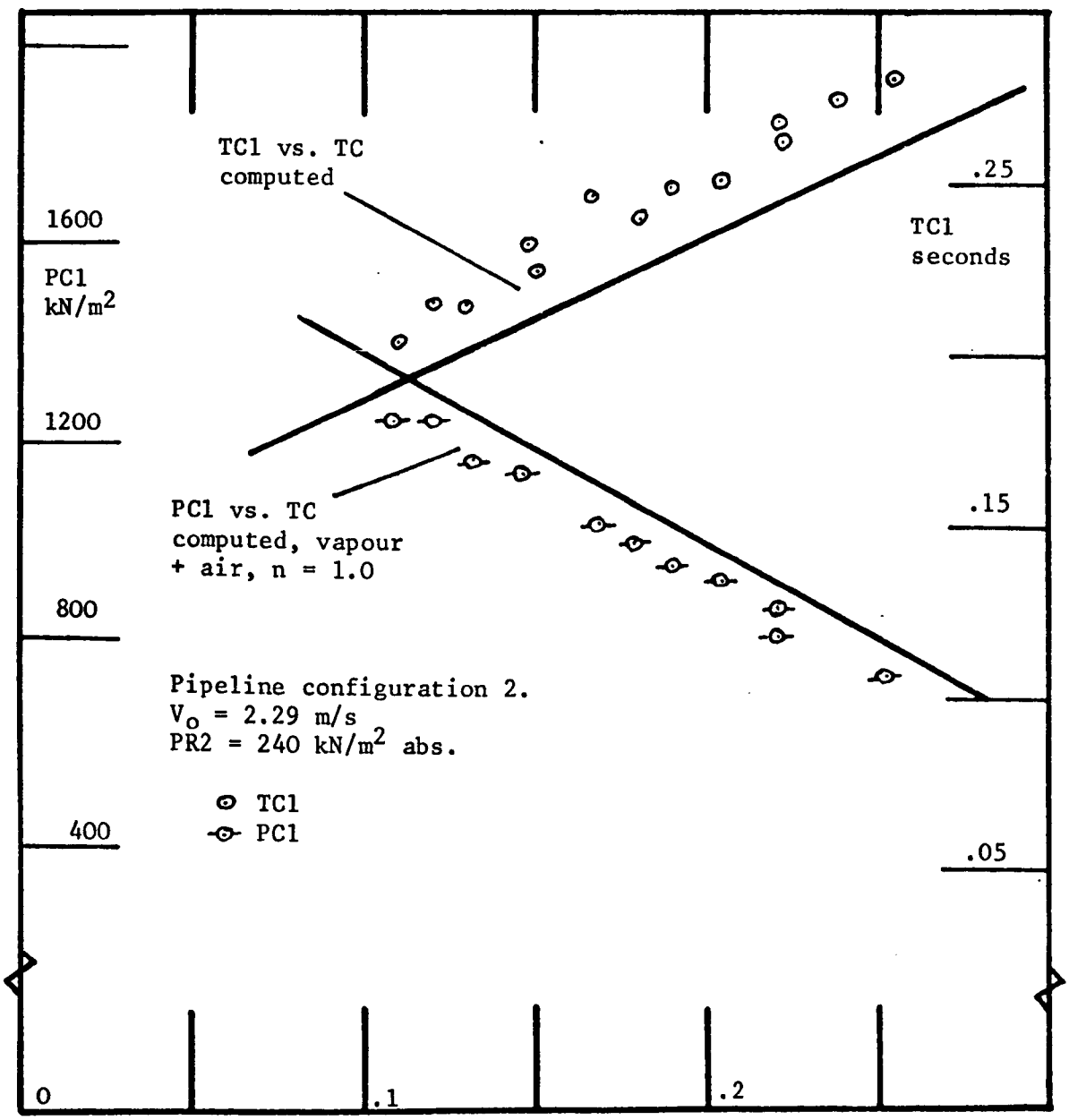

Fig. 106 Peak pressures recorded at the valve downstream face following first cavity collapse (PC1) and cavity collapse time (TC1) for a range of overall valve closure times (TC). Initial flow velocity and line pressure constant, pressures expressed as variations from steady state.

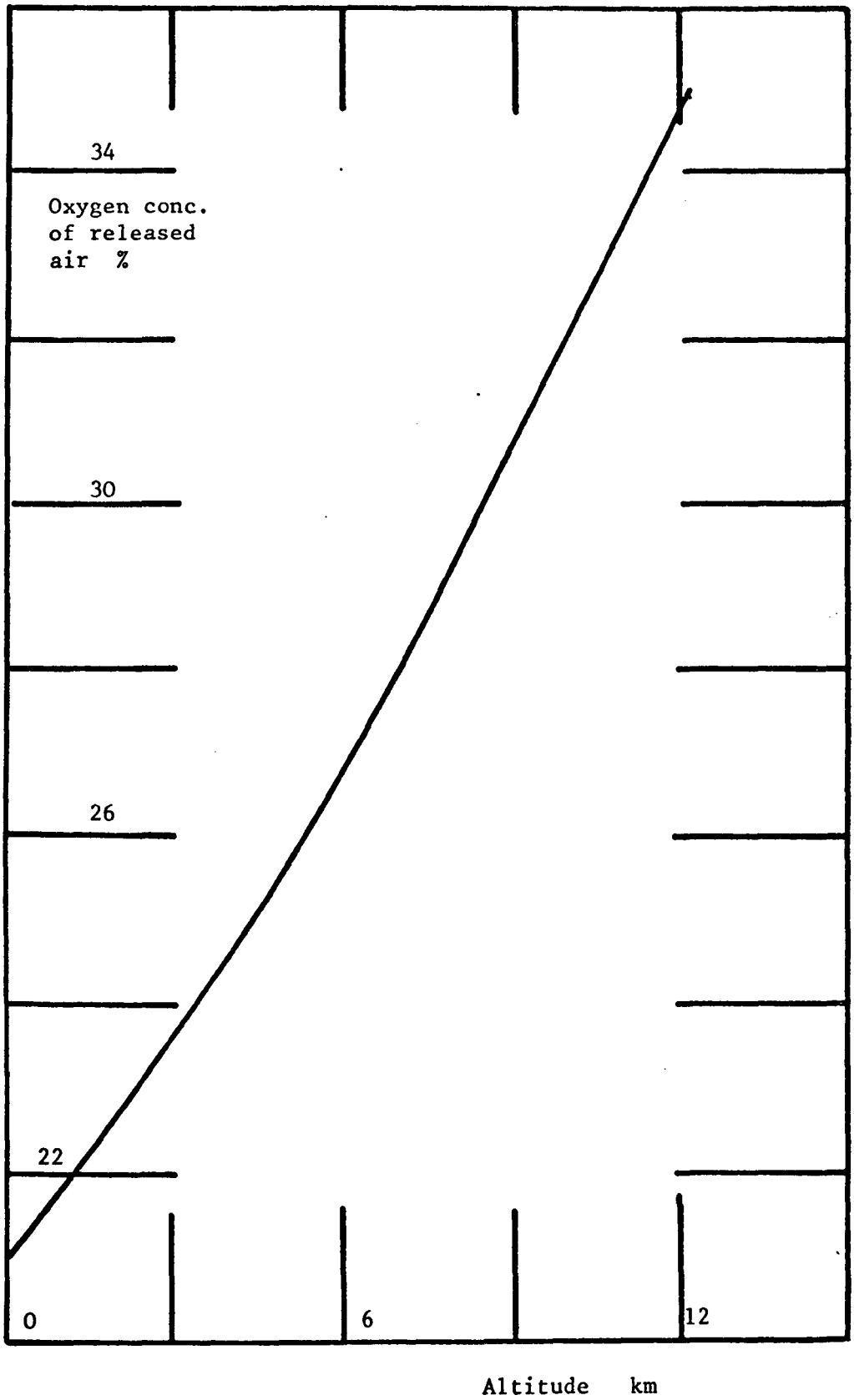

Fig. 107 Oxygen concentration of released air for Aviation Kerosene 2494 (B.A.C. data)

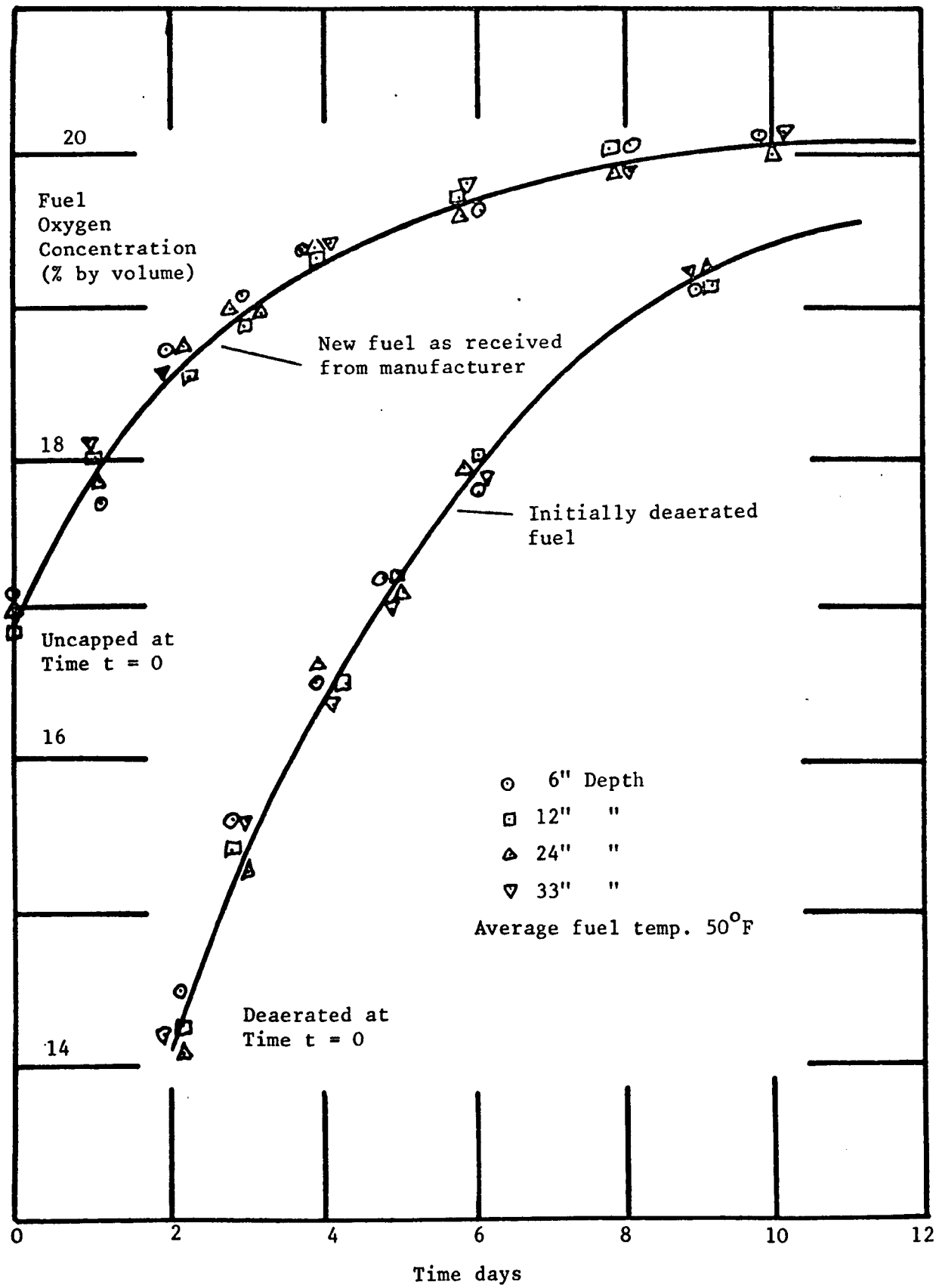

Fig. 108 Oxygen solubility in Aviation Kerosene 2494 with time (B.A.C. Data)

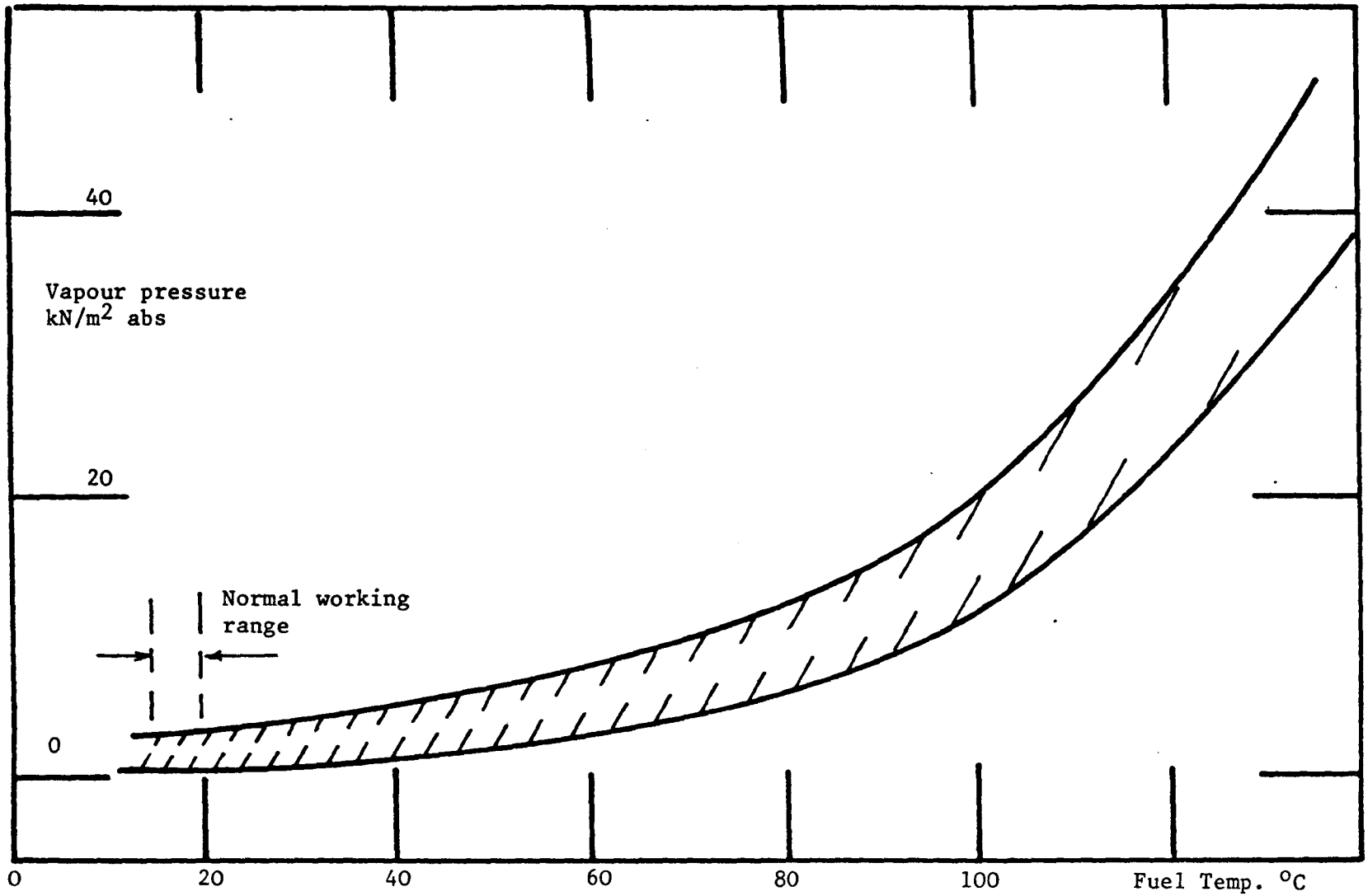

Fig. 109 Variation of the vapour pressure of Aviation Kerosene (Spec. 2494) with temperature and typical sample scatter. (Shell, B.A.C. data)

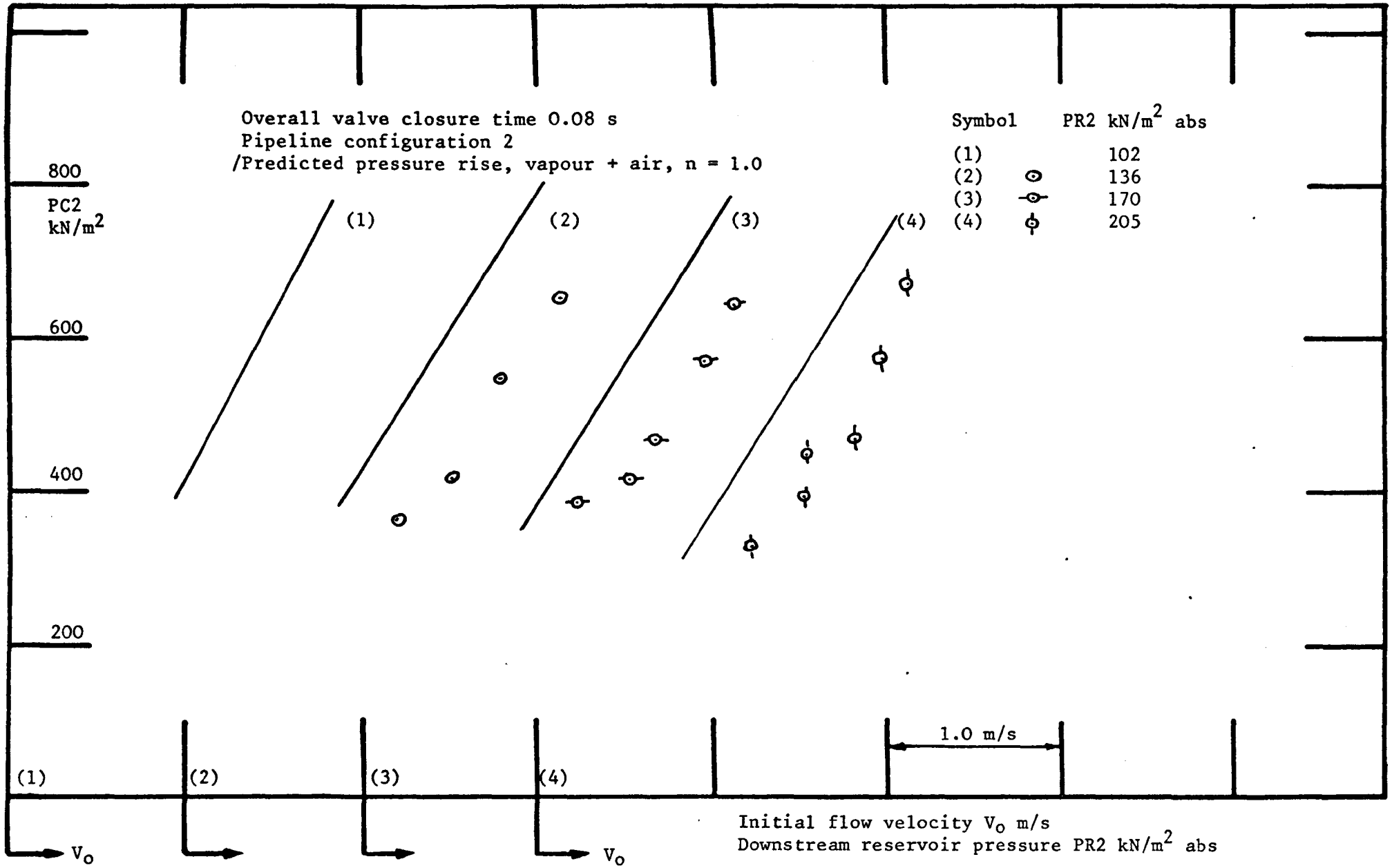

Fig. 110 Pressure rise PC2, above steady state, on the downstream face of the valve following the collapse of the second vapour cavity for a range of initial flow velocities (V_o) and downstream reservoir pressures (PR2).

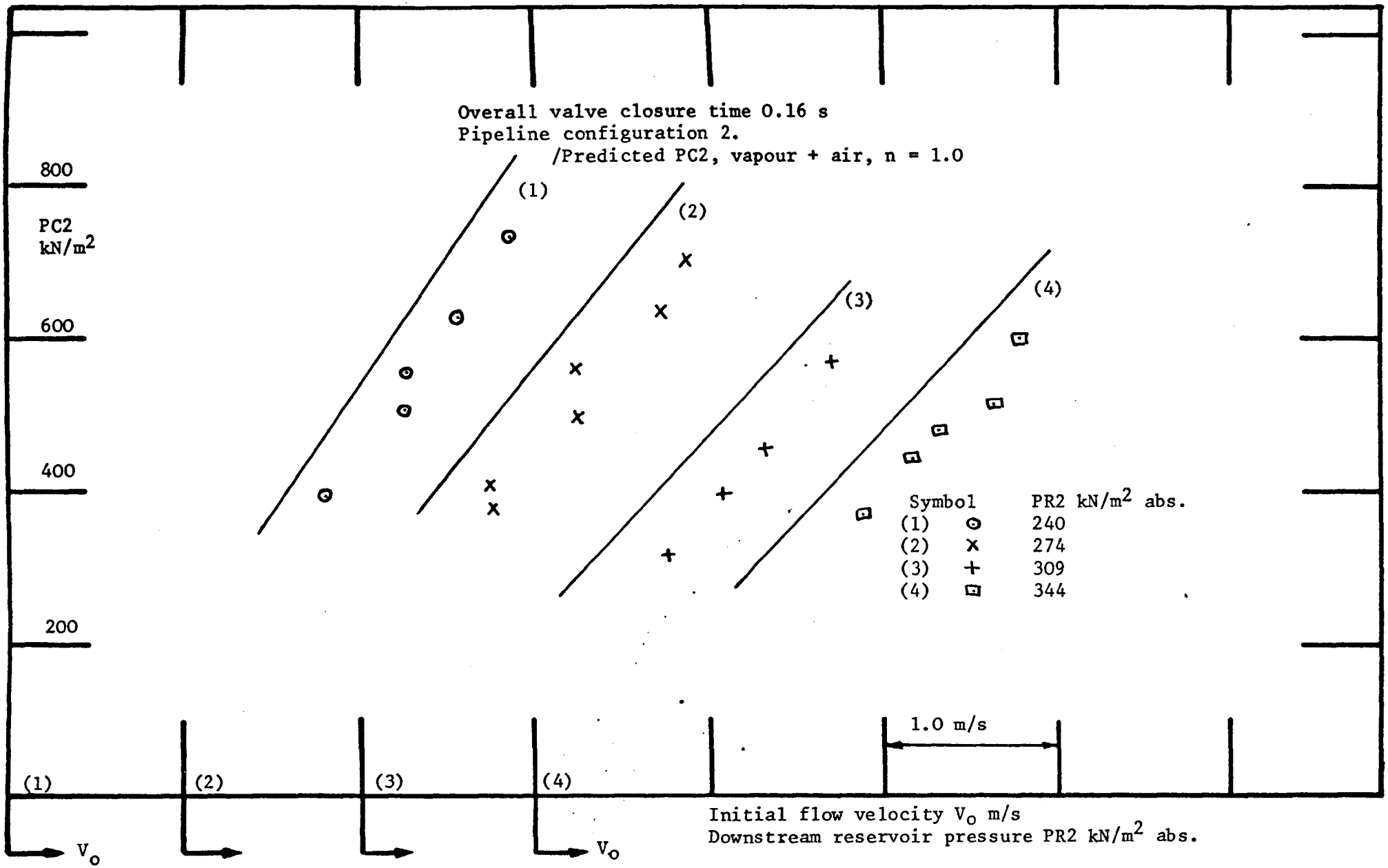

Fig. 111 Pressure rise PC2, above steady state, on the downstream face of the valve following the collapse of the second vapour cavity for a range of initial flow velocities (V_o) and downstream reservoir pressures (PR2).

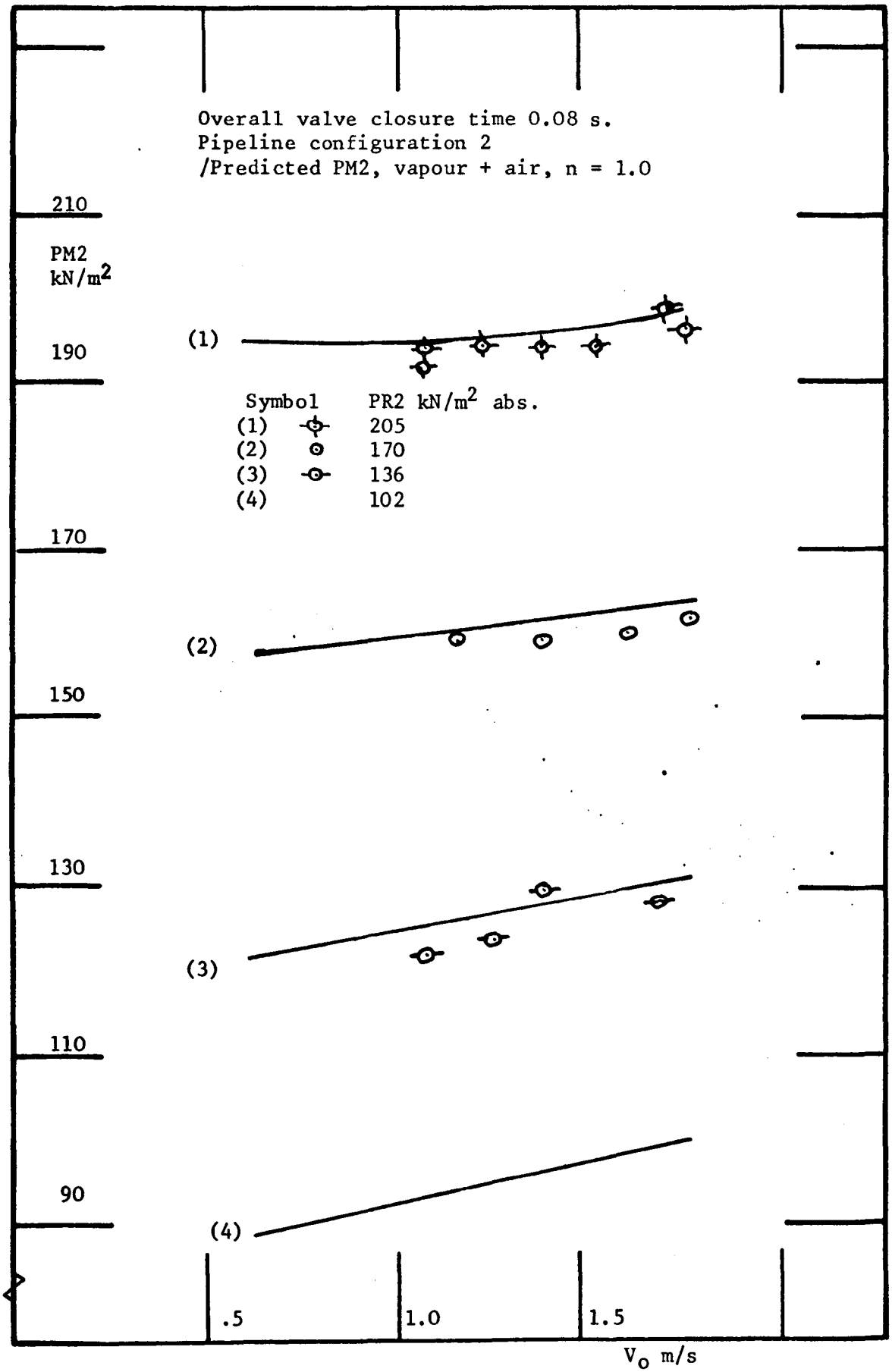

Fig. 112 Minimum pressure (PM2) expressed as a drop below steady state, at the valve downstream face, during the growth of the second cavity formed downstream of the valve for a range of initial flow velocities (V_o) and downstream reservoir pressures (PR2).

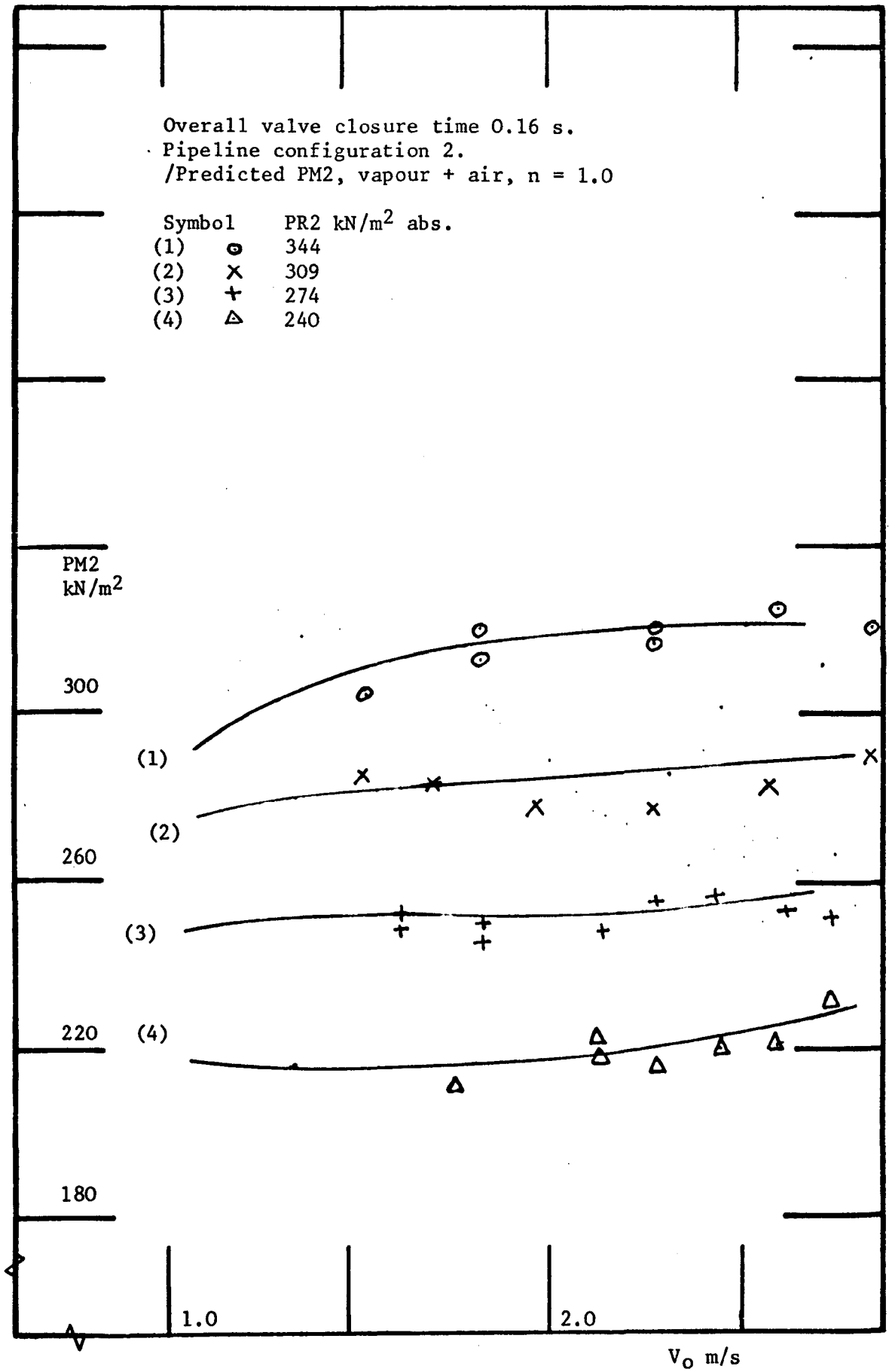

Fig. 113 Minimum pressure (PM2), expressed as a drop below steady state, at the downstream face of the valve during the growth of the second cavity downstream of the valve for a range of initial flow velocities (V_o) and downstream reservoir pressures (PR2).

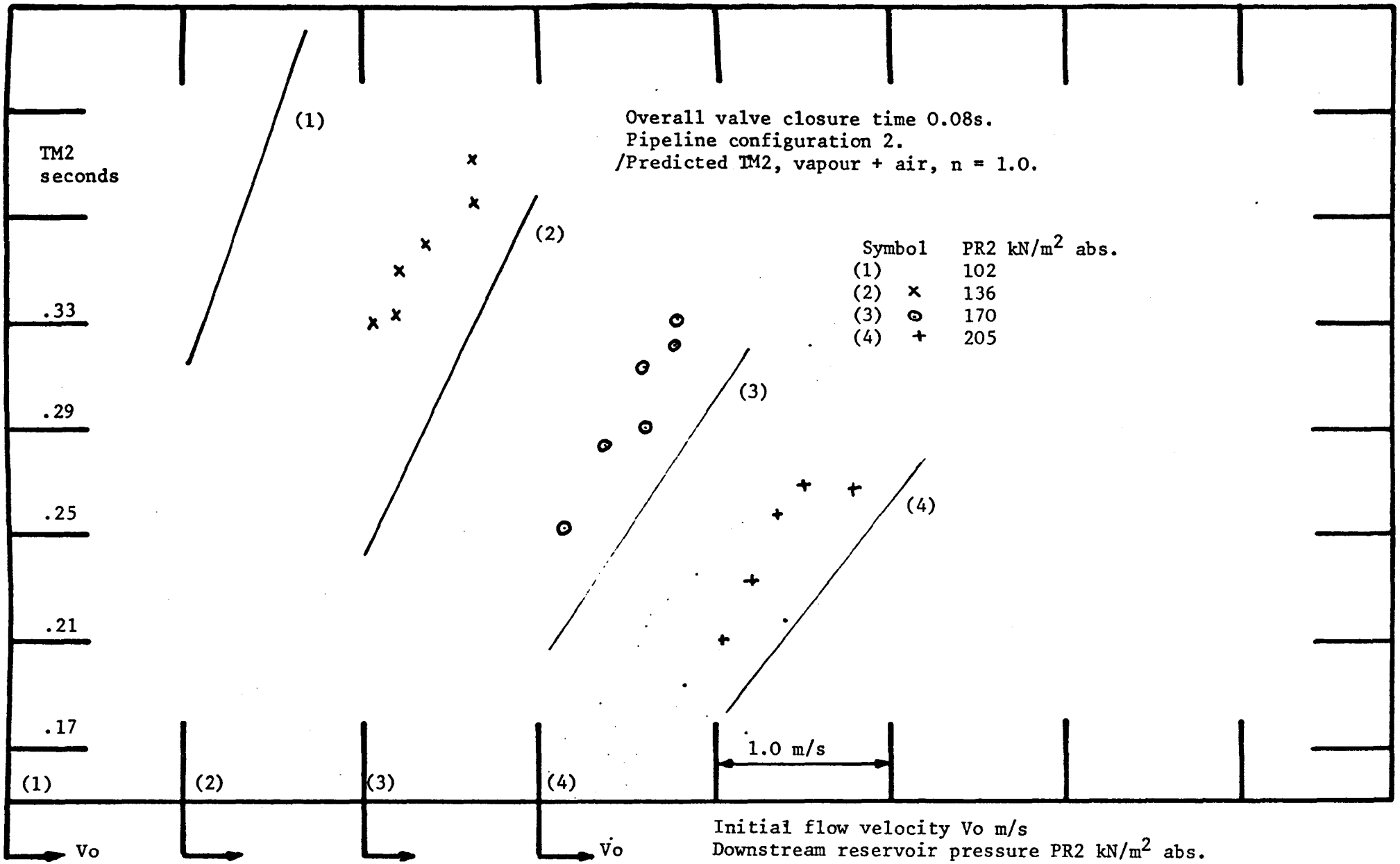

Fig. 114 Time to minimum pressure (TM2) for the second cavity formed downstream of the valve, for a range of initial flow velocities (Vo) and downstream reservoir pressures (PR2).

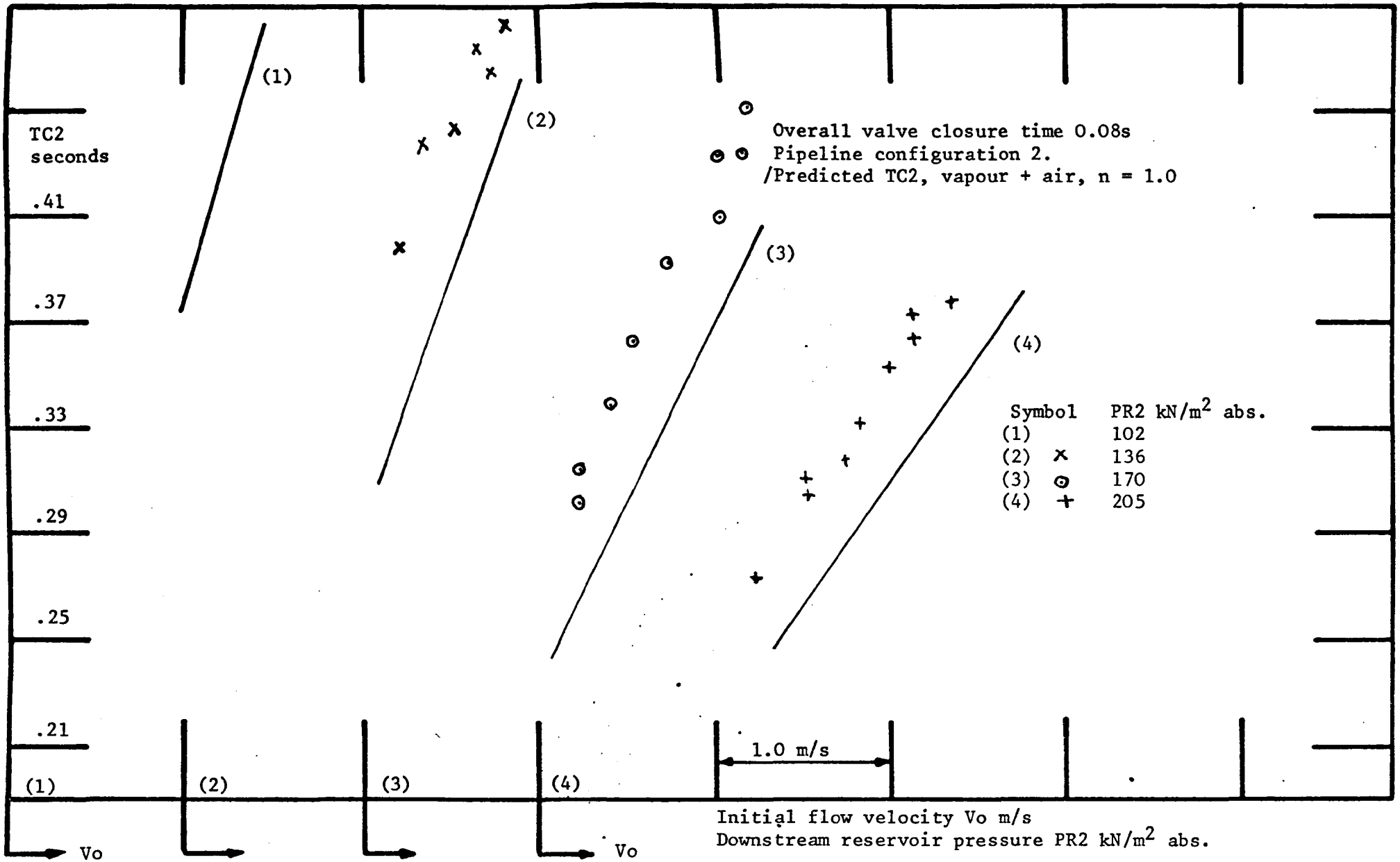

Fig. 115 Time to cavity collapse (TC2), for the second cavity formed downstream of the valve, for a range of initial flow velocities (Vo) and downstream reservoir pressures (PR2).

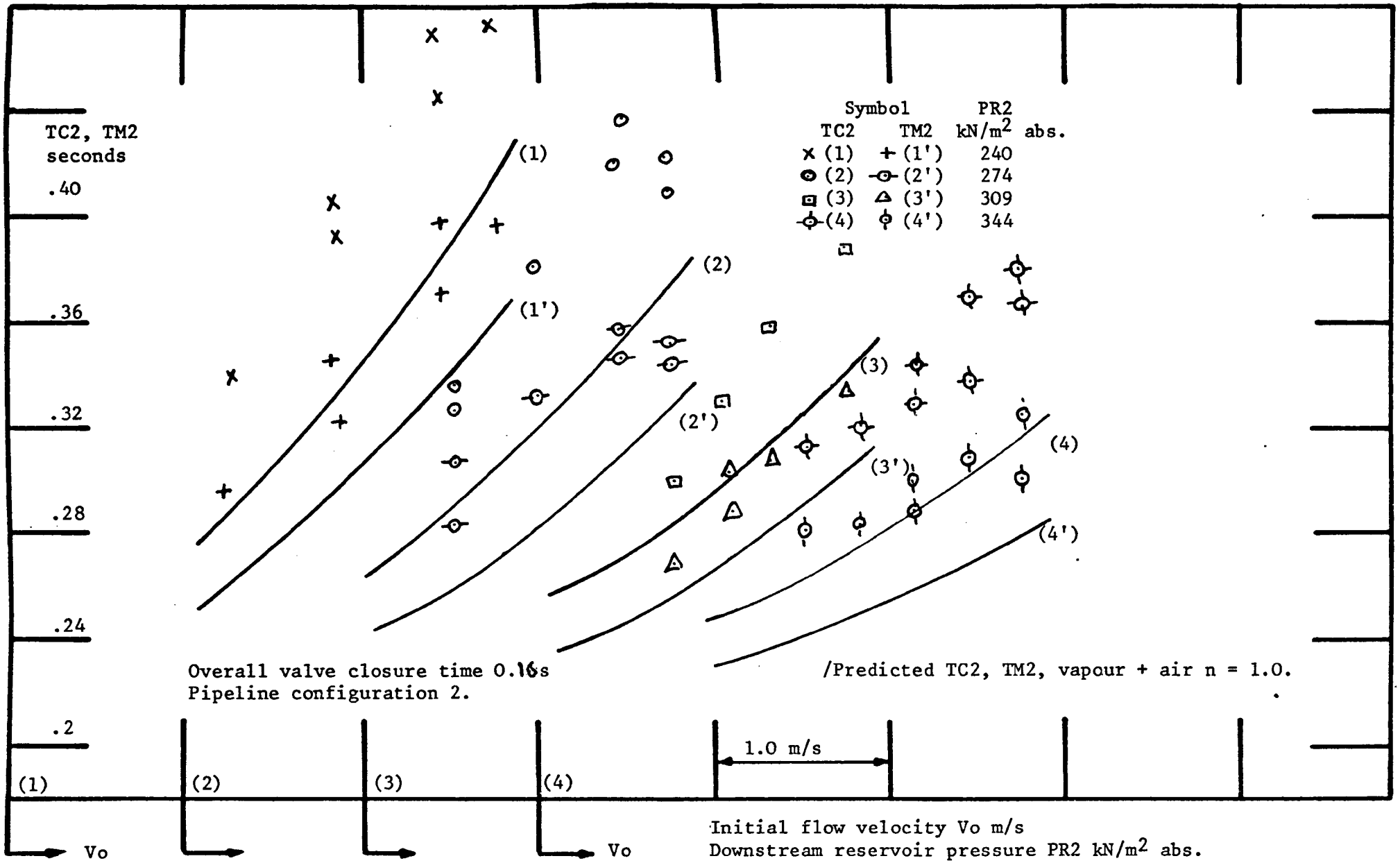

Fig. 116 Time to minimum pressure (TM2) and subsequent cavity collapse (TC2) for the second cavity formed downstream of the valve for a range of initial flow velocities (Vo) and downstream reservoir pressures (PR2).

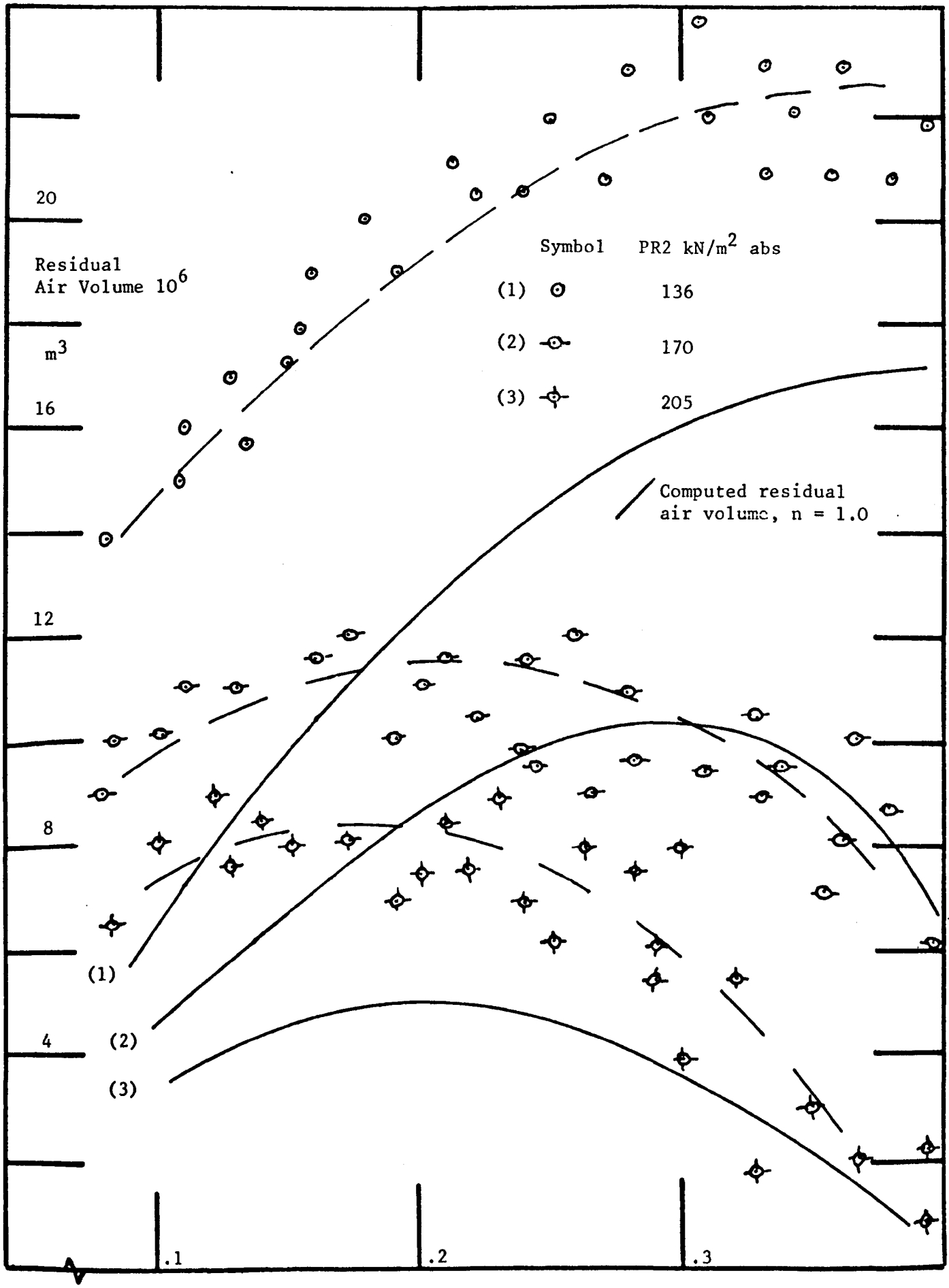

Fig. 117 Residual air volume vs. valve closure time (TC) for a range of downstream reservoir pressures (PR2). Initial flow velocity constant at 1.75 m/s. Pipeline configuration 2.

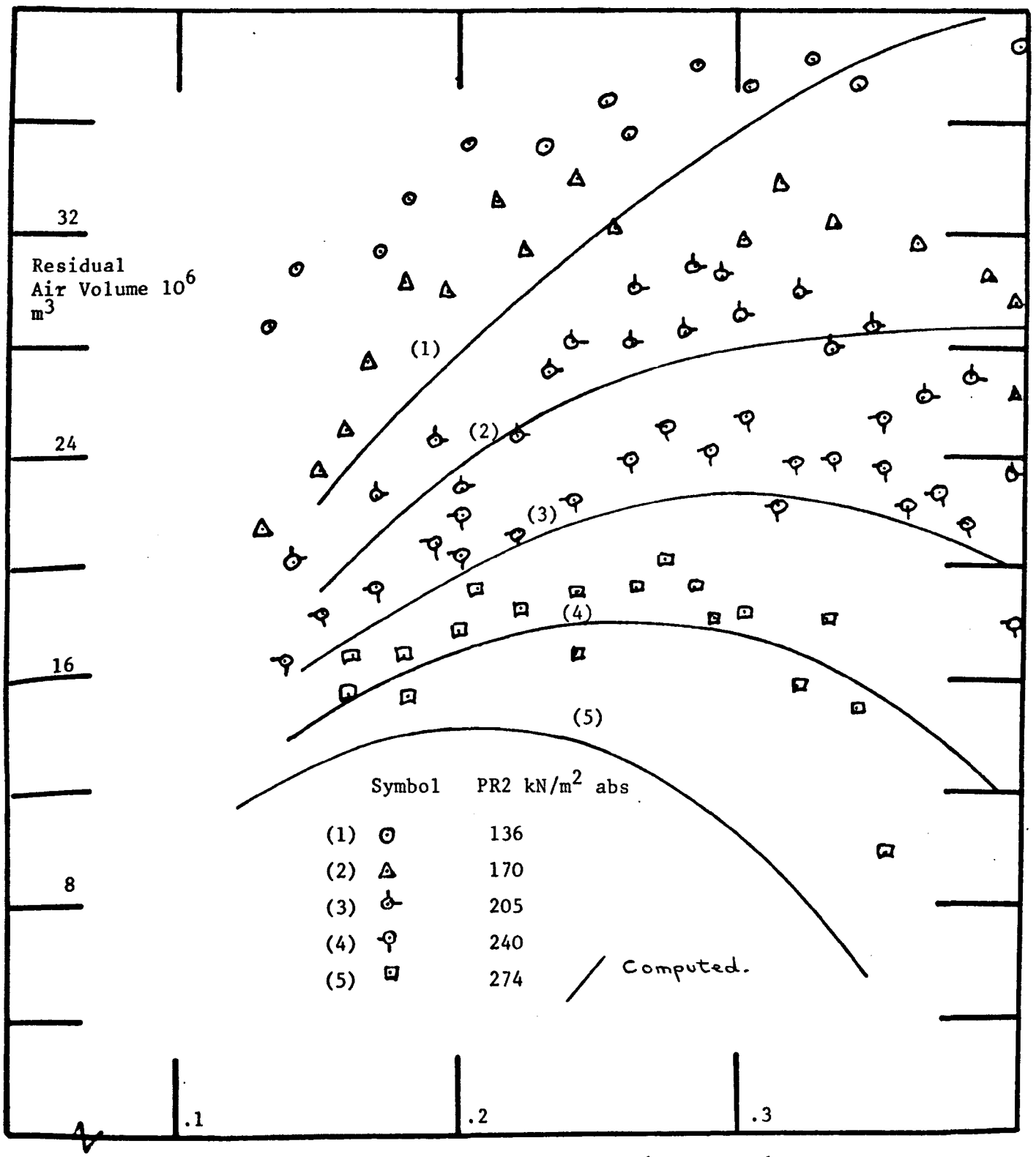

Fig. 118 Residual air volume vs. valve closure time (TC) for a range of downstream reservoir pressures (PR2). Initial flow velocity constant at 2.74 m/s. Pipeline configuration 2.

Fig. 119 Plates 1 - 4 illustrate the velocity variations recorded with a DISA hot-film anemometer mounted 1 m downstream of the valve, on the pipe centre line. Probe output linearized by use of a DISA 55D10 unit.

Common scales for plates 1 - 4:

L.D.T. .5 volts/y div.
DISA probe 2 volts/y div.

Trace layout:

1. L.D.T.
2. Hot-film probe.
3. Pressure transducer 5.08 cm downstream of valve.
4. " " 4.04 m " " "

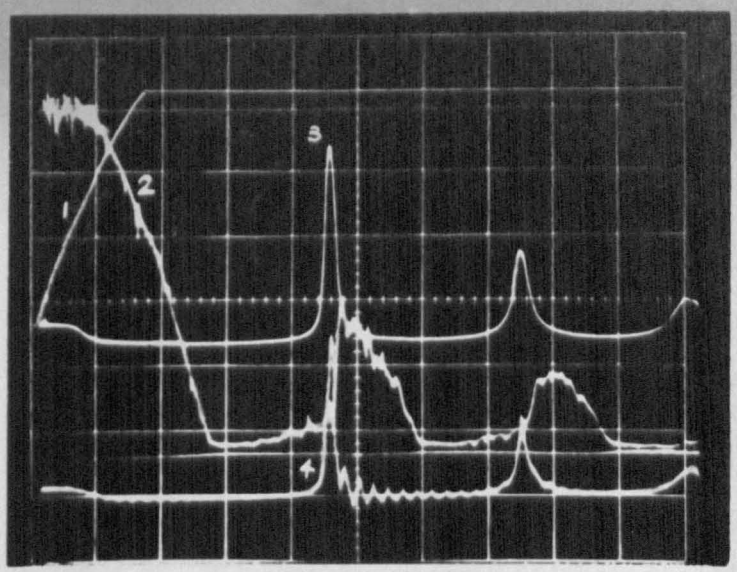

Fig. 119 Plate 1. Probe directed upstream.

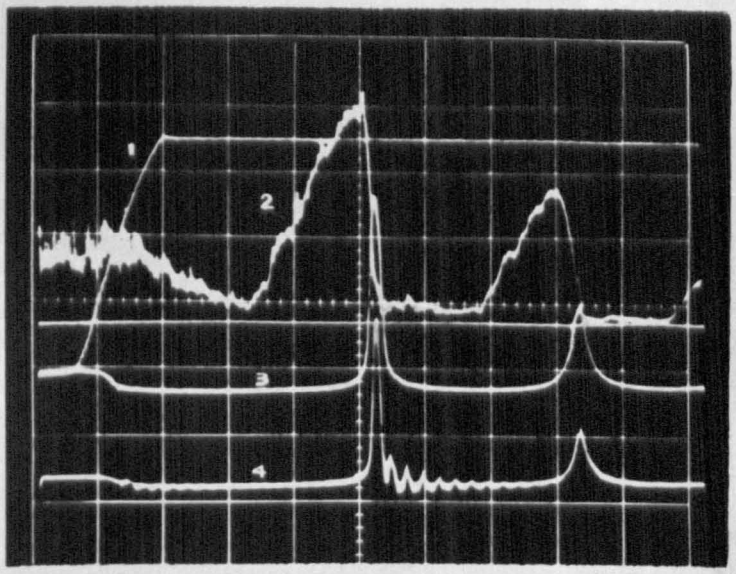

Fig. 119 Plate 2. Probe directed downstream.

V_o = 2.66 m/s TC = 0.14 s
PR2 = 120 kN/m^2 abs.

Scale: 450 kN/m^2/y div. for pressure-time traces 3, 4.
Time base = 0.1 s / x div.

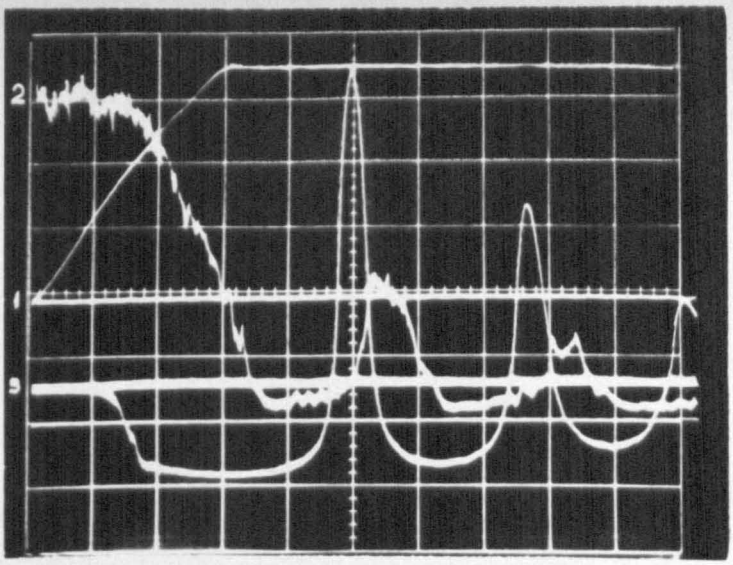

Fig. 119 Plate 3. Probe directed upstream.

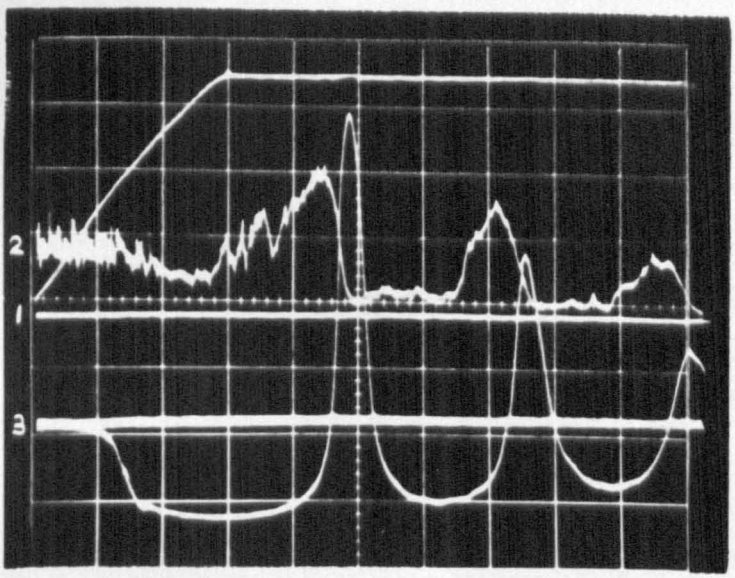

Fig. 119 Plate 4. Probe directed downstream.

V_o = 2.743 m/s TC = 0.16 s
PR2 = 309 kN/m^2 abs.

Scale: 225 kN/m^2/y div. for pressure trace 3.
Time base = 0.05 s / x div.

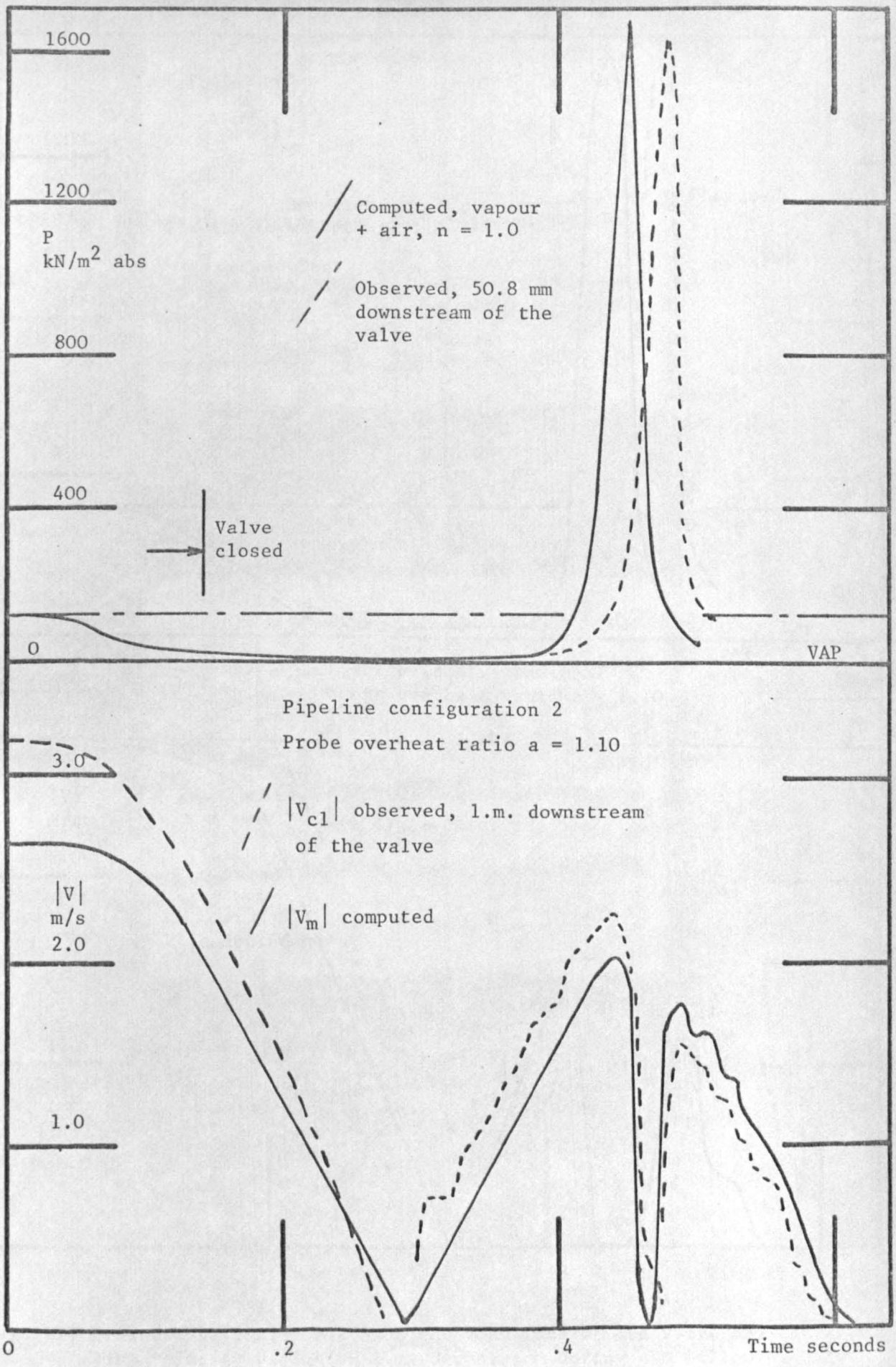

Fig.120 Pressure and velocity variations downstream of the valve during and following valve closure and the growth and collapse of the first cavity. Initial conditions, V_o = 2.67 m/s, PR2 = 120 kN/m^2 abs, TC = 0.14 s.

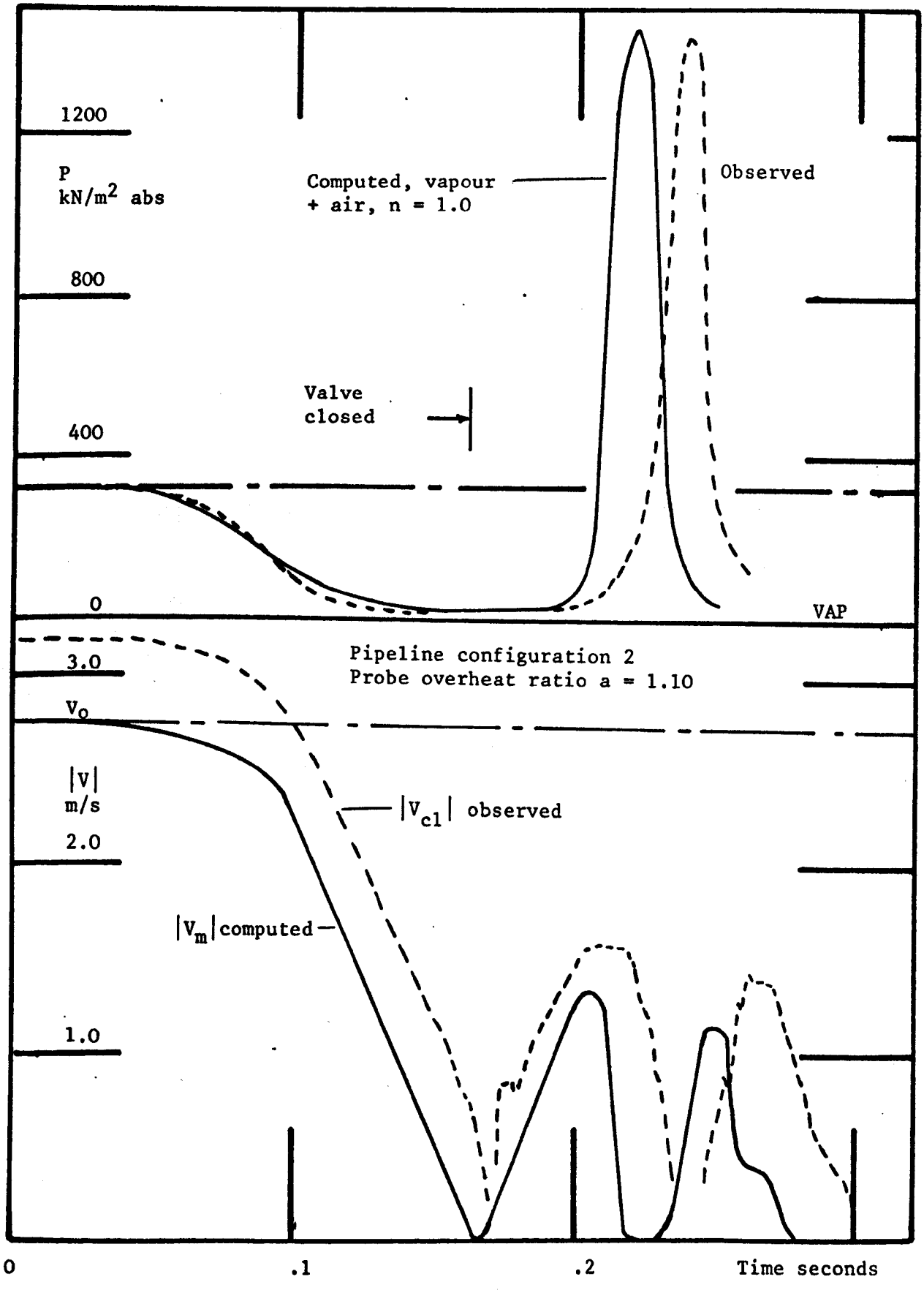

Fig. 121 Pressure variation on the downstream face of the valve and centre line velocity variation 1.m. downstream during and following valve closure and the growth and collapse of the first cavity. V_o = 2.74 m/s, PR2 = 309 kN/m^2 abs.

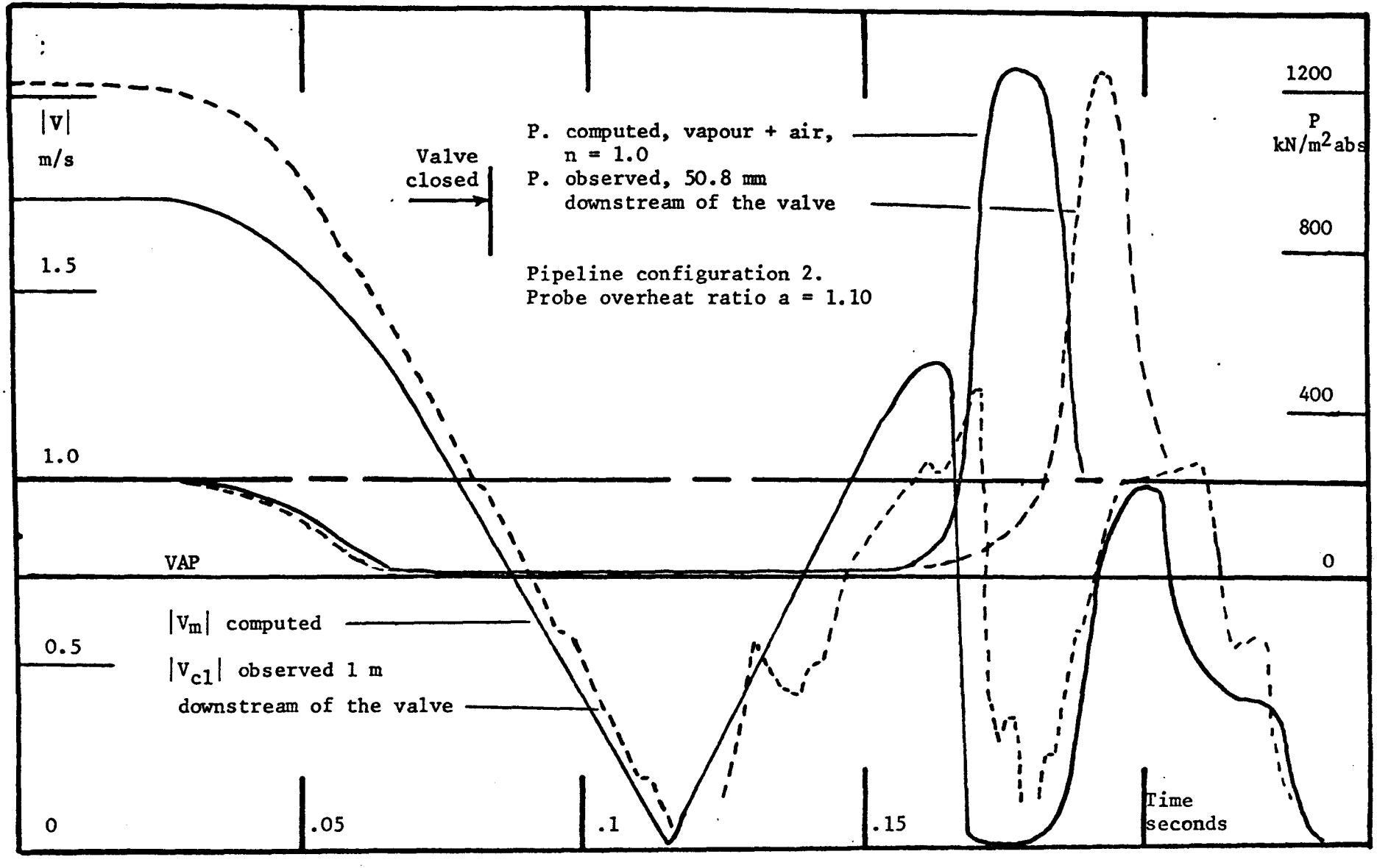

Fig. 122 Pressure and velocity variation downstream of the valve up to first cavity collapse.
Initial test conditions, V_o = 1.75 m/s, PR2 = 222 kN/m^2 abs.

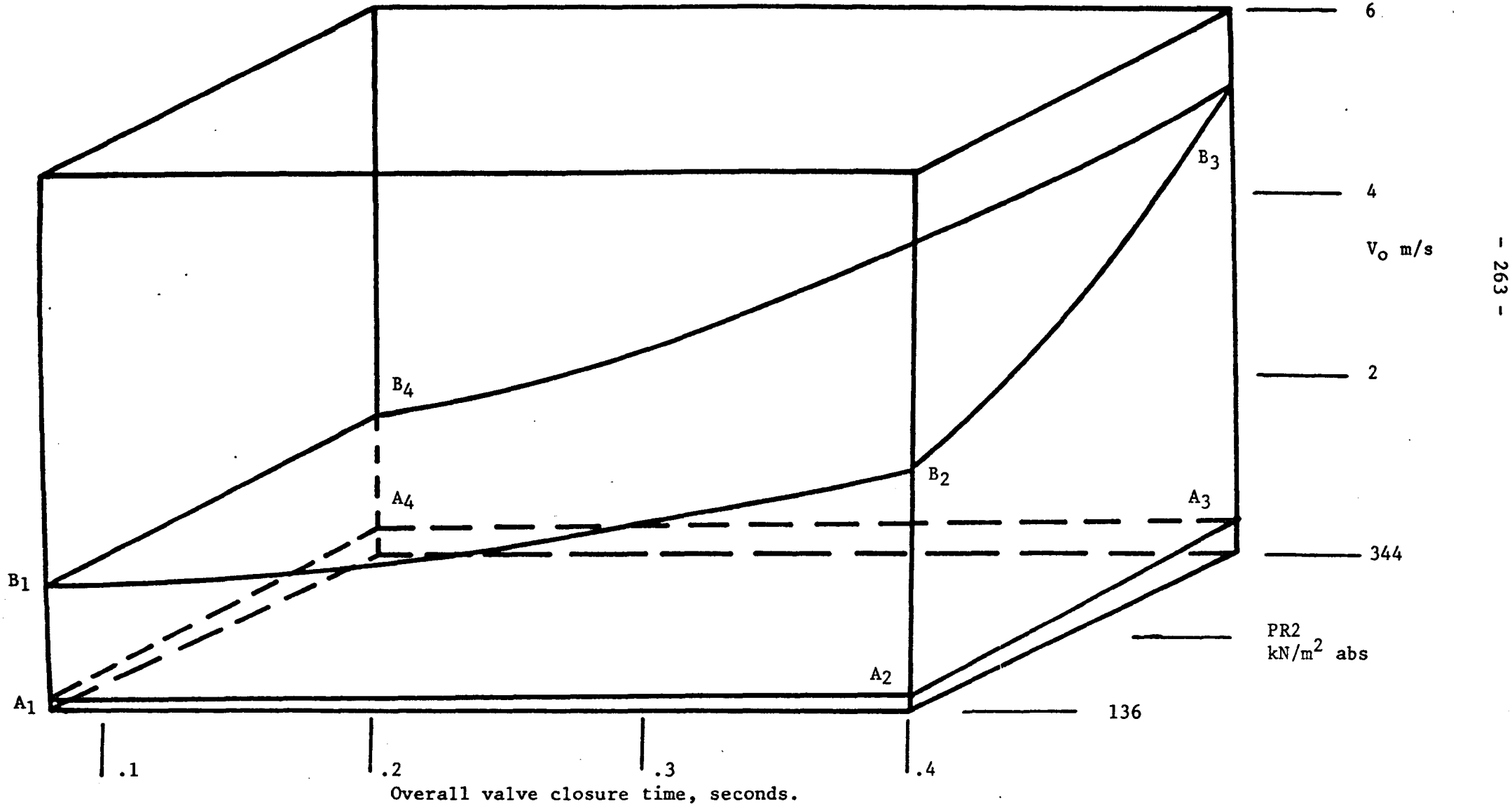

Fig. 123 Design envelope for simple pipeline to either avoid downstream separation on valve closure (conditions below A_{1-4}) or to limit pressure variation on cavity collapse to 1000 kN/m^2 above line pressure (volume A_{1-4}, B_{1-4}). *Pipeline configuration 2.*

Fig. 124 Plates 1 - 3 illustrate pressure variations on both sides of the valve during closure for a range of initial flow velocities (V_o) and valve closure times (TC).

Common scales for plates 1 - 3.

1. L.D.T. .5 volts/y div.
2. Pressure transducers 225 kN/m^2/y div.

Common trace layout from the top of each plate.

1. L.D.T.
2. Pressure transducer 5.08 cm upstream of valve.
3. " " 5.08 cm downstream of valve.

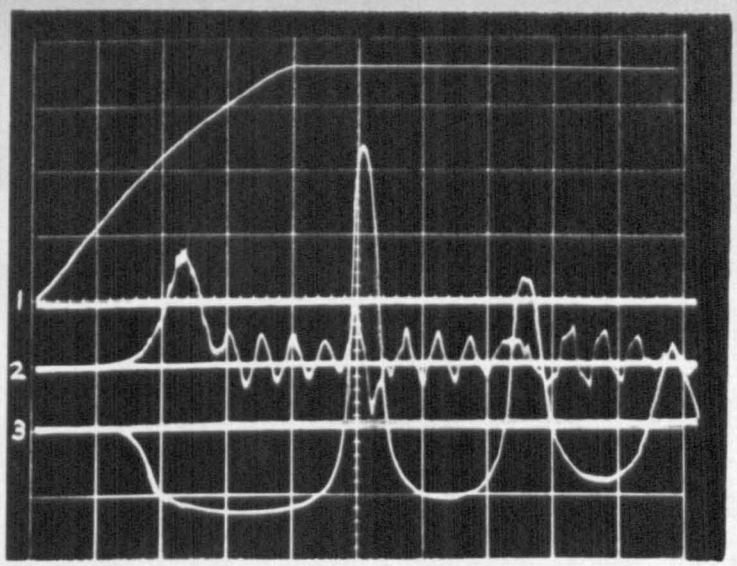

Fig. 124 Plate 1.

V_o = 2.743 m/s PR2 = 309 kN/m^2 abs.
Time base = 0.05 s / x div.

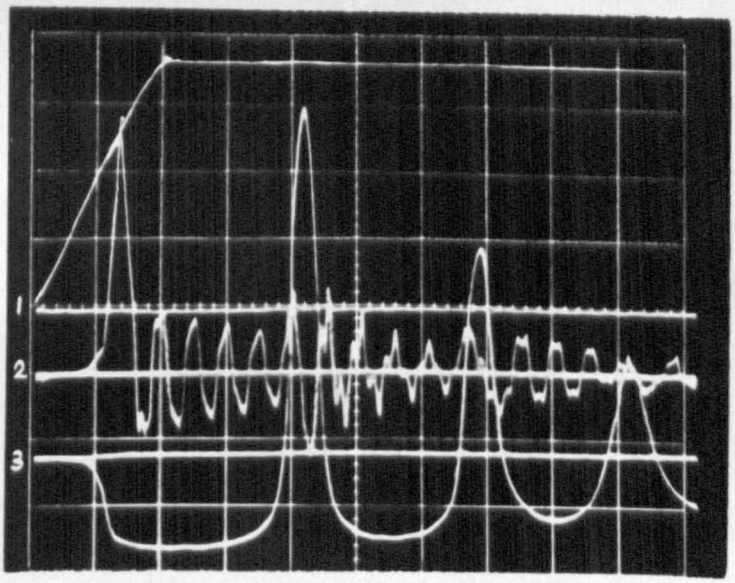

Fig. 124 Plate 2.

V_o = 2.29 m/s PR2 = 309 kN/m^2 abs.
Time base = 0.05 s / x div.

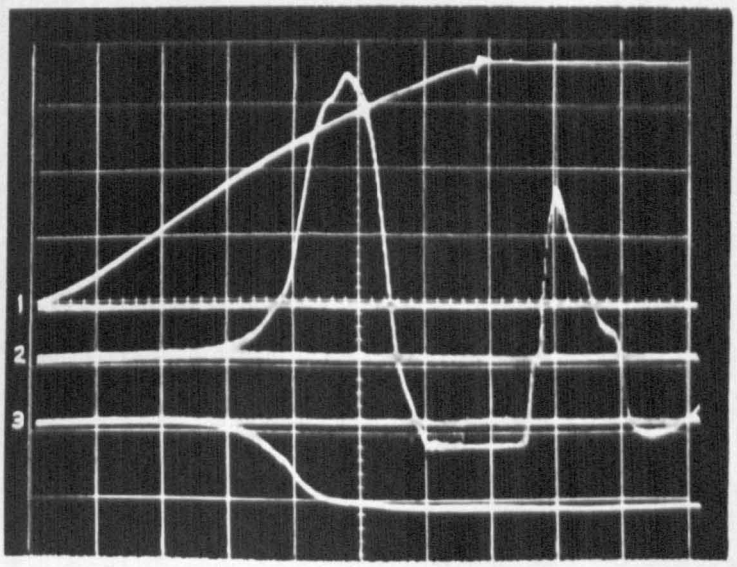

Fig. 124 Plate 3.

V_o = 1.75 m/s PR2 = 309 kN/m^2 abs.
Time base = 0.01 s / x div.

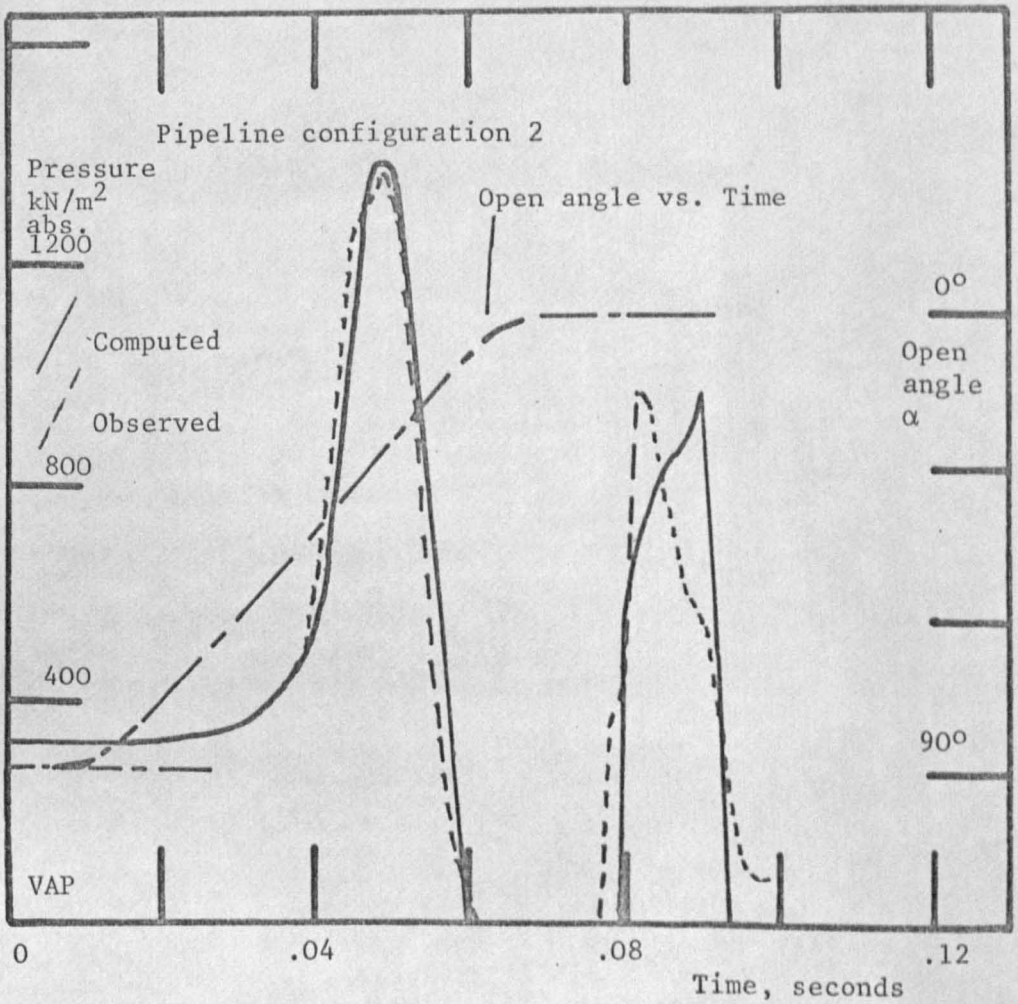

Fig. 125 Comparison between the observed and computed pressure variation on the upstream face of the valve following closure.
Initial conditions:- V_o = 1.75 m/s,
PR2 = 309 kN/m^2, valve closure in 0.07 s.

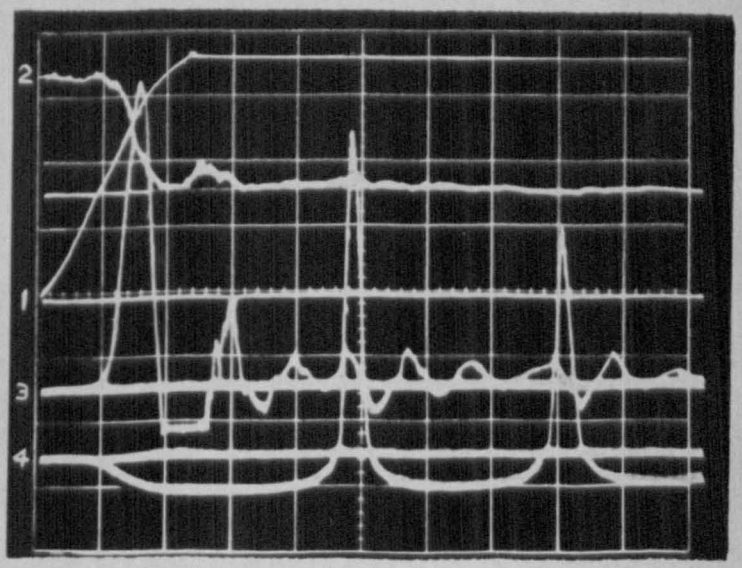

Fig. 126 Pressure variations on either side of the valve, together with the centre line velocity variation recorded by the DISA probe, following valve operation. For the above test the pipeline configuration was changed by initially pumping kerosene in the normal 'reverse flow' direction by means of the pump bypass system.

V_o = 2.43 m/s PR2 = 136 kN/m^2 abs.

Scale:
L.D.T. .5 volts/y div.
DISA probe 5 volts/y div.
Pressure transducers 225 kN/m^2/y div.
Time base = 0.05 s / x div.

Traces
1. L.D.T.
2. DISA probe, directed upstream, 1 m upstream of the valve.
3/4. Pressure transducers 5.08 cm on either side of the valve.

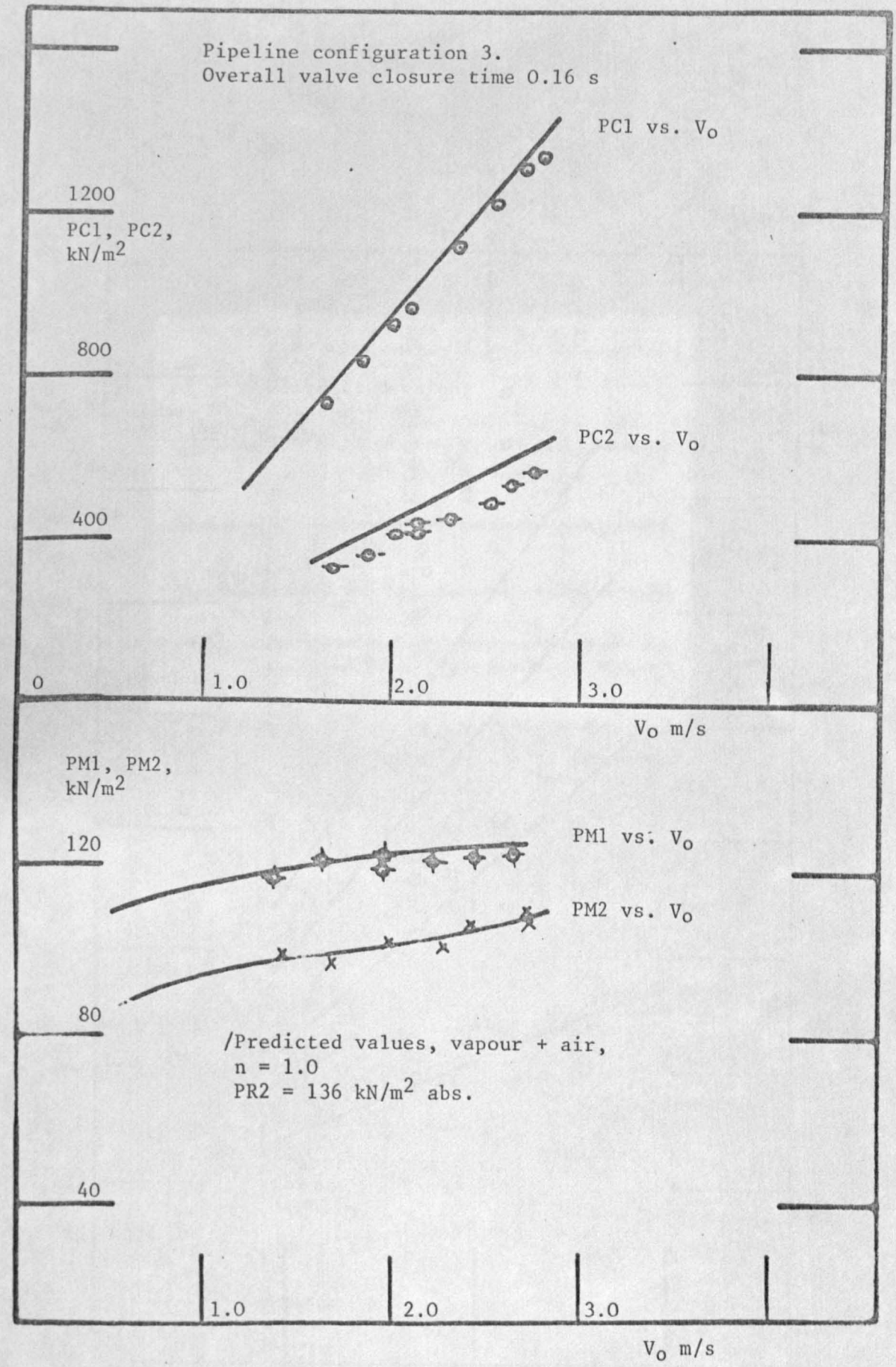

Fig. 127 Minimum pressure and cavity collapse pressure at the valve downstream face, for the first and second cavities formed, for a range of initial flow velocities. Pressures expressed as variations from steady state.

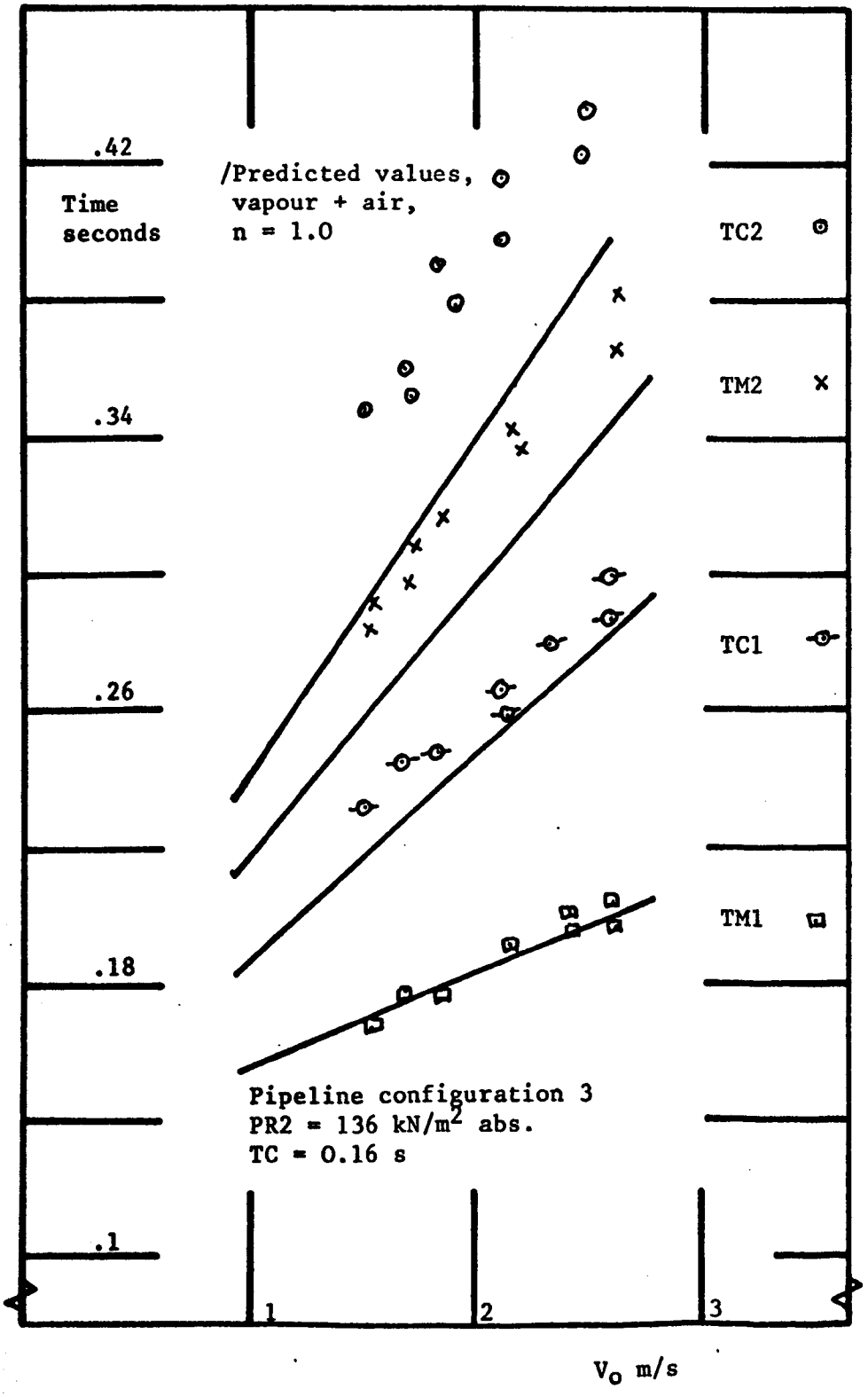

Fig. 128 Minimum pressure and cavity collapse times for the first and second cavities formed downstream of the valve following valve closure. Note that this figure refers to the 'reversed' test rig, i.e. shorter pipeline downstream.

PIPELINE CONFIGURATIONS					
1		2		2G	
	X1 m		X1 m		X1 m
Reservoir	0	Reservoir	0	Reservoir	0
T5	1.67	T5	1.67	T5	1.67
T4	4.10	T4	4.10	T4	4.10
T3	7.44	Valve	5.8	Valve	5.8
T2	11.30		X2 m		X2 m
T1	13.99	Valve	0	Valve	0
Valve	15.24	T3	1.0	T2	4.3
		T2	4.04	T1	7.41
		T1	7.15	Reservoir	9.74
		Reservoir	9.74		

Table 1 Layout of pressure transducer stations T_{1-5} for pipeline configurations 1, 2, 2G.
Note that on 2, 2G, 3 there were two additional tappings 50.8 mm on either side of the valve centre line. Pipeline 3 is the reverse of 2.
X1 measured from upstream reservoir
X2 measured downstream from valve.

LIQUID	TEMP.	SEPARATION SOURCE AND REFLECTOR.	REFLECTIONS MEASURED	DISTANCE TRAVELLED	TIME BASE	TIME TAKEN	EXPECTED ERROR	WAVE SPEED
	°C	m		m	µs/D	ms	± %	m/s
DISTILLED WATER	22.30	0.3048	1 - 2	0.6096	50	4.1000	1.22	1490.0
	22.30	0.3048	2 - 3	0.6096	50	4.1000	1.22	1490.0
	22.30	0.3048	1 - 2	0.6096	50	4.1250	1.21	1482.0
	22.30	0.3048	2 - 3	0.6096	50	4.1250	1.21	1482.0
	22.30	0.3048	1 - 3	1.2182	100	8.2000	1.22	1490.0
KEROSENE 2494	17.50	0.3048	1 - 2	0.6096	50	4.7500	1.05	1285.0
	17.50	0.3048	2 - 3	0.6096	50	4.7750	1.04	1275.0
	17.50	0.1524	1 - 3	0.6096	50	4.7750	1.04	1275.0
	17.50	0.1524	1 - 3	0.6096	100	4.8000	2.09	1270.0
	17.50	0.1524	1 - 4	0.9144	100	7.1500	1.40	1280.0
	17.50	0.1524	1 - 5	1.2182	100	9.5000	1.05	1285.0

TABLE 2 ACOUSTIC VELOCITY MEASUREMENTS CARRIED OUT TO DETERMINE BULK MODULUS OF KEROSENE.

LIQUID	TEMP	ACOUSTIC VELOCITY MEASURED	ACOUSTIC VELOCITY QUOTED	ERROR
	°C	m/s	m/s	%
DISTILLED WATER	22.3	1486.00 ± 0.274%	1489.00	0.202
AVIATION KEROSENE 2494.	17.5	1278.33 ± 0.700%	NO RELIABLE FIGURE.	

TABLE 3 AVERAGE RESULTS FOR THE ACOUSTIC VELOCITY IN DISTILLED WATER AND ASSO AVIATION KEROSENE SPEC. 2494 (AVTUR 50).

METHOD No.	DESCRIPTION	APPROX. TIME MEASURED.	TIME BASE	EXPECTED SCATTER
1	MEASUREMENT OF THE TIME TAKEN FOR A TRANSIENT TO TRAVEL FROM T1 TO RESERVOIR AND BACK -27.98 m	30 ms	5 ms/D	± 0.2D.
2	T1 TO T3 TRANSIT TIME -6.55 m	- DELAY TIME BASE USED.	2 ms/D	± 0.1D.
3			1 ms/D	± 0.1D.
4		NO TIME DELAY USED.	5 ms/D	± 0.1D.

TABLE 4 SUMMARY OF THE METHODS USED TO MEASURE THE TRANSIENT PROPAGATION VELOCITY THROUGH THE TEST SECTION.

Pipeline configuration 1, transducer stations T1, T3 refer to Table 1.

DATE	V_o m/s	α_o	WAVE SPEED	NUMBER OF READINGS	METHOD OF MEASUREMENT
10/10/68	0.170	22.5	910	4	1
			917	4	1
			880	2	1
11/10/68	0.170	22.5	934	4	3
			895	2	2
17/10/68	0.352	25.0	915	8	1
			932	9	1
			900	7	1
			910	2	1
			885	2	1
			940	4	4
			910	2	4
17/10/68	0.323	25.0	914	2	1
29/10/68	0.365	25.0	885	4	1
			914	2	1
			900	2	1
			920	4	2
			896	2	2
			935	2	4
30/10/68	0.299	25.0	914	2	1
			935	2	1
			903	2	2
			910	2	2
			919	4	2
			923	2	2
			935	2	4
			907	4	2
			919	2	2
6/11/68	0.327	25.0	930	12	2
			934	6	2
			915	8	2
			922	2	2
			912	12	2
			938	6	2
			932	2	2
			926	4	2
			917	4	2
			924	12	2
			940	4	2
			916	2	2
			908	2	2
7/11/68	0.285	24.0	933	14	2
			924	28	2
			916	12	2
			912	20	2
			938	2	2

TABLE 5 SUMMARY OF WAVE SPEED MEASUREMENTS. TEMP. = 17.5°C

WAVE SPEED COMPUTED	WAVE SPEED OBSERVED	AVERAGE DIFF.	METHOD	SCATTER OBSERVED	SCATTER EXPECTED
m/s	m/s	%		%	± %
917.113	919.850	0.295	1	1.3,-4.35	3.3
			2	1.96,-2.72	2.8
			3	1.52.	1.4
			4	2.18.	5.0

TABLE 6 COMPARISON BETWEEN THE OBSERVED AND COMPUTED VALUES OF THE TRANSIENT PROPAGATION VELOCITY THROUGH THE TEST SECTION. TEMP.=17.5°C.

DATE	RUN No.	α_o	Vo m/s	PR1 kN/m^2	Tc s	POSITION 1st. CAVITY.	POSITION 2nd. CAVITY.
13/11/68	1	90.0	0.989	6.05	.08	X/L=0.5-VALVE	VALVE.
	2	42.5	0.413	6.05	.04	VALVE	VALVE.
	3	25.0	0.293	27.6	.03	VALVE	---
18/11/68	1	20.0	0.150	57.7	.03	-----	-----
26/11/68	1	27.0	0.503	54.0	.04	VALVE	VALVE
	2	27.0	0.503	54.0	.072	VALVE	VALVE
	3	27.0	0.503	54.0	.100	---	---
17/2/69	1	50.0	1.096	18.4	.07	VALVE	VALVE
	2	42.5	0.790	18.4	.065	VALVE	VALVE
	3	32.5	0.487	18.4	.050	VALVE	VALVE
	4	57.5	1.40	18.4	.085	VALVE	VALVE
	5	57.5	1.40	18.4	.095	VALVE	VALVE
18/2/69	1	36.0	0.67	20.4	.065	VALVE	VALVE
	2	36.0	0.67	20.4	.065	VALVE	VALVE
	3	52.5	1.26	20.4	.090	VALVE	VALVE
	4	52.5	1.26	20.4	.100	VALVE	---
26/2/69	1	65.0	1.21	11.9	.085	X/L=0.4-VALVE	VALVE
	2	70.0	1.38	12.3	.080	X/L=0.4-VALVE	VALVE
	3	75.0	1.45	12.3	.090	X/L=0.5-VALVE	VALVE
	4	75.0	1.45	12.3	.130	VALVE	VALVE
	5	80.0	1.50	12.3	.130	VALVE	VALVE
27/2/69	1	45.0	0.487	5.44	.080	X/L=0.6-VALVE	VALVE
	2	45.0	0.615	8.50	.080	X/L=0.5-VALVE	VALVE
	3	45.0	0.785	13.60	.080	VALVE	VALVE
	4	45.0	0.868	17.00	.080	VALVE	VALVE
	5	45.0	1.100	27.20	.080	VALVE	VALVE
	6	45.0	1.144	30.60	.080	VALVE	VALVE
	7	45.0	0.980	22.40	.080	VALVE	VALVE
	8	45.0	0.968	22.10	.080	VALVE	VALVE
28/2/69	1	90.0	0.970	5.10	.096	X/L=0.7-VALVE	VALVE
	2	90.0	0.970	5.10	.142	X/L=0.4-VALVE	VALVE
	3	90.0	0.970	5.10	.200	X/L=0.6-VALVE	VALVE
	4	90.0	1.500	11.90	.124	VALVE	VALVE
	5	90.0	1.500	11.90	.144	X/L=0.7-VALVE	VALVE

TABLE 7 SUMMARY OF RECORDED TESTS AND THE PREDICTED POSITIONS OF THE VAPOUR CAVITIES FORMED.

Pipeline configuration 1. L = 15.24 m, X measured from reservoir.
All pressures kN/m^2 gauge.

		X/L	SEPP	SEPB	SEPD	OBSERVED.
1ST PEAK	PRESSURE	0.9	694.35	694.20	694.35	690.00
	PHASE		0.0768	0.0768	0.0768	0.0750
2ND PEAK	PRESSURE	0.9	456.00	455,40	455.40	385.00
	PHASE		0.2579	0.2579	0.2579	0.2600
3RD PEAK	PRESSURE	0.9	295.60	284.70	284.70	207.00
	PHASE		0.3791	0.3788	0.3788	0.3900
1ST PEAK	PRESSURE	0.5	594.16	594.16	594.16	572.20
	PHASE		0.0833	0.0833	0.0833	0.076
2ND PEAK	PRESSURE	0.5	413.38	412.69	412.76	372.60
	PHASE		0.2531	0.2530	0.2530	0.2500
3RD PEAK	PRESSURE	0.5	255.37	254.47	254.48	200.10
	PHASE		0.3742	0.3739	0.3739	0.3800
1ST CAVITY		X/L=	0.5	0.5	0.5	
	PHASE		0.0997	0.0997	0.0997	0.1000
	DURATION		0.0381	0.0381	0.0381	0.0400
	CLOSING PRESSURE		92.53	92.46	92.46	69.00
1ST VALVE CAVITY	PHASE		0.1015	0.1015	0.1015	0.1000
	DURATION		0.1353	0.1346	0.1352	0.1400
2ND VALVE CAVITY	PHASE		0.2718	0.2717	0.2717	0.2900
	DURATION		0.0863	0.0850	0.0851	0.0800

PRESSURE IN kN/m^2, PHASE-DURATION IN SECONDS.

TABLE 8 COMPARISON BETWEEN THE OUTPUT OF SEPP, SEPB, SEPD AND THE OBSERVED RESULTS FOR RUN 1, 13/11/68.

Pipeline configuration 1, L = 15.24 m,
X measured from upstream reservoir.

		X/L	SEPP	SEPB	SEPD	OBSERVED.
1ST PEAK	PRESSURE	0.9	242.05	242.05	242.12	236.33
	PHASE		0.0325	0.0325	0.0325	0.0340
2ND PEAK	PRESSURE	0.9	180.40	180.30	180.30	175.95
	PHASE		0.1136	0.1136	0.1136	0.1150
3RD PEAK	PRESSURE	0.9	138.90	138.80	138.80	127.65
	PHASE		0.1754	0.1754	0.1754	0.1700
1ST PEAK	PRESSURE	0.5	196.65	196.58	196.65	
	PHASE		0.0374	0.0374	0.0374	
2ND PEAK	PRESSURE	0.5	147.87	147.80	147.80	
	PHASE		0.1071	0.1071	0.1071	
3RD PEAK	PRESSURE	0.5	108.60	108.60	108.60	
	PHASE		0.1738	0.1738	0.1738	
1ST VALVE CAVITY	PHASE		0.0572	0.0572	0.0572	0.0600
	DURATION		0.0312	0.0312	0.0312	0.0280

PRESSURE IN kN/m^2, PHASE-DURATION IN SECONDS.

TABLE 9 COMPARISON BETWEEN THE OUTPUT OF SEPP, SEPB, SEPD AND THE OBSERVED RESULTS FOR RUN 3, 13/11/68.

Pipeline configuration 1, L = 15.24 m,
X measured from upstream reservoir.

		Z=	1.0	0.8	0.6	0.4	0.2	OBSERVED.
		X/L						
1ST PEAK	PRESSURE	0.9	694.20					690.00
	PHASE		0.0768					0.0768
2ND PEAK	PRESSURE	0.9	488.00	473.00	462.50	447.00	434.00	385.00
	PHASE		0.2648	0.2608	0.2582	0.2572	0.2551	0.2600
3RD PEAK	PRESSURE	0.9	443.50	345.00	310.50	277.50	250.00	207.00
	PHASE		0.4128	0.3924	0.3824	0.3751	0.3700	0.3900
1ST PEAK	PRESSURE	0.5	594.00					572.20
	PHASE		0.0833					0.0760
2ND PEAK	PRESSURE	0.5	467.60	441.00	418.00	404.50	387.00	372.60
	PHASE		0.2599	0.2556	0.2533	0.2526	0.2516	0.2500
3RD PEAK	PRESSURE	0.5	366.60	318.00	271.50	238.00	220.00	200.10
	PHASE		0.4047	0.3882	0.3775	0.3699	0.3645	0.3800
1ST CAVITY		X/L=	0.5	0.5	0.5	0.5	0.5	
	PHASE		0.0997	0.0997	0.0997	0.0997	0.0997	0.1000
	DURATION		0.0375	0.0377	0.0380	0.0381	0.0387	0.0400
	CLOSING PRESSURE		87.00	92.00	92.40	92.80	95.30	69.00
1ST VALVE	PHASE		0.1015	0.1015	0.1015	0.1015	0.1015	0.1000
CAVITY	DURATION		0.1355	0.1358	0.1352	0.1344	0.1340	0.1400
2ND VALVE	PHASE		0.2693	0.2712	0.2714	0.2716	0.2714	0.2900
CAVITY	DURATION		0.1120	0.0987	0.0884	0.0813	0.0800	0.0800

PRESSURE IN kN/m^2, PHASE-DURATION IN SECONDS.
PRIOR TO COLUMN SEPARATION DT =Dx/c,
FOLLOWING SEPARATION DT = Z*Dx/c.

TABLE 10 EFFECT OF VARYING THE TIME INCREMENT FOLLOWING THE 1ST. INDICATION OF VAPOUR PRESSURE. RUN 1. 13/11/68.

Pipeline configuration 1, L = 15.24 m, X measured from upstream reservoir.

		Z=	1.0	0.8	0.6	0.4	0.2	OBSERVED.
		X/L						
1ST PEAK	PRESSURE	0.9	240.05					236.33
	PHASE		0.0325					0.0340
2ND PEAK	PRESSURE	0.9	176.80	205.50	190.00	175.80	167.50	175.95
	PHASE		0.1180	0.1146	0.1138	0.1131	0.1123	0.1150
3RD PEAK	PRESSURE	0.9	176.50	144.40	143.20	132.20	124.00	127.65
	PHASE		0.1823	0.1798	0.1759	0.1748	0.1747	0.1700
1ST PEAK	PRESSURE	0.5	196.65					
	PHASE		0.0374					
2ND PEAK	PRESSURE	0.5	212.00	166.00	152.50	144.00	136.80	
	PHASE		0.1115	0.1081	0.1070	0.1066	0.1068	
3RD PEAK	PRESSURE	0.5	173.40	128.40	114.00	103.80	96.400	
	PHASE		0.1758	0.1746	0.1730	0.1735	0.1741	
1ST VALVE CAVITY	PHASE		0.0572	0.0572	0.0572	0.0572	0.0572	0.0600
	DURATION		0.0315	0.0314	0.0313	0.0312	0.0313	0.0280

PRESSURE IN kN/m^2, PHASE-DURATION IN SECONDS.
PRIOR TO COLUMN SEPARATION DT = Dx/c,
FOLLOWING SEPARATION DT = Z*Dx/c.

TABLE 11 EFFECT OF VARYING THE TIME INCREMENT FOLLOWING THE 1ST. INDICATION OF VAPOUR PRESSURE, RUN 3, 13/11/68.

Pipeline configuration 1, L = 15.24 m, X measured from upstream reservoir.

	Vapour only	Vapour + air			Observed
		n = 1.0	n = 1.2	n = 1.4	
V_o m/s	1.75				1.75
TC s	0.08				0.08
PR2 kN/m^2 abs	102.6				103.2
T (separation) s	0.051	0.03	0.03	0.03	-
V (separation) m/s	1.59	1.74	1.74	1.74	-
P (separation) kN/m^2 abs	0.7	101.5	101.5	101.5	-
Minimum pressure kN/m^2 abs	0.7	6.07	3.86	2.55	7.0
T (minimum pressure) s	0.173	0.198	0.195	0.192	0.20
T (cavity collapse) s	0.284	0.338	0.325	0.317	-
V (cavity collapse) m/s	-1.45	-1.522	-1.522	-1.525	-
Maximum pressure kN/m^2 abs	1200	1265	1272	1280	1180
T (maximum pressure) s	0.298	0.348	0.339	0.335	0.365
AIRVOL 10^6 m^3	-	12.0	12.2	12.4	-
FUELVOL 10^6 m^3	-	93.2	93.21	93.23	-
Maximum cavity volume 10^6 m^3	154.5	212.0	217.0	212.5	-

Table 12 Comparison between the 'vapour only' and released air boundary conditions at the valve during the existence of the 1st cavity formed.

Note: V (cavity collapse) is the maximum velocity of the returning column prior to cavity collapse.

T (minimum pressure) is the time of maximum cavity volume.

	Vapour only	Vapour + air			Observed
		n = 1.0	n = 1.2	n = 1.4	
V_o m/s	1.75				1.75
TC s	0.08				0.08
PR2 kN/m^2 abs	222				222
T (separation) s	0.056	.052	0.052	0.052	-
V (separation) m/s	1.41	1.56	1.56	1.56	-
P (separation) kN/m^2 abs	0.7	101.5	101.5	101.5	-
Minimum pressure kN/m^2 abs	0.7	6.50	4.14	2.7	7.0
T (minimum pressure) s	0.11	0.114	0.114	0.113	0.12
T (cavity collapse) s	0.155	0.162	0.16	0.159	-
V (cavity collapse) m/s	-1.29	-1.26	-1.25	-1.25	-
Maximum pressure kN/m^2 abs	1255	1250	1245	1252	1242
T (maximum pressure) s	0.170	0.178	0.176	0.175	0.19
AIRVOL 10^6 m^3	-	3.84	3.96	4.04	-
FUELVOL 10^6 m^3	-	30.3	30.4	30.4	-
Maximum cavity volume 10^6 m^3	56.6	68.0	66.6	65.8	-

Table 13 Comparison between the various boundary conditions applied at the valve during the existence of the 1st cavity.

	Vapour only	Vapour + air			Observed
		n = 1.0	n = 1.2	n = 1.4	
V_o m/s	1.75				1.75
TC s	0.16				0.16
PR2 kN/m^2 abs	222				222
T (separation) s	0.116	0.104	.104	0.104	-
V (separation) m/s	1.18	1.452	1.452	1.452	
P (separation) kN/m^2 abs	0.7	101.5	101.5	101.5	
Minimum pressure kN/m^2 abs	0.7	14.40	10.45	7.8	13.8
T (minimum pressure) s	0.158	0.167	0.167	0.166	0.16
T (cavity collapse) s	0.190	0.204	0.203	0.196	-
V (cavity collapse) m/s	-0.878	-0.907	-0.912	-0.902	-
Maximum pressure kN/m^2 abs	960	1010	1020	1018	995
T (maximum pressure) s	0.205	0.221	0.220	0.218	0.23
AIRVOL 10^6 m^3	-	5.78	6.0	6.2	-
FUELVOL 10^6 m^3	-	4.93	4.94	4.94	-
Maximum cavity volume 10^6 m^3	26.9	43.4	42.10	41.3	-

Table 14 Comparison between the various boundary conditions applied at the valve during the existence of the 1st cavity.

V_o m/s	PR2 kN/m^2 abs.	TC s.	Number of valve closures	Volume collected cc	Volume following treatment with alkaline pyrogallol cc				% Oxygen
					1	2	3	4	
2.74	240	.16	2	35.7	31.5	29.5	29.2	29.0	19.0
"	240	.14	2	32.5	28	26.5	26.3	26.3	19.9
"	309	.14	2	29.0	24.6	24.0	23.2	23.2	20.5
"	170	.24	1	25.5	22.5	21.0	20.0	20.0	21.3
"	170	.12	1	31.5	29.10	27.5	25.0	25.0	20.6
"	136	.14	1	28.0	24.0	23.2	22.5	22.4	20.0
"	205	.12	2	36.5	30.0	29.0	28.8	28.8	20.8
"	119	.17	1	25.5	22.0	21.0	20.5	20.5	19.8
"	188	.16	1	24.0	22.0	20.0	19.3	19.2	20.5
2.74	102	.16	1	38.0	34.0	33.0	30.2	30.0	20.8
1.75	136	.08	2	32.0	29.0	27.0	25.8	25.4	21.2
"	136	.12	1	18.0	16.0	15.0	14.6	14.6	19.6
"	136	.16	1	23.0	20.0	19.0	18.8	18.6	19.7
"	136	.20	1	22.0	19.0	18.0	17.5	17.5	20.4
"	170	.10	2	24.0	22.0	20.0	19.0	19.0	20.8
"	170	.14	2	26.0	22.0	20.7	20.7	20.7	20.2
"	170	.18	2	28.0	24.0	22.8	22.4	22.4	20.0
"	170	.24	2	26.0	22.0	21.5	20.9	20.9	19.7
"	205	.12	3	30.0	27.0	26.5	24.5	24.1	19.9
"	205	.16	3	30.0	28.0	25.0	24.0	23.5	21.5
"	205	.20	2	22.0	20.0	18.0	17.5	17.5	20.8
1.75	205	.28	3	25.0	22.0	20.5	20.5	19.9	20.3

Table 15 % Oxygen concentration of the residual air collected downstream of the valve following final cavity collapse.

V_o m/s	PR2 kN/m^2 abs.	TC s.	Predicted		Observed	
			P_c kN/m^2 abs.	T s.	P_c kN/m^2 abs.	T s.
1.75	222	.08	1035	0.067	1070	0.065
1.75	104	.08	895	0.062	930	0.060
2.74	309	.16	750	0.123	760	0.120
1.75	222	.16	600	0.133	600	0.140
2.74	222	.16	650	0.124	625	0.120
2.66	119	.18	400	0.135	410	0.130
1.75	309	.07	1340	0.050	1320	.048
2.74	309	.20	720	0.120	720	.115
2.29	309	.10	1100	0.062	1130	0.06
0.655	104	.11	350	0.082	360	0.08
0.655	104	.08	500	0.053	480	0.05
0.990	104	.12	618	0.079	600	0.08
0.990	104	.08	773	0.061	780	0.06
1.25	104	.14	500	0.101	470	0.10
1.25	104	.08	898	0.057	900	0.06
1.57	104	.13	618	0.102	630	.10
1.57	104	.08	1038	0.057	1050	.055

Table 16 Comparison between the observed and predicted pressure rise during valve closure immediately upstream of the valve in pipeline configuration 2.

V_o m/s	PR2 kN/m^2 abs	TC s	TSEP s	VSEP m/s	FUELVOL cc	VOL cc	AIRVOL cc	PMIN kN/m^{2}abs	TM1 s	VCLOS m/s	TCLOS s	ρcVCLOS kN/m^2	PMAX kN/m^{2}abs	TC1 s
2.743	135.827	0.081	0.038	2.676	100.693	356.131	13.096	4.431	0.207	2.307	0.353	1696.4	1888.4	0.368
2.743	204.774	0.081	0.043	2.573	76.595	203.860	9.841	5.602	0.152	2.155	0.240	1584.1	1871.9	0.255
2.743	273.722	0.081	0.047	2.469	59.176	135.904	7.545	6.339	0.126	2.036	0.188	1496.5	1869.7	0.201
2.743	342.670	0.081	0.051	2.359	42.129	96.467	5.370	6.355	0.110	1.934	0.156	1422.0	1873.1	0.170
2.743	135.827	0.162	0.075	2.645	180.082	316.856	22.573	7.939	0.257	2.071	0.394	1522.4	1713.2	0.410
2.743	204.774	0.162	0.086	2.514	134.413	154.588	16.229	11.374	0.199	1.766	0.276	1298.1	1596.2	0.292
2.743	273.722	0.162	0.094	2.359	105.374	83.867	12.149	15.437	0.174	1.474	0.221	1083.8	1485.8	0.237
2.743	342.670	0.162	0.103	2.121	68.852	46.686	7.741	17.572	0.159	1.214	0.190	892.7	1395.7	0.206
2.743	411.617	0.162	0.110	1.862	47.349	27.688	5.184	19.770	0.150	1.014	0.172	745.3	1337.3	0.188
2.743	135.827	0.243	0.113	2.606	245.403	276.041	29.560	11.588	0.304	1.844	0.432	1355.6	1541.8	0.449
2.743	204.774	0.243	0.130	2.425	180.115	109.166	19.855	19.208	0.248	1.375	0.312	1011.2	1310.0	0.329
2.743	273.722	0.243	0.145	2.144	124.396	42.977	12.040	29.233	0.223	0.932	0.257	685.3	1100.5	0.274
2.743	342.670	0.243	0.168	1.537	50.155	14.580	4.607	32.927	0.210	0.578	0.227	425.2	957.8	0.245
2.743	411.617	0.243	0.174	1.300	35.048	4.208	2.207	54.515	0.206	0.292	0.213	215.0	849.0	0.230
2.743	135.827	0.324	0.150	2.576	315.549	239.180	36.116	16.061	0.352	1.624	0.472	1193.8	1371.3	0.490
2.743	204.774	0.324	0.176	2.310	213.498	69.292	20.293	30.530	0.297	0.986	0.348	725.0	1014.7	0.365
2.743	273.722	0.324	0.218	1.496	72.071	11.661	5.272	46.876	0.275	0.397	0.291	292.0	706.2	0.309
2.743	342.670	0.324	0.252	0.503	17.934	0.073	0.042	72.760	0.269	0.016	0.269	12.0	378.0	0.281

Table 17 Output from SEPI, pipeline configuration 2.

V_o m/s	PR2 kN/m^2 abs	TC s	TSEP s	VSEP m/s	FUELVOL cc	VOL cc	AIRVOL cc	PMIN kN/m^{2}abs	TM1 s	VCLOS m/s	TCLOS s	ρcVCLOS kN/m^2	PMAX kN/m^{2}abs	TC1 s
2.743	135.827	0.041	0.019	2.685	52.903	222.461	6.921	3.855	0.121	2.394	0.210	1759.6	1934.7	0.217
2.743	204.774	0.041	0.022	2.586	38.649	130.984	5.018	4.588	0.087	2.267	0.142	1666.4	1916.4	0.149
2.743	273.722	0.041	0.024	2.487	29.721	88.783	3.839	5.091	0.072	2.161	0.110	1589.0	1906.6	0.117
2.743	342.670	0.041	0.026	2.383	23.093	28.596	2.810	10.689	0.052	1.253	0.072	920.9	1370.8	0.080
2.743	411.617	0.041	0.027	2.283	17.487	6.583	1.730	27 792	0.040	0.845	0.045	621.3	722.1	0.046
2.743	135.827	0.081	0.038	2.665	100.546	205.183	12.730	7.003	0.149	2.194	0.234	1613.0	1796.2	0.242
2.743	204.774	0.081	0.044	2.550	73.497	105.428	9.065	9.441	0.114	1.926	0.162	1416.0	1688.3	0.170
2.743	135.827	0.162	0.078	2.625	181.675	171.832	21.444	13.392	0.202	1.847	0.280	1357.9	1536.5	0.290
2.743	204.774	0.162	0.093	2.380	113.645	64.752	12.382	20.160	0.165	1.359	0.204	999.1	1279.9	0.212
2.743	273.722	0.162	0.108	1.916	52.330	25.649	5.527	22.652	0.149	0.980	0.169	720.4	1096.3	0.178
2.743	342.670	0.162	0.112	1.771	41.699	10.946	3.703	35.198	0.142	0.648	0.153	476.7	954.6	0.162
2.743	411.617	0.162	0.117	1.475	26.509	3.454	1.739	52.656	0.138	0.329	0.143	242.0	827.0	0.153
2.743	135.827	0.243	0.120	2.552	233.505	135.820	25.543	19.839	0.253	1.516	0.323	1114.5	1271.9	0.335
2.743	204.774	0.243	0.155	1.918	90.363	28.471	8.513	31.163	0.216	0.800	0.241	588.5	872.7	0.250
2.743	273.722	0.243	0.172	1.381	52.274	4.479	2.711	62.785	0.206	0.274	0.214	201.5	592.7	0.224
2.743	135.827	0.324	0.160	2.499	288.070	104.301	28.250	28.280	0.305	1.197	0.367	880.3	982.1	0.381
2.743	204.774	0.324	0.210	1.684	97.432	8.966	5.282	60.991	0 274	0.326	0.287	239.7	514.3	0.297

Table 18 Output from SEPI, pipeling configuration 3.

10. APPENDICES

Appendices 1 to 6 cover the derivation of equations not provided in the main text, together with print out of the computer programs and their flow diagrams.

10.1 Appendix 1 Schnyder-Bergeron graphical method

The method is based on the d'Alembert solution of the wave equations defining transient propagation:

$$p_{(x,t)} - p_o = F(t + x/c) + f(t - x/c) \quad (1.1)$$

$$V_{(x,t)} - V_o = -\frac{1}{\rho c}\left\{F(t + x/c) - f(t - x/c)\right\} \quad (1.2)$$

where V and p are the flow velocity and pressure at a section x at time t. F( ), f( ) are pressure waves moving in the -ve and +ve x directions respectively at the wave speed c.

Eliminating f( ) from (1.1), (1.2):

$$p_{(x,t)} - p_o = \rho c\,(V_{(x,t)} - V_o) + 2F\,(t + \frac{x}{c}) \quad (1.3)$$

Consider particular values X, T for the variables x, t and re-write (1.3) as:

$$p_{(X,T)} - p_o = \rho c(V_{(X,T)} - V_o) + 2F(T + \frac{X}{c}) \quad (1.4)$$

If an observer is assumed to travel in the -ve x direction with velocity c, the F( ) function will be constant as the observer travels with the wave, thus:

$$F(t + \frac{x}{c}) = F(T + \frac{X}{c}) \quad (1.5)$$

The F( ) function may now be eliminated from (1.3), (1.4):-

$$p_{(x,t)} - P_{(X,T)} = \rho c(V_{(x,t)} - V_{(X,T)}) \quad (1.6)$$

Referring to Figure 1.1, equation (1.6) represents line I.

By an identical process the second transient line, II, on Figure 1.1 can be shown to represent an observed travelling in the +ve x direction at velocity c. Line II is represented by the equation:

$$p_{(x,t)} - p_{(X,T)} = -\rho c\,(V_{(x,t)} - V_{(X,T)}) \quad (1.7)$$

In order to calculate the (V, p) unknowns it is necessary to solve a pair of equations. Two possibilities exist.

1. Either equation (1.6) or (1.7) may be solved graphically with a boundary condition known in terms of p and V, i.e. a valve discharge relationship, a closed end where V = 0 or a reservoir where p is a constant.
2. Internal points along a pipeline may be solved by the intersection of lines I and II on Figure 1.1.

A combination of 1 and 2 together with the application of continuity at junctions allows complex problems to be investigated.

Friction losses may be incorporated by the inclusion of a number of discrete pressure drops along each pipeline.

The above method has been shown to be accurate, however it does suffer from possible graphical errors which may be cumulative. Further it is an analysis method with little or no design capability. It is in the design of systems that the computer based method of characteristics is preferable.

It will have been noticed that the sign convention used has been +ve x in +V direction. This is contrary to the standard practice on the Schnyder Bergeron method but was adopted in order to agree with the convention employed in the numerical solution.

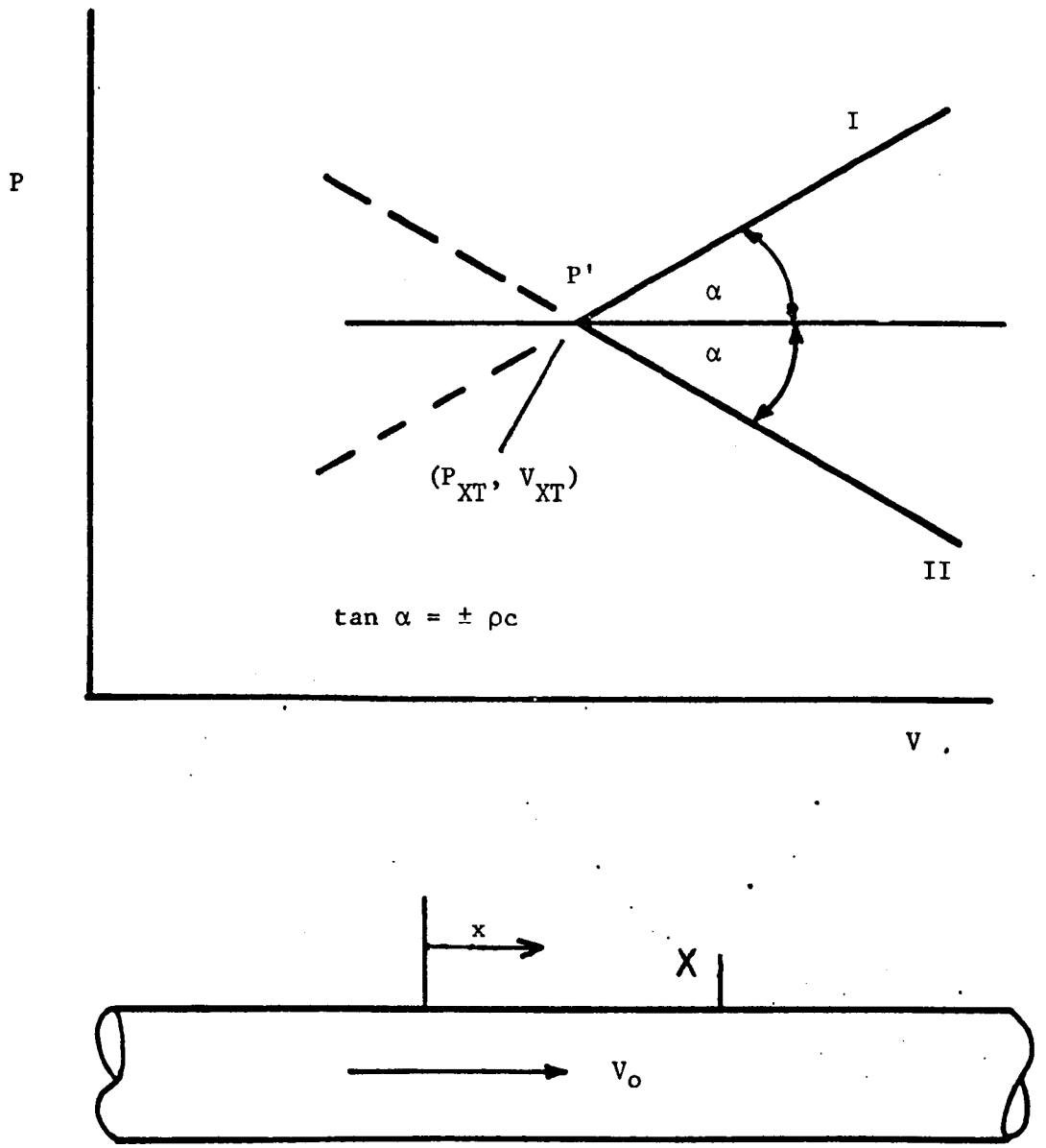

Fig. 1.1 Characteristic transient lines in the (P,V) plane used in the Schnyder-Bergeron graphical method.

10.2 Appendix 2 Preparation of the valve discharge - pressure characteristic for input into the programs during valve closure.

The valve steady state discharge coefficient was known as a function of the valve open angle. During closure the open angle of the valve was monitored by a Linear Displacement Transducer connected to the valve closing ram. Two curves are therefore available, Figure 2.1, to define the relationship between time, t, and valve discharge coefficient, τ.

During the analysis of column separation upstream of the valve by programs SEPP, SEPB, SEPC and SEPD the following procedure was followed.

1. Each curve was fed into the program as a series of points having (τ, α) and (α, t) co-ordinates respectively.
2. Values of α for each time step ΔT from t = 0 to t = TC (valve closure) were calculated by linear interpolation from the (α - t) data co-ordinates.
3. Using the α array set up by (2) a τ array was similarly produced from the (τ - α) data by linear interpolation between the two data points bracketting the α value concerned.

These procedures were carried out in the MASTER segment of SEPP, B, C and D.

A different method was chosen for the programs employed to analyse separation downstream of the valve in order to improve on the linear interpolations necessary above.

The method chosen was to fit polynomial curves to both the angle-τ and angle-time lines. Each curve was split into a number of sections and a polynomial fitted, by the method of least squares, to each section.

If the angle-τ curve is split into n sections and each is fitted with a polynomial of order m then a series of n equations are

obtained of the form:-

$$\tau_\alpha = C(i, 1) + \sum_{j=2}^{m+1} C(i, j).\alpha^{j-1} \qquad (2.1)$$

where α is the open angle of the valve.

Similarly for the time-angle curve, if it is split into p sections each represented by a polynomial of order q then

$$\alpha_t = D(k, 1) + \sum_{\ell=2}^{q+1} D(k, \ell).t^{\ell-1} \qquad (2.2)$$

represent a series of equations defining the angle vs. time curve.

In the programs presented in Appendix 5 these sets of equations are produced by Subroutines PRELIM and CURFIT.

During the valve closure procedure it is necessary to calculate the value of τ for each time step. The value of time t is substituted into the appropriate equation in set (2.2). The value of α_t is then substituted into the appropriate equation in set (2.1) and this yields a value for τ_t. The search and substitution procedures involved here are carried out by Subroutines INTER which deals with both substitutions.

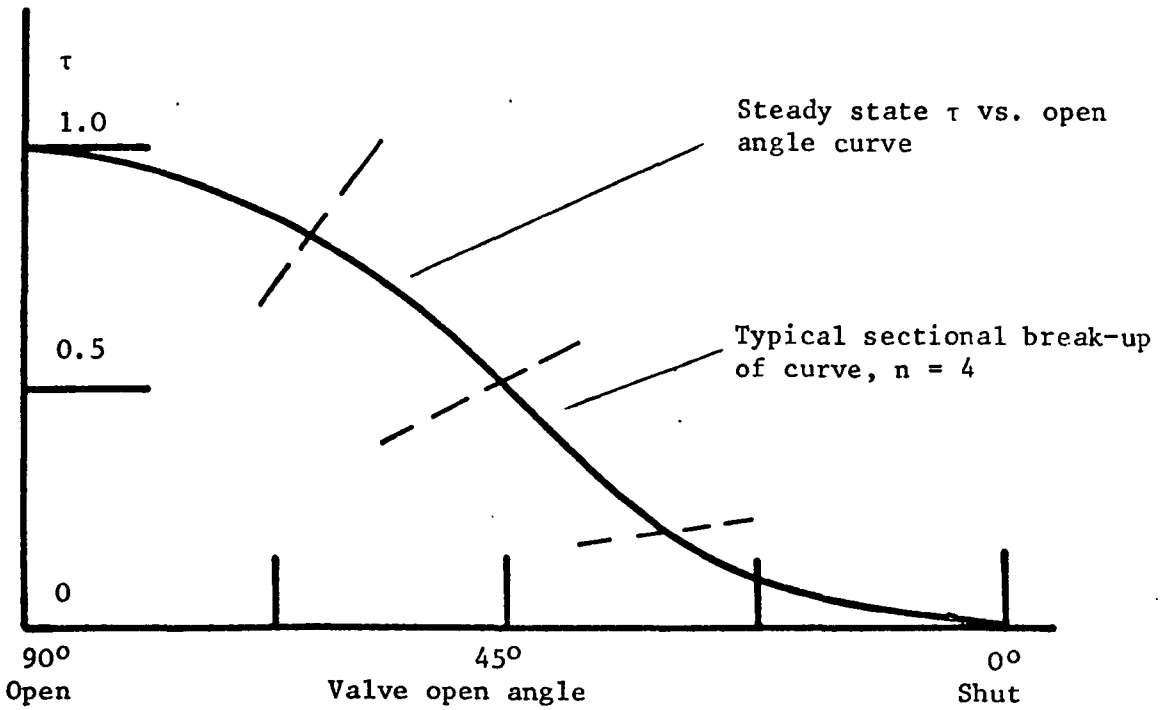

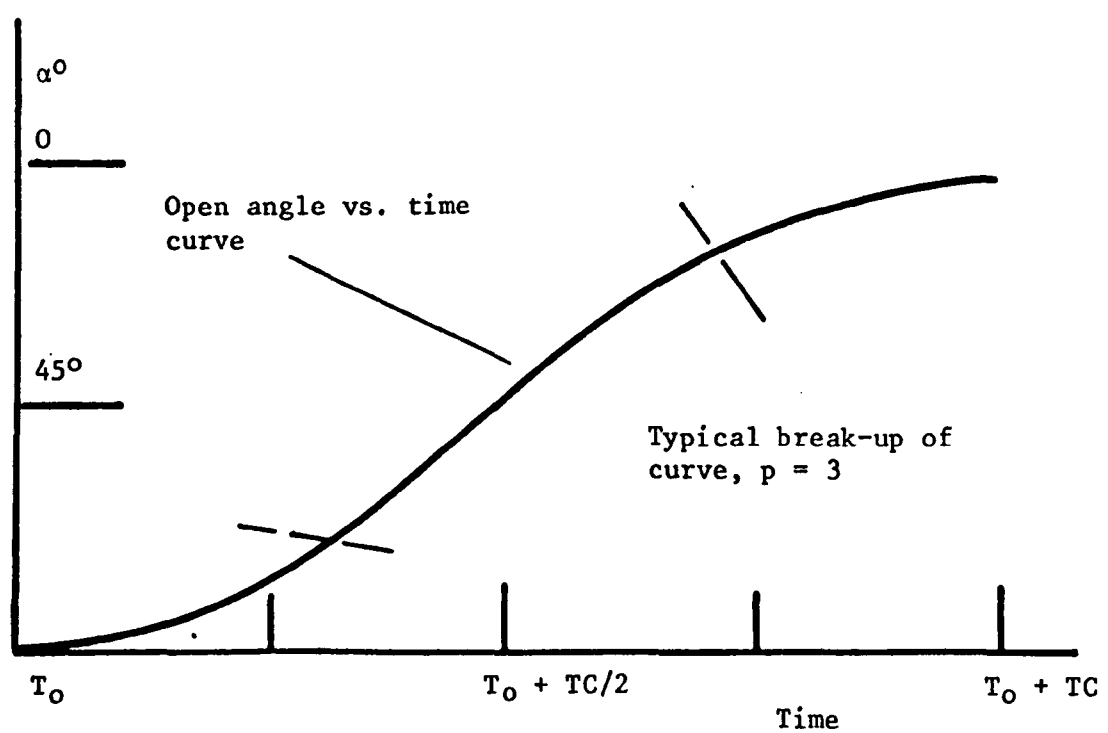

Fig. 2.1 Illustration of cross plot procedure for valve characteristic.

10.3 Appendix 3 Computer programs written to predict column separation upstream of a closed valve

Four programs were written in Fortran IV, based on the method of characteristics solution, to predict pressure variations upstream of a closed valve during and following column separation.

1. SEPP 1st order finite difference equations, friction factor based on the initial flow Reynold's Number. Time increment reduced following column separation from $\Delta x/c$ to $\Delta x/2c$ by interpolation. Vapour cavities allowed for either at some internal pipe section or at the valve.
2. SEPB Identical procedures to SEPP except that the friction factor at each section was calculated for each time step from the local Reynold's Number.
3. SEPC Identical procedures to SEPB. Program designed to investigate the effect of a variation in the time increment following separation, i.e. $\Delta T = Z\Delta x/c$, where $1 > Z > 0$.
4. SEPD 2nd order finite difference equations, friction factor calculated for each section at each time step from the local Reynold's Number. Vapour cavities again allowed for at the valve and at an internal pipe section.

All these programs accepted pressure data in gauge pressures and similarly all output pressures were gauge values. A linear interpolation technique was used to produce the $\tau \alpha t$ array needed as a boundary condition at the closing valve.

This appendix contains a complete print-out of SEPD together with flow diagram and notation. The second order C^+ C^- equations may be written as:

$$V_P - V_R + \frac{1}{\rho c}(P_P - P_R) + \frac{\Delta T}{D}\left((fV|V|)_P + (fV|V|)_R\right) = 0$$

$$V_P - V_S - \frac{1}{\rho c}(P_P - P_S) + \frac{\Delta T}{D}\left((fV|V|)_P + (fV|V|)_S\right) = 0$$

i.e. in a similar form to the 1st order equations, the (P, R, S) notation referring to Figure 5 in the text.

or, for the C^+ characteristic:

$$Y_P \, V_P |V_P| + V_P = K1 - K2 \, P_P \tag{3.1}$$

and for the C^- characteristic:

$$Y_P \, V_P |V_P| + V_P = K3 + K4 \, P_P \tag{3.2}$$

All internal points can be solved from (3.1), (3.2) above as they reduce to:

$$Y_P \, V_P |V_P| + V_P - K = 0 \tag{3.3}$$

however as $Y_P = f(V_P)$ it is necessary to employ an iterative procedure. The value of Y_P may be approximated by:

$$Y_P \triangleq \frac{1}{2} \frac{\Delta T}{D} (f_R + f_S) \tag{3.4}$$

and a value of V_P calculated from (3.3). This value may be used to calculate f_P from either:

$$f_P = 16/Re_P \qquad Re_P < 2300$$

or $$f_P = 0.079/Re_P^{\frac{1}{4}} \qquad Re_P > 2300$$

and a comparison made with the assumed value of Y_P.

The various boundary conditions may be solved directly with either (3.1) or (3.2), the above iterative procedure being incorporated into the solutions, which have already been fully described for the 1st order equations.

Notation employed in SEPD

AC	Valve open angle
AN	Values of the open angle of the valve during closure
BA, BB, BX, VC	Values of discharge-pressure characteristic during valve closure
C	Transient propagation velocity
D	Pipe bore
DT	Time increment used in the solution prior to cavity formation
DTR	Correction for exact time of cavity closure
F	Friction factor
FACT	Interpolation factor
F1, F1D	Frictional loss terms within the pipe sections upstream and downstream of an internal cavity
INTM, ICAV, JY	Route markers
JS	Section at which vapour cavity first formed
KINV1S	Fuel kinematic viscosity
MA, ZMA	Number of points on the valve characteristic vs. open angle curve
M, ZM	Number of points on the valve open angle vs. time curve
NRUN	Number of data sets
N, ZN	Number of pipe sections
PO, PR	Reservoir pressure
PL	Pipe length
P, PP, P1	Pressure at a section
REN	Reynolds Number
ROUTE	Route marker
RHO	Fuel density
TC	Valve closure time

TRANS	Transition Reynolds Number -2300
TS	Time of occurrence of vapour pressure at each of the pipe sections displaying pressures below vapour pressure at the end of a time step
TSMAX	Maximum value of TS for that time step
TMAX	Run time of solution
VAP, VAPI	Fuel vapour pressure
VOL, VOLX	Volume vapour cavities
VO	Initial flow velocity
V, VV, V1	Velcoity at a section
VCLOS	Cavity collapse velocity
VD VU	Velocity conditions downstream and upstream of an internal cavity
Y2	Slope of characteristic

FLOW DIAGRAM FOR SEPD

Read in values of valve discharge-pressure characteristic for a number of valve settings.

↓

Read in valve open angle for a series of time steps during closure.

↓

Crossplot to give valve characteristic vs. time curve. Interpolate at DT intervals.

↓

Read in basic program parameters, PL, RHO, VAP, D, N etc.

↓

Calculate steady state conditions at T = 0.

↓

Print out column headings.

↓

Print out calculated values of pressure, velocity, time, valve characteristic and cavity volume and position.

↓

Update time T = T + DT

↓

If T > TMAX go to FINISH

↓

Transfer values in VV, PP arrays into V, P as base conditions for next calculation.

↓

If DT < Dx/c interpolate between V,P(i) and V,P(i ± 1) to obtain arrays PU, PD, VU, VD.

↓

If DT < Dx/c go to B else A.

A. Solution prior to cavity formation.

↓

CALL FRICT to calculate friction factor at each internal section.

↓

CALL INTERNAL to calculate pressure and velocity conditions along the pipe.

↓

CALL VALVE to calculate conditions at the valve

Check all pressure values for results equal to or below vapour pressure.

No vapour pressure indicated Goto write Statements.

Values of TS(i) calculated to give times at which vapour pressure was reached at each section.

CALL SORTER to yield TSMAX and JS, the position of the 1st cavity.

If JS < N + 1, ICAV = 1 else 2.

Interpolate VV, PP arrays back to (T - TSMAX)

CALL CAVITY to calculate interface velocity on cavity formation.

Put DT = DT/2 if this is 1st cavity formed.

Goto write statements.

B. Solution following cavity formation.

CALL INTERNAL. If ICAV = 1 then CALL CAVITY for interface velocities.

Calculate pressure at closed valve if ICAV = 1.

Calculate TS(i) for any new section displaying vapour pressure.

ICAV = 1

Separation at an internal section.

ICAV = 2

Separation at the closed valve.

CALL CAVITY for interface velocity.

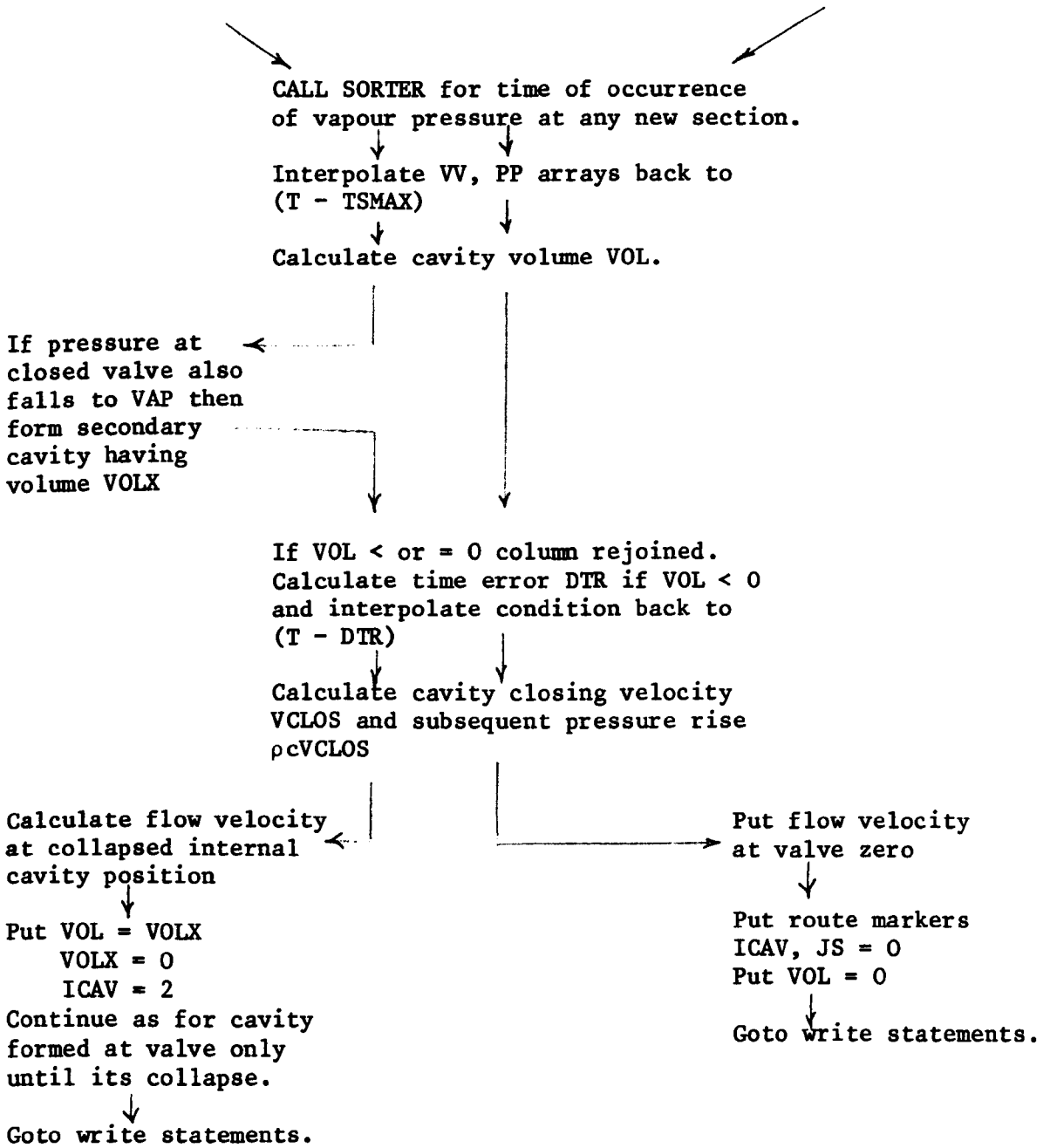
CALL SORTER for time of occurrence of vapour pressure at any new section.
Interpolate VV, PP arrays back to (T - TSMAX)
Calculate cavity volume VOL.
If pressure at closed valve also falls to VAP then form secondary cavity having volume VOLX
If VOL < or = 0 column rejoined. Calculate time error DTR if VOL < 0 and interpolate condition back to (T - DTR)
Calculate cavity closing velocity VCLOS and subsequent pressure rise ρcVCLOS
Calculate flow velocity at collapsed internal cavity position
Put VOL = VOLX
VOLX = 0
ICAV = 2
Continue as for cavity formed at valve only until its collapse.
Goto write statements.
Put flow velocity at valve zero
Put route markers ICAV, JS = 0
Put VOL = 0
Goto write statements.

FINISH.

```
      MASTER SEPD
C
C     SEPD IS THE 4TH IN A SERIES OF PROGRAMS WRITTEN IN FORTRAN 4
C     DESIGNED TO PREDICT PRESSURE AND VELOCITY VARIATIONS IN A
C     SIMPLE PIPELINE FOLLOWING VALVE CLOSURE. IN PARTICULAR
C     SEPD IS DESIGNED TO PREDICT THE PRESSURE VARIATIONS DURING
C     AND FOLLOWING THE FORMATION OF VAPOUR CAVITIES IN THE FLUID
C     COLUMN. THE APPROACH TO THE SOLUTION OF THE QUASI-LINEAR
C     HYPERBOLIC PARTIAL DIFFERENTIAL EQUATIONS DEFINING THE
C     PROPAGATION OF PRESSURE TRANSIENTS ALONG THE PIPELINE IS
C     VIA THE NUMERICAL METHOD OF CHARACTERISTICS. THE EXISTANCE
C     OF MORE THAN ONE VAPOUR CAVITY IN THE PIPE AT ONE TIME IS
C     DEALT WITH BY A SORTING AND INTERPOLATION PROCEEDURE WHICH
C     ALSO ENABLES ACCURATE PREDICTION OF THE VELOCITY AND
C     PRESSURE CONDITIONS IN THE PIPELINE DURING THE FORMATION
C     OF THE VAPOUR CAVITIES.

C     THE PROGRAM CAN BE SPLIT INTO A NUMBER OF SECTIONS:-
C     1.    INPUT OF THE VALVE DISCHARGE-PRESSURE
C           CHARACTERISTIC VS. VALVE OPEN ANGLE CURVE.
C           INPUT OF THE VALVE OPEN ANGLE VS. TIME CURVE.
C     2.    CROSS-PLOT OF THESE TWO CURVES TO GIVE VALVE
C           CHARACTERISTIC VS. TIME CURVE WHICH IS USED
C           AS THE OPEN VALVE BOUNDARY CONDITION IN THE
C           SUBSEQUENT SOLUTION.
C     3.    SOLUTION OF THE WAVE EQUATIONS, THREE POSSIBILITIES
C           ARE DEALT WITH:-
C     A.    NO VAPOUR CAVITIES PREDICTED AS THE PRESSURE REMAINED
C           ABOVE VAPOUR FORMATION LEVEL.
C     B.    A VAPOUR CAVITY IS FIRST PREDICTED AT THE CLOSED
C           VALVE.
C     C.    THE FIRST CAVITY IS PREDICTED AT SOME INTERNAL
C           SECTION.

C     FOR THE SOLUTION THE PIPELINE IS SPLIT INTO 10 EQUAL
C     SECTIONS AND PRESSURE AND VELOCITY CONDITIONS AT EACH
C     OF THESE ARE PRINTED OUT BY THE PROGRAM AT THE END OF
C     EACH TIME STEP TOGETHER WITH THE VOLUME OF ANY
C     CAVITIES PRESENT.

C     SEPD EMPLOYS 2ND ORDER OR TRAPEZOIDAL RULE APPROX.
C     IN THE FINITE DIFFERENCE EQUATIONS. FRICTION FACTOR IS
C     CONSIDERED DEPENDANT ON REYNOLDS NUMBER AND IS
C     CALCULATED AT EACH SECTION FOR EACH TIME STEP.

      REAL KINVIS
      DIMENSION T(800),B(800),BA(800),BB(800),VC(800),A(250),AN(250),
     1   P1(31), V1(31), UV(31), DV(31), VVU(31), VVD(31), F1D(31),
     1  AP(50), P(50), PP(50), V(50), VV(50), AX(500), BX(500), TS(110),
     2FF(50), F1(50), RE(50), XL(50) ,VU(30),PU(30),VD(30),PD(30)
      COMMON N, DT,KINVIS, TRANS, D,Y2,Y5,PF,VAP,VCHAR,JS,VCLOS
C
```

```
C       SECTION 1 -CROSSPLOT OF INPUT DATA - COMMON TO ALL TESTS ON
C       ONE VALVE SETTING.
C
        READ ( 1, 115 ) NRUN, KINVIS, TRANS
 115    FORMAT ( I3, 2F10.4 )
        KINVIS = KINVIS / 100000.0
        NX = 0
 45     NX = NX + 1
        READ ( 1, 100 ) MA, ZMA, AC
 100    FORMAT ( I4, 2F10.4 )
        DANG = AC / ZMA
        DO 1 I = 1, MA+1
                IF ( I-1 ) 2,2,3
 2              A(I) = AC
                GOTO 1
 3              A(I) = A(I-1) - DANG
 1      READ ( 1, 101 ) BX(I)
 101    FORMAT ( F10.4 )
        READ ( 1, 103 ) PL, C, ZN, N, D, RHO
        READ ( 1, 110 ) VAPI
 110    FORMAT ( F10.4 )
        AREA = 3.1417 * ( D**2 ) / 4.0
        VAP = VAPI * 144.0

C       REMAINDER OF PROGRAM REPEATED FOR EACH DATA SET.
        READ (1,102) IA
        IB = 0
 4      IB = IB + 1
        READ ( 1, 111 ) IDAY, IMTH, IYEAR, INUM
 111    FORMAT ( 4I4 )
        WRITE ( 2, 5001) IDAY, IMTH, IYEAR, INUM
 5001   FORMAT ( 5X, 94HTRANSIENT TESTS ON CONCORDE 2IN. O. D. 20 SWG. L56
       1. FUEL PRPE AND SAUNDERS E60F16 S. P. VALVE., //5X, 8HDATE =  ,
       2I2,3H / ,I2,3H / ,I4, 1H., /5X, 12HRUN NUMBER = , I4, 1H., // )
 102    FORMAT (I3 )
 103    FORMAT ( 3F10.4, I3, 2F10.4 )
        VOLX = 0.0
        VOL = 0.0
        ROUTE = 0.0
        NPATH = 0
        DO 50 I = 1, MA + 1
 50     BB(I) = BX(I)
        READ ( 1, 100 ) M, ZM, TC
        GDT = TC / ZM
        DO 8 IC = 1,M+1
                IF ( IC - 1 ) 6,6,7
 6              T(IC) = 0.0
                GOTO 8
 7              T(IC) = T(IC-1 ) + GDT
                GOTO 8
 8      READ ( 1, 101 ) AN(IC)
        DO 9 ID = 1, M-1
                DO 10 IE = 1, MA
                IG = IE + 1
                        IF ( AN(ID) - A(IG) ) 10, 11, 12
 11                     B(ID) = BB(IG)
```

```
                GOTO 9
 12         S = ( BB(IE) - BB(IG)) / DANG
            B(ID) = BB(IG) + S * ( AN(ID) - A(IG))
                GOTO 9
 10         CONTINUE
 9      CONTINUE
C
C       PRINTED CHECK ON CROSSPLOT
       WRITE ( 2, 200 )
 200   FORMAT ( /5X, 5HT(IP), 4X, 6HAN(IP), 2X/ )
       DO 3009IQ = 1, M+1
 3009  WRITE ( 2, 2019) T(IQ), AN(IQ)
 2019  FORMAT ( 2F10.4 )
       WRITE ( 2, 2029)
 2029  FORMAT ( /5X, 5HA(IR), 4X, 6HBB(IR), 2X/ )
       DO 3019IS = 1, MA+1
 3019  WRITE ( 2, 2019) A(IS), BB(IS)
       WRITE ( 2,2039)
 2039  FORMAT ( /5X, 5HT(IT), 5X, 5HB(IT), 3X/ )
       DO 3029IV = 1, M+1
       BB(IV) = B(IV)
 3029  WRITE ( 2, 2019) T(IV),BB(IV)



C       SECTION 2 - INTERPOLATION OF VALVE CHARACTERISTIC FOR THE
C       REQUIRED NUMBER OF TIME INTERVALS.

       DT =PL / ( C*ZN )
       U = ( TC / DT ) + 2.0
       IU = U
       JA = 1
       Y = 1.
       DO 900 IT = 1, M+1
       T(IT) = T(IT) * 1000.0
 900   BB(IT) = BB(IT) * 1000.0
       DT = DT * 1000.0
       GDT = GDT * 1000.0
       TC = TC * 1000.0
       DO 13 J = 1, IU
            IF ( J -1 ) 14, 14, 15
 14         T(J) = 0.0
            GOTO 16
 15         T(J) = T(J-1) + DT
            GOTO 16
 16         S = ( BB(JA)-BB(JA+1))/GDT
            IF ( T(J) - Y*GDT ) 17,18,19
 17         BA(J) = BB(JA)-S*(T(J)-(Y-1.0) * GDT)
            GOTO 20
 18         BA(J) = BB (JA+1)
            JA = JA+1
            Y = Y + 1.0
            GOTO 20
 19    BA(J)= BB(JA+1)-((BB(JA+1)-BB(JA+2))*(T(J)-Y*GDT)/GDT)
            JA = JA + 1
            Y = Y + 1.0
```

```
            GOTO 20
 20         IF ( T(J) - TC ) 13, 21,22
 22         J=J-1
            GOTO 21
 13    CONTINUE
 21    DO 23 JB = 1, J
       T(JB) = T(JB) / 1000.0
 23    B(JB) = BA(JB)  /1000.0
       DT = DT / 1000.0
       GDT = GDT / 1000.0
       TC = TC / 1000.0
C
C      INTERPOLATION CHECK -
       WRITE ( 2, 2049)
 2049  FORMAT ( /3X, 4HTIME, 7X,4HB(I) )
       WRITE ( 2, 205 ) ( T(JC), B(JC), JC=1, J )
 205   FORMAT ( 2F10.4 )




C      SECTION 3 - SOLUTION OF THE WAVE EQUATIONS.
C      ALL LENGTHS MEASURED FROM RESERVOIR.

       READ ( 1, 104 ) PO, VO, TMAX
 104   FORMAT ( 3F10.4 )

C      STEADY STATE CONDITIONS.

       WRITE ( 2, 105 ) N
 105   FORMAT ( 5X, 45HTRANSIENT PRESSURE AND FLUID VELOCITY AT 1 / ,
     1          I2, 49HPOINTS ALONG A SINGLE PIPE FOLLOWING VALVE MOTIWN,
     2        // )
       REN = ABS( VO ) * D / KINVIS
       IF ( REN - TRANS ) 81, 82, 82
 81    F = 16.0 / REN
       GOTO 83
 82    F = 0.79 / REN ** 0.25
 83    WRITE ( 2, 106 )
 106   FORMAT ( 5X, 29HINITIAL CONDITIONS:-, 2X// )
       WRITE ( 2, 107 ) PO, VO, PL, C, RHO, D, N, F , VAPI
 107   FORMAT (  5X, 3HPO=, F6.2, 6HP.S.I., 4X, 3HVO=, F6.2, 6HFT/SEC,
     1         4X, 3HPL=, F6.2, 2HFT, 4X/5X, 2HC=, F8.2, 6HFT/SEC, 4X, 4X,
     2      4HRHO=,F6.2,11HSLUGS/CU.FT, /5X, 2HD=, F6.2,3HFT.,
     3         4X, 2HN=, I3, 4X, 2HF=, F6.4, 4X,4HVAP=,F6.4,6HP.S.I., //)
       WRITE ( 2, 1000 ) AC, TC
 1000  FORMAT(5X,13HOPEN ANGLE = ,F5.1,5X,11HCLOSURE IN ,F6.3,4HSECS,//)
       XL(1) = 0.0
       DO 84 I = 2, N+1
       XL(I) = XL(I-1) + 1.0 / ZN
 84    CONTINUE
       WRITE ( 2, 108 ) ( XL(I), I= 1, N+1 )
 108   FORMAT (5X,4HTIME,6X,2HVL,5X,4HX/L=,11F7.4,3X,12HVOLUME VALVE,
     1         /99X, 13HCAVITY CU.FT., // )
       PO = PO * 144.0
       FDR = 2.0 * RHO * F * PL * ( VO**2 ) / ( D * ZN )
```

```
      PR = PO
      AA= 0.0
      DO 24 KA = 1, N+1
            AA = AA+ 1.0
            V(KA) = VO
            P(KA) = PR - (AA-1.0 ) * FDR
 24   AP(KA) = P(KA) / 144.0
      TIME = 0.0
      VC(1) = 1.0
      WRITE (2,109) TIME,VC(1),(V(KA),KA=1,N+1), (AP(KA),KA=1,N+1) ,VOL
 109  FORMAT(2F1 .4,2X,2HV=,10F7.2,F7.2/22X,2HP=,11F7.2,F13.8/ )
      Y2 =  1.0 / ( C * RHO )
      Y5 = ( VO**2 ) / ( Y2 * P(N+1) )
      KB = 1
      JS = 0
      ICAV = 0
      INTM = 0
      JY = 0



C     CALCULATION OF INTERIOR POINTS.

 25   TIME = TIME + DT
      KB = KB + 1
      VC(KB) = B(KB) / B(1)
      DO 91 LX = 1, N+1
91       TS(LX) = 0.0

      IF ( INTM - 1 ) 56, 57, 57

C     INTM DENOTES WHETHER DT=DX/C OR =DX/2C.

 56     CALL FRICT ( V, 1, N+1, F1 )
        DO 26 L = 1, N-1
             LA = L + 1
             CALL INTERNAL (1,LA,P,V,P,V,F1,F1,VV,PP)
 26   CONTINUE
C

C     BOUNDARY CONDITIONS:-
C     1.      CONSTANT PRESSURE RESERVOIR.
       CALL INTERNAL (1,1,P,V,P,V,F1,F1,VV,PP)
C
C     2.      VALVE BOUNDARY-
      IF ( TIME - TC ) 27, 28, 28
C     2A.     OPEN VALVE-
 27    VCHAR = VC(KB)
       CALL VALVE (P,V,F1,VV,PP)
        GOTO 29
C
C     2B.     CLOSED VALVE-
 28   VC(KB) =  .0
      IF ( ROUTE - 1.0 ) 34, 35, 38
 34    VV(N+1) = 0.0
       PP(N+1) = P(N) + (V(N)-0.5*F1(N)*V(N)*ABS(V(N)))/Y2
       IF ( INTM. LE. 1 )   GOTO 9000
```

```
C      CALC. INTERNAL POINTS WHEN DT=DX/AC,THIS SECTION
C      ONLY USED IF A CAVITY HAS BEEN INDICATED.

 57     CALL FRICT ( VU, 2, N+1, F1 )
        CALL FRICT ( VD,   1,   N,  F1D )
        DO 261 I = 2, N
       IF ( I-JS ) 571,572,571
 572   PP(JS) = VAP
       TS(JS) = 0.0
        CALL CAVITY (-1.0,1,I,VD,PD,F1D,VVD)
        CALL CAVITY ( 1.0,1,I,VU,PU, F1,VVU)
       GOTO 261
 571    CALL INTERNAL (2,I,PU,VU,PD,VD,F1,F1D,VV,PP)
 261    CONTINUE
        CALL INTERNAL (2,1,PU,VU,PD,VD,F1,F1D,VV,PP)
       VC(KB) = 0.0
       IF ( ICAV - 1 ) 264, 264, 263
 264   VV(N+1) = 0.0
       PP(N+1)=(VU(N+1)+Y2*PU(N+1)-0.5*F1(N+1)*VU(N+1)*ABS(VU(N+1)))/Y2
 263   IF ( ROUTE - 1.0 ) 9000, 35, 29
 9000  KZ = 0
        IF ( TIME - 0.2680)  573, 574, 574
 574    KZ=0
 573    KZ=0

C      THE NEXT PROCEEDURE CALCULATES VALUES OF TS(I) THE
C      TIME OF  OCCURENCE OF VAPOUR PRESSURE AT ANY SECTION.

       DO 201 I = 1, N+1
       VX = PP(I) + ABS(VAP)
       IF ( VX - 0.0 ) 202, 201, 203
 202   TS(I) = DT*(VAP-PP(I))/(P(I)-PP(I))
       IF ( P(I) - VAP ) 2021, 2021, 201
 2021  TS(I) = 0.0
       PP(I) = VAP
       GOTO 201
 203   KZ = KZ + 1
 201   CONTINUE
       IF ( KZ - ( N+1 )) 204, 29, 29
 204     CALL SORTER ( TS, TSMAX, J1 )

       IF ( J1 - N+1 ) 206, 207, 207
 206   ICAV = 1
       JS = J1
       GOTO 208
 207   ICAV = 2
 208   TIME = TIME - TSMAX
C      THE FOLLOWING INTERPOLATION GIVE THE PRESSURE AND VELOCITY
C      CONDITIONS IN THE PIPELINE AT THE INSTANT THAT VAPOUR
C      PRESSURE WAS FIRST REACHED.

       FACT = ( DT - TSMAX ) / DT
       DO 209 I = 1, N+1
       VV(I) = V(I) + FACT*(VV(I)-V(I))
       PP(I) = P(I) + FACT *(PP(I)-P(I))
       P(I) = P1(I) + FACT*(P(I)-P1(I))
       V(I) = V1(I) + FACT * ( V(I)-V1(I))
 209   CONTINUE
```

```
      IF ( INTM. EQ. 1 )   GOTO 9001
       CALL FRICT ( V, 1, N+1, F1 )
      IF ( ICAV - 1 ) 210, 210, 211
  210  CALL CAVITY ( 1.0,0,JS,V,P,F1,VVU)
       CALL CAVITY (-1.0,0,JS,V,P,F1,VVD)
      PP(JS) = VAP
      GOTO 212
  211 PP(N+1) = VAP
       CALL CAVITY (1.0,0,N+1,V,P,F1,VV)
      GOTO 212
 9001 IF ( ICAV. GT. 1 )   GOTO 9002
      VD(JS) = 0.5*(V(JS)+V(JS+1))
      VU(JS) = 0.5 * ( V(JS) + V(JS-1) )
      PU(JS) = 0.5*(P(JS)+P(JS-1))
      PD(JS) = 0.5*(P(JS)+P(JS+1))
       CALL FRICT ( VU, JS, JS, F1 )
       CALL FRICT ( VD, JS, JS, F1D )
       CALL CAVITY ( 1.0,1,JS,VU,PU,F1,VVU)
       CALL CAVITY (-1.0,1,JS,VD,PD,F1D,VVD)
      PP(JS) = VAP
      GOTO 212
 9002 PP(N+1) = VAP
      VU(N+1)=0.5*(V(N)+V(N-1))
      PU(N+1)=0.5*(P(N)+P(N-1))
       CALL FRICT ( VU, N+1, N+1, F1 )

       CALL CAVITY (1.0,1,N+1,VU,PU,F1,VV)
       GOTO 212
  212 ROUTE = 1.0
      INTM = 1
      IF(JY-1) 99, 29, 29
   99 DT = DT / 2.0
      GOTO 29



C     THE NEXT SECTION DEALS WITH CAVITY FORMATION AT SOME
C     INTERNAL PIPE SECTION AND WITH THE FORMATION OF A
C     SECONDARY CAVITY AT THE CLOSED VALVE. THE PRESSURE
C     RISE DUE TO THE COLLAPSE OF THIS INTERNAL CAVITY
C     IS CALCULATED IN THIS SECTION AS IS THE SUBSEQUENT
C     VELOCITY AT ITS LOCATION.

   35 DO 2611 I = 1, N+1
      IF ( I - JS ) 352, 353, 352
  353 PP(JS) = VAP
      TS(JS) = 0.0
      GOTO 2611
  352 IF ( PP(I) - VAP ) 262, 1261, 261 1
  262 TS(I) = DT*(VAP-PP(I))/(P(I)-PP(I))
      IF ( P(I) - VAP ) 2621, 2621, 261 1
 2621 PP(I) = VAP
 1261 TS(I) = 0.0
 2611 CONTINUE
      IF ( ICAV - 1 ) 773, 773, 73
  773 CALL SORTER ( TS, TSMAX, J1 )
      IF ( TSMAX - 0.0 ) 477, 477, 488
  488 FACT = ( DT - TSMAX)/ DT
      TIME = TIME - TSMAX
```

```
      DO 499 I = 1, N+1
      IF ( I - JS ) 491, 492, 491
  491 VV(I) = V(I) + FACT*(VV(I)-V(I))
      PP(I) = P(I) +  FACT*(PP(I)-P(I))
      GOTO 499
  492 VVD(I) = DV(I) + FACT*(VVD(I)-DV(I))
      VVU(I) = UV(I) + FACT *(VVU(I)-UV(I))
      PP(I) = VAP
  499 CONTINUE
  477 VOL = VOL-AREA*(DT-TSMAX)*(VVU(JS)+UV(JS)-VVD(JS)-DV(JS))/2.0
      IF ( PP(N+1)-VAP) 500, 500, 600
  500  CALL CAVITY (1.0,1,N+1,VU,PU,F1,VV)
       VOLX = VOLX -AREA*(DT-TSMAX)*(VV(N+1)+V(N+1))/2.0
  600 IF ( VOL - 0.0 ) 377, 388, 399
  399 ROUTE = 1.0
      GOTO 29
  377 DTR = -VOL/(AREA*0.5*(VVU(JS)+UV(JS)-VVD(JS)-DV(JS)))
      IF(VOLX.GT.0.0)VOLX=VOLX-DTR*AREA*0.5*(VV(N+1)-V(N+1))
      TIME = TIME - DTR
      FACT = ( DT - DTR ) / DT
      DO 400 I = 1, N+1
      IF ( I - JS ) 401, 402, 401
  401 VV(I) = V(I) + FACT*(VV(I)-V(I))
      PP(I) = P(I) + FACT*(PP(I)-P(I))
      GOTO 400
  402 VVD(I) = DV(I) + FACT*(VVD(I)-DV(I))
      VVU(I) = UV(I) + FACT*(VVU(I)-UV(I))
      PP(I) = VAP
  400 CONTINUE
  388 VCLOS =(VVU(JS) - VVD(JS)) / 2.0
      PP(JS) = VAP + VCLOS / Y2

       CALL  INTERNAL (2,JS,PU,VU,PD,VD,F1,F1D,VV,PP)
      IF ( PP(N+1)-VAP ) 601, 601, 602
  601 VOL = VOLX
      ICAV = 2
      ROUTE = 1.0
      GOTO 603
  602 VOL = 0.0
      ICAV = 0
      ROUTE = 0.0
  603 JY=1
      JS = 0
      GOTO 29
```

```
C     THIS SECTION DEALS WITH THE FORMATION OF A VAPOUR
C     CAVITY AT THE CLOSED VALVE. THE GROWTH AND DECAY
C     OF A SECONDARY VALVE CAVITY AND ITS CLOSING PRESSURE
C     ARE DEALT WITH IN THIS SECTION FOLLOWING THE COLLAPSE
C     OF THE INTERNAL PIPE SECTION VAPOUR CAVITY MENTIONED
C     ABOVE.
```

```
C       SEPARATION AT CLOSED VALVE.

 73     PP(N+1) = VAP
        CALL CAVITY (1.0,1,N+1,VU,PU,F1,VV)
        CALL SORTER ( TS, TSMAX, J1 )
        IF ( TSMAX - 0.0 ) 47, 47, 48
 48     FACT = ( DT- TSMAX ) / DT
        TIME = TIME - TSMAX
        DO 49 I = 1, N+1
        VV(I) = V(I) + FACT*(VV(I)-V(I))
        PP(I) = P(I) + FACT*(PP(I)-P(I))
 49     CONTINUE
 47     VOL = VOL - AREA*(DT-TSMAX)*(VV(N+1)+V(N+1))/2.0
        IF ( VOL - 0.0 ) 37, 38, 39
 39     ROUTE = 1.0
        GOTO 29
 37     DTR = -VOL/(AREA*0.5*(VV(N+1)+V(N+1)))
        TIME = TIME - DTR
        FACT = ( DT - DTR ) / DT
        DO 40 IX = 1, N+1
        VV(IX) = V(IX) + FACT * ( VV(IX) - V(IX))
        PP(IX) = P(IX) + FACT * ( PP(IX) - P(IX))
 40     CONTINUE
C       COLUMN REJOINED.
 38     VCLOS = VV(N+1)
        VV(N+1) = 0.0
        PP(N+1) = VAP + VCLOS / Y2
        NPATH = 0
        VOL = 0.0
        ICAV = 0
        JS = 0
        ROUTE = 0.0
        JY = 1
        GOTO 29




C       THE FOLLOWING SECTION DEALS WITH THE PRINTING OUT OF
C       RESULTS AND THE CALCULATION OF THE BASE CONDITIONS
C       FOR THE NEXT TIME STEP.

 29     IF ( ICAV - 1 ) 291, 292, 291
 291    DO 30 LC = 1, N+1
        V1(LC) = V(LC)
        P1(LC) = P(LC)
               V(LC) = VV(LC)
               AP(LC) = PP(LC)/ 144.0
 30     P(LC) = PP(LC)
        WRITE(2,1 9)TIME,VC(KB),(V(LD),LD=1,N+1),(AP(LD),LD=1,N+1),VOL
        GOTO  303
 292    DO 31 LC = 1, N+1
        UV(LC) = 0.0
        DV(LC) = 0.0
        P(LC) =PP(LC)
        AP(LC) = PP(LC) / 144.0
        IF ( LC - JS ) 302, 303, 304
```

```
 302  V(LC) = VV(LC)
      UV(LC) = VV(LC)
      GOTO 3,1
 303  V(LC) = VVU(LC)
      UV(LC) = VVU(LC)
      DV(LC) = VVD(LC)
      GOTO 3,1
 304  V(LC) = VV(LC)
      DV(LC) = VV(LC)
 301  CONTINUE
      WRITE(2,1091)TIME,VC(KB),(UV(I),I=1,N+1),(DV(I),I=1,N+1),
     1             (AP(I),I=1,N+1),VOL,JS
 1091 FORMAT(2F10.4,1X,3HUV=,10F7.2,F7.2/21X,3HDV=,10F7.2,F7.2/22X,
     1       2HP=, 11F7.2,F10.8,I3/ )
 300  PU(1) = 0.0
      VU(1) = 0.0
      PD(N+1) = 0.0
      VD(N+1) = 0.0
      DO 74 I = 1, N
      PD(I) = 0.5* (P(I)+P(I+1))
      IF( I - JS ) 741,742,741
 741  VD(I) = 0.5* (V(I) + V(I+1))
      GOTO 74
 742  VD(I) = 0.5 * ( DV(I) + V(I+1 ))
 74   CONTINUE
      DO 75 I = 2, N+1
       PU(I) = PD(I-1)
       VU(I) = VD(I-1)
 75   CONTINUE
C
C     RUN TIME CHECK -
      IF ( TIME - TMAX ) 25, 31, 31
C     NUMBER OF DATA SETS CHECK -
 31   IF ( IB - IA ) 4, 32, 32
 32   IF ( NX - NRUN ) 45, 46, 46
 46   PAUSE
      STOP
      END
```

```
      SUBROUTINE VALVE ( P,V,A1,XV,XP )


C     VALVE SOLVES THE OPEN VALVE BOUNDARY CONDITION.

      DIMENSION P(11),V(11),A1(11),XV(11),XP(11),A3(11)
      COMMON N,DT,KINVIS,TRANS,D,Y2,Y5,PR,VAP,VCHAR,JS,VCLOS
      XK = V(N)+Y2*P(N)-0.5*A1(N)*V(N)*ABS(V(N))
      IF ( VCHAR )  6,5,6
    5 XV( N+1 ) = 0.0
      XP (N+1 ) = XK / Y2
      GOTO  7
    6 Z1 = 1.0/(Y5*VCHAR**2)
      AX = A1(N+1)/2.0
    4 Z2 = 1.0/(Z1+AX)
      XV(N+1) = SQRT(((Z2/2.0)**2)+Z2*XK)-0.5*Z2
      CALL FRICT ( XV,N+1,N+1,A3 )
      A3(N+1) = A3(N+1)/2.0
      EROR = ((A3(N+1)/AX)-1.0)*100.0
      IF ( ABS(EROR) - 5.0 ) 2,2,3
    3 AX = A3(N+1)
      GOTO 4

    2 XP(N+1) = ( XK-XV(N+1)*(1.0+A3(N+1)*ABS(XV(N+1))))/Y2
    7 RETURN
      END
```

```
      SUBROUTINE CAVITY ( SLOPE,INTM,I,V,P,A1,XV )
C     CAVITY CALCULATES THE VELOCITIES AT WHICH THE
C     COLUMN SEPARATES.

      DIMENSION V(11),P(11),A1(11),XV(11),A2(11)
      COMMON N,DT,KINVIS,TRANS,D,Y2,Y5,PR,VAP,VCHAR,JS,VCLOS

      IF ( INTM - 1 ) 1,2,2

2     A = V(I)
      B = P(I)
      C = A1(I)
      GOTO 3
1     IF ( SLOPE ) 11,12,12
12    A = V(I-1)
      B = P(I-1)
      C = A1(I-1)
      GOTO 3
11    A = V(I+1)
      B = P(I+1)
      C = A1(I+1)

3     XK = A-SLOPE*Y2*(VAP-B)-0.5*C*A*ABS(A)
      CX = A1(I)/2.0
      IF (CX) 13,14,13
13    IF (XK) 4,5,5
4     SIGN = 1.0
      GOTO 6
5     SIGN = -1.0
6     XV(I) = (SIGN/(2.0*CX))-SIGN*SQRT(((1.0/(2.0*CX))**2+ABS(XK)
     1 /CX))
      IF ( XV(I) ) 9,7,9
9     CALL FRICT ( XV,I,I,A2 )
     A2(I) = A2(I)/2.0
      EROR = ((A2(I)/CX)-1.0)*100.0
      IF ( ABS(EROR) - 5.0 ) 7,7,8
8     CX = A2(I)
      GOTO 6
14    XV(I) = XK
7     RETURN
      END
```

```
      SUBROUTINE FRICT ( U, I1, I2, A1 )
C     FRICT CALCULATES FRICTION FACTOR AS A FUNCTION OF
C     REYNOLDS NUMBER.

      REAL KINVIS
      DIMENSION U(31), A1(31)
      COMMON N, DT, KINVIS, TRANS, D
      DO 1 I = I1, I2
      IF ( U(I)) 3, 2, 3
 2    A = 0.0
      GOTO 4
 3    RE= ABS(U(I)) * D / KINVIS
      IF ( RE - TRANS ) 5, 6, 6
 5    A = 16.0 / RE
      GOTO 4
 6    A = 0.079 / RE ** 0.25
 4    A1(I) = 2.0 * A * DT /D
 1    CONTINUE
      RETURN
      END
```

```
      SUBROUTINE SORTER ( U, W, J )
C     SORTER DETERMINES THE TIME AND SECTION WITHIN THE PIPE
C     AT WHICH VAPOUR PRESSURE WAS FIRST REACHED.

      DIMENSION U(110)
      COMMON N ,DT
      DT = DT * 1000.0
      W = 0.0
      DO 2 I = 1, N+1
      U(I) = U(I) * 1000.0
      IF ( U(I).EQ.DT )    U(I) = 0.0
      IF ( W - U(I) ) 3, 2, 2
 3    J = I
      W = U(I)
 2    CONTINUE
      W = W / 1000.0
      DT = DT / 1000.0
      RETURN
      END
```

```
      SUBROUTINE INTERNAL ( INTM,I,P,V,P1,V1,E,E1,XV,XP )

C     INTERNAL SOLVES THE CHARACTERISTIC EQUATIONS ◊( AT EACH
C     INTERNAL PIPE SECTION. DUE TO THE 2ND ORDER APPROX.
C     INTEGRATION AND THE VARIABLE FRICTION FACTOR
C     AN ITERATIVE PROCEEDURE IS NEEDED TO CALCULATE VELOCITY.

      DIMENSION P(11),P1(11),V(11),V1(11),E(11),E1(11),C3(11),
     1 XP(11),XV(11)
      COMMON N,DT,KINVIS,TRANS,D,Y2,Y5,PR,VAP,VCHAR,JS,VCLOS
      IF ( I - 1 ) 1,10,1
    1 IF ( INTM. GT. 1 ) GOTO 2
      A = P(I-1)
      B = V(I-1)
      C = E(I-1)
      A1 = P1(I+1)
      B1 = V1(I+1)
      C1 = E1(I+1)
      GOTO 3
    2  IF ( I-JS ) 21,22,21
   22 XP(I) = VAP + VCLOS/Y2
      XK = V(I) - Y2*(XP(I)-P(I))-0.5*E(I)*V(I)*ABS(V(I))
      CX = E(I)/2.0
      GOTO 15
   21  A = P(I)
      B = V(I)
      C = E(I)
      A1 = P1(I)
      B1 = V1(I)
      C1 = E1(I)
      GOTO 3
   10 IF ( INTM. GT. 1 ) GOTO 12
      XK = V(2)+Y2*(PR-P(2))-E(2)*0.5*V(2)*ABS(V(2))
      CX = E(1)/2.0
      GOTO 16

   12 XK=V1(1)+Y2*(PR-P1(1))-0.5*E1(1)*V1(1)*ABS(V1(1))
      CX = E1(1)/2.0

   16 XP(1) = PR
      GOTO 15
    3 XP(I) = .5*((A+A1)+((B-B1)-0.5*(C*B*ABS(B)
     1 -C1*B1*ABS(B1)))/Y2)
      XK = .5*(B+B1+Y2*(A-A1)-0.5*(C*B*ABS(B)
     1 +C1*B1*ABS(B1)))
      CX = (C+C1)/4.0
   15 IF ( XK ) 4,5,5
    4 SIGN = 1.0
      GOTO 6
    5 SIGN = -1.0
    6 XV(I)=(SIGN/(2.0*CX))-SIGN*SQRT(((1.0/(2.0*CX))**2+ABS(XK)/CX))
      CALL FRICT ( XV,I,I,C3 )
      C3(I) = C3(I)/2.0
      EROR = ((C3(I)/CX)-1.0)*100.0
      IF ( ABS (EROR) - 5.0 ) 7,7,8
    8 CX = C3 (I)
      GOTO 6
    7 RETURN
      END
```

FINISH

10.4 Appendix 4 Valve boundary equations during column separation on its downstream face

The four equations necessary to define the boundary conditions on both sides of a closing valve in the presence of an air/vapour cavity on its downstream face are:

$$PP_{2,1} = VAP + PA \tag{4.1}$$

$$\tau = \frac{VV_{1,N1+1}}{V_{01}} \sqrt{\left(\frac{\Delta P_o}{PP_{1,N1+1} - PP_{2,1}}\right)} \tag{4.2}$$

$$VV_{1,N1+1} = K1 - K3\, PP_{1,N1+1} \tag{4.3}$$

$$VV_{2,1} = K2 + K4\, PP_{2,1} \tag{4.4}$$

where $K3 = 1/\rho c_1$, note that K2, K3 notation is reversed relative to the main text.

$$K4 = 1/\rho c_2$$

$$K1 = V_{1,N1}\,(1 - 2f\,\frac{\Delta T}{D}|V_{1,N1}|) + P_{1,N1}\,K3$$

$$K2 = V_{2,2}\,(1 - 2f\,\frac{\Delta T}{D}|V_{2,2}|) - P_{2,2}\,K4$$

$$K5 = (\Delta P_o/(V_{01}\,\tau)^2)^{-1}$$

The expression for PA, the partial pressure of the released air, may be written as

$$PA = \left(\frac{AIRVOL}{VOL}\right)^n ATM \tag{4.5}$$

where n is the polytropic coefficient of expansion.

Two cases will be dealt with, namely n = 1 and n > 1.

Case 1: n > 1

The available equations may be written as:

$$A^2 = K5\,(B - (C + VAP)) \tag{4.6}$$

$$A = K1 - K3\,B \tag{4.7}$$

$$D = K2 + K4\ (C + VAP) \tag{4.8}$$

$$C = PA \tag{4.9}$$

where $A = VV_{1,N1+1}$, $B = PP_{1,N1+1}$, $D = VV_{2,1}$, and C = partial pressure released air.

The volume of the cavity (VOL) and its air content (AIRVOL) may be calculated as:

$$VOL_T = VOL_{T-\Delta T} + \frac{AR}{2}\,\Delta T\ (D-A+V_{2,1} - V_{1,N1+1}) \tag{4.10}$$

where AR is the pipe cross sectional area and ΔT is the time increment.

Put $$K8 = VOL_{T-\Delta T} + K9\ (V_{2,1} - V_{1,N1+1})$$

$$K9 = \frac{AR}{2}\ \Delta T$$

and substituting for A, D in (4.10) from (4.7), (4.8) yields

$$VOL_T = K12 + K13\ C + K14\ B \tag{4.11}$$

where

$$K12 = K8 + K9\ (K2 + K4\ VAP - K1)$$

$$K13 = K9\ K4,\ K14 = K9\ K3.$$

The quantity of air present at any time is assumed to have been released by the fuel that passed through the valve between the instant considered and the time at which the pressure first fell below atmosphere. This quantity of fuel may be expressed as:

$$FUELVOL_T = FUELVOL_{T-\Delta T} + \frac{AR}{2}\,\Delta T(A + V_{1,N1+1})$$

and the quantity of released air:

$$AIRVOL_T = FUELVOL_T\ (ATM - 0.5\ (C + VAP + P_{2,1}))\frac{K}{ATM}$$

where K is the Bunsen solubility coefficient at the working temperature. Substitution in (4.9) then yields:

$$C = \left\{\frac{(K18 + K9\ A)(W1 - W2\ C)}{K12 + K13\ C + K14\ B}\right\}^n\ ATM \tag{4.12}$$

where

$$K18 = FUELVOL_{T-\Delta T} + K9\ V_{1,N1+1}$$

$$W1 = (ATM - 0.5\ (VAP + P_{2,1}))\ K/ATM$$

$$W2 = 0.5\ K/ATM$$

Substituting for A in (4.12) yields an expression in terms of B, C

$$C = \left\{\frac{(K10 - K11\ B)\ (W1 - W2\ C)}{K12 + K13\ C + K14\ B}\right\}^{n} ATM \qquad (4.13)$$

where

$$K10 = K18 + K9\ K1$$

$$K11 = K9\ K3$$

Equation (4.13) may be expressed as:

$$X_o\ C^{\frac{n+1}{n}} + X_1\ C^{1/n} + X_2 C + X3 = 0 \qquad (4.14)$$

if B is known.

Similarly from (4.6) and (4.7) a quadratic may be formed in terms of B and C:

$$B^2 - B\left\{\frac{K5 + 2K1\ K3}{K3^2}\right\} + \frac{1}{K3^2}\ (K1^2 + K5(C + VAP)) = 0 \qquad (4.15)$$

The method of solution is as follows:

1. Use $C = P_{2,1}$ as a starting value as the change in pressure across any one time step is small.
2. Substitute for C in (4.15) and solve for B.
3. Substitute for B in (4.14) and solve for C.
4. Compare the two values of C, if the difference is too great, say above 0.5% repeat the above procedure using the new C value as a starting value.

The procedures in program SEPG are carried out by Subroutines VALVE and AIRV. The remaining unknowns can be calculated by substituting C into equations (4.6) to (4.9). New values of FUELVOL, VOL, and AIRVOL may also be calculated.

If the valve is closed at the end of the time step being considered A = 0 in equation (4.10) and the cavity volume becomes:

$$VOL_T = K12 + K13\ C$$

where K12 = K8 + K9 (K2 + K4 VAP).

Equation (4.13) becomes:

$$C = \left\{\frac{K18\ (W1 - W2\ C)}{K12 + K13\ C}\right\}^{n} \text{ ATM} \qquad (4.16)$$

which may be solved directly for C. The pressure in the cavity $PP_{2,1}$ and the interface velocity $VV_{2,1}$ may now be calculated. The upstream conditions may be calculated using $VV_{1,N1+1} = 0$ as the boundary.

Following valve closure the calculations of the cavity boundary conditions may be split into the opening and closing phases.

1. Opening phase: Air continues to be given up by the maximum value of the FUELVOL term:

   hence AIRVOL = FUELVOL_{MAX} (W1 - W2 C)

   and VOL_T = K8 + K9 D

   where K8 = $\text{VOL}_{T-\Delta T}$ + K9 $V_{2,1}$

   $$\therefore \quad C = \left\{\frac{K10 - K11\ C}{K12 + K13C}\right\}^{n} \text{ ATM} \qquad (4.17)$$

   where K10 = FUELVOL_{MAX} W1

   K11 = K10 W2/W1.

   Equation (4.17) may be solved for C and values obtained for the cavity pressure and interface velocity during the opening phase.

2. Closing phase: No air is allowed back into solution, hence

   AIRVOL = FUELVOL_{MAX} $(W1 - W2\ C)_{MAX}$

   and $$C = \left\{\frac{\text{AIRVOL}}{K12 + 13\ C}\right\}^{n} \text{ ATM} \qquad (4.18)$$

   thus yielding the required boundary conditions at the cavity.

Case 2: n = 1

Equations (4.6) to (4.9) may be written as:

$$A^2 = K5\ (B - C) \tag{4.19}$$

$$A = K1 - K3\ B \tag{4.20}$$

$$D = K2 + K4\ C \tag{4.21}$$

$$C = VAP + \frac{AIRVOL}{VOL}\ ATM \tag{4.22}$$

where $C = PP_{2,1}$ and A, B, D, K1-5 have the same values as in case 1.

Following case 1 the cavity volume may be written as:

$$VOL_T = K12 + K13\ C + K14\ B \tag{4.23}$$

where $K12 = K8 + K9\ (K2 - K1)$

and K8, K9, K13, K14 have the same values as in case 1.

The quantity of air released may be expressed as:

$$AIRVOL_T = FUELVOL_T\ (ATM - 0.5(C + P_{2,1}))\ \frac{K}{ATM}$$

Substitution in (4.22) yields:

$$C = VAP + \left(\frac{K6 + K7A + K18}{VOL}\right)(W1 - W2\ C) \tag{4.24}$$

where $K6 = FUELVOL_{T-\Delta T}\ ATM$

$K7 = AR\ \Delta T\ ATM/2$

$K18 = K7\ V_{1,N1+1}$

$W1 = (ATM - 0.5\ P_{2,1})\ K/ATM$

$W2 = 0.5\ K/ATM$

Substituting for A in (4.24) from (4.20) yields:

$$C = VAP + \left(\frac{K20 - K21C - K22B - K23BC}{K12 + K13C + K14B}\right) \tag{4.25}$$

where $K20 = W1\ (K18 + K6 + K7\ K1)$

$K21 = K20\ W2/W1$

$K22 = W1\ K7\ K3$

$K23 = W2\ K7\ K3$

Similarly, from (4.19) and (4.20)

$$C = B - A^2/K5$$

$$C = B\left(1 + 2K1\,\frac{K3}{K5}\right) - \frac{K3^2}{K5}\,B^2 - \frac{K1^2}{K5} \qquad (4.26)$$

Equation (4.26) can be used to calculate C^2 and values of C and C^2 may then be substituted into (4.25) yielding a quartic in B:

$$CO\,B^4 + C1\,B^3 + C2\,B^2 + C3\,B + C4 = 0 \qquad (4.27)$$

where

$$CO = K13\,\frac{K3^4}{K5^2}$$

$$C1 = -2\,K13\,K17\,\frac{K3^2}{K5} - K14\,\frac{K3^2}{K5} + K23\,\frac{K3^2}{K5}$$

$$C2 = -K12\,\frac{K3^2}{K5} + K13\,K17^2 + 2K13\,K1^2\,\frac{K3^2}{K5^2}$$

$$+K14\,K17 + VAP\,K13\,\frac{K3^2}{K5} - K21\,\frac{K3^2}{K5} - K23\,K17$$

$$C3 = K12\,K17 - 2K13\,K17\,\frac{K1^2}{K5} - K14\,VAP - K14\,\frac{K1^2}{K5}$$

$$- K13\,K17\,VAP + K22 + K21\,K17 + K23\,\frac{K1^2}{K5}$$

$$C4 = -K12\,\frac{K1^2}{K5} + K13\,\frac{K1^4}{K5^2} - K12\,VAP + VAP\,K13\,\frac{K1^2}{K5}$$

$$-K20 - K21\,\frac{K1^2}{K5}$$

and

$$K17 = 1 + 2\,K1\,\frac{K3}{K5}$$

Equation (4.27) may be solved by Newton's Method, the required root is known as the pressure change across one time step is small so that $B = P_{1,N1+1}$ may be used as a starting value.

These procedures in programs SEPF, SEPH, SEPI, SEPJ and SEPK are carried out in Subroutine VALVE. The remaining unknowns may be calculated by substituting B into equations (4.19) to (4.22). New values of AIRVOL, FUELVOL and VOL may also be calculated.

If the valve is closed at the end of the time step being calculated a different procedure is required as $\tau = 0$ implies K5 = 0 and the program would fail at equation (4.27). In this case, put A = 0 so that:

$$VOL_T = K8 + K9\ D$$

and

$$AIRVOL_T = (K6 + K18)(W1 - W2\ C)$$

Substituting in (4.21) and (4.22) yields:

$$C = VAP + \frac{(K6 + K18)(W1 - W2\ C)}{K8 + K9\ (K2 + K4\ C)} \qquad (4.28)$$

which reduces to a quadratic in C. This procedure is also allowed for in Subroutine VALVE.

Following valve closure the calculations of the cavity boundary conditions may be split into the opening and closing phases:

1. Opening phase: air continues to be given up by the maximum value of the FUELVOL term; hence from equations (4.21), (4.22)

$$PP_{2,1} = VAP + \frac{K6\ (W1 - W2\ PP_{2,1})}{K24 + K9(K2 + K4\ PP_{2,1})} \qquad (4.29)$$

where $K24 = VOL_{T-\Delta T} + K9\ V_{2,1}$

and $K6 = ATM\ FUELVOL_{MAX}$

Equation (4.29) may then be solved for $PP_{2,1}$.

2. Closing phase: the air content is assumed constant at its maximum value. This effectively reduces equation (4.29) to

$$PP_{2,1} = VAP + \frac{AIR.ATM}{K24 + K9(K2 + K4\ PP_{2,1})}$$

where $AIR = FUELVOL_{MAX}\ (W1 - W2\ C_{min})$

These procedures are carried out in Subroutine CAVITY.

10.5 Appendix 5 Computer programs written to predict column separation downstream of the valve

Two models of this phenomena were studied, namely cavity formation with and without air release from the fuel passing through the closing valve. All the programs, SEPE - SEPK employed the 1st order finite difference equations, with friction factors based on local Reynolds Number at each section at each time step. A polynomial curve fitting technique was used to provide the τ vs time data during valve closure. The programs, SEPF-K employing the released air model accepted input pressures in absolute values due to the introduction of the $pVol^n = k$ expression.

1. SEPE Vapour only case. Cavity assumed to form when pressure falls to fluid vapour pressure. Pressure rise on cavity collapse instantaneous.
2. SEPF Released air case, cavity opens at atmospheric pressure due to air release. Coefficient of expansion taken as n = 1.0.
3. SEPG Identical to SEPF except that $1 < n \leq 1.4$.
4. SEPH Investigation of column separation upstream of a valve positioned between two reservoirs. Upstream cavity unaffected by released air. n = 1.0 assumed downstream as in SEPF.
5. SEPI Identical to SEPF except that output statements at every time step replaced by a sorting procedure designed to select maximum and minimum pressures, their event times and maximum cavity volume values etc.
6. SEPJ Version of SEPI designed to investigate the limits of steady state parameters necessary to either avoid or restrict column separation.
7. SEPK Identical to SEPF but including a glass/aluminium junction 3 m downstream of the valve.

This appendix contains flow diagrams for SEPE, SEPF and SEPG together with flow diagrams for the VALVE and CAVITY subroutines dealing with the boundary conditions at the cavity interface.

The notation included in this report has been kept close to that employed in the programs. Additional notation, together with descriptions of all the subroutines employed in SEPE-K are also included.

A.5.1 Description of subroutines used in SEPE-K

Subroutine PRELIM.

This procedure transforms the input data from the valve characteristic - angle and angle - time curves into a form suitable for use in the following procedure CURFIT.

Subroutine CURFIT.

This procedure is designed to fit a polynomial of any given order to a suitable number of points. The coefficients of each polynomial curve are stored by PRELIM.

Subroutine INTER.

This is a cross plotting procedure. For any given time INTER calculates the valve angle and can then be called a second time to calculate the value of valve characteristic appropriate to that angle.

Subroutine FRICT.

FRICT calculates the friction factor at each section of the pipeline at each time step.

Subroutine VALVE.

This subroutine calculates the pressure and velocity conditions on each side of the valve during closure. If separation occurs on the downstream side of the valve the procedures outlined in this report are employed to calculate the cavity pressure, air content, volume and interface velocity. A flow diagram for VALVE is included in this appendix.

Subroutine RESERVOIR.

RESERVOIR calculates the velocity at the inlet to each reservoir tank, the constant pressure boundary condition being assumed.

Subroutine INTERNAL.

This procedure calculates the pressure - velocity conditions at each internal section along the pipeline by solution of the C^+ and C^- characteristic equations.

Subroutine CAVITY.

This subroutine calculates the pressure and interface velocities at the cavity. For a cavity forming at the valve the effect of released air is included. A flow diagram for this subroutine is included in this appendix.

Subroutine VAPOUR.

The pressures at each section of the pipeline are checked for calculated values at or below the vapour pressure of the liquid. If the calculated pressure is less than vapour pressure the time during the preceding time step at which it passed through the vapour level is calculated.

Subroutine SORTER.

This procedure uses information from VAPOUR to determine the first section to display pressure below or equal to the fluid vapour pressure.

Subroutine FACTOR.

This subroutine is used to interpolate all pressure-velocity results back to the time of first occurrence of vapour pressure. The necessary interpolation factor is calculated from the output of SORTER.

Subroutine AIRV

This procedure is called by VALVE and CAVITY in SEPG to solve an equation of the form $ax^{(n+1)/n} + bx^{1/n} + cx + d = 0$.

A.5.2 Notation employed in SEPE - SEPK.

The notation below is arranged in the order in which the terms appear in SEPH

NRUN	Number of test cases to be computed
IJ	Counter
KINVIS	Kinematic viscosity fluid
TRANS	Transition Reynolds number
VAPI, VAP	Vapour pressure fluid
RHO	Density fluid
N, ZN	Number of sections in each pipe
PL	Length of each pipe
C	Wave speed
D	Pipe bore
VO	Initial velocity
A	Area of each pipe
DT, DTO	Time increment
ICAV	Marker indicating presence of a cavity
PR1, PR2	Reservoir pressures
TMAX	Maximum time for each test case
ZDT, ZDTO	Interpolation factor
M	Order of polynomials to be fitted by CURFIT
NSAVC	Number of sections in angle-valve characteristic curve
NPAVC	Number of points in each section of above curve
VC, B, VCHAR	Valve characteristic
AN, A1, AX	Valve angle
NSAT	Number of sections in angle-time curve
NPAT	Number of points in each section of above curve
T, TIME, T1	Time measured from start of valve motion
C1, C2	Coefficients of polynomials fitted to VC-AN and T-A1 curves.
TC	Valve closure time

V	Velocity at a pipe section at time T
REN	Reynolds Number
FF, F1, F1D	Friction factor
FDR	Frictional loss per pipe section
AP, P	Pressure at a section at time T
RO	Marker indicating cavity condition, i.e. opening or closing
ATM	Atmospheric pressure
VOLX	Maximum volume cavity
FUELVOL	Fuel giving up its air
AIRVOL	Volume of released air at N.T.P.
VOL	Cavity volume at time T
VOL2	Cavity volume at T-ΔT
KB	Counter
INTM	Marker indicating whether $\Delta T = \Delta x/c$ or $< \Delta x/c$
V1, P1	Velocity and pressure at time T-ΔT
VV, PP	Velocity and pressure at time T+ΔT
TS	Time at which vapour pressure was reached at each section
TSMAX	Maximum value of TS array in each time step
J1	Section having maximum TS value in each time step
FACT	Interpolation factor
W1, W2	Constants relating to air concentration

The notation in the subroutines follows the above list closely.

A.5.3 Flow diagram for SEPE, SEPF, SEPG

Read data: pipe lengths, bore, wave speed, No. of sections in each pipe, initial flow velocity, fluid density and viscosity, transition Reynolds Number and maximum calculation time TMAX.

Read in interpolation factor ZDT to be used if separation occurs.

Read in order of the polynomials to be fitted to the τ - angle, angle - time curves for the valve closure.

Read in number of sections, the number of points in each section and their co-ordinates for the above curves.

CALL PRELIM and CURFIT to fit the required polynomials which are stored in the form

$$\tau_\alpha = C(i,1) + \sum_{j=2}^{m+1} C(i,j)\,\alpha^{j-1}$$

$$\alpha_t = D(k,1) + \sum_{\ell=2}^{q+1} D(k,\ell)\,t^{\ell-1}$$

Calculate steady state values (V,P) as arrays along both pipelines.

Calculate time step $\Delta T = \Delta x/c$

Assign steady state values to VCHAR, VOL, VOLX, AIRVOL, FUELVOL, etc.

A. WRITE τ, TIME, (V,P) for both pipes.

Update time, TIME + ΔT

CALL INTER to calculate τ_T

CALL VALVE

CALL INTERNAL, RESERVOIR for both pipes.

Check valve position at end of time step:

Valve open	Valve closed
Goto B	Goto C

B. Re assign VV, PP arrays into V,P arrays as a base for next time step and goto A.

D. Update time, TIME + ΔT

Check state of cavity - if 'vapour only' case (SEPE), Goto E.

1st cavity opening:	1st cavity closing
$VOL_T > VOL_{T-\Delta T}$	and subsequent boundary conditions
FUELVOL is assumed to continue to release air. Marker RO in CAVITY call statement = 2	AIRVOL held constant at its maximum value, RO = 3
CALL CAVITY	CALL CAVITY

G CALL INTERNAL and RESERVOIR for downstream pipeline.

Check PP (2,2 → N 2 + 1) for values below or equal to vapour pressure by calling VAPOUR and SORTER.

If positive CALL FACTOR to interpolate conditions back to instant of vapour formation

If a cavity exists at the valve calculate its volume.

Goto C.

E. If PP(2,1) > VAP Goto F
If VOL > 0 cavity open, call CAVITY with RO = 1 and calculate new value of VOL.
If VOL ≤ 0 cavity shut, VV(2,1) = 0 and
PP(2,1) = VAP + ρcVCLOS.
Goto G.

F. Calculate PP(2,1) from C^- characteristic and boundary equation
VV(2,1) = 0.0.
Goto G.

C. WRITE TIME, (VV, PP) for downstream pipeline and cavity volume.

Check rate of volume growth.

If $|VOL_T| < |0.5 * (VOL_T - VOL_{T-\Delta T})|$

then divide time increment by 2.

If $|VOL_T| > |VOL_{T-\Delta T}|$ revert to original time increment.

Reassign (VV,PP) arrays as (V,P) as a base for next time step.

If $\Delta T < \Delta x/c$ then carry out interpolation procedure using value of ZDT to give PU, VU, PD, VD arrays as a base for the next time step.

If TIME < TMAX Goto D

FINISH

A5.4 Flow diagram for Subroutine VALVE

VALVE calculates valve boundary conditions at time T.
Check valve position at time T:

Open	Closed
Check pressure P(2,1) at time T - ΔT against atmospheric pressure ATM.	No flow boundary on upstream side of valve. Goto A

P(2,1) > ATM	P(2,1) < ATM
Goto C	Goto A

C. Calculate conditions on both sides of the valve assuming no separation.

Check pressure PP(2,1) at time T against ATM.

PP(2,1) < ATM	PP(2,1) $\geq$ ATM
Column separated at valve CALL FACTOR to interpolate conditions along both pipelines to time at which column separated. Goto B	Goto B

A. Check valve position at time T, if 'vapour only' case Goto D.

Open:	Closed:
Calculate boundary conditions on both sides of the valve using valve characteristics τ, C^+ and C^- lines and PP(2,1) = VAP + PA as the four required equations.	Calculate downstream conditions only from C^- line and PP(2,1) = VAP + PA

Calculate FUELVOL, AIRVOL and cavity VOL.

Goto B.

B. Return to Master Segment.

D. If PP(2,1) $\geq$ VAP, Goto B.
If PP(2,1) < VAP, calculate boundary conditions on both sides of the valve using τ, C^+ and C^- lines and PP(2,1) = VAP, as the required equations, then Goto B.

A5.5 Flow diagram for Subroutine CAVITY

CAVITY calculates pressure and interface velocity at a cavity boundary.

Check value INTM

INTM > 1
PU, VU, PD, VD arrays are used as base conditions.

INTM = 1
P, V arrays are used as base conditions.

SLOPE indicates which cavity interface velocity is to be calculated. Applies only to internal cavity.

Check value RO.

RO $\leq$ 1 :
No air in vapour cavity,
PP(2,1) = VAP, VV(2,1) direct from C^- characteristic.

RO = 2
Cavity opening,
FUELVOL is still assumed to be releasing air.

RO = 3
Cavity closing,
AIRVOL held at its maximum value.

Return to Master Segment.

A.5.6 SEPE master segment and VALVE and CAVITY subroutines

```
TASKA/SEPE52616SWAFFIELD/
SPACE19697'
SECONDS500
PRINT6000
COMPILER FORTRAN
      LIST(LP)
      PROGRAM(SEPE52212)
      INPUT1=CR0
      OUTPUT2=LP0
      TRACE'
      END
```

```
      MASTER SEPE
      REAL KINVIS
      DIMENSION NPAVC(10),VC(10,50),AN(10,50),C1(10,10),NPAT(10),C2(10,
     1          10),A1(10,10),T(10,10),T1(500),AX(500),B(500), TS(2,41),
     2AP(2,41), V1(2,41),P1(2,41),V(2,41),P(2,41),PP(2,41),VV(2,41),
     3Z(2,41),  VU(2,41),PU(2,41),VD(2,41),PD(2,41),F1(2,41),F1D(2,41),
     4       A(2),D(2),C(2),DT(2),ICAV(2),PL(2),ZN(2),N(2),VO(2)
      COMMONM,KINVIS,TRANS,VCHAR,DP,RHO,PR1,PR2,N,VD2,Z2    ,VAP
     5          , TIME     ,DT
      READ(1,101)NRUN
      IJ = 0
      NPATH = 0
  98  IJ = IJ + 1
      READ(1,102) KINVIS,TRANS
      READ(1,102) VAPI,RHO
      VAP = VAPI
      DO 9 I = 1, 2
      READ (1,101) N(I)
      READ(1,103)PL(I),C(I),ZN(I),D(I),VO(I)
 103  FORMAT(5F10.4)
      A(I) = 3.1417 * (D(I)**2)/ 4.0
      DT(I)= PL(I)/(C(I)*ZN(I))
      ICAV(I) = 0
  9   CONTINUE
      READ (1,102) PR1,DP
      READ (1,102) TMAX,ZDT
      KINVIS = KINVIS/100000.0
      READ ( 1,101 ) M
      READ ( 1,101 ) NSAVC
      DO 1 I =1, NSAVC
      READ ( 1,101 ) NPAVC(I)
      READ ( 1, 102 ) ( VC(I,K),AN(I,K),K=1,NPAVC(I) )
1     CONTINUE
```

```
      CALL PRELIM ( AN,VC,NSAVC,NPAVC,C1 )
      READ ( 1,101 ) NSAT
      DO 2 I=1, NSAT
      READ (1,101 ) NPAT(I)
      READ(1,102) (A1(I,K),T(I,K),K=1,NPAT(I))
2     CONTINUE
      CALL PRELIM (T,A1,NSAT,NPAT,C2)
      DTX = DT(1)
      TC = T( NSAT, NPAT(NSAT))
      KMAX = TC/DTX + 1.0
101   FORMAT(I3)
102   FORMAT(2F10.4)
      READ(1,111)IDAY,IMTH,IYEAR,INUM
  111 FORMAT (4I4)
      WRITE(2,204)IDAY,IMTH,IYEAR,INUM
  204 FORMAT(8HDATE =  ,I2,3H / ,I2,3H / ,I4,/,12HRUN NUMBER = ,I4,1H.,
     1       //)
C     INITIAL CONDITIONS ALONG BOTH PIPE SECTIONS.
      DO 22 I = 1, 2
      DO 22 K = 1, N(I)+1
      V(I,K) = VO(I)
   22 CONTINUE
      CALL FRICT (D,DT,1,V,1,N(1)+1,F1)
      CALL FRICT (D,DT,2,V,1,N(2)+1,F1)
      DO 23 I = 1, 2
      REN = ABS(VO(I))*D(I)/KINVIS
      FF = 0.079/REN**0.25
      FDR = 2.0*RHO*FF*PL(I)*(VO(I)**2)/(D(I)*ZN(I))
      AA = 0.0
      DO 23 K =1, N(I)+1
      XR = PR1
      IF ( I. EQ. 2 )   XR= P(1,N(1)+1) - DP
      AA = AA + 1.0
      P(I,K) =  XR - (AA - 1.0)* FDR
      AP(I,K) = P(I,K)/1000.0
   23 CONTINUE
      PR2 = P(2,N(2)+1)
      TIME=0.0
      Z2 = 0.0
      VOL = 0.0
      VCHAR=1.0
      WRITE(2,200)
C     CALCULATION INTERNAL POINTS DURING VALVE CLOSURE
      KB = 1
      INTM = 1
      WRITE(2,201)TIME,VCHAR,(V(1,K),K=1,N(1)+1,3),(V(2,K),K=1,N(2)+1,
     1                2),(AP(1,K),K=1,N(1)+1,3),(AP(2,K),K=1,N(2)+1,2)
   30 TIME = TIME + DT(2)
      KB = KB + 1
      T1(KB) = TIME
      CALL INTER ( KB,T1,T,NSAT,NPAT,KMAX,C2,AX )
      CALL INTER ( KB,AX,AN,NSAVC,NPAVC,KMAX,C1,B )
      VCHAR = B(KB)
      DO 31 I = 1, 2
      CALL INTERNAL (1,N,I,C,V,P,F1,P,V,F1,VV,PP)
      CALL RESERVOIR (I,1,C,V,P,F1,VV,PP)
   31 CONTINUE
```

```
      CALL VALVE ( V,P,F1,C,A,VD,VV,PP )
      IF ( Z2. GT. 0.0 )   GOTO 38
      GOTO   39
   38 VV(2,1)=V(2,2)+(PP(2,1)-P(2,2))/(RHO*C(2))
     1          -F1(2,2) * V(2,2) * ABS(V(2,2))
      VOL = VOL + A(2)*DT(2)*0.5*(VV(2,1)+V(2,1)-VD2-VD1)
   39 IF (VCHAR) 32,32,33
   32 IF (PP(2,1) - VAP) 34,34,33
   34 PP(2,1) = VAP
      VV(2,1) = V(2,2) + (VAP - P(2,2))/(RHO * C(2))
     1           -F1(2,2) * V(2,2) * ABS (V(2,2))
      ICAV(2) = 2
      VD2 = 0.0
      NPATH = 1
      DT(2) = DT(2) * ZDT
      GO TO 33
   33 DO 35 I = 1, 2
      DO 36 K = 1, N(I)+1
      V1(I,K) = V(I,K)
      P1(I,K) = P(I,K)
      V (I,K) = VV(I,K)
      P (I,K) = PP(I,K)
      AP(I,K) = P(I,K)/1000.0
   36 CONTINUE
      CALL FRICT (D,DT,I,V,1,N(I)+1,F1)
   35 CONTINUE
      VD1 = VD2
      WRITE(2,201)TIME,VCHAR,(V(1,K),K=1,N(1)+1,3),(V(2,K),K=1,N(2)+1,2
     1            ),(AP(1,K),K=1,N(1)+1,3),(AP(2,K),K=1,N(2)+1,2)
      IF ( NPATH. EQ. 1 )     GOTO  83
   84 IF ( VCHAR)  37,37,30
   37 IF(ICAV(2)) 40,40,41
C     LABEL 40 DENOTES NO VAPOUR FORMED UP TO VALVE CLOSURE TIME
   40 CALL RESERVOIR (2,1,C,V,P,F1,VV,PP)
C     VALVE BOUNDARY, NO VAPOUR POCKET.
      VV(2,1)= 0.0
      PP(2,1) = RHO*C(2)*(F1(2,2)*V(2,2)*ABS(V(2,2))-V(2,2)) + P(2,2)
      CALL INTERNAL (1,N,2,C,V,P,F1,P,V,F1,VV,PP )
      CALL VAPOUR (2,N,DT,VAP,P,PP,KZ,PP,TS)
      IF (KZ - (N(2)+1)) 43, 33, 33
C     LABEL 43  INDICATES PRESENCE OF FUEL VAPOUR.
   43 FACT = (DT(2)-TS(2,1))/DT(2)
      DO 45 K = 2, N(2)+1
      CALL FACTOR (2,K,K,K,K,K,V,P,V1,P1,VV,PP,V,P,FACT,VV,PP,V,P)
   45 CONTINUE
      CALL FRICT ( D,DT,2,V,2,2,F1 )
      PP(2,1) = VAP
      VV(2,1) = V(2,2)+(VAP-P(2,2))/(RHO*C(2))-F1(2,2)*V(2,2)*ABS(V(2,2)
     1          )
      TIME = TIME - TS(2,1)
      ICAV(2) = 2
      DT(2) = DT(2)* ZDT
      INTM  =  2
      VOL   =  0.0
      GOTO 50
   41 TIME = TIME + DT(2)
      NPATH = 2
      IF (ICAV(2))60,60,61
```

```
C       LABEL 61 DENOTES VAPOUR POCKET AT VALVE.
  61    CALL RESERVOIR (2,2,C,VU,PU,F1,VV,PP)
        CALL INTERNAL  (2,N,2,C,VU,PU,F1,PD,VD,F1D,VV,PP)
        CALL CAVITY (-1.0,2,C,2,1,VAP,VD,PD,F1D,VV,PP)
        CALL VAPOUR (2,N,DT,VAP,P,PP,KZ,PF,TS)
        CALL SORTER (N(2)+1,TS,2,DT,TSMAX,J1)
        FACT = (DT(2)-TSMAX)/DT(2)
        TIME = TIME - TSMAX
        DO 63  K =1,N(2)+1
        CALL FACTOR(2,K,K,K,K,K,V,Z,P,Z,VV,Z,PP,Z,FACT,VV,Z,PP,Z)
    63  CONTINUE
        VOL = VOL + A(2)*(DT(2)-TSMAX)*(VV(2,1)+V(2,1))/2.0
        IF (VOL) 64,65,50
  64    DTR = -VOL/(A(2)*0.5*(VV(2,1)+V(2,1))   )
        TIME = TIME -DTR
        FACT = (DT(2)- DTR)/DT(2)
        DO 67 K = 1,N(2)+1
        CALL FACTOR(2,K,K,K,K,K,V,Z,P,Z,VV,Z,PP,Z,FACT,VV,Z,PP,Z)
  67    CONTINUE
C       COLUMN REJOINED.
  65    VCLOS = - VV(2,1)
        VV(2,1) = 0.0
        PP(2,1) = VAP + VCLOS*RHO*C(2)
        VOL = 0.0
        ICAV(2) = 0
        GOTO 50
C       LABEL 60 INDICATES THAT THE VAPOUR CAVITY AT THE VALVE HAS
C       COLLAPSED.
  60    CALL RESERVOIR (2,2,C,VU,PU,F1,VV,PP)
C       VALVE BOUNDARY,NO VAPOUR PRESENT.
        VV(2,1) = 0.0
        PP(2,1) = RHO*C(2)*(F1D(2,1)*VD(2,1)*ABS(VD(2,1))-VD(2,1))+PD(
     1      2,1)
        CALL INTERNAL  (2,N,2,C,VU,PU,F1,PD,VD,F1D,VV,PP)
        CALL VAPOUR    (2,N,DT,VAP,P,PP,KZ,PP,TS)
        IF(KZ -(N(2)+1)) 73,50,50
C       LABEL 73 INDICATES VAPOUR PRESENT.
  73    FACT =((DT(2)-TS(2,1))/DT(2))
        DO 75 K = 2, N(2)+1
        CALL FACTOR ( 2,K,K,K,K,K,V,Z,P,Z,VV,Z,PP,Z,FACT,VV,Z,PP,Z)
  75    CONTINUE
        DO 78 I = 1, 2
        Z(2,I)=P1(2,I)+FACT*(P(2,I)-P1(2,I))
        Z(2,I+2)=V1(2,I)+FACT*(V(2,I)-V1(2,I))
  78    CONTINUE
        PD(2,1) = Z(2,1)+ZDT*(Z(2,2)-Z(2,1))
        VD(2,1) = Z(2,3)+ZDT*(Z(2,4)-Z(2,3))
        WRITE ( 2,102) PD(2,1), VD(2,1)
        CALL FRICT(D,DT,2,VD,1,1,F1D)
        PP(2,1) = VAP
        VV(2,1) = VD(2,1) + ( VAP - PD(2,1))/(RHO*C(2))
     1            -F1D(2,1) * VD(2,1) * ABS(VD(2,1))
        TIME = TIME - TS(2,1)
        ICAV(2) = 2
        INTM = 2
        VOL = 0.0
        GOTO 50
```

```
C     LABEL 50 DENOTES WRITE OUT OF RESULTS SECTION.
 50   DO 51 K = 1, N(2)+1
      V1(2,K) = V(2,K)
      P1(2,K) = P(2,K)
      P(2,K)  = PP(2,K)
      V(2,K)  = VV(2,K)
      AP(I,K) = P(I.K)/1000.0
 51   CONTINUE
 83   VU(2,1) = 0.0
      PU(2,1) = 0.0
      VD(2,N(2)+1)= 0.0
      PD(2,N(2)+1)= 0.0
      DO 52 K=2,N(2)+1
      VU(2,K) = V(2,K) + ZDT * (V(2,K -1) - V(2,K))
      PU(2,K) = P(2,K) + ZDT * (P(2,K -1) - P(2,K))
 52   CONTINUE
      DO 53 K = 1,N(2)
      VD(2,K) = V(2,K) +ZDT * (V(2,K+1) - V(2,K))
      PD(2,K) = P(2,K) +ZDT * (P(2,K+1) - P(2,K))
 53   CONTINUE
      CALL FRICT (D.DT,2,VU,1,N(2)+1,F1)
      CALL FRICT (D,DT,2,VD,1,N(2)+1,F1D)
      WRITE(2,203)TIME, (V(2,K),K=1,N(2)+1,2),(AP(2,K),K=1,N(2)+1,2),
     1        VOL
      IF ( TIME. GT. TMAX )  GOTO 99
      IF ( NPATH. EQ . 1)   GOTO  84
      GOTO 41
200   FORMAT(      1H1,10HTIME VCHAR,5X,18H(0.5*L1) SECTIONS,,11H   VALVE
     1  ,,18H(0.2*L2) SECTIONS.,//)
201   FORMAT(2F5.3,4HV = ,3F7.2,7X,6F7.2,/,10X,4HP = ,3F7.2,7X,6F7.2,//)
202   FORMAT(F5.3,5X,4H V= ,28X,6F7.2,/10X,4HP = ,28X,6F7.2,//)
203   FORMAT(F5.3,5X,4H V= ,28X,6F7.2,/10X,4HP = ,28X,6F7.2,F12.8,//)
 99   IF ( IJ. EQ. NRUN )   GOTO 98
      STOP
      END
```

```
      SUBROUTINE VALVE ( V,P,A1,C,A,VO,VV,PP )
      DIMENSION V(2,41),P(2,41),A1(2,41),N(2),VO(2),C(2),A(2),
     1          PP(2,41),VV(2,41)
     1     ,DT(2)
     1     , Z(2,41)
      COMMON M,KINVIS,TRANS,VCHAR,DP,RHO  ,PR1,PR2,N,VD2,Z2  ,VAP
     5     , TIME   , DT
      X1=V(1,N(1))-A1(1,N(1))*V(1,N(1))*ABS(V(1,N(1)))+P(1,N(1))
     1   /(RHO*C(1))
      X3=V(2,2)-A1(2,2)*V(2,2)*ABS(V(2,2))-P(2,2)/(RHO*C(2))
      IF ( VCHAR. GT. 0.0 )   GOTO  10
      VD2 = 0.0
      VV(1,N(1)+1) = 0.0
      PP(1,N(1)+1) = RHO*C(1)*X1
      GOTO  13
   10 X5=((VCHAR*VO(1) )**2)/DP
      IF ( P(2,1). LE. VAP )  GOTO 12
      X6=RHO*((C(2)*A(1)/A(2))+C(1))
      X7=RHO*((C(2)*X3)+(X1*C(1)))
      VV(1,(N(1)+1))=-(X7/ABS(X7))*X5*X6/2.0 +(X7/ABS(X7))*SQRT
     1              (((X5*X6)/2.0)**2.0 +X5*ABS(X7))
      VV(2,1) = VV(1,(N(1)+1))*A(1)/A(2)
      VD2 = VV(2,1)
   11 PP(1,(N(1)+1)) = RHO*C(1)*(X1-VV(1,(N(1)+1)))
      PP(2,1) = RHO * C(2) * (VV(2,1)-X3)
      IF ( PP(2,1).LE.VAP )     GOTO 12 2
      GOTO  13
  122 TS = DT(1)* ( VAP-PP(2,1))/(P(2,1)-PP(2,1))
      FACT = ( DT(1)-TS)/DT(1)
      DO 15 I = 1,2
      DO 15 K = 1,N(I)+1
      CALL FACTOR(I,K,K,K,K,K,P,V,Z,Z,PP,VV,Z,Z,FACT,PP,VV,Z,Z)
   15 CONTINUE
      TIME = TIME - TS
      GOTO 13
   12 X6 = X5* RHO * C(2)
      X7 = X5 * ( VAP - RHO*C(2) * X1 )
      VV(1,N(1)+1) = -X6/2.0 +(SQRT((X6**2)-4.0*X7))/2.0
      VD2 = VV(1,N(1)+1)
      PP(1,N(1)+1) = RHO*C(1)*(X1-VV(1,N(1)+1))
      Z2 = 1.0
   13 RETURN
      END
      SUBROUTINE RESERVOIR (I,INTM,C,V,P,A1,VV,PP)
      DIMENSION C(2),V(2,41),P(2,41),A1(2,41),VV(2,41),PP(2,41) ,N(2)
      COMMON M,KINVIS,TRANS,VCHAR,DP,RHO,PR1,PR2 ,N
      Y2= 1.0/(RHO *C(I))
      IF (I-1) 1,1,2
    1 PP(1,1) = PR1
      IF(INTM - 1) 3,3,4
    3 VV(I,1) = V(I,2)+Y2*(PR1-P(I,2))-A1(I,2)*V(I,2)*ABS(V(I,2))
      GOTO 5
    4 VV(I,1) = V(I,1)+Y2*(PR1-P(I,1)) -A1(I,1)*V(I,1)*ABS(V(I,1))
      GOTO 5
    2 PP(2,(N(I)+1)) = PR2
      IF(INTM - 1) 6,6,7
    6 VV(I,(N(I)+1)) = V(I,N(I))-Y2*(PR2-P(I,N(I)))-A1(I,N(I))*V(I,N(I))
     1                  *ABS(V(I,N(I))   )
      GOTO  5
    7 VV(I,(N(I)+1))= V(I,N(I)+1)-Y2*(PR2-P(I,(N(I)+1)))
     1                -A1(I,(N(I)+1))*V(I,(N(I)+1))*ABS(V(I,(N(I)+1)) )
    5 RETURN
      END
```

```
      SUBROUTINE CAVITY (SLOPE,INTM,CC,I,J,VAP,V,P,A1,XV,XP)
      DIMENSION V(2,41),P(2,41),A1(2,41),XV(2,41),XP(2,41),CC(2)
       COMMON M,KINVIS,TRANS,VCHAR,DP,RHO
      Y2 = 1.0/(RHO *CC(I))
      IF (INTM - 1) 1,2,2
    2 A = V(I.J)
      B = P(I,J)
      C = A1(I,J)
      GOTO 3
    1 IF (SLOPE) 4,5,5
    5 A = V(I,J-1)
      B = P(I,J-1)
      C = A1(I,J-1)
      GOTO 3
    4 A = V(I,J+1)
      B = P(I,J+1)
      C = A1(I,J+1)
    3 XP(I,J) = VAP
      XV(I,J) = A - SLOPE * Y2 * (VAP - B) - C*A*ABS(A)
      RETURN
      END
```

```
      SUBROUTINE VAPOUR (I,N,DT,VAP,P,PP,KZ,PPX,TS )
      DIMENSION P(2,41),PP(2,41),PPX(2,41),TS(2,41),N(2),DT(2)
      KZ = 0
      DO 3 K = 1, N(I)+1
      TS(I,K) = 0.0
      X = PP(I,K) + ABS(VAP)
      X1= P(I,K) + ABS(VAP)
      IF (X) 2,6,4
    2 TS(I,K) = DT(I)*(VAP-PP(I,K))/(P(I,K)-PP(I,K))
      IF (X1) 5,5,3
    5 TS(I,K) = 0.0
    6 PPX(I,K)= VAP
      GOTO 3
    4 KZ = KZ +1
      PPX(I,K) = PP(I,K)
    3 CONTINUE
      RETURN
      END
```

A.5.7 SEPF master segment and VALVE and CAVITY subroutines

```
TASKA/SEPF52616SWAFFIELD/
SPACE18900
SECONDS500
PRINT9000
COMPILER FORTRAN
      LIST(LP)
      PROGRAM(SEPF52616)
      INPUT1=CR0
      OUTPUT2=LP0
      TRACE2
      END
```

```
      MASTER SEPF
      REAL KINVIS
      DIMENSION NPAVC(10),VC(10,50),AN(10,50),C1(10,10),NPAT(10),C2(10,
     1     10),A1(10,10),T(10,10),T1(200),AX(200),B(200),TS(2,21),
     2AP(2,41), V1(2,41),P1(2,41),V(2,41),P(2,41),PP(2,41),VV(2,41),
     3Z(2,41),  VU(2,41),PU(2,41),VD(2,41),PD(2,41),F1(2,41),F1D(2,41),
     4      A(2),D(2),C(2),DT(2),ICAV(2),PL(2),ZN(2),N(2),VO(2)
      COMMONM,KINVIS,TRANS,VCHAR,DP,RHO,PR1,PR2,N,VD2,Z2    ,VAP
     1      , VOL, FUELVOL, VD1
     2       ,DT,AIRVOL
     3       ,Z
     4      , TIME
      READ(1,101)NRUN
      IJ = 0
  98  IJ = IJ + 1
      READ(1,102) KINVIS,TRANS
      READ(1,102) VAPI,RHO
      VAP = VAPI
      DO 9 I = 1, 2
      READ (1,101) N(I)
      READ(1,103)PL(I),C(I),ZN(I),D(I),VO(I)
 103  FORMAT(5F10.4)
      A(I) = 3.1417 * (D(I)**2)/ 4.0
      DT(I)= PL(I)/(C(I)*ZN(I))
      ICAV(I) = 0
  9   CONTINUE
      DTO = DT(2)
      READ (1,102) PR1,DP
      READ (1,102) IMAX,ZDT
      ZDTO = ZDT
```

```
      KINVIS = KINVIS/100000.0
      READ ( 1,101 ) M
      READ ( 1,101 ) NSAVC
      DO 1 I =1, NSAVC
      READ ( 1,101 ) NPAVC(I)
      READ ( 1, 102 ) ( VC(I,K),AN(I,K),K=1,NPAVC(I) )
1     CONTINUE
      CALL PRELIM ( AN,VC,NSAVC,NPAVC,C1 )
      READ ( 1,101 ) NSAT
      DO 2 I=1, NSAT
      READ (1,101 ) NPAT(I)
      READ(1,102) (A1(I,K),T(I,K),K=1,NPAT(I))
2     CONTINUE
      CALL PRELIM (T,A1,NSAT,NPAT,C2)
      DTX = DT(1)
      TC = T( NSAT, NPAT(NSAT))
101   FORMAT(I3)
102   FORMAT(2F10.4)
      READ(1,111)IDAY,IMTH,IYEAR,INUM
  111 FORMAT (4I4)
      WRITE(2,204)IDAY,IMTH,IYEAR,INUM
  204 FORMAT(8HDATE =  ,I2,3H / ,I2,3H / ,I4,/,12HRUN NUMBER = ,I4,1H.,
     1      //)
C     INITIAL CONDITIONS ALONG BOTH PIPE SECTIONS.
      DO 22 I = 1, 2
      DO 22 K = 1, N(I)+1
      V(I,K) = VO(I)
   22 CONTINUE
      CALL FRICT (D,DT,1,V,1,N(1)+1,F1)
      CALL FRICT (D,DT,2,V,1,N(2)+1,F1)
      DO 23 I = 1, 2
      REN = ABS(VO(I))*D(I)/KINVIS
      FF = 0.079/REN**0.25
      FDR = 2.0*RHO*FF*PL(I)*(VO(I)**2)/(D(I)*ZN(I))
      AA = 0.0
      DO 23 K =1, N(I)+1
      XR = PR1
      IF ( I. EQ. 2 )   XR= P(1,N(1)+1) - DP
      AA = AA + 1.0
      P(I,K) =  XR - (AA - 1.0)* FDR
      AP(I,K) = P(I,K)        /1000.0
   23 CONTINUE
      PR2 = P(2,N(2)+1)
      TIME=0.0
      ATM = 14.7*6894.76
      RO = 3.0
      Z2 = 0.0
      Z4 = 0.0
      VOLX = 0.0
      FUELVOL = 0.0
      AIRVOL = 0.0
      VOL = 0.0
      VCHAR=1.0
      WRITE(2,200)
C     CALCULATION INTERNAL POINTS DURING VALVE CLOSURE
      KB = 1
      INTM = 1
      WRITE(2,201)TIME,VCHAR,(V(1,K),K=1,N(1)+1,3),(V(2,K),K=1,N(2)+1,
     1                2),(AP(1,K),K=1,N(1)+1,3),(AP(2,K),K=1,N(2)+1,2)
   30 TIME = TIME + DT(2)
      KB = KB + 1
      T1 (KB) = TIME
      CALL INTER ( KB,T1,T,NSAT,NPAT,KMAX,C2,AX )
      CALL INTER ( KB,AX,AN,NSAVC,NPAVC,KMAX,C1,B )
      VCHAR = B(KB)
      DO 31 I = 1, 2
```

```
      CALL INTERNAL (1,N,I,C,V,P,F1,P,V,F1,VV,PP)
      CALL RESERVOIR (I,1,C,V,P,F1,VV,PP)
   31 CONTINUE
      CALL VALVE ( V,P,F1,C,A,VU,VV,PP )
      IF ( VCHAR. EQ. 0.0 ) DT(2) = DTO*ZDTO
   38 VOL1 = VOL
   33 DO 35 I = 1, 2
      DO 36 K = 1, N(I)+1
      V1(I,K) = V(I,K)
      P1(I,K) = P(I,K)
      V (I,K) = VV(I,K)
      P (I,K) = PP(I,K)
      AP(I,K) = P(I,K)/1000.0
   36 CONTINUE
      CALL FRICT (D,DT,I,V,1,N(I)+1,F1)
   35 CONTINUE
      VD1 = VD2
      WRITE(2,201)TIME,VCHAR,(V(1,K),K=1,N(1)+1,3),(V(2,K),K=1,N(2)+1,2
     1            ),(AP(1,K),K=1,N(1)+1,3),(AP(2,K),K=1,N(2)+1,2)
      IF ( VCHAR )   83,83,30
   41 TIME = TIME + DT(2)
C     LABEL 61 DENOTES VAPOUR POCKET AT VALVE.
   61 CALL RESERVOIR (2,2,C,VU,PU,F1,VV,PP)
      CALL INTERNAL  (2,N,2,C,VU,PU,F1,PD,VD,F1D,VV,PP)
      IF ( VOLX. GT. 0.0 )  GOTO 184
      IF ( VOL. LT. VOL2 )      VOLX = VOL2
      IF ( VOL. LT. VOL2 )   . RO = 2.0
      IF ( VOL. LT. VOL2 )      Z4 = 1.0
  184 IF ( Z4. EQ. 1.0 )   GOTO  183
      VCHAR = FUELVOL
      CALL CAVITY ( -1.0,2,C,2,1,VAP,RO,A,DT,AIRVOL,VOL,VD,PD,F1D,
     1              VV,PP)
       VOL2 = VOL
      VOL = VOL + 0.5*A(2)*DT(2)*(VV(2,1)+V(2,1))
      W1 = ( ATM - 0.5*P(2,1))*0.136/ATM
      W2 = 0.5*0.136/ATM
      AIRVOL = ( W1 - W2 * PP(2,1)) * FUELVOL
      VOL1 = VOL
      WRITE ( 2, 701 ) AIRVOL,  FUELVOL
  701 FORMAT ( 2F 12.8 )
      GOTO 50
  183 Z4 = 1.0
      CALL CAVITY ( -1.0, 2, C, 2, 1, VAP,2.0, A, DT, AIRVOL, VOL,
     1                          VD, PD, F1D, VV, PP )
      CALL VAPOUR (2,N,DT,VAP,P,PP,KZ,PF,TS)
      CALL SORTER (N(2)+1,TS,2,DT,TSMAX,J1)
      FACT = (DT(2)-TSMAX)/DT(2)
      TIME = TIME - TSMAX
      DO 63  K =1,N(2)+1
      CALL FACTOR(2,K,K,K,K,K,V,Z,P,Z,VV,Z,PP,Z,FACT,VV,Z,PP,Z)
   63 CONTINUE
      VOL2 = VOL
      VOL = VOL + 0.5* A(2)*(DT(2)-TSMAX)*(VV(2,1)+V(2,1))
      GOTO 50
C     LABEL 50 DENOTES WRITE OUT OF RESULTS SECTION.
   50 DO 51 K = 1, N(2)+1
      V1(2,K) = V(2,K)
      P1(2,K) = P(2,K)
      P(2,K)  = PP(2,K)
      AP(I,K) = P(I,K)/1000.0
      V(2,K)  = VV(2,K)
   51 CONTINUE
      IF ( ABS( VOL2 - VOL), GT. ( 0.33*VOL))    GOTO 91
      IF ( VOL. GT. VOL2 )  GOTO 92
      GOTO 83
   91 DT(2) = DT(2) / 2.0
```

```
      ZDT = DT(2) / DTO
      GOTO 83
   92 DT(2) = DTO * ZDTU
      ZDT = ZDTO
   83 VU(2,1) = 0.0
      PU(2,1) = 0.0
      VD(2,N(2)+1)= 0.0
      PD(2,N(2)+1)= 0.0
      DO 52 K=2,N(2)+1
      VU(2,K) = V(2,K) + ZDT * (V(2,K -1) - V(2,K))
      PU(2,K) = P(2,K) + ZDT * (P(2,K -1) - P(2,K))
   52 CONTINUE
      DO 53 K = 1,N(2)
      VD(2,K) = V(2,K) +ZDT * (V(2,K+1) - V(2,K))
      PD(2,K) = P(2,K) +ZDT * (P(2,K+1) - P(2,K))
   53 CONTINUE
      CALL FRICT (D,DT,2,VU,1,N(2)+1,F1)
      CALL FRICT (D,DT,2,VD,1,N(2)+1,F1D)
      NL = N(2) / 5
      WRITE(2,203)TIME,(V(2,K),K=1,N(2)+1,NL),(AP(2,K),K=1,N(2)+1,NL),
     1       VOL
      IF ( TIME. GT. TMAX )  GOTO 99
      GOTO 41
  200 FORMAT(     1H1,10HTIME VCHAR,5X,18H(0.5*L1) SECTIONS.,11H   VALVE
     1  ,,18H(0.2*L2) SECTIONS.,//)
  201 FORMAT(2F5.3,4HV = ,3F7.2,7X,6F7.2,/,10X,4HP = ,3F7.2,7X,6F7.2,//)
  202 FORMAT(F5.3,5X,4H V= ,28X,6F7.2,/10X,4HP = ,28X,6F7.2,//)
  203 FORMAT(F5.3,5X,4H V= ,28X,6F7.2,/10X,4HP = ,28X,6F7.2,F12.8,//)
   99 IF ( IJ. EQ. NRUN )   GOTO 98
      STOP
      END
```

```
      SUBROUTINE VALVE ( V,P,A1,C,A,VO,VV,PP )
      DIMENSION V(2,41),P(2,41),A1(2,41),N(2),VO(2),C(2),A(2),
     1          PP(2,41),VV(2,41)
     2        , DT(2)
     3          ,Z(2,41)
      COMMON M,KINVIS,TRANS,VCHAR,DP,RHO   ,PR1,PR2,N,VD2,Z2   ,VAP
     1    , VOL, FUELVOL, VD1
     2              ,DT,AIRVOL
     3        ,Z
     1      , TIME
      ATM = 14.7*6894.76
      X1=V(1,N(1))-A1(1,N(1))*V(1,N(1))*ABS(V(1,N(1)))+P(1,N(1))
     1   /(RHO*C(1))
      X3=V(2,2)-A1(2,2)*V(2,2)*ABS(V(2,2))-P(2,2)/(RHO*C(2))
      Z3 = 0.0
      IF ( VCHAR. GT. 0.0 )   GOTO  10
      VV(1,N(1)+1) = 0.0
      PP(1,N(1)+1) = RHO*C(1)*X1
      Z3 = 1.0
      GOTO 121
   10 X5=((VCHAR*VO(1) )**2)/DP
      IF ( P(2,1).GT.ATM)     VOL = 0.0
      IF ( P(2,1).LE.ATM )  GOTO 121
      X6=RHO*((C(2)*A(1)/A(2))+C(1))
      X7=RHO*((C(2)*X3)+(X1*C(1)))
      VV(1,(N(1)+1))=-(X7/ABS(X7))*X5*X6/2.0 +(X7/ABS(X7))*SQRT
     1               (((X5*X6)/2.0)**2.0 +X5*ABS(X7))
   11 PP(1,(N(1)+1)) = RHO*C(1)*(X1-VV(1,(N(1)+1)))
      VV(2,1) = VV(1,(N(1)+1))*A(1)/A(2)
      PP(2,1) = RHO * C(2) * (VV(2,1)-X3)
      IF ( PP(2,1). LE. ATM )   GOTO 122
      DPDT = PP(1,N(1)+1) - P(1,N(1)+1)
      GOTO  13
  122 TS = DT(1)*(ATM-PP(2,1))/(P(2,1)-PP(2,1))
      FACT = ( DT(1)-TS)/DT(1)
      DO 15 I = 1,2
      DO 15 K = 1,N(I)+1
      CALL FACTOR(I,K,K,K,K,K,P,V,Z,Z,PP,VV,Z,Z,FACT,PP,VV,Z,Z)
   15 CONTINUE
      TIME = TIME - TS
      GOTO 13
  121 Z2 = 1.0
      Y1 = X1
      Y2 = X3
      Y3 = 1.0 / ( RHO*C(1) )
      Y4 = 1.0 / ( RHO*C(2) )
      Y6 = FUELVOL * ATM
      Y7 = 0.5*A(1)*DT(1)*ATM
      Y18 = Y7*V(1,N(1)+1)
      Y18 = Y18 + Y6
      Y6 = 0.0
      W1 = ( ATM-0.5*P(2,1))*0.136/ATM
      W2 = 0.5*0.136/ATM
      Y8 = VOL + 0.5*A(2)*DT(2)*(V(2,1)-V(1,N(1)+1))
      Y9 = 0.5*A(2)*DT(2)
      IF ( Z3. EQ. 1.0)   GOTO125
```

```
      Y5 = X5
      Y10 = Y7*Y1 +Y18
      Y11 = Y7*Y3
      Y12 = Y8 + Y9*(Y2-Y1)
      Y13 = Y9*Y4
      Y14 = Y9*Y3
      Y15 = 0.0
      Y16 = 0.0
      Y17 = 1.0 + 2.0*Y1*Y3*1.0/Y5
      Y20 = Y10 * W1 + Y6
      Y21 = Y10*W2
      Y22 = Y11*W1
      Y23 = Y11*W2
      AX = ( Y3**4)*Y13/(Y5**2)
      C1 = (((-2.0*Y17*Y13*Y3**2)/Y5)-(Y14*Y3**2)/Y5)/AX
     1      -((-Y23*Y3**2)/Y5)/AX
      C2=(((-Y12*Y3**2)/Y5)+Y13*2.0*((Y3*Y1/Y5)**2)+Y17*(Y13*Y17+Y14))
     1         / AX
     1          - ((Y21*Y3**2)/Y5  +Y23*Y17)/AX
     2        +(Y13*VAP*(Y3**2)/Y5)/AX
      C3 = (Y12*Y17-(2.0*Y13*Y17+Y14)*(Y1**2)/Y5+Y16)/AX
     1       -((-Y21*Y17)- Y22 - (Y23*Y1**2)/Y5)/AX
     2         +VAP*(-Y14-Y13*Y17)/AX
      C4 = (((Y1**2)/Y5)*(Y13*((Y1**2)/Y5)-Y12)-Y15)/AX
     1      -(Y20+(Y21*Y1**2)/Y5)/AX
     2        +VAP*((Y13*(Y1**2)/Y5)-Y12)/AX
      B1 = P(1,N(1)+1) + DPDT
   50 B = B1
      FB = B**4+C1*B**3+C2*B**2+C3*B+C4
      FDB = 4.0*B**3+3.0*C1*B**2+C2*2.0*B*1.0+C3
      B1 = B - FB/FDB
      IF ( ABS((B-B1)/B).GT.0.005)     GOTO 50
      PP(1,N(1)+1) = B1
      VV(1,N(1)+1)= X1-Y3*B1
      PP(2,1) = B1 - (VV(1,N(1)+1)**2)/X5
      VV(2,1) = X3+Y4*PP(2,1)
      GOTO  6
  125 Z3 = 0.0
      B2 = ( VAP*(Y8+Y9*Y2)+Y6+Y18*W1)/(Y9*Y4)
      B1 = ( Y8+Y9*Y2-VAP*Y9*Y4+Y18*W2)/(Y9*Y4)
      PP(2,1) = - ( B1/2.0)+SQRT(((B1/2.0)**2)+B2)
      VV(2,1) = Y2 +Y4*PP(2,1)
      GOTO 6
    6 FUELVOL = FUELVOL + 0.5*A(1)*DT(1)*(VV(1,N(1)+1)+V(1,N(1)+1))
      VD2 = VV(1,N(1)+1)
      ACON = W1 - W2 * PP(2,1)
      AIRVOL = ACON * FUELVOL
      VOL = Y8 + Y9*(VV(2,1)-VV(1,N(1)+1))
      DPDT = PP(1,N(1)+1) - P(1,N(1)+1)
   13 RETURN
      END
```

```
      SUBROUTINE CAVITY ( SLOPE,INTM,CC,I,J,VAP,RO,AR,DT,AIR,VOL,V,P,
     1     A1,                  XV,XP )
      DIMENSION V(2,41),P(2,41),A1(2,41),XV(2,41),XP(2,41),CC(2)
     1     ,        DT(2),        AR(2)
       COMMON M,KINVIS,TRANS,VCHAR,DP,RHO
      ATM = 14.7*6894.76
      Y2 = 1.0/(RHO *CC(I))
      IF (INTM - 1) 1,2,2
    2 A = V(I,J)
      B = P(I,J)
      C = A1(I,J)
      GOTO 3
    1 IF (SLOPE) 4,5,5
    5 A = V(I,J-1)
      B = P(I,J-1)
      C = A1(I,J-1)
      GOTO 3
    4 A = V(I,J+1)
      B = P(I,J+1)
      C = A1(I,J+1)
    3 IF ( RO. GT. 1.0 )    GOTO6
      XP(I,J) = VAP
      XV(I,J) = A - SLOPE * Y2 * (VAP - B) - C*A*ABS(A)
      GOTO  7
    6 IF ( RO. EQ. 3.0 )   GOTO 8
      Y6 = AIR * 14.7 * 144.0
      Y16 = 0.0
      GOTO 9
    8 Y6 = VCHAR      * 144.0 * 14.7
      W2 = 0.5*0.136/ATM
      W1 = ( ATM - 0.5 * XP(I,J)) * 0.136 / ATM
      Y16 = Y6 * W2
      Y6 = Y6 * W1
    9 Y25 = 0.5 * AR(1) * DT(2)
      Y24 =  VOL + 0.5*AR(2)*DT(2)*XV(I,J)
      Y24 = Y24 + Y16
      Y4 = Y2
      Y2 = A*(1.0-C*ABS(A))+SLOPE*Y4*B
      B1 = ( Y24+Y2*Y25-VAP*Y25*Y4)/(Y25*Y4)
      B2 = ( VAP*(Y24+Y25*Y2)+Y6)/(Y25*Y4)
      XP(I,J) = -(B1/2.0)+SQRT(((B1/2.0)**2)+B2)
      XV(I,J) = Y2+Y4*XP(I,J)
      IF ( RO . EQ . 3.0 )  DP = W1 -W2 * XP (I, J)
    7 RETURN
      END
```

A.5.8 SEPG master segment and VALVE, AIRV and CAVITY subroutines

```
TASKA/SEPG52616SWAFFIELD/
SECONDS500
SPACE19697
PRINT9000
COMPILER FORTRAN
      LIST(LP)
      PROGRAM(SEPF52616)
      INPUT1=CR0
      OUTPUT2=LP0
      TRACE2
      END
```

```
      MASTER SEPG
      REAL KINVIS
      DIMENSION NPAVC(10),VC(10,50),AN(10,50),C1(10,10),NPAT(10),C2(10,
     1     10),A1(10,10),T(10,10),T1(200),AX(200),B(200),TS(2,21),
     2AP(2,41), V1(2,41),P1(2,41),V(2,41),P(2,41),PP(2,41),VV(2,41),
     3Z(2,41),  VU(2,41),PU(2,41),VD(2,41),PD(2,41),F1(2,41),F1D(2,41),
     4      A(2),D(2),C(2),DT(2),ICAV(2),PL(2),ZN(2),N(2),VO(2)
      COMMONM,KINVIS,TRANS,VCHAR,DP,RHO,PR1,PR2,N,VD2,Z2    ,VAP
     1      , VOL, FUELVOL, VD1
     2       ,DT,AIRVOL
     3       ,Z
     4      , TIME
      READ(1,101)NRUN
      IJ = 0
      NPATH = 0
   98 IJ = IJ + 1
      READ(1,102) KINVIS,TRANS
      READ(1,102) VAPI,RHO
      VAP = VAPI
      DO 9 I = 1, 2
      READ (1,101) N(I)
      READ(1,103)PL(I),C(I),ZN(I),D(I),VO(I)
  103 FORMAT(5F10.4)
      A(I) = 3.1417 * (D(I)**2)/ 4.0
      DT(I)= PL(I)/(C(I)*ZN(I))
      ICAV(I) = 0
    9 CONTINUE
      DTO = DT(2)
      READ (1,102) PR1,DP
      READ (1,102) TMAX,ZDT
      ZDTO = ZDT
      KINVIS = KINVIS/100000.0
      READ ( 1,101 ) M
      READ ( 1,101 ) NSAVC
      DO 1 I =1, NSAVC
      READ ( 1,101 ) NPAVC(I)
      READ ( 1, 102 ) ( VC(I,K),AN(I,K),K=1,NPAVC(I) )
      CONTINUE
```

```
      CALL PRELIM ( AN,VC,NSAVC,NPAVC,C1 )
      READ ( 1,101 ) NSAT
      DO 2 I=1, NSAT
      READ (1,101 ) NPAT(I)
      READ(1,102) (A1(I,K),T(I,K),K=1,NPAT(I))
2     CONTINUE
      CALL PRELIM (1,A1,NSAT,NPAT,C2)
      DTX = DT(1)
      TC = T( NSAT, NPAT(NSAT))
      KMAX = TC / DTX + 1.0
101   FORMAT(I3)
102   FORMAT(2F10.4)
      READ(1,111)IDAY,IMTH,IYEAR,INUM
  111 FORMAT (4I4)
      WRITE(2,204)IDAY,IMTH,IYEAR,INUM
  204 FORMAT(8HDATE =  ,I2,3H / ,I2,3H / ,I4,/,12HRUN NUMBER = ,I4,1H.,
     1       //)
C     INITIAL CONDITIONS ALONG BOTH PIPE SECTIONS.
      DO 22 I = 1, 2
      DO 22 K = 1, N(I)+1
      V(I,K) = VO(I)
   22 CONTINUE
      CALL FRICT (D,DT,1,V,1,N(1)+1,F1)
      CALL FRICT (D,DT,2,V,1,N(2)+1,F1)
      DO 23 I = 1, 2
      REN = ABS(VO(I))*D(I)/KINVIS
      FF = 0.079/REN**0.25
      FDR = 2.0*RHO*FF*PL(I)*(VO(I)**2)/(D(I)*ZN(I))
         AA = 0.0
      DO 23 K =1, N(I)+1
      XR = PR1
      IF ( I. EQ. 2 )   XR= P(1,N(1)+1) - DP
      AA = AA + 1.0
      P(I,K) =  XR - (AA - 1.0)* FDR
      AP(I,K) = P(I,K)/1000.0
   23 CONTINUE
      PR2 = P(2,N(2)+1)
      TIME=0.0
      NT = 2
      RO = 3.0
      Z2 = 0.0
      Z4 = 0.0
      VOLX = 0.0
      FUELVOL = 0.0
      AIRVOL = 0.0
      XN = 1.0
      VOL = 0.0
      VCHAR=1.0
      WRITE(2,200)
C     CALCULATION INTERNAL POINTS DURING VALVE CLOSURE
      KB = 1
      INTM = 1
      WRITE(2,201)TIME,VCHAR,(V(1,K),K=1,N(1)+1,3),(V(2,K),K=1,N(2)+1,
     1                2),(AP(1,K),K=1,N(1)+1,3),(AP(2,K),K=1,N(2)+1,2)
   30 TIME = TIME + DT(2)
      KB = KB + 1
      T1 (KB) = TIME
      CALL INTER ( KB,T1,T,NSAT,NPAT,KMAX,C2,AX )
      CALL INTER ( KB,AX,AN,NSAVC,NPAVC,KMAX,C1,B )
      VCHAR = B(KB)
```

```
      DO 31 I = 1, 2
      CALL INTERNAL (1,N,I,C,V,P,F1,P,V,F1,VV,PP)
      CALL RESERVOIR (I,1,C,V,P,F1,VV,PP)
   31 CONTINUE
      CALL VALVE ( V,P,F1,C,A,VU,VV,PP )
      IF ( VCHAR. EQ. 0.0 ) DT(2) = DTO*ZDTO
   38 VOL1 = VOL
   33 DO 35 I = 1, 2
      DO 36 K = 1, N(I)+1
      V1(I,K) = V(I,K)
      P1(I,K) = P(I,K)
      V (I,K) = VV(I,K)
      P (I,K) = PP(I,K)
      AP(I,K) = P(I,K) / 1000.0
   36 CONTINUE
      CALL FRICT (D,DT,I,V,1,N(I)+1,F1)
   35 CONTINUE
      VD1 = VD2
      WRITE(2,201)TIME,VCHAR,(V(1,K),K=1,N(1)+1,3),(V(2,K),K=1,N(2)+1,2
     1            ),(AP(1,K),K=1,N(1)+1,3),(AP(2,K),K=1,N(2)+1,2)
      IF ( VCHAR )   83,83,30
   41 TIME = TIME + DT(2)
C     LABEL 61 DENOTES VAPOUR POCKET AT VALVE.
   61 CALL RESERVOIR (2,2,C,VU,PU,F1,VV,PP)
      CALL INTERNAL  (2,N,2,C,VU,PU,F1,PD,VD,F1D,VV,PP)
      IF ( VOLX. GT. 0.0 )  GOTO 184
      IF ( VOL. LT. VOL2 )     VOLX = VOL2
      IF ( VOL. LT. VOL2 )    RO = 2.0
      IF ( VOL. LT. VOL2 )     Z4 = 1.0
  184 IF ( Z4. EQ. 1.0 )   GOTO  183
      VCHAR = FUELVOL
      CALL CAVITY ( -1.0,2,C,2,1,VAP,RO,A,DT,AIRVOL,VOL,VD,PD,F1D,
     1              VV,PP)
       VOL2 = VOL
      VOL = VOL + 0.5*A(2)*DT(2)*(VV(2,1)+V(2,1))
      W1 = ( ATM - 0.5*P(2,1))*0.136/ATM
      W2 = 0.5*0.136/ATM
      AIRVOL = ( W1 - W2 * PP(2,1)) * FUELVOL
      VOL1 = VOL
      WRITE ( 2, 701 ) AIRVOL,  FUELVOL
  701 FORMAT ( 2F 12.8 )
      GOTO 50
  183 Z4 = 1.0
      CALL CAVITY ( -1.0, 2, C, 2, 1, VAP,2.0, A, DT, AIRVOL, VOL,
     1                        VD, PD, F1D, VV, PP )
      VOL2 = VOL
      CALL VAPOUR (2,N,DT,VAP,P,PP,KZ,PP,TS)
      CALL SORTER (N(2)+1,TS,2,DT,TSMAX,J1)
      FACT = (DT(2)-TSMAX)/DT(2)
      TIME = TIME - TSMAX
      DO 63  K =1,N(2)+1
      CALL FACTOR(2,K,K,K,K,K,V,Z,P,Z,VV,Z,PP,Z,FACT,VV,Z,PP,Z)
   63 CONTINUE
      VOL = VOL + 0.5* A(2)*(DT(2)-TSMAX)*(VV(2,1)+V(2,1))
      GOTO 50
C     LABEL 50 DENOTES WRITE OUT OF RESULTS SECTION.
   50 DO 51 K = 1, N(2)+1
      V1(2,K) = V(2,K)
      P1(2,K) = P(2,K)
      P(2,K)  = PP(2,K)
      V(2,K)  = VV(2,K)
      AP(I,K) = P(I,K) / 1000 .0
   51 CONTINUE
```

```
      IF ( ABS( VOL2 - VOL). GT. ( 0.33*VOL))     GOTO 91
      IF ( VOL. GT. VOL2 )  GOTO 92
      GOTO 83
   91 DT(2) = DT(2) / 2.0
      ZDT = DT(2) / DTO
      GOTO 83
   92 DT(2) = DTO * ZDTO
      ZDT = ZDTO
   83 VU(2,1) = 0.0
      PU(2,1) = 0.0
      VD(2,N(2)+1)= 0.0
      PD(2,N(2)+1)= 0.0
      DO 52 K=2,N(2)+1
      VU(2,K) = V(2,K) + ZDT * (V(2,K -1) - V(2,K))
      PU(2,K) = P(2,K) + ZDT * (P(2,K -1) - P(2,K))
   52 CONTINUE
      DO 53 K = 1,N(2)
      VD(2,K) = V(2,K) +ZDT * (V(2,K+1) - V(2,K))
      PD(2,K) = P(2,K) +ZDT * (P(2,K+1) - P(2,K))
   53 CONTINUE
      CALL FRICT (D,DT,2,VU,1,N(2)+1,F1)
      CALL FRICT (D,DT,2,VD,1,N(2)+1,F1D)
      NL = N(2) / 5
      WRITE(2,203)TIME,(V(2,K),K=1,N(2)+1,NL),(AP(2,K),K=1,N(2)+1,NL),
     1        VOL
      IF ( TIME. GT. TMAX )  GOTO 99
      GOTO 41
  200 FORMAT(      1H1,10HTIME VCHAR,5X,18H(0.5*L1) SECTIONS.,11H   VALVE
     1  ,,18H(0.2*L2) SECTIONS.,//)
  201 FORMAT(2F5.3,4HV = ,3F7.2,7X,6F7.2,/,10X,4HP = ,3F7.2,7X,6F7.2,//)
  202 FORMAT(F5.3,5X,4H V= ,28X,6F7.2,/10X,4HP = ,28X,6F7.2,//)
  203 FORMAT(F5.3,5X,4H V= ,28X,6F7.2,/10X,4HP = ,28X,6F7.2,F12.8,//)
   99 IF ( IJ. EQ. NRUN )   GOTO 98
      STOP
      END
```

```
      SUBROUTINE VALVE ( V,P,A1,C,A,VD,VV,PP )
      DIMENSION V(2,41),P(2,41),A1(2,41),N(2),VD(2),C(2),A(2),
     1          PP(2,41),VV(2,41)
     2        , DT(2)
     3          ,Z(2,41)
      COMMON M,KINVIS,TRANS,VCHAR,DP,RHO   ,PR1,PR2,N,VD2,Z2   ,VAP
     1    , VOL, FUELVOL, VD1
     2             ,DT,AIRVOL
     3       ,Z
     1     , TIME
      XN = 1.4
      ATM = 14.7*6894.76
      X1=V(1,N(1))-A1(1,N(1))*V(1,N(1))*ABS(V(1,N(1)))+P(1,N(1))
     1   /(RHO*C(1))
      X3=V(2,2)-A1(2,2)*V(2,2)*ABS(V(2,2))-P(2,2)/(RHO*C(2))
      Z3 = 0.0
      IF ( VCHAR. GT. 0.0 )   GOTO  10
      VV(1,N(1)+1) = 0.0
      PP(1,N(1)+1) = RHO*C(1)*X1
      Z3 = 1.0
      GOTO 121
   10 X5=((VCHAR*VD(1) )**2)/DP
      IF ( P(2,1).GT.ATM)     VOL = 0.0
      IF ( P(2,1).LE.ATM )  GOTO 121
      X6=RHO*((C(2)*A(1)/A(2))+C(1))
      X7=RHO*((C(2)*X3)+(X1*C(1)))
      VV(1,(N(1)+1))=-(X7/ABS(X7))*X5*X6/2.0 +(X7/ABS(X7))*SQRT
     1               (((X5*X6)/2.0)**2.0 +X5*ABS(X7))
   11 PP(1,(N(1)+1)) = RHO*C(1)*(X1-VV(1,(N(1)+1)))
      VV(2,1) = VV(1,(N(1)+1))*A(1)/A(2)
      PP(2,1) = RHO * C(2) * (VV(2,1)-X3)
      IF ( PP(2,1). LE. ATM )   GOTO 122
      DPDT = PP(1,N(1)+1) - P(1,N(1)+1)
      GOTO  13
  122 TS = DT(1)*(ATM-PP(2,1))/(P(2,1)-PP(2,1))
      FACT = ( DT(1)-TS)/DT(1)
      DO 15 I = 1,2
      DO 15 K = 1,N(I)+1
      CALL FACTOR(I,K,K,K,K,K,P,V,Z,Z,PP,VV,Z,Z,FACT,PP,VV,Z,Z)
   15 CONTINUE
      TIME = TIME - TS
      GOTO 13
  121 Z2 = 1.0
      Y1 = X1
      Y2 = X3
      Y3 = 1.0 / ( RHO*C(1) )
      Y4 = 1.0 / ( RHO*C(2) )
      Y7 = 0.5*A(1)*DT(1)
      Y18 = FUELVOL + Y7*V(1,N(1)+1)
      W1 = ( ATM-0.5*(P(2,1)+VAP))*0.136/ATM
      W2 = 0.5*0.136/ATM
      Y8 = VOL + 0.5*A(2)*DT(2)*(V(2,1)-V(1,N(1)+1))
      Y9 = 0.5*A(2)*DT(2)
      Y10 = Y7*Y1 +Y18
      Y11 = Y7*Y3
      Y12 = Y8 + Y9*(Y2-Y1+Y4*VAP)
      Y13 = Y9*Y4
      Y14 = Y9*Y3
      IF ( Z3. EQ. 1.0)   GOTO 125
```

```
      Y5 = X5
      C2 = PP(2,1)
      D1 = ( 2.0*Y1*Y3+Y5)/Y3**2
 50   C1 = C2
      D2 =  (Y5*(C1+VAP)+Y1**2)/Y3**2
      B = ( D1/2.0) - SQRT((D1/2.0)**2 - D2 )
      D4 = (Y10-Y11*B)*W1*ATM**(1.0/XN)
      D5 = ( Y10-Y11*B)*W2*ATM**(1.0/XN)
      D6 = Y12+Y14*B
      CALL AIRV ( D6,Y13,D4,D5,C2 )
      IF ( ABS((C1-C2)/C1).GT.0.005)   GOTO 50
      PP(2,1) = C2 + VAP
      D2 =(Y5*(C2+VAP)+Y1**2)/Y3**2
      B1 = (D1/2.0) - SQRT((D1/2.0)**2 - D2)
      PP(1,N(1)+1) = B1
      VV(1,N(1)+1)= X1-Y3*B1
      PP(2,1) = B1 - (VV(1,N(1)+1)**2)/X5
      VV(2,1) = X3+Y4*PP(2,1)
      GOTO  6
 125  Z3 = 0.0
      Y12 = Y8 + Y9*(Y2+Y4*VAP)
      Y20 = Y18*W2*ATM**(1.0/XN)
      Y21= Y18*W1*ATM**(1.0/XN)
      X1 = PP(2,1)
      CALL AIRV ( Y12, Y13, Y21,Y20,X1    )
      PP(2,1) = X1 + VAP
      VV(2,1) = Y2 +Y4*PP(2,1)
      GOTO 6
  6   FUELVOL = FUELVOL + 0.5*A(1)*DT(1)*(VV(1,N(1)+1)+V(1,N(1)+1))
      VD2 = VV(1,N(1)+1)
      ACON = W1 - W2 * PP(2,1)
      AIRVOL = ACON * FUELVOL
      VOL = Y8 + Y9*(VV(2,1)-VV(1,N(1)+1))
  13  RETURN
      END
```

```
      SUBROUTINE CAVITY ( SLOPE,INTM,CC,I,J,VAP,RO,AR,DT,AIR,VOL,V,P,
     1     A1,              XV,XP )
      DIMENSION V(2,41),P(2,41),A1(2,41),XV(2,41),XP(2,41),CC(2)
     1     ,        DT(2),        AR(2)
      COMMON M, KINVIS, TRANS,FUELVOL, DP, RHO
      ATM = 14.7*6894.76
      XN = 1.4
      Y2 = 1.0/(RHO *CC(I))
      IF (INTM - 1) 1,2,2
    2 A = V(I,J)
      B = P(I,J)
      C = A1(I,J)
      GOTO 3
    1 IF (SLOPE) 4,5,5
    5 A = V(I,J-1)
      B = P(I,J-1)
      C = A1(I,J-1)
      GOTO 3
    4 A = V(I,J+1)
      B = P(I,J+1)
      C = A1(I,J+1)
    3 IF ( RO. GT. 1.0 )     GOTO6
      XP(I,J) = VAP
      XV(I,J) = A - SLOPE * Y2 * (VAP - B) - C*A*ABS(A)
      GOTO  7
    6 IF ( RO. EQ. 3.0 )   GOTO 8
      W1 = AIR*ATM**(1.0/XN)
      W2 = 0.0
      GOTO 9
    8 W2 =  0.5*0.136*FUELVOL*ATM**(1.0/XN)/ATM
      W1 =  ((ATM-0.5*(XP(2,1)+VAP))*0.136/ATM)*FUELVOL*ATM**(1.0/XN)
    9 Y25 = 0.5 * AR(1) * DT(2)
      Y24 =  VOL + 0.5*AR(2)*DT(2)*XV(I,J)
      Y4 = Y2
      Y2 = A*(1.0-C*ABS(A))+SLOPE*Y4*B
      Y12 = Y24+Y25*(Y2+Y4*VAP)
      Y13= Y25*Y4
      X1 = XP(I,J)
      CALL AIRV ( Y12, Y13, W1,W2, X1 )
      XP(2,1) = X1 + VAP
      XV(I,J) = Y2+Y4*XP(I,J)
      IF ( RO . EQ . 3.0 )  DP = W1 -W2 * XP (I, J)
    7 RETURN
      END
```

```
      SUBROUTINE  AIRV ( A, B, C, D, X1   )
      XN = 1.4
      ITN = 1
1     X = X1
      FX = B*X**((XN+1.0)/XN) +A*X**(1.0/XN) - C
     1        + D * X
      DFX = ((XN+1.0)*B/XN)*X**(1.0/XN)+(A/XN)*1.0/(X**((XN-1.0)/XN))
     2      + D
      X1 = X - FX / DFX
      IF ( ABS((X1-X)/X). LE. 0.005 )       GOTO 2
      ITN = ITN + 1
      GOTO 1
2     RETURN
      END
```

A.5.9 Subroutines common to programs SEPE, SEPF, SEPG

```
      SUBROUTINE CURFIT(X,Y,N,M,C)
      DIMENSION X(50),Y(50),YY(50),ERROR(50),P(20),C(11),B(11),A(11,11)
C     THIS SUBROUTINE FITS EXPERIMENTAL DATA TO A POLYNOMIAL
C     FUNCTION. IT ALSO CALCULATES THE ERROR BETWEEN EXPERIMENTAL
C     VALUES AND CALCULATED VALUES.
29    MX2=M*2
      DO 1 I=1,MX2
      P(I)=0.0
      DO 1 J=1,N
1     P(I)=P(I)+X(J)**I
      NXY=N
      NI=M+1
      DO 2 I=1,NI
      DO 2 J=1,NI
      K=I+J-2
      IF(K-0) 3,3,4
4     A(I,J)=P(K)
      GOTO 2
3     A(1,1)=NXY
2     CONTINUE
      B(1)=0.0
      DO 5 J=1,NXY
5     B(1)=B(1)+Y(J)
      DO 6 I=2,NI
      B(I)=0.0
      DO 6 J=1,NXY
6     B(I)=B(I)+Y(J)*X(J)**(I-1)
C     PIVOTAL CONDENSATION
      NM1=NI-1
      DO 7 K=1,NM1
      KPI=K+1
      L=K
      DO 8 I=KPI,NI
      IF(ABS(A(I,K))-ABS(A(L,K))) 8,8,9
9     L=I
8     CONTINUE
      IF(L-K) 10, 10, 11
 11   DO 12 J=K,NI
      TEMP=A(K,J)
      A(K,J)=A(L,J)
12    A(L,J)=TEMP
      TEMP=B(K)
      B(K)=B(L)
      B(L)=TEMP
C     ELIMINATION, BACK SOLUTION, RESULTS.
 10   DO 7 I= KPI,NI
      FACTOR = A(I,K)/A(K,K)
      A(I,K) = 0.0
      DO 13 J=KPI,NI
 13   A(I,J)=A(I,J)-FACTOR*A(K,J)
 7    B(I)=B(I)-FACTOR*B(K)
      C(NI)=B(NI)/A(NI,NI)
      I=NM1
 14   IP1=I+1
      SUM=0.0
      DO 15 J=IP1,NI
 15   SUM=SUM+A(I,J)*C(J)
      C(I) = (B(I)-SUM)/A(I,I)
      I = I-1
      IF(I-0) 21,21,14
 21   DO 22 J=1,NXY
      YY(J)=C(1)
      DO 22 K=2,M+1
      YY(J)=YY(J)+C(K)*X(J)**(K-1)
 22   CONTINUE
```

```
      DO 51 J=1,NXY
51    QR=QR+(Y(J)-YY(J))**2
      KDEGR = ( NXY - 1 )
      DEGR=KDEGR
      VARIN = QR / DEGR
      DO 25 I=1,NXY
      IF ( Y(I)) 251, 252, 251
252   EROR(I) = 0.0
      GOTO 25
251   EROR(I)=(Y(I)-YY(I))/Y(I)
25    CONTINUE
      WRITE(2,104) M
104   FORMAT(1H1,//5X,30HORDER OF PROPOSED POLYNOMIAL =, I3,//6X,
     1       21HPOLYNOMIAL CONSTANTS.,/)
      WRITE(2,105) (I, C(I), I=1,M+1)
105   FORMAT( 10X, 1HC,I2,2H=, F10.4)
      WRITE(2,106) VARIN
106   FORMAT(10X, 10HVARIANCE =, F10.5)
      WRITE(2,107)
107   FORMAT(10X,10HINPUT DATA,5X,8HCALC. Y.,5X,5HERROR,/9X,1HX,9X,
     1       1HY,9X,2HYY,5X,6H1-YY/Y,//)
      WRITE(2,108) (X(I),Y(I),YY(I),EROR(I), I=1,NXY)
108   FORMAT(5X,4F10.4)
      RETURN
      END
```

```
      SUBROUTINE PRELIM ( X1,Y1,N1,N2,C1 )
      COMMON M
      DIMENSION X1(10,50),Y1(10,50),N2(10),C1(10,10),
     1                X(50),Y(50),C(10)
      DO 1 I = 1, N1
      NXY = N2(I)
      DO 2 K = 1, N2(I)
      X(K) = X1(I,K)
      Y(K) = Y1(I,K)
2     CONTINUE
      CALL CURFIT ( X,Y,NXY,M,C )
      DO 1 K = 1, M+1
      C1(I,K) = C(K)
1     CONTINUE
      RETURN
      END


      SUBROUTINE INTER ( K, X,X1,N1,N2,KMAX,C1,Y )
      COMMON M
      DIMENSION X(200),X1(10,50),N2(10),C1(10,10),Y(200)
      X(1) = X1(1,1)
      DO 1 I = 1, N1
      IF ( X(1) - X(K) ) 4,4,5
4     IF ( X(K). GT. X1(I,N2(I))) GOTO 1
      GOTO 3
5     IF ( X(K) - X1(I,N2(I))) 1, 3,3
3     Y(K) = C1(I,1)
      DO 2 J = 2, M+1
      Y(K) = Y(K) + C1(I,J)*X(K)**(J-1)
2     CONTINUE
      I = N1
1     CONTINUE
      RETURN
      END


      SUBROUTINE FRICT (D,DT,I,U,I1,I2,A1 )
      REAL KINVIS
      DIMENSION D(2),DT(2),U(2,41),A1(2,41)
      COMMON M,KINVIS, TRANS
      DO 1 K = I1, I2
      IF (U(I,K)) 3,2,3
2     A = 0.0
      GOTO 4
3     RE = ABS(U(I,K))*D(I)/KINVIS
      IF (RE - TRANS) 5,6,6
5     A = 16.0/RE
      GOTO 4
6     A = 0.079/RE**0.25
4     A1(I,K)= 2.0*A*DT(I)/D(I)
1     CONTINUE
      RETURN
      END
```

```
      SUBROUTINE INTERNAL (INTM,N,I,C,V,P,A1,P1,V1,A1D,VV,PP)
      DIMENSION V(2,41),P(2,41),A1(2,41),V1(2,41),P1(2,41),A1D(2,41),
     1          VV(2,41),PP(2,41),C(2),N(2)
      COMMON M,KINVIS,TRANS,VCHAR,DP,RHO
      Y2 = 1.0/(RHO * C(I))
      IF (INTM - 1) 1,1,2
    1 DO 3 L = 1, N(I)-1
      L1 = L+1
      L2 = L+2
      VV(I,L1) = 0.5*(V(I,L)+V(I,L2)+Y2*(P(I,L)-P(I,L2))-(A1(I,L)*V(I,L)
     1           *ABS(V(I,L))+A1(I,L2)*V(I,L2)*ABS(V(I,L2))))
      PP(I,L1) = 0.5*((P(I,L)+P(I,L2)+(V(I,L)-V(I,L2))/Y2)-(A1(I,L)
     1           *V(I,L)*ABS(V(I,L))-A1(I,L2)*V(I,L2)*ABS(V(I,L2)))/Y2)
    3 CONTINUE
      GOTO 4
    2 DO 5 L = 2, N(I)
      VV(I,L) = 0.5*(V(I,L)+V1(I,L)+Y2*(P(I,L)-P1(I,L))    -(A1(I,L)*
     1       V(I,L)*ABS(V(I,L))+A1D(I,L)*V1(I,L)*ABS(V1(I,L))))
      PP(I,L) =0.5*((P(I,L)+P1(I,L)+ (V(I,L)-V1(I,L))/Y2)-(A1(I,L)*V(I,L
     1       )*ABS(V(I,L))-A1D(I,L)*V1(I,L)*ABS(V1(I,L)))/Y2)
    5 CONTINUE
    4 RETURN
      END
```

```
      SUBROUTINE RESERVOIR (I,INTM,C,V,P,A1,VV,PP)
      DIMENSION C(2),V(2,41),P(2,41),A1(2,41),VV(2,41),PP(2,41) ,N(2)
      COMMON M,KINVIS,TRANS,VCHAR,DP,RHO,PR1,PR2 ,N
      Y2= 1.0/(RHO *C(I))
      IF (I-1) 1,1,2
    1 PP(1,1) = PR1
      IF(INTM - 1) 3,3,4
    3 VV(I,1) = V(I,2)+Y2*(PR1-P(I,2))-A1(I,2)*V(I,2)*ABS(V(I,2))
      GOTO 5
    4 VV(I,1) = V(I,1)+Y2*(PR1-P(I,1)) -A1(I,1)*V(I,1)*ABS(V(I,1))
      GOTO 5
    2 PP(2,(N(I)+1)) = PR2
      IF(INTM - 1) 6,6,7
    6 VV(I,(N(I)+1)) = V(I,N(I))-Y2*(PR2-P(I,N(I)))-A1(I,N(I))*V(I,N(I))
     1                  *ABS(V(I,N(I))    )
      GOTO  5
    7 VV(I,(N(I)+1))= V(I,N(I)+1)-Y2*(PR2-P(I,(N(I)+1)))
     1                 -A1(I,(N(I)+1))*V(I,(N(I)+1))*ABS(V(I,(N(I)+1)) )
    5 RETURN
      END
```

```
      SUBROUTINE VAPOUR (I,N,DT,VAP,P,PP,KZ,PPX,TS )
      DIMENSION P(2,41),PP(2,41),PPX(2,41),TS(2,41),N(2),DT(2)
      KZ = 0
      DO 3 K = 1, N(I)+1
      TS(I,K) = 0.0
      X1 = P(I,K) - VAP
      X = PP(I,K) - VAP
      IF (X) 2,6,4
    2 TS(I,K) = DT(I)*(VAP-PP(I,K))/(P(I,K)-PP(I,K))
      IF (X1) 5,5,3
    5 TS(I,K) = 0.0
    6 PPX(I,K)= VAP
      GOTO 3
    4 KZ = KZ +1
      PPX(I,K) = PP(I,K)
    3 CONTINUE
      RETURN
      END
```

```
      SUBROUTINE SORTER (K,U,I,DT,W,J)
      DIMENSION U(2,41), DT(2)
      J = K + 1
      W = 0.0
      DO 2 IA = 1, K
      IF (U(I,IA).EQ.DT(I))  U(I,IA) = 0.0
      IF (W - U(I,IA)) 3,2,2
    3 J = IA
      W = U(I,IA)
    2 CONTINUE
      RETURN
      END
      FINISH
```

```
      SUBROUTINE FACTOR  (I,J1,J2,J3,J4,J5,X1,X2,X3,X4,Y1,Y2,Y3,Y4,
     1              FACT,   XA,XB,XC,XD )
      DIMENSION X1(2,41),X2(2,41),X3(2,41),X4(2,41),
     1          Y1(2,41),Y2(2,41),Y3(2,41),Y4(2,41),
     2          XA(2,41),XB(2,41),XC(2,41),XD(2,41)
      XA(I,J5) = X1(I,J5) + FACT*(Y1(I,J1)-X1(I,J5))
      XB(I,J5) = X2(I,J5) + FACT*(Y2(I,J2)-X2(I,J5))
      XC(I,J5) = X3(I,J5) + FACT*(Y3(I,J3)-X3(I,J5))
      XD(I,J5) = X4(I,J5) + FACT*(Y4(I,J4)-X4(I,J5))
      RETURN
      END
```

10.6 Appendix 6

The City University Symposium on Pressure Transients
November 25th, 1970

Paper No. 2

PRESSURE TRANSIENT ANALYSIS OF THE B.A.C./S.N.I.A.S. CONCORDE REFUELLING SYSTEM

By: T.J. Doyle, J.A. Swaffield & W.J. Wood

of British Aircraft Corporation

SUMMARY

A pressure transient analysis of the Concorde refuelling system is reported. The theoretical approach is via the method of characteristics applied to solve the partial differential equations defining transient propagation. A computer program written in Fortran IV for use on an IBM 360/50 machine is presented together with representative predicted pressure variations following closure of all tank inlet valves. It is hoped that this program will be a useful tool in the continuing development of the system.

NOTATION

A	Pipe cross sectional area
ACON	% dissolved air released at any pressure
AIRV	Quantity of air released from the fuel during column separation downstream of a valve
ATM	Atmospheric pressure
C1, C2, C3	Constants in relation for inwards relief valve characteristic
c	Wave speed
D	Pipe bore
DP	Pressure drop across a valve in steady state condition
FULV	Quantity of fuel giving up its dissolved air
FK1, FK2	Minor loss coefficients at a pipe junction
f	Steady state friction factor
I, J, K	Pipe identification markers
K	Bunsen solubility coefficient
K1, K2, K3, K4	Constants calculated at each time step from known P, V, and pipe properties ΔT earlier
P	Pressure at a pipe section
PP	Pressure at a pipe section to be calculated at time $T + \Delta T$
Pav	Average pressure at one section over one time step used in air release volume calculation
PR	Pressure at aircraft R.C.U.
QR	Discharge through relief valve
RHO	Fluid density
t, T	Time
V	Mean sectional velocity
V_o	Initial flow velocity
VV	Velocity to be calculated at $T + \Delta T$
V_{CLOS}	Cavity collapse velocity
VOL	Volume of cavity formed upstream of a valve
VOLA	Volume of an air/vapour cavity at time $T + \Delta T$

VOLB	Volume of an air/vapour cavity at time T
x	Distance measured along the pipeline in the direction of initial flow
ρ	Fluid density
τ	Valve discharge coefficient
Δx	Length of a pipe section within a pipelength
Δt	Time step
ΔP	Pressure differential across the relief valve

INTRODUCTION

The possible occurrence of pressure transients in a piping network following any change in the steady state boundary conditions has been recognised for many years as a major design criterion. In the past the most common cases related to large scale water distribution systems and hydro-electric schemes and it is in these fields that much of the pioneer work on the subject is to be found.

Recently the application of computing techniques (1, 2, 3) to pressure transient analysis has enabled a much wider range of problems to be dealt with, particularly small scale systems which would be too complex for an accurate application of the more traditional graphical methods (4, 5).

Similarly the vast majority of the work reported relates to water as the working fluid. It is the purpose of this paper to report the application of computing techniques to predict pressure transient phenomena in the B.A.C./ SNIAS Production Concorde refuelling system. This system contains a large number of tanks and inter connecting pipelines in a relatively small area, the working fluid being Aviation Kerosene Spec. 2494.

The reasons for the propagation of possibly destructive transients together with a full description of the system, the mathematical models employed and a flow diagram for the computer program are presented. It will be noted that the system has a relatively low operating head so that column separation is a distinct possibility and recent work on column separation by one of the present authors is heavily drawn on (6, 7, 8).

DESCRIPTION OF REFUELLING SYSTEM

The Concorde is refuelled by use of a composite Fuel Sub-system which is used also as a means of adjusting the aircraft C of G (Trim Transfer) and discharging fuel overboard (Jettison). The sub-system is in two halves, right and left hand, the main feature of each half being a 2½/3"bore pipe which runs between the front and rear trim tanks. This pipe is known as the main trim transfer pipe. The layout of the system is shown in Figure 1.

To form the refuelling installation each main trim transfer pipe is connected to a Refuelling Control Unit, through which the external refuelling supply is delivered to the aircraft and thence to fuel tanks via valve-controlled branch pipes of 1" to 2" diameter.

Fuel, from either bowser or hydrant supply, is delivered to each Refuelling Control Unit through two flexible 2½" hoses, hose end pressure controllers maintaining a constant 50 p.s.i.g. at the aircraft inlets.

Each Refuelling Control Unit contains a valve which shuts off the flow under certain failure conditions. Correct fuel distribution is obtained by the use of an appropriately sized restrictor in each refuelling branch pipe so that nominally all tanks become full at the same time. The refuel valves in each branch pipe are electrically operated open or shut spherical plug type, controlled by tank level and/or quantity sensors.

An inward (tank to pipe) relief valve is sited in each main trim transfer pipe adjacent to the R.C.U. This is to alleviate the separation effect which may occur when the Refuelling Control Unit is closed, following a failure, under full flow conditions.

The left hand side refuels 7 tanks and the right hand 6 tanks. The asymmetry is due to the inclusion of some fuselage cells.

Typical flow rates are 40 to 400 igpm in the main pipes and 40 to 200 igpm in the branch pipes.

Velocities vary from 3 to 30 ft/s in the main pipes and 5 to 70 ft/s. in the branch pipes.

The length of each main trim transfer pipe is approximately 100 ft. and the branch pipes are up to 10 ft. long.

Most of the piping is Aluminium Alloy but some use is made of Stainless Steel. A typical pipe wall thickness is 0.8 mm.

Design Criteria

Consistent with a short "turn-around" time the refuelling of the aircraft will take approximately 20 minutes. Hence the fuel flow rates and velocities already mentioned.

With an obvious need for pipes to weigh as little as possible and yet fulfill stringent airworthiness and maintainability requirements, the surge pressures that may be imposed on the fuel system form important design criteria.

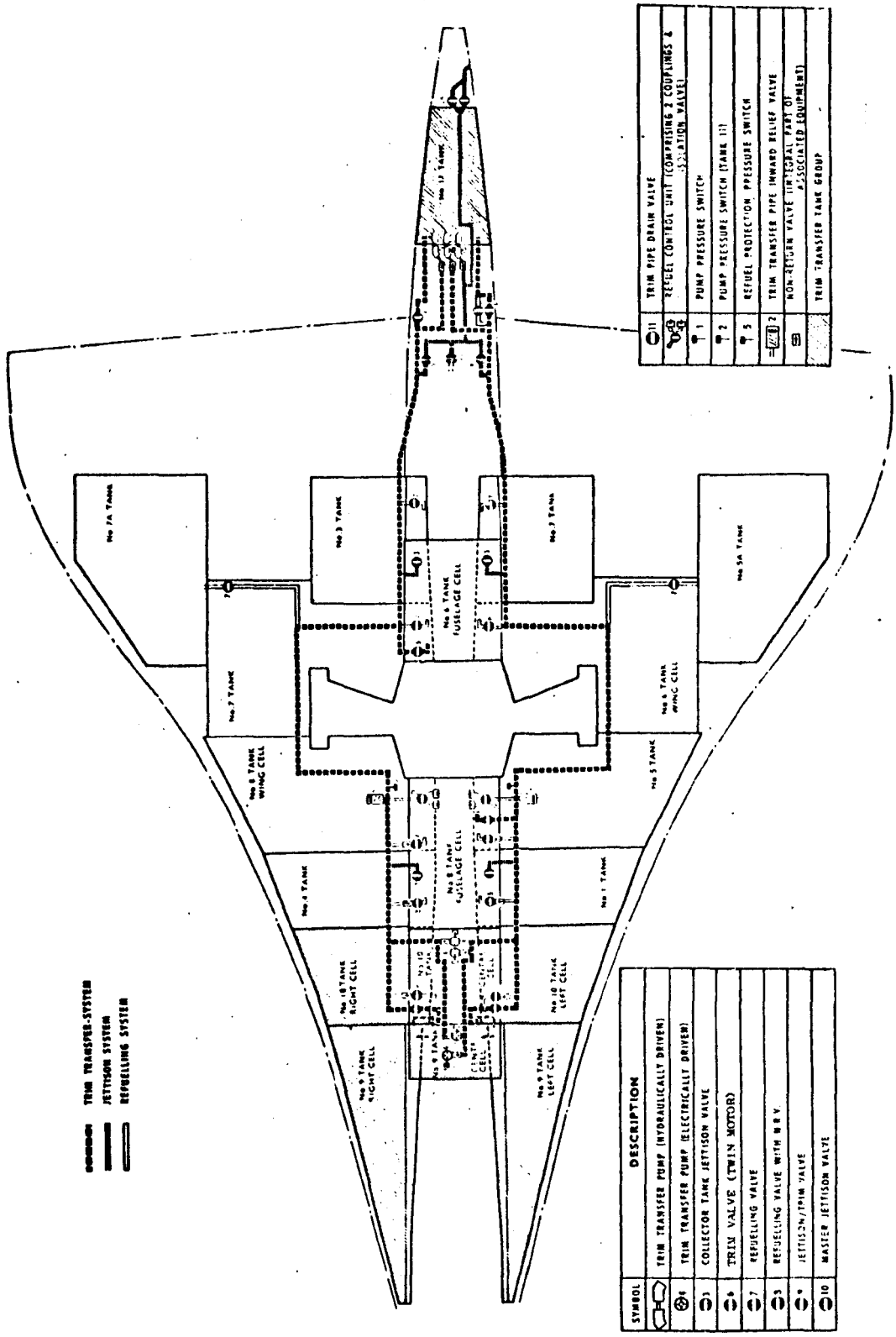

Fig. 1 CONCORDE REFUELLING SYSTEM

Fuel tank shut-off levels have to be controlled accurately over a wide range of possible conditions, e.g. normal or single tank refuelling, fuel uplift temperatures from -30°C to +45°C, aircraft busbar voltage variation, etc. Consequently, it is necessary for tank inlet valves to shut in as short a time as possible consistent with the control of surge pressures.

If certain failures occur during refuelling (e.g. loss of electric power) it is imperative that flow into the aircraft shall cease. Again this must be achieved in as short a time as possible consistent with the control of surge pressures.

Development Problems

In order to achieve an optimum time of closure the valve manufacturers are required to demonstrate, during development, that valve closure produces a surge pressure that is within the piping limitations. This is done with the valve(s) mounted in a pipe of representative length proportions and material , and the maximum design rate of flow applied. At the same time measurement is made of the amount of fuel passed through the valve after initiation of closure.

Complete fuel system testing is carried out on a special full size Total Fuel System Rig (T.F.S.R.) which is used to verify designed performance and to detect any unusual conditions. For example, testing on the Prototype standard T.F.S.R. revealed that closing of the Refuelling Control Unit resulted in a high transient pressure being recorded in the main trim transfer pipe. After consultation it was realised that this was due to a"separation effect" adjacent to the Refuelling Control Unit. Subsequent testing with an inwards relief valve showed that this alleviated the problem.

Program Objectives

In the past remedial design action has been taken following further testing on a system rig. However this is an expensive and time consuming process. An alternative approach would be to employ a computerised model of the aircraft system to highlight possible problems in advance of the rig test program, investigating fully the effects of various possible design actions which could later be verified on the test rig.

As this is a relatively new application of the techniques described in this paper it is important at this stage to obtain a confidence level for the calculations from parallel rig and computer results.

Program Capabilities

The following cases are considered in the initial computer program :-

(a) Normal refuelling

- all reasonable sequences of refuelling valves closure.
- abnormal sequence of all refuelling valves closing simultaneously.

(b) Single tank refuelling - each refuelling valve closing under individual refuelling conditions.

(c) Refuel Control Unit closure - under conditions varying from minimum to maximum flow.

Various inputs such as valve closing characteristics can be changed to investigate their effects.

THEORY

Derivation of basic equations

Transient pressure phenomena are commonly described by a one dimensional model with time, t, and distance, x, as independent variables and pressure, P, and mean sectional velocity, V, as dependent variables. By applying momentum and continuity principles to an untapered section, Δx, of a pipeline the equations governing transient propagation may be derived.

Equation of motion: $$\frac{\partial P}{\partial x} + \rho \left(\frac{\partial V}{\partial t} + V \frac{\partial V}{\partial x}\right) + 2\rho f \frac{V|V|}{D} = 0 \qquad (1)$$

Continuity of equation: $$\frac{\partial P}{\partial t} + V \frac{\partial P}{\partial x} + \rho c^2 \frac{\partial V}{\partial x} = 0 \qquad (2)$$

These equations are a pair of quasi-linear hyperbolic partial differential equations which may be transformed into a pair of total differential equations whose validity is restricted to certain lines in an x-t plane known as characteristics. The necessary mathematical procedures have been fully reported elsewhere (9, 10) and lead to the following equations:

$$\frac{dV}{dt} \pm \frac{1}{c} \frac{dP}{dt} + 2f \frac{V|V|}{D} = 0 \qquad (3)$$

valid along $$\frac{dx}{dt} = V \pm c \qquad (4)$$

In most practical cases $V << c$ so that the above relation may be reduced to

$$\frac{dx}{dt} = \pm c \qquad (5)$$

which corresponds to neglecting the non-linear convective terms $V\partial V/\partial x$ and $V\,\partial P/\partial x$ in equations (1, 2).

Application of a first order finite difference approximation to equations (3, 5) yields the following relationships, referring to Fig. 2 below.

$$V_P = V_A \left(1 - 2f \frac{V_A|V_A|\Delta T}{D}\right) + \frac{1}{\rho c} (P_A - P_P) \qquad (6)$$

$$V_P = V_B \left(1 - 2f \frac{V_B|V_B|\Delta T}{D}\right) - \frac{1}{\rho c} (P_B - P_P) \qquad (7)$$

$$x_p - x_A = c\,(t_p - t_A) \qquad (8)$$

$$x_p - x_B = -\,c\,(t_p - t_B) \qquad (9)$$

where all necessary values at A and B are known.

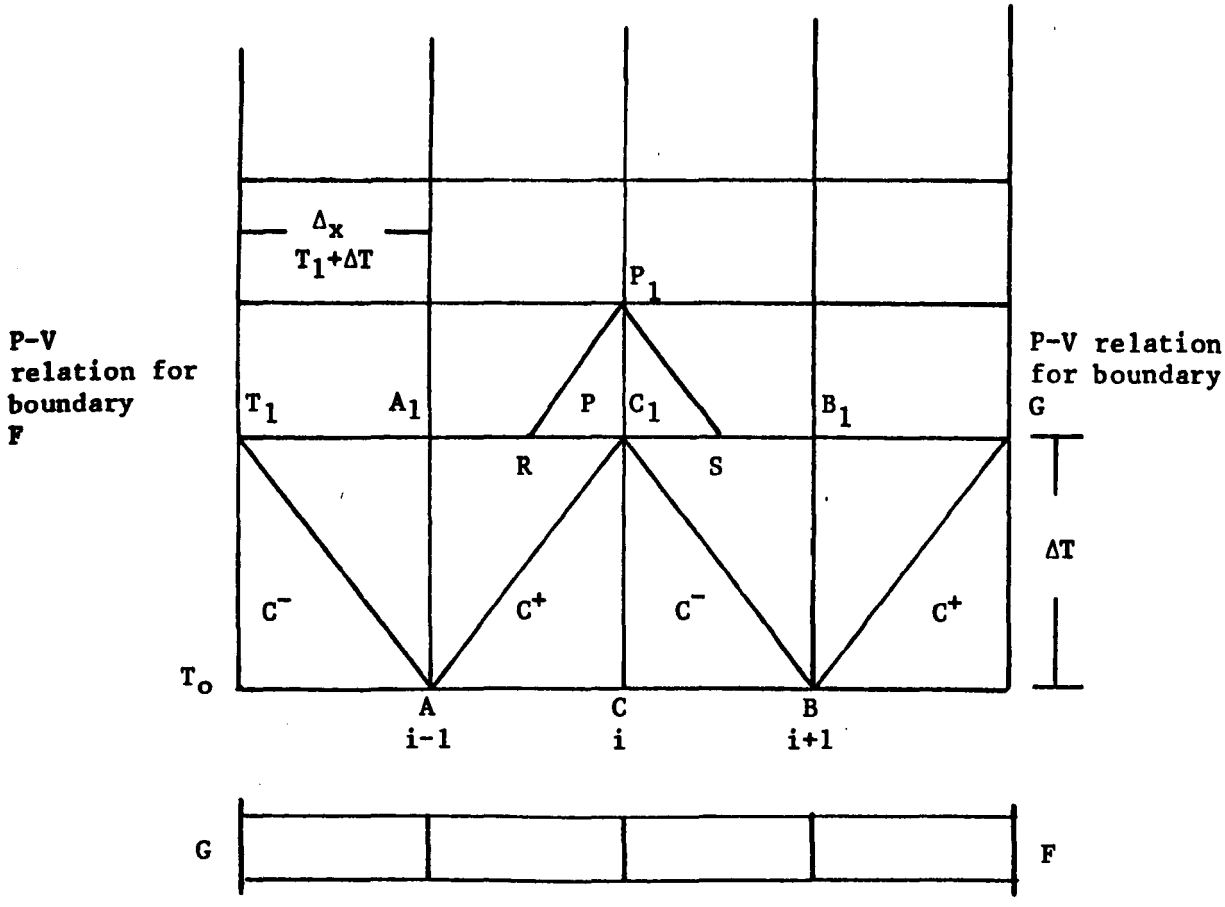

Fig. 2 Development of the solution in the (x,t) plane

Equations (6) and (7) are referred to as the C^+ and C^- equations between points (i) and (i $\pm$ 1) and may be expressed in the form

$$V_P = K1 - K2\ P_P \qquad (8)$$

$$V_P = K_3 + K4\ P_P \qquad (9)$$

which will be used for the remainder of this paper.

Values of V and P at all internal points along the pipeline may be calculated directly from equations (6) and (7). The conditions at the boundaries of the pipe may be similarly calculated from the appropriate characteristic (C^+ at G, C^- at F) and a P-V linking boundary equation, e.g. a valve discharge coefficient relation or for a junction of two or more pipelines the continuity of pressure and flow equations.

The friction factor, f, included in the above equations is assumed to be the steady state friction factor calculated at each section from the usual Reynolds Number expressions.

Choice of time step

In order to maintain a stable solution the value of ΔT must obey the relation

$$\Delta T \leqslant \Delta x/c \qquad (10)$$

If $\Delta T = \Delta x/c$ then the conditions at P at time $T_o + \Delta T$ can be calculated from the known values of pressure and velocity at sections A, B at time T_o. Similarly if $\Delta T < \Delta x/c$ the conditions at P_1 at time $T_1 + \Delta T$ can be calculated from known values at R, S at time T_1. The values of pressure and velocity at R, S can be found by interpolating between A_1C_1, $C_1 B_1$.

In a multiple pipe network the time step employed must satisfy the relation

$$\Delta T < \Delta x_{(i)}/c_{(i)} \qquad (11)$$

where suffix (i) refers to each pipe in the system. Generally as the value of wave speed is likely to vary through a piping network it follows that the value of ΔT is dictated by the fastest wave speed in the shortest pipe.

Similarly as it is necessary for each pipe to have an integer number of sections slight adjustments in pipe length are required, although these can be minimised if the acceptable time step is very small. Figures 3 and 4 and Tables 1 and 2 illustrate this procedure.

Allocation of base conditions for each time step

Referring to Fig. 2 it will be seen that each time step uses the results of the previous set of calculations as a base condition. In order to conserve storage space it is common practice to overwrite the base arrays P, V at time T with the values of PP and VV calculated for time $T + \Delta T$ to allow the solution to advance to $T + 2\Delta T$ etc.

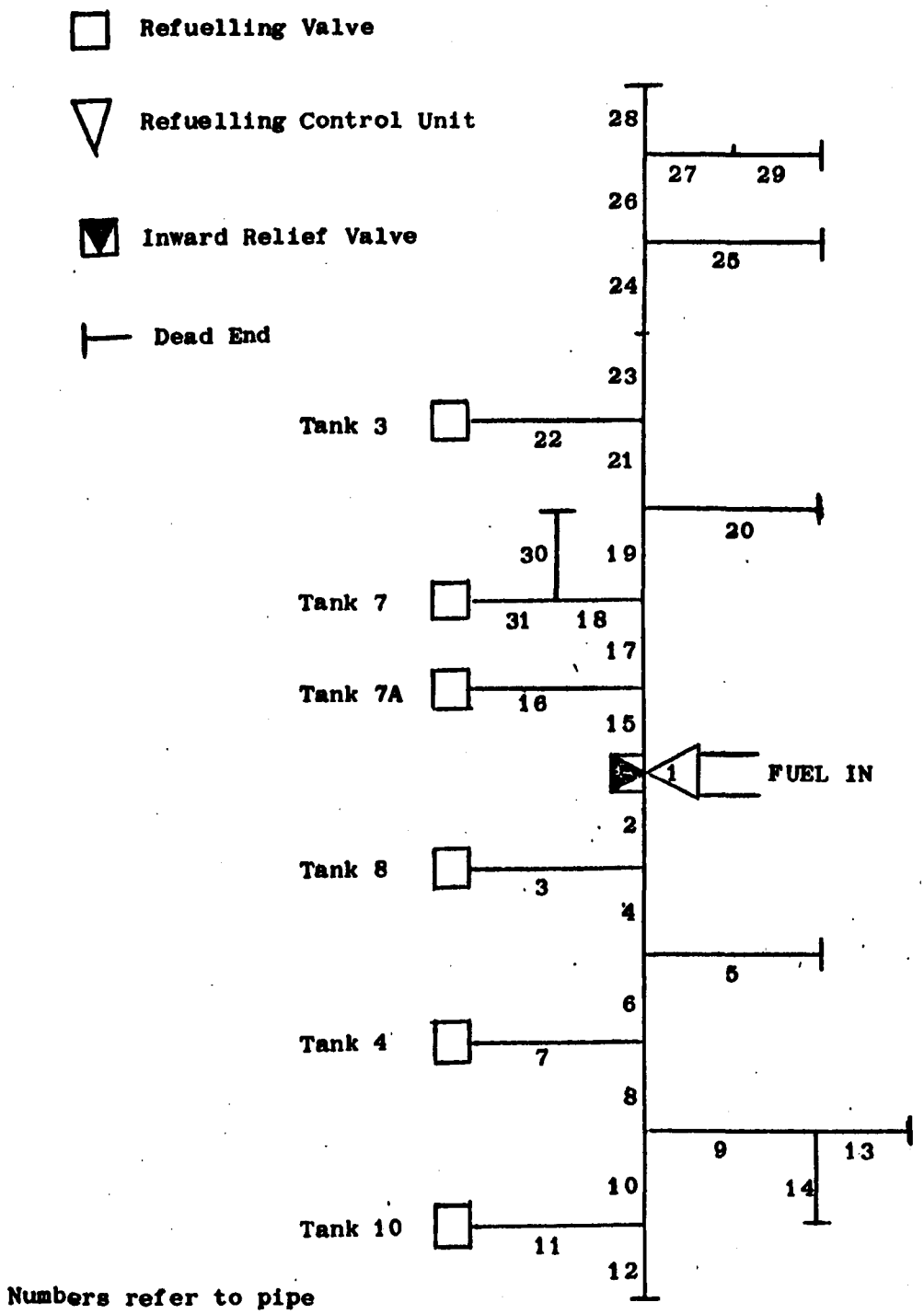

Fig. 3 - SCHEMATIC REFUELLING SYSTEM - RIGHT HAND

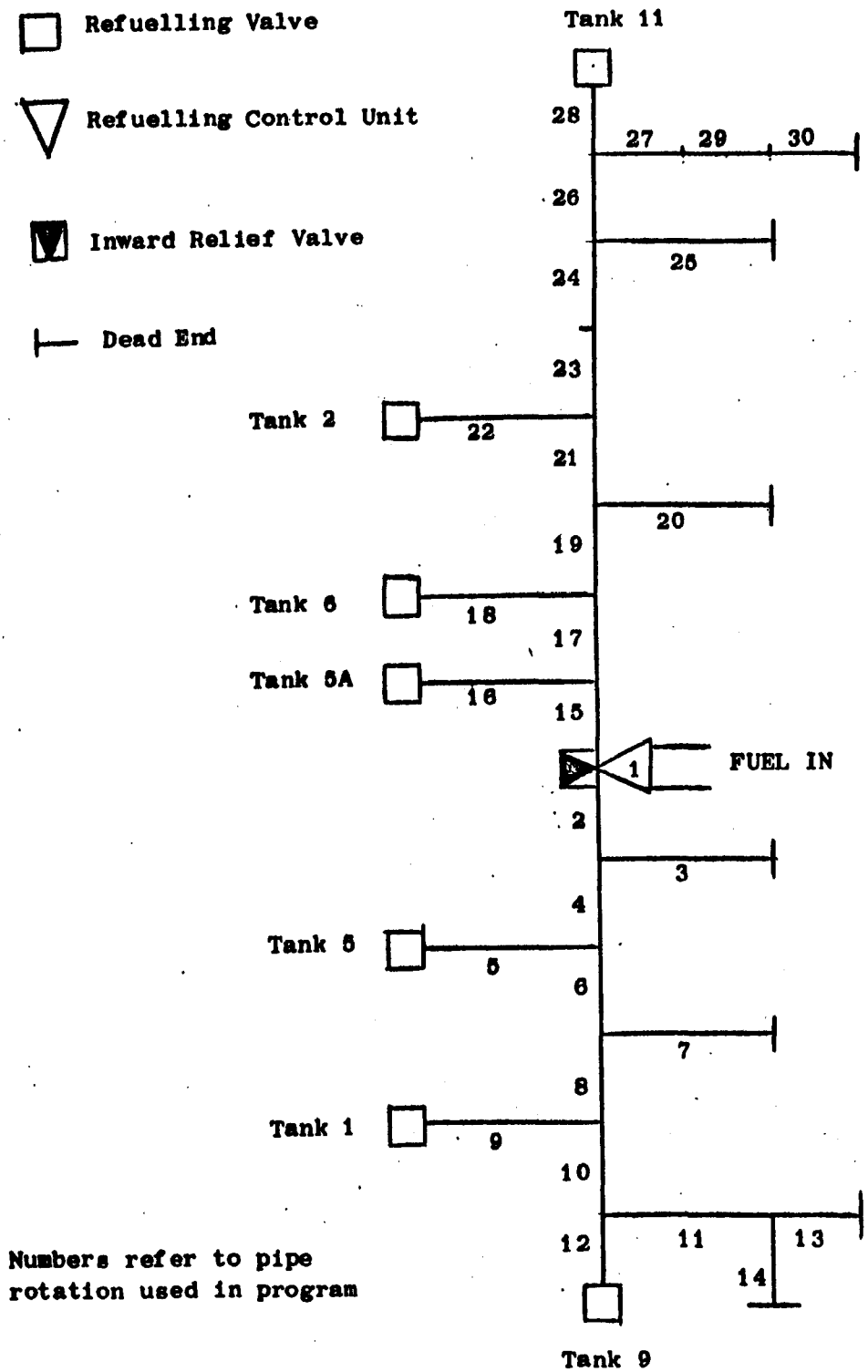

Fig. 4 - SCHEMATIC REFUELLING SYSTEM - LEFT HAND

Pipe Number	Bore ft.	Flow $ft^3/s.$	Length ft. Actual	Length ft. Assumed	No. of sections.	Wave speed ft/s.
1	0.26	1.975	0.5	0.0000	NIL	ZERO
2	0.20	0.940	1.50	2.8498	1	2600
3	0.16	ZERO	1.00	2.9597	1	2700
4	0.20	0.940	2.00	2.8498	1	2600
5	0.16	0.328	0.75	2.9597	1	2700
6	0.20	0.612	2.40	2.8498	1	2600
7	0.16	ZERO	1.00	2.9597	1	2700
8	0.20	0.612	3.60	2.8498	1	2600
9	0.16	0.100	0.75	2.9597	1	2700
10	0.20	0.512	2.50	2.8498	1	2600
11	0.20	ZERO	3.00	2.8498	1	2600
12	0.20	0.512	5.50	5.6996	2	2600
13	0.20	ZERO	11.50	11.3992	4	2600
14	0.20	ZERO	2.25	2.8498	1	2600
15	0.20	1.035	25.00	25.6483	9	2600
16	0.08	0.097	9.50	9.6990	3	2950
17	0.20	0.938	9.00	8.5494	3	2600
18	0.16	0.534	3.00	2.9597	1	2700
19	0.20	0.404	6.00	5.6996	2	2600
20	0.16	ZERO	1.00	2.9597	1	2700
21	0.25	0.404	5.00	5.5897	2	2550
22	0.08	0.114	0.75	3.2330	1	2950
23	0.25	0.290	10.00	8.3845	3	2550
24	0.25	0.290	5.00	3.6166	1	3300
25	0.25	ZERO	1.25	3.9463	1	3600
26	0.20	0.290	1.23	4.0000	1	3650
27	0.12	ZERO	1.00	3.9463	1	3600
28	0.25	0.290	1.25	3.6166	1	3300
29	0.20	ZERO	4.50	3.3979	1	3100
30	0.20	ZERO	3.00	2.9597	1	2700

Table 1 - LEFT HAND SYSTEM

Pipe Number	Bore ft.	Flow $ft^3/s.$	Length ft.		No. of sections	Wave speed ft/s.
			Actual	Assumed		
1	0.26	1.777	0.50	0.0000	NIL	ZERO
2	0.20	1.222	1.50	2.8893	1	2600
3	0.16	0.588	1.00	3.0000	1	2700
4	0.20	0.634	3.50	2.8893	1	2600
5	0.16	ZERO	1.00	3.0000	1	2700
6	0.20	0.634	3.60	2.8893	1	2600
7	0.16	0.100	1.00	3.0000	1	2700
8	0.20	0.534	2.40	2.8893	1	2600
9	0.20	ZERO	3.00	2.8893	1	2600
10	0.20	0.534	5.40	5.7787	2	2600
11	0.16	0.534	1.00	3.0000	1	2700
12	0.20	ZERO	7.30	8.6680	3	2600
13	0.20	ZERO	8.00	8.6680	3	2600
14	0.20	ZERO	3.00	2.8893	1	2600
15	0.20	0.555	25.00	26.0040	9	2600
16	0.08	0.097	9.50	9.8328	3	2950
17	0.20	0.458	9.00	8.6680	3	2600
18	0.16	0.344	3.00	3.0000	1	2700
19	0.20	0.114	6.00	5.7787	2	2600
20	0.16	ZERO	1.00	3.0000	1	2700
21	0.25	0.114	5.00	5.6673	2	2550
22	0.08	0.114	0.75	3.2776	1	2950
23	0.25	ZERO	10.00	11.3346	4	2550
24	0.25	ZERO	5.00	3.6670	1	3300
25	0.16	ZERO	2.00	3.0000	1	2700
26	0.25	ZERO	1.50	4.0000	1	3600
27	0.20	ZERO	5.40	6.8894	2	3100
28	0.25	ZERO	0.50	4.0000	1	3600
29	0.20	ZERO	3.00	3.0000	1	2700
30	0.16	ZERO	2.00	3.0000	1	2700
31	0.12	0.344	1.00	2.9446	1	2650

Table 2 - RIGHT HAND SYSTEM

Application of the method of characteristics to the Concorde refuelling system

The major advantage of the method of characteristics is that boundary conditions can be dealt with in isolation enabling, by an efficient use of subroutines, the same procedures to be used for a range of different piping configurations.

Apart from the internal pipeline sections the necessary calculations for the Concorde refuelling system involve the following boundary conditions:

(1) Closure of tank valves and possible column separation in the upstream pipeline (6).

(2) Closure of the Refuelling Control Unit under failure conditions involving the possibility of column separation in the downstream pipeline (8) and the operation of an inwards relief valve.

(3) Series (2 pipe) and branch (3 pipe) junctions.

(4) Tank valves left open or fully shut during refuelling, these tank inlets possibly fitted with non-return valves.

(5) Dead ended branch pipes. The possibility of upstream column separation to be allowed for in cases (4) and (5).

Refuelling Control Unit

Two assumptions were made with regard to the R.C.U.

(1) The supply to the aircraft is assumed to be represented by a constant pressure source located upstream of the R.C.U. (11).

(2) The R.C.U. is assumed to be mounted directly onto the main trim transfer pipe opposite the inwards relief valve.

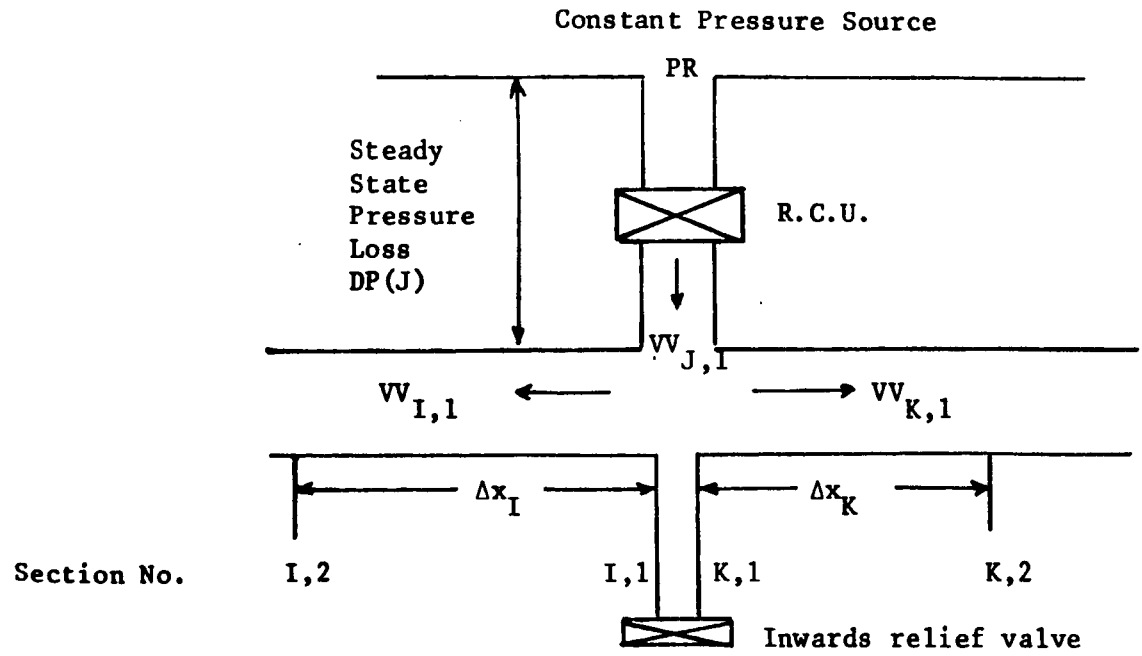

Fig. 5 Layout of R.C.U. and main trim transfer pipeline

The available boundary equations at the above junction, in the absence of column separation are:

Valve discharge coefficient:

$$PP(J,1) = PR - \frac{DP(J)}{(\tau\, V_o(J))^2}\, VV(J,1)|VV(J,1)| \qquad (12)$$

Flow and pressure continuity at the junction:

$$VV(J,1)A(J) = VV(K,1)A(K) + VV(I,1)A(I) \qquad (13)$$

$$PP(J,1) = PP(K,1) = PP(I,1) \qquad (14)$$

These four equations may be solved with the two C^- characteristics drawn between points (K,1) and (K,2) and (I,2).

Solution yields a quadratic equation solvable for VV(J,1) in terms of known pressure and velocity values one time step earlier, pipeline characteristics such as wave speed, and the discharge coefficient (τ) for the valve. If the R.C.U. is open throughout the solution the value of τ is held at 1.0. If the flow reverses through the inlet pipe the R.C.U. acts at a non return valve and the expression VV(J,1) = 0 replaces equation (12).

Column separation downstream of the closing R.C.U.

If column separation occurs downstream of the R.C.U. during closure then the flow continuity equation (13) above must be replaced by a relation governing the pressure within the forming cavity. It has been found (8) that air release from the kerosene cannot be ignored and it is reasonable to consider that the column separates, due to air release, at atmospheric pressure (7).

The necessary equation is:

$$PP(K,1) = VAP + \frac{AIRV}{VOLA} \cdot ATM \qquad (15)$$

where AIRV is the quantity of released air at N.T.P. and VOLA is the cavity volume.

The cavity volume is calculated from

$$VOLA = VOLB + \tfrac{1}{2}\Delta T(A(K)(VV(K,1) + V(K,1)) + A(I)(VV(I,1) + V(I,1)) -$$

$$A(J)(VV(J,1) + V(J,1))) \qquad (16)$$

at time T where VOLB is its volume at T - ΔT. The values of the interface velocities VV(K,1), VV(I,1) can be calculated directly from the two C^- characteristics previously mentioned once PP(J,1) is known.

The quantity of air released up to time T at any pressure below atmosphere is calculated from

$$AIRV_T = FULV \times ACON \qquad (17)$$

where FULV is the quantity of fuel giving up its dissolved air and is assumed to be that volume of fuel passing through the valve between the instant of column separation and the time T. ACON is the % of dissolved

air released at any pressure calculated from Henry's Law and the Bunsen Solubility Coefficient i.e.:-

$$ACON = ((ATM - P_{av})\ K/ATM \qquad (18)$$

where P_{av} is the average pressure across one time step.

The value of FULV can be calculated from an equation similar to (16):

$$FULV_T = FULV_{T-\Delta T} + \tfrac{1}{2}\Delta T\ A(J)(VV(J,1) + V(J,1)) \qquad (19)$$

Solution of equations 12, 14, 15 together with the two C^- characteristics between (K,1) and (K,2) and (I,2) yields a pair of equations in PP(J,1), VV(J,1) which can be solved by an iterative process.

Inwards Relief Valve

In the event of column separation following the closure of the main inlet valve an inwards relief valve passes fuel from an adjacent tank into the main transfer pipe. The action of this valve is assumed instantaneous and the quantity of fuel passed is assumed to be given by the valve's steady state discharge coefficient.

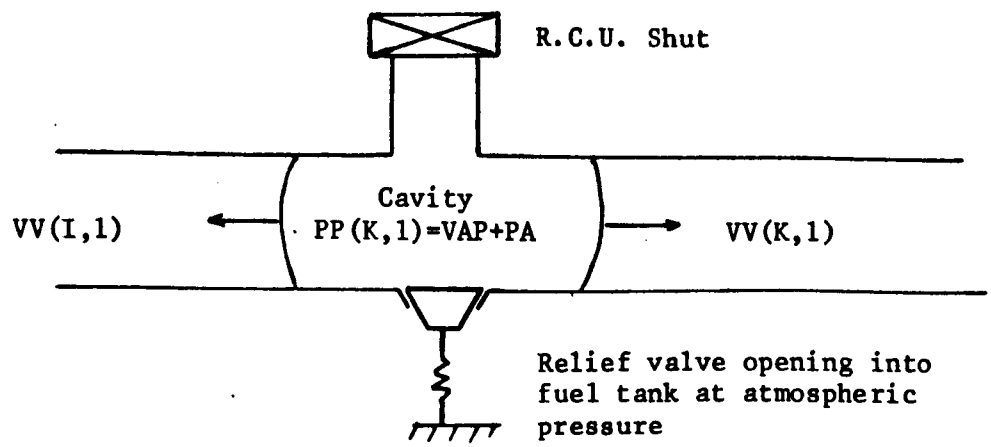

Fig. 6 Layout of Relief Valve

The discharge through the relief valve is assumed to be of the form:

$$Q_R = C_1 + C_2\ \Delta P + C_3\ \Delta P^2$$

During the growth of the cavity, i.e. pressure PP(K,1) falling, it will be assumed that the volume of fuel FULV mentioned above continues to give up its dissolved air in accordance with Henry's Law. If the pressure drops sufficiently to open the relief valve then the fuel passing into the area of the cavity will also be assumed to give up its dissolved air. As the cavity collapses, but with the relief valve still open, the fuel passing into the pipe will be assumed to release its air but none of the previously released air will be allowed back into solution. Recent high speed filming

(7) of cavity formation in kerosene pipelines support this assumption. Following the closure of the relief valve the released air will be assumed to remain out of solution and form the boundary condition at this location.

It is necessary to calculate the cavity interface velocities VV(I,1), VV(K,1) and the cavity pressure PP(K,1). The available equations are the two C^- curves for pipes I and K referred to previously together with equation (15).

The value of AIRV can be calculated from

$$AIRV = (FULV + QR.DT)ACON \qquad (20)$$

The volume of the cavity may be calculated as:

$$VOLA = VOLB + \frac{DT}{2}(A(K)(VV(K,1) + V(K,1)) + A(I)(VV(I,1) + V(I,1))) - Q_R\,DT \qquad (21)$$

Series and Branch Junctions

The values of pressure and velocity at a pipeline junction can be calculated from the appropriate flow continuity and pressure continuity equations solved with the C^+ and C^- characteristic equations joining the junction conditions at time T to the adjacent pipe section conditions at T - ΔT.

Tank Inlet Valves

Generally during valve operation only two equations are necessary, the valve discharge coefficient relation and the C^+ characteristic joining section (J, N(J)) at time T - ΔT to (J, N(J) + 1) at T.

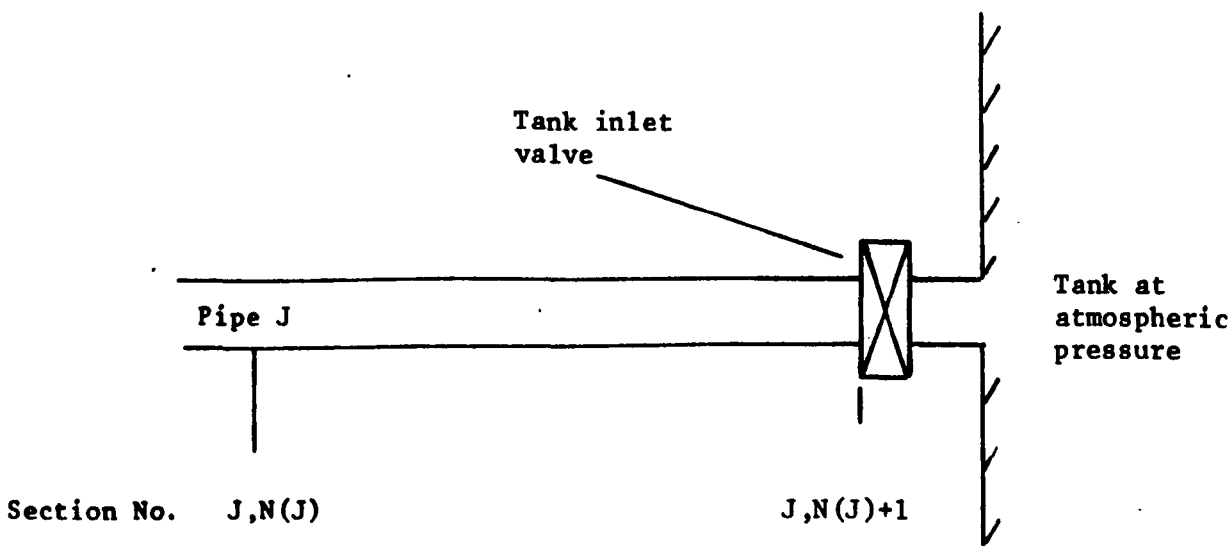

Fig. 7 Tank Inlet Valves

The available equations are:

$$VV(J,N(J)+1) = \tau\, V_o(J) \sqrt{\frac{PP(J,N(J)+1) - ATM}{DP(J)}} \qquad (22)$$

where DP(J) is the pressure drop across the fully open valve at an initial flow velocity $V_o(J)$,

and

$$VV(J,N(J)+1) = K1(J) - K2(J)PP(J,N(J)+1) \qquad (23)$$

Substitution yields a quadratic solvable for VV(J,N(J) + 1).

A number of separate operating conditions were considered and these are outlined below:

(1) Valve closing:

Solution of (22), (23) above together with the values of τ as the valve closes.

(2) Valve open, no non-return valve fitted:

Solution of (22), (23) with $\tau = 1.0$.

(3) Valve open, fitted with a non-return valve:

The non-return valve is assumed to act instantaneously so that if the flow reverses through the tank inlet the valve is considered shut and the no-flow boundary equation (24) solved with the characteristic (23)

$$VV(J,N(J)+1) = 0.0 \qquad (24)$$

(4) Valve closed or dead ended branch:

The no-flow boundary equation (24) is again solved with the appropriate C^+ characteristic equation.

(5) Column separation upstream of a closed valve or in a dead ended branch:

If the pressure at the closed valve falls to the liquid vapour pressure then equation (24) is replaced by a pressure boundary relation:

$$PP(J,N(J)+1) = VAP \qquad (25)$$

which may be solved with the C^+ characteristics (23) to give the cavity interface velocity. The growth of the cavity may be monitored and the pressure on its collapse calculated from

$$PP(J,N(J)+1) = VAP + \rho c\, V_{CLOS} \qquad (26)$$

where V_{CLOS} is the final interface velocity before cavity collapse. The no-flow boundary equation can then be re-employed.

If column separation occurs upstream of a closed non-return valve then the collapse of the cavity is assumed to open the valve and the applicable boundary equation is equation (22) with $\tau = 1.0$.

Valve discharge characteristics

In the above approach it has been assumed that a relation of the form

$$\tau = f(\text{time})$$

was known. Normally τ is known in terms of valve open angle or area ratio, which in turn can be monitored against time during closure. This results in two sets of curves,

$$\tau = f(\text{angle}),$$

$$\text{angle} = f(\text{time}).$$

These may be cross plotted and values of τ interpolated for each time step.

Concorde Refuelling Computer Programs

Two programs have been written, the first calculates the pressure transients in the system and outputs the pressures to the line printer and to a temporary file, the second reads this file and plots the pressure variations against time for each tank inlet.

Both programs have been written in FORTRAN IV and have been tested on an IBM System/360 Model 50 Computer with an offline Calcomp X-Y digital plotter. The larger program requires 40,000 words (160,000 bytes), plus buffer space, for execution.

A flow diagram for the pressure transient program is set out below.

FLOW DIAGRAM FOR CONCORDE REFUELLING PROGRAM

Begin

↓

Assign steady state values for VOL(I), VOL1(I), FULV, AIRV, ACON

↓

Read data: order of polynomials to be fitted to valve characteristics,
number of fuel tanks,
pressure of constant source,
pressure loss through refuelling control unit.

↓

For each tank valve input :-
parameter to define valve state (e.g. always open, closing, etc.),
parameter to define existence of non-return valve,
pressure discharge coefficients/valve angle coordinates
valve angle/closure time coordinates

↓

For each tank valve call PRELIM and CURFIT to fit required polynomials to the above coordinates.

↓

Input relief valve characteristics in terms of gall/min versus pressure differential

↓

Input vapour pressure of fuel, density, air solubility, maximum computing time, kinematic viscosity of the fuel, number of pipes, interpolation factor for separation.

↓

For each pipe in the system input:-

pipe length,
fuel velocity,
pipe diameter,
wave speed,
number of sections,
pressure losses due to bends and couplings in the pipe

↓

Calculate the time step $\Delta t = \frac{\Delta x_L}{C_L}$

↓

Working downstream from the main inlet call LOSS for each pipe to obtain the steady-state values of velocity (VV) and pressure (PP) at each section.

↓

Transfer values in VV, PP arrays into V, P arrays as base conditions for calculation at the next time step.

↓

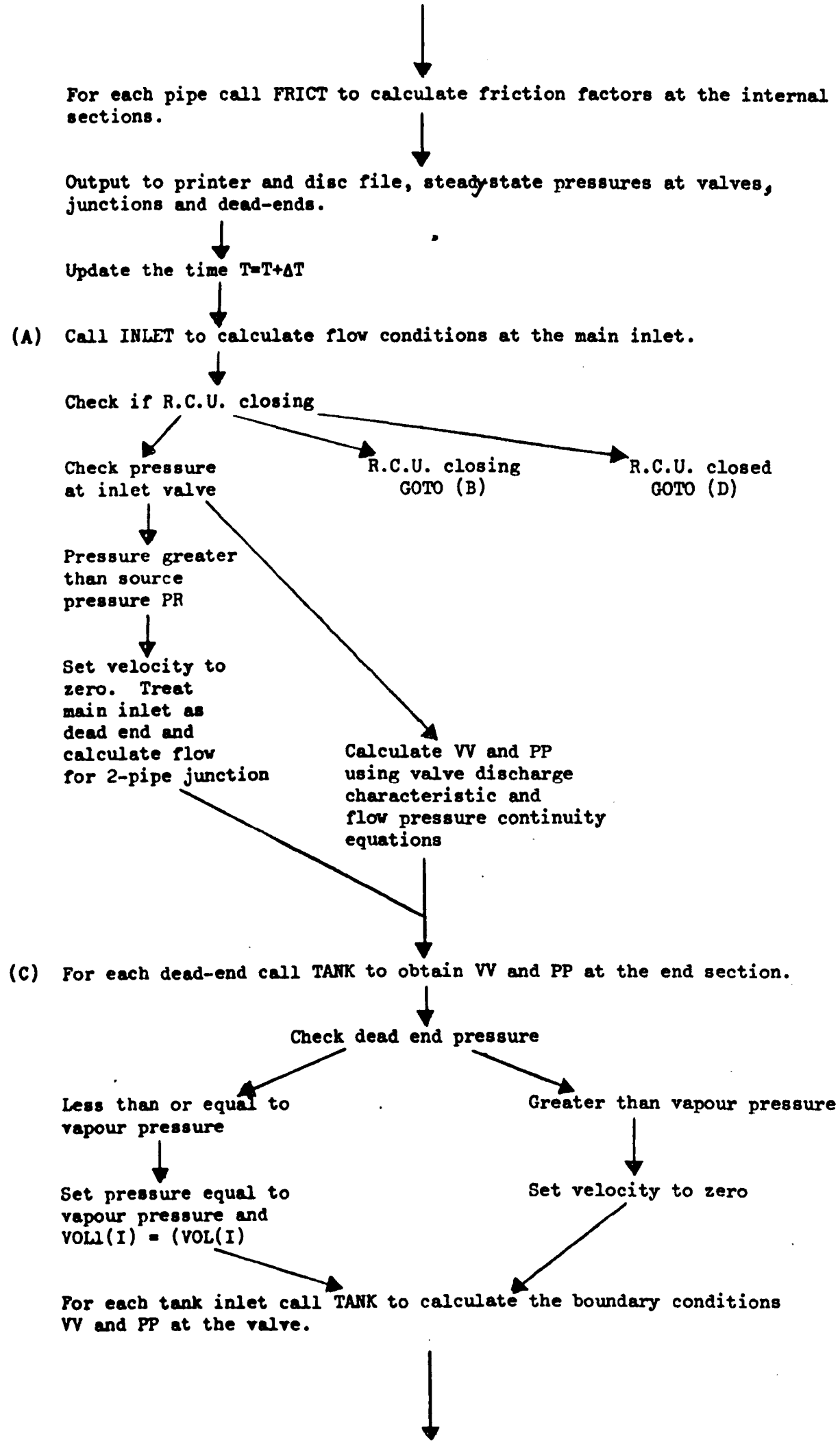
For each pipe call FRICT to calculate friction factors at the internal sections.
Output to printer and disc file, steady-state pressures at valves, junctions and dead-ends.
Update the time T=T+ΔT
(A) Call INLET to calculate flow conditions at the main inlet.
Check if R.C.U. closing
Check pressure at inlet valve
R.C.U. closing GOTO (B)
R.C.U. closed GOTO (D)
Pressure greater than source pressure PR
Set velocity to zero. Treat main inlet as dead end and calculate flow for 2-pipe junction
Calculate VV and PP using valve discharge characteristic and flow pressure continuity equations
(C) For each dead-end call TANK to obtain VV and PP at the end section.
Check dead end pressure
Less than or equal to vapour pressure
Greater than vapour pressure
Set pressure equal to vapour pressure and VOL1(I) = (VOL(I)
Set velocity to zero
For each tank inlet call TANK to calculate the boundary conditions VV and PP at the valve.

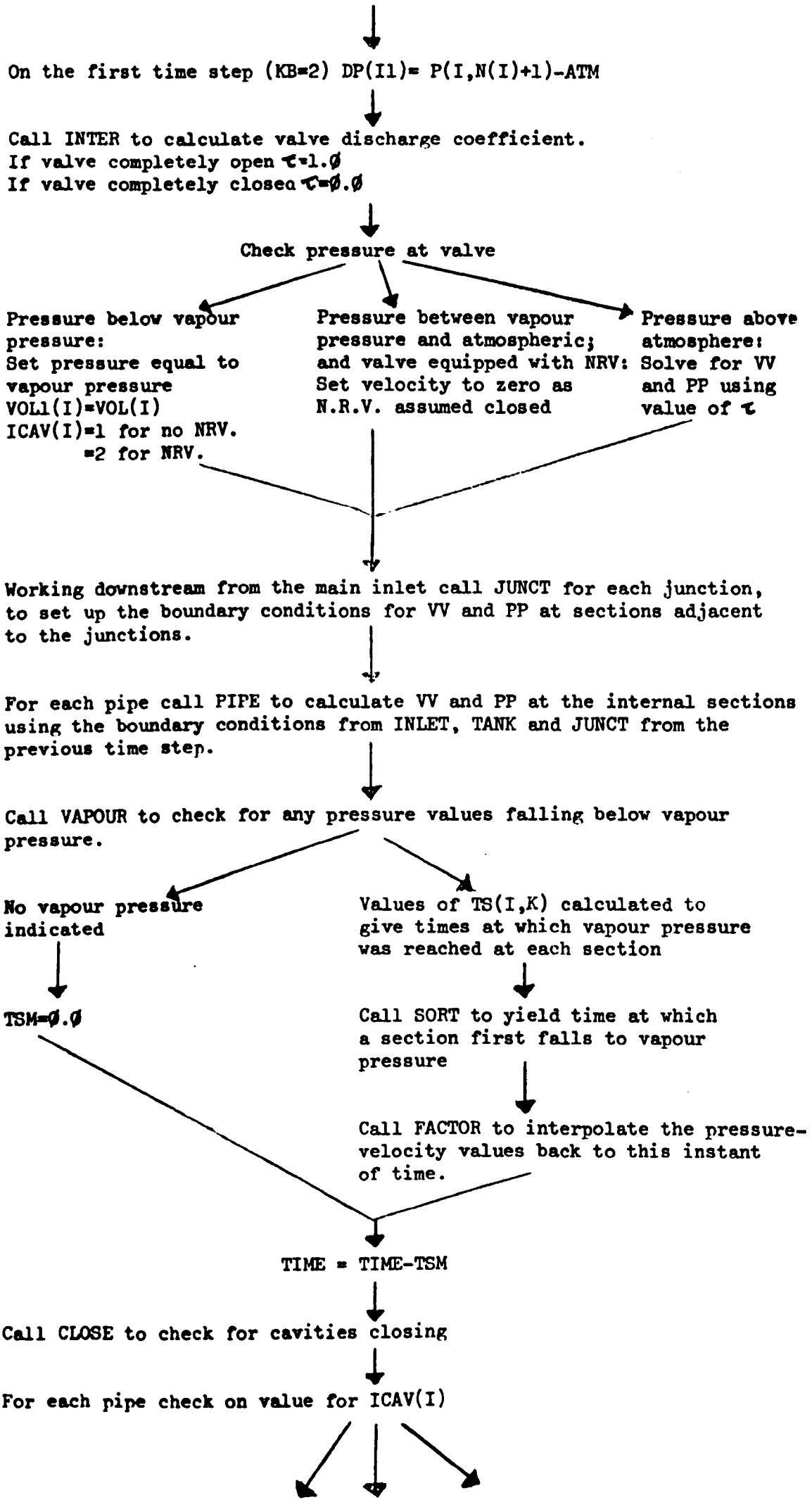
On the first time step (KB=2) DP(I1)= P(I,N(I)+1)-ATM
Call INTER to calculate valve discharge coefficient.
If valve completely open τ=1.Ø
If valve completely closed τ=Ø.Ø
Check pressure at valve
Pressure below vapour pressure:
Set pressure equal to vapour pressure
VOL1(I)=VOL(I)
ICAV(I)=1 for no NRV.
=2 for NRV.
Pressure between vapour pressure and atmospheric; and valve equipped with NRV:
Set velocity to zero as N.R.V. assumed closed
Pressure above atmosphere:
Solve for VV and PP using value of τ
Working downstream from the main inlet call JUNCT for each junction, to set up the boundary conditions for VV and PP at sections adjacent to the junctions.
For each pipe call PIPE to calculate VV and PP at the internal sections using the boundary conditions from INLET, TANK and JUNCT from the previous time step.
Call VAPOUR to check for any pressure values falling below vapour pressure.
No vapour pressure indicated
TSM=Ø.Ø
Values of TS(I,K) calculated to give times at which vapour pressure was reached at each section
Call SORT to yield time at which a section first falls to vapour pressure
Call FACTOR to interpolate the pressure-velocity values back to this instant of time.
TIME = TIME-TSM
Call CLOSE to check for cavities closing
For each pipe check on value for ICAV(I)

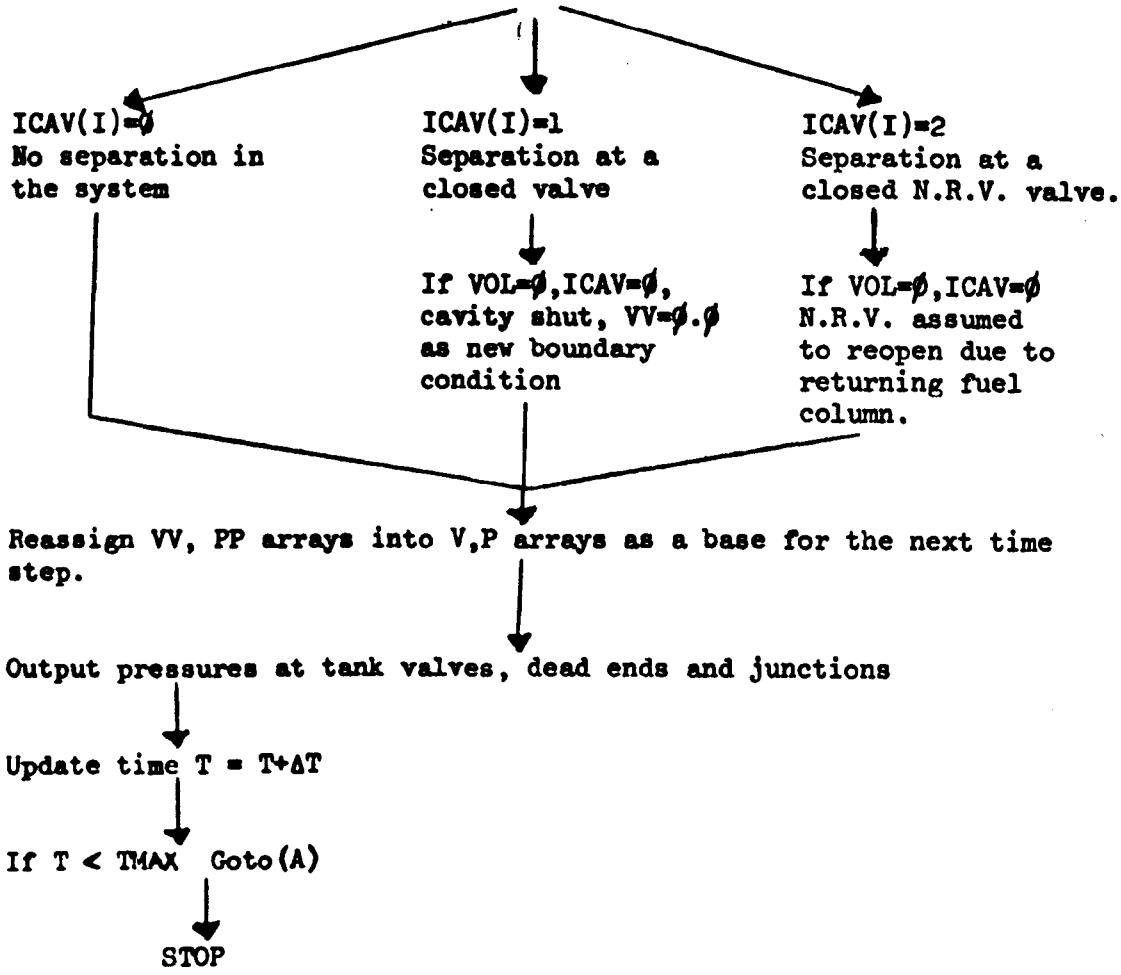
ICAV(I)=ϕ
No separation in the system
ICAV(I)=1
Separation at a closed valve
ICAV(I)=2
Separation at a closed N.R.V. valve.
If VOL=ϕ,ICAV=ϕ, cavity shut, VV=ϕ.ϕ as new boundary condition
If VOL=ϕ,ICAV=ϕ N.R.V. assumed to reopen due to returning fuel column.
Reassign VV, PP arrays into V,P arrays as a base for the next time step.
Output pressures at tank valves, dead ends and junctions
Update time T = T+ΔT
If T < TMAX Goto(A)
STOP

(B)

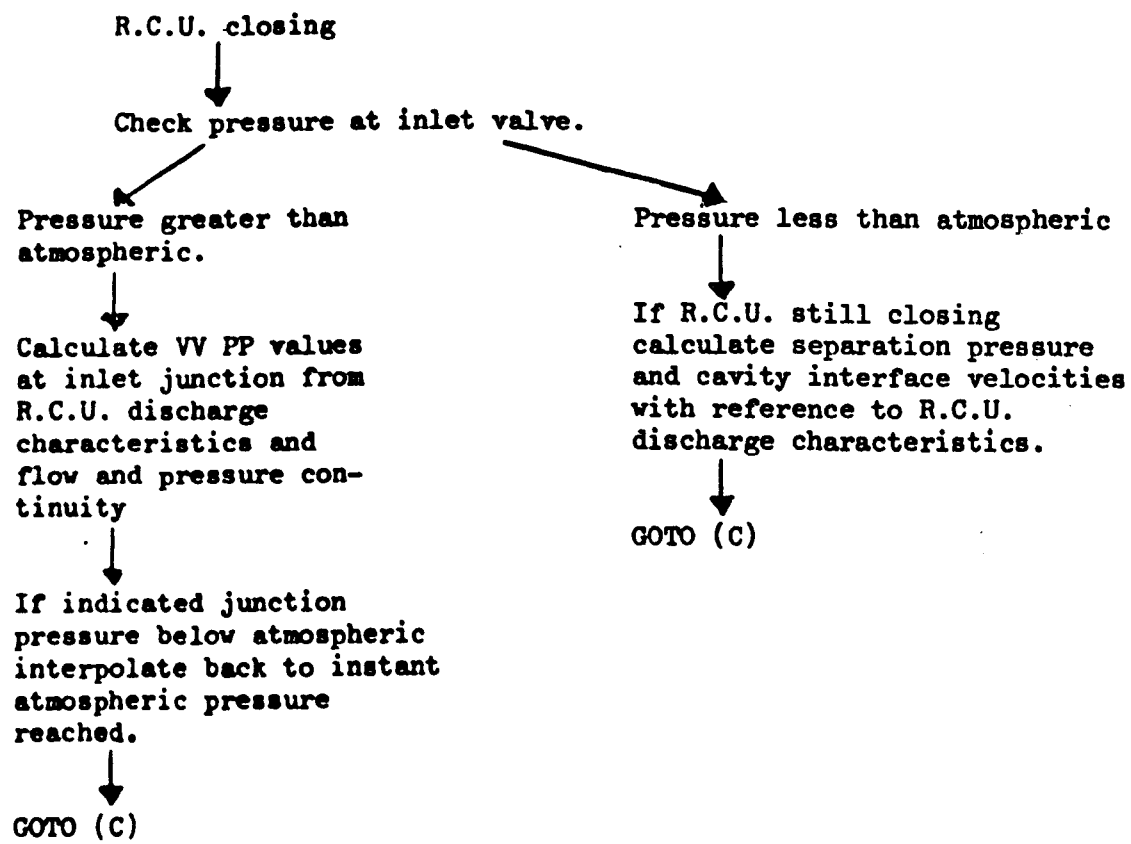
R.C.U. closing
Check pressure at inlet valve.
Pressure greater than atmospheric.
Calculate VV PP values at inlet junction from R.C.U. discharge characteristics and flow and pressure continuity
If indicated junction pressure below atmospheric interpolate back to instant atmospheric pressure reached.
GOTO (C)
Pressure less than atmospheric
If R.C.U. still closing calculate separation pressure and cavity interface velocities with reference to R.C.U. discharge characteristics.
GOTO (C)

(D)

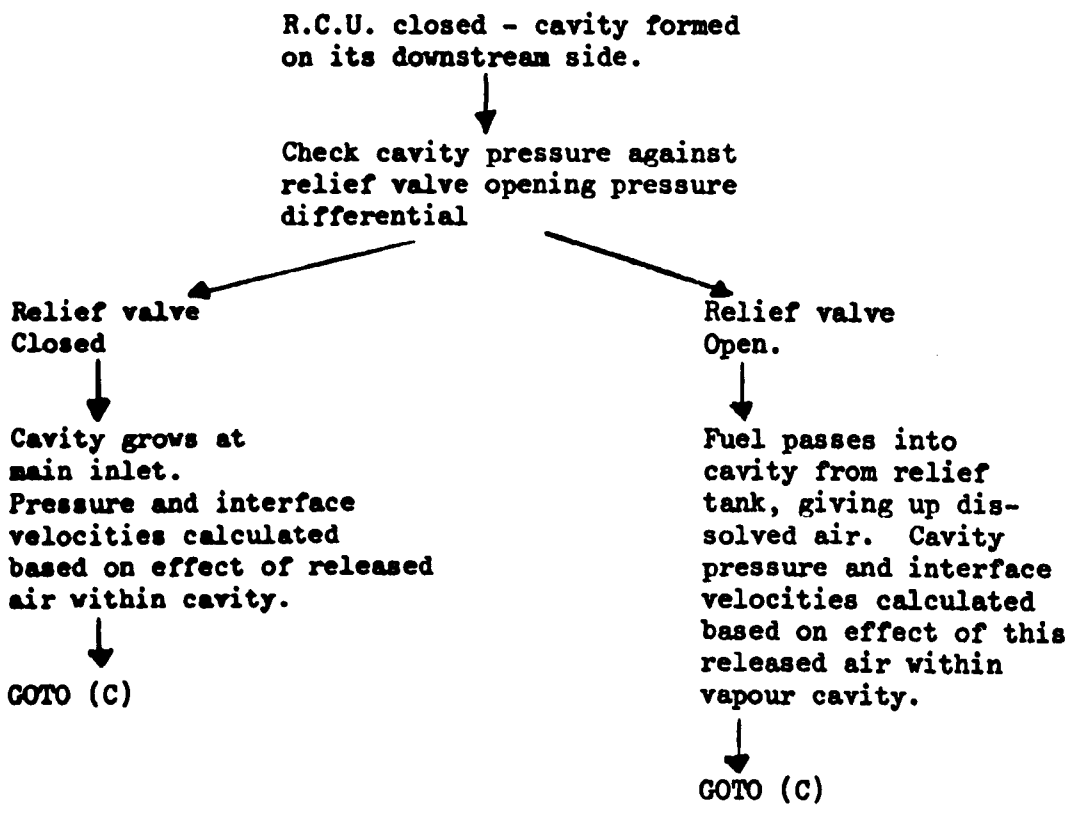
R.C.U. closed - cavity formed on its downstream side.
Check cavity pressure against relief valve opening pressure differential
Relief valve Closed
Cavity grows at main inlet. Pressure and interface velocities calculated based on effect of released air within cavity.
GOTO (C)
Relief valve Open.
Fuel passes into cavity from relief tank, giving up dissolved air. Cavity pressure and interface velocities calculated based on effect of this released air within vapour cavity.
GOTO (C)

Discussion of Results

Figures 8 to 15 represent the predicted pressure variations at the RCU and tank inlet valves during and following the simultaneous closure of all the tank inlet valves in an overall closure time of 1.29 seconds. The curves clearly split into two distinct sections, pressure variations up to and following tank inlet valve closure.

Up to valve closure the system is subjected to positive pressure waves propagating away from each valve, however as the valve closure times are far in excess of the local pipe periods, from both the adjacent junctions and the main inlet, negative reflections from these boundaries will tend to give the pressure variation at the valve its characteristic 'maximum pressure before valve closure' shape. The presence of positive pressure waves from the other closing valves does tend to cloud the picture, however the curves are of a shape that can be expected from an analysis of the system based on known boundary reflection coefficients.

The supply to the aircraft has been assumed to be represented by a constant pressure reservoir. This is justified by the fact that the Hose End Pressure Controller maintains a constant pressure at the inlet to the RCU. This assumption would lead to a reverse flow through the RCU following tank inlet valve closure, however this could not occur on the aircraft so that the RCU has also been assumed to act as a non-return valve. This explains the pressure fluctuations predicted following tank inlet valve closure as the system becomes a piping network with all boundaries represented by closed valves and dead ends so that the pressure waves present at valve closure are reflected internally with very little damping. In practice this pressure variation would damp quickly due to natural wave front dispersion, which is not included in the model, system vibration and fluid friction.

Two interesting points emerge from the curves obtained, namely the dependence of spherical plug valves on a small central part of their rotation for flow stoppage and the effect of the change in valve characteristic obtained by the use of the restrictor plates, particularly on tank 6. Figures 16 to 19 illustrate the valve characteristics for all the tank inlet valves on the aircraft and the normal one speed rotation closure mode. It will be appreciated that a two speed valve motion could be used to reduce transient pressures while keeping the valve overall closing time constant.

An important consideration is the likely accuracy of these results. In the absence of any test rig results, the appropriate point in the system testing programme will not be reached till next year, the only measure of accuracy is that supplied by work on transients in kerosene reported elsewhere (6, 7, 8). In this case accuracy within 10% could be expected, but depending entirely on the accuracy of the assumptions made relating to the RCU and the accuracy of the valve characteristics measured by one of the authors at Flight Refuelling. During later program runs to consider the effect of column separation following RCU shut down the accuracy would be expected to decrease due to the complexity of the solution caused by the release of dissolved air.

Conclusions and Further Work

A computer program has been written and found to give an acceptable qualitative picture of pressure transients in the Concorde refuelling system following tank inlet valve closure. The quantitative results appear reasonable but an estimate of the program accuracy will have to await the appropriate full scale tests on the fuel system test rig.

The program will also be used to investigate column separation on closure of the Refuelling Control Unit.

It is hoped to extend the work to include the Trim Transfer and jettison sub-systems of the aircraft.

Acknowledgements

Much of the analysis reported was based on work carried out at The City University under a Science Research Council award BSR 5832. This award and the facilities made available by Professor J.C. Levy are gratefully acknowledged.

The authors wish to thank the British Aircraft Corporation for permission to publish this paper.

References

1. Gray, C.A.M. "Analysis of waterhammer by a method of characteristics" Proc. A.S.C.E. 1953 Vol. 79.

2. Streeter, V.L. and Wylie, E.B. "Hydraulic Transients" McGraw-Hill 1967.

3. Fox, J.A. "Use of a digital computer in the solution of water-hammer problems" Inst. Civil Eng. Proc. Vol. 39 1968.

4. Bergeron, L. "Waterhammer in hydraulics and wave surges in electricity" Wiley, London 1957.

5. Angus, R.W. "Waterhammer in pipes" Procs. I.Mech.E. Vol. 136, 1937.

6. Swaffield, J.A. "Column separation following valve closure in a kerosene pipeline" Procs. I.Mech.E. 1970 and T.C.U. Research Memo. ML.5 June 1969.

7. Swaffield, J.A. "Visualization of column separation in a kerosene pipeline" TCU Research Memo. ML 18 April 1970.

8. Swaffield, J.A. "The influence of air release on column separation in a kerosene pipeline" TCU Research Memo. ML 21 June 1970.

9. Lister, Mary "Numerical solution of hyperbolic partial differential equations by the method of characteristics" in Vol. 1 of "Mathematical Methods for Digital Computers" Ed. Ralston and Wilf. Wiley, London 1960.

10. Evangelisti, G. "Waterhammer analysis by the method of characteristics" Energia Electrica 46, 10, 11, 12. 1969-70.

11. B.A.C. (Systems Lab.) "Ground Refuelling Surge Pressures" Test Note 50, 1967.

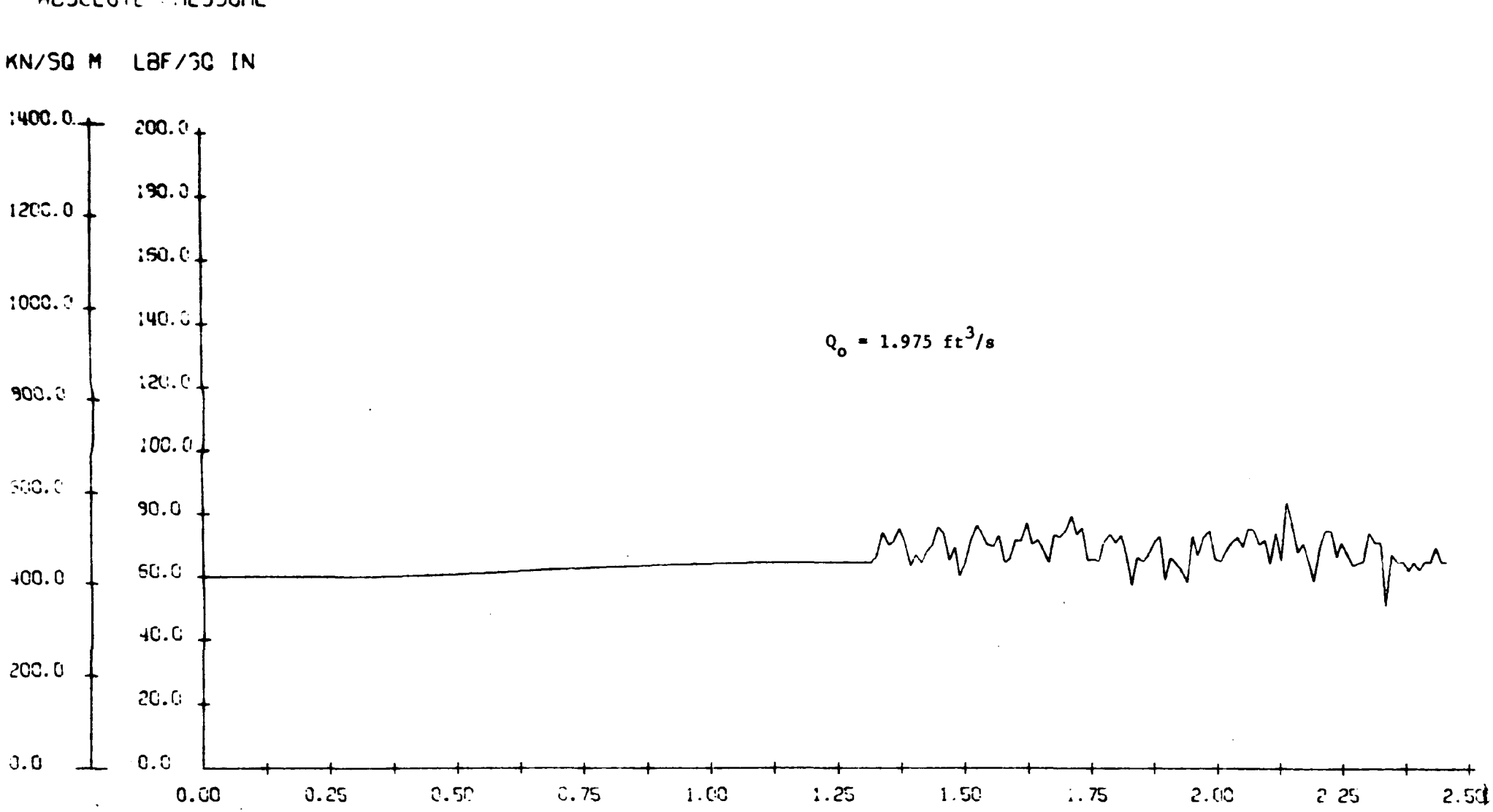

Fig. 8 PRESSURE VARIATION RECORDED AT MAIN INLET DURING TEST CASE 1

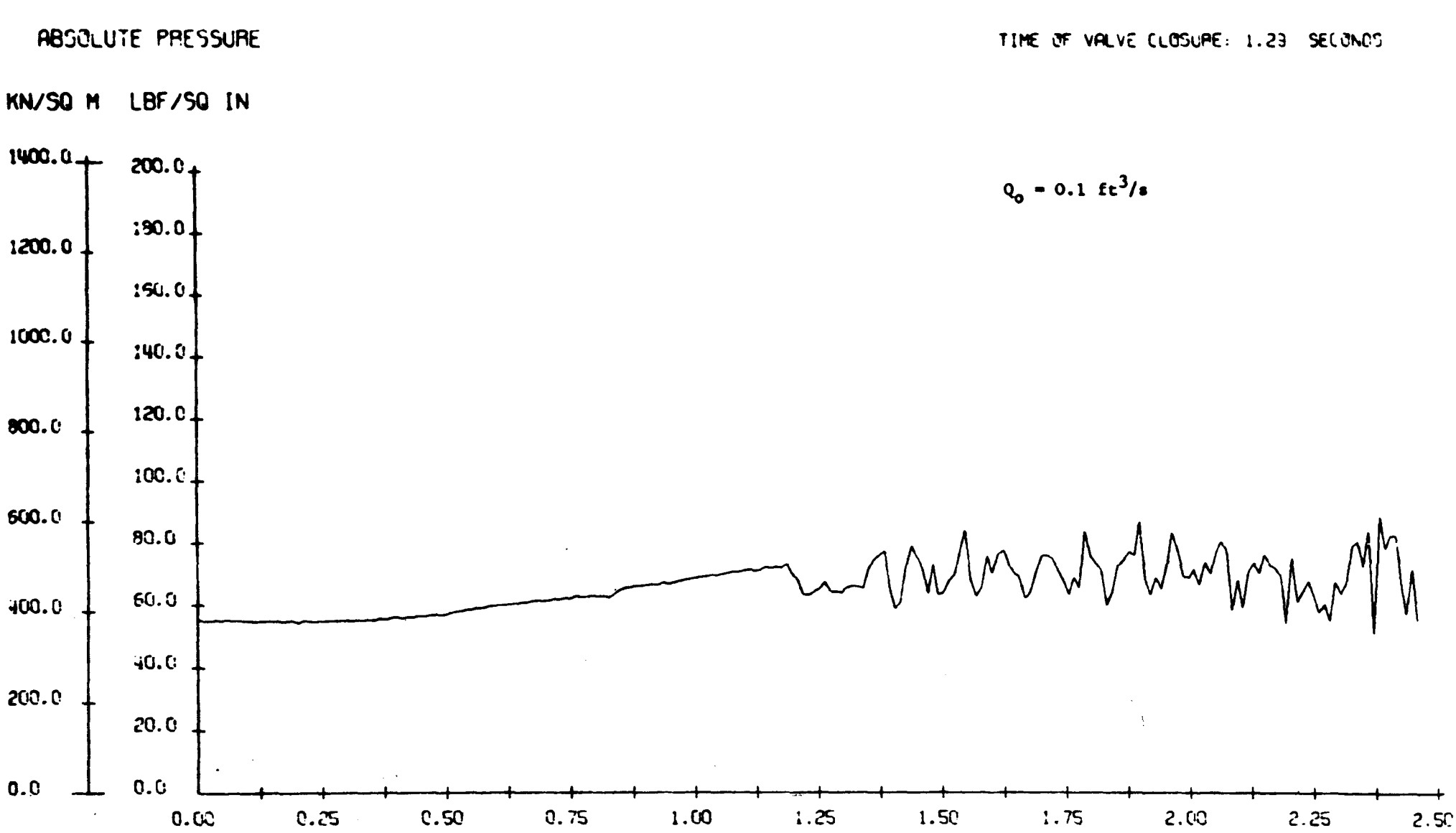

Fig. 9 PRESSURE VARIATION RECORDED AT TANK 1 DURING TEST CASE 1

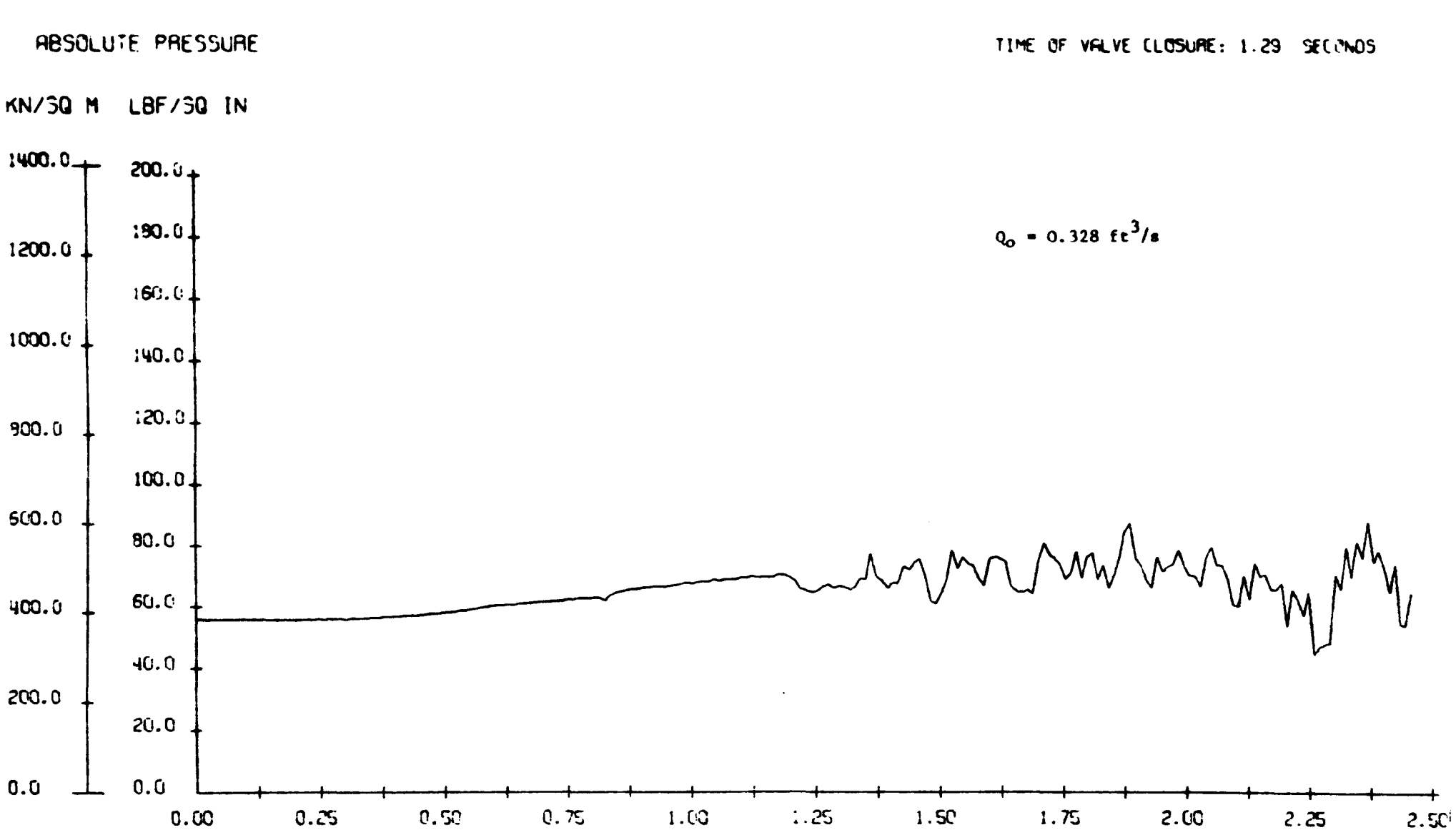

Fig. 10 PRESSURE VARIATION RECORDED AT TANK 5 DURING TEST CASE 1

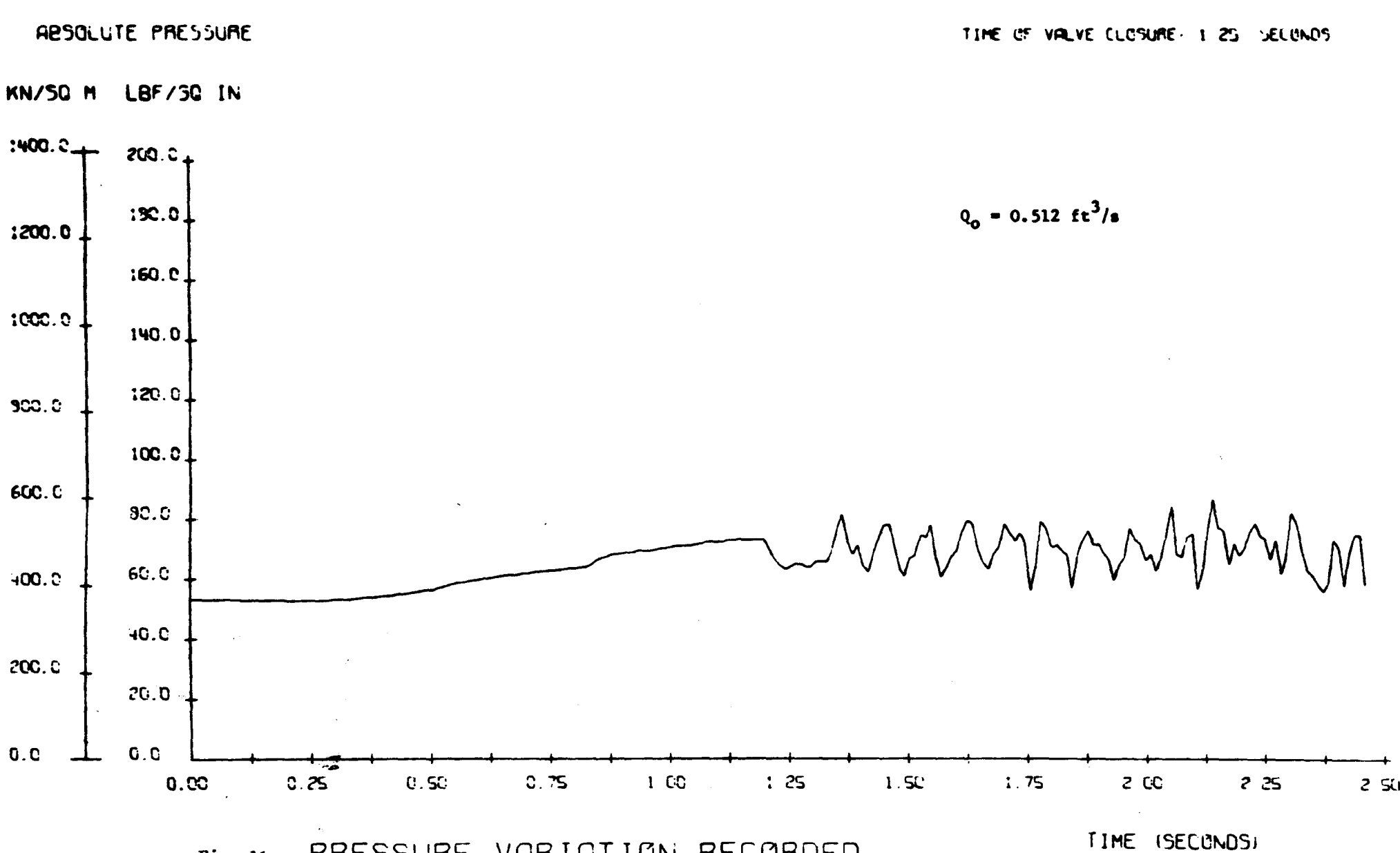

Fig. 11 PRESSURE VARIATION RECORDED AT TANK 9 DURING TEST CASE 1

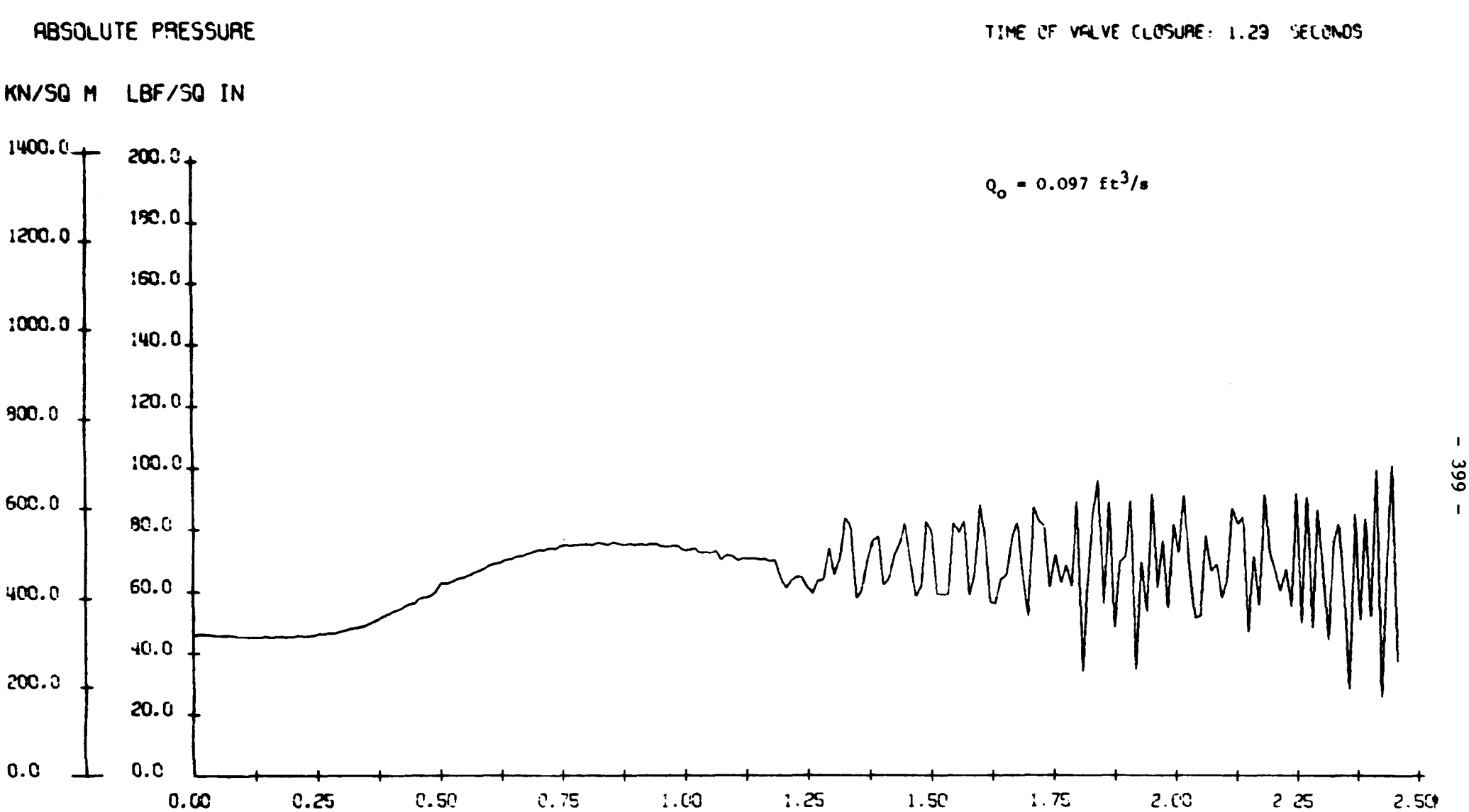

Fig. 12 PRESSURE VARIATION RECORDED AT TANK 5A DURING TEST CASE 1

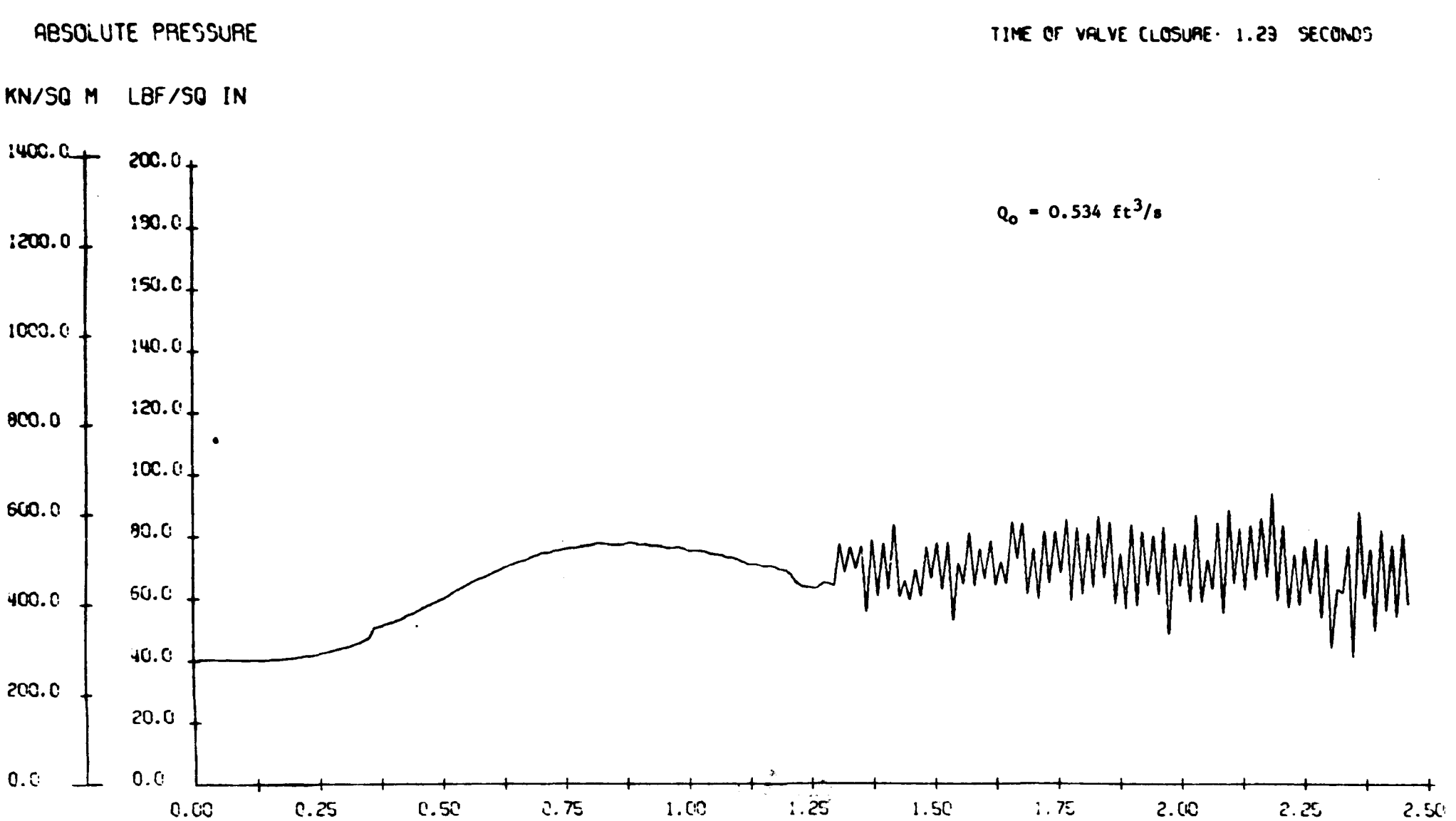

Fig. 13 PRESSURE VARIATION RECORDED AT TANK 6 DURING TEST CASE 1

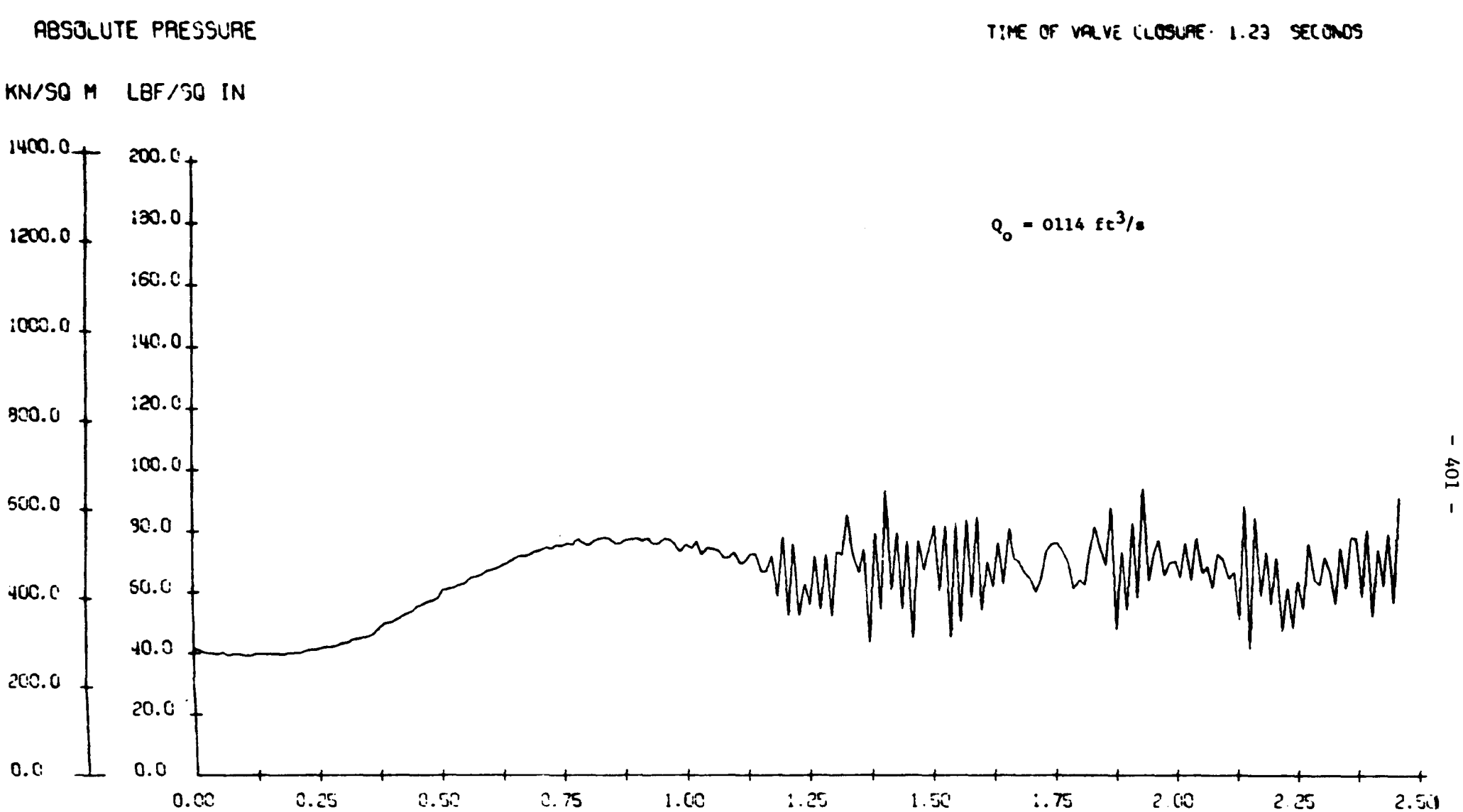

Fig. 14 PRESSURE VARIATION RECORDED AT TANK 2 DURING TEST CASE 1

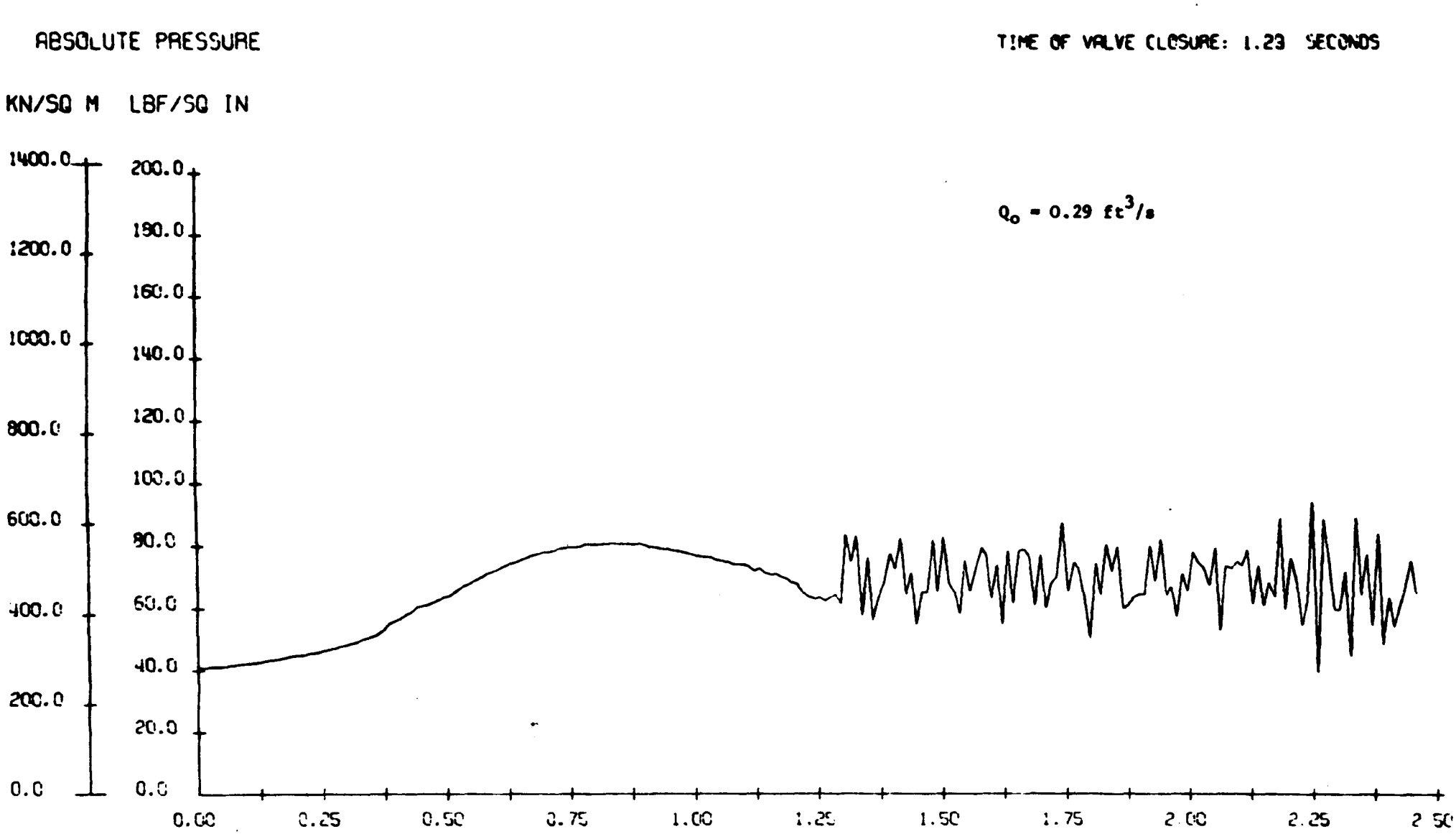

Fig. 15 PRESSURE VARIATION RECORDED AT TANK 11 DURING TEST CASE 1

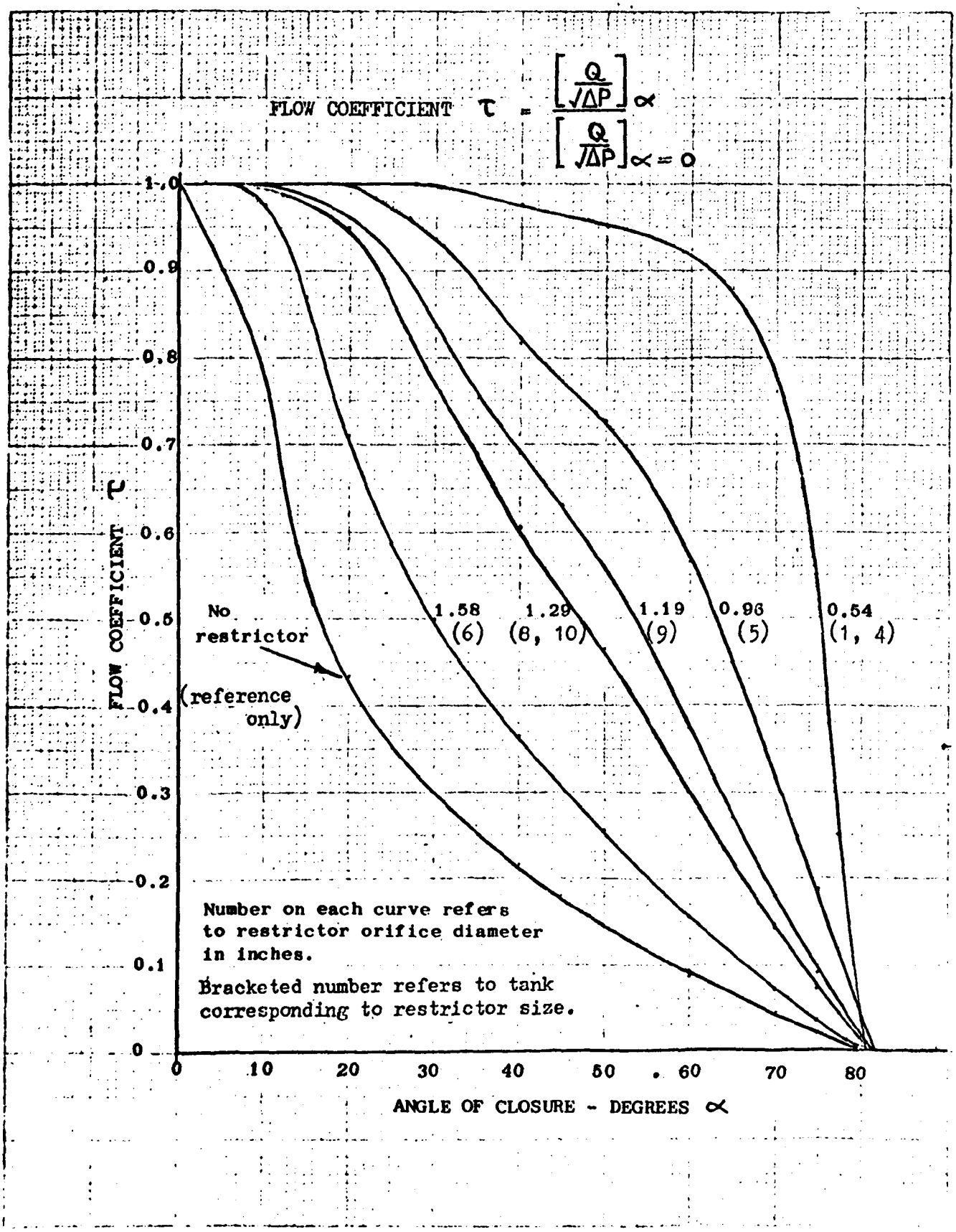

2" Refuelling Valve

Fig. 16 CLOSURE CHARACTERISTICS - FLOW v ANGLE

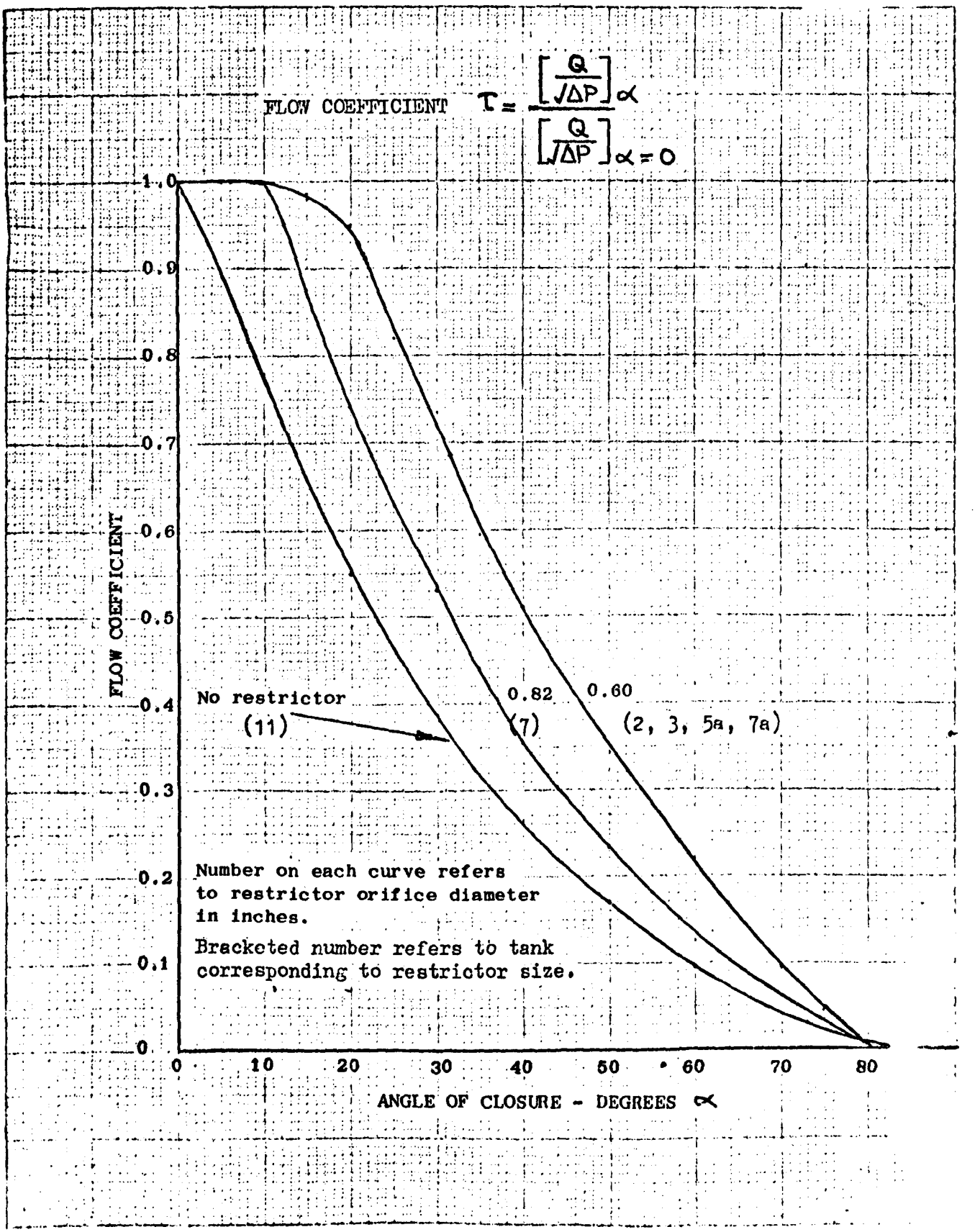

1" Refuelling Valve

Fig. 17 CLOSURE CHARACTERISTICS - FLOW v ANGLE

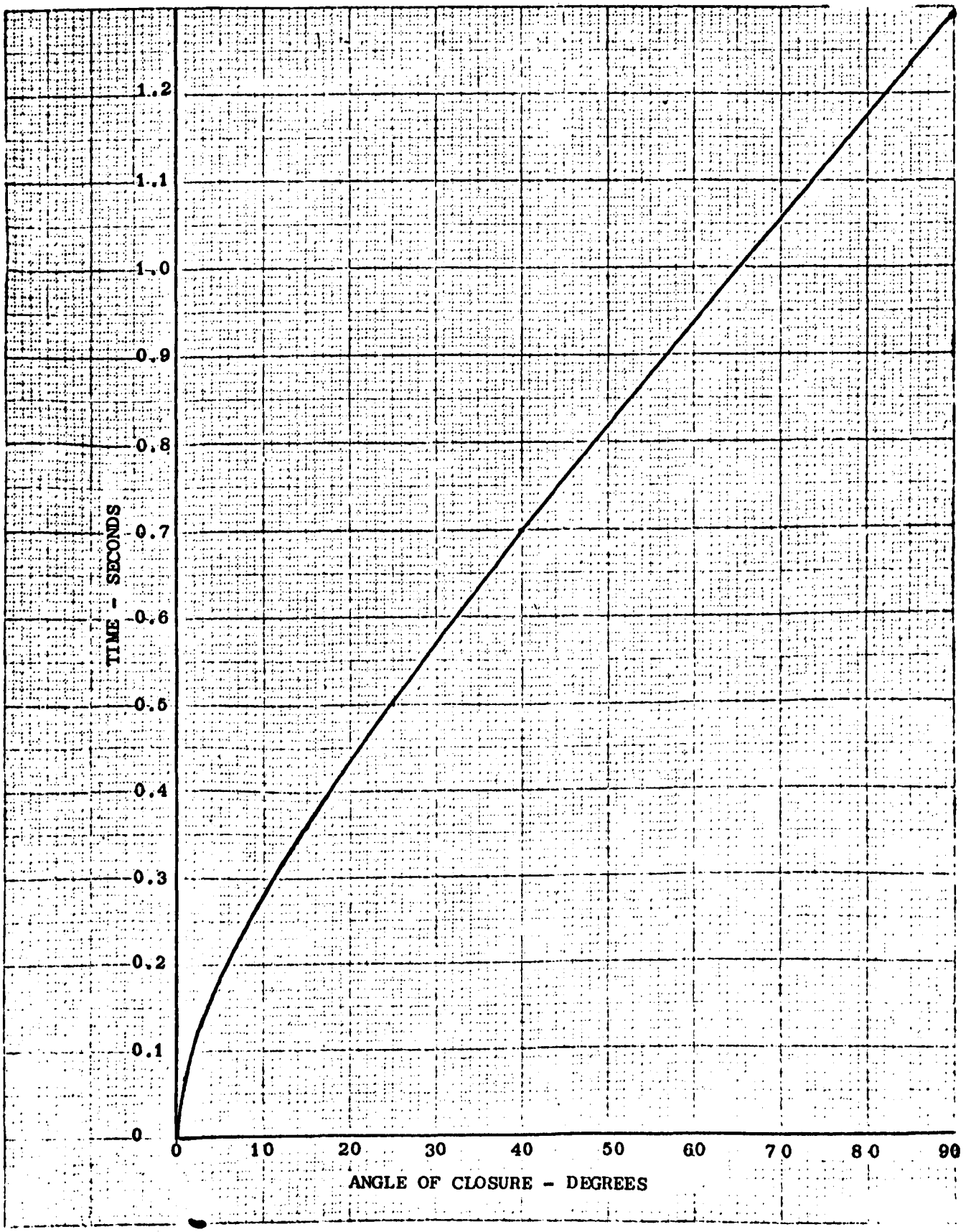

1" and 2" Refuelling Valve

Fig. 18 CLOSURE CHARACTERISTICS - TIME v ANGLE

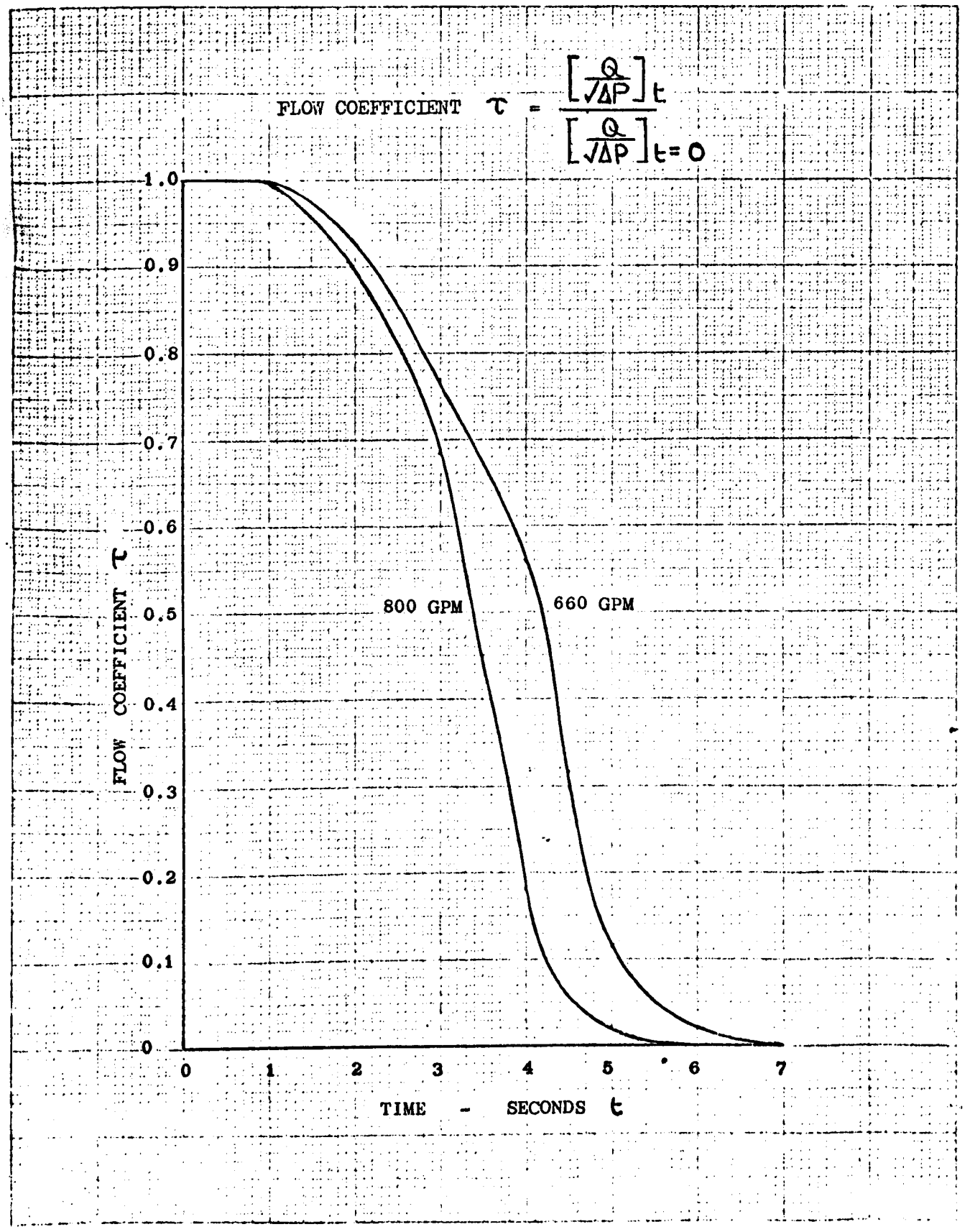

Refuelling Control Unit

Fig. 19 REFUEL CLOSURE CHARACTERISTIC - FLOW COEFF v TIME